

การจำแนกยีนที่เกี่ยวข้องกับการพัฒนาการรังไข่ของกิ้งกูดำ *Penaeus monodon*



นางสาว รชนิมุข ปรีชาผล

ศูนย์วิทยทรัพยากร
จุฬาลงกรณ์มหาวิทยาลัย

วิทยานิพนธ์นี้เป็นส่วนหนึ่งของการศึกษาตามหลักสูตรปริญญาวิทยาศาสตรดุษฎีบัณฑิต

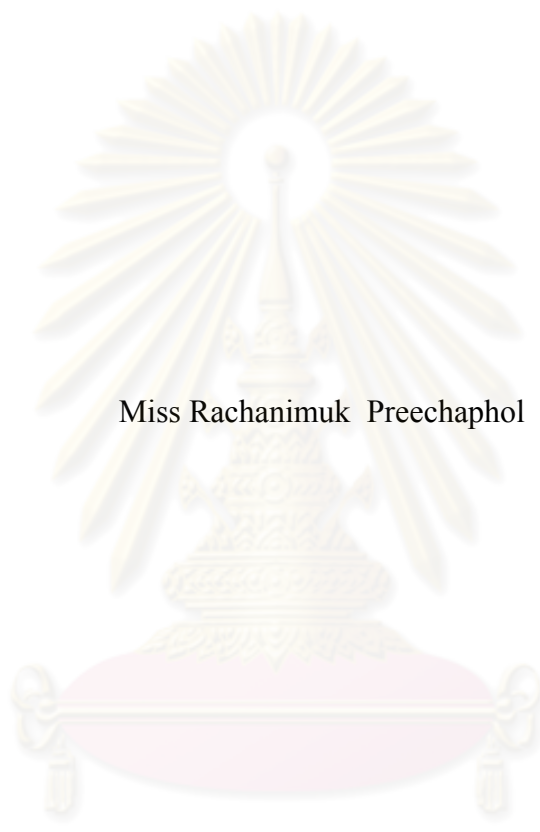
สาขาวิชาเทคโนโลยีชีวภาพ

คณะวิทยาศาสตร์ จุฬาลงกรณ์มหาวิทยาลัย

ปีการศึกษา 2551

ลิขสิทธิ์ของจุฬาลงกรณ์มหาวิทยาลัย

IDENTIFICATION OF GENES RELATED TO OVARIAN DEVELOPMENT OF
THE GIANT TIGER SHRIMP *Penaeus monodon*



Miss Rachanimuk Preechaphol

ศูนย์วิทยทรัพยากร
จุฬาลงกรณ์มหาวิทยาลัย
A Dissertation Submitted in Partial Fulfillment of the Requirements
for the Degree of Doctor of Philosophy Program in Biotechnology

Faculty of Science


Chulalongkorn University

Academic year 2008


Copyright of Chulalongkorn University

Thesis Title Identification of genes related to ovarian development of the giant tiger shrimp *Penaeus monodon*
By Miss Rachanimuk Preechaphol
Field of Study Biotechnology
Advisor Professor Piamsak Menasveta, Ph.D.
Co-Advisor Sirawut Klinbunga, Ph.D.


Accepted by the Faculty of Science, Chulalongkorn University in Partial Fulfillment of the Requirements for the Doctoral Degree

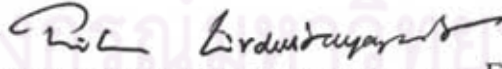

..... Dean of the Faculty of Science
(Professor Supot Hannongbua, Dr.rer.nat.)


THESIS COMMITTEE



..... Chairman
(Associate Professor Sirirat Rengpipat, Ph.D.)


..... Advisor
(Professor Piamsak Menasveta, Ph.D.)


..... Co-Advisor
(Sirawut Klinbunga, Ph.D.)


..... Examiner
(Associate Professor Thaithaworn Lirdwittayaprasit, Ph.D.)


..... Examiner
(Associate Professor Warawut Chulalaksananukul, Ph.D.)


..... External Examiner
(Sittiruk Roytrakul, Ph.D.)

รชนิมุข ปรีชาผล : การจำแนกยีนที่เกี่ยวข้องกับการพัฒนาการรังไข่ของกุ้งกุลาดำ *Penaeus monodon* (IDENTIFICATION OF GENES RELATED TO OVARIAN DEVELOPMENT OF THE GIANT TIGER SHRIMP *Penaeus monodon*) อ.ที่ปรึกษาวิทยานิพนธ์หลัก : ศ.ดร. เปี่ยมศักดิ์ เมณะเศวต, อ. ที่ปรึกษาวิทยานิพนธ์ร่วม : ดร. ศิราวุธ กลิ่นบุหงา, 353 หน้า.

สร้างห้องสมุดยีนจากรังไข่ของกุ้งกุลาดำเพื่อสืบค้นยีนที่เกี่ยวข้องกับการพัฒนาการรังไข่ในกุ้งกุลาดำ จากการโคลนและหาลำดับนิวคลีโอไทด์ของอีเอสทีทั้งหมด 4560 อีเอสที (จากห้องสมุดยีนปกติจำนวน 2,330 อีเอสที, ห้องสมุดยีน normalized จำนวน 1,778 อีเอสที และห้องสมุดยีน forward และ reverse subtraction จำนวน 452 อีเอสที) พบว่า 3482 อีเอสที (76.4% ประกอบด้วย 692 singletons; 15.2% และ 331 contigs) มีลำดับนิวคลีโอไทด์ที่เหมือนกับยีนในฐานข้อมูล NCBI (E-value < 10⁻⁴) โดยมีจำนวน contigs ที่พบทั้งหมด 441 contigs และ 1231 (27.0%) singletons โดย TSP (452 อีเอสที, 9.9%) และ *peritrophin* (470 อีเอสที, 10.3%) เป็นยีนที่พบมากในห้องสมุดอีเอสทีจากรังไข่ของกุ้งกุลาดำ

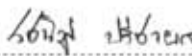

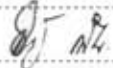
จากการสืบค้นเครื่องหมายที่แสดงออกแตกต่างกันระหว่างการพัฒนาการรังไข่ของกุ้งกุลาดำ ด้วยวิธี RAP-PCR ได้คัดเลือกเครื่องหมาย RAP-PCR จำนวน 14 เครื่องหมายมาออกแบบไพรเมอร์เพื่อตรวจสอบรูปแบบการแสดงออกของยีน และพบว่า 7 ยีน (*B cell RAG associated protein*, *hypothetical protein W02B8.3*, *DNA replication licensing factor MCM5*, *APEX nuclease*, *U5 snRNP-specific protein*, *ABC transporter* และ *Moira CG18740-PA*) แสดงแนวโน้มของรูปแบบการแสดงออกที่แตกต่างกันในรังไข่ระยะต่างๆของกุ้งกุลาดำ จึงตรวจสอบการแสดงออกของยีนด้วยวิธี Semiquantitative RT-PCR พบว่ายีน *B cell RAG associated protein* และ *APEX nuclease* มีระดับการแสดงออกในรังไข่ระยะที่ 1 สูงกว่าระยะอื่นๆ ($P < 0.05$) ส่วน *U5 snRNP-specific protein* มีระดับการแสดงออกลดลงที่รังไข่ระยะที่ 4 ($P < 0.05$) บ่งชี้ว่ายีนดังกล่าวน่าจะมีความสำคัญต่อการพัฒนาการรังไข่ของกุ้งกุลาดำ

หาลำดับนิวคลีโอไทด์ที่สมบูรณ์ของยีนต่างๆ จากห้องสมุดอีเอสทีจากรังไข่ของกุ้งกุลาดำจำนวน 18 ยีน ประกอบด้วย *SARIP*, *PGMRC1*, *p23*, *Cdc42*, *PSR*, *Bystin*, *chk1*, *carbonyl reductase*, *Protein disulfide-isomerase precursor (PDI)* (*Prolyl 4-hydroxylase subunit beta*) (*Cellular thyroid hormone-binding protein*) (*p55*) (*Erp59*), *gonadotropin-regulated long chain acyl-CoA synthetase*, *Cdc20*, *protein mago nashi*, *actin depolymerizing factor*, *I-box and wd-40 domain protein*, *Cyclin-dependent kinase 7*, *selenoprotein M precursor* และ *anaphase promoting complex subunit 11 homolog*) ด้วยวิธี RACE-PCR และการหาลำดับนิวคลีโอไทด์เพิ่มจากโคลนที่มียีนที่สมบูรณ์

ตรวจสอบการแสดงออกด้วยวิธี quantitative real-time PCR พบว่า *Pm-p23* มีระดับการแสดงออกเพิ่มขึ้นตั้งแต่วัยระยะที่ 1 ($P < 0.05$) ในขณะที่ *Pm-Cdc42* มีระดับการแสดงออกลดลงตั้งแต่วัยระยะที่ 3 ($P < 0.05$) อย่างไรก็ตาม การตัดดาวน์ส่งผลต่อระดับการแสดงออกของยีน *Pm-p23* ($P > 0.05$) แต่ส่งผลให้ *Pm-Cdc42* มีระดับการแสดงออกเพิ่มขึ้นในวัยระยะที่ 3 และ 4 ($P < 0.05$) รูปแบบการแสดงออกของยีน *Pm-SARIP* และ *Pm-PGMRC1* มีระดับการแสดงออกแตกต่างกันในรังไข่ของกุ้งกุลาดำปกติ ($P < 0.05$) การตัดดาวน์ส่งผลให้การแสดงออกของยีนดังกล่าวมีระดับสูงขึ้นเมื่อรังไข่มีการเจริญมากขึ้น และระดับการแสดงออกยิ่งสูงกว่าในรังไข่ของกุ้งกุลาดำปกติที่ระยะเดียวกันอีกด้วย ($P < 0.05$) บ่งชี้ว่ายีนดังกล่าวตอบสนองต่อการกระตุ้นการเจริญพันธุ์ระยะสุดท้ายด้วยการตัดดาวน์หรือการกำจัด GIH แสดงให้เห็นว่าสามารถใช้อินดิวเตอร์เป็นเครื่องหมายโมเลกุลเพื่อตรวจสอบความสมบูรณ์พันธุ์ของแม่พันธุ์กุ้งกุลาดำโดยวิธีการกระตุ้นการเจริญพันธุ์ด้วยการให้อาหาร การฉีดกระตุ้นด้วยฮอร์โมน และ/หรือสารจำพวก neurotransmitter ได้

นอกจากนี้ได้ตรวจสอบตำแหน่งการแสดงออกของยีนและโปรตีนที่สนใจในรังไข่ของกุ้งกุลาดำด้วยวิธี *in situ* hybridization และ immunohistochemistry โดยพบว่ายีน *Pm-Cdc42*, *Pm-PGMRC1*, *Pm-SARIP* และ *Pm-p23* แสดงออกที่โอโอพลาสซึมของเซลล์ไข่ระยะ previtellogenic โดยโปรตีน *Pm-PGMRC1* พบที่ชั้น follicle และผนังของเซลล์ follicle เท่านั้น โดยไม่พบที่เซลล์ไข่ของกุ้งกุลาดำส่วนโปรตีน *Pm-Cdc42* นั้นพบที่โอโอโกเนีย (oogonia), โอโอพลาสซึมของเซลล์ไข่ระยะ previtellogenic และ ชั้น follicle

สร้างโปรตีนลูกผสมของ *Cdc42* และ *p23* ในแบคทีเรีย ทำให้บริสุทธิ์และใช้ผลิต polyclonal antibody จากการศึกษา western blot แสดงว่าโปรตีน *p23* มีระดับสูงในรังไข่ระยะ previtellogenic และลดลงเมื่อรังไข่มีพัฒนาการสูงขึ้น ซึ่งเป็นการบ่งชี้ว่า *p23* มีความสำคัญในช่วงต้นของการพัฒนาการรังไข่ของกุ้งกุลาดำ

สาขาวิชา.....เทคโนโลยีชีวภาพ.....ลายมือชื่อผู้นิสิต.....
ปีการศึกษา.....2551.....ลายมือชื่อ อ.ที่ปรึกษาวิทยานิพนธ์หลัก.....
ลายมือชื่อ อ.ที่ปรึกษาวิทยานิพนธ์ร่วม.....

4773865323 : MAJOR BIOTECHNOLOGY

KEYWORDS *Penaeus monodon* / GIANT TIGER SHRIMP / OVARIAN MATURATION / cDNA LIBRARY / *IN SITU* HYBRIDIZATION

RACHANIMUK PREECHAPHOL : IDENTIFICATION OF GENES RELATED TO OVARIAN DEVELOPMENT OF THE GIANT TIGER SHRIMP *Penaeus monodon*. ADVISOR : PROF. PIAMSAK MENASVETA, Ph.D., CO-ADVISOR : SIRAWUT KLINBUNGA, Ph.D., 353 pp.

Reproduction-related genes in ovaries of the giant tiger shrimp (*Penaeus monodon*) were identified and characterized. A total of 4560 clones (2330 clones from typical, 1778 clones from normalized and 452 clones from subtraction ovarian cDNA libraries) were unidirectional sequenced and 2167 (47.5%) ESTs significant matched known genes previously deposited in the GenBank (E-value < 10⁻⁴) were obtained. *TSP* (452 clones, 9.9% of ESTs sequenced) and *peritrophin* (470 clones, 10.3%) predominated among known transcripts. Sequence assembly of all ESTs resulted in 441 contigs and 1231 (27.0%) singletons.

RNA-arbitrary primed (RAP)-PCR was carried out for identification of differentially expressed transcripts during ovarian development of *P. monodon*. Fourteen candidate RAP-PCR markers were cloned and sequenced. Seven genes (*B cell RAG associated protein*, *hypothetical protein W02B8.3*, *DNA replication licensing factor MCM5*, *APEX nuclease* and *U5 snRNP-specific protein*, *ABC transporter* and *moira CG18740-PA*) showed a trend of differential expression between different ovarian developmental stages. Semiquantitative RT-PCR indicated that the expression level of *B cell RAG associated protein* and *APEX nuclease* at stage I ovaries was greater than that of other stages ($P < 0.05$). In contrast, *U5 snRNP-specific protein* was down-regulated at stage IV ovaries ($P < 0.05$). Accordingly, these transcripts should functionally contribute in ovarian development of *P. monodon*.

The full length cDNA of *SARIP*, *PGMRC1*, *p23* and *Cdc42* transcripts and other functional important transcripts; *phosphatidyl serine receptor (PSR)*, *bystin*, *chk1*, *carbonyl reductase*, *protein disulfide-isomerase precursor (PDI)* (*prolyl 4-hydroxylase subunit beta*) (*cellular thyroid hormone-binding protein*) (*p55*) (*Erp59*), *gonadotropin-regulated long chain acyl-CoA synthetase*, *Cdc20*, *protein mago nashi*, *actin depolymerizing factor*, *f-box* and *wd-40 domain protein*, *cyclin-dependent kinase 7*, *selenoprotein M precursor* and *anaphase promoting complex subunit 11*) were successfully identified by RACE-PCR or sequencing of the original cDNA clones.

Quantitative real-time PCR indicated that *Pm-p23* was up-regulated at the early stage ($P < 0.05$) whereas *Cdc42* was down-regulated at stage III ($P < 0.05$) of ovarian development. Eyestalk ablation did not alter the expression pattern of *Pm-p23* ($P > 0.05$) but caused increasing levels of *Pm-Cdc42* at stage III and IV ovaries of *P. monodon* ($P < 0.05$). *Pm-SARIP* and *Pm-PGMRC1* were differentially expressed in ovaries of normal broodstock ($P < 0.05$). Eyestalk ablation resulted in earlier and greater upregulation of these genes in ovaries of eyestalk ablated broodstock than normal broodstock ($P < 0.05$). This indicated that expression of *Pm-SARIP* and *Pm-PGMRC1* was influenced by the downstream effects of GIH. Results suggested that *Pm-SARIP* and *Pm-PGMRC1* may be used as bioindicators for monitoring progression of oocyte maturation as a consequent effects of maturation-inducing feed, hormone and/or neurotransmitter administration in *P. monodon* broodstock.

In situ hybridization and immunohistochemistry were applied to examine localization of mRNA and proteins during ovarian development of *P. monodon*. All transcripts (*Pm-Cdc42*, *Pm-PGMRC1*, *Pm-SARIP* and *Pm-p23*) were localized in the ooplasm of previtellogenic oocytes. Immunohistochemistry revealed positive signals of the *Pm-PGMRC1* protein only in the follicular layer and cell membrane of follicular cells. Nevertheless, the false positive signal was also detected when tissue sections were incubated with normal sera. *Pm-Cdc42* was detected in oogonia, cytoplasm of previtellogenic oocytes and follicular layer.

Recombinants *Cdc42* and *p23* proteins were successfully expressed *in vitro*. Polyclonal antibodies of these recombinant proteins were successfully produced. Western blot analysis indicated that the level of *p23* was increased at the previtellogenic stage and decreased as oocyte development progressed. Results confirmed functional important of *p23* gene products during oogenesis of *P. monodon*.

Field of Study : Biotechnology

Student's Signature *Rachanimuk Preechaphol*

Academic Year : 2008

Advisor's Signature *Prof. Piamsak Menasveta*

Co-Advisor's Signature *S. Klinbunga*

ACKNOWLEDGMENTS

I would like to express my deepest gratitude to my advisor Professor Dr. Piamsak Menasveta and my co-advisor Dr. Sirawut Klinbunga for their guidance, supervision, encouragement, invaluable suggestion and supports throughout my study.

My gratitude is also extended to Associate Professor Dr. Sirirat Rengpipat, Associate Professor Dr. Thaithaworn Lirdwitayaprasit, Associate Professor Dr. Warawut Chulalaksananukul and Dr. Sittiruk Roytrakul for serving as thesis committee, for their recommendations and also useful suggestion.

I would particularly like to thank The Golden Jubilee Ph D program, The Thailand Research Funds (TRF) and Commission of Higher Education Staff Development Project, Ministry of Education, Thailand for a student grant (RP).

I would particularly like to extend my thank to the Marine Biotechnology Research Unit, Aquatic Molecular Genetics and Biotechnology laboratory, National Center for Genetic Engineering and Biotechnology (BIOTEC), National Science and Technology Development Agency (NSTDA) and Program in Biotechnology, Faculty of Science, Chulalongkorn University for providing some facilities.

I would like to special thanks to Dr. Keisuke Yamano, Dr. Atushi Fujiwara and Dr. Takuji Okumura, National Research Institute of Aquaculture, Fisheries Research Agency, Minamihara, Mie, Japan for technical training, invaluable suggestion and taking care of me during stay in Japan.

Many thanks are also excessively to Dr. Bavornlak Khamnamtong, Ms. Thidathip Wongsurawat, Ms. Kanchana Sittikhankeaw, Ms. Natechanok Thamneamdee, Ms. Sirikarn prasertlux, Ms. Sasithon Petkon, Ms. Patchari Yocawibun and everyone in the laboratory for their help, suggestion and kindness friendship that give a happy time during a study periods.

Finally, I would like to express my deepest gratitude to my beloved parents, all members of my family and my dearest friend, Mr. Norawat Hiransuchalart, for their love, care, understanding and encouragement extended throughout my study.

CONTENTS

	Page
THAI ABSTRACT.....	iv
ENGLISH ABSTRACT.....	v
ACKNOWLEDGEMENTS.....	vi
CONTENTS.....	vii
LIST OF TABLES.....	xv
LIST OF FIGURES.....	xx
LIST OF ABBREVIATIONS.....	xxxi
CHAPTER I INTRODUCTION	1
1.1 Background information	1
1.2 Objectives	3
1.3 General introduction	3
1.4 Penaeid shrimp biology.....	8
1.4.1 Taxonomy	8
1.4.2 Morphology.....	8
1.4.3 Distribution and life cycle.....	10
1.4.4 Sexual dimorphism	12
1.5 Female reproductive system	12
1.5.1 Morphology of female reproductive system	12
1.5.2 Visual assessment of ovarian development	14
1.5.2.1 Immature ovaries (stage 0).....	14
1.5.2.2 Previtellogenic ovaries (stage I).....	14
1.5.2.3 Early vitellogenic ovaries (stage II)	14
1.5.2.4 Late vitellogenic ovaries (stage III)	14
1.5.2.5 Mature ovaries (stage IV)	15
1.5.2.6 Spent (stage V).....	16
1.5.3 Changes of ovarian morphology during oogenesis.....	16
1.5.3.1 Oogenesis	16
1.5.3.2 Spawning and egg activation	22
1.6 Hormones involving shrimp reproduction	23
1.7 Molecular biological approaches used in this thesis	25

	Page
1.7.1 Polymerase chain reaction (PCR)	25
1.7.2 Expressed Sequence Tags (ESTs).....	26
1.7.3 Normalized ESTs	29
1.7.4 Suppression subtractive hybridization (SSH)	30
1.7.5 DNA sequencing	32
1.7.6 Reverse transcription-polymerase chain reaction (RT-PCR)	33
1.7.7 RNA arbitrary-primed (RAP)-PCR	33
1.7.8 Rapid amplification of cDNA ends-polymerase chain reaction RACE-PCR	35
1.7.9 Quantitative real-time PCR	37
1.7.10 <i>In situ</i> hybridization	37
1.8 EST analysis for isolation of reproduction-related genes in <i>P. monodon</i>	40
1.9 Functionally important genes related to ovarian development of <i>P. monodon</i>	42
1.9.1 Progesterone receptor.....	42
1.9.2 Cell division cycle.....	45
1.9.3 Carbonyl reductase and small androgen receptor-interacting protein	47
CHAPTER II MATERIALS AND METHODS	49
2.1 Experimental animals... ..	49
2.2 Nucleic acid extraction	50
2.2.1 DNA extraction	50
2.2.2 RNA extraction	51
2.2.3 Purification of mRNA	51
2.3 Measuring concentrations of extracted DNA and RNA using spectrophotometry and electrophoresis	52
2.4 Construction of typical, normalized and subtractive ovaries cDNA libraries of <i>P. monodon</i>	53
2.4.1 The typical ovary cDNA library of <i>P. monodon</i>	53
2.4.1.1 First and second strand cDNA synthesis	53
2.4.1.2 Blunting the cDNA termini.....	54
2.4.1.3 Ligation of <i>EcoR</i> I adapters	54
2.4.1.4 Phosphorylation of <i>EcoR</i> I ends	54
2.4.1.5 <i>Xho</i> I digestion	55
2.4.1.6 Size fractionation	55
2.4.1.7 Processing the cDNA fractions	56

	Page
2.4.1.8 Ligation of the cDNA insert	57
2.4.1.9 Packaging and titring.....	57
2.4.1.10 Amplifying the cDNA library	58
2.4.1.11 <i>In vivo</i> excision to convert the lambda library to the phagemid library	59
2.4.2 Construction of the normalized ovary cDNA library of <i>P. monodon</i>	60
2.4.2.1 Preparing of single-stranded phagemid	60
2.4.2.2 Preparing of driver	61
2.4.2.3 Hybridization between single-stranded phagemid and the labeled driver	62
2.4.2.4 Discover the remaining single-stranded plasmids of rare expressed genes... ..	63
2.4.2.5 Double-stranded cDNA synthesis	64
2.4.3 Construction of suppression subtractive hybridization (SSH) cDNA libraries	65
2.4.3.1 First strand cDNA synthesis	66
2.4.3.2 Second strand cDNA synthesis	66
2.4.3.3 <i>Rsa</i> I Digestion.....	68
2.4.3.4 Adaptor-ligated Tester cDNA preparation... ..	68
2.4.3.5 First Hybridization	69
2.4.3.6 Second Hybridization.....	69
2.4.3.7 Primary and secondary PCR amplification	72
2.4.3.8 Ligation of PCR products to pGEM®-T easy vector	73
2.4.3.9 Transformation of ligation products to <i>E. coli</i> host cells	73
2.4.4 Identification of the positive clones using colony PCR	74
2.4.5 Plasmid DNA extraction	75
2.4.6 DNA sequencing and EST analysis	76
2.5 Isolation and characterization of differentially displayed transcripts during ovarian development of <i>P. monodon</i> using RNA arbitrary primed (RAP)-PCR... ..	77
2.5.1 cDNA synthesis	77
2.5.2 Preparation of denaturing polyacrylamide gel electrophoresis.....	77
2.5.3 Electrophoresis	79
2.5.4 Silver staining	79

	Page
2.5.5 Cloning and characterization of candidate differential/stage-specific of differential ovarian development expression markers of RAP-PCR fragments.....	80
2.5.5.1 Elution of DNA from polyacrylamide gels... ..	80
2.5.5.2 Elution of RAP-PCR fragments from agarose gels	80
2.5.5.3 Ligation and cloning of the RAP-PCR products... ..	81
2.5.5.4 DNA sequencing and sequence similarity	81
2.6 Isolation and characterization of the full length cDNA and genomic DNA of functionally important gene homologues of <i>P. monodon</i>	81
2.6.1 Isolation and characterization of the full length cDNA using 3' end terminal sequencing.....	81
2.6.2 Isolation and characterization of the full length cDNA using Rapid Amplification of cDNA Ends-Polymerase Chain Reaction (RACE - PCR).....	81
2.6.2.1 Preparation of the 5' and 3' RACE template	81
2.6.2.2 Primer designed for RACE-PCR and primer walking	83
2.6.2.3 RACE-PCR and cloning of RACE-PCR products.....	83
2.6.3 Genomic DNA organization of functionally important gene homologues of <i>P. monodon</i>	85
2.6.4 DNA sequencing and sequence assembly.....	88
2.7 Northern blot analysis	89
2.7.1 RNA sample preparation and blotting	89
2.7.2 Post-Northern hybridization washing and detection	90
2.8 Examination of expression patterns of genes related to ovarian development by RT-PCR and tissue distribution analysis	91
2.8.1 Primer design	91
2.8.2 First strand cDNA synthesis	97
2.8.3 RT-PCR analysis.....	98
2.8.4 Tissue distribution analysis	99
2.8.4.1 Total RNA extraction and first strand cDNA synthesis.....	99
2.8.4.2 Tissue distribution analysis by RT-PCR	99
2.9 Semiquantitative RT-PCR of functionally important gene homologues in ovaries of broodstock <i>P. monodon</i>	100
2.9.1 Experiment animals and the first strand cDNA synthesis	100
2.9.2 Primers	100
2.9.3 Optimization of semi-quantitative RT-PCR conditions.....	100

	Page
2.9.3.1 Primer concentration	100
2.9.3.2 MgCl ₂ concentration	101
2.9.3.3 Cycle numbers	101
2.9.4 Agarose gel electrophoresis, semiquantitative RT-PCR and data analysis	101
2.10 Examination of expression levels of interesting genes in ovaries of <i>P. monodon</i> by quantitative real-time PCR	102
2.10.1 Effects of serotonin on expression of genes in ovaries of juvenile <i>P. monodon</i>	102
2.10.2 Primer design	102
2.10.3 Quantitative real-time PCR analysis	104
2.11 <i>In situ</i> hybridization (ISH)	104
2.11.1 Sample preparation	104
2.11.2 Preparation of cRNA probes	106
2.11.2.1 Addition of RNA polymerase recognition sequence (RPRS) by PCR... ..	106
2.11.2.2 Synthesis of cRNA probes	108
2.11.2.3 Dot blot analysis (<i>Cdc42</i> , <i>PGMRC1</i> and <i>TSP</i>)	108
2.11.3 Hybridization and detection	109
2.12 Production of the polyclonal antibody and western blot analysis.....	109
2.12.1 Polyclonal antibody raise against <i>Cdc42</i>	109
2.12.2 Production of the polyclonal antibody against <i>PGMRC1</i>	109
2.12.3 Sample preparation	111
2.12.4 Western blot analysis	111
2.13 Immunohistochemistry	112
2.14 <i>In vitro</i> expression of the full length cDNA using the bacterial expression system	112
2.14.1 Primers design... ..	112
2.14.2 Construction of recombinant plasmid in cloning and expression vectors	112
2.14.3 Expression of recombinant proteins.....	114
2.14.4 Detection of recombinant proteins	114
2.14.5 Purification of recombinant proteins	115
2.14.6 Polyclonal antibody production	115
CHAPTER III RESULTS	116

	Page
3.1 Construction of typical, normalized and suppression subtractive hybridization (SSH) cDNA libraries from ovaries of <i>P. monodon</i> ...	116
3.1.1 A typical ovarian cDNA library of <i>P. monodon</i>	116
3.1.2 Construction of a normalized ovarian cDNA library of <i>P. monodon</i>	133
3.1.3 Construction of suppression subtractive hybridization (SSH) cDNA libraries from mature and immature ovaries of <i>P. monodon</i> broodstock	139
3.1.4 ESTs from all libraries	151
3.2 Isolation and characterization of differentially displayed transcripts during ovarian development of <i>P. monodon</i> using RNA arbitrary primed (RAP)-PCR.....	160
3.2.1 Identification of candidate differential/stage-specific of differential ovarian development expression markers of RAP-PCR fragments	160
3.2.2 Preliminary examining expression patterns of genes related to ovarian development by RT-PCR	170
3.2.3 Semiquantitative RT-PCR to evaluate expression of different gene homologues in ovaries of broodstock <i>P. monodon</i>	173
3.2.4 Tissue distribution analysis	174
3.3 Isolation and characterization of the full length cDNA of functionally important gene homologues of <i>P. monodon</i>	178
3.3.1 3' end terminal sequencing of original EST clones	178
3.3.2 Rapid Amplification of cDNA Ends-Polymerase Chain Reaction (RACE - PCR).....	191
3.4 Expression profiles of <i>Pm-PGMRC1</i> and <i>Pm-Cdc42</i> in different ovarian stages and various tissues of <i>P. monodon</i> examined by northern blot analysis	212
3.5 Genomic DNA organization of functionally important gene homologues of <i>P. monodon</i>	212
3.5.1 Genomic DNA preparation	212
3.5.2 Characterization of genomic sequence of <i>Pm-Cdc42</i>	213
3.5.3 Characterization of the <i>SARIP</i> genes	216
3.6 Examination of expression patterns of genes functionally related to ovarian development of <i>P. monodon</i> by RT-PCR	220
3.6.1 Total RNA extraction.....	220
3.6.2 RT-PCR and tissue distribution analysis of genes functionally related to ovarian development	221

	Page
3.6.3 Determining expression patterns of ovarian and testicular forms <i>PGMRC1</i> in ovaries and testes of <i>P. monodon</i> broodstock	231
3.7 Semiquantitative RT-PCR of functionally important genes during ovarian development of <i>P. monodon</i>	236
3.7.1 Optimization of primer concentration, MgCl ₂ concentration and cycle numbers	237
3.7.2 Semi-quantitative RT-PCR analysis	238
3.7.2.1 <i>keratinocytes associated protein 2</i>	238
3.7.2.2 <i>Ser/Thr kinase chk1</i>	239
3.7.2.3 <i>DNA replication licensing factor mcm2</i>	240
3.7.2.4 <i>Selenoprotein M precursor</i>	241
3.7.2.5 <i>Egalitarian</i>	242
3.8 Examination of expression levels of interesting genes related with ovarian development of <i>P. monodon</i> by Quantitative real-time PCR	243
3.9 Localization of sex-related transcripts in ovaries of <i>P. monodon</i> broodstock	252
3.9.1 Quantification of the cRNA probes	252
3.9.2 <i>In situ</i> hybridization (ISH)	252
3.10 Expression profiles and localization of Cdc42 and PGMRC1 proteins during ovarian development of <i>P. monodon</i>	258
3.11 <i>In vitro</i> expression of recombinant Cdc42 and p23 proteins using the bacterial expression system	264
3.11.1 Construction of recombinant plasmids	264
3.11.2 <i>In vitro</i> expression of recombinant protein	265
3.11.3 Purification of recombinant proteins	269
3.11.4 Expression profiles of p23 protein during ovarian development of <i>P. monodon</i>	272
CHAPTER IV DISCUSSION	274
CHAPTER V CONCLUSION	291
REFERENCES... ..	293
APPENDICES	308
APPENDIX A	309
APPENDIX B	321
APPENDIX C	333
APPENDIX D	338
APPENDIX E	341

	Page
APPENDIX F	349
BIOGRAPHY.....	351



ศูนย์วิทยทรัพยากร
จุฬาลงกรณ์มหาวิทยาลัย

LIST OF TABLES

	Page
Table 1.1 The exportation of the chilled and frozen <i>P. monodon</i> from Thailand to world wide countries since 2002-20076
Table 2.1 Compositions of the single-strand DNA driver labeling.....	62
Table 2.2 Compositions of the first strand cDNA synthesis for construction of SSH libraries66
Table 2.3 Compositions of the second strand cDNA synthesis for for construction of SSH libraries67
Table 2.4 Sequences of the PCR select cDNA synthesis primer, adaptors and PCR primers and control primers69
Table 2.5 Ligation reactions of the tester cDNA of forward (tester 1-1 and 1-2) and reverse (tester 2-1 and 2-2) subtraction libraries70
Table 2.6 Compositions of the first hybridization reaction of each subtraction70
Table 2.7 Preparation of the primary PCR master mix72
Table 2.8 Preparation of the secondary PCR master mix73
Table 2.9 Sequences of arbitrary primers used for screening of differential expression markers in ovaries of <i>P. monodon</i> using RAP-PCR analysis78
Table 2.10 Internal primers used for primer walking of the full length cDNA of functionally important gene homologues in <i>P. monodon</i>82
Table 2.11 Primer sequences for the first strand cDNA synthesis for RACE-PCR83
Table 2.12 Gene-specific primers (GSPs) used for characterization of the full length cDNA of functionally important gene homologues in <i>P. monodon</i> using RACE-PCR84
Table 2.13 Internal primers used for primer walking of the full length cDNA fragments of functionally important gene homologues in <i>P. monodon</i> using RACE-PCR84
Table 2.14 Composition of 5'- and 3'- RACE-PCR85
Table 2.15 The amplification conditions for RACE-PCR of various gene homologues of <i>P. monodon</i>86
Table 2.16 Lists of primers and primer sequences used for isolation of genomic DNA sequence of <i>Cdc42</i> and <i>SARIP</i> genes87
Table 2.17 The amplification conditions for amplification of genomic DNA sequences of <i>Cdc42</i> and <i>SARIP</i> genes88
Table 2.18 Sample buffer for RNA preparation before electrophoresis and Northern blot analysis90

	Page
Table 2.19 Profile and condition of post-northern blot hybridization wash (DIG wash and block buffer set)	91
Table 2.20 Primer sequences and the expected size of the PCR product of gene homologue of <i>P. monodon</i> initially isolated by EST analysis ...	92
Table 2.21 Primer sequences, melting temperature and the expected product sizes of gene homologue designed from RAP-PCR fragments of <i>P. monodon</i>	95
Table 2.22 Primer sequences, melting temperature and the expected product sizes from primers designed from <i>PGMRC1</i> homologues of ovarian and testicular forms of <i>P. monodon</i>	97
Table 2.23 DNase I digestion reaction for elimination of genomic DNA from total RNA	97
Table 2.24 Nucleotide sequences of primers used for quantitative real-time PCR analysis of <i>PGRMC1</i> , <i>SARIP</i> , <i>progesterone receptor-related protein p23</i> and <i>Cdc42</i> in <i>P. monodon</i>	105
Table 2.25 Primer sequences for preparation of templates for synthesis of <i>Cdc42</i> , <i>PGMRC1</i> and <i>TSP</i> antisense and sense cRNA probes of <i>P. monodon</i>	107
Table 2.26 Primer sequences for preparation of <i>SARIP</i> and <i>VTG</i> antisense and sense cRNA probes of <i>P. monodon</i>	107
Table 2.27 Detailed information of the polyclonal antibody against <i>Cdc42</i> and <i>PGMRC1</i>	110
Table 2.28 Nucleotide sequences of primers used for <i>in vitro</i> expression of <i>Cdc42</i> and <i>progesterone receptor-related protein p23</i> of <i>P. monodon</i>	113
Table 3.1 The percentage and number of clones found in the first phase of EST analysis of a typical ovarian cDNA library of <i>P. monodon</i>	118
Table 3.2 Classification of sequences according to three principal GO categories of the first phase of EST analysis (1051 ESTs) of a typical ovarian cDNA library of <i>P. monodon</i>	121
Table 3.3 A summary of contigs and singletons creation and BLASTX score in the first phase of EST analysis (1051 ESTs) of a typical ovarian cDNA library of <i>P. monodon</i>	122
Table 3.4 A summary of homologues of sex-linked or sex differentiation-related transcripts found in the first phase of EST analysis of an ovarian cDNA library of <i>P. monodon</i>	124
Table 3.5 The percentage and number of clones found in the second phase of EST analysis of a typical ovarian cDNA library of <i>P. monodon</i>	125
Table 3.6 Classification of sequences according to three principal GO categories of the second phase of EST analysis (1279 ESTs) of an ovarian cDNA library of <i>P. monodon</i>	127

	Page
Table 3.7 A summary of contigs and singletons creation and BLASTX score in the second phase of EST analysis (1279 ESTs) of a typical ovarian cDNA library of <i>P. monodon</i> ...	129
Table 3.8 The percentage and number of clones found in the both phases of a typical ovaries cDNA library ...	129
Table 3.9 Classification of sequences according to three principal GO categories in the first and second phases (2330 ESTs) of typical ovaries cDNA library ...	130
Table 3.10 A summary of contigs and singletons creation and BLASTX score in the first and second phases (2330 ESTs) of a typical ovarian cDNA library ...	131
Table 3.11 The percentage and number of clones found in the normalized ovaries cDNA library ...	135
Table 3.12 Classification of sequences according to three principal GO categories in the normalized ovaries cDNA library (1778 ESTs) ...	136
Table 3.13 A summary of contigs and singletons creation and BLASTX score in the normalized ovaries cDNA library (1778 ESTs)...	138
Table 3.14 The percentage and number of clones found in the forward SSH ovarian cDNA library of <i>P. monodon</i> ...	142
Table 3.15 Classification of sequences according to three principal GO categories in the forward SSH ovaries cDNA library (220 ESTs) ...	143
Table 3.16 A summary of contigs and singletons creation and BLASTX score in the forward SSH ovarian cDNA library (220 ESTs) ...	145
Table 3.17 The percentage and number of clones found in the reverse SSH ovaries cDNA library of <i>P. monodon</i> ...	146
Table 3.18 Classification of sequences according to three principal GO categories in the reverse SSH ovaries cDNA library (232 ESTs) ...	146
Table 3.19 A summary of contigs and singletons creation and BLASTX score in the reverse SSH ovarian cDNA library (232 ESTs) ...	147
Table 3.20 The percentage and number of clones found in the forward and reverse SSH ovarian cDNA libraries of <i>P. monodon</i> ...	149
Table 3.21 Classification of sequences according to three principal GO categories in the forward and reverse SSH ovarian cDNA libraries (452 ESTs) ...	150
Table 3.22 A summary of contigs and singletons creation and BLASTX score in the forward and reverse SSH ovarian cDNA libraries (452 ESTs)...	151
Table 3.23 The percentage and number of clones found in all ESTs ovarian cDNA libraries ...	152
Table 3.24 Classification of sequences according to three principal GO categories in all ESTs ovaries cDNA libraries (4560 ESTs) ...	154

	Page
Table 3.25 A summary of contigs and singletons creation and BLASTX score in all ESTs ovaries cDNA libraries (4560 ESTs)	155
Table 3.26 Ontological function of ESTs functionally involving reproduction in homologue species	157
Table 3.27 Ontological function of ESTs functionally involving growth in homologue species	159
Table 3.28 A summary of candidate RAP-PCR fragments converted to SCAR markers.....	162
Table 3.29 Candidate differentially expressed SCAR markers in <i>P. monodon</i> initially generated from RAP-PCR using an oligo-dT ₍₁₆₎ -overhang with A, C or G in combination with each of 45 arbitrary primers	169
Table 3.30 A summary of expression patterns of various gene homologues or unknown transcripts analyzed by RT-PCR using primers derived from RAP-PCR	170
Table 3.31 A trend of expression levels of various genes isolated by RAP-PCR	172
Table 3.32 Optimal primer and MgCl ₂ concentrations and the number of PCR cycles for semiquantitative analysis of various genes in <i>P. monodon</i>	173
Table 3.33 A summary of full length cDNA of genes expressed inn ovaries of <i>P. monodon</i> characterized by 3' primer walking of original ESTs	208
Table 3.34 A summary of full length cDNA of genes expressed inn ovaries of <i>P. monodon</i> characterized by RACE-PCR	209
Table 3.35 GO ontology function, probability site in the cells and signal peptide prediction of the full length cDNA characterized in this study	210
Table 3.36 N-link glycosylation site, cAMP dependent protein kihase site and the percentage of hydrophobic amino acid of the full length cDNA characterized in this study.....	211
Table 3.37 GC content and length of exons and introns in <i>Pm-Cdc42</i> genes	216
Table 3.38 GC content and length of exons and introns in <i>Pm-SARIP</i> gene	219
Table 3.39 A summary of expression patterns of various gene homologues during ovarian development of <i>P. monodon</i> preliminary analyzed by RT-PCR.....	225
Table 3.40 Expression profiles and tissue distribution analysis of various genes during ovarian development of <i>P. monodon</i>	229
Table 3.41 Optimal primer and MgCl ₂ concentrations and the number of PCR cycles for semiquantitative analysis of expression levels of functionally important genes in <i>P. monodon</i>	237

	Page
Table 3.42 Localization of sex-related transcripts in ovaries of <i>P. monodon</i> visualized by <i>in situ</i> hybridization.	258
Table 3.43 Titers of polyclonal antibodies after rabbits were immunized with recombinant Cdc42 and p23 for 3 times	271
Table 3.44 Titers of polyclonal antibodies after rabbits were immunized with recombinant Cdc42 and p23 for 4 times	271
Table 3.45 The intensity of p23 signals in different stages of ovaries of <i>P. monodon</i> from western blot analysis	273



ศูนย์วิทยทรัพยากร
จุฬาลงกรณ์มหาวิทยาลัย

LIST OF FIGURES

	Page
Figure 1.1 The Chilled and frozen <i>P. monodon</i> exported from Thailand to world wide Countries since 2002-2007	4
Figure 1.2 Taxonomy of the giant black tiger shrimp, <i>Penaeus monodon</i> , Fabricius, 1798.....	8
Figure 1.3 Lateral view of the external morphology of <i>P. monodon</i>	9
Figure 1.4 Lateral view of the internal anatomy of a female <i>Penaeus monodon</i>	10
Figure 1.5 The life history of <i>Penaeus monodon</i> shrimp. Eggs hatch within 16 hours after fertilization.....	11
Figure 1.6 Development of thelycum	13
Figure 1.7 Development of petasma	13
Figure 1.8 The dorsal view observed by hatchery operators when female broodstock are graded for ovarian development by torchlight	15
Figure 1.9 Light microscopy showing an immature ovaries.....	17
Figure 1.10 Light microscopy showing a previtellogenic ovaries	18
Figure 1.11 Light microscopy showing an early vitellogenic ovaries	19
Figure 1.12 Light microscopy showing an late vitellogenic ovaries	20
Figure 1.13 Light microscopy showing mature ovaries.....	20
Figure 1.14 Various stages of oocyte development in <i>M. japonicus</i>	21
Figure 1.15 Reproductive cycle of the close-thelycum penaeid shrimp	22
Figure 1.16 General illustration of the polymerase chain reaction (PCR) for amplifying DNA	26
Figure 1.17 Overview for construction of cDNA inserts (A) and automated DNA sequencing (single-pass) of randomly selected cDNA clones	28
Figure 1.18 Schematic diagram of the normalized-subtracted cDNA preparation protocol	30
Figure 1.19 The PCR-Select cDNA subtraction technique.....	31
Figure 1.20 A schematic diagram illustrating principles of Automated DNA sequencing.....	32
Figure 1.21 Overall concepts of the RT-PCR procedure. During first-strand cDNA synthesis an oligo d(T) primer anneals and extends from sites present within the total RNA	34
Figure 1.22 Overview of RACE-PCR. A; Mechanism of 5' and 3' RACE cDNA synthesis	36
Figure 1.23 The principle of SYBR Green detection in real-time	38

	Page
Figure 1.24 Digoxigenin-UTP/dUTP/ddUTP, alkali-stable	39
Figure 1.25 Schematic overview of proposed mechanisms of non-genomic P4 actions mediated by the classical (or nuclear) PR or through the non-classical putative P4 receptors PGRMC1 (possibly complex with SERBP1) and mPRs.....	44
Figure 1.26 Checkpoint pathways controlling Cdc25 isoforms in mammalian cells	46
Figure 2.1 Assembly of the drip column for size-fractionation of synthesized cDNA	56
Figure 2.2 Overview of the PCR-Selected procedure based on a PCR-Select™ cDNA Subtraction Kit (Clontech) (A) and the preparation of adaptor-ligated tester cDNA for hybridization and suppression PCR (B, C)	71
Figure 2.3 A typical downward nucleic acid transfer system	90
Figure 2.4 Two approaches of primer design to prevent amplification of the residual genomic DNA in the template for quantitative real-time RT-PCR.....	103
Figure 3.1 Estimation of insert sizes by colony PCR	117
Figure 3.2 Recombinant plasmid DNA of the typical cDNA libraries of <i>P. monodon</i> digested with <i>Eco</i> RI- <i>Xho</i> I (or <i>Eco</i> RI- <i>Apa</i> I).....	117
Figure 3.3 Classification of genes identified in the first phase of EST analysis of an ovarian cDNA libraries of <i>P. monodon</i> (E-value < 10 ⁻⁴) owing to functional categories of their homologues ...	119
Figure 3.4 Number of unique sequences plotted as a function of the accumulative number of sequenced clones from the first phase of an ovarian cDNA library of <i>P. monodon</i>	122
Figure 3.5 The percent distribution of nucleotide sequences according to three principal GO categories from the first phase of EST analysis (1051 ESTs) of a typical ovarian cDNA library of <i>P. monodon</i>	123
Figure 3.6 The percent distribution of nucleotide sequences according to three principal GO categories in the second phase of EST analysis (1279 ESTs) of a typical ovarian cDNA library of <i>P. monodon</i>	128
Figure 3.7 The percent distribution of nucleotide sequences according to three principal GO categories in both phases of typical ovaries cDNA library (2330 ESTs).....	132
Figure 3.8 Colony PCR for determining recombinant clones carrying insert sizes greater than 500 bp from the normalized ovarian cDNA libraries of <i>P. monodon</i>	134
Figure 3.9 Digestion of plasmid DNA containing positive clones of the normalized ovarian cDNA libraries of <i>P. monodon</i>	134

Figure 3.10 The percent distribution of nucleotide sequences among the three principal GO categories in the normalized ovaries cDNA library (1778 ESTs)	137
Figure 3.11 Agarose gel electrophoresis showing <i>RsaI</i> digestion for SSH ovarian cDNA libraries of <i>P. monodon</i>	139
Figure 3.12 An agarose gel electrophoresis showing primary (A) and secondary (B) PCR amplification of subtracted (lanes 1 and 3) and unsubtracted (lanes 2 and 4) for forward (lanes 1-2; A and B) and reverse (lanes 3-4; A and B) SSH ovaries cDNA libraries of <i>P. monodon</i>	140
Figure 3.13 Colony PCR for determining recombinant clones carrying insert sizes greater than 300 bp the forward (lines 1-2) and reverse (lines 3-4) SSH ovarian cDNA libraries of <i>P. monodon</i>	140
Figure 3.14 Digestion of plasmid DNA containing positive clones of the forward (lines 1-2) and reverse (lines 3-4) SSH ovarian cDNA libraries of <i>P. monodon</i>	141
Figure 3.15 The percent distribution of nucleotide sequences according to three principal GO categories in the forward SSH ovaries cDNA library	144
Figure 3.16 The percent distribution of nucleotide sequences according to three principal GO categories in the reverse SSH ovaries cDNA library	148
Figure 3.17 The percent distribution of nucleotide sequences according to three principal GO categories in the forward and reverse SSH ovaries cDNA library	153
Figure 3.18 The percent distribution of nucleotide sequences according to three principal GO categories in the ESTs ovaries cDNA libraries.....	156
Figure 3.19 RAP-PCR patterns of transcripts expressed in mature (lanes 1 - 2, 6 - 7, 11 - 12 and 16 - 17; A - C and lanes 1, 4, 7, 10 and 13; D and E) and immature (lanes 5, 10, 15 and 20; A - C and lanes 2, 5, 8, 11 and 14; D and E) ovaries of wild broodstock and those of juveniles (lanes 3 - 4, 8 - 9, 13 - 14 and 18 - 19; A - C and lanes 3, 6, 9, 12 and 15; D and E) <i>P. monodon</i>	161
Figure 3.20 Nucleotide sequence of a candidate stage-specific RAP-PCR fragment (mature ovaries, 381 bp) generated from oligo-dT ₍₁₆₎ G-UBC 299 primers.	162
Figure 3.21 Nucleotide sequence of a candidate stage-specific RAP-PCR fragment (mature ovaries, 831 bp) generated from oligo-dT ₍₁₆₎ G-OPA17 primers.	162
Figure 3.22 Nucleotide sequence of a candidate stage-specific RAP-PCR fragment (mature ovaries, 621 bp) generated from oligo-dT ₍₁₆₎ G-OPB08 primers.....	163

	Page
Figure 3.23 Nucleotide sequence of a candidate stage-specific RAP-PCR fragment (immature ovaries, 329 bp) generated from oligo-dT ₍₁₆₎ A-OPB10 primers.....	163
Figure 3.24 Nucleotide sequence of an another candidate stage-specific RAP-PCR fragment (immature ovaries, 331 bp) generated from oligo-dT ₍₁₆₎ G-OPB10 primers.	163
Figure 3.25 Nucleotide sequence of an additional candidate stage-specific RAP-PCR fragment (immature ovaries, 330 bp) generated from oligo-dT ₍₁₆₎ G-OPB08 primers. ...	163
Figure 3.26 Nucleotide sequence of a candidate stage-specific RAP-PCR fragments (immature ovaries, 294 bp) generated from oligo-dT ₍₁₆₎ G-OPA01 primers.	164
Figure 3.27 Nucleotide sequence of an another candidate stage-specific RAP-PCR fragments (immature ovaries, 308 bp) generated from oligo-dT ₍₁₆₎ G-OPA01 primers.	164
Figure 3.28 Nucleotide sequence of additional candidate stage-specific RAP-PCR fragments (immature ovaries, 335 bp) generated from oligo-dT ₍₁₆₎ G-OPA01 primers.	164
Figure 3.29 Nucleotide sequence of a RAP-PCR fragment (294 bp) found in mature ovaries and those of juvenile generated from oligo-dT ₍₁₆₎ G-UBC268 primers.	164
Figure 3.30 Nucleotide sequence of an another RAP-PCR fragment (474 bp) found in mature ovaries and those of juvenile generated from oligo-dT ₍₁₆₎ G-UBC268 primers. ...	165
Figure 3.31 Nucleotide sequence of a RAP-PCR fragment (435 bp) found in immature ovaries and those of juvenile generated from oligo-dT ₍₁₆₎ G-UBC135 primers.	165
Figure 3.32 Nucleotide sequence of an another RAP-PCR fragment (437 bp) found in immature ovaries and those of juvenile generated from oligo-dT ₍₁₆₎ G-UBC135 primers. ...	165
Figure 3.33 Nucleotide sequence of a RAP-PCR fragment (385 bp) found in immature ovaries and those of juvenile generated from oligo-dT ₍₁₆₎ G-UBC191 primers.	166
Figure 3.34 Nucleotide sequence of an another RAP-PCR fragment (377 bp) found in immature ovaries and those of juvenile generated from oligo-dT ₍₁₆₎ G-UBC191 primers. ...	166
Figure 3.35 Nucleotide sequence of a RAP-PCR fragment (403 bp) found in immature ovaries and those of juvenile generated from oligo-dT ₍₁₆₎ G-OPA02 primers.	166
Figure 3.36 Nucleotide sequence of an aother RAP-PCR fragment (334 bp) found in immature ovaries and those of juvenile generated from oligo-dT ₍₁₆₎ G-OPA02 primers.....	166

Figure 3.37 Nucleotide sequence of a candidate up-regulated RAP-PCR fragment (499 bp) generated from oligo-dT ₍₁₆₎ G-OPB08 primers.....	167
Figure 3.38 Nucleotide sequence of a candidate up-regulated RAP-PCR fragment (361 bp) generated from oligo-dT ₍₁₆₎ G-UBC459 primers.....	167
Figure 3.39 Nucleotide sequence of a candidate up-regulated RAP-PCR fragment (349 bp) generated from oligo-dT ₍₁₆₎ G-UBC459 primers.	167
Figure 3.40 Nucleotide sequence of a candidate up-regulated RAP-PCR fragment (284 bp) generated from oligo-dT ₍₁₆₎ G-UBC457 primers. Positions of RAP-PCR primers were illustrated in boldface and underlined.	167
Figure 3.41 Nucleotide sequence of a candidate down-regulated RAP-PCR fragment (560 bp) generated from oligo-dT ₍₁₆₎ G-UBC138 primers.	168
Figure 3.42 Nucleotide sequence of a candidate differentially expressed marker (380 bp) generated from oligo-dT ₍₁₆₎ G-OPA14 primers.	168
Figure 3.43 A 1.5% ethidium bromide-stained agarose gel showing RT-PCR result of <i>B cell RAG associated protein</i> (oligo-dT ₍₁₆₎ G-UBC 299) (A) and <i>hypothetical protein W02B8.3</i> (oligo-dT ₍₁₆₎ G-OPA 17) (B) using the first strand cDNA of <i>P. monodon</i> with different Gonado-Somatic Index (GSI).	171
Figure 3.44 A 1.5% ethidium bromide-stained agarose gel showing RT-PCR result of <i>APEX nuclease</i> (oligo-dT ₍₁₆₎ A-OPA02) (A), DNA replication licensing factor <i>MCM5</i> (oligo-dT ₍₁₆₎ G-OPB 08) (B) and <i>U5 snRNP-specific protein</i> (oligo-dT ₍₁₆₎ G-UBC 457) (C) using the first strand cDNA of <i>P. monodon</i> with different Gonadosomatic Index (GSI). ..	171
Figure 3.45 Histograms showing the relative expression levels of <i>B cell RAG associated protein</i> in different ovarian developmental stages of normal <i>P. monodon</i> broodstock.	174
Figure 3.46 Histograms showing the relative expression levels of <i>APEX nuclease</i> in different ovarian developmental stages of normal <i>P. monodon</i> broodstock.	175
Figure 3.47 Histograms showing the relative expression levels of <i>U5 snRNP-specific protein</i> in different ovarian developmental stages of normal <i>P. monodon</i> broodstock.	175
Figure 3.48 Histograms showing the relative expression levels of <i>hypothetical protein W02B8.3</i> in different ovarian developmental stages of normal <i>P. monodon</i> broodstock.	176
Figure 3.49 Histograms showing the relative expression levels of <i>DNA replication licensing factor MCM5</i> in different ovarian developmental stages of normal <i>P. monodon</i> broodstock.	176

	Page
Figure 3.50 Tissue distribution analysis of <i>B cell RAG-associated protein</i> (A), <i>APEX nuclease</i> (B) and <i>U5 snRNP-specific protein</i> (C).	177
Figure 3.51 The full length cDNA and deduced protein sequences of <i>Pm-Cdc20</i>	179
Figure 3.52 The full length cDNA and deduced protein sequences of <i>Pm-SARIP</i>	181
Figure 3.53 The full length cDNA and deduced protein sequences of <i>Pm-Cdc42</i>	182
Figure 3.54 The full length cDNA and deduced protein sequences of <i>Pm-cytochrome B5</i>	183
Figure 3.55 Diagrams showing outside, inside and transmembrane probability (A) and hydrophobicity analysis of deduced <i>Pm-cytochrome B5</i> protein according to Kyte and Doolittle (1982).	184
Figure 3.56 The full length cDNA and deduced protein sequences of <i>Pm-Protein mago nashi</i>	185
Figure 3.57 The full length cDNA and deduced protein sequences of <i>Pm-actin depolymerizing factor</i>	186
Figure 3.58 The full length cDNA and deduced protein sequences of <i>Pm-F-box and wd40 repeat domain binding protein</i>	187
Figure 3.59 The full length cDNA and deduced protein sequences of <i>Pm-Cdk 7</i>	189
Figure 3.60 The full length cDNA and deduced protein sequences of <i>Pm-SEPM</i>	190
Figure 3.61 The full length cDNA and deduced protein sequences of <i>Pm-APC11</i>	190
Figure 3.62 3' RACE-PCR products of <i>Pm-PSR</i> (A) and <i>Pm-p23 like protein</i> (B) and 5' RACE-PCR products of <i>Pm-bystin</i> (C).	192
Figure 3.63 The full length cDNA and deduced protein sequences of <i>Pm-PSR</i> (1862 bp, ORF of 1170 bp corresponding to a deduced polypeptide of 389 aa) further characterized by 3' RACE-PCR. ..	193
Figure 3.64 The full length cDNA and deduced protein sequences of <i>Pm-p23</i> (1943 bp, ORF of 495 bp corresponding to a deduced polypeptide of 164 aa) further characterized by 3' RACE-PCR.	194
Figure 3.65 The full length cDNA and deduced protein sequences of <i>Pm-bystin isoform 1</i> (1553 bp, ORF of 1365 bp corresponding to a deduced polypeptide of 454 aa) further characterized by 5' RACE-PCR and 3' primer walking of the original EST clone. ..	195
Figure 3.66 3' RACE-PCR products of <i>Pm-Chk1</i> (A), 5' RACE-PCR products of <i>Pm-PGMRC1</i> (B) and 3' RACE-PCR products of <i>Pm-carbonyl reductase</i> (C). Arrowheads indicate bands selected for further analysis.	197

Figure 3.67 The full length cDNA and deduced protein sequences of <i>Pm-Chk1</i> (2078 bp, ORF of 1455 bp corresponding to a deduced polypeptide of 484 aa) further characterized by 3' RACE-PCR.....	198
Figure 3.68 The full length cDNA and deduced protein sequences of <i>Pm-PGMRC1</i> (2040 bp, ORF of 573 bp corresponding to a deduced polypeptide of 190 aa) further characterized by 5' RACE-PCR and 3' primer walking of the original EST clone.	199
Figure 3.69 Diagrams showing outside, inside and transmembrane probability (A) and hydrophobicity analysis (B) of deduced <i>Pm-PGMRC1</i> protein according to Kyte and Doolittle (1982).....	200
Figure 3.70 Multiple alignment of <i>PM-PGMRC1</i> and other vertebrates and invertebrates <i>PGMRC1</i> proteins. Identical residues across taxa are highlighted. Cysteine residues in each protein sequence are shaded.	201
Figure 3.71 The full length cDNA and deduced protein sequences of <i>Pm-carbonyl reductase</i>	202
Figure 3.72 5' RACE-PCR products of <i>Pm-PDI Erp59</i> (A) and <i>Pm-gonadotropin-regulated long chain acyl-CoA synthetase</i> (B). C is the amplified transcript of <i>Pm-gonadotropin-regulated long chain acyl-CoA synthetase</i> using proof-reading DNA polymerase that were re-sequenced to clarify the missing amino acids sequences 330 th - 519 th of this gene initially obtained from RACE-PCR.	204
Figure 3.73 The full length cDNA and deduced protein sequences of <i>Pm-PDI Erp59</i>	205
Figure 3.74 The full length cDNA and deduced protein sequences of <i>Pm-gonadotropin-regulated long chain acyl-CoA synthetase</i>	207
Figure 3.75 Northern blot analysis of <i>Pm-PGRMC1</i> (upper) and <i>Pm-Cdc42</i> (middle) transcripts.	212
Figure 3.76 A 1.0% ethidium bromide-stained agarose gel showing genomic DNA extracted from pleopods of <i>P. monodon</i> (lanes 1 - 4) and 100 ng of λ DNA (lane M).	213
Figure 3.77 Organization of genomic sequence of <i>Pm-Cdc42</i>	215
Figure 3.78 Organization of the <i>Pm-SARIP</i> gene.	218
Figure 3.79 A 1.0% ethidium bromide-stained agarose gel showing the quality of total RNA extracted from ovaries of <i>P. monodon</i> broodstock (A) and the synthesized first strand cDNA (B).	220
Figure 3.80 RT-PCR of <i>keratinocytes-associated protein 2</i> , <i>26S proteasome regulatory subunit rpn2</i> , <i>Chk1</i> , <i>selenoprotein M precursor</i> , <i>Neuralized protein</i> , <i>Egalitarian</i> and <i>carbonyl reductase</i> using the first strand cDNA template of <i>P. monodon</i> having different GSI values.	222

Figure 3.81 RT-PCR of <i>DNA replication - licensing factor mcm2</i> and <i>CWF19-like 2</i> (A) and <i>OV-N-ST01-0012-W</i> and <i>OV-N-ST02-0010W</i> regarded as unknown transcripts, <i>cytochrome c oxidase polypeptide IV</i> (A) using the first strand cDNA template of <i>P. monodon</i> having with different GSI values.	223
Figure 3.82 RT-PCR of <i>procollagen-proline</i> (A) and <i>citrate synthase, GA17699-PA</i> (B) using the first strand cDNA of <i>P. monodon</i> having different GSI values.	224
Figure 3.83 RT-PCR of <i>gonadotropin-regulated long chain Acyl-CoA synthetase, vitellogenin receptor</i> and <i>OV-N-ST01-0022-W</i> using the first strand cDNA template of ovaries <i>P. monodon</i>	225
Figure 3.84 A 1.5% ethidium bromide-stained agarose gel showing results from tissue distribution analysis of <i>SARIP</i> (A), <i>VTG</i> (B) and <i>Cdc42</i> (C) transcripts....	226
Figure 3.85 A 1.5% ethidium bromide-stained agarose gel showing results from tissue distribution analysis of <i>PGMRC1</i> (A), <i>p23-like protein</i> (B) and <i>carbonyl reductase</i> (C) transcripts....	228
Figure 3.86 A 1.5% ethidium bromide-stained agarose gel showing RT-PCR of <i>PGMRC1</i> using the first strand cDNA of testes and ovaries of juveniles and broodstock of <i>P. monodon</i>	231
Figure 3.87 The sequence alignments between the full length cDNA of <i>Pm-PGMRC1</i> initially characterized one isoform from ovaries (OVPM-PGMRC12040) and three isoforms from testes (TPM-PGMRC1-S, -M and -L) of <i>P. monodon</i>	235
Figure 3.88 A 1.5% ethidium bromide-stained agarose gel showing RT-PCR of <i>PGMRC1</i> transcript using primers specifically amplified an ovarian form (A) and testicular forms (B) of <i>PGMRC1</i> against the first strand cDNA from ovaries and testes of <i>P. monodon</i>	236
Figure 3.89 Histograms showing relative expression levels of <i>keratinocytes associated protein 2</i> in different ovarian developmental stages of <i>P. monodon</i>	238
Figure 3.90 Histograms showing relative expression levels of <i>chk1</i> in different ovarian developmental stages of <i>P. monodon</i>	239
Figure 3.91 Histograms showing relative expression levels of <i>DNA replication licensing factor mcm2</i> in different ovarian developmental stages of <i>P. monodon</i>	240
Figure 3.92 Histograms showing relative expression levels of selenoprotein M precursor in different ovarian developmental stages of <i>P. monodon</i>	241
Figure 3.93 Histograms showing relative expression levels of <i>Egalitarian</i> in different ovarian developmental stages of <i>P. monodon</i>	242
Figure 3.94 Standard curves of <i>Pm-p23</i> and <i>EF-1α</i>	243

	Page
Figure 3.95 Standard curve of <i>Pm-PGMRC1</i> , <i>Pm-SARIP</i> and <i>EF-1α</i>244
Figure 3.96 Standard curve of <i>Pm-PGMRC1</i> and <i>EF-1α</i> for examined expression profiles of <i>PGMRC1</i> transcript in ovaries of 5-HT treated juvenile <i>P. monodon</i>244
Figure 3.97 Standard curve of <i>Pm-Cdc42</i> and <i>EF-1α</i> for examined expression profiles of <i>Pm-Cdc42</i> transcript using 10-fold dilution of plasmid DNA of <i>Pm-Cdc42</i> and <i>EF-1α</i> (10^3 - 10^8 copy).....	.245
Figure 3.98 Histograms showing the relative expression profiles of <i>Pm-p23</i> during ovarian maturation of normal (A), unilateral eyestalk ablated (B) <i>P. monodon</i> broodstock.....	246
Figure 3.99 Histograms showing the relative expression profiles of <i>Pm-PGMRC1</i> during ovarian maturation of normal (A), unilateral eyestalk ablated (B) <i>P. monodon</i> broodstock.247
Figure 3.100 Histograms showing the relative expression profiles of <i>Pm-SARIP</i> during ovarian maturation of normal (A), unilateral eyestalk ablated (B) <i>P. monodon</i> broodstock.249
Figure 3.101 Histograms showing the relative expression profiles of <i>Pm-Cdc42</i> during ovarian maturation of normal (A), unilateral eyestalk ablated (B) <i>P. monodon</i> broodstock.250
Figure 3.102 Expression profiles of <i>PM-PGMRC1</i> in ovaries of 5-HT treated juvenile <i>P. monodon</i>251
Figure 3.103 Dot blot hybridization using the antisense <i>Pm-TSP</i> probe (A), antisense <i>Pm-PGMRC1</i> probe (B), sense <i>Pm-PGMRC1</i> probe (C), antisense <i>Pm-Cdc42</i> probe (D) and sense <i>Pm-Cdc42</i> probe (E).252
Figure 3.104 Localization of <i>Pm-TSP</i> transcript during ovarian development of normal <i>P. monodon</i> broodstock visualized by <i>in situ</i> hybridization using the sense <i>Pm-TSP</i> probe (A), antisense <i>Pm-TSP</i> probe (B and C).253
Figure 3.105 Localization of <i>Pm-TSP</i> transcript during ovarian development of eyestalk-ablated <i>P. monodon</i> broodstock visualized by <i>in situ</i> hybridization using the sense <i>Pm-TSP</i> probe (A), antisense <i>Pm-TSP</i> probe (B and C).254
Figure 3.106 Localization of <i>Pm-VTG</i> transcript during ovarian development of normal <i>P. monodon</i> broodstock visualized by <i>in situ</i> hybridization using the sense <i>Pm-VTG</i> probe (A), antisense <i>Pm-VTG</i> probe (B and C).254
Figure 3.107 Localization of <i>Pm-VTG</i> transcript during ovarian development of eyestalk-ablated <i>P. monodon</i> broodstock visualized by <i>in situ</i> hybridization using the sense <i>Pm-VTG</i> probe (A), antisense <i>Pm-VTG</i> probe (B and C).255

Figure 3.108 Localization of <i>Pm-Cdc42</i> transcript during ovarian development of normal <i>P. monodon</i> broodstock visualized by <i>in situ</i> hybridization using the sense <i>Pm-Cdc42</i> probe (A), antisense <i>Pm-Cdc42</i> probe (B).255
Figure 3.109 Localization of <i>Pm-PGMRC1</i> transcript during ovarian development of normal <i>P. monodon</i> broodstock visualized by <i>in situ</i> hybridization using the sense <i>Pm-PGMRC1</i> probe (A), antisense <i>Pm-PGMRC1</i> probe (B).256
Figure 3.110 Localization of <i>Pm-SARIP</i> transcript during ovarian development of normal <i>P. monodon</i> broodstock visualized by <i>in situ</i> hybridization using the sense <i>Pm-SARIP</i> probe (A), antisense <i>Pm-SARIP</i> probe (B and C). ..	.256
Figure 3.111 Localization of <i>Pm-SARIP</i> transcript during ovarian development of eyestalk-ablated <i>P. monodon</i> broodstock visualized by <i>in situ</i> hybridization using the sense <i>Pm-SARIP</i> probe (A), antisense <i>SARIP</i> probe (B and C).....	.257
Figure 3.112 Localization of <i>Pm-p23</i> transcript during ovarian development of normal <i>P. monodon</i> broodstock visualized by <i>in situ</i> hybridization using the sense <i>Pm-PGMRC1</i> probe (A), antisense <i>Pm-p23</i> probe (B and C). ..	.257
Figure 3.113 Western blotting analysis of purified anti-PGMRC1 PcAb.259
Figure 3.114 Western blotting analysis of anti-Cdc42 PcAb.....	.260
Figure 3.115 Immunohistochemical localization of PGMRC1 protein in ovaries of wild <i>P. monodon</i> broodstock using purified anti-PGMRC1 PcAb (D-F).....	.261
Figure 3.116 Immunohistochemical localization of PGMRC1 protein in ovaries of eyestalk-ablated broodstock <i>P. monodon</i> using purified anti-PGMRC1 PcAb (D-F). ..	.262
Figure 3.117 Immunohistochemical localization of Pm-Cdc42 protein in ovaries of <i>P. monodon</i> broodstocks using commercially available anti-Cdc42 PcAb (B and D). ..	.263
Figure 3.118 RT-PCR of the mature transcript of <i>Cdc42</i> (A) and <i>p23</i> (B). Fragments were cloned and sequenced264
Figure 3.119 A 15% SDS-PAGE showing <i>in vitro</i> expression of three recombinant clones of Cdc42 (A) and p23 (B) of <i>P. monodon</i> at 0 hr (lanes 1; A and B), 3 hours (lanes 2-4; A and B) and 6 hours (lanes 5-7; A and B) after IPTG induction (1 mM)265
Figure 3.120 <i>In vitro</i> expression of Cdc42 of <i>P. monodon</i> at 0, 1, 2, 3, 4, 6 hours and overnight after induction with 1 mM IPTG (lanes 1-7) analyzed by 15% SDS-PAGE (A) and western blot analysis (B).....	.266
Figure 3.121 <i>In vitro</i> expression of Cdc42 of <i>P. monodon</i> at 0, 1, 2, 3, 4, 6 hours and overnight after induction with 1 mM IPTG (lanes 1-7) analyzed by 15% SDS-PAGE (A) and western blot analysis (B).....	.266

Figure 3.122 A 15% SDS-PAGE (A) and western blot analysis (B) showing expression of recombinant Cdc42 in a recombinant clone cultured at 30°C for 6 hours after IPTG induction (1 mM)	267
Figure 3.123 A 15% SDS-PAGE (A) and western blot analysis (B) showing expression of recombinant p23 in a recombinant clone cultured at 30°C for 6 hours after IPTG induction (1 mM)	267
Figure 3.124 A 15% SDS-PAGE (A) and western blot analysis (B) showing expression of recombinant Cdc42 in the clone cultured at 20°C overnight after IPTG induction (1 mM).....	268
Figure 3.125 A 15% SDS-PAGE (A) and western blot analysis (B) showing expression of recombinant p23 in a clone cultured at 25°C overnight after IPTG induction (1 mM).....	268
Figure 3.126 Purification of recombinant Cdc42 of <i>P. monodon</i> (cultured overnight at 20°C)	269
Figure 3.127 Purification of recombinant p23 of <i>P. monodon</i> (cultured overnight at 20°C)	270
Figure 3.128 SDS-PAGE (A) and western blotting analysis of anti-p23 PcAb (dilution 1:300, expected MW approximately 19.04 kDa; B and C) using total protein extracted from ovaries of <i>P. monodon</i> broodstock	272
Figure 4.1 A diagram proposing functional involvement of various reproduction-related genes during ovarian development of normal and eyestalk-ablated <i>P. monodon</i> broodstock.....	286

LIST OF ABBREVIATIONS

bp	base pair
°C	degree Celsius
DEPC	Diethylpyrocarbonate
dATP	deoxyadenosine triphosphate
dCTP	deoxycytosine triphosphate
dGTP	deoxyguanosine triphosphate
dTTP	deoxythymidine triphosphate
DNA	deoxyribonucleic acid
EDTA	ethylene diamine tetraacetic acid (disodium salt)
EtBr	ethidium bromide
HCl	hydrochloric acid
IPTG	isopropyl-thiogalactoside
kb	kilobase pair
M	Molar
mg	milligram
mRNA	Messenger-Ribonucleic acid
ml	millilitre
mM	millimolar
ng	nanogram
OD	optical density
PCR	polymerase chain reaction
RNA	Ribonucleic acid
rpm	revolution per minute
RNase A	Ribonuclease A

SDS	sodium dodecyl sulfate
T _m	melting temperature
Tris	Tris (hydroxy methyl) aminomethane
U	unit
UV	ultraviolet
w/v	weight/volume
μg	Microgram
μl	Microlitre
μM	Micromolar



ศูนย์วิทยทรัพยากร
จุฬาลงกรณ์มหาวิทยาลัย

CHAPTER I

INTRODUCTION

1.1 Background information

The giant tiger shrimp (*Penaeus monodon* Fabricius 1798) is one of the world's most economically important cultured crustaceans. Still, *P. monodon* farming relies almost entirely on ocean-caught females for farm seed supply. This open reproductive cycle and reliance on wild stocks of *P. monodon* results in heavy exploitation of female broodstock from wild populations (Klinbunga, 1996).

Perhaps as important, at least for the shrimp culture industry, selective breeding for improved culture performance, disease resistance, and other desirable traits cannot be achieved until this species is domesticated and seed are mass produced using closed-life-cycle, captive populations (Jarayabhand *et al.*, 1998). This will require the use of high quality pond-reared broodstock rather than ocean-caught broodstock (Benzie, 1997; Ibarra *et al.*, 2007).

Farming of *P. monodon* presently faces several problems such as the reduction of high quality wild broodstock and loss of the cultured production due to bacterial and viral infections and large size differences of cultivated *P. monodon* in the same cultured pond. The annual production of *P. monodon* was significantly reduced from approximately 200,000 MT during 1992 - 2002 to about 30,000 MT in 2006 (Limsuwan, 2004; FAO Fishery Statistic, 2009).

The domestication and selective breeding programs of penaeid shrimp would provide a more reliable supply of seed stock and the improvement of their production efficiency (Coman *et al.*, 2006). The use of selectively bred stocks having improved culture performance (e.g. disease resistance and/or other commercially desired traits) rather than the reliance on wild-caught stocks is a major determinant of sustainability of the shrimp industry (Clifford and Preston, 2006). Despite the potential benefits, the domestication of *P. monodon* has been remarkably slow in

Thailand and is still at the initial stage because the previous stocks (Withyachumnarnkul *et al.*, 1998) were recently collapsed by WSSV infection.

Reduced spawning potential and low degree of maturation of *P. monodon* in captivity crucially prohibit several possible applications including development of effective selective breeding programs of this species. Genetic improvement of *P. monodon* cannot be achieved without knowledge on the control of reproduction. Mechanisms controlling ovarian maturation of *P. monodon* at the molecular level are important and can be directly applied to the industry.

The development of oocytes consists of a series of complex cellular events, in which different genes express to ensure the proper development of oocytes and to store transcripts and proteins as maternal factors for early embryogenesis (Qiu *et al.*, 2005). Different biotechnological approaches, for example; injection of vertebrate steroid hormones, neurotransmitters and ecdysteroids (Benzie 1998; Okumura, 2004) and the use of specially formulated feed (Harrison, 1990) have been applied to induce the ovarian maturation of female shrimp but results are inconsistent owing to limited knowledge on genetic and hormonal control of penaeid species (Meusy and Payen, 1988; Okumura, 2004).

In penaeid shrimp, the final maturation with germinal vesicle breakdown (GVBD) immediately precedes spawning in a closed thelycum species (Yano, 1988). Two phases are involved: the appearance of ripe ovaries and germinal vesicle breakdown (GVBD), in preparation for fertilization after spawning. It remains unknown whether crustaceans possess a gonad-stimulating hormone or gonadotropin homologue that can trigger the meiotic resumption during final oocyte maturation as those in most vertebrate animals such as mammals, fishes and amphibians. Additionally, there is no report associated with the characterization of maturation promoting factor (MPF) and its regulatory mechanism of final oocyte maturation, which is an obviously important aspect towards artificial control of maturation of penaeid shrimp species (Qiu and Yamano, 2005).

It was pointed out that ovaries of the kuruma shrimp, *Marsupenaeus japonicus*, in most cases, start to develop in the reproductive season but fail to reach the necessary stage required by the formation of cortical rods. Accordingly, ovaries

are degenerate without spawning. Ovarian development of penaeid shrimps may not pass through to the accumulation of yolk substances or in some cases to the stage after yolk accumulation is achieved (Yamano *et al.*, 2004). Further studies about mechanisms controlling formation of CRs is, therefore, required to control maturation of *P. monodon* in captivity successfully.

Progress in genetic and biotechnology researches in penaeid shrimps have been slow because a lack of knowledge on fundamental aspects of their biology (Benzie, 1998). Molecular mechanisms involving gonad development of *P. monodon* have long been of interest by aquaculture industries (Benzie, 1998). Identification, characterization and expression analysis of genes involving gonad maturation and sex differentiation can be directly applied for selection of high quality pond-reared *P. monodon*. Accordingly, an initial step toward understanding molecular mechanisms of ovarian (and oocyte) maturation in *P. monodon* is the identification and characterization of reproductively related genes that are differential expressed during ovarian development of this economically important species

1.2 Objectives

The objectives of this thesis were isolation, characterization and expression analysis of genes functionally related to ovarian development of *P. monodon*. A large number of genes were identified by EST analysis. Moreover, differentially expressed transcripts during ovarian development of normal *P. monodon* broodstock were also identified by RNA arbitrary primed (RAP)-PCR and RT-PCR. The full length cDNA of interesting genes was isolated. Expression levels of various genes were examined by semiquantitative RT-PCR or quantitative real-time PCR. Localization of mRNA and/or proteins of functional important genes of *P. monodon* were determined by *in situ* hybridization and/or immunohistochemistry. Recombinant proteins of functionally important gene homologues were expressed *in vitro* and used to produce of polyclonal antibody.

1.3 General introduction

Shrimp farming has become one of the most important food product industry of the world. Total aquaculture production of the giant tiger shrimp, *Penaeus monodon* increased gradually from 21,000 tons in 1981 to 200,000 tons in 1988; then

it sharply increased to nearly 500,000 tons in 1993. Since then, the production has been quite variable, ranging from a low of 480,000 tons in 1997 to a high of 676,000 tons in 2001 (FAO Fishery Statistic, 2009). The major producers of *P. monodon* are Thailand, Viet Nam, Indonesia, India, the Philippines, Malaysia and Myanmar. The exportation of the chilled and frozen *P. monodon* from Thailand world wide since 2002-2007 was reported (Table 1.1)

Marine shrimp farms and hatcheries are located along the coastal areas of Thailand where Nakorn Sri Thammarat and Surat Thani in Peninsular Thailand are the major parts of shrimp cultivation. In addition, Chanthaburi (eastern Thailand), Samut Sakhon and Samut Songkhran (central region) also significantly contribute on the country production. The intensive farming system has resulted in consistent production of marine shrimp of Thailand. Thailand has been regarded as the leading shrimp producer of cultivated shrimp for over a decade.

Farming of *P. monodon* has achieved a considerable economic and social importance in the region, constituting a significant source of income and employment. In Thailand, *P. monodon* had been intensively cultured for more than two decades.

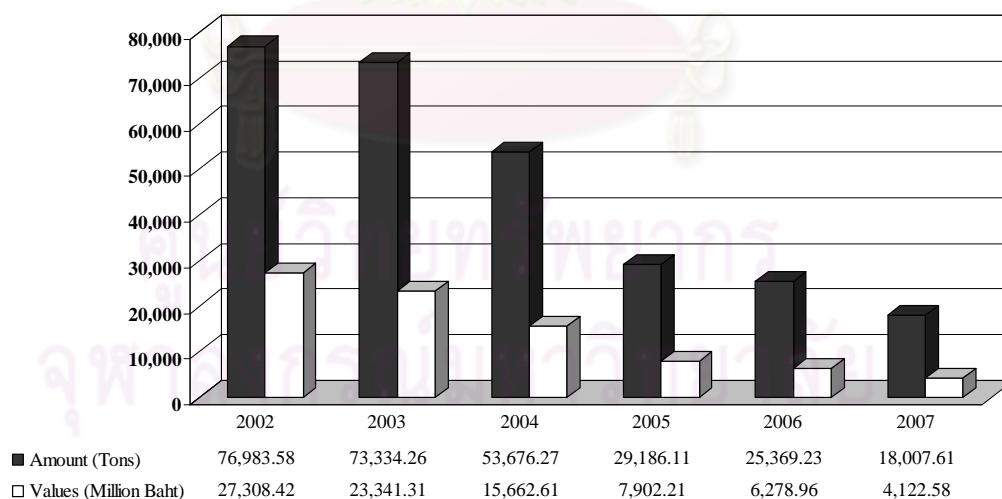


Figure 1.1 The Chilled and frozen *P. monodon* exported from Thailand to world wide Countries since 2002-2007 (Source: Department of Fisheries).

Culture of *P. monodon* had increased the national revenue, therefore, *P. monodon* was, until recently, the most economically important cultured species in Thailand. Since 2002, production of *P. monodon* in Thailand has been reported to have declined (Figure 1.1), and its production is replaced by the farming of the Pacific white shrimp (*Litopenaeus vannamei*).

However, the price of *L. vannamei* is quite low and broodstock used relies almost entirely on genetic improved stocks brought from different sources. In addition, the labor costs in Thailand are higher than other countries (e.g. Vietnam and China) preventing the advantage of competition for the world market. In contrast, the market of premium-sized *P. monodon* is still open for Thailand because *L. vannamei* is not suitable for that market. Accordingly, *P. monodon* culture is currently promoted for increasing the production of this species.

Shrimp hatchery operations rely on the availability of wild-caught broodstock from the sea, which is seasonal and limited. In order to meet the increasing and growing demand for seed, it is essential to develop techniques for maintaining a captive broodstock and induce them to mature under controlled conditions, for sustained production of quality seed (Rao *et al.*, 1995).

The fundamental problem in shrimp culture industry is lack of predictably abundant supplies of offspring's of known heritage. Development of the suitable biotechnology for controlled induction of reproduction in *P. monodon* is the prime requisite to overcome this problem. In order to develop such a technology, basic information on morphology, anatomy, physiology, cytology, and molecular biology of the reproductive systems of *P. monodon* is the most essential.

จุฬาลงกรณ์มหาวิทยาลัย

Table 1.1 The exportation of the chilled and frozen *P. monodon* from Thailand to world wide countries since 2002-2007

Chilled and frozen shrimp COUNTRY	Year 2002		Year 2003		Year 2004		Year 2005		Year 2006		Year 2007	
	Amount (T)	Values (MB)	Amount (T)	Values (MB)	Amount (T)	Values (MB)	Amount (T)	Values (MB)	Amount (T)	Values (MB)	Amount (T)	Values (MB)
ALL COUNTRY	76,983.58	27,308.42	73,334.26	23,341.31	53,676.27	15,662.61	29,186.11	7,902.21	25,369.23	6,278.96	18,007.61	4,122.58
U.S.A.	36,609.45	13,690.15	37,700.69	12,156.86	22,623.97	6,534.96	12,146.95	2,992.49	15,248.38	3,599.27	6,822.45	1,498.44
JAPAN	17,131.66	6,476.46	15,237.90	5,380.86	12,725.46	4,304.66	6,662.47	2,260.72	2,523.07	801.97	1,871.61	528.38
KOREA, REPUBLIC OF	3,732.61	1,072.74	5,141.09	1,345.48	5,471.74	1,358.88	3,704.20	864.16	2,738.61	657.02	1,732.33	364.38
CANADA	4,748.05	1,760.06	5,452.53	1,766.59	3,520.70	1,174.95	1,965.59	578.14	2,003.42	528.09	1,725.49	455.28
HONG KONG	1,023.94	259.98	515.66	139.50	707.92	233.90	588.91	169.30	618.16	142.41	1,526.43	352.24
CHINA	942.41	256.76	361.16	73.89	631.25	140.61	663.80	104.85	581.67	71.37	1,520.22	203.63
TAIWAN	2,839.83	757.73	1,886.25	514.63	2,952.10	496.22	1,469.41	381.39	456.40	144.62	633.49	165.04
MALAYSIA	15.16	2.44	44.06	10.22	306.08	97.64	83.38	18.05	7.81	1.62	562.80	136.56
GERMANY, FEDERAL REPUBLIC	258.32	92.50	71.05	23.10	102.37	47.24	11.22	4.18	8.20	2.97	323.49	85.48
AUSTRALIA	2,544.18	818.20	2,668.64	717.87	1,478.74	398.87	295.99	107.53	317.05	107.25	246.39	69.67
VIETNAM	-	-	9.86	3.37	28.95	6.20	265.89	54.66	49.20	4.70	204.37	43.41
U. KINGDOM	242.17	70.76	-	-	284.72	118.55	94.74	33.05	65.88	19.65	198.68	59.61
CYPRUS	64.67	22.77	125.49	44.05	110.67	35.21	96.17	31.16	85.39	27.50	135.64	39.53
RUSSIAN FEDERATION	20.81	10.76	99.84	42.27	97.87	39.49	125.47	46.86	36.72	14.82	98.24	31.12
SINGAPORE	4,139.36	1,181.92	2,366.43	611.73	1,141.54	219.52	379.47	65.82	237.65	37.87	71.66	16.70
U. ARAB EMIRATES	0.01	0.01	14.10	5.29	2.78	1.45	1.66	0.64	4.00	2.08	38.54	5.00
KOREA (NORTH)	1,082.36	343.35	304.23	98.10	77.69	24.05	41.32	14.49	42.73	16.44	31.53	6.39
FRANCE	189.40	74.88	78.27	42.73	136.06	64.92	11.49	5.25	0.27	0.12	30.74	7.43
ITALY	13.20	3.31	10.36	2.49	68.03	9.28	23.46	6.17	12.55	4.11	30.32	4.86
POLAND	30.63	13.15	40.16	14.41	17.32	6.69	2.74	0.98	-	-	24.90	7.94
NETHERLANDS (HOLLAND)	81.66	26.24	45.44	13.59	3.44	1.29	0.32	0.19	30.18	13.48	23.13	6.91
UKRAINE	4.00	1.60	8.95	3.57	21.34	8.10	39.67	14.21	12.38	5.18	21.06	5.53
NEW ZEALAND	315.07	102.24	392.89	120.03	391.39	112.96	174.70	52.47	76.78	19.58	19.47	5.03
MAURITIUS	-	-	-	-	-	-	-	-	-	-	19.16	3.81

Table 1.1 (Cont.)

Chilled and frozen shrimp COUNTRY	Year 2002		Year 2003		Year 2004		Year 2005		Year 2006		Year 2007	
	Amount (T)	Values (MB)	Amount (T)	Values (MB)	Amount (T)	Values (MB)	Amount (T)	Values (MB)	Amount (T)	Values (MB)	Amount (T)	Values (MB)
BELGIUM	278.17	83.05	80.25	24.51	16.50	5.23	4.57	1.11	113.35	27.72	16.40	4.17
NEW CALEDONIA	-	-	-	-	-	-	-	-	-	-	12.14	1.21
SAUDI ARABIA	-	-	-	-	-	-	-	-	-	-	11.09	1.80
ISRAEL	25.31	9.45	55.32	21.00	12.44	4.35	10.08	3.39	12.01	4.67	8.48	2.56
SWEDEN	-	-	2.61	0.61	0.36	0.21	0.25	0.11	0.50	0.30	6.72	1.04
SWITZERLAND	37.82	14.56	38.91	11.51	138.85	47.47	92.57	30.77	34.01	12.02	5.13	1.18
QATAR	-	-	-	-	-	-	-	-	-	-	5.00	0.57
CHILE	-	-	-	-	-	-	-	-	-	-	4.93	2.30
LEBANON	-	-	0.40	0.24	14.44	8.11	-	-	0.56	0.27	4.90	1.72
CROATIA	12.20	2.57	4.00	0.73	-	-	4.32	1.73	1.50	0.36	2.24	0.97
LAO PEOPLES DEMOCRATIC	10.80	0.55	13.20	0.65	19.60	0.93	18.00	0.85	16.80	0.76	1.51	0.52
INDONESIA	41.00	10.32	39.49	9.10	60.05	17.60	-	-	-	-	1.47	0.20
DENMARK	16.95	5.80	-	-	-	-	-	-	0.02	0.00	0.53	0.06
PHILIPPINES	58.70	8.03	-	-	0.95	0.33	-	-	0.01	0.00	-	-
GUAM	50.93	18.34	69.46	23.44	36.92	8.16	45.84	14.09	6.92	1.95	-	-
SPAIN	44.49	6.84	28.72	9.94	1.28	0.90	34.12	7.04	0.00	0.00	-	-
FRENCH POLYNESIA (TAHITI)	238.44	65.08	287.62	69.61	322.90	87.88	84.74	23.41	-	-	-	-
INDIA	0.09	0.00	34.04	11.80	57.38	18.14	20.48	7.96	-	-	-	-
OTHER COUNTRIES	139.75	45.84	105.19	27.56	92.48	27.63	22.16	4.99	27.05	8.80	14.94	1.91

Source: Department of Fisheries

1.4 Penaeid shrimp biology

1.4.1 Taxonomy

Penaeid shrimp belong to the largest phylum in the animal kingdom, the Arthropoda. This group of animals is characterized by the presence of paired appendages and a protective cuticle or exoskeleton that covers the whole animal. The subphylum Crustacea is made up of 42,000, predominantly aquatic species, that belong to 10 different classes. Within the class Malacostraca, shrimp, together with crayfish, lobsters and crabs, belong to the order Decapoda (Figure 1.2). Taxonomical recognition of *P. monodon* is illustrated below.

Phylum Arthropoda

Subphylum Crustacea

Class Malacostraca

Order Decapoda

Superfamily Penaeoidea

Family Penaeidae Rafinesque, 1815

Genus *Penaeus* Fabricius, 1798

Subgenus *Penaeus*

Species *monodon*

Figure 1.2 Taxonomy of the giant black tiger shrimp, *Penaeus monodon*, Fabricius, 1798 (Brusca and Brusca, 1990).

1.4.2 Morphology

The exterior of penaeid shrimp is distinguished by a cephalothorax with a characteristic hard rostrum, and by a segmented abdomen (Figure 1.3). Most organs, such as gills, digestive system and heart, are located in the cephalothorax, while the

muscles concentrate in the abdomen. Appendages of the cephalothorax vary in appearance and function. In the head region, antennules and antennae perform sensory functions. The mandibles and the two pairs of maxillae form the jaw-like structures that are involved in food uptake. In the thorax region, the maxillipeds are the first three pairs of appendages, modified for food handling, and the remaining five pairs are the walking legs (pereiopods). Five pairs of swimming legs (pleopods) are found on the abdomen.

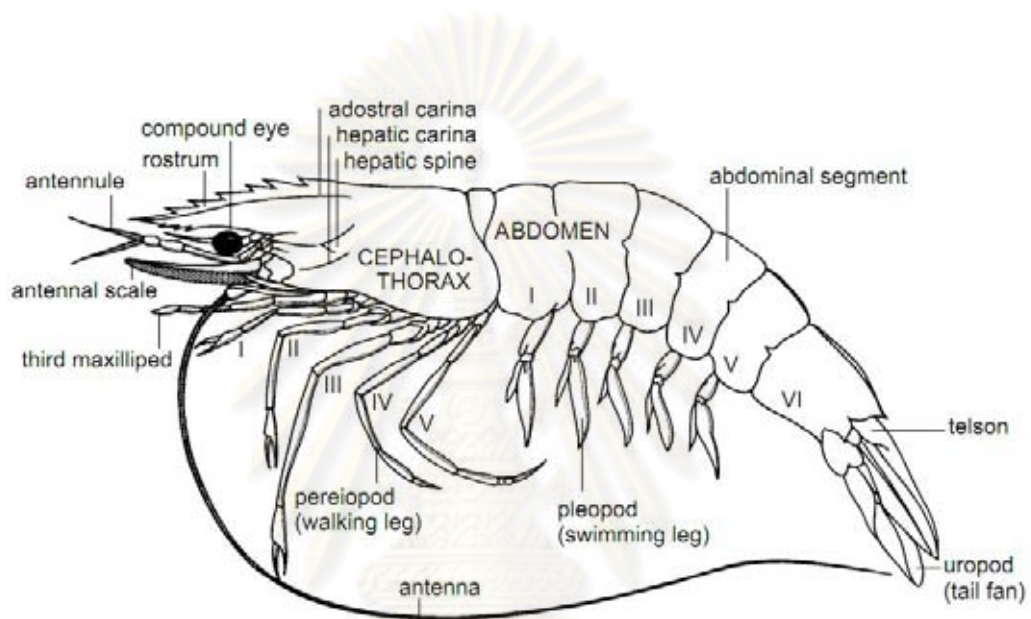


Figure 1.3 Lateral view of the external morphology of *P. monodon* (Source: Primavera, 1990).

The internal morphology of penaeid shrimp is outlined in Figure 1.4. Penaeids and other arthropods have an open circulatory system and, therefore, the blood and the blood cells are called haemolymph and haemocytes, respectively. Crustaceans have a muscular heart that is dorsally located in the cephalothorax. The valved haemolymph vessels leave the heart and branch several times before the haemolymph arrives at the sinuses that are scattered throughout the body, where exchange of substances takes place. After passing the gills, the haemolymph returns in the heart by means of three wide non-valved openings (Bauchau, 1981). A large part of the cephalothorax in penaeid shrimp is occupied by the hepatopancreas. This digestive

gland consists of diverticula of the intestine. Spaces between these hepatopancreatic tubules are haemolymph sinuses. The main functions of the hepatopancreas are the absorption of nutrients, storage of lipids and production of digestive enzymes (Johnson, 1980). One of the haemolymph vessels that leaves the heart ends in the lymphoid organ, where the haemolymph is filtered. This organ is located ventro-anteriorly to the hepatopancreas. The haemocytes are produced in haematopoietic tissue. This organ is dispersed in the cephalothorax, but mainly present around the stomach and in the onset of the maxillipeds. Lymphoid organ and haematopoietic tissue are not shown in Figure 1.4.

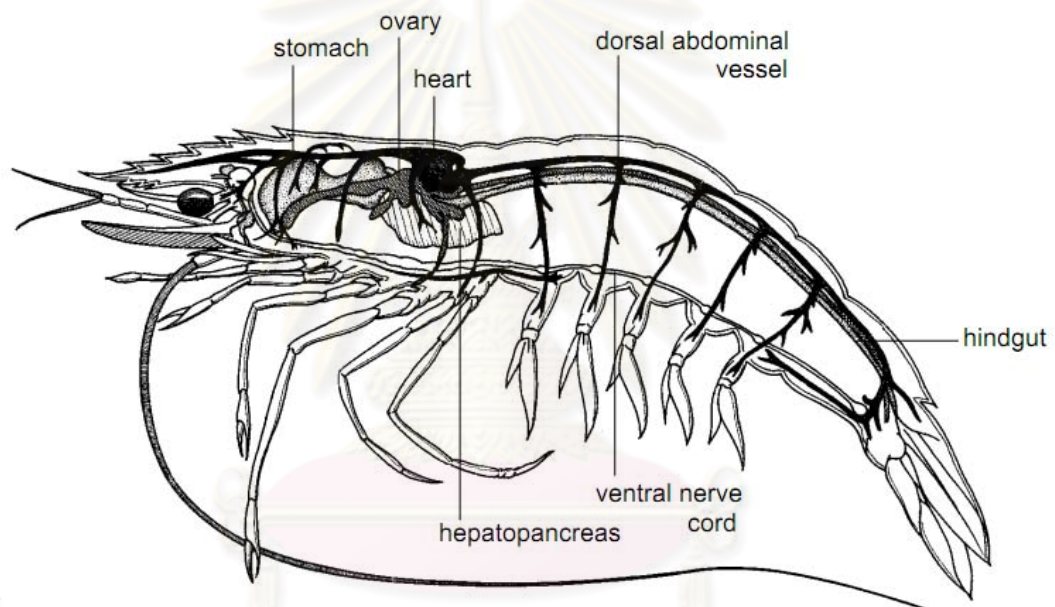


Figure 1.4 Lateral view of the internal anatomy of a female *Penaeus monodon* (Source: Primavera, 1990).

1.4.3 Distribution and life cycle

The giant black tiger shrimp is widely distributed throughout the greater part of the Indo-Pacific region, ranging northward to Japan and Taiwan, eastward to Tahiti, southward to Australia and westward to Africa. Penaeid shrimp life cycle include several distinct stages that are found in a variety of habitats (Figure 1.5).

Juveniles prefer brackish shore areas and mangrove estuaries in their natural environment. Most of the adults migrate to deeper offshore areas at higher salinities, where mating and reproduction takes place. Females produce between 50,000-1,000,000 eggs per spawning (Rosenberry, 1997). The eggs hatch into the first larval stage, which is the nauplius. The nauplii feed on their reserves for a few days and develop into the protozoae. The protozoae feed on algae and metamorphose into mysids. The mysids feed on algae and zooplankton and have many of the characteristics of adult shrimp and develop into megalopas, the stage commonly called postlarvae (PLs). Larval stages inhabit plankton-rich surface waters offshore, with a coastal migration as they develop.

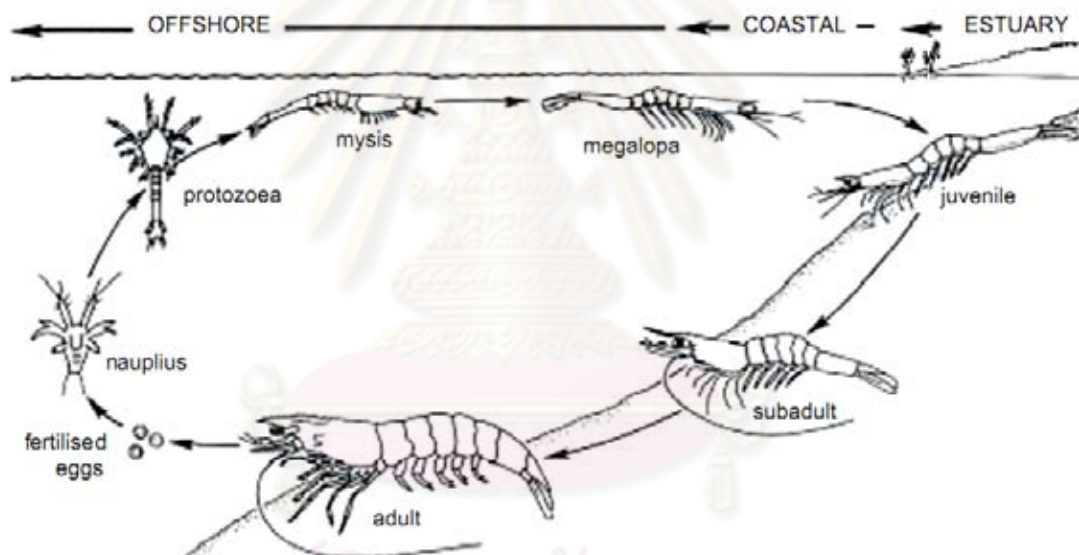


Figure 1.5 The life history of *Penaeus monodon* shrimp. Eggs hatch within 16 hours after fertilization. The larval stages comprise nauplius (6 stages in 2 days), protozoa (3 stages in 5 days), mysis (3 stages in 4-5 days) and megalopa (6-35 days). The megalopa and early juvenile are called postlarvae. Transition from juvenile to subadult takes 135-255 days and subsequently completion of sexual maturity occurs within 10 months (Motoh, 1984). The picture is not in proportion to actual size.

P. monodon is the largest, reaching 330 mm or more in body length, and exhibits the highest growth rate of all cultured penaeid shrimps (Lee and Wickins, 1992). Generally, *P. monodon* can reach a market size up to 25-30 g. within 3-4 months after PL stocking in the culture ponds and tolerates a wide range of salinities (Rosenberry, 1997). Those facts together make *P. monodon* a leading species to culture.

1.4.4 Sexual dimorphism

Motoh and Buri (1980) reported that *P. monodon* can be sexually distinguished with the first appearance of gonopores in juveniles, at 11 mm (carapace length; CL) for both female (thelycum, Figure 1.6) and male (petasma, Figure 1.7) *P. monodon*.

The diploid chromosome numbers in *P. monodon* have been reported ($2n = 88$) (Benzie, 1998). Recently, Staelens *et al.* (2008) constructed sex-specific high-density AFLP linkage maps of *P. monodon*. The female and male linkage maps, incorporating 494 and 757 markers, which have a median intermarker distance of 2.8 and 2.1 cM, respectively. Six sex-linked AFLP marker were inherited from female parents in the three families. One sex-linked AFLP marker was converted into an allele-specific assay, confirmed their association with sex in a panel of 52 genetically unrelated animals suggesting that the *P. monodon* adopts a WZ-ZZ sex-determining system

1.5 Female reproductive system

1.5.1 Morphology of female reproductive system

The female reproductive system consists of paired ovaries, paired oviducts and a single thelycum. The first two are internal and the last is an external organ. The ovaries are partly fused, bilaterally symmetrical bodies extending in the mature female for almost its entire length, from the cardiac region of the stomach to the anterior portion of the telson. In cephalothorax region the organ bears a slender anterior lobe and five finger-like lateral projections (King, 1948). A pair of lobes, one from each ovary, extends over the length of the abdomen. The anterior lobes lie close

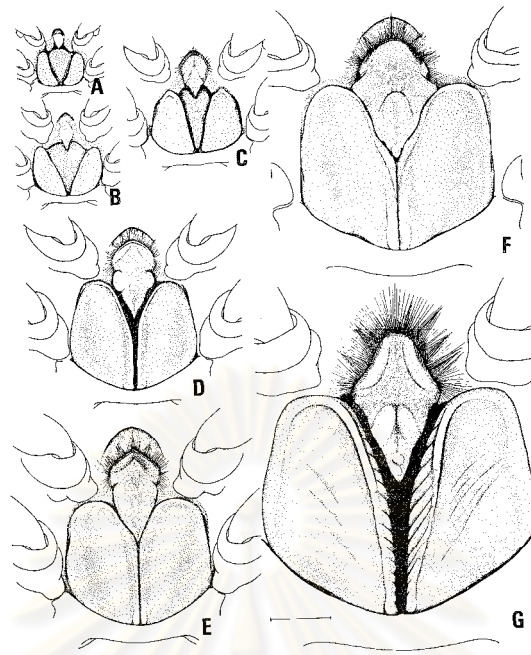


Figure 1.6 Development of theelycum. A; 11.7 mm in CL, B; 15.2 mm in CL; C 22.4 mm in CL, D; 31.4 mm in CL, E; 36.5 mm in CL, F; 46.8 mm in CL, G; 62.6 mm in CL. Thelyca F and G are inseminated. Scales represent 2 mm (Source: Motoh and Buri, 1980).

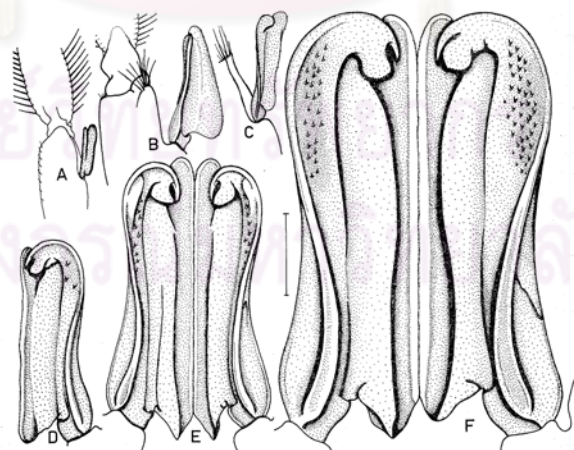


Figure 1.7 Development of petasma. A; 11.2 mm in CL, B; 21.6 mm in CL; C 23.5 mm in CL, D; 26.9 mm in CL, E; 34.2 mm in CL, F; 46.8 mm in CL (Source: Motoh and Buri, 1980).

1.5.2 Visual assessment of ovarian development

Generally, shrimp farmer visualize the ovarian development of female *P. monodon* broodstock by torchlight. These oocytes phases correspond to the stages 0 to V based on morphological characters (Rao *et al.*, 1995) (Figure 1.8).

1.5.2.1 Immature ovaries (stage 0)

The ovaries are not visible externally through the dorsal exoskeleton. The ovaries in this stage appear as a thin, translucent, and unpigmented band with small finger like linear lobules over the hepatopancreas. The posterior lobes are rudimentary.

1.5.2.2 Previtellogenic ovaries (stage I)

The ovary is not visible through the exoskeleton, as it is not developed. The paired ovaries at this stage lose its transparency and appear opaque. The colour of the ovarian lobules varies from white to cream and appears a bit granular especially in the anterior and middle lobes. The anterior and middle lobes appear larger in this stage but no increase in size in the posterior lobes.

1.5.2.3 Early vitellogenic ovaries (stage II)

Ovaries are faintly visible through the exoskeleton as a thick linear solid band due to its expansion in the posterior thoracic and anterior abdominal regions. The diameter of the posterior lobes becomes longer than that of the intestine. The dissected ovaries appear firm and granular in texture with a light yellow to greenish yellow colour due to the accumulation of yolk. The visibility of the ovary through the exoskeleton is due to the granular nature and the increased colouration in the ovarian lobules.

1.5.2.4 Late vitellogenic ovaries (stage III)

A diamond shaped expansion of the ovary at the first abdominal segment. Ovaries are visible through the exoskeleton as a thick solid and dark linear band due to its further expansion in all of its lobules. The ovaries are light to dark green in colour with a firm and granular texture.

1.5.2.5 Mature ovaries (stage IV)

Ovaries are clearly visible through the exoskeleton as a thick band on the entire dorsal side of the animal. The fully diamond shaped or butterfly shaped expansion of the first abdominal segment is clearly visible. The ovarian lobes are considerably larger, and these fully developed ovaries fill up all the available space in the body cavity, both in the cephalothoracic and abdominal region. The olive green to dark green ovaries is highly granular in texture.

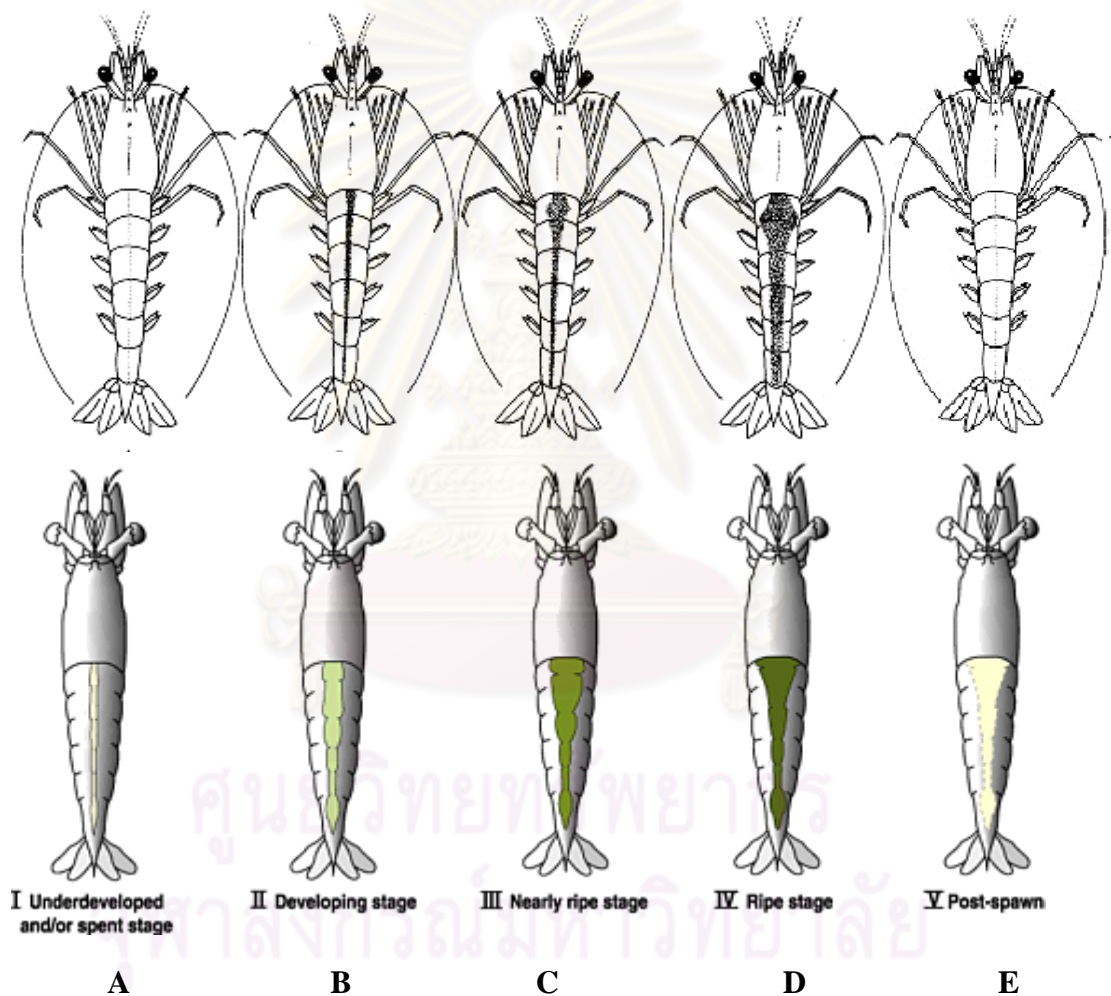


Figure 1.8 The dorsal view observed by hatchery operators when female broodstock are graded for ovarian development by torchlight (Upper) A; stage I-immature, B; stage II-developing, C; stage III-early mature, D; stage IV-mature and E; stage V-spent (Rao *et al.*, 1995). The wide saddle of ovarian tissue directly behind the carapace (Stage IV) is indicative of an immediate pre-spawning female. Colours of each ovarian developmental stage was illustrated in the lower line (AIMS, 2009).

1.5.2.6 Spent (stage V)

Ovaries are not visible through the exoskeleton. Externally it is indistinguishable from those in the previtellogenic stage. But the ovaries are flaccid and reduced in size but remained opaque, with less coloration, distinctive than the previtellogenic stage. In incomplete spawns, portions of ovaries, particularly posterior lobes, retain the coloration of the matured ovary.

1.5.3 Changes of ovarian morphology during oogenesis

The reproductive cycle of *P. monodon* includes a series of events starting from activation of primordial germ cells to the differentiation of highly yolk-equipped ova. Staging of reproductive development based on the morphological characters of ovaries is not appropriate. Correct staging of reproductive maturity requires more detailed characteristics like size of the germ cells, nature and arrangement of oogonial cells in ovaries, which is possible through microscopical investigations (Diwan *et al.*, 2009). Light microscopic examinations of ovaries of *P. monodon* at different stages of their maturity revealed the chain of nuclear and cytoplasmic changes that occur inside the developing ovaries. Oogonial cells developed from the primordial germ cells get transformed into the mature ova with sufficient yolk for the development of the embryo. A series of dramatic as well as complicated changes take place in the developing oocyte during its developmental phase. Based on the changes that occur inside the cytoplasm and nucleus of the growing oocytes, process of oogenesis may be classified into six different phases, such as immature, previtellogenic, early vitellogenic, late vitellogenic, mature or gravid and spent oocytes (Diwan *et al.*, 2009).

1.5.3.1 Oogenesis

The light microscopic studies in the ovarian tissue of *P. monodon* revealed, a thin ovarian wall, encompass the ovaries. It consists of 3 layers; a thin outer most pavement epithelium, an inner layer of germinal epithelium and a relatively thick layer of connective tissue in between. Blood capillaries are also present in the ovarian wall. A germinal zone (GZ) is found on the lateral periphery in the form of a thin band and this is the "zone of proliferation" from which the displacement of oogonial

cells takes place (Figure 1.9). Invasion of this zone into the ovarian lobes is observed from the ventral portion of the ovary. The young oocytes moved farther from the germinal zone upon maturation so the developing oocytes and ova are found towards the center of each ovarian lobe.

Immature stage

An active zone of proliferation with clusters of developing oogonial cells is the characteristic feature of immature ovaries (Figure 1.9). The primary and secondary oogonial cells are arranged in a graded manner in the ovaries so that the growing secondary oogonial cells are shifted to the interior. The nuclei of the primary oogonial cells are not conspicuous. These primary oogonial undergo mitotic division and gives rise to the secondary oogonia. The secondary oogonial cells possess a conspicuous nucleus.

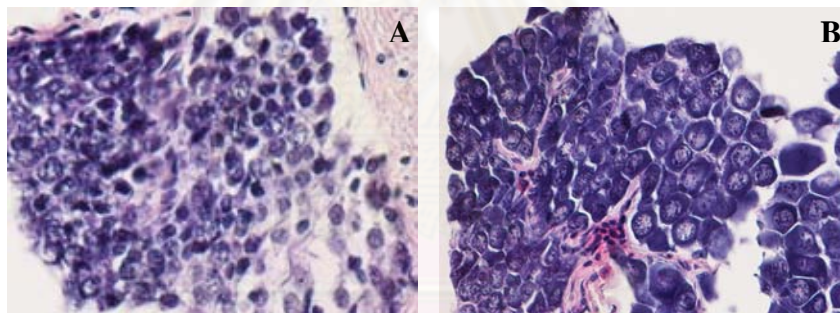


Figure 1.9 Light microscopy showing an immature ovaries; A: germinal zone with developing oogonial cells and B: the oogonial cells. Hymatoxylin and Eosin (HE) staining (40 x).

The oogonial cells appear round ultrastructurally and their large nucleus occupies approximately 80% of the cell volume (Figure 1.9). The oolemma is smooth and without any particular morphological specializations at this stage. The diffused electron-dense chromatin materials as well as small granule like round nucleoli are not present in the nucleolemma of these oogonial cells. Electron-loose cytoplasm in these oogonial cells contains only some small granules and filamentous materials (Figure 1.9). Other cell organelles are not at all visible at this stage of development.

Previtellogenic stage (stage I ovaries)

The most striking feature of previtellogenic ovaries is the presence of highly basophilic primary oocytes with much more increased cytoplasmic volume than that of the oogonial cells. These primary oocytes develop from the secondary oogonial cells through meiotic division. The nuclei contain 10 to 18 centrally located, deeply stained granules like nucleoli and prominent chromatin materials in their nucleoplasm. These oocytes are devoid of individual follicle cell layers. The early previtellogenic oocytes are characterized by the displacement of nucleoli towards the periphery of the nucleoplasm (Figure 1.10).

At the late of this stage, oocytes begin their folliculogenesis around the outer surface of each oocyte. The follicle cells in this stage are rectangular or cubical and a highly vacuolated conspicuous nucleus is also present.

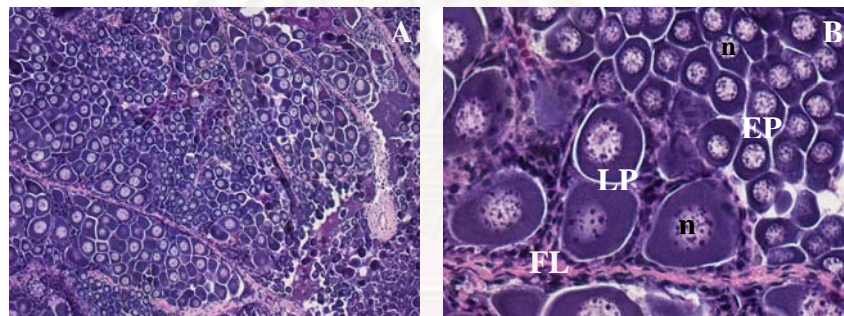


Figure 1.10 Light microscopy showing a previtellogenic ovaries. Hymatoxylin and Eosin (HE) staining (10 x; A and 40 x; B). EP = early previtellogenic oocyte, LP = late previtellogenic oocyte, n = nucleus, FL = follicular layers.

Early vitellogenic stage (stage II ovaries)

Early vitellogenic ovaries are sudden two fold increase in the size of the oocytes. The nature of the cytoplasm changes suddenly from homogenous to vesicular and little bit granular. From the granular nature of the cytoplasm and its sudden increase in the cytoplasmic volume it is seen that during this stage onwards the oocytes started its active accumulation of yolk. The granular nature is due to the

accumulation of oil globules in the cytoplasm, which is the characteristic feature of the primary vitellogenic oocytes. Consequently the nucleolar materials made a halo around the nucleus due to their circular arrangements in the peripheral karyoplasms (Figure 1.11).

During this stage, the formation of follicle cells around each individual oocyte occurs. Because of the sudden increase in the cytoplasmic volume the follicle cells stretched considerably and consequently their thickness decreased (Figure 1.11).

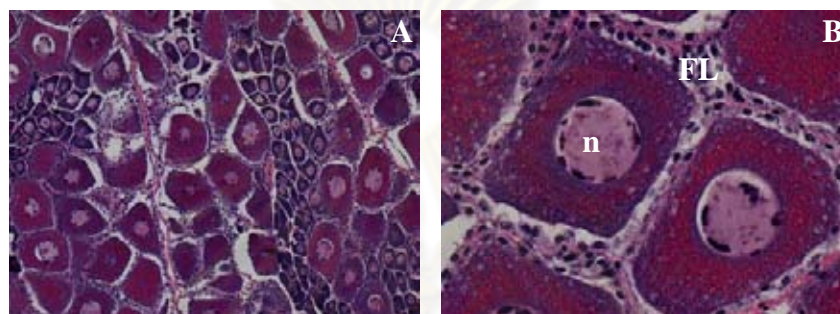


Figure 1.11 Light microscopy showing an early vitellogenic ovaries. Hymatoxylin and Eosin (HE) staining (10 x; A and 40 x; B). n = nucleus, FL = follicular layers.

Late vitellogenic stage (stage III ovaries)

Late vitellogenic oocytes are characterized by the appearance of radially arranged well developed of the oocytes. The ooplasm of which is full of eosinophilic yolk granules. The hypertrophied nucleus as well as nucleolus of follicle cells becomes conspicuous during this stage. Due to the increase in the volume of the oocytes, the follicle cells encompassing them stretch further and appear as a narrow band of flattened cells around each oocyte (Figure 1.12).

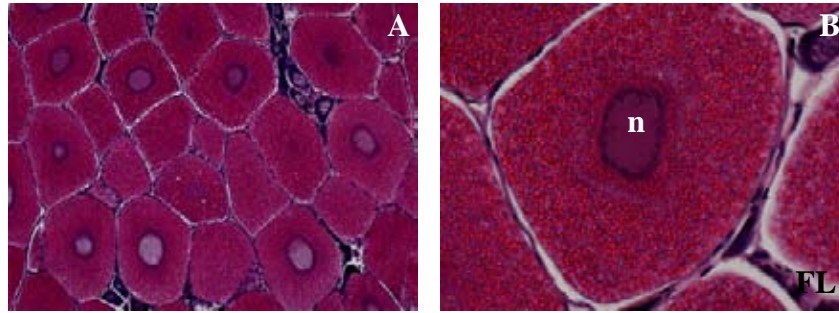


Figure 1.12 Light microscopy showing an late vitellogenic ovaries. Hymatoxylin and Eosin (HE) staining (10 x; A and 40 x; B). n = nucleus, FL = follicular layers.

Mature stage (stage IV ovaries)

Mature oocytes develop club shaped structures of the cortical rods in the peripheral ooplasm. The vitellin envelope is visible just at the top of the cortical crypts (Figure 1.13). At early of this stage, the oocytes appear with a very thin rim of follicle cells around it. follicle cells disappear from around the oocytes when reach to the late of this stage. Final maturation is finish when germinal vesicle breakdown (GVBD) (Figure 1.13). After GVBD, the spawning immediately proceeds.

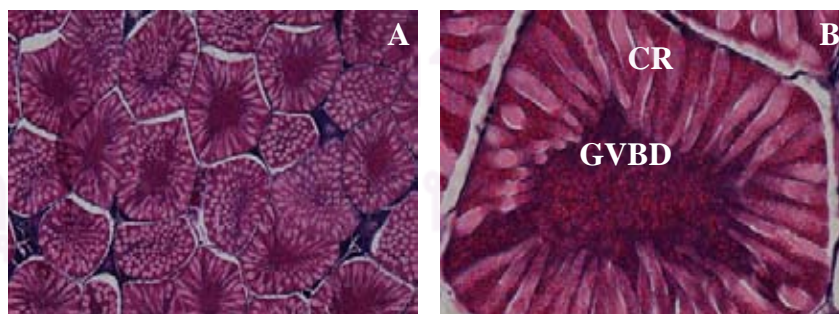


Figure 1.13 Light microscopy showing mature ovaries. Hymatoxylin and Eosin (HE) staining (10 x; A and 40 x; B). CR = cortical granules, GVBD = germinal vesical breakdown.

Spent stage (Stage V Ovaries)

Oocytes of the spent ovary are mostly primary oocytes similar to those of pre-vitellogenic oocytes in the immature ovary. Resorbing oocytes are also observed in between the empty thicker follicle cells caused by the retraction of the follicle cells from the oocytes. The zone of proliferation is active with irregular primary oogonial cells and developing oocytes at certain portions of the spent ovary. Some regressing atretic oocytes were commonly observe in the spent ovary.

The morphological characters of oocytes at each stage of oogenesis and the morphological changes occurring in the follicle cells during oocyte development have been investigated in the kuruma shrimp, *M. japonicus* (Yano, 1988) (Figure 1.14).

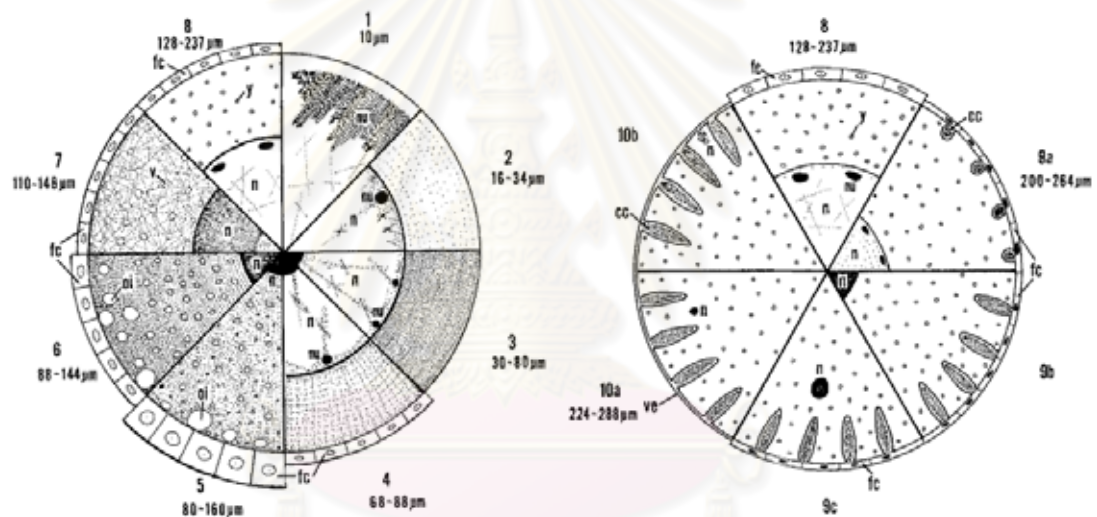


Figure 1.14 Various stages of oocyte development in *M. japonicus*. Oocyte diameters are given for each stage. 1; Synapsis stage (formation of typically half-moon shaped nucleolus). 2; Chromatin nucleolus stage (appearance of a round nucleoli in the nucleus). 3; Early perinucleolus stage (increase of nucleoli in the nucleus). 4; Late perinecleolus stage (follicle cells surround oocytes). 5; Oil globule stage I (rapid expansion of follicle cell and shrinking of nucleus; appearance of oil globule). 6; Oil globule stage II (slight shrinking of follicle cell and reexpansion of shrunken nucleus). 7; Yolkless stage (shrink of follicle cell and appearance of vesicles; further expansion of nucleus). 8; Yolk granule stage (accumulation of yolk granule and further expansion of nucleus). 9a; Prematuration stage (appearance of cortical crypts and shrinking of follicle cell and nucleus). 9b; Prematuration stage (further shrinking of the nucleus). 9c; Prematuration stage (migration and further shrinking of the nucleus and completion of club-shaped cortical crypts). 10a; Maturation stage (ovulation and further migration of nucleus and formation of vitellin envelope). 10b; Progression of meiotic division to metaphase of primary maturation division. Nu: nucleolus; n: nucleus; fc: follicle cell; oi: oil globule; v: vesicle; y: yolk granule; cc: cortical crypts; ve: vitellin envelope (Yano, 1988).

1.5.3.2 Spawning and egg activation

Penaeid shrimp are classified into two groups; open thelycum and closed thelycum species. The final phase of maturation, spawning, mating and their interrelationships differ significantly between the groups. The giant tiger shrimp, *P. monodon* is one of the closed thelycum species. Typically, mature males mate by insert in their spermatophore into the soft thelycum of newly molted immature females. In penaeid shrimp, the development of oocyte arrests at the first meiotic prophase (prophase I). After completion of yolk accumulation, the full-grown maturation oocyte resumes meiosis, the germinal vesicle begins to disintegrate and migrates towards the peripheral cytoplasmic membrane from the center of oocyte. Eventually, the mature oocyte arrests at the first meiotic metaphase (metaphase I) until fertilization or activated artificially by chemical agents (Yano, 1998).

Final maturation with germinal vesicle breakdown (GVBD) immediately precedes spawning in a closed thelycum species (Yano, 1988). Two phases are involved: the appearance of ripe ovaries and germinal vesicle breakdown (GVBD) in preparation for fertilization after spawning (Figure 1.15).

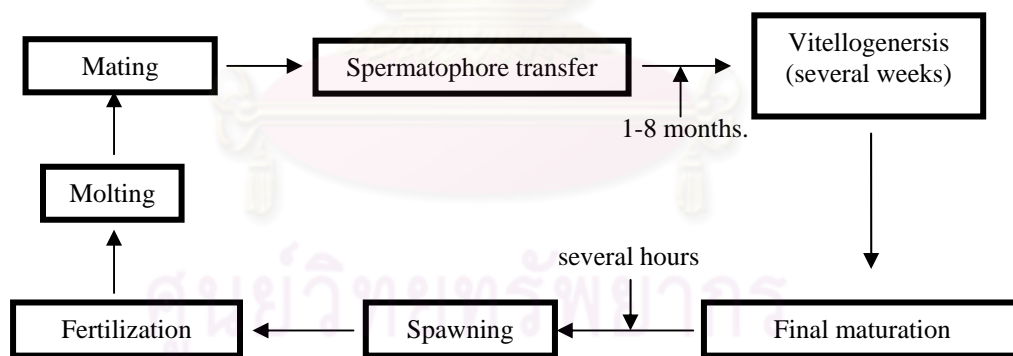


Figure 1.15 Reproductive cycle of the close-thelycum penaeid shrimp.

Immediately after release from the female gonopore, the mature eggs, still in metaphase (for example in *M. japonicus*), are fertilized by sperm released into the seawater from the spermatophore held in the thelycum. Once begun, spawning is continuous, females releasing batches of eggs from the ripe ovaries and sperm from

the spermatophore into the seawater, where fertilization takes place. Female shrimp repeat the process of molting, mating, and sexual maturation in order to achieve several spawnings during their life.

Egg activation, morphological changes in the eggs upon contact with seawater, in *P. monodon* were investigated by microscopy (Pongtippatee-Taweepreda *et al.*, 2004). The cortical rods began to emerge from the crypts on the periphery of the egg immediately when the egg was released into seawater and were completely expelled out within 45 seconds. Immediately after complete extrusion, the cortical rods began to break up and formed the jelly layer around the egg. By this time, the interaction between the sperm at the second phase of the acrosome reaction and egg began. The hatching envelope had started formation at 1-minute post-spawning to protect the additional sperm enter the egg, and was completed within 13-15-minutes post-spawning. The first and second polar bodies extruded from the egg at 3-5- and 10–15-minutes post-spawning, respectively.

1.6 Hormones involving shrimp reproduction

Neurosecretory structures in crustacean eyestalks are known to produce the crustacean hyperglycemic hormone (CHH), molting-inhibiting hormone (MIH) and gonad-inhibiting hormone (GIH) of the CHH/MIH/GIH gene family which secreted from brain and thoracic ganglion as well as other steroids and terpenoids (Chan *et al.*, 2003). These neuropeptides are involved in blood sugar regulation, inhibition of ecdysteroid synthesis, and regulation of reproduction, respectively (Chang, 1993).

A number of physiological processes in decapod crustaceans are known to be regulated by diverse neuropeptides synthesized by a neurosecretory system called X-organ-sinus gland complex (XOSG) located in the optic ganglia of the eyestalks (De and Van, 1995). In penaeid shrimp, GIH is produced in the X-organs and stored in the sinus glands of eyestalks (Gu *et al.*, 2002).

Treerattrakool *et al.* (2007) characterized a cDNA encoding a GIH (Pem-GIH) from the eyestalk of *Penaeus monodon*. *Pem-GIH* cDNA is 861 bp in size with an ORF of 288 bp. The deduced Pem-GIH consists of a 17-residue signal peptide and a mature peptide region of 79 amino acids with features typical of type II peptide hormones from the CHH family. Pem-GIH transcript was detected in eyestalk, brain,

thoracic and abdominal nerve cords of *P. monodon* adults. The gonad-inhibiting activity of Pem-GIH was investigated using the RNA interference technique. Double-stranded RNA, corresponding to the mature Pem-GIH sequence, triggered a decrease in *Pem-GIH* transcript levels both *in vitro* (eyestalk ganglia and abdominal nerve cord culture) and *in vivo* (female *P. monodon* broodstock). The conspicuous increase in *Vg* transcript level in the ovary of GIH-knockdown shrimp suggests a negative influence for Pem-GIH on *Vg* gene expression, and thus implies its role as the gonad-inhibiting hormone.

Steroid and steroid-like compounds ingested in the diet may have direct effects on reproduction and development (Benzie, 1997). While these can have unintended negative effects, it also means that inclusion of appropriate hormone in the diet may provide the means for a more controlled endocrine manipulation than eyestalk ablation. Since shrimp cannot synthesize cholesterol, an important precursor of steroid hormones (Cuzon *et al.*, 1994), diet is the only source of this substance.

An understanding the roles of steroid hormones on vitellogenesis may lead to the development of ways to induce ovarian maturation in decapod crustaceans. Progesterone has been shown to stimulate ovarian maturation of penaeid shrimp (Yano, 1985) and yolk protein synthesis in the ovary of white shrimp (Quackenbush, 2001). In addition, 17α -hydroxy-progesterone induces spawning in prawn; *P. stylifera* (Nagabhushanam *et al.*, 1980), *Vg* secretion into hemolymph of kuruma prawn *M. japonicus* (Yano, 1987) and oocyte developments in white shrimp *P. vannamei* and red swamp crayfish *Procambarus clarkii* (Tsukimura and Kamemoto, 1991; Rodriguez *et al.*, 2002).

Several steroid hormones have been detected in *P. monodon* (Young *et al.*, 1992). It has been reported that 17β -oestradiol and oestrone increase in the early stages of ovary growth demonstrated that 17β -estradiol stimulated *in vitro* yolk protein synthesis in white shrimp which suggests that 17β -estradiol may also stimulate vitellogenesis in decapod crustaceans. Pregnenolone as well as testosterone have been document from various organs such as the mandibular organ, kidney, hepatopancreas, hemolymph, ovary and testis (Quinitio *et al.*, 1994).

1.7 Molecular biological approaches used in this thesis

1.7.1 Polymerase chain reaction (PCR)

The introduction of the polymerase chain reaction (PCR) has revolutionized molecular biological researches. PCR is a technique for the *in vitro* amplification of specific DNA sequences by the simultaneous primer extension of complementary strands of DNA (Figure 1.16). The technique was originally reported by Saiki *et al.* (1986), who employed a heat-stable DNA polymerase-*Taq* polymerase with two primers that are complementary to DNA sequence at 3' ends of the region of the DNA to be amplified. The oligonucleotides serve as primers to which nucleotides are added during the subsequent replication step. Because a DNA strand can only add nucleotides at the 3' hydroxyl terminus of an existing strand, a strand of DNA that provides the necessary 3'-OH terminus, in this case, is also called a primer. All DNA polymerases require a template and a primer.

The PCR technique involves three steps

- (a) Denaturation of double stranded DNA by heating.
- (b) Annealing of extension primers to the target sites.
- (c) Primer extension, in which strands complementary to the region between the flanking primers are synthesised under the influence of a thermostable DNA polymerase (usually *Taq* polymerase).

The PCR is well established as the default method for DNA and RNA analysis. More robust formats have been introduced, improved thermal cycles developed, and new labeling and detection methods developed. Because gene expression profiling relies on mRNA extraction from defined types and number of cells, in some cases the use of small number of cells or even a few cells is necessary. In this situation, the PCR technique has been used to allow synthesis of cDNAs from a small amount of mRNA. For instance, the cDNA can be generated by mRNA extracted and amplified by poly (A) reverse transcription and PCR.

The use of PCR for molecular genetic studies in aquatic organisms is increased dramatically. This technique has facilitated the analysis of sequence

variation and has enabled a new PCR-based technique to develop for wider applications. The basic knowledge of a particular region from a few taxa (conserved but, however specific sequences) permits the amplification of the same DNA sequences from distant related species.

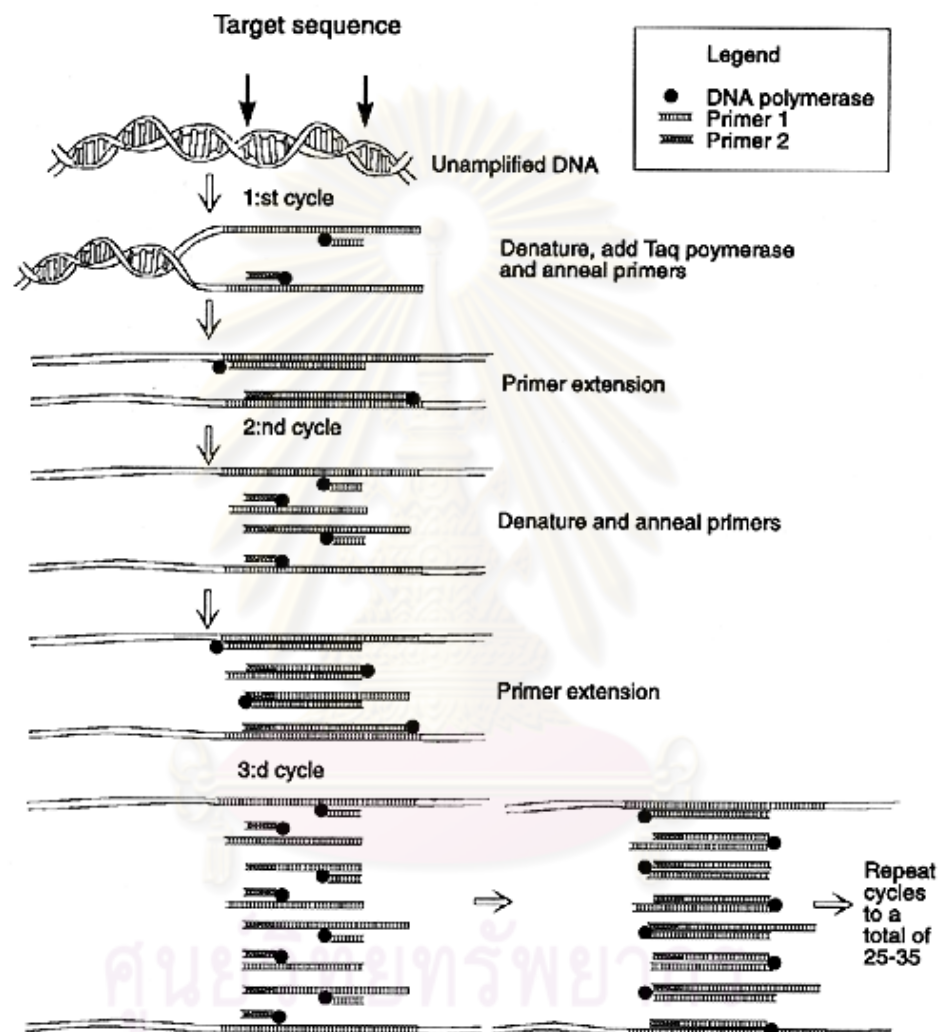


Figure 1.16 General illustration of the polymerase chain reaction (PCR) for amplifying DNA.

1.7.2 Expressed Sequence Tags (ESTs)

Functional genomic approaches may provide powerful tools for identifying and discovery of novel expressed genes. ESTs are DNA molecules reverse-transcribed

from a cellular mRNA population (MacIntosh *et al.*, 2001). They are generated by large-scale single-pass sequencing of randomly picked cDNA clones and have proven to be efficient and rapid means to identify novel genes (Adams *et al.*, 1991). ESTs thus represent informative source of expressed genes and provide a sequence resource that can be exploited for large-scale gene discovery (Whitefield *et al.*, 2002). By using comparative genomic approaches, the putative functions for some of these new cDNA clones may be found and thereby constitute an important tool for a better understanding of plant genome structure, gene expression and function (Lopez *et al.*, 2005).

Basically, construction of a cDNA library start with the purified target mRNA are reverse transcribed to the first-strand cDNA using the oligo (dT) primer as the synthesizing primer (Figure 1.17). The second-strand DNA is then copied from the first-strand cDNA using *E. coli* DNA polymerase I. The double-strand cDNA is ligated to adapter and subsequently to an appropriate vector using T4 DNA ligase. The recombinant vector-cDNA molecules are packaged (λ vector) *in vitro* and transfected to the appropriate host. If a plasmid is used recombinant plasmid is transformed into *E. coli* host cells to generate a cDNA library.

ESTs can be sequenced from either 5' or 3' ends of cloned cDNA. The 3' end of the cloned insert is usually marked by the poly A stretch which is often problematic for thermostable polymerase sequencing, and sequencing through poly T can reduce the length and quality of the subsequent sequence. Nevertheless, 3' UTR usually exhibit high polymorphism and is a promising location for SNP identification. The 5' ESTs have the advantage of being more likely to include some of the open reading frame (ORF) of the cDNA and thus facilitate identification of the encoded product.

EST sequences are used as the tag to homology search through the sequence data in the GenBank (Altschl *et al.*, 1990). The BlastN program uses nucleotide sequence to compare against the NCBI nucleotide database whereas the BLASTX uses the translated protein products to compare against the NCBI protein database in all possible 6 reading frames. Sequences are considered to be significantly matched when the possibility value (E-value) is less than 10^{-4} and the match length is > 100 nucleotides for BlastN and a match length is > 10 amino acid residues for BlastX, respectively, (Anderson and Brass, 1998).

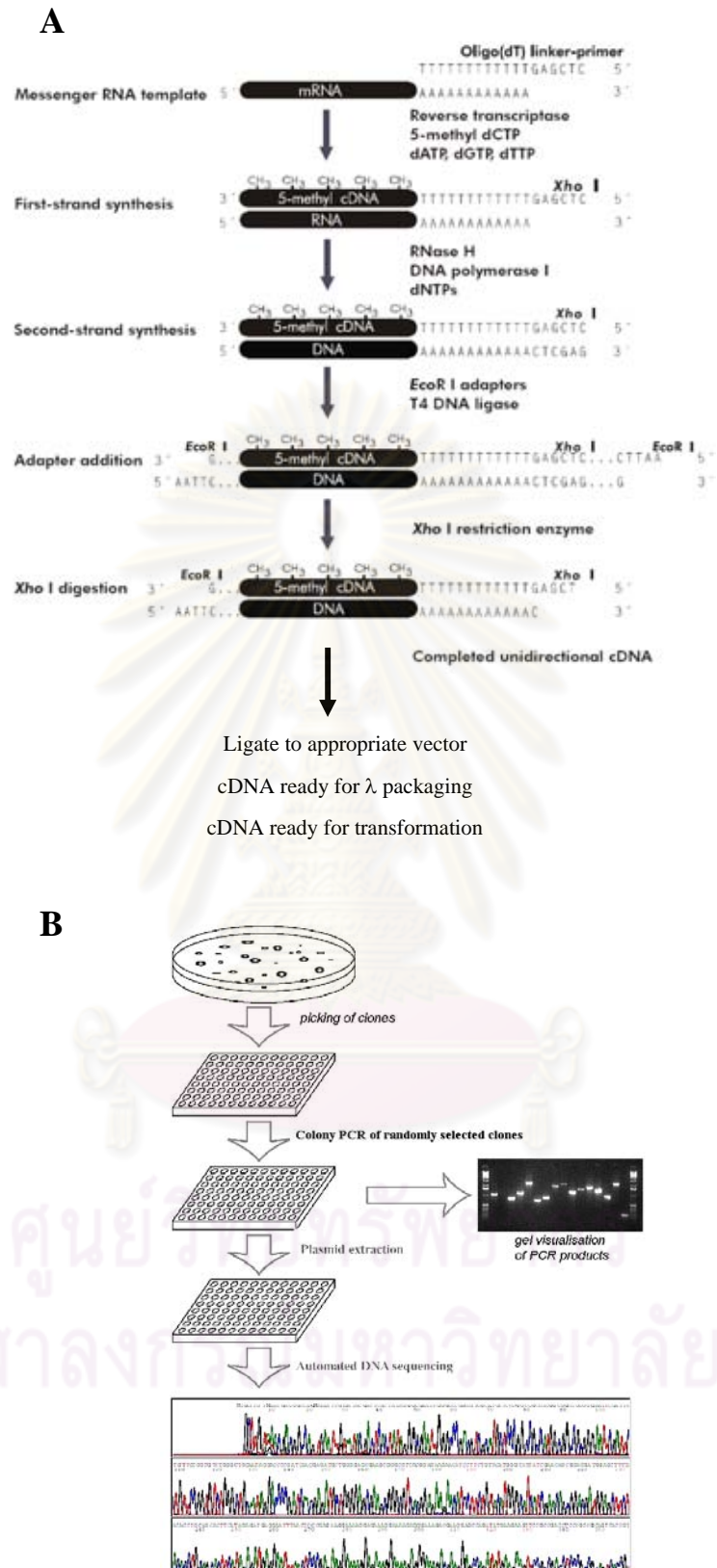


Figure 1.17 Overview for construction of cDNA inserts (A) and automated DNA sequencing (single-pass) of randomly selected cDNA clones (the entire process simply called EST analysis).

EST analysis is an important tool for several applications. They have mainly applied for rapid gene discovery of genes, comparative genomics and functional genomics in various organisms. After characterization and annotation, cDNA or designed oligonucleotides of transcripts can be further used for microarray analysis. Construction of genetic linkage maps and/or physical maps of interesting species can be carried out by development and sequencing of EST-derived markers using genomic DNA of species under investigation (Liu and Cordes, 2004).

1.7.3 Normalized ESTs

The problem associated with gene discovery reflects the redundancy of the cellular mRNA. Depending on their expression, mRNAs can be defined as abundant, intermediate, or rare. In a typical cell, 5 - 10 species of abundantly expressed cDNA comprise at least 20% of the mass of mRNA, 500 - 2000 species of intermediately expressed mRNA comprise 40 - 60% of the RNA mass, and 10,000 - 20,000 rare messages may account for < 20 - 40% of the mRNA mass (Carninci *et al.*, 2000). This average distribution may vary markedly between tissue sources, and the presence of numerous highly expressed genes may further unbalance this distribution. Sequencing cDNAs from standard cDNA libraries is ineffective for discovering rarely expressed genes, when intermediately and highly expressed cDNAs would be sequenced redundantly.

A normalized cDNA library could be constructed from a typical cDNA library established previously. The normalization method is a reassociation-kinetics-based approach involving hybridization of a many fold excess of cDNA inserts excised from a plasmid DNA preparation of the standard EST library with the library itself in the form of single-stranded circles (Bonaldo *et al.*, 1996; Carninci *et al.*, 2000). Biotinylation of the mRNA driver is an easy alternative that is amenable to up scaling. Further, biotinylation can be coupled easily to streptavidin-phenol extraction (Barr and Emanuel, 1990) or using magnetic beads techniques, provided that the reported cDNA degradation caused by photo-biotinylated drivers (Fargnoli *et al.* 1990) is prevented (Figure 1.18).

1.7.4 Suppression subtractive hybridization (SSH)

Suppression subtractive hybridization (SSH) is a widely used method for separating DNA molecules that distinguish (differentially expressed) two closely related DNA samples (call tester and driver). In fact, SSH is one of the most powerful and popular methods for generating subtracted cDNA or genomic DNA libraries. The SSH method is based on a suppression PCR effect and combines normalization and subtraction in a single procedure. The normalization step equalizes the abundance of DNA fragments within the target population, and the subtraction step excludes sequences that are common to the populations being compared.

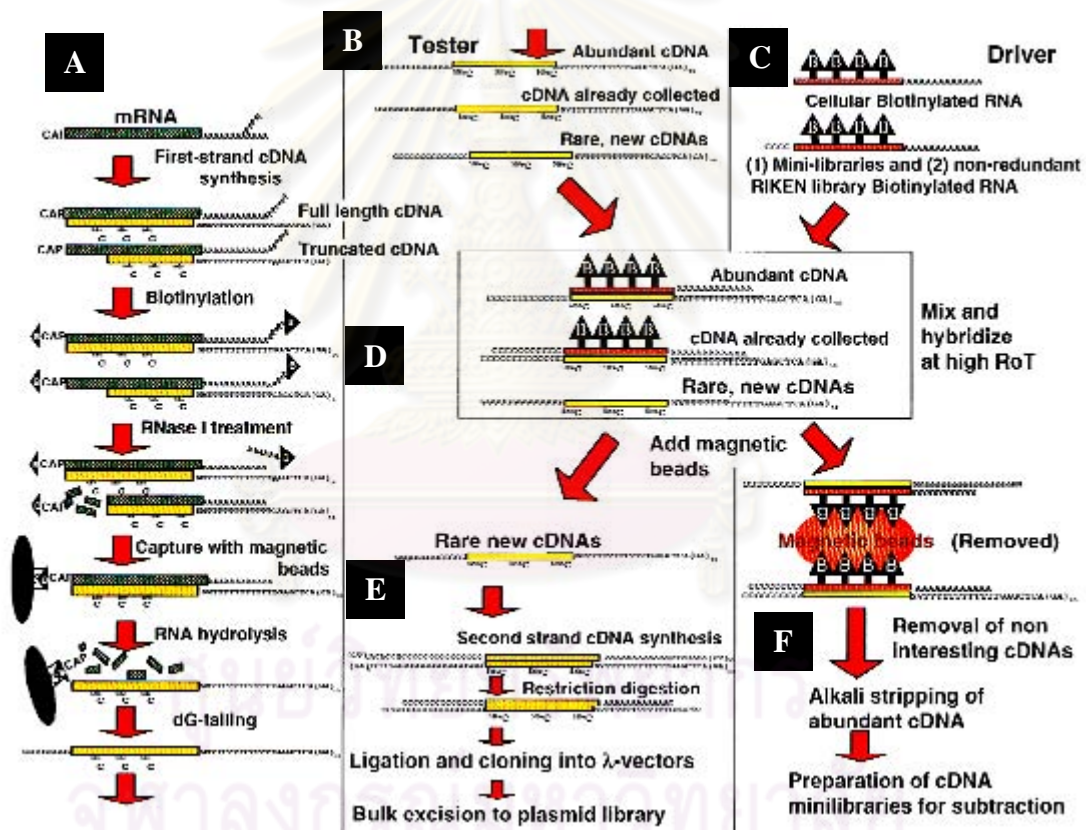
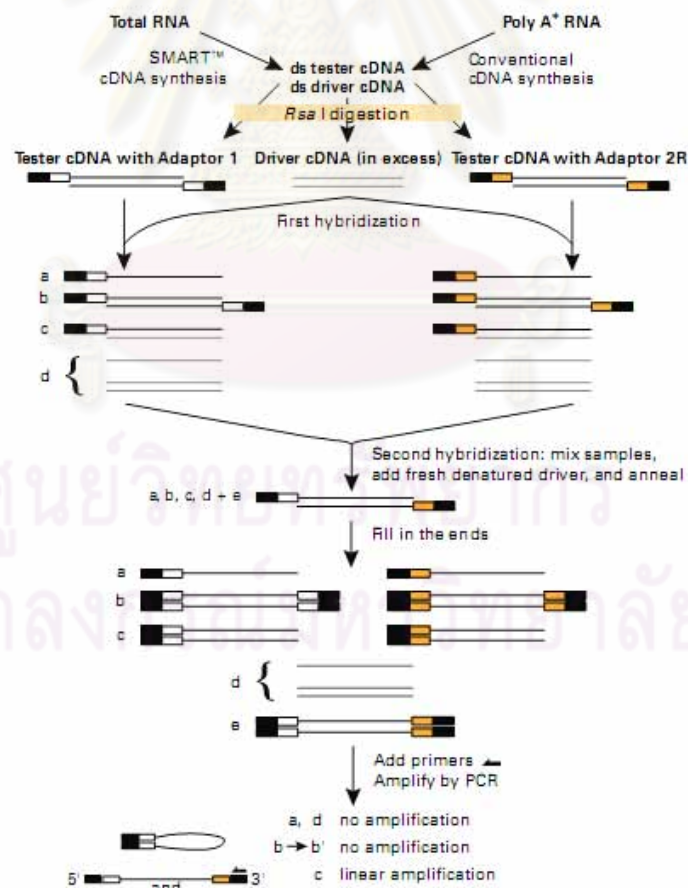


Figure 1.18 Schematic diagram of the normalized-subtracted cDNA preparation protocol. (A) general scheme for preparing full-length single-strand cDNA; (B) representation of various populations of tester cDNAs; (C) normalizing driver (cellular mRNA) and subtracting drivers (run-off transcripts); (D) hybridization; (E) rare/new cDNAs used for second-strand cDNA preparation (normalized/subtracted cDNA library); (F) abundant cDNAs/unwanted cDNAs are removed and maybe used for the preparation of mini-libraries to implement subtraction.

This dramatically increases the probability of obtaining low-abundance differentially expressed cDNA or genomic DNA fragments, and simplifies analysis of the subtracted library. The SSH technique has enriched over 1000-fold for rare sequences in a single round of subtractive hybridization (Figure 1.19).

One potential disadvantage of the SSH technique is the fact that under our standard procedure, a few micrograms of poly(A)⁺ RNA from the two cell populations are needed. In some special cases, such quantity of RNAs may be difficult to obtain. To circumvent this problem, an amplification step for both the driver and tester cDNAs can be incorporated to generate sufficient quantities of both cDNA samples before initiating the SSH procedure. In such cases, separate adapter/primers will be ligated to the cDNA fragments and subsequently used for the PCR amplification. Nevertheless, avoiding the preamplification step is desirable because it may result in the loss of some sequences (Diatchenko *et al.*, 1996).



(BD PCR-Select[™] cDNA Subtraction Kit User Manual, Clontech)

Figure 1.19 The PCR-Select cDNA subtraction technique

1.7.5 DNA sequencing

Polymorphism at the DNA level can be studied by several methods but the direct strategy is determination of nucleotide sequences of a defined region. There are two general methods for sequencing of DNA segments: the “chemical cleavage” procedure (Maxam and Gilbert, 1977) and the “chain termination” procedure (Sanger, 1977). Nevertheless, the latter method is more popular because chemical cleavage procedure requires the use of several hazardous substances.

DNA sequencing is the most optimal method for several genetic applications. This technique provides high resolution and facilitating interpretation. DNA fragments generated from PCR can be directly sequenced or alternatively, those fragments can be cloned and sequenced. This eliminates the need to establish a genome library and searching of a particular gene in the library.

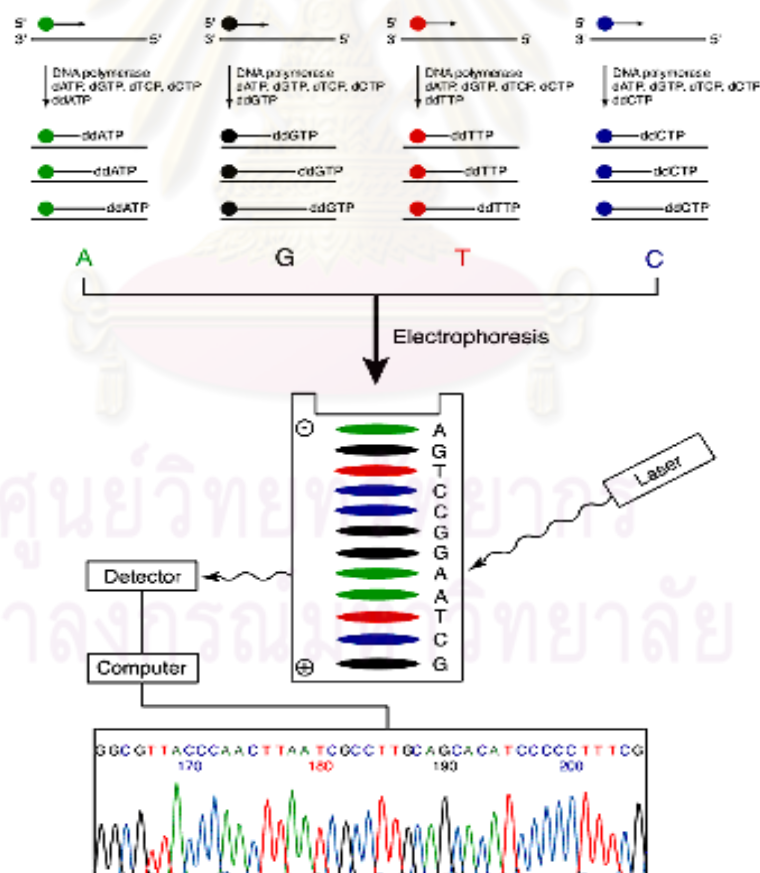


Figure 1.20 A schematic diagram illustrating principles of Automated DNA sequencing.

The enzymatic sequencing approach has presently been developed to automated method (Figure 1.20). DNA sequences can be detected using a fluorescence-based system following labeling with a fluorescence dye. PCR allow the possibility to isolate homologous DNA sequences from any organism of interest with unprecedented speed. This greatly allows wider application of DNA sequencing analysis for population genetic and systematic studies.

1.7.6 Reverse transcription-polymerase chain reaction (RT-PCR)

RT-PCR is a comparable method of conventional PCR but the first strand cDNA template rather than genomic DNA was used as the template in the amplification reaction (Figure 1.21). It is a direct method for examination of gene expression of known sequence transcripts in the target species. Alternatively, RT-PCR can also be used to identify homologues of interesting genes by using degenerate primers and/or conserved gene-specific primers from the original species and the first strand cDNA of the interesting species as the template. The amplified product is further characterized by cloning and sequencing.

1.7.7 RNA arbitrary-primed (RAP)-PCR

RAP-PCR is a comparable method of conventional randomly amplified polymorphic DNA (RAPD; Williams *et al.*, 1990 and Welsh and McClelland, 1990) but the first strand cDNA template rather than genomic DNA was used as the template in the amplification reaction.

The amplification conditions in RAPD differ from the standard PCR in that only single random primer (usually 10 mer with GC content usually at least 50%) is employed. RAPD is utilized to amplified target DNA on the basis that the nuclear genome may contain several priming sites closed to one another that is located in an inverted orientation. Accordingly, the primer is utilized to scan genome for the small inverted sequences resulting in amplification of DNA segments of variable length.

Subsequently, RNA fingerprinting by arbitrary primed PCR (RAP-PCR) (Welsh *et al.*, 1992) was introduced. The technique required reverse transcription of the target total RNA (or mRNA) to the first strand cDNA (by oligo dT or short and long random nucleotides). The synthesized cDNA was included as the template in the PCR reaction

composing of the single primer or a combination of primers. The amplification products are size-fractionated through agarose or denaturing polyacrylamide gels and detected by either radiolabeled or non-radiolabeled (Etbr or silver staining) detection methods.

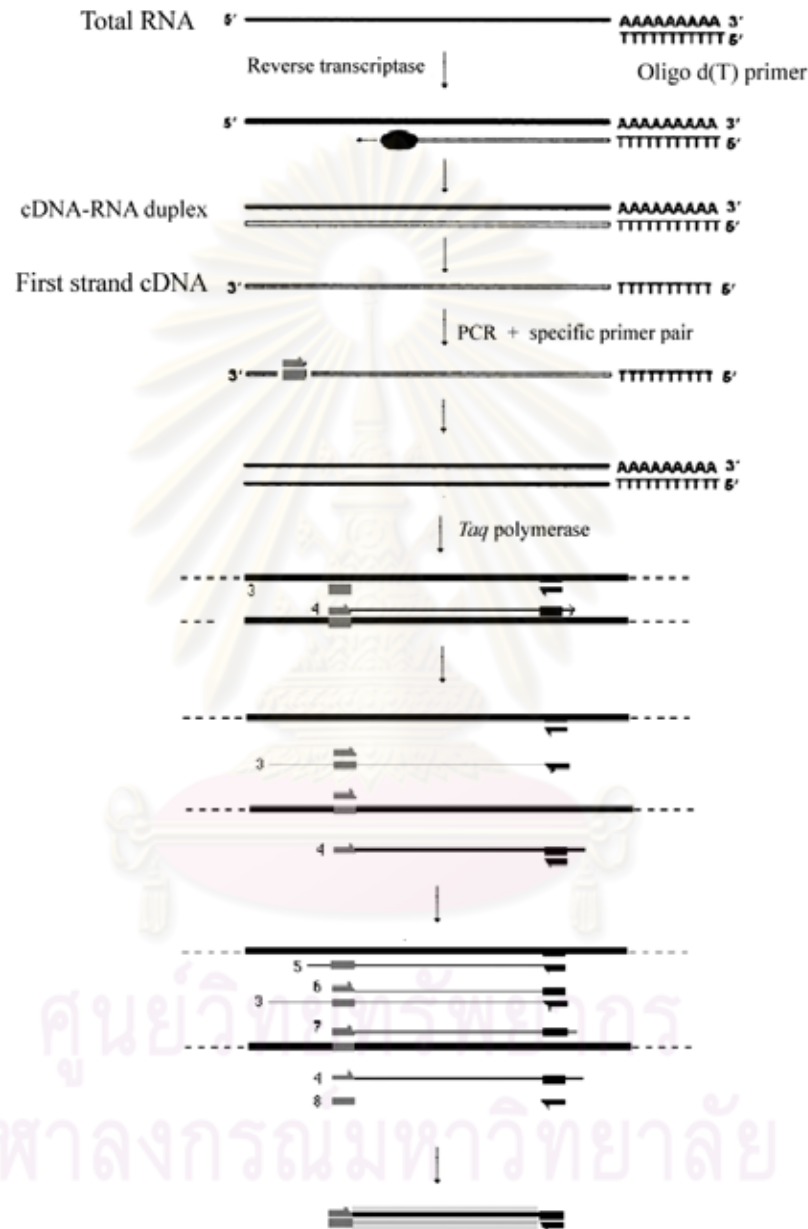


Figure 1.21 Overall concepts of the RT-PCR procedure. During first-strand cDNA synthesis an oligo d(T) primer anneals and extends from sites present within the total RNA. Second strand cDNA synthesis primed by the 18 - 25 base specific primer proceeds during a single round of DNA synthesis catalyzed by *Taq* polymerase. These DNA fragments serve as templates for PCR amplification.

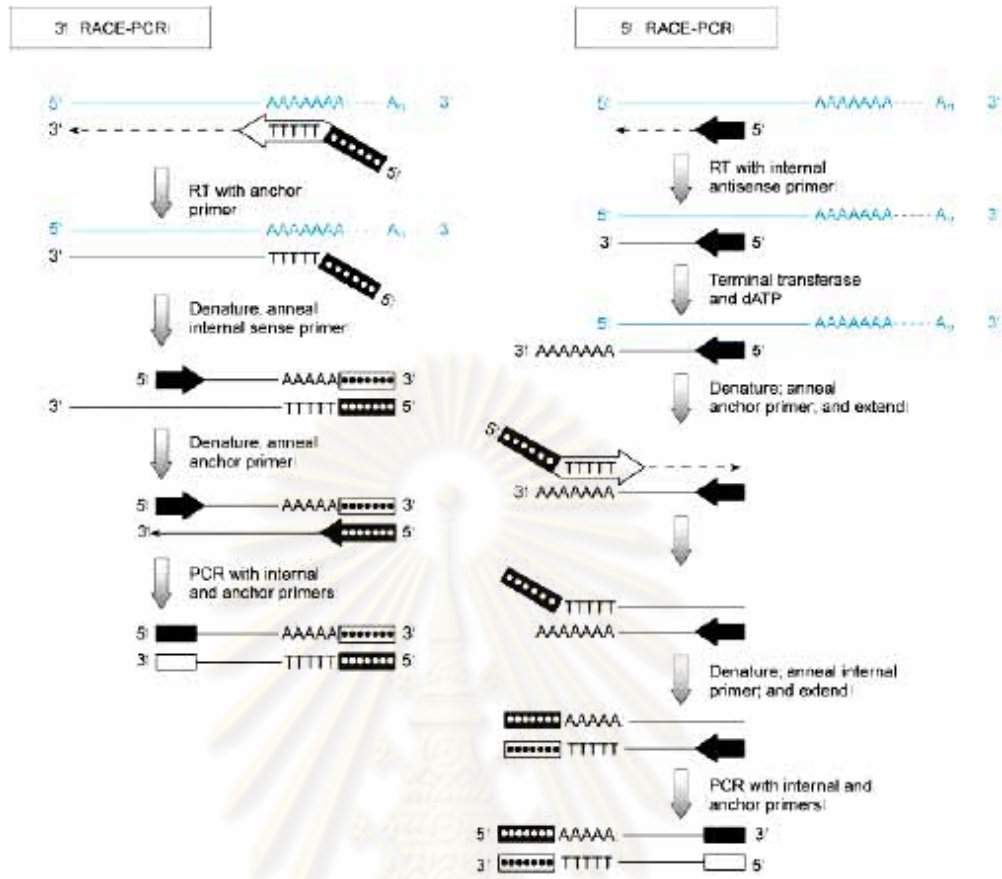
The intensity of RAP-PCR bands produced from different experimental samples is considered. Bands that are present in one sample and absent in another or bands that exhibit large differences in the intensity across the experimental treatments should represent potentially differentially expressed mRNA transcripts and required further characterization. The fragments can be cloned and sequenced. The expression levels of interesting bands are then examined using specific primers.

1.7.8 Rapid amplification of cDNA ends-polymerase chain reaction RACE-PCR

Rapid amplification of complementary DNA (cDNAs) ends (RACE) is a powerful technique for obtaining the ends of cDNAs when only partial sequences are available. Using SMART (Switching Mechanism At 5' end of RNA Transcript) technology, terminal transferase activity of Powerscript Reverse Transcriptase (RT) adds 3-5 nucleotides (predominantly dC) to the 3' end of the first-strand cDNA. This activity is harnessed by the SMART oligonucleotides whose terminal stretch of dG can anneal to the dC-rich cDNA tail and serve as an extended template for reverse transcriptase. A complete cDNA copy of original mRNA is synthesized with the additional SMART sequence at the end.

Essentially, an adaptor with a defined sequence is attached to one end of the cDNA; then the region between the adaptor and the known sequences is amplified by polymerase chain reaction (PCR). Since the initial publication in 1988 (Frohman *et al.*, 1988), RACE has greatly facilitated the cloning of new genes. Currently, RACE remains the most effective method of cloning cDNAs ends. It is especially useful in the studies of the temporal and spatial regulation of transcription initiation and differentiation splicing of mRNA. A linker at the 3' end and an adaptor at the 5' end are added to the first strand of cDNA during reverse transcription; amplification of virtually any transcript to either end can then make use of this same pool of cDNAs (Figure 1.22). In addition to being simple, the efficiency of 5'-RACE is dramatically increased because the adaptor is added only to the full-length cDNAs.

A



Source: www.e-biolearning.com

B

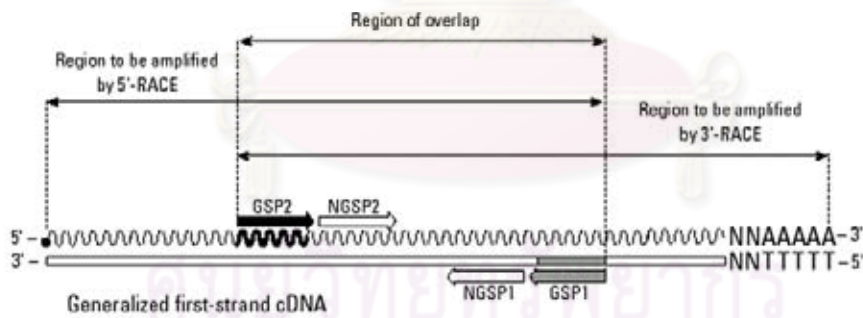


Figure 1.22 Overview of RACE-PCR. A; Mechanism of 5' and 3' RACE cDNA synthesis. First strand synthesis is primed using a modified oligo (dT) primer. After reverse transcriptase reaches the end of the mRNA template, it added several dC residues. The oligonucleotide adaptor anneals to the tail of the cDNA and serves as an extended template for RACE-PCR. B; Relationships of gene-specific primers to the cDNA template. This diagram shows a generalized first strand cDNA template.

1.7.9 Quantitative real-time PCR

Real-time polymerase chain reaction, also called “quantitative real time polymerase chain reaction” (Q-PCR/qPCR) or “kinetic polymerase chain reaction”, is a laboratory technique based on the polymerase chain reaction, which is used to amplify and simultaneously quantify a target DNA molecule. It enables both detection and quantification (as absolute number of copies or relative amount when normalized to DNA input or additional normalizing genes) of a specific sequence in a DNA sample (Figure 1.23).

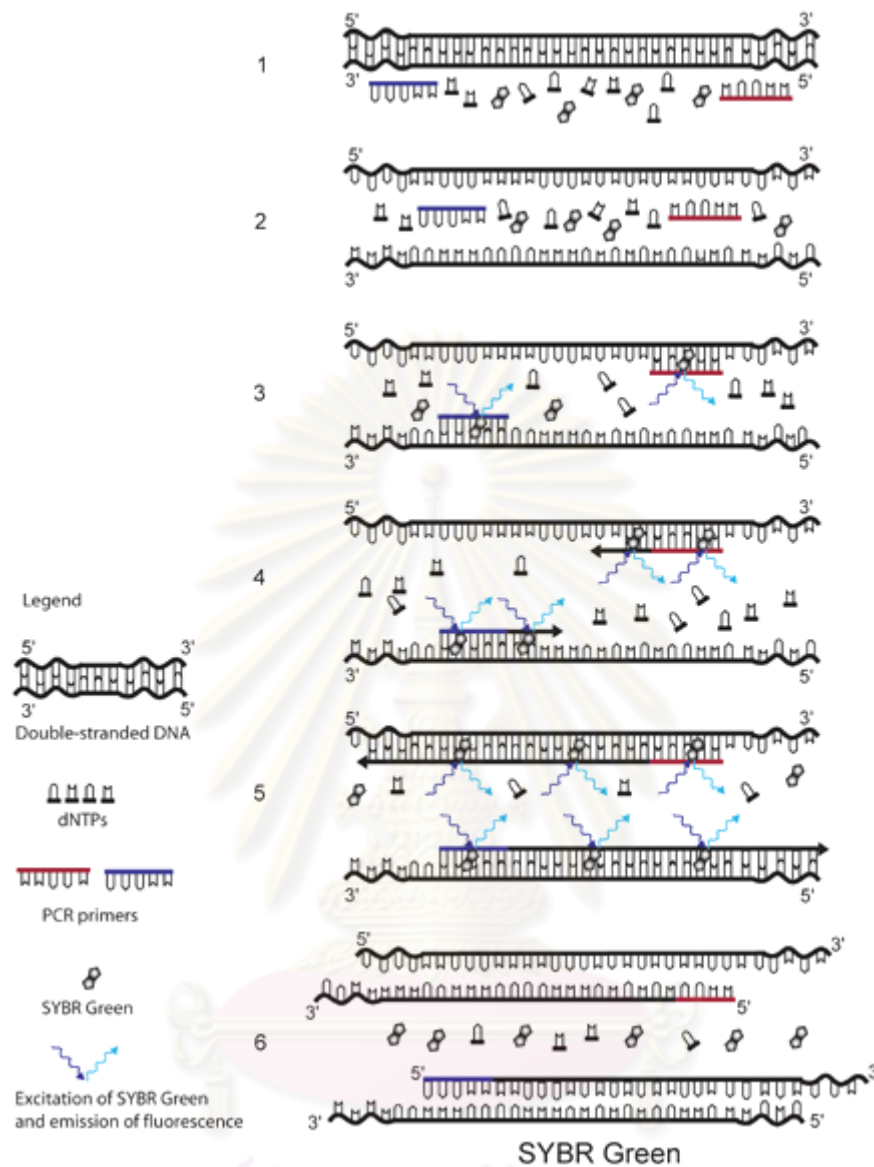
The procedure follows the general principle of polymerase chain reaction; its key feature is that the amplified DNA is quantified as it accumulates in the reaction in *real time* after each amplification cycle. Two common methods of quantification are: (1) the use of fluorescent dyes that intercalate with double-stranded DNA, and (2) modified DNA oligonucleotide probes that fluoresce when hybridized with a complementary DNA (VanGuilder *et al.*, 2008).

Typically, the reaction is prepared as usual, with the addition of fluorescent dsDNA dye. The reaction is run in a thermocycler and after each cycle, the levels of fluorescence are measured with a detector; the dye only fluoresces when bound to the dsDNA (i.e., the PCR product). With reference to a standard dilution, the dsDNA concentration in the PCR can be determined.

A DNA-binding dye binds to all double-stranded (ds) DNA in PCR, causing fluorescence of the dye. An increase in DNA product during PCR therefore leads to an increase in fluorescence intensity and is measured at each cycle, thus allowing DNA concentrations to be quantified. However, dsDNA dyes such as SYBR Green bind to all dsDNA PCR products, including nonspecific PCR products (such as "primer dimers"). This can potentially interfere with or prevent accurate quantification of the intended target sequence.

1.7.10 *In situ* hybridization

In situ hybridization allows specific nucleic acid sequences to be detected in morphologically preserved chromosomes, cells or tissue sections.



Source: www.dpd.cdc.gov

Figure 1.23 The principle of SYBR Green detection in real-time. The fluorescent dye SYBR Green is added to the PCR mixture. SYBR Green is a DNA binding dye that fluoresces strongly when bound to double-stranded DNA. At the start of the reaction, very little double stranded DNA is present, and so the fluorescent signal detected by the thermocycler is low. As the reaction proceeds and PCR product accumulates, the amount of double-stranded DNA increases and with it the fluorescence signal. The signal is only detectable during annealing and extension, since the denaturation step contains predominantly single-stranded DNA.

In combination with immunocytochemistry, *in situ* hybridization can relate microscopic topological information to gene localization at the DNA, mRNA, and protein level. The technique was originally developed by Pardue and Gall (1969). At that time radioisotopes were the only labels available for nucleic acids, and autoradiography was applied of detecting hybridized sequences. Furthermore, as molecular cloning was not possible in those days, *in situ* hybridization was restricted to those sequences that could be purified and isolated by conventional biochemical methods (e.g., mouse satellite DNA, viral DNA, ribosomal RNAs).

At present, non-radioactive labeling using the digoxigenin (DIG) system is commonly applied for *in situ* hybridization. Digoxigenin is linked to the C-5 position of uridine nucleotides via a spacer arm containing eleven carbon atoms (Figure 1.23). The DIG-labeled nucleotides may be incorporated, at a defined density, into nucleic acid probes by DNA polymerases (such as *E. coli* DNA Polymerase I, T4 DNA Polymerase, T7 DNA Polymerase, Reverse Transcriptase, and Taq DNA Polymerase) as well as RNA Polymerases (SP6, T3, or T7 RNA Polymerase), and Terminal Transferase.

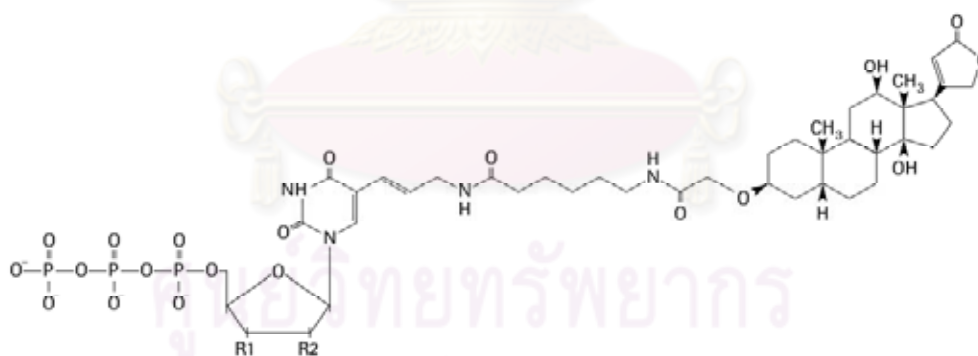


Figure 1.24 Digoxigenin-UTP/dUTP/ddUTP, alkali-stable. Digoxigenin-UTP (R1 = OH, R2 = OH) Digoxigenin-dUTP (R1 = OH, R2 = H) Digoxigenin-ddUTP (R1 = H, R2 = H)

DIG label may be carried out by random primed labeling, nick translation, PCR, 3'-end labeling/tailing, or *in vitro* transcription. Hybridized DIG-labeled probes may be detected with high affinity anti-digoxigenin (anti-DIG) antibodies that are conjugated to alkaline phosphatase, peroxidase, fluorescein, rhodamine, or colloidal gold. Alternatively, unconjugated anti-digoxigenin antibodies and conjugated secondary antibodies may be used.

Detection sensitivity depends upon the method used to visualize the anti-DIG antibody conjugate. For instance, when an anti-DIG antibody conjugated to alkaline phosphatase is visualized with colorimetric (NBT; blue tetrazolium chloride and BCIP; 5-Bromo-4-chloro-3-indolyl phosphate, toluidine salt) or fluorescent (HNPP) alkaline phosphatase substrates, the sensitivity of the detection reaction is routinely 0.1 pg of the target on a Southern blot.

1.8 EST analysis for isolation of reproduction-related genes in *P. monodon*

Subtractive cDNA libraries of ovaries and testes of *P. monodon* were constructed. A total of 218 clones (157 clones from subtractive cDNAs of ovaries and 61 clones from those of testes) were unidirectionally sequenced. Most of the expressed genes in ovaries encoded thrombospondin (TSP, 45 clones accounting for 28.7% of total expressed sequence tags, ESTs), peritrophin (17 clones, 10.8%), and unknown transcripts (78 clones, 49.7%) (Leelatanawit *et al.*, 2004). Conversely, almost all of the ESTs in *P. monodon* testes were unknown transcripts (59 clones, 96.7%). Rapid amplification of cDNA ends–polymerase chain reaction (RACE–PCR) was carried out for further characterization of *TSP*. Homologues of *elongation factor-2*, *oxidoreductase*, *peritrophin*, *transketolase*, *hypothetical protein FLJ23251*, and *sex-linked ENSANGP00000010123* and *X-linked protein 1 (XNP-1)* were also isolated. Gender-specific expression of candidate sex-linked gene homologs was examined by reverse transcriptase–polymerase chain reaction (RT-PCR). While *XNP-1* and *peritrophin* were expressed in both ovaries and testes, *TSP* and *ENSANGP00000010123* homologues revealed sex-specific expression in female *P. monodon* (Leelatanawit *et al.*, 2004).

Low degrees of reproductive maturation of captive *P. monodon* females and low quality of spermatozoa of captive males have limited the potential of genetic

improvement that resulted in remarkably slow domestication and selective breeding programs of *P. monodon* in Thailand (Withyachumnarnkul *et al.*, 1998). Practically, breeding of *P. monodon* using spermatozoa of captive males yields low quality offspring. The use of spermatozoa from wild males with either wild or pond-reared females has resolved that problem successfully (Withyachumnarnkul, B., personal communication).

Spermatogenesis is a complex cell differentiation process required a coordinated series of both mitosis and meiosis cycle events (Abe, 1987). Spermiation and sperm maturation occur during the final stage of spermatogenesis and are critical steps for successful fertilization (Callard, 1991; Zirkin, 1993). Mechanisms governing gonadal maturation and sex differentiation processes of *P. monodon* at the molecular level are important and can be directly applied to the shrimp industry (Benzie, 1998). Accordingly, an initial step towards understanding molecular mechanisms of testicular and sperm development in *P. monodon* is to identify and characterize sex-related genes expressed in testes of this economically important species.

Recently, suppression subtractive hybridization (SSH) testis cDNA libraries of *P. monodon*, were constructed (Leelatanawit *et al.*, 2008). In total, 178 and 187 clones from the forward and reverse SSH libraries, respectively, of *P. monodon* were unidirectionally sequenced. From these, 37.1% and 53.5% Expressed Sequence Tags (ESTs) significantly matched known genes (E-value $< 1 \times 10^{-4}$). Three isoforms of *P. monodon* progesterin membrane receptor component 1: *PM-PGMRC1-s* (1980 bp), *PM-PGMRC1-m* (2848 bp), and *PM-PGMRC1-l* (2971 bp), with an identical ORF of 573 bp corresponding to a deduced polypeptide of 190 amino acids, were successfully identified by RACE-PCR. Interestingly, *PM-PGMRC1* showed a greater expression level in testes of juvenile than broodstock *P. monodon* ($P < 0.05$). Dopamine administration (10^{-6} mol/shrimp) resulted in up-regulation of *PM-PGMRC1* in testes of juveniles at 3 hrs post treatment ($P < 0.05$), but had no effect on *PM-Dmc1* ($P > 0.05$).

Isolation and characterization of genes involving gonadal development are an initial step towards understanding reproductive maturation and sex determination of the giant tiger shrimp (*Penaeus monodon*). Accordingly, 896 clones from the testis cDNA library were sequenced. A total of 606 ESTs (67.6%) significantly matched

sequences in the GenBank (E-value $< 1 \times 10^{-4}$) whereas 290 ESTs (32.4%) were newly unidentified transcripts. The full length cDNA of genes functionally involved in testicular development including *cyclophilin A (PMCYA)*, *small ubiquitin-like modifier 1 (PMSUMO-1)*, *ubiquitin conjugating enzyme E2*, *dynactin subunit 5*, *cell division cycle 2 (cdc2)* and *mitotic checkpoint BUB3* were discovered. In addition, *Tra-2*, a gene involving sex determination cascades, was successfully characterized by RACE-PCR and first reported in crustaceans. Expression analysis indicated that a homologue of *low molecular weight neurofilament protein XNF-L* (termed *P. monodon testis-specific transcript 1, PMTST1*; $N = 8$ for each sex) was only expressed in testes but not ovaries. *PMCYA*, *thyroid hormone receptor-associated protein complex 240 kDa component (Trap240)*, *multiple inositol polyphosphate phosphatase 2 (MIPP2)* and *heat shock-related 70 kDa protein 2 (HSP70-2)*, but not *PMSUMO-1*, *PMTra-2* and *prohibitin2* were differentially expressed between ovaries and testes of *P. monodon*. Expression of *PMTST1* was up-regulated but that of the remaining genes in testes of *P. monodon* broodstock was down-regulated after shrimp were molted (Pb0.05). Significant reduction of *PMSUMO-1* and increment of *prohibitin2* transcripts in domesticated broodstock (Pb0.05) suggested that these reproductively related genes may be used as biomarkers to evaluate reduced degrees of the reproductive maturation in domesticated *P. monodon*.

1.9 Functionally important genes related to ovarian development of *P. monodon*

1.9.1 Progesterone receptor

Progestins (progesterone, P4 and its derivatives) are sex steroid hormones that play important roles in gametogenesis (Miura *et al.*, 2006). The actions of P4 are mediated through binding to its nuclear receptor, the progesterone receptor (PGR) as the classical pathway (Rao *et al.*, 1974). However, P4 retains its actions in a variety of PGR negative cells and in mutant mice devoid of classical PGRs leading to the finding that progestins elicit their actions via interactions with other proteins (Zhu *et al.*, 2003a and 2003b).

Progestins have a broad range of functions in reproductive biology. Many rapid nongenomic actions of progestins have been identified, including induction of oocyte maturation, modulation of reproductive signaling in the brain, rapid activation

of breast cancer cell signaling, induction of the acrosomal reaction and hypermotility in mammalian sperm. Currently, there are three receptor candidates for mediating progestin actions: (1) membrane progestin receptors (mPRs); (2) progestin receptor membrane components (PGRMCs); and (3) nuclear progestin receptors (nPRs). The recently-described mPR family of proteins has seven integral transmembrane domains and mediates signaling via G-protein coupled pathways. The PGRMCs have a single transmembrane with putative Src homology domains for potential activation of second messengers. The classical nPRs, in addition to having well defined transcriptional activity, can also mediate activation of intracellular signaling pathways. However, details of the mechanisms by which these three classes of progestin receptors mediate rapid intracellular signaling and their subcellular localization remain unclear. In addition, mPRs, nPRs and PGRMCs exhibit overlapping expression and functions in multiple tissues, implying potential interactions during physiological processes in individual cells (Zhu *et al.*, 2008).

Two totally distinct classes of putative membrane-bound progestin receptors have been reported in vertebrates: membrane progestin receptors (mPR, subtypes α , β , γ also called progestin and adipoQ receptors; PAQR, VII, VIII and V, respectively) and progestin membrane receptor component (PGMRC subtypes 1 and 2) (Mourot *et al.*, 2006; Cahill, 2007).

The nuclear progesterone receptor, p23, is a ubiquitous and highly conserved protein from yeast to humans. It was first discovered as part of the complex of Hsp90 with the progesterone receptor (Johnson *et al.*, 1994). Recently, p23 has been claimed to possess a prostaglandin synthase activity (Tanioka *et al.*, 2000), and the core-folding motif of p23 has been shown in a number of proteins that lack any known relationship to chaperoning (Garcia-Ranea *et al.*, 2002). Thus, the range of possible activities for this simple protein is surprisingly large. p23 (and, to a lesser extent, Hsp90) may be localized to the chromatin of hormone-responsive genes and there function, in a very dynamic way, to facilitate the disassembly of transcriptional regulatory complexes. This localization of p23 may enhance the mobility of functional receptors, allowing the cell to respond quickly to changes in transcriptional needs. This chaperone function may apply to other signal transduction systems where a rapid response to changes in external stimuli required (Morimoto, 2002).

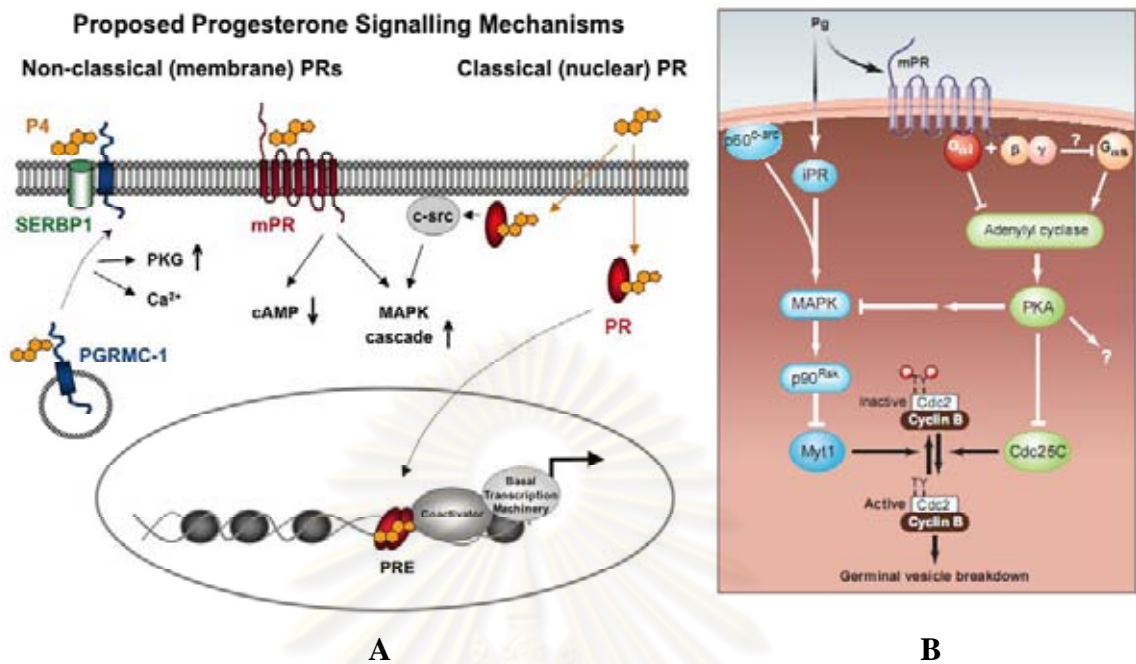


Figure 1.25 A; Schematic overview of proposed mechanisms of non-genomic P4 actions mediated by the classical (or nuclear) PR or through the non-classical putative P4 receptors PGRMC1 (possibly complex with SERBP1) and mPRs. PRE denotes progesterone response element in the promoter region of target genes (Fernandes *et al.*, 2008). B; A pair of progesterone receptors. Progesterone (Pg) binds to both intracellular iPR and plasma membrane-bound mPR. (Left) After binding to Pg, iPR is recruited to the membrane-associated protein tyrosine kinase $p60^{c-src}$, which induces activation of the MAPK signaling pathway. This results in activation of $p90^{Rsk}$ and the subsequent phosphorylation and inactivation of Myt1, which favors formation of the activated cell cycle complex cyclin B-Cdc2. Activation of cyclin B-Cdc2 causes breakdown of the germinal vesicle and the initiation of oocyte maturation. (Right) In contrast, binding of Pg to mPR leads to inhibition of adenylyl cyclase through activation of G_{oi} or inhibition of G_{os} . This leads to a decrease in the cAMP-dependent kinase PKA, which relieves inhibition of Cdc25C (the phosphatase that dephosphorylates and activates cyclin B-Cdc2) and also indirectly promotes the activation of MAPK signaling. PKA also regulates the initiation of oocyte maturation through other effects that are independent of PKA activity (Maller, 2003).

P4 and 17α -hydroxyprogesterone administration induced ovarian maturation and spawning in *Metapenaeus ensis* (Yano, 1985 and 1987). In *P. monodon*, the titers of conjugated pregnenolone and unconjugated and conjugated dehydroepiandrosterone (DHEA) were found to be maximal at stages II (early vitellogenesis) and III (late vitellogenesis) of ovarian development. Unconjugated progesterone was found in ovary at the late stages (III and IV) of maturation whereas conjugated testosterone was only detected in the mature (IV) ovaries (Fairs *et al.*, 1990).

1.9.2 Cell division cycle

In eukaryotic cells, the initiation of DNA replication and entry into mitosis requires members of the cyclin-dependent kinase (Cdk) family. Cdk1 is necessary for mitotic onset and shares an overlapping role with Cdk2 in controlling S phase initiation (Murray, 2004). DNA structure check points provide a mechanism to block cell cycle progression if DNA is damaged or not fully replicated and they are necessary for the maintenance of genome integrity. In eukaryotic cells, the three major points at which this occurs are the G1-S, the intra-S and the G2-M check points. Cell cycle arrest is imposed by activation of two down stream kinases, Chk1 and Chk2. Chk1 is activated by DNA damage during interphase, whereas Chk2 is activated in response to stalled replication forks during S phase. However, when Chk2 is absent, collapsed replication forks give rise to single stranded DNA, which results in inactivation of Chk1 (Karlsson-Rosenthal and Jonathan, 2006).

Cdc25 is a specialized phosphatase that dephosphorylates cyclin B-cdk1 complex and so controls the entry into mitosis. In mammalian cells, Cdc25 activates both Cdk1 and Cdk2 by dephosphorylating Tyr15 and Thr14. Mammalian cells have three Cdc25 isoforms: Cdc25A, Cdc25B (splice variants 1, 2 and 3) and Cdc25C (Figure 1.26). Cdc25A controls progression through S phase and entry into mitosis, whereas Cdc25B and Cdc25C primarily control entry into meiosis (Donzelli and Draetta, 2003). Cdc25A dephosphorylates and activates Cyclin E-Cdk2, Cyclin A-Cdk2 and CyclinB-Cdk1, whereas Cdc25B and Cdc25C primarily target CyclinB-Cdk1. Surprisingly, *Cdc25B^{-/-} Cdc25C^{-/-}* mice develop normally, suggesting that Cdc25A can catalyze all somatic cell cycle transitions. However, Cdc25B is essential

for meiotic resumption in female mice, indicating that substitution between various Cdc25 isoforms cannot occur during oocyte meiotic divisions (Donzelli and Draetta, 2003).

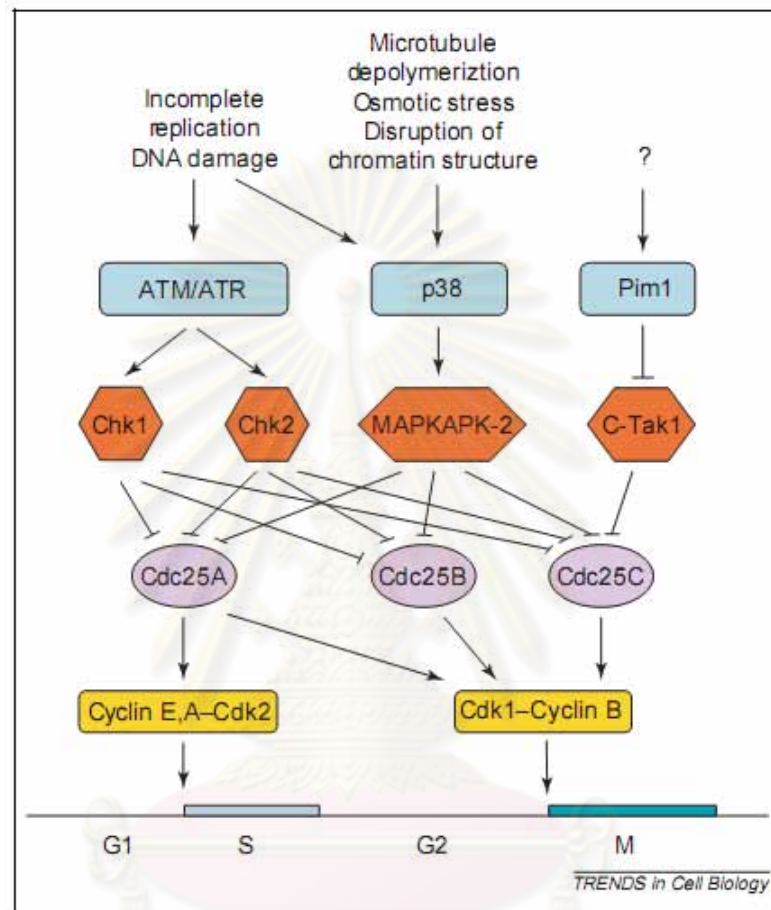


Figure 1.26 Checkpoint pathways controlling Cdc25 isoforms in mammalian cells. Different checkpoint pathways converge on the inactivation of Cdc25 phosphatases, leading to failure to activate Cdk-cyclin complexes and therefore cell cycle arrest. Genotoxic stress induces the ATM/ATR checkpoint pathways, causing phosphorylation and inactivation of Cdc25 by the Chk1/Chk2 kinases. The p38 MAPK pathway has recently been suggested to inactivate Cdc25 activity in response to various environmental insults, including osmotic stress, heat stress, UV irradiation and microtubule depolymerization. C-TAK1 is keeping Cdc25C inactive during the unperturbed cell cycle but might also function in a pathway involving the Pim1 oncoprotein. Although Cdc25A, Cdc25B and Cdc25C all contain phosphorylation sites for Chk1, Chk2 and MAPKAPK-2, not all phosphorylation events have been demonstrated (Karlsson-Rosenthal and Jonathan, 2006).

Cdc42, a member of the small GTPases superfamily (Verlhac and Dumont, 2008), acts in the control of the oocyte maturation pathway. The GDP-bound Cdc42 greatly facilitates progesterone-induced maturation, whereas its GTP-bound form completely blocks meiotic maturation of oocytes (Cau *et al.*, 2000). In mouse, Cdc42 also involved in MI spindle assembly and migration completion of meiosis I (Na and Zernicka-Goetz, 2006) but it was involved in control of spindle organization and positioning in *Xenopus* Cdc42 is also required for the cortical polarization that occurs prior to polar body extrusion (Ma *et al.*, 2006).

Anaphase-promoting complex (APC) is also important for oocyte maturation. The APC activity is regulated by two related WD repeat-containing proteins, Cdc20 and Cdh1, which function as substrate-specific activators. Cdc20 promotes degradation of early substrates such as an anaphase inhibitor (Pds1), mitotic arrest-deficient (MAD) family genes, whereas Cdh1 promotes degradation of late substrates such as cyclin B. The precise mechanism by which Cdc20 activates the APC remains unclear. Cdc20 does not appear to affect the phosphorylation state of the APC but may induce a structural change upon binding that promotes substrate-specific activation of the APC (Zhang and Lees, 2001).

1.9.3 Carbonyl reductase and small androgen receptor-interacting protein

The physiological role of carbonyl reductase was thought to be in the NADPH-dependent reduction in a variety of endogenous and foreign carbonyl compounds. However, evidence for its involvement in steroid metabolism is increasing. It has been suggested that two classes of carbonyl reductase exist, one with high activity and steroid specificity and the other with low activity and broad specificity. Several lines of evidence including localization in ovaries, enzymatic characteristics, and increase in transcripts with oocyte maturation, suggested that ayu carbonyl reductase also functions as 20 β -HSD in the production of maturation inducing hormone (MIH) (Tanaka *et al.*, 2002). The existing knowledge confirms that ayu ovary carbonyl reductase is the carbonyl reductase-like 20 β -HSD.

The small androgen receptor-interacting protein (SARIP) which was first identified in rat interacts with the androgen receptor and contained RWD domain.

This domain was identified in WD40 (Trp-Asp dipeptide) repeat proteins and Ring finger domain proteins. WD-repeat proteins are a large family found in all eukaryotes and are implicated in a variety of functions ranging from signal transduction and transcription regulation to cell cycle control and apoptosis. The underlying common function of all WD-repeat proteins is coordinating multi-protein complex assemblies, where the repeating units serve as a rigid scaffold for protein interactions (Rouleau *et al.*, 1999). In mice, Rwd1 (or SARIP) is a thymus involution related protein that may indirectly affect AR signaling pathway (Kang *et al.*, 2008).



ศูนย์วิทยทรัพยากร
จุฬาลงกรณ์มหาวิทยาลัย

CHAPTER II

MATERIALS AND METHODS

2.1 Experimental animals

Wild female *P. monodon* broodstock purchased from Satun (Andaman Sea) was used for construction of typical and normalized ovaries cDNA library and RACE-PCR. In addition, broodstock-sized male and female *P. monodon* were purchased from Angsila, Chonburi (Gulf of Thailand, east). Juvenile *P. monodon* males and females (approximately 20 g body weight, 4-month-old) were purchased from local farms in Chachengsao, eastern Thailand. These samples were used for construction of suppression subtractive hybridization (SSH) cDNA libraries and RNA arbitrary primed (RAP)-PCR, RT-PCR or semiquantitative RT-PCR.

For quantitative RT-PCR analysis, female broodstock were wild-caught from the Andaman Sea and acclimated under the farm conditions for 2-3 days. Ovaries were dissected out from normal broodstock shrimps and weighed ($N = 41$). In addition, ovaries of post-spawned normal broodstock shrimps originated from the Andaman Sea were also collected at after spawning ($N = 6$). For the eyestalk ablation group, shrimp were acclimated for 7 days prior to unilateral eyestalk ablation. Ovaries of ablated shrimp were collected at 2-7 days after ablation ($N = 32$). The gonadosomatic index (GSI, ovarian weight/body weight \times 100) of each shrimp was calculated. Ovarian maturation stages of broodstock *P. monodon* were grouped as describe by Yamano *et al.* (2004) and Marsden *et al.* (2007). The gonadosomatic index (GSI, ovarian weight/body weight \times 100) of each shrimp was calculated. Ovarian developmental stages were divided to previtellogenic (stage I, GSI $<$ 1.5%), vitellogenic (stage II, GSI $>$ 2-4%), early cortical rod (stage III, GSI $>$ 4-6%) and mature (IV, GSI $>$ 6%) ovaries, respectively.

To confirm developmental stages of *P. monodon* ovaries, ovaries of several shrimp from each group according to the GSI values were dissected out and divided to 2 halves; one for isolation of total RNA which is subsequently used for real-time RT-PCR analysis and the other ($N = 23$ and 22 for normal and eyestalk ablation groups,

respectively) for *in situ* hybridization/immunochemistry. The latter portion was excised to small pieces and fixed with the 4% paraformaldehyde prepared in 0.1 M phosphate buffer pH 7.2 (*in situ* hybridization) or Davidson's solution for 16-24 hours (immunochemistry), washed 3 times with 0.1 M phosphate buffer pH 7.2 and 3 times with 50% ethanol for ovaries fixed in 4% paraformaldehyde and 3 times with 50% ethanol for ovaries fixed in Davidson's solution. Tissues were subsequently stored in 70% ethanol before subjected to the standard paraffin section. Ovarian developmental stages were classified by conventional histology slightly modified from Qiu *et al.* (2005).

2.2 Nucleic acid extraction

2.2.1 DNA extraction

Genomic DNA was extracted from a piece of pleopod of each *P. monodon* individual using a phenol-chloroform-proteinase K method (Klinbunga *et al.*, 1999). A piece of pleopod tissue was dissected out from a frozen pleopod and placed in a prechilled microcentrifuge tube containing 500 μ l of the extraction buffer (100 mM Tris-HCl, 100 mM EDTA, 250 mM NaCl; pH 8.0) and briefly homogenized with a micropestle. SDS (10%) and RNase A (10 mg/ml) solutions were added to a final concentration of 1.0 % (w/v) and 100 μ g/ml, respectively. The resulting mixture was then incubated at 37°C for 1 hour. At the end of the incubation period, a proteinase K solution (10 mg/ml) was added to the final concentration of 100 μ g/ml and further incubated at 55°C for 3-4 hours. An equal volume of buffer-equilibrated phenol was added and gently mixed for 15 minutes. The solution was centrifuged at 10000 rpm for 10 minutes at room temperature. The upper aqueous phase was transferred to a newly sterile microcentrifuge tube. This extraction process was then repeated once with phenol:chloroform:isoamylalcohol (25:24:1) and twice with chloroform:isoamylalcohol (24:1). The aqueous phase was transferred into a sterile microcentrifuge. One-tenth volume of 3 M sodium acetate, pH 5.2 was added. DNA was precipitated by an addition of two volume of prechilled absolute ethanol and mixed thoroughly. The mixture was incubated at -20°C for 2 hours. The precipitated DNA was recovered by centrifugation at 12000 rpm for 10 minutes at room temperature and washed twice with 1 ml of 70% ethanol (5 minutes and brief washes, respectively). After centrifugation, the supernatant was removed. The DNA pellet was

air-dried and resuspended in 100 μ l of TE buffer (10 mM Tris-HCl, pH 8.0 and 0.1 mM EDTA). The DNA solution was incubated at 37°C for 1 - 2 hours and kept at 4°C until further needed.

2.2.2 RNA extraction

Total RNA was extracted from ovaries (or other tissues) of each shrimp using TRI REAGENT[®] (Molecular Research Center). A piece of tissues was immediately placed in mortar containing liquid nitrogen and ground to the fine powder. The tissue powder was transferred to a microcentrifuge tube containing 500 μ l of TRI-REAGENT[®] (Molecular Research Center) (1 ml/50-100 mg tissue) and homogenized. Additional 500 μ l of TRI REAGENT[®] were added. The homogenate were left for 5 minutes, before adding 0.2 ml of chloroform. The homogenate was vortexed for 15 seconds and left at room temperature for 2-15 minutes before centrifuged at 12000g for 15 minutes at 4°C. The mixture was separated into the lower red, phenol-chloroform phase, the interphase, and the colorless upper aqueous phase. The aqueous phase (inclusively containing RNA) was transferred to a new 1.5 ml microcentrifuge tube. RNA was precipitated by an addition of 0.5 ml of isopropanol and mixed thoroughly. The mixture were left at room temperature for 10-15 minutes and centrifuged at 12000g for 10 minutes at 4-25°C. The supernatant was removed. The RNA pellet was washed with 1 ml of 75% ethanol and centrifuged at 12000g for 5 minutes at 4°C. The ethanol was removed. The RNA pellet was air-dried for 5-10 minutes. RNA was dissolved in DEPC-treated H₂O for immediately used. Alternatively, the RNA pellet was kept under absolute ethanol in a -80 °C freezer for long storage.

Total RNA was also extracted from other tissues including testes, eyestalks, gills, heart, hemocytes, hepatopancreases, lymphoid organs, intestine, stomach, pleopods and thoracic ganglion of *P. monodon* using the same extraction procedure.

2.2.3 Purification of mRNA

Total RNA was extracted from ovaries of wild broodstock-sized of female *P. monodon* using TRI-REAGENT[®]. Messenger (m) RNA was further purified using a QuickPrep *micro* mRNA Purification Kit (GE Healthcare).

Four hundred microliters of the extraction buffer were added to a microcentrifuge tube containing 25 µl of total RNA and mixed by pipetting. Two volumes (0.8 ml) of the elution buffer were added and mixed thoroughly. The mixture was centrifuged at 16000g for 1 minute. Concurrently, the tube containing 1 ml of oligo(dT)-cellulose for each purification was centrifuged at the same speed for 1 minute. The supernatant was removed. The homogenate was transferred into the microcentrifuge tube containing the oligo(dT)-cellulose pellet. The tube was gently inverted to resuspend the oligo(dT)-cellulose for 3 minutes and centrifuged at 16000g for 10 seconds at room temperature. The supernatant was carefully removed. The high salt buffer (1 ml) was added to a microcentrifuge tube and spun for 10 seconds at 16000g. The supernatant was carefully removed. The wash was repeated four more times, as described above. The low salt buffer (1 ml) was added to the oligo(dT)-cellulose pellet. The tube was inverted and spun at 16000g for 10 seconds. This wash was repeated once. The pellet from the final wash was resuspended in 0.3 ml of the low salt buffer. The slurry was transferred to a MicroSpin column and spun for 5 seconds. The flow-through solution was discarded. The low salt buffer (0.5 ml) was added and further spun for 5 seconds. This step was repeated twice. The column was then placed into a sterile 1.5 ml microcentrifuge tube and briefly centrifuged. The mRNA was eluted out by an addition of 0.2 ml of the pre-warmed elution buffer (55°C) to the top of column and centrifuged at 16000g for 5 seconds. Additional 0.2 ml of the pre-warmed elution buffer was added to the top of column to elute residual mRNA and centrifuged as described above.

2.3 Measuring concentrations of extracted DNA and RNA using spectrophotometry and electrophoresis

The concentration of extracted DNA or RNA samples is estimated by measuring the optical density at 260 nanometre (OD_{260}). An OD_{260} of 1.0 corresponds to a concentration of 50 µg/ml of double stranded DNA, 40 µg/ml of single stranded RNA and 33 µg/ml of single stranded (ss) DNA (Sambrook and Russel, 2001). Therefore, the concentration of DNA/RNA samples were estimated in µg/ml by using the following equation,

$$[\text{DNA/RNA}] = OD_{260} \times \text{dilution factor} \times 50 \text{ (40 or 33 for RNA or ssDNA, respectively)}$$

The purity of DNA samples can be evaluated from a ratio of OD_{260} / OD_{280} . The ratios of appropriately purified DNA and RNA were approximately 1.8 and 2.0, respectively (Sambrook and Russel, 2001).

2.4 Construction of typical, normalized and subtractive ovaries cDNA libraries of *P. monodon*

2.4.1 The typical ovary cDNA library of *P. monodon*

The typical ovary cDNA library of *P. monodon* was constructed from vitellogenic ovaries of a broodstock with GSI = 5.689% using a ZAP-cDNA Synthesis and Cloning Kit (BD Biosciences Clontech).

2.4.1.1 First and second strand cDNA synthesis

Five micrograms of mRNA was combined with 5 μ l of 10X first-strand buffer, 3 μ l of first-strand methyl nucleotide mixture (10 mM dATP, dGTP, and dTTP supplemented with 5 mM 5-methyl dCTP), 2 μ l of linker-primer (1.4 μ g/ μ l), and 1 μ l of (40 units/ μ l) RNase Block Ribonuclease Inhibitor. DEPC-treated H₂O was added to a final volume of 50 μ l. The reaction was gently vortexed and briefly centrifuged. The reaction was incubated at room temperature for 10 minutes and 1.5 μ l of (50 units/ μ l) StrataScript RT was added to the first strand synthesis reaction. The reaction was gently vortexed and briefly centrifuged. Five microliters of the first-strand synthesis reaction was transferred to a separate tube and served as the first-strand synthesis control reaction. The reaction was incubated at 42°C for 1 hour. The tubes were placed on ice to terminate the first strand cDNA synthesis.

The components of second-strand synthesis reaction including 20 μ l of 10X second-strand buffer, 6 μ l of second-strand dNTP mixture (10 mM dATP, dGTP, and dTTP plus 26 mM dCTP), 116 μ l of Sterile distilled H₂O, 2 μ l of (1.5 units/ μ l) RNase H, and 11 μ l of DNA polymerase (9.0 units/ μ l) were added to the first-strand synthesis reaction on ice. The reaction was gently vortexed, briefly centrifuged, and incubated at 16°C for 2.5 hours. After second-strand synthesis reaction, immediately placed the reaction tube on ice.

2.4.1.2 Blunting the cDNA termini

Twenty-three microliters of blunting dNTP mix and 2 μ l of (2.5 units/ μ l) cloned *Pfu* DNA polymerase were added to the second-strand synthesis reaction. The reaction was gently vortexed, briefly centrifuged, and incubated at 72°C for 30 minutes.

An equal volume (200 μ l) of phenol-chloroform [1:1 (v/v)] was added. The mixture was vortexed and centrifuged at 14000g for 2 minutes at room temperature. The upper aqueous layer was transferred to a new tube. An equal volume of chloroform:isoamyl alcohol (24:1) was added and vortexed. The mixture was centrifuged at 14000g for 2 minutes at room temperature and the upper aqueous layer was transferred to a new tube. The cDNA was precipitated by adding 20 μ l of 3M sodium acetate and 400 μ l of absolute ethanol. The reaction was vortexed and kept overnight at -20°C.

The synthesized cDNA was recovered by centrifugation at 14000g at 4°C for 60 minutes. The cDNA pellet was gently washed by adding 500 μ l of 75% (v/v) ethanol to the side of the tube away from the precipitate and centrifuged at 14000g for 2 minutes at room temperature. The pellet was air-dried, resuspended in 9 μ l of *EcoR* I adapters, and incubated at 4°C for at least 30 minutes.

2.4.1.3 Ligation of *EcoR* I adapters

One microliter of 10X ligase buffer, 1 μ l of 10 mM rATP, and 1 μ l of T4 DNA ligase (4 units/ μ l) were added to the tube containing the blunted cDNA and the *EcoR* I adapters. The reaction was centrifuged and incubated overnight at 8°C or 16°C for 2 days. After ligation reaction, the ligase activity was heat-inactivated at 70°C for 30 minutes. The reaction was spun down for 30 seconds and cooled at room temperature for 5 minutes.

2.4.1.4 Phosphorylation of *EcoR* I ends

The components including 1 μ l of 10X ligase buffer, 2 μ l of 10 mM rATP, 5 μ l of sterile H₂O, and 2 μ l of T4 polynucleotide kinase (5 units/ μ l) were added to the

reaction and incubated at 37°C for 30 minutes. The kinase activity was heat-inactivated at 70°C for 30 minutes. The reaction was spun down for 30 seconds and cooled at room temperature for 5 minutes.

2.4.1.5 *Xho* I digestion

Twenty-eight microliters of *Xho* I buffer supplement and 3 µl of *Xho* I (40 units/µl) were added. The reaction was incubated at 37°C for 1.5 hours. Digested cDNA was precipitated by adding 5 µl of 10X STE buffer (1M NaCl, 200 mM Tris-HCl, pH 7.5, and 100 mM EDTA) and 125 µl of absolute ethanol and incubated overnight at -20°C. Following precipitation, the reaction was centrifuged at 14000g for 60 minutes at 4°C. The pellet was dried, resuspended in 14 µl of 1X STE buffer and 3.5 µl of the column loading dye (50% (v/v) glycerol, 10% (v/v) 10X STE buffer, and 40% (w/v) saturated bromophenol blue). The resuspended sample was ready to be size-fractionated through a drip column containing sepharose CL-2B gel filtration medium.

2.4.1.6 Size fractionation

Assembling and loading the drip column

A sterile 1-ml pipette was used as column. Small piece (about 8 millimeters) of the connecting tubing was used to connect the 1 ml pipette to the 10 ml syringe (Figure 2.1). Prior to loading the drip column, sepharose CL-2B gel filtration medium was gently mixed until the resin was uniformly suspended and 2 ml of 1X STE buffer (100 mM NaCl, 20 mM Tris-HCl pH 7.5, and 10 mM EDTA) and added to a column until the surface of the packed bed was approximately 0.25 inch below the “lip of the pipette” (the point where the pipette and the syringe were joined). The drip column was washed with 10 ml of 1X STE buffer. When about 50 µl of the 1X STE buffer remained above the surface of the resin, cDNA sample was immediately loaded using an automatic pipette.

Collecting the sample fractions

Sephacrose CL-2B gel filtration medium separated molecules on the basis of size. Three drops per fraction were collected to a fresh microcentrifuge tube. The

fractions began to collect when the leading edge of the dye reached the .4 ml graduation of the pipette (Figure 2.1), and stopped when trailing edge of the dye reached the .3 ml graduation. Before processing the fractions and recovering the size-fractionated cDNA, 8 μ l of each collected fraction was electrophoresed in a 5% nondenaturing polyacrylamide gel to determine the appropriate fractions used for ligation.

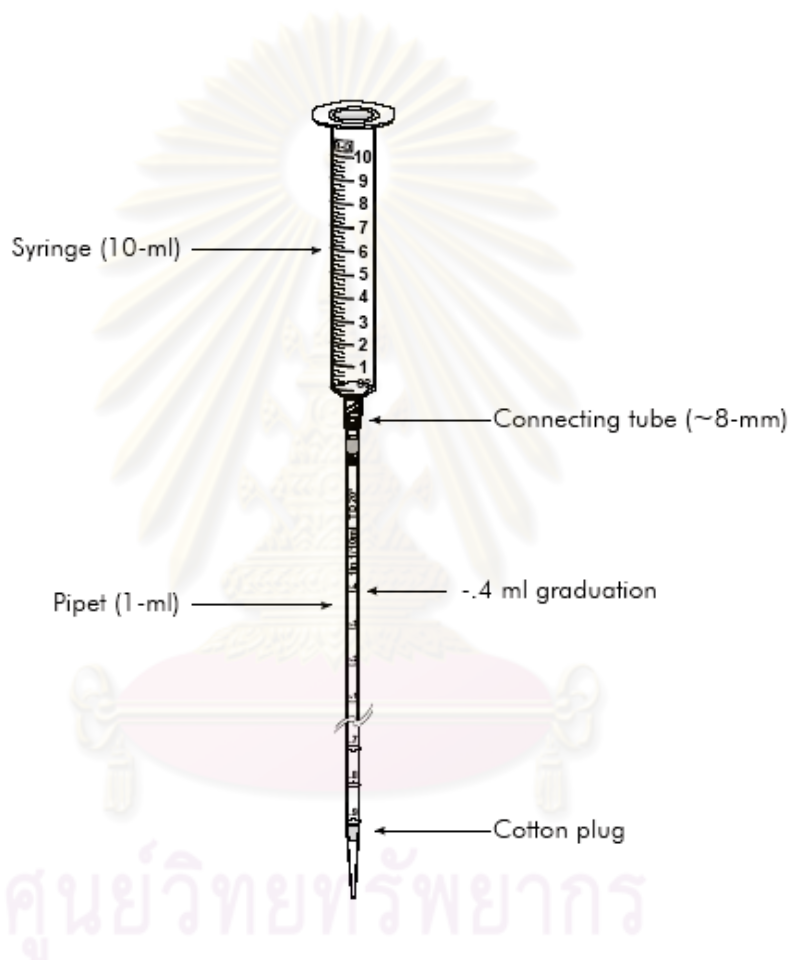


Figure 2.1 Assembly of the drip column for size-fractionation of synthesized cDNA

2.4.1.7 Processing the cDNA fractions

The collected fractions that did not contain linkers (>500 bp fragments) were selected and extracted with an equal volume of phenol-chloroform [1:1 (v/v)], vortexed, and spun in a microcentrifuge at the maximum speed for 2 minutes at room

temperature. The upper aqueous layer was transferred to a fresh microcentrifuge tube. An equal volume of chloroform:isomyl alcohol (24:1) was added, vortexed, and spun in a microcentrifuge at the maximum speed for 2 minutes at room temperature. Two volume of absolute ethanol was added to extracted sample and cDNA was precipitated overnight at -20°C. The sample was centrifuged at the maximum speed for 60 minutes at 4°C. The pellet was carefully washed with 200 µl of 80% (v/v) ethanol. The sample was centrifuged at the maximum speed for 2 minutes at room temperature. The pellet was air-dried and resuspended in 3.5-5 µl of sterile water.

2.4.1.8 Ligation of the cDNA insert

Size-selected cDNAs (>500 bp) were ligated into dephosphorylated *Eco*RI/*Xho*I-digested UNI-ZAP XR. The ligation reaction contained 100 ng of resuspended cDNA, 0.5 µl of 10X ligase buffer, 0.5 µl of 10 mM rATP (pH 7.5), 1.0 µl of the predigested Uni-ZAP XR vector (1 µg), sterile water for a final volume of 4.5 µl, and 0.5 µl of T4 DNA ligase (4 units/µl). The ligated reaction was incubated overnight at 12°C or for up to 2 days at 4 °C.

2.4.1.9 Packaging and titering

Packaging

The packaging extract was removed from a -80°C freezer and placed on the ice. Three microliters (containing 0.1-1.0 µg) of the ligation product was added to the packaging extract, gently stirred the tube with a pipette, and briefly centrifuged. The tube was incubated at room temperature for 2 hours and 500 µl of SM buffer and 20 µl of chloroform were added to the tube and mixed gently. The tube was centrifuged briefly and the supernatant was transferred to a newly sterile tube. The supernatant containing the phage was ready for titering. The supernatant may be stored at 4°C for up to 1 month.

Titering of the Packaging

E. coli XL1-Blue MRF' cells were cultured in LB broth with supplements (0.2% (w/v) maltose and 10 mM MgSO₄) with shaking at 37 °C for 4-6 hours (OD₆₀₀ < 1.0), or overnight at 30 °C. The bacterial cells were centrifuged at 1000g for 10 minutes, and the cell pellet was resuspended in 25 ml of sterile 10 mM MgSO₄. After

OD determination, the culture was diluted to an OD₆₀₀ of 0.5 with sterile 10 mM MgSO₄.

To determine the titer of the primary library, 1 µl of the final packaged reaction and 200 µl of *E. coli* XL1-Blue MRF' cells at an OD₆₀₀ of 0.5. In addition, 1 µl of a 1:10 dilution of the final packaged reaction was also combined with 200 µl of *E. coli* XL1-Blue MRF' cells. The phage/bacteria mixture was incubated at 37°C for 15 minutes to allow the phage to attach to the cells. The component was added into 3 ml of the melted NZY top agar that was pre-cooled to approximately 48°C, and plated immediately onto dry, the prewarmed NZY agar plate. The plate was incubated at 37°C about 6-8 hours. The plaques were counted and the titer of the library was estimated and expressed in plaque-forming units per milliliter (pfu/ml).

2.4.1.10 Amplifying the cDNA library

The *E. coli* XL1-Blue MRF' cells were overnight cultured in LB broth with supplements at 30°C with shaking. The cells were gently centrifuged and resuspended in 25 ml of 10 mM MgSO₄. The cell suspensions were measured at 600 mM and then diluted to an OD₆₀₀ of 0.5 using 10 mM MgSO₄.

Aliquots of the packaged mixture containing about 5×10^4 pfu of bacteriophage (< 300 µl of phage) with 600 µl of *E. coli* XL1-Blue MRF' cells at OD₆₀₀ of 0.5 were combined in polypropylene tubes. To amplify 1×10^6 plaques, a total of 20 aliquots were combined (each aliquot contained 5×10^4 plaques/150-mm plate).

Each aliquot tube was incubated at 37°C for 15 minutes and 6.5 ml of the NZY top agar, melted and cooled to 48°C, was mixed with each aliquot of infected bacteria and evenly spread onto a 150-mm NZY agar plate. Plates were incubated at 37°C for 6-8 hours. After that plates were overlaid with 5-10 ml of SM buffer and stored overnight at 4°C.

The bacteriophage suspension from each plate was recovered and pooled into a sterile polypropylene container. Each plate was rinsed with additional 2 ml of SM buffer and pooled. Chloroform was added to a 5% (v/v) final concentration, mixed well, and incubated at room temperature for 15 minutes. The cell debris was removed

by centrifugation for 10 minutes at 500g. Chloroform was added to a final concentration of 0.3% (v/v). Aliquots of the amplified library were stored in 7% (v/v) DMSO at -80°C.

2.4.1.11 *In vivo* excision to convert the lambda library to the phagemid library

The lambda library was converted into the pBluescript library by *in vivo* excision. *E. coli* XL1-Blue MRF' and SOLR cells were grown separately in 50-ml LB broth with supplements (0.2% (w/v) maltose and 10 mM MgSO₄) overnight at 30°C. *E. coli* XL1-Blue MRF' and SOLR cells were gently spun down (1000g) and resuspended each of the cell pellets in 25 ml of 10 mM MgSO₄. Measure the OD₆₀₀ of the cell suspensions and adjust the concentration of the cells to an OD₆₀₀ of 1.0 (8 x 10⁸ cells/ml) using 10 mM MgSO₄.

Combine a portion of the amplified lambda bacteriophage library with XL1-Blue MRF' cells at a 1:10 lambda phage-to-cell ratio (10⁷ pfu of the lambda phage: 10⁸ cells of *E. coli* XL1-Blue MRF') using a 50-ml conical tube. Add ExAssist helper phage at a 10:1 helper phage-to-cells ratio (10⁹ pfu of ExAssist helper phage: 10⁸ cells of *E. coli* XL1-Blue MRF') to ensure that every cell is co-infected with lambda phage and helper phage. The mixture was then incubated at 37°C for 15 minutes to allow the phage to attach to the cells. Twenty microliters of LB broth with supplements were added and the conical tube was incubated for 2.5 hours at 37°C with shaking. The conical tube was heated at 68°C for 20 minutes to lyse the lambda phage particles and the cells, centrifuged at 1000g for 10 minutes, and the supernatant was transferred into a sterile conical tube.

One microliter of the supernatant containing excised phagemids was combined with 200 µl of *E. coli* SOLR cells in a 1.5 ml microcentrifuge tube, and incubated at 37°C for 15 minutes. The cell mixtures were plated onto LB ampicillin (50 µg/ml) agar plates and incubated overnight at 37°C. Recombinant clones were selected by a lacZ' system following standard protocols (Sambrook and Russell, 2001).

2.4.2 Construction of the normalized ovary cDNA library of *P. monodon*

Normalized cDNA library was constructed from a typical cDNA library established previously. The normalization method is a reassociation kinetics-based approach involving hybridization of an excess of cDNA inserts (e.g. 20 folds) excised from a plasmid DNA preparation of the standard EST library with the library itself in the form of single-stranded circles (Bonaldo, Lennon and Soares, 1996; Carninci *et al.*, 2000). The cDNA inserts were labeled with biotin. The remaining single-stranded plasmids of rare expressed genes were removed from the hybrid by using streptavidin beads and were converted to double-strands using Pfu polymerase (Promega, U.S.A.). The double-stranded cDNA inserts were then cloned into the bacterial host *Escherichia coli* stain XL-1blue to propagate the normalized library.

2.4.2.1 Preparing of single-stranded phagemid

The supernatant containing excised phagemid was used to prepare single-stranded phagemid. Single-stranded phagemid was precipitated and capsid proteins were digested.

One microliter of the supernatant was removed to a fresh tube and 150 μ l of a solution containing 20% PEG8000 and 2.5 M NaCl was added. The phage particles were allowed to precipitate overnight at 4°C. The tube containing phage particles was centrifuged at 12000 rpm for 20 minutes in a microcentrifuge tube. After the supernatant as removed, the PEG pellet was centrifuged for a few seconds to collect the residual liquid. The pellet was resuspended in 400 μ l of 0.01 M Tris-HCl (pH 7.8), 0.5% SDS, 0.005 M EDTA and 50 μ g/ml proteinase K by vortexing vigorously. The mixture was incubated at 56°C for 1-2 hours. The solution was extracted with an equal volume of phenol-chloroform and centrifuged at 7000 rpm for 5-10 minutes to separate phases. The aqueous phase was transferred to a fresh tube. To precipitate the single-stranded phagemid DNA 1/10 volume of 3 M of KOAc and 2 volumes of ice cold 100% EtOH and 1/40 volume of glycogen (10 mg/ml) was sequentially added, thoroughly mixed and incubated overnight at -20°C. The solution was centrifuged at 12000 rpm for 10 minutes and the supernatant was discarded. The pellet was washed with 70% EtOH and centrifuged at 12000 rpm for 5 minutes. The supernatant was removed and air-dried. The pellet was dissolved in 25 μ l of TE buffer. The

concentration was spectrophotometrically estimated. Two microliters of single-stranded phagemid were analyzed by agarose gel electrophoresis.

2.4.2.2 Preparing of driver

One microliter of the supernatant containing excised phagemids was combined with 200 μ l of *E. coli* SOLR cells in a 1.5 ml microcentrifuge tube, and incubated at 37°C for 15 minutes. The cell mixtures were plated onto LB ampicillin (50 μ g/ml) agar plates and further incubated overnight at 37°C. The colonies were rinsed with LB broth and then cultured 37°C for 2 hours. Plasmid DNA was isolated using a HiYield™ Plasmid Mini Kit (RBC; Real Biotech Corporation). The concentration of extracted plasmid DNA was spectrophotometrically measured.

Approximately 60 μ g of plasmid DNA was digested with *Eco* RI and *Xho* I (Promega). Three digestion reactions were carried out separately in a 100 μ l containing 1x restriction buffer (buffer D; 6 mM Tris-HCl; pH 7.9, 6 mM MgCl₂, 150 mM NaCl and 1 mM DTT), 0.1 mg/ml of BSA, 20 μ g of plasmid DNA, 40 unit of *Eco* RI and *Xho* I. The reaction mixture was incubated overnight at 37°C. The digested plasmid DNA was electrophoresed in an agarose gel and the digested plasmid DNA was excised from the gel. Plasmid DNA was purified using a HiYield™ Gel/PCR DNA Extraction Kit according to the manufacturer's instructions (RBC; Real Biotech Corporation). The purified plasmid DNA was precipitated by adding 1/10 volume of 3 M of KOAc, 2 volumes of ice cold 100% EtOH and 1/40 volume of glycogen (10 mg/ml), mixed and incubated overnight at -20°C. The mixture was centrifuged at 12000 rpm for 10 minutes at room temperature. The supernatant was removed. The DNA pellet was air-dried and dissolved in 25 μ l of TE buffer. The concentration was estimated by spectrophotometry and the concentration of driver was adjusted to 125 ng/ μ l.

Driver labeling

Five micrograms (40 μ l) of driver were labeled with biotin using a *Label IT*® Nucleic Acid Labeling Kit, Biotin according to the manufacturer's instructions (Mirus, Madison).

Labeling reaction

Labeling reaction was prepared as described in Table 2.1. The reaction was incubated at 37°C for 2 hours. A quick spin was performed after 30 minutes of incubation to minimize the effect of evaporation and to maintain the appropriate concentration of the reaction components.

Purification of the labeled driver using ethanol precipitation

The labeled driver was purified by adding 1/8 volume of 4 M NaCl, 2 volumes of ice cold 100% ethanol, thoroughly mixed and incubated at -20°C overnight. The mixture was centrifuged at 12000 rpm for 10 minutes. The supernatant was removed. The pellet was washed once with 500 µl nuclease-free 70% EtOH. After an additional centrifugation at 12000 rpm for 10 minutes at 4°C, the supernatant was removed and the pellet was air-dried. The labeled driver was resuspended in 50 µl 1X Labeling Buffer A and kept at -20°C until used.

Table 2.1 Compositions of the single-strand DNA driver labeling.

Labeling Reaction	
Molecular biologygrade H ₂ O	Up to 50 µl
10X labeling Buffer A	5.0 µl
Single-strand DNA driver	5.0 µg
<i>Label IT</i> [®] Reagent	5.0 µl
Total volume	50.0 µl

2.4.2.3 Hybridization between single-stranded phagemid and the labeled driver

Two micrograms of single-stranded phagemid were combined with 150 µl of deionized formamide in a 1.5 ml microcentrifuge tube and incubated at 80°C for 3 minutes. Then, 1 mM Tris-HCl (pH 7.5), 10 mM EDTA, 0.5 M NaCl and 20 µg of denatured oligo-dT₁₅ (heated at 95°C for 5 minutes, chilled on ice) were added and further incubated at 42°C for 1 hour with gently shaking.

For 50 μ l of labeled driver, 1/10 volume of the Denaturation Reagent D1 (*Label IT*[®] Nucleic Acid Labeling Kit, Biotin; Mirus, Madison) was added, mixed thoroughly and incubated for 5 minutes at room temperature. After that, 1/10 volume of the Neutralization Buffer N1 was added, mixed and incubated on ice for at least 5 minutes. The mixture was incubated in 42°C for 3 minutes and then transferred to the single-stranded phagemid mixture. The reaction volume was adjusted to 300 μ l with nuclease-free H₂O and further incubated overnight at 42°C.

2.4.2.4 Discover the remaining single-stranded plasmids of rare expressed genes

The streptavidin MagneSphere[®] Paramagnetic Particles (SA-PMPs) (streptavidin beads MagneSphere[®] Magnetic Separation Products; Promega) were used to remove the remaining single-stranded plasmids of rare expressed genes from the hybrid.

Bead preparing and washing of SA-PMPs

Aliquots of a 0.6 ml of SA-PMPs were resuspended by gently flicking the bottom of the tube until the particles are completely dispersed. The tube was placed in the magnetic stand until the SA-PMPs were collected at the side of the tube (approximately 30 seconds). The supernatant was carefully removed. The captured SA-PMPs were washed three times with 500 μ l of 0.5X SSC. After mixing for each wash, the SA-PMPs were captured using the magnetic stand and the wash solution was removed. The SA-PMPs was then washed twice with 500 μ l of 1 M NaCl and 10 mM EDTA. The washed SA-PMPs was resuspended in 500 μ l of the solution containing 1 M NaCl, 10 mM EDTA and 100 ng of tRNA. After incubation at room temperature for 10-20 minutes, the SA-PMPs were washed three times with 500 μ l of 1 M NaCl and 10 mM EDTA. The washed SA-PMPs were then resuspended in 300 μ l of the solution containing 0.01 M Tris-HCl (pH 7.5), 0.1 M EDTA and 4 M NaCl.

Capture and washing of annealed single-stranded plasmids-driver hybrids

After removing the wash solution, the hybridized reaction was added into the SA-PMPs tube and further incubated at 42°C for 1 hour with gently shaking. The SA-PMPs was captured by placing the tube in the magnetic stand for 3 minutes. The

supernatant was carefully removed by pipetting without contamination of beads (solution I).

The SA-PMPs were washed with 50 μ l of 1 M NaCl and 10 mM EDTA. The SA-PMPs were washed by placing the tube in the magnetic stand for 10 minutes. The supernatant was carefully removed by pipetting without contamination of beads (solution II).

The washed SA-PMPs were resuspended with 200 μ l of 0.5X SSC and further incubate at 65°C for 7 minutes. Capture the SA-PMPs by placing the tube in the magnetic stand for 10 minutes. The supernatant was carefully removed by pipetting without contamination of beads (solution III).

The washed SA-PMPs were resuspended with 200 μ l of 0.1X SSC and further incubate at 65°C for 15 minutes. The SA-PMPs were removed by placing the tube in the magnetic stand for 10 minutes. The supernatant was carefully removed by pipetting without contamination of beads (solution IV).

Precipitation of remaining single-stranded plasmids of rare expressed genes from the hybrid

To precipitate the remaining single-stranded plasmids, 1/10 volume of 3 M NaOAc, 1/40 volume of glycogen and 2 volumes of ice cold 100% EtOH were added and mixed thoroughly. After incubated at -20°C for 1 hour, the solution was centrifuged at 12000 rpm for 10 minutes. The supernatant was removed and the pellet was gently washed once with 500 μ l nuclease-free 70% EtOH. After centrifuged at 12000 rpm for 10 minutes, the supernatant was removed and the pellet was air-dried. The pellet was dissolved in 20 μ l of dH₂O and the concentration was electrophotometrically estimated.

2.4.2.5 Double-stranded cDNA synthesis

The double-stranded cDNA was synthesized from the recovered single-stranded plasmid cDNA using a PCR-based method. PCR was performed in a 20 μ l reaction mixture containing 1X reaction buffer (20 mM Tris-HCl, pH 8.8, 10 mM KCl, 10 mM (NH₄)₂SO₄, 2 mM MgSO₄, 0.01% Triton X-100 and 0.1 mg/ml nuclease-free BSA), 0.36 mM of each dNTP, 4 μ M of an M13 reverse primer (5'-GGA AAC AGC

TAT GAC CAT GA-3'), 3 unit of *Pfu Taq* DNA Polymerase (Promega) and 9 μ l of single-strand plasmid DNA.

PCR was carried out in a thermocycler consisting 1 cycle of denaturation at 94°C for 3 minutes followed by annealing at 50°C for 1 minutes and extension at 72°C for 15 minutes. After the extension step, 1 μ l of 0.5 M EDTA was added. The double-stranded cDNA was precipitated by adding 1/10 volume of 3 M of NaOAc, 2 volumes of ice cold 100% EtOH and 1/40 volume of glycogen and incubated overnight at -20°C. The mixture was centrifuged at 12000 rpm for 10 minutes. The supernatant was removed and the pellet was air-dried. The pellet was then dissolved in 20 μ l of TE buffer.

The double-stranded cDNA were then cloned into the bacterial host *Escherichia coli* stain XL-1 blue MRF to propagate the normalized library. The cell mixtures were plated onto LB-amplicilin (50 μ g/ml) agar plates and incubated overnight at 37°C. Recombinant clones were selected by a lacZ' system following standard protocols (Sambrook and Russel, 2001).

2.4.3 Construction of suppression subtractive hybridization (SSH) cDNA libraries

PCR-based cDNA subtraction method, termed suppression subtractive hybridization (SSH) (Diatchenko *et al.*, 1996) were carried out using a PCR-Select™ cDNA Subtraction Kit (Clontech, U.S.A.) to constructed the forward (cDNA extracted from vitellogenic ovaries of female broodstock shrimp having GSI = 5.689% as the tester) and the reverse (cDNA extracted from previtellogenic ovaries of female broodstock shrimp having GSI =1.434% as the tester) subtractive cDNA libraries of *P. monodon* broodstock.

Tester (forward library; vitellogenic ovaries and reverse library; previtellogenic ovaries) and driver (forward library; previtellogenic ovaries and reverse library; vitellogenic ovaries) were synthesized from mRNA of the target ovarian stages. Then, cDNA was digested with *Rsa* I. This digested driver cDNA was served as the experimental driver. The tester cDNA was ligated with adapters to create tester cDNAs for subtraction. The cDNAs from the tester (target) and those from the driver were subjected to subtractive hybridization and selective PCR

amplification using a PCR-Select cDNA Subtraction Kit (Clontech). The subtractive fragments were cloned into the pGEM[®]-T vector (Promega, U.S.A.)

2.4.3.1 First strand cDNA synthesis

Two micrograms of each tester and driver poly A (m) RNA was combined with 1 μ l of 10 μ M cDNA synthesis primer in a sterile 0.5 ml-microcentrifuge tube. Sterile H₂O was added to a final volume of 5 μ l. The mixture was mixed by briefly centrifuged incubated at 70°C for 2 minutes, chilled on ice for 2 minutes and briefly centrifuged.

The first strand tester and driver cDNA synthesis was carried out by adding the components in order as described in Table 2.2. The reaction was gently mixed and briefly centrifuged. The reaction was further incubated at 42°C for 1.5 hours and chilled on ice to terminate the first strand cDNA synthesis.

Table 2.2 Compositions of the first strand cDNA synthesis for construction of SSH libraries

Reaction component	
Molecular biologygrade H ₂ O	1.0 μ l
5X First-Strand Buffer (250 mM Tris-HCl, pH 8.5, 40 mM MgCl ₂ , 150 mM KCl and 5 mM DTT)	2.0 μ l
dNTPs Mix (10 mM each)	1.0 μ l
AMV Reverse Transcriptase (20 units/ μ l)	1.0 μ l
Total volume	5.0 μl

2.4.3.2 Second strand cDNA synthesis

The second strand cDNA synthesis was performed by adding components in order according to Table 2.3 into the first strand tester and driver cDNA synthesis reaction tubes. The reaction was gently mixed, briefly centrifuged and further incubated at 16°C for 2 hours. Two microliters of T4 DNA Polymerase (3 units/ μ l) were added to the second strand reaction mixture and further incubated at 16°C for 30 minutes.

The reaction was added with 4 μ l of 20X EDTA/Glycogen (0.2 mM EDTA; 1 mg/ml glycogen) and mixed thoroughly. The second strand cDNA was purified by adding 100 μ l of phenol:chloroform:isoamyl alcohol (25:24:1) and thoroughly vortexed. The mixture was centrifuged at 14000 rpm for 10 minutes at room temperature. The top aqueous layer was carefully transferred to a sterile microcentrifuge tube.

Table 2.3 Compositions of the second strand cDNA synthesis for for construction of SSH libraries

Reaction component	
Molecular biologygrade H ₂ O	48.4 μ l
5X Second-Strand Buffer (100 mM Tris-HCl, pH 7.5, 25 mM MgCl ₂ , 500 mM KCl, 50 mM ammonium sulfate, 0.75 mM β -NAD and 0.25 mg/ml BSA)	16.0 μ l
dNTPs Mix (10 mM each)	1.6 μ l
20X second strand enzyme cocktail (DNA polymerase I, 6 units/ μ l; RNase H, 0.25 units/ μ l; and <i>E. coli</i> DNA ligase, 1.2 units/ μ l)	4.0 μ l
Total volume	70.0 μl

The solution was extract again with 100 μ l of chloroform:isoamyl alcohol (24:1). The extraction steps were repeated. The second strand cDNA was precipitated by adding 40 μ l of 4 M NH₄OAc and 300 μ l of ice cold 100% EtOH, thoroughly mixed and centrifuged at 14000 rpm for 20 minutes at room temperature. The supernatant was carefully removed. The pellet was washed with 500 μ l of 80% EtOH and centrifuged at 14000 rpm for 10 minutes. After the supernatant was removed, the pellet was air-dried for 10 minutes to evaporate residual ethanol and the pellet was dissolved in 50 μ l of sterile H₂O. The synthesized cDNA were further analyzed by agarose gel electrophoresis to estimated yield and size range of double strand cDNA products synthesized.

2.4.3.3 *Rsa* I Digestion

The blunt-ended double strand cDNA fragments which are optimal for subtraction and required for adaptor ligation was carried out by performing the digestion mixture containing 43.5 μ l of double strand tester or driver cDNA, 5 μ l of 10X *Rsa* I restriction buffer (100 mM Bis Tris Propane-HCl; pH 7.0, 100 mM MgCl₂ and 1 mM DTT) and 1.5 μ l of *Rsa* I (10 units/ μ l). The mixture was incubated at 37°C for 1.5 hours. Five microliters of the digested solution were collected for analysis of *Rsa* I digestion efficiency by agarose gel electrophoresis. The digested cDNA was added with 2.5 μ l of 20X EDTA/glycogen to terminate the reaction. The purification of the digested cDNA was performed by adding 50 μ l of phenol:chloroform:isoamyl alcohol (25:24:1) was added and thoroughly vortexed. The mixture was centrifuged at 14000 rpm for 10 minutes at room temperature. The top aqueous layer was carefully removed and placed in a sterile microcentrifuge tube. The solution was extract again with 50 μ l of chloroform:isoamyl alcohol (24:1). The extraction steps were repeated. The digested cDNA was precipitated by adding 25 μ l of 4 M NH₄OAc and 187.5 μ l of ice cold 100% EtOH. The tube was thoroughly mixed and centrifuged at 14000 rpm for 10 minutes at room temperature. The supernatant was carefully removed. The pellet was washed with 200 μ l of 80% EtOH and centrifuged at 14000 rpm for 5 minutes. The pellet was air-dried for about 10 minutes and dissolved in 5.5 μ l of sterile H₂O and stored at -20°C.

This *Rsa* I-digested cDNA was served as the experimental driver cDNA. Furthermore, the sample was ligated with adapters to create tester cDNAs for forward and reverse subtractions. One microliter of *Rsa* I-digested cDNA was diluted with 5 μ l of sterile H₂O to used as template for tester cDNA ligation reaction.

2.4.3.4 Adaptor-ligated Tester cDNA preparation

A ligation master mix was prepared by adding 3 μ l of sterile H₂O, 2 μ l of 5X ligation buffer (250 mM Tris-HCl; pH 7.8, 50 mM MgCl₂, 10 mM DTT and 0.25 mg/ml BSA) and 1 μ l of T4 DNA ligase (400 units/ μ l) into the diluted *Rsa* I-digested cDNA tube. For each experimental tester cDNA, the reagents were combined in the order shown in Table 2.5. The tubes were briefly centrifuged and further incubated

overnight at 16°C. The ligation reactions were stopped by adding 1 µl of the EDTA/glycogen mix, heated at 72°C for 5 minutes to inactivate the ligase activity.

2.4.3.5 First Hybridization

The first hybridization reaction mixture was prepared in the order shown Table 2.6. Samples were overlaid with a drop of mineral oil and briefly centrifuged. The samples were incubated in a thermal cycler at 98°C for 1.5 minutes. The first hybridization was carried out at 68°C for 9 hours. The two hybridization samples (Tester 1-1 and 1-2 or Tester 2-1 and 2-2) were mixed together and proceed immediately to the second hybridization step. A fresh denatured driver DNA was added to further enrich for differentially expressed cDNAs with different adaptors on each end.

Table 2.4 Sequences of the PCR select cDNA synthesis primer, adaptors and PCR primers and control primers.

Primer/Adaptor	Sequence
cDNA synthesis primer	5'- TTTTGTACAAGCTT ₃₀ N ₁ N -3'
Adaptor 1	5'- CTAATACGACTCACTATAGGGCTCGAGCGGCCCGCCCGGGCAGGT -3' 3'- GGCCCGTCCA -5'
Adaptor 2R	5'-CTAATACGACTCACTATAGGGCAGCGTGGTCGCGGCCGAGGT-3' 3'-GCCGGCTCCA-5'
PCR primer 1	5'- CTAATACGA CTCCATATAGGGC -3'
Nested PCR primer 1	5'- TCGAGCGGCCCGCCCGGGCAGGT -3'
Nested PCR primer 2R	5'- AGCGTGGTCGCGGCCGAGGT -3'
Control Primers:	
EF-1alpha 5' Primer	5'- ATGGTTGTCAACTTTGCCCC -3'
EF-1alpha 3' Primer	5'- TTGACCTCCTTGATCACACC -3'

2.4.3.6 Second Hybridization

The two samples from the first hybridization of each library were mixed together and fresh denatured driver cDNA was added to further enrich for differentially expressed sequence. To carry out the second hybridization: 1 µl of *Rsa* I -digested driver cDNA, 1 µl of 4X Hybridization Buffer and 2 µl of sterile H₂O were added to a new 0.5 ml microcentrifuge tube. One microliter of mixture was placed in another 0.5 ml microcentrifuge tube and overlaid with a drop of mineral oil.

Table 2.5 Ligation reactions of the tester cDNA of forward (tester 1-1 and 1-2) and reverse (tester 2-1 and 2-2) subtraction libraries

Component	cDNA for forward library		cDNA for reverse library	
	Tube 1	Tube 2	Tube 3	Tube 4
	Tester 1-1*	Tester 1-2*	Tester 2-1*	Tester 2-2*
	(μ l)	(μ l)	(μ l)	(μ l)
Diluted <i>Rsa</i> I-digested cDNA	2.0	2.0	2.0	2.0
Adaptor 1 (10 μ M)	2.0	-	2.0	-
Adaptor 2R (10 μ M)	-	2.0	-	2.0
Master Mix	6.0	6.0	6.0	6.0
Final volume	10.0	10.0	10.0	10.0

* The solution was mixed. Two microliters of Tester 1-1, 1-2, 2-1 2-2 were taken and subsequently served as unsubtracted tester control 1-C and 2-C, respectively.

Table 2.6 Compositions of the first hybridization reaction of each subtraction

Component	cDNA for a forward library		cDNA for a reverse library	
	Tube 1	Tube 2	Tube 3	Tube 4
	Tester 1-1*	Tester 1-2*	Tester 2-1*	Tester 2-2*
	(μ l)	(μ l)	(μ l)	(μ l)
<i>Rsa</i> I-digested Driver cDNA	1.5	1.5	1.5	1.5
Adaptor 1-ligated Tester 1-1	1.5	-	-	-
Adaptor 2R- ligated Tester 1-2	-	1.5	-	-
Adaptor 1- ligated Tester 2-1	-	-	1.5	-
Adaptor 2R- ligated Tester 2-2	-	-	-	1.5
4x Hybridization Buffer	1.0	1.0	1.0	1.0
Final volume	4.0	4.0	4.0	4.0

The mixture was incubated in a thermal cycler at 98°C for 1.5 minutes and simultaneously mixed with the combination of two hybridization samples (Tester 1-1 and 1-2 or Tester 2-1 and 2-2 from the first hybridization, Table 2.6) by pipetting. The reaction was incubated overnight at 68°C. Two hundred microliters of the dilution buffer (20 mM HEPES, pH 6.6, 20 mM NaCl and 0.2 mM EDTA, pH 8.0) were added and mixed by pipetting. The reaction mixture was heated in a thermal cycler at 68°C for 7 minutes and stored at -20°C until used.

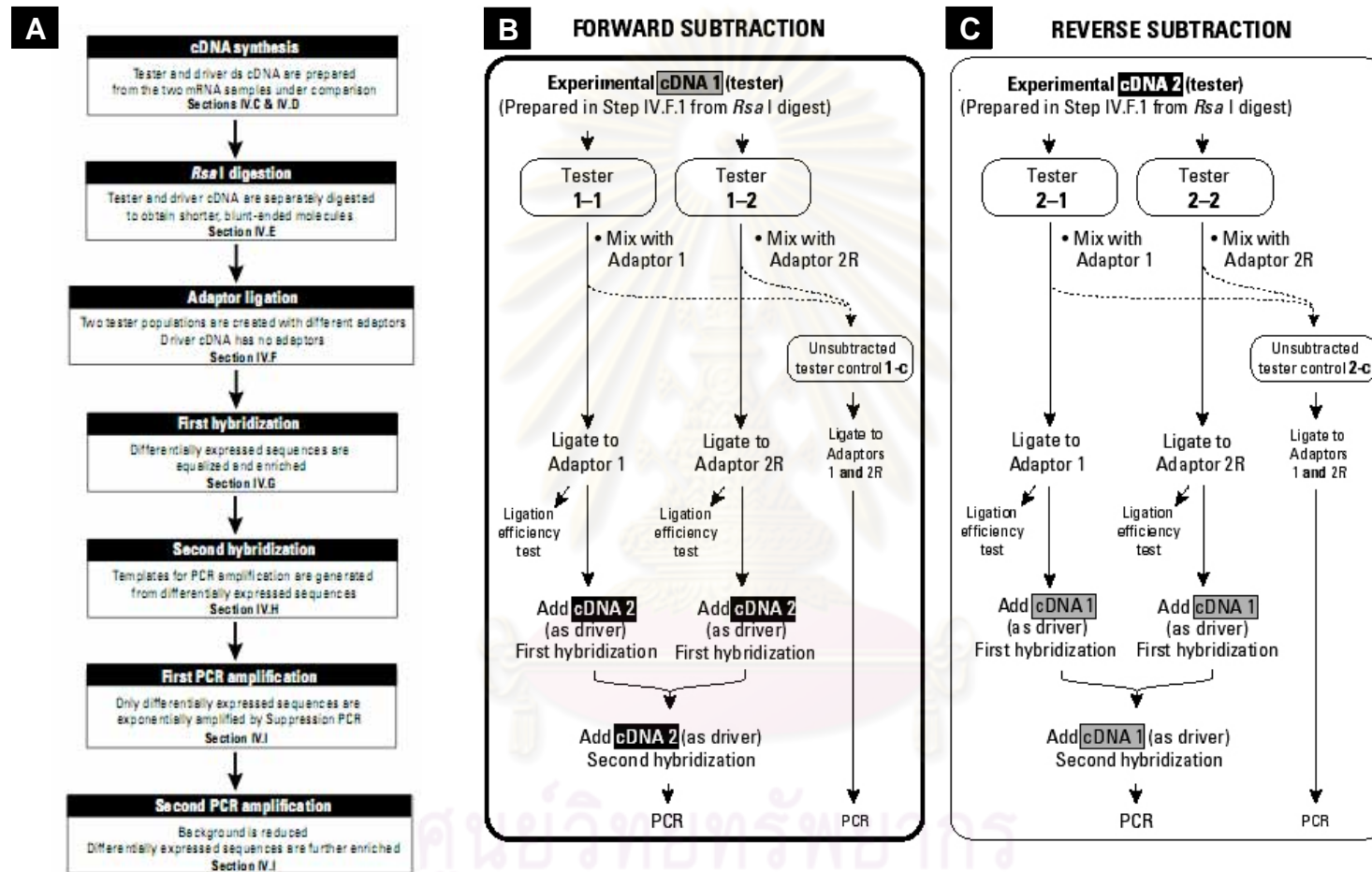


Figure 2.2 Overview of the PCR-Selected procedure based on a PCR-Select™ cDNA Subtraction Kit (Clontech) (A) and the preparation of adaptor-ligated tester cDNA for hybridization and suppression PCR (B and C).

2.4.3.7 Primary and secondary PCR amplification

One microliter of each diluted subtracted cDNA samples or unsubtracted cDNA control was aliquoted into an appropriately labeled tube. A master mix enough for the primary PCR reactions was prepared (Table 2.7).

Table 2.7 Preparation of the primary PCR master mix

Reagent	Amount per reaction (μ l)
Sterile H ₂ O	19.5
10X PCR reaction buffer	2.5
dNTP Mix (10 mM)	0.5
PCR primer 1 (10 μ M)	1.0
50X Advantage cDNA Polymerase Mix	0.5
Total volume	24.0

The reaction was mixed well and briefly centrifuged. An aliquot of 24 μ l of the master mix was dispensed to each samples tube and overlaid with a drop of mineral oil. The reaction mix was incubated in a thermal cycler at 75°C for 5 minutes to extend the adaptors. The amplification reaction was carried out for 27 cycles composing of a 94°C for 10 s, 66°C for 30 seconds and a 72°C for 1.5 minutes. After amplification, 8 μ l of each tube were electrophoretically analyzed through 2.0% agarose gel.

A ten-fold dilution was performed using 3 μ l of each primary PCR mixture in 27 μ l H₂O. One microliter of each diluted primary PCR product mixture was added into an appropriately labeled tube. A master mix for secondary PCR was prepared (Table 2.8).

The reaction was mixed well and briefly centrifuged. An aliquot of 24 μ l of the second master mix was dispensed to each samples tube and overlaid with a drop of mineral oil. The reaction mix was carried out for 10 cycles composing of 94°C for 30 s, 68°C for 30 seconds and 72°C for 1.5 minutes. The final extension was carried out at 72°C for 7 minutes. After amplification, 8 μ l of each tube were

electrophoretically analyzed through 2.0% agarose gel. The amplification product was recovered by spinning through Microcon YM-100 centrifugal filter devices (Millipore) at 1000 g for 15 minutes.

Table 2.8 Preparation of the secondary PCR master mix

Reagent	Amount per reaction (µl)
Sterile H ₂ O	18.5
10X PCR reaction buffer	2.5
Nested PCR primer 1 (10 µM)	1.0
Nested PCR primer 2R (10 µM)	1.0
dNTP Mix (10 mM)	0.5
50X Advantage cDNA Polymerase Mix	0.5
Total volume	24.0

2.4.3.8 Ligation of PCR products to pGEM[®]-T easy vector

The resulting products from the forward (cDNA from vitellogenic ovaries as tester) and reverse (cDNA from previtellogenic ovaries as tester) subtraction were separately ligated to pGEM[®]-T Easy vector (Promega) in a 15 µl reaction volume containing 7.5 µl of 2X Rapid Ligation Buffer (60 mM Tris-HCl, pH 7.8, 20 mM MgCl₂, 20 mM DTT, 2 mM ATP and 10% polyethylene glycol; MW 8000), 3 Weiss units of T4 DNA ligase, 50 ng of pGEM[®]-T easy vector and 3 µl of eluted subtraction cDNA. The reaction mixture was incubated overnight at 4 °C and cloned into *Escherichia coli* JM109 to propagate the forward and reverse subtractive libraries. The cell mixtures were plated onto LB ampicillin (50 µg/ml) agar plates and incubated overnight at 37°C. Recombinant clones were selected by a lacZ' system following standard protocols (Sambrook and Russel, 2001).

2.4.3.9 Transformation of ligation products to *E. coli* host cells

Preparation of competent cells

A single colony of *E. coli* JM109 was inoculated in 10 ml of LB broth (1% Bactotryptone, 0.5% Bactoyeast extract and 0.5% NaCl, pH 7.0) with vigorous

shaking at 37°C overnight. The starting culture was then inoculated into 50 ml of LB broth and continued culture at 37°C with vigorous shaking to an OD₆₀₀ of 0.5 to 0.8. The cells were briefly chilled on ice for 10 minutes, and recovered by centrifugation at 2700g for 10 minutes at 4°C. The pellets were resuspended in 30 ml of ice-cold MgCl₂/CaCl₂ solution (80 mM MgCl₂ and 20 mM CaCl₂) and centrifuged as above. After resuspended in 2 ml of ice-cold 0.1 M CaCl₂, the concentrated cell suspension was divided to 200 µl aliquots. These competent cells were either used immediately or stored at -80 °C for subsequently used.

Transformation

The competent cells were thawed on ice for 5 minutes. Two to four microlitres of the ligation mixture were added and gently mixed by pipetting and left on ice for 30 minutes. The transformation reaction was heat-shocked in a 42°C water bath for exactly 45 seconds without shocking. The reaction tube was immediately placed in ice for 2-3 minutes. The mixture were removed from the tubes and added to a new tube containing 1 ml of prewarmed SOC (2% Bacto tryptone, 0.5% Bacto yeast extract, 10 mM NaCl, 2.5 mM KCl, 10 mM MgCl₂, 10 mM MgSO₄ and 20 mM glucose). The cell suspension was incubated with shaking at 37°C for 90 minutes. The mixture were centrifuged for 20 seconds at room temperature, and gently resuspended in 100 µl of SOC medium and spreaded onto a selective LB agar plates containing 50 µg / ml of ampicillin, 25 µg/ml of IPTG and 20 µg/ml of X-gal and further incubated at 37°C overnight (Sambrook and Russell, 2001). The recombinant clones containing inserted DNA are white whereas those without inserted DNA are blue.

2.4.4 Identification of the positive clones using colony PCR

Recombinant clones carrying insert sizes greater than 500 bp (typical and normalized ovaries cDNA libraries) or 300 bp (SSH ovaries cDNA libraries) were randomly selected by colony PCR. The colony PCR was performed in a 25 µl reaction mixture containing 75 mM Tris-HCl, pH 8.8, 20 mM (NH₄)₂SO₄, 0.01% Tween 20, 0.2 mM of each dNTP, 2 mM MgCl₂, 0.1 µM each of pUC1 (5'-TCC GGC TCG TAT GTT GTG TGG A-3') and pUC2 (5'-GTG CTG CAA GGC GAT TAA GTT GG-3'), 0.5 unit of *Taq* DNA Polymerase (recombinant) (Fermentas Life Sciences). A colony was picked by a sterile toothpick and used as the template in the reaction. PCR was

carried out in a thermocycler consisting of predenaturation at 94°C for 3 minutes followed by 35 cycles of denaturation at 94°C for 30 s, annealing at 50°C for 1 minutes and extension at 72°C for 3 minutes. The final extension was carried out at 72°C for 7 minutes. The amplicon was electrophoretically analyzed through 1.2% agarose gel and visualized with a UV transilluminator after ethidium bromide staining (Sambrook and Russel, 2001).

2.4.5 Plasmid DNA extraction

Plasmid DNA was extracted from approximately 1,500 and 2,000 clones from typical and normalized ovary cDNA libraries and 250 clones from each SSH library of *P. monodon*, respectively.

Plasmid DNA was isolated from each recombinant clone using a HiYield™ Plasmid Mini Kit (RBC; Real Biotech Corporation). A recombinant clone was inoculated into 3 ml of LB broth (1% tryptone, 0.5% yeast extract, 1.0 % NaCl) containing 50 µg/ml of ampicillin and incubated at 37°C with constant shaking at 250 rpm overnight. The cultured was transferred into 1.5 ml microcentrifuge tube and centrifuged at 13,000 rpm for 1 minute. The supernatant was removed and the bacterial cell pellet was resuspended in 200 µl of the PD1 buffer containing RNaseA by vortexing. The resuspended cell was lysed by adding 200 µl of the PD2 buffer and mixed gently by inverting the tube for 10 times and then placed the mixture for 2 minutes at room temperature. Neutralize the alkaline lysis by adding 300 µl of the buffer PD3 to and mixed immediately by inverting the tube for 10 times. The mixture was centrifuged at 14,000 rpm for 15 minutes to separate the cell debris. The supernatant was then applied into the PD column and centrifuged at 8000 rpm for 1 minute. The flow-through was discarded and the PD column was placed back in the collection tube. The PD column was washed by adding 400 µl of the W1 buffer and centrifuged at 8000 rpm for 1 minute. The flow-through was discarded and then 600 µl of the ethanol-added Wash buffer was added and centrifuged at 8000 rpm for 1 minute. The flow-through was discarded and the column was centrifuged for an additional 2 minutes at the full speed (14000 rpm) to remove the residual Wash buffer. The dried PD column was transferred onto a new 1.5 ml microcentrifuge tube. Approximately 50 µl of the Elution buffer was added into the centre of the column

matrix. The column was placed for 2 minutes at room temperature and centrifuged at 14000 rpm for 2 minutes. The concentration of extracted plasmid DNA was also spectrophotometrically measured.

For typical and normalized cDNA libraries, the insert size of each recombinant plasmid was examined by digestion of the plasmid with *Eco* RI-*Xho* I (or *Eco* RI-*Apa* I) (Promega). The digest was carried out in a 12 μ l containing 1X restriction buffer (buffer D; 6 mM Tris-HCl; pH 7.9, 6 mM MgCl₂, 150 mM NaCl and 1 mM DTT for *Eco* RI-*Xho* I or MULTI-CORE™ buffer; 25 mM Tris-HCl; pH 7.5, 100 mM Potassium acetate, 10 mM Magnesium acetate and 1 mM DTT for *Eco* RI-*Apa* I), 0.1 mg/ml of BSA, 1 μ l of recombinant plasmid, 3 unit of each *Eco* RI and *Xho* I (or *Apa* I). For SSH cDNA libraries, each recombinant plasmid was digested with *Eco* RI (Promega). The digestion was carried out in a 10 μ l containing 1X restriction buffer (buffer H; 90 mM Tris-HCl; pH 7.5, 10 mM MgCl₂ and 50 mM NaCl), 0.1 mg/ml of BSA, 1 μ l of recombinant plasmid, 3 unit of each *Eco* RI. The reaction was incubated at 37 °C for 3 hours (or overnight) before electrophoretically analyzed by agarose gel electrophoresis.

2.4.6 DNA sequencing and EST analysis

Plasmid DNA was unidirectional sequenced by a dideoxy-chain termination sequencing reaction using the MegaBace1000 DNA Analysis System (Amersham Bioscience). The cDNA inserts were partially sequenced from the 5' end direction for non-subtractive cDNA libraries and the random end for subtractive cDNA libraries. The raw sequence data were polished automatically to remove unwanted vector sequence, various contaminants and low quality sequence information using Seqclean). The sequence identities were determined by comparing each sequence with the sequences in the GenBank mirror site using the BLASTX program (Altschul *et al.*, 1990; available at <http://www.ncbi.nih.gov>) and blast2go (<http://www.blast2go.de>). Clustering and assembling of sequences were performed using TIGR Gene Indices Clustering Tools (TGICL) (Pertea *et al.*, 2003) with CAP3 (Huang and Madan, 1999). Significant probabilities and numbers of matched proteins were considered when the e-values were less than 10^{-4} . Gene ontology (GO) of examined ESTs was also examined.

2.5 Isolation and characterization of differentially displayed transcripts during ovarian development of *P. monodon* using RNA arbitrary primed (RAP)-PCR

2.5.1 cDNA synthesis

Total RNA was extracted from stages III (GSI = 5.689%) and I (GSI = 1.434%) ovaries of female broodstock originating from Satun (Andaman Sea) and Angsila (Gulf of Thailand) and from ovaries of juvenile *P. monodon* (approximately 20 g body weight purchased from local farms in Chachengsao, eastern Thailand) using TRI-REAGENT[®] as described previously. Messenger (m) RNA was further purified using a QuickPrep *micro* mRNA Purification Kit (Amersham Pharmacia Biotech) as described previously.

Two hundred and fifty nanograms of the first strand cDNA was synthesized from 1.5 µg of purified mRNA from mature and immature ovaries of broodstock and premature ovaries of juvenile *P. monodon* and used as the template for PCR amplification. The reaction was carried out in a 25 µl reaction volume containing 10 mM Tris-HCl, pH 8.8 at 25°C, 50 mM KCl and 0.1% Triton X - 100, 1.5 mM MgCl₂, 200 µM each of dNTPs, 1 unit of Dynazyme[™] DNA Polymerase (FINNZYMES, Finland), 1 µM each of the oligo-dT₍₁₆₎-overhang with A, C or G primer (that used for the first strand cDNA synthesis) and the second arbitrary primers (Table 2.9).

PCR was performed by pre-denaturation at 94°C for 3 minutes, followed by 40 cycles of denaturation at 94°C for 15 seconds, annealing at 42°C for 60 seconds, and extension at 72°C for 90 seconds. The final extension was carried out for 7 minutes at 72°C. Five microlitres of the amplification product were electrophoretically analyzed in 2.0% agarose gel to verify whether the amplification was successful.

2.5.2 Preparation of denaturing polyacrylamide gel electrophoresis

Denaturing polyacrylamide gels are used for the separation of single-stranded RAP-PCR fragments. These gels are polymerized in the presence of urea that suppresses base pairing in nucleic acids. Denatured DNA migrates through these gels at a rate that is almost completely independent of its base composition and sequence.

Five percent denaturing polyacrylamide gels were prepared by combining 40 ml of the degassed acrylamide solution (19:1 acrylamide: bisacrylamide with 7 M

urea in TBE buffer) with 240 µl of freshly prepared 10% ammonium persulphate and 24 µl of TEMED.

Table 2.9 Sequences of arbitrary primers used for screening of differential expression markers in ovaries of *P. monodon* using RAP-PCR analysis

Primer name	Sequence	Primer name	Sequence
UBC 101	GCGCCTGGAG	OPA 01	CAGGCCCTTC
UBC 119	ATTGGGCGAT	OPA 02	TGCCGAGCTG
UBC 122	GTAGACGAGC	OPA 07	GAAACGGGTG
UBC 128	GCATATTCCG	OPA 09	GGGTAACGCC
UBC 135	AAGCTGCGAG	OPA 11	CAATCGCCGT
UBC 138	GCTTCCCCTT	OPA 14	TCTGTGCTGG
UBC 158	TAGCCGTGGC	OPA 15	TTCCGAACCC
UBC 159	GAGCCCGTAG	OPA 16	AGCCAGCGAA
UBC 169	ACGACGTAGG	OPA 17	GACCGCTTGT
UBC 174	AACGGGCAGC	OPA 18	AGGTGACCGT
UBC 191	CGATGGCTTT	OPB 01	GTTTCGCTCC
UBC 217	ACAGGTAGAC	OPB 02	TGATCCCTGG
UBC 222	AAGCCTCCCC	OPB 03	CATCCCCCTG
UBC 228	GCTGGGCCGA	OPB 04	GGACTGGAGT
UBC 263	TTAGAGACGG	OPB 07	GGTGACGCAG
UBC 268	AGGCCGCTTA	OPB 08	GTCCACAGGG
UBC 273	AATGTCGCCA	OPB 09	TGGGGGACTC
UBC 299	TGTCAGCGGT	OPB 10	CTGCTGGGAC
UBC 428	GGCTGCGGTA	OPB 12	CCTTGACGCA
UBC 456	GCGGAGGTCC	OPB 16	TTTGCCCGGA
UBC 457	CGACGCCCTG	OPZ 04	AGGCTGTGCT
UBC 459	GCGTCGAGGG	OPZ 08	GGGTGGGTAA
		OPZ 09	CACCCAGTC

The acrylamide solution was then gently injected into one side of the assembled plates using a 50 ml syringe. The filled plate sandwich was left in the horizontal position. The flat edge of the shark-tooth comb was then inserted. The gel was left at room temperature for 1 hour. After that, the polymerized gel was covered by the water-soaked tissue paper and left at room temperature for at least 4 hours (or

overnight) for complete polymerization. When required, the spring clips and the sealing tapes were carefully removed. The top of the gel was rinsed with 1X TBE. The sharkstooth comb was rinsed with water.

2.5.3 Electrophoresis

The gel sandwich was placed in the vertical sequencing apparatus with the short glass plate inward. The gel sandwich was securely clamped with the integral gel clamps along the sides of the sequencing apparatus. The upper and lower buffer chambers were filled with approximately 300 ml of 1X TBE. The sharkstooth comb was reinserted into the gel until the teeth just touched the surface of the gel. Six microlitres of the acrylamide gel loading dye (98% formamide, 200 μ l EDTA, 0.25% bromophenol blue and 0.25% xylene cyanol) was loaded into each well. The gel was prerun at 35-40 W for 20 minutes.

Six microlitres of the amplification products were mixed with 3 μ l of the loading buffer and heated at 95°C for 5 minutes before snapped cooled on ice for 3 minutes. The sample was carefully loaded into the well. Electrophoresis was carried out at 35-40 W for approximately 2.5 hours (xylene cyanol moved out from the gel for approximately 10 minutes).

2.5.4 Silver staining

The gel plates were carefully separated using a plastic wedge. The long glass plate with the gel was placed in a plastic tray containing 1.5 litres of the fix/stop solution and agitates well for 40 minutes. The gel was soaked with shaking 3 times for 2 minutes with deionized water. The gel was lifted out from the tray between each wash and allowed the washed water draining out of the gel for 4 seconds. The gel was transferred to 0.1% silver nitrate (1.5 liters) and incubated with agitation at room temperature for 30 minutes. The gel was soaked in 1.5 liters off deionized water with shaking (10 forward and 10 backward agitation) and immediately placed in the tray containing 1.5 liters of the chilled developing solution. This step is crucial and the time taken to soak the gel in the water and transfer it to chilled developing solution should be no longer than 5-10 s. The gel was well agitated until the first bands are visible (usually 1.5-2 minutes). The gel was then transferred to another tray containing 1.5 liters of chilled developer and shake until bands from every lane were

observed (usually 2-3 minutes). One liter of the fix/stop solution was directly added to the developing solution and continued shaking for 3 minutes. The stained gel was soaked in deionized water twice for 3 minutes each. The gel was left at 80°C for 2-3 hours.

2.5.5 Cloning and characterization of candidate differential/stage-specific of differential ovarian development expression markers of RAP-PCR fragments

2.5.5.1 Elution of DNA from polyacrylamide gels

RAP-PCR fragments showing presence/absence between different stages and those exhibiting differential expression profiles (at least 2-3 times differences in band intensity) were considered. Candidate RAP-PCR fragments were excised from the gel using a sterile razor blade and washed 3 times for 30 min each at room temperature with 200 µl of sterile deionized H₂O. Twenty microliters of H₂O was then added and incubated overnight at 37°C.

Reamplification of the target fragment was carried out using the same PCR recipes as those for selective amplification with the exception that 0.2 µM of each primer and 5 µl of the eluted RAP-PCR product were used. The amplification conditions were composed of 1 cycle of 94°C for 3 minutes; follow by additional 35 cycles at 94°C for 15 s, 42°C for 60 seconds and 72°C for 90 s. The final extension was performed at 72°C for 7 minutes. The reamplified product was electrophoretically analyzed through a 1.25-1.6 % agarose gel.

2.5.5.2 Elution of RAP-PCR fragments from agarose gels

The desired RAP-PCR fragments were excised from the agarose gel using a sterile scalpel and placed in a preweighed microcentrifuge tube. DNA was isolated using HiYield™ Gel/PCR DNA Extraction Kit (RBC; Real Biotech Corporation). Five hundreds microlitres of DF buffer was added and mixed by vortexing. The mixture was incubated at 55°C for 10-15 minutes or until the gel slice was completely dissolved. The mixture was transferred into a DF column inserted in a collection tube and centrifuged at 8000 rpm for 30 s. The flow-through solution was discarded. After this step, 0.5 ml of wash buffer was added to the DF column and centrifuged as above.

The flow-through solution was discarded. The column was recentrifuged to remove the trace amount of the washing solution. The DF column was then placed into a sterile 1.5 ml microcentrifuge tube. DNA was eluted out by an addition of 15 μ l of the Elution buffer or H₂O to the center of the DF membrane and left for 1 minute, before centrifuged at 12000 rpm for 2 minutes.

2.5.5.3 Ligation and cloning of the RAP-PCR products

The eluted RAP-PCR fragments were ligated to pGEM[®]-T Easy vector (Promega) in a 10 μ l reaction volume as described previously and cloned into *Escherichia coli* JM109. Colony PCR was carried out. Recombinant clones carrying desired DNA fragments were sequenced.

2.5.5.4 DNA sequencing and sequence similarity

The recombinant clone was unidirectional sequenced using the M13 forward and/or reverse primer on an automatic sequencer. Nucleotide sequences were blasted against data in GenBank using BlastN (nucleotide similarity) and BlastX (translated protein similarity). Significant similarity was considered when the probability value was $<10^{-4}$.

2.6 Isolation and characterization of the full length cDNA and genomic DNA of functionally important gene homologues of *P. monodon*

2.6.1 Isolation and characterization of the full length cDNA using 3' end terminal sequencing

For sequencing of genes that showed the full length from the 5' direction, the product from colony PCR was considered. If the insert of a particular gene was larger than that of its homologues, the 3' direction was further sequenced. Internal forward primers were designed for primer walking of the inserted cDNA (Table 2.10).

2.6.2 Isolation and characterization of the full length cDNA using Rapid Amplification of cDNA Ends-Polymerase Chain Reaction (RACE – PCR)

2.6.2.1 Preparation of the 5' and 3' RACE template

Full length cDNAs of interesting gene homologues were characterized using a SMART™ RACE cDNA Amplification Kit (Clontech). Total RNA was extracted from ovaries of *P. monodon* broodstock using TRI-REAGENT®. Messenger (m) RNA was purified using a QuickPrep *micro* mRNA Purification Kit (Amersham Pharmacia Biotech) as described previously. RACE-Ready cDNA was prepared by combining 1 µg of ovarian mRNA with 1 µl of 5'-CDS primer and 1 µl of 10 µM SMART II A oligonucleotide for 5'- RACE-PCR or 1 µg of ovarian mRNA with 1 µl of 3'-CDS primer A for 3'- RACE-PCR (Table 2.11). The components were mixed and spun briefly. The reaction was incubated at 70°C for 2 minutes and immediately cooled on ice for 2 minutes. The reaction tube was spun briefly. After that, 2 µl of 5X First-Strand buffer, 1 µl of 20 mM DTT, 1 µl of dNTP Mix (10 mM each) and 1 µl of PowerScript Reverse Transcriptase were added. The reactions were mixed by gently pipetting and centrifuged briefly to collect the contents at the bottom.

The tubes were incubated at 42°C for 1.5 hours in a thermocycler. The first strand reaction products were diluted with 125 µl of TE buffer and heated at 72°C for 7 minutes. The first strand cDNA template was stored at -20°C.

Table 2.10 Internal primers used for primer walking of the full length cDNA of functionally important gene homologues in *P. monodon*

Primer	Sequence	T _m (°C)
<i>Cell division cycle 20</i> (OV-N-S01-0197-W)		
Cdc20seq internal 3'-F1	5'- CGCCACCCCACATAACCAGCAAG -3'	70.2
Cdc20seq internal 3'-F2	5'- CGCAGGAGGTCTGTGGTCTA -3'	58.3
<i>Cell division cycle 42</i> (OV-N-S01-1131-W)		
Cdc42seq internal 3'-F	5'- GATGAAGCAATTCTCGCAGC -3'	58.4
<i>cofilin/actin-depolymerizing factor homolog (D61 protein) (Twinstar protein)</i> (OV-N-N01-0526-W)		
cofilinseq internal 3'-F	5'- CAGCATCAGGGGACTCATTG -3'	58.4

2.6.2.2 Primer designed for RACE-PCR and primer walking

Gene-specific primers (GSPs) were designed from interesting transcripts obtained from ovaries (and haemocyte) cDNA libraries and the subtraction ovaries cDNA libraries of *P. monodon*. The antisense and/or sense primers were designed for 5'- and 3'- RACE-PCR, respectively (Table 2.12). Internal forward and/or reverse primers were also designed for further sequencing of the internal regions of large RACE-PCR fragments (Table 2.13).

2.6.2.3 RACE-PCR and cloning of RACE-PCR products

The master mix which is sufficient for 5'- or 3'- RACE-PCR was prepared as described in Tables 2.14. The 5'- and 3'- RACE-PCR were set up as described in Table 2.15.

The desired RACE-PCR fragments were isolated using HiYield™ Gel/PCR DNA Extraction Kit (RBC; Real Biotech Corporation). The DNA fragments were ligated to pGEM®-T Easy vector (Promega) in a 10 µl reaction volume and cloned into *Escherichia coli* JM109. Recombinant clones were selected by a lacZ' system following standard protocols (Sambrook and Russel, 2001) and randomly selected by colony PCR. Recombinant clones carrying desired DNA fragments were selected. Plasmid DNA was extracted and subjected to unidirectional sequencing.

Table 2.11 Primer sequences for the first strand cDNA synthesis for RACE-PCR

Primer	Sequence
BD SMART II™ A Oligonucleotide (12 µM)	5'- AAGCAGTGGTATCAACGCAGAGTACGCGGG -3'
3'-RACE CDS Primer A (3'-CDS; 12 µM)	5'- AAGCAGTGGTATCAACGCAGAGTAC(T) ₃₀ V N -3' (N = A, C, G or T; V = A, G or C)
5'-RACE CDS Primer (5'-CDS; 12 µM)	5'- (T) ₂₅ V N -3' (N = A, C, G or T; V = A, G or C)
10X Universal Primer A Mix (UPM)	Long : 5'- CTAATACGACTCACTATAGGGCAA GCAGTGGTATCAACGCAGAGT -3' Short : 5'- CTAATACGACTCACTATAGGGC -3'
Nested Universal Primer A (NUP; 12 µM)	5'- AAGCAGTGGTATCAACGCAGAGT -3'

Table 2.12 Gene-specific primers (GSPs) used for characterization of the full length cDNA of functionally important gene homologues in *P. monodon* using RACE-PCR

Primer	Sequence	Tm (°C)
Phosphatidylserine receptor (PSR) (OV-N-S01-0046-W)		
3'-RACE	5'- GAGGATAGACGCCCCCTTACCGCTGG -3'	76.6
Procollagen-proline, 2-oxoglutarate 4-dioxygenase (protein disulfide isomerase; thyroid hormone binding protein p55) (P4HB) (OV-N-S01-0280-W)		
5'-RACE	5'- CGACAGATTTGCCAGAACGGAAGA-3'	67.5
Progesterone receptor-related protein p23 (OV-N-S01-0802-W)		
3'-RACE	5'- GCAAGTGATGCGTCGTGGTA -3'	60.1
Bystin isoform 1 (OV-N-S01-1377-W)		
5'-RACE	5'- TTGGCAAGGGTCCACTTCTGTAT -3'	62.6
Progesterin receptor membrane component 1 (PGMRC1) (OV-N-N01-0057-W)		
5'-RACE	5'- TGTCCTGTCGTTTCATCTTGGGCAC -3'	66.7
Serine/threonine-protein kinase chk1 (OV-N-ST01-0032-W)		
3'-RACE	5'- CCGAATTTGTGGTGGGGTGGAAACG-3'	72.8
Carbonyl reductase (OV-N-ST02-0071-W)		
3'-RACE	5'- CGCAGTTTGTCCCACTCCTTAGACCA -3'	70.6
Gonadotropin-regulated long chain acyl-CoA synthetase (GL-H-S01-0591-LF)		
5'-RACE	5'- GATGAGTTCTTTGATGCGTCCCGTG -3'	68.8
Nested 5'-RACE	5'- GCCTTCTCCAGGTGATGTTGTCGTG -3'	68.8

Table 2.13 Internal primers used for primer walking of the full length cDNA fragments of functionally important gene homologues in *P. monodon* using RACE-PCR

Primer	Sequence	Tm (°C)
Progesterone receptor-related protein p23 (OV-N-S01-0802-W)		
PGRp23seq internal 3'-F	5'- GCAAGTGATGCGTCGTGGTA -3'	60.1
Progesterin receptor membrane component 1 (PGMRC1) (OV-N-N01-0057-W)		
PGMRC1seq internal 3'-F	5'- CACCAAAGCGAAGACGGATG -3'	61.3
Serine/threonine-protein kinase chk1 (OV-N-ST01-0032-W)		
Chk1seq internal 3'-F	5'- GGACAAAGGTGGACAATCTG -3'	54.8
Gonadotropin-regulated long chain acyl-CoA synthetase (GL-H-S01-0591-LF)		
Gonado-seq internal 3'-F	5'- TGGCTCCTCCAATGCTCAG -3'	60.9
internal gonadotropin-F	5'- GAGTTGGGAAGATGTCTGTA -3'	55.2
internal gonadotropin-R	5'- GCATTGGAAGGAGCCAGTTTA -3'	59.6

Table 2.14 Composition of 5'- and 3'- RACE-PCR

Component	5'-RACE Sample	3'-RACE Sample	GSP1+UPM (-Control)	GSP2+UPM (-Control)
5'-RACE-Ready cDNA	1.25 µl	-	-	-
3'-RACE-Ready cDNA	-	1.25 µl	-	-
UPM (10X)	2.5 µl	2.5 µl	2.5 µl	2.5 µl
GSP1 (10 µM)	1.0 µl	-	1.0 µl	-
GSP2 (10 µM)	-	1.0 µl	-	1.0 µl
10X BD advantage [®] 2 PCR Buffer	2.5 µl	2.5 µl	2.5 µl	2.5 µl
10 µM dNTP mix	0.5 µl	0.5 µl	0.5 µl	0.5 µl
50X BD Advantage [®] 2 polymerase mix	0.5 µl	0.5 µl	0.5 µl	0.5 µl
H ₂ O	Up to 25 µl	Up to 25 µl	Up to 25 µl	Up to 25 µl
Final volume	25µl	25µl	25µl	25µl

2.6.3 Genomic DNA organization of functionally important gene homologues of *P. monodon*

The full length genomic DNA of *cell division cycle 42 (Cdc42)* and *Small androgen receptor interacting protein (SARIP)* were characterized using PCR-base technique. Genomic DNA was amplified using overlapping regions primer pairs (Table 2.16). The amplification conditions for isolation of genomic DNA sequence of *Cdc42* and *SARIP* were described in Table 2.17. Amplicons were electrophoretically analyzed through 1.5% agarose gel.

The desired DNA fragments were excised from the agarose gel using a sterile scalpel and placed in a preweighed microcentrifuge tube. The products were purified from agarose gel using Wizard[®] SV Gel and PCR clean-up System. Membrane Binding Solution was added to the gel slice at a ratio of 10:1 of solution per 10 mg of agarose gel slice and mixed by vortexing. The mixture was incubated at 50-65°C for 10 minutes or until the gel slice was completely dissolved. The mixture was transferred into a SV Minicolumn assembly with a collection tube and incubated for 1 minute at room temperature. The column was centrifuged at 14000 rpm for 1 minute, the SV Minicolumn was removed from the spin column assembly and the collected

liquid was discarded. The SV Minicolumn was placed to the collection tube. After this step, 0.7 ml of a Membrane Wash Solution was added to the SV Minicolumn and

Table 2.15 The amplification conditions for RACE-PCR of various gene homologues of *P. monodon*

Gene homologue	Amplification condition
<i>Phosphatidylserine receptor (PSR)</i> (OV-N-S01-0046-W)	
3' RACE	5 cycles of 94°C for 30 seconds and 72°C for 3 minutes 5 cycles of 94°C for 30 seconds, 70°C for 30 seconds and 72°C for 3 minutes 20 cycles of 94°C for 30 seconds, 68°C for 30 seconds and 72°C for 3 minutes and the final extension at 72°C for 7 minutes
<i>Procollagen-proline, 2-oxoglutarate 4-dioxygenase (protein disulfide isomerase; thyroid hormone binding protein p55) (P4HB)</i> (OV-N-S01-0280-W)	
5' RACE	20 cycles of 94°C for 30 seconds, 68°C for 30 seconds, 72°C for 3 minutes and the final extension at 72 °C for 7 minutes
<i>Progesterone receptor-related protein p23</i> (OV-N-S01-0802-W)	
3' RACE	20 cycles of 94°C for 30 seconds, 65°C for 3 minutes and the final extension at 65°C for 10 minutes
<i>Bystin isoform 1</i> (OV-N-S01-1377-W)	
5' RACE	5 cycles of 94°C for 30 seconds and 72°C for 2 minutes 5 cycles of 94°C for 30 seconds, 70°C for 30 seconds and 72°C for 2 minutes 20 cycles of 94°C for 30 seconds, 68°C for 30 seconds and 72°C for 2 minutes and the final extension at 72°C for 7 minutes
<i>Progesterin receptor membrane component 1 (PGMRC1)</i> (OV-N-N01-0057-W)	
5' RACE	5 cycles of 94°C for 30 seconds and 72°C for 3 minutes 5 cycles of 94°C for 30 seconds, 70°C for 30 seconds and 72°C for 3 minutes 20 cycles of 94°C for 30 seconds, 68°C for 30 seconds and 72°C for 3 minutes and the final extension at 72°C for 7 minutes
<i>Serine/threonine-protein kinase chk1</i> (OV-N-ST01-0032-W)	
3' RACE	5 cycles of 94°C for 30 seconds and 72°C for 3 minutes 5 cycles of 94°C for 30 seconds, 70°C for 30 seconds and 72°C for 3 minutes 20 cycles of 94°C for 30 seconds, 68°C for 30 seconds and 72°C for 3 minutes and the final extension at 72°C for 7 minutes
<i>Carbonyl reductase</i> (OV-N-ST02-0071-W)	
5' RACE	5 cycles of 94°C for 30 seconds and 72°C for 3 minutes 5 cycles of 94°C for 30 seconds, 70°C for 30 seconds and 72°C for 3 minutes 20 cycles of 94°C for 30 seconds, 68°C for 30 seconds and 72°C for 3 minutes and the final extension at 72°C for 7 minutes
<i>Gonadotropin-regulated long chain acyl-CoA synthetase</i> (GL-H-S01-0591-LF)	
5' RACE	30 cycles of 94°C for 30 seconds, 65°C for 3 minutes and the final extension at 65°C for 10 minutes
Nested 5' RACE	20 cycles of 94°C for 30 seconds, 65°C for 3 minutes and the final extension at 65°C for 10 minutes

centrifuged as above. The flow-through solution was discarded. The wash step was repeated by adding 0.5 ml of the Membrane Wash Solution to the column and centrifuged at 14000 rpm for 5 minutes. The flow-through solution was discarded and the SV Minicolumn was recentrifuged at 14000 rpm for 1 minute to remove the trace amount of the washing solution. The SV Minicolumn was then placed into a sterile 1.5 ml microcentrifuge tube. DNA was eluted out by an addition of 20 µl of sterile H₂O to the center of the SV Minicolumn and left for 1 minute, before centrifuged at 14000 rpm for 1 minute.

Table 2.16 Lists of primers and primer sequences used for isolation of genomic DNA sequence of *Cdc42* and *SARIP* genes

Primer	Sequence (5'-3')	Amplified region
<i>Isolation of genomic DNA sequence</i>		
<i>Cdc42</i> -F1	AAATGCAGACCATTAAATGCGTAGT	Coding region; positions 1 st -259 th
<i>Cdc42</i> -F2 (nested F1)	TCCTCATCTCCTACACAACAAACAA	
<i>Cdc42</i> -R1	GGGATACCACTGAGAAGCAGACTAA	
<i>Cdc42</i> -F3	CTGGTCAGGAGGATTATGACAGACT	Coding region; positions 176 th -565 th
<i>Cdc42</i> -R2	TACATTTCCCTTCGTCTCTGAGGTTC	
<i>Cdc42</i> -F4	CATTCCTCCTAGTAGGCACACAGAT	Coding region (position 323 rd
<i>Cdc42</i> -R3	GAAAGTCAAAGGACACTCGACCTAA	to 3' UTR (position 502 nd
<i>Cdc42</i> -F5	GAATGTGAGCAATCTAAGCACAAGA	3' UTR (positions 271 st -1,166 th
<i>Cdc42</i> -R4	GACTGGCTTCATACCCACTATGACT	
<i>Cdc42</i> -F6	AATCCTTGAGACGAGACCAGTTATG	3' UTR (positions 925 th -1,533 th
<i>Cdc42</i> -R5	ATTTGTATCTCCCTCCATAACACCA	
<i>SARIP</i> -F1	CAAGGAAGAACAGAATAACGAAATTG	Coding region; positions 12 nd -111 st
<i>SARIP</i> -R1	AGTAATTCTGAACTTGTGCCTTGGT	
<i>SARIP</i> -F2	AACCAAGGCACAAGTTCAGAATTAC	Coding region; positions 86 th -263 rd
<i>SARIP</i> -R2	TCATCCAGCTCTTCCTCTTCTATGT	
<i>SARIP</i> -F3	ACATAGAAGAGGAAGAGCTGGATGA	Coding region; positions 239 th -574 th
<i>SARIP</i> -R3	TGAAGAGCTCTCTACCAGTTGGTTT	
<i>SARIP</i> -F4	TTTGAATGAGTCGGATCTTAGCTTC	Coding region; positions 588 th -712 rd
<i>SARIP</i> -R4	CTGGAACATAATCCTCGTCATCTTC	
<i>SARIP</i> -F5	GGTGAAGGAGAAGGTGAGGT	Coding region (position 616 th)
<i>SARIP</i> -R5	TGCATCATACTGACTCCTCTA	to 3' UTR (position 510 th)

Table 2.17 The amplification conditions for amplification of genomic DNA sequences of *Cdc42* and *SARIP* genes

Gene homologue	Amplification condition	Component
I. <i>Cdc42</i> (F1/R1, F2/R1;used fifty-fold dilution of PCR products derived from F1/R1 as template), F3/R2	94°C for 5 minutes followed by 35 cycles of 94°C for 30 seconds, 60°C for 1 minute and 72°C for 3 minutes and the final extension at 72°C for 7 minutes	1X BD advantage [®] 2 PCR Buffer, 0.2 mM each of dNTPs, 0.5 μM of each primer, 1X BD Advantage [®] 2 polymerase mix
II. <i>Cdc42</i> (F4/R3, F5/R4, F6/R5)	As described in I.	1X <i>Ex Taq</i> Buffer (plus 2.0 mM MgCl ₂), 0.2 mM of each dNTPs, 0.5 μM of each primer and 0.5 unit of <i>TaKaRa Ex Taq</i> [™]
III. <i>SARIP</i> (F1/R1, F2/R2, F3/R3, F3/R4, F4/R4)	As described in I.	As described in I.
IV. <i>SARIP</i> (F4/R5, F5/R5;used fifty-fold dilution of PCR products derived from F4/R5 as template)	94°C for 3 minutes followed by 35 cycles of 94°C for 30 seconds, 50°C for 1 minute and 72°C for 3 minutes and the final extension at 72°C for 7 minutes	As described in I.

Purified DNA fragments were ligated with pGEM[®]-T easy (for DNA fragment smaller than 2.0 kb) (Promega) or pCR[®]-XL-TOPO (for DNA fragment larger than 2.0 kb) (Invitrogen) vector, transformed into Premade Z-competent[™] *E. coli* DH5α cell (Zymo Research) or competent *E. coli* stain JM109 and sequenced.

2.6.4 DNA sequencing and sequence assembly

The recombinant clones were unidirectional sequenced using the M13 forward and reverse primer on an automatic sequence. Nucleotide sequence from RACE-PCR product was assembled with the EST sequence to generate the completed full length cDNA of a particular transcript. Exon-intron boundaries were characterized followed the GT/AG rule (Bon *et al.*, 2003). Nucleotide sequences were

blasted against data in GenBank (<http://www.ncbi.nlm.nih.gov>) using BlastN (nucleotide similarity) and BlastX (translated protein similarity). Significant similarity was considered when the probability (E) value was $<10^{-4}$.

The transmembrane helices, protein domain, pI and molecular weight and hydrophobicity of deduced amino acids of transcripts were searched using TMHMM (<http://www.cbs.dtu.dk/services/TMHMM/>), SMART (<http://smart.embl-heidelberg.de/>), Protparam (<http://www.expasy.org/tools/protparam.html>) and ProtScale (<http://www.expasy.org/tools/protscale.html>), respectively.

2.7 Northern blot analysis

2.7.1 RNA sample preparation and blotting

Five microgram of total RNA extracted from various stages of ovaries and from other tissues of normal and eyestalk-ablated shrimp was mixed with the one-fourth volume of the 1.25X sample buffer (Table 2.18). The mixture was heat at 65°C for 10 minutes and immediately chilled on ice before electrophoresed through a 1.2% agarose gel containing 1X MOPS buffer and 3.7% formaldehyde. The electrophoresis was performed in 1X MOPS buffer. The gel was photographed under a UV illuminator.

The agarose gel containing RNA was downward transfer onto a positively-charge nylon membrane using 10X SSC; pH 7.0 (167 mM sodium citrate and 167 mM NaCl) for 3 hours (Figure 2.3). After blotting, the membrane was rinsed in 2X SSC for 10 minutes and UV-crosslinked at 0.12 joules/cm². The membrane was prehybridized with preheated at 68°C of DIG EasyHyb solution (Roche) for 30 minutes.

One microgram of the digoxigenin-labeled antisense cRNA probes (prepared as cRNA probes for *In situ* hybridization, please see 2.11.2.2) were denatured at 65°C for 5 minutes, immediately chilled on ice and transferred to preheated at 68°C of DIG EasyHyb to made a final concentration of 100 ng/ml. The probes solution was added and incubated at 68°C overnight.

Table 2.18 Sample buffer for RNA preparation before electrophoresis and Northern blot analysis

Component (1.25X)	
10X MOPS buffer; pH 7.0 (200 mM 3-(N-morpholino) propanesulphonic acid, 50 mM sodium acetate; pH 5.2, 10 mM EDTA)	100 μ l
37% formaldehyde	100 μ l
Formamide (deionized)	500 μ l
10X loading dye (0.4% Bromophenol blue, 50% glycerol, 1 mM EDTA)	100 μ l
Ethidium bromide (10 mg/ml)	2 μ l
Total volume	802 μl

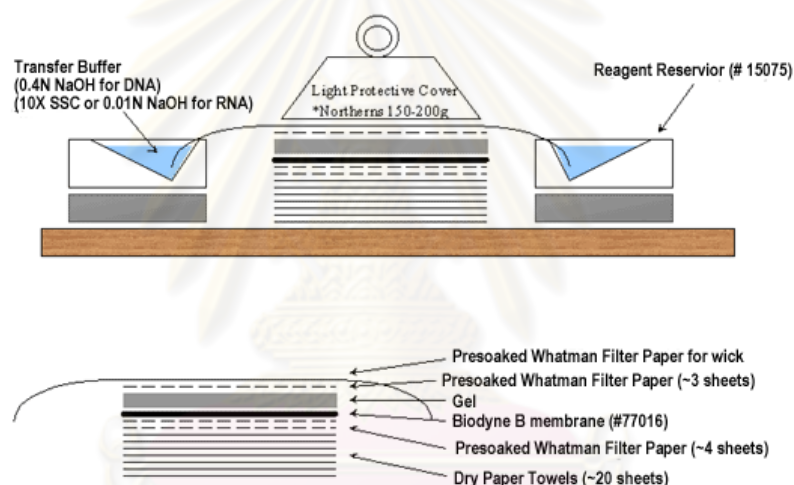


Figure 2.3 A typical downward nucleic acid transfer system. (available at <http://www.piercenet.com/Objects/>)

2.7.2 Post-Northern hybridization washing and detection

The membrane was washed twice in 2X SSC, 0.1% SDS for 5 minutes each at room temperature and twice in 0.1X SSC, 0.1% SDS for 15 minutes at 68°C. The washing was performed using a DIG wash and block buffer set and immunologically detected (anti-Digoxigenin-AP Fab fragment conjugated with alkaline phosphatase and NBT/BCIP) according to the manufacturer's instructions (Table 2.19) (Roche). 18S RNA of various tissues was used as the control.

Table 2.19 Profile and condition of post-northern blot hybridization wash (DIG wash and block buffer set)

Step	Condition
DIG washing buffer	2 minutes at room temperature, with shaking
DIG blocking buffer	30 minutes (or longer) at room temperature, with shaking
DIG blocking buffer with AP-labeled anti-DIG antibody (1:5000 dilution)	30 minutes at room temperature, with shaking
DIG washing buffer	15 minutes at room temperature, with shaking; twice
DIG detection buffer	2 minutes at room temperature, with shaking

2.8 Examination of expression patterns of genes related to ovarian development by RT-PCR and tissue distribution analysis

2.8.1 Primer design

Forward and reverse primers of each gene were designed from nucleotide sequence obtained from ESTs of typical, normalized and subtractive ovary cDNA libraries and libraries from other tissues of *P. monodon* (Table 2.20). Forward and reverse primers were also designed from RAP-PCR derived markers using Primer Premier 5.0 or Primer3 (Available at <http://frodo.wi.mit.edu/>) programs (Table 2.21).

In addition, forward and reverse primers were also designed from nucleotide sequence of ovary and testes forms of *PGMRC1* to identify whether *PGMRC1* in gonads of *P. monodon* were encoded from different loci. The sequence of primers were illustrated in Table 2.22

Table 2.20 Primer sequences and the expected size of the PCR product of gene homologue of *P. monodon* initially isolated by EST analysis

Gene/Primer	Sequence	T _m (°C)	Size (bp)
1. Phospholipid phospholipase C beta isoform (OV-N-S01-0075-W)			
F:	5'- CAGGTGGAGCAGGAGGC -3'	56.1	201
R:	5'- TCTGGAATAGACAAGCGTTC -3'	52.7	
2. Progesterone receptor-related protein p23 (OV-N-S01-0802-W)			
F:	5'- GCACAGGAGGCACTGAAAG -3'	52.5	155
R:	5'- CCATCGGCTGAAATCTACT -3'	55.5	
3. Small androgen receptor interacting protein (SARIP) (OV-N-S01-1107-W)			
F:	5'- GAACGAAACTTAACGAGCAGTGTGA -3'	62.9	157
R:	5'- ATCTCTTCCTGCTCTTTCTTCTTGC -3'	62.8	
4. cell division cycle 42 (Cdc42) (OV-N-S01-1131-W)			
F:	5'- AAATGCAGACCATTAAATGCGTAGT -3'	61.8	261
R:	5'- GGGATAACCACTGAGAAGCAGACTAA -3'	61.2	
5. M-phase inducer phosphatase (String protein Cdc25-like protein) (OV-N-S01-1905-W)			
F:	5'- TACCTGCTGGAGGGCGGCT -3'	65.1	172
R:	5'- GCGTGCTTCTGCTCTTGGC -3'	61.7	
6. Progesterin receptor membrane component 1 (PGMRC1) (OV-N-N01-0057-W)			
F:	5'- TTAATGGCAAGATCTTTGATGTCAC -3'	61.5	147
R:	5'- CACTGAGGTCATCGTACTCTTCCTT -3'	62.2	
7. Vitellogenin (OV-N-N01-0265-W)			
F:	5'- AGGCATCACAGTAACTGAGACCGAT -3'	64.5	172
R:	5'- CAGGTGTTGGGTAACGTTCTTGAC -3'	64.0	
8. Gonadotropin-regulated long chain acyl-CoA synthetase (GL-H-S01-0591-LF)			
F:	5'- TTATTGGTGACAAGCGGAAGTT -3'	59.3	232
R:	5'- GCATTGGAAGGAGCCAGTTTA -3'	59.6	
9. Low density lipoprotein receptor; vitellogenin receptor (HC-V-S01-0308-LF)			
F:	5'- TGAAGAGGGCTGTAGCGTGA -3'	59.1	224
R:	5'- ACCGAAACTCGTTCTGATTG -3'	55.0	

Table 2.20 (cont.)

Gene/Primer	Sequence	Tm (°C)	Size (bp)
10. keratinocytes associated protein 2 (OV-N-ST01-0003-W)			
F:	5'- CTGCTGTAAACAATCTGGAAAAC -3'	56.6	207
R:	5'- GGGACACCTGAGCGGAAGT -3'	59.4	
11. unknownST01-012 (OV-N-ST01-0012-W)			
F:	5'- CAACCTTTCATTTTCCTACGA -3'	55.0	481
R:	5'- TCTGCTGGGTCTTCCTCTGC -3'	60.0	
12. GAI7699-PA (OV-N-ST01-0013-W)			
F:	5'- GCTCAGTATGGCTGGTATG -3'	50.8	195
R:	5'- TTAGAGGAATCCGACAATG -3'	50.4	
13. unknownST01-022 (OV-N-ST01-0022-W)			
F:	5'- TCGGCTGAGTCAATAGAAGTAA -3'	55.0	163
R:	5'- CCTAACGCAAGGACAAACAA -3'	56.4	
14. CG17161-PA: Ser/Thr kinase chk1 (OV-N-ST01-0032-W)			
F:	5'- CTCCCAGTGTCTTATTGATTAG -3'	59.3	269
R:	5'- TGGCTTTCATTCCTCGCTG -3'	60.5	
15. 26S proteasome regulatory subunit rpn2 (OV-N-ST01-0048-W)			
F:	5'- AGTGATGAGTCGGTCTGCCT -3'	56.6	205
R:	5'- TCCTTTCCAAGATGATGCTGT -3'	57.1	
16. cytochrome c oxidase polypeptide IV (OV-N-ST01-0049-W)			
F:	5'- GCAGCAATGAGACTAAGACCAATA -3'	58.6	188
R:	5'- GGTGTTTCGCTTCAAGGAAAATA -3'	59.1	
17. coatomer protein complex (OV-N-ST01-0069-W)			
F:	5'- GGCAGCCAAGTCAGAGGA -3'	56.1	240
R:	5'- GGGTCGCTAAAGCCAGTG -3'	56.2	
18. procollagen-proline, 2-oxoglutarate 4-dioxygenase (protein disulfide isomerase; thyroid hormone binding protein p55) (P4HB) (OV-N-ST01-0105-W)			
F:	5'- AAGCAGCACCTTCTGTCTCA -3'	55.5	233
R:	5'- ACTGTAGCATCCATTTTCGC -3'	55.4	
19. DNA replication licensing factor mcm2 (OV-N-ST01-0123-W)			
F:	5'- TCAAGCGAGACAACAACGAACT -3'	60.1	321
R:	5'- TTGGACCATCACTGGGCATC -3'	61.0	

Table 2.20 (cont.)

Gene/Primer	Sequence	T _m (°C)	Size (bp)
20. <i>CWF19-like 2</i> (OV-N-ST01-0181-W)			
F:	5'- ATGTCTGTTTGCCTCCCCAC -3'	59.4	193
R:	5'- CTCAGCCGTTTCACTGTCTCA -3'	58.5	
21. <i>citrate synthase</i> (OV-N-ST01-0196-W)			
F:	5'- ACCTCAAAGATTGGTCGGC -3'	59.1	235
R:	5'- GCAGCACCTCCTGGTTAGCA -3'	61.0	
22. <i>unknownST02-006</i> (OV-N-ST02-0006-W)			
F:	5'- AAAGTAGACAGATACGCCAAGC -3'	56.2	348
R:	5'- ACAAGCAGCACCAATGTAATAA -3'	55.7	
23. <i>unknownST02-010</i> (OV-N-ST02-0010-W)			
F:	5'- TGGACAAACAACATCGCAGTA -3'	57.3	405
R:	5'- GCACCATTACCGACATCTT -3'	57.9	
24. <i>selenoprotein M precursor</i> (OV-N-ST02-0024-W)			
F:	5'- GACATCCCCTCTTCCATAAT -3'	53.1	240
R:	5'- TTTCATCTACAGTTCTTCCCTC -3'	53.2	
25. <i>Neuralized protein</i> (OV-N-ST02-0046-W)			
F:	5'- CTGACTTAGAACTGAGATTTGGGC -3'	59.5	351
R:	5'- AGTGGCGTGGTCGTGGAGGT -3'	64.7	
26. <i>thioesterase superfamily member 2</i> (OV-N-ST02-0057-W)			
F:	5'- AGAAATGACTGTGGAGAAAGA -3'	51.3	174
R:	5'- TCCCGATGTTGCTGCTGTT -3'	59.5	
27. <i>carbonyl reductase</i> (OV-N-ST02-0071-W)			
F:	5'- CAGTTTGTTCCTCCTTAG -3'	54.2	264
R:	5'- ATGCGTGTGAGAGCCGATAC -3'	58.3	
28. <i>Selenophosphate synthetase</i> (OV-N-ST02-0118-W)			
F:	5'- GAGGAGGATGTTCCGAAAGC -3'	59.7	313
R:	5'- CAGCCTGTTACGGGGTAG -3'	58.6	
29. <i>Egalitarian</i> (OV-N-ST02-0133-W)			
F:	5'- CACTTGTGCCCACTGTCTATG -3'	60.7	445
R:	5'- CCTCCACTGCCAACACTACTC -3'	59.8	

Table 2.20 (cont.)

Gene/Primer	Sequence	T _m (°C)	Size (bp)
30. RNA polymerase I associated factor 53 isoform 1 (OV-N-ST02-0147-W)			
F:	5'- CGTCGCACAAGGCAAAGAG -3'	60.0	387
R:	5'- CAAATCAACAGCAGAAGCAGC -3'	58.7	
31. Neutral alpha-glucosidase AB precursor (OV-N-ST02-0181-W)			
F:	5'- GTGCTGTGAAACCAGGGGAA -3'	60.5	448
R:	5'- GGAAGGGCATTGGGCTCTC -3'	61.6	

Table 2.21 Primer sequences, melting temperature and the expected product sizes of gene homologue designed from RAP-PCR fragments of *P. monodon*

Gene/Primer	Sequence	T _m (°C)	Size (bp)
1. B cell RAG associated protein (oligo-dT ₍₁₆₎ G-UBC 299)			
F:	5'- CTTGAAATGTGGGAAAACC -3'	52.6	258
R:	5'- TACCTCTTCTTCGTCATCTGT -3'	51.3	
2. hypothetical protein W02B8.3 (oligo-dT ₍₁₆₎ G-OPA 17)			
F:	5'- TGACATTCCCTCCAGACGCT -3'	60.1	318
R:	5'- GCTTCACTTACTTTAGGCACA -3'	52.9	
3. DNA replication licensing factor MCM5 (oligo-dT ₍₁₆₎ G-OPB 08)			
F:	5'- GCCAAGGAGGTAGCAGATGA -3'	57.6	343
R:	5'- CAGGGACAATGAAGAAGGGAT -3'	58.1	
4. Unknown (oligo-dT ₍₁₆₎ A-OPA 01)			
F:	5'- GCTGTCTTGATTCCCTCTCGG -3'	57.1	217
R:	5'- AACGGCTTCATAACCCCAT -3'	56.9	
5. ABC transporter (oligo-dT ₍₁₆₎ A-OPA 01)			
F:	5'- GGTGATCTATCCATTACTGTACG -3'	53.8	215
R:	5'- AGAATCCCGAGAAGAGCAAC -3'	55.9	
6. β-ketoacyl synthase (oligo-dT ₍₁₆₎ G-UBC 268)			
F:	5'- ATTGGGCAACCGAGTTATCA -3'	57.9	237
R:	5'- ACAAAGCCACCCGCAGTA -3'	56.9	

Table 2.21 (cont.)

Gene/Primer	Sequence	T _m (°C)	Size (bp)
7. Unknown (oligo-dT ₍₁₆₎ G-UBC 268)			
F:	5'- GGAGGACAGCAGAGTAAAA -3'	49.6	344
R:	5'- CAAAGCAGACAGTCAACATTC -3'	53.0	
8. alpha -1,6-mannosyl-glycoprotein beta-1,2-N-acetylglucosaminyltransferase, putative (oligo-dT ₍₁₆₎ A-UBC135)			
F:	5'- CAGGGACAGTGACCAAGAC -3'	52.3	347
R:	5'- GAAACGAGGAGTGATAGTAGAT -3'	50.0	
9. lysyl-tRNA synthetase (oligo-dT ₍₁₆₎ A-UBC135)			
F:	5'- ATAGTTGGAGGTATTGACAG -3'	46.3	260
R:	5'- ATTCTTCGGTAGGGAGGTT -3'	52.8	
10. Unknown (oligo-dT ₍₁₆₎ A-UBC191)			
F:	5'- CCTTCACTGTCCAGATTTCC -3'	54.1	321
R:	5'- CTTTTCTTTCCAACCGCTTC -3'	57.0	
11. APEX nuclease (apurinic/aprimidinic endonuclease) 2 (oligo-dT ₍₁₆₎ A-OPA02)			
F:	5'- ATGATTATTTTGGGCGGACT -3'	56.5	289
R:	5'- CCCTGAGAAACCAGAGCG -3'	55.9	
12. cystathionine gamma-lyase (oligo-dT ₍₁₆₎ G-OPB 08)			
F:	5'- GCCACAACCTTCAAGCAGG -3'	56.3	219
R:	5'- GCCGCCATACAGGTCATC -3'	56.4	
13. Thrombospondin (oligo-dT ₍₁₆₎ A-UBC 459)			
F:	5'- GGGCACGGATACATCTACAA -3'	55.8	170
R:	5'- TTACCCTGGAGACCTTCACT -3'	53.5	
14. U5 snRNP-specific protein (oligo-dT ₍₁₆₎ G-UBC 457)			
F:	5'- GAAGCCAAGTGTGTCCTCAT -3'	54.5	192
R:	5'- GCGGTATAAGAAAGTCCAAG -3'	52.2	
15. Moira CG18740-PA (oligo-dT ₍₁₆₎ G-UBC 138)			
F:	5'- TGTGGCTTCCTTGGCATCTG -3'	61.6	141
R:	5'- GCATTATCTGCGACATTCTTG -3'	56.1	
16. WD-repeat protein 1 (Actin-interacting protein 1) (AIP1) (oligo-dT ₍₁₆₎ G-OPA 14)			
F:	5'- CACCAAGGCTATCAACTCAG -3'	53.0	201
R:	5'- TTGCCATCAAATCCACCC -3'	56.6	

Table 2.22 Primer sequences, melting temperature and the expected product sizes from primers designed from *PGMRC1* homologues of ovarian and testicular forms of *P. monodon*

Gene/Primer	Sequence	T _m (°C)	Size (bp)
<i>PGMRC1</i>			
PGMRC1-OVTT-F:	5'- CTCCTCTATGCAGATGGACTCTGTC -3'	62.8	
PGMRC1-OV-R:	5'- GACCACCTTCGTCGTCAACA -3'	58.7	493
PGMRC1-TT-R:	5'- TGCTGTGTTTCAATGGGACC -3'	58.8	727

2.8.2 First strand cDNA synthesis

The first strand cDNA was synthesized from 1.5 µg of total RNA extracted from various tissues of each shrimp using TRI REAGENT® (Molecular Research Center). Fifth-teen micrograms of total RNA were treated with a RQ1 RNase-Free DNase I (Promega) to eliminate possible contamination of genomic DNA. DNase I digestion reaction was set up as described in Table 2.23. The reaction mixture was incubated at 37°C for 30 minutes.

Table 2.23 DNase I digestion reaction for elimination of genomic DNA from total RNA

Component	Volume
RNA in water or TE buffer (15µg)	up to 28.5 µl
RQ1 RNase-Free DNase 10X Reaction Buffer (400 mM Tris HCl; pH 8.0, 100 mM MgSO ₄ and 10 mM CaCl ₂)	4 µl
RQ1 RNase-Free DNase (0.5 Unit/1 µg RNA)	7.5 µl
Nuclease-free water	to a final volume of 40µl

An equal volume of phenol:chloroform:isoamylalcohol (25:24:1) was added to the mixture, mixed thoroughly and placed at room temperature for 10 minutes. The mixture was centrifuged at 12000 rpm for 10 minutes at 4°C. The aqueous phase was

transferred into a sterile microcentrifuge and extraction was repeated once with an equal volume of chloroform:isoamylalcohol. One-tenth volume of 3 M sodium acetate, pH 5.2 was added. DNA was precipitated by an addition of 2.5 volume of prechilled absolute ethanol and mixed thoroughly. The mixture was incubated at -80°C for 30 minutes. The precipitated DNA was recovered by centrifugation at 12000 rpm for 10 minutes at 4°C . After remove the supernatant, the DNA pellet was washed with 1 ml of 75% ethanol and centrifuged at 12000 rpm for 5 minutes at 4°C . After removed the supernatant, the DNA pellet was air-dried and resuspended in 12 μl of DNase-free H_2O and kept at -20°C until further needed.

One and a half micrograms of DNase-treated total RNA were reverse-transcribed to the first strand cDNA using an ImProm- IITM Reverse Transcription System Kit (Promega, U.S.A.). Total RNA was combined with 0.5 μg of oligo dT₁₂₋₁₈ and appropriate DEPC-treated H_2O in final volume of 5 μl . The reaction was incubated at 70°C for 5 minutes and immediately placed on ice for 5 minutes. Then 5X reaction buffer, MgCl_2 , dNTP Mix, RNasin were added to final concentrations of 1X, 2.25 mM, 0.5 mM and 20 units, respectively. Finally, 1 μl of ImProm- IITM Reverse transcriptase was add and gently mixed by pipetting. The reaction mixture was incubated at 25°C for 5 minutes and at 42°C for 90 minutes. The reaction mixture was incubated at 70°C for 15 minutes to terminate the reverse transcriptase activity. Concentration and rough quality of the newly synthesized first strand cDNA was spectrophotometrically examined ($\text{OD}_{260}/\text{OD}_{280}$) and electrophoretically analyzed by 1.0% agarose gels, respectively. The first stranded cDNA was 10 fold-diluted and kept at 20°C until required.

2.8.3 RT-PCR analysis

Typically, the amplification reactions were performed in a 25 μl reaction volume containing 10 mM Tris-HCl, pH 8.8 at 25°C , 50 mM KCl and 0.1% Triton X-100, 1.5-2.0 mM MgCl_2 , 100 or 200 μM each of dNTPs, 0.2 μM of each primer, 1 unit of DynazymeTM DNA Polymerase (FINNZYMES, Finland) and 2 μl of a 10 fold-diluted first strand cDNA (about 200 ng). RT-PCR was initially performed by predenaturation at 94°C for 3 minutes followed by 20, 25 and 30 cycles of denaturation at 94°C for 30 seconds, annealing at 53 (or 55°C) for 45 seconds and extension at 72°C for 30 seconds. The final extension was carried out at 72°C for 7

minutes. Five microlitres of the amplification products were electrophoretically analyzed though 1.0-2.0% agarose gel.

2.8.4 Tissue distribution analysis

2.8.4.1 Total RNA extraction and first strand cDNA synthesis

Total RNA was extracted from eyestalks, gills, heart, hemocytes, hepatopancreas, lymphoid organs, intestine, pleopods, stomach, testes and thoracic ganglion and ovaries of female broodstock *P. monodon* using TRIzol (Invitrogen). Ten micrograms of total RNA was treated with a TURBO DNA-free™ kit (Ambion) to eliminate possible contamination of genomic DNA. The First strand cDNA was synthesized from 1 µg DNase-treated total RNA using a QuantiTech Reverse® Transcription (Qiagen) according to the manufacturer's instructions. The synthesized cDNA was diluted to final concentration 5 ng/µl.

2.8.4.2 Tissue distribution analysis by RT-PCR

Twenty five nanograms of the DNase-treated first strand cDNA was used as the template for amplification of functionally important genes in a 20 µl reaction volume containing 1X *Ex Taq*™ Buffer (2.0 mM MgCl₂), 0.2 mM of each dNTPs, 0.5 µM of each primer and 0.5 unit of *TaKaRa Ex Taq*™ (Takara, Japan) RT-PCR was initially performed by predenaturation at 94°C for 5 minutes followed by 35 cycles of denaturation at 94°C for 30 seconds, annealing at 60°C for 30 seconds and extension at 72°C for 1 minute.

Althenatively, PCR was performed in a 20 µl reaction volume containing 10 mM Tris-HCl, pH 8.8 at 25°C, 50 mM KCl and 0.1% Triton X-100, 1.5 mM MgCl₂, 100 µM each of dNTPs, 0.2 µM of each primer and 1 unit of Dynazyme™ DNA Polymerase (FINNZYMES, Finland). RT-PCR was initially performed by predenaturation at 94°C for 3 minutes followed by 30 cycles of denaturation at 94°C for 30 seconds, annealing at 55°C for 45 seconds, extension at 72°C for 30 seconds minutes and the final extension at 72°C for 7 minutes. *Elongation factor-1α* was included as a positive control. Five microlitres of the amplification product was electrophoretically analyzed though 1.5-2.0% agarose gels.

2.9 Semiquantitative RT-PCR of functionally important gene homologues in ovaries of broodstock *P. monodon*

2.9.1 Experiment animals and the first strand cDNA synthesis

Male and female *P. monodon* broodstock were live-caught from Satun (Andaman Sea) and Angsila (Chonburi, Gulf of Thailand) and domesticated broodstock obtained from Banchong Farm. In addition, juvenile *P. monodon* males and females (approximately 20 g body weight, 4-month-old) were purchased from a local farm in Chachengsao.

Total RNA was extracted from stages I ($N = 10$), II ($N = 7$), III ($N = 7$) and IV ($N = 10$) ovaries of shrimp broodstock using TRI REAGENT[®]. The first strand cDNA was synthesized as described previously.

2.9.2 Primers

Expression levels of 5 genes related to ovarian development primers initially identified from subtractive ovaries cDNA libraries; *keratinocytes associated protein 2*, *Ser/Thr kinase chk1*, *DNA replication licensing factor mcm2*, *selenoprotein M precursor* and *Egalitarian*, and 5 transcripts identified from RAP-PCR; *B cell RAG associated protein*, *hypothetical protein W02B8.3*, *DNA replication licensing factor MCM5*, *APEX nuclease (apurinic/aprimidinic endonuclease) 2* and *U5 snRNP-specific protein* were determined. *EF-1 α* was used as an internal control.

2.9.3 Optimization of semi-quantitative RT-PCR conditions

Amplification was performed in a 25 μ l reaction volume containing 2 μ l of the first strand cDNA template diluted ten-fold, 1 x PCR buffer (10 mM Tris-HCl pH 8.8, 50 mM KCl and 0.1% Triton X – 100), 200 μ M each of dATP, dCTP, dGTP and dTTP and 1 unit of Dynazyme[™] DNA Polymerase (FINNZYMES, Finland). PCR was carried out using the conditions described in the standard RT-PCR.

2.9.3.1 Primer concentration

The optimal primer concentration for each primer pair (between 0.1-0.4 μ M) was examined using PCR conditions described above. The resulting product was

electrophoretically analyzed. The primer concentration that gave product specificity and clear results were selected for further optimization of PCR conditions.

2.9.3.2 MgCl₂ concentration

The optimal MgCl₂ concentration of each primer pair (between 1.0-4.0 mM MgCl₂) was examined using the standard PCR conditions and the optimized primer concentration. The concentration that gave the highest specificity was chosen.

2.9.3.3 Cycle numbers

The PCR amplifications were carried out at different cycles (e.g. 22, 24, 26 and 28 cycles) using the optimized concentration of primers MgCl₂ and analyzed by gel electrophoresis. The number of cycles that still provided the PCR product in the exponential range and did not reach a plateau level of amplification was chosen.

2.9.4 Agarose gel electrophoresis, semiquantitative RT-PCR and data analysis

An appropriate amount of agarose was weighed out and mixed with an appropriate volume of 1X TBE buffer (89 mM Tris-HCl, 89 mM boric acid and 2 mM EDTA, pH 8.3). The gel slurry was boiled in a microwave oven to complete solubilization, and allowed to lower than 60°C before poured into the gel mold. A comb was inserted. The gel was left to solidified. When needed, the comb was carefully removed. The agarose gel was submerged in a chamber containing an enough amount of 1X TBE buffer covering the gel for approximately 0.5 cm.

Appropriate volumes of PCR products were mixed with the one-fourth volume of the 10X loading dye (0.25% bromophenol blue and 25% Ficoll in water) and loaded into the well. A 100 bp DNA ladder was used as the standard DNA marker. Electrophoresis was carried out at 5-6 volts/cm until bromophenol blue moved to approximately one-half of the gel. The electrophoresed gel was stained with an ethidium bromide solution (2.5 µg/ml) for 5 minutes and destained in running tap water to remove unbound ethidium bromide from the gel. DNA fragments were visualized under a UV transilluminator through Molecular Imager[®] Gel Doc XR (Bio-Rad Laboratories, U.S.A). The intensity of target and control bands was quantified

from photographs of the gels using the Quantity One version 4.6.2 program (Bio-Rad Laboratories, U.S.A).

The expression level of each transcript was normalized by that of *EF-1 α* . Significantly different expression levels between different groups of *P. monodon* were tested using one way analysis of variance (ANOVA) followed by Duncan multiple range test ($P < 0.05$).

2.10 Examination of expression levels of interesting genes in ovaries of *P. monodon* by quantitative real-time PCR

Expression levels of several transcripts related to ovarian development, such as; *progesterin membrane receptor component 1 (PGRMC1)*, *small androgen receptor interacting protein (SARIP)*, *progesterone receptor-related protein p23* and *cell division cycle 42 (Cdc42)* were examined using quantitative real-time PCR analysis. The same set of cDNA templates was used for semiquantitative RT-PCR and quantitative real-time PCR of various genes.

2.10.1 Effects of serotonin on expression of genes in ovaries of juvenile *P. monodon*

The acclimated female juveniles of *P. monodon* (with the average body weight of 33.9 ± 6.40 g) were treated with serotonin ($50 \mu\text{g g}^{-1}$ body weight). Five groups of shrimp are single injected intramuscularly into the first abdominal segment of each shrimp and specimens are collected at 0 hr, 12, 24, 48 and 72 hr post injection (Treatment A). The normal saline control (0.85% at 0 hr, control A) is also included. In addition, other five groups of shrimp are repeatedly injected with the same amount of serotonin. The second injection is carried out at 3 days post initial injection and the specimens are collected at 0 hr, 12, 24, 48 and 72 hr after the second injection (Treatment B). The normal saline control (0.85% at 0 hr, control B) is also included. Ovaries of each sample were sampling and immediately placed in liquid N₂. The samples were stored at -80°C prior to RNA extraction and first-stand cDNA synthesis.

2.10.2 Primer design

The intron/exon structure of the target gene was characterized. Several primer pairs were designed from cDNA sequence of each gene and used to PCR

against genomic DNA as the template. The PCR fragment was cloned and sequenced. The forward or reverse primer covering intron/exon boundaries or alternatively, a primer pairs sandwiching the large intron was designed (Figure 2.4). A size of the expected PCR product size was approximately 100-200 bp or less than 500 bp (Table 2.24).

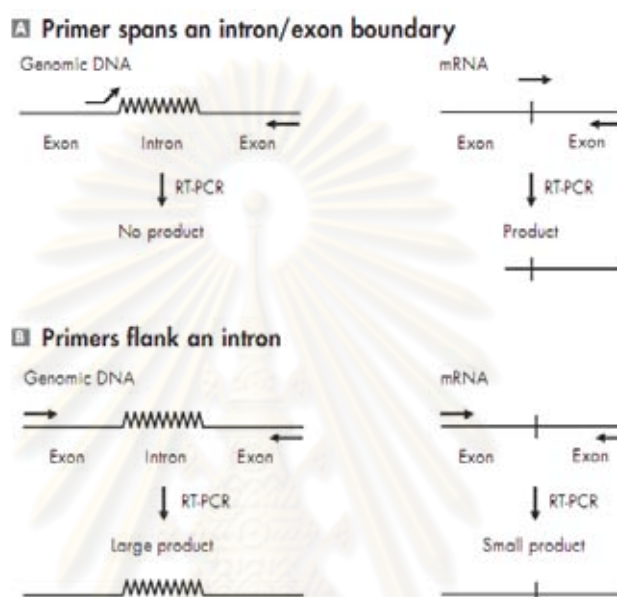


Figure 2.4 Two approaches of primer design to prevent amplification of the residual genomic DNA in the template for quantitative real-time RT-PCR based on primers spanning exon-intron boundaries (A) or primers flanking an intron (B).

For construction of the standard curve of each gene, the DNA segment covering the target PCR product and *EF-1 α* were amplified from primers for quantitative real-time PCR. The PCR products were cloned Plasmid DNA were extracted and used as the template for estimation of the copy number. A 10 fold-serial dilution was prepared corresponding to 10^3 - 10^8 molecules/ μ l. The copy number of standard DNA molecules can be calculated using the following formula:

$$X \text{ g}/\mu\text{l DNA} / [\text{plasmid length in bp} \times 660] \times 6.022 \times 10^{23} = Y \text{ molecules}/\mu\text{l}$$

The standard curves (correlation coefficient = 0.995-1.000 or efficiency higher than 95%) were drawn for each run. The standard samples were carried out in a 96 well plate and each standard point was run in duplicate.

2.10.3 Quantitative real-time PCR analysis

The target transcripts and the internal control *EF-1 α* of the synthesized cDNA were amplified in a reaction volume of 10 μ l using 2X LightCycler[®] 480 SYBR Green I Master (Roche, Germany). The specific primer pairs were used at a final concentration of 0.3 μ M (0.2 μ M for *progesterone receptor-related protein p23*). The thermal profile for SYBR Green real-time PCR was 95°C for 10 minutes followed by 40 cycles of 95°C for 15 seconds, 58°C for 30 seconds and at 72°C for 30 seconds. Cycles for the melting curve analysis was 95°C for 15 seconds, 65°C for 1 minute and at 98°C for continuation and cooling was 40°C for 10 seconds. The real-time RT-PCR assay was carried out in a 96 well plate and each sample was run in duplicate using a LightCycler[®] 480 Instrument II system (Roche).

For serotonin treatment, the target transcripts and the internal control *EF-1 α* of the synthesized cDNA were amplified in a reaction volume of 20 μ l using a QuantiTect[™] SYBR[®] Green PCR (Qiagen). Real-time PCR was carried out containing 10 μ l of 2x SYBR Green Master Mix (Qiagen). The thermal profile for SYBR Green real-time PCR was 95°C for 10 minutes followed by 40 cycles of 95°C for 30 s, 58°C for 1 min and at 72°C for 1 min. The real-time RT-PCR assay of each sample is run in duplicate using a Mx3000 QPCR system (Stratagene).

A ratio of the absolute copy number of the target gene and that of *EF-1 α* was calculated. The relative expression level between shrimp possessing different ovarian development (or treatment) were statistically tested using one way analysis of variance (ANOVA) followed by a Duncan's new multiple range test. Significant comparisons were considered when the *P* value was < 0.05.

2.11 *In situ* hybridization (ISH)

2.11.1 Sample preparation

Ovaries of normal and eyestalk-ablated *P. monodon* broodstock were fixed in 4% paraformaldehyde prepared in 0.1 M sodium phosphate buffered (pH 7.2) overnight at 4°C. The fixed was washed four times with PBS at room temperature and stored in 70% ethanol at -20°C until use. Tissues were histologically prepared, embedded in paraffin and sectioned onto silane-coated slides.

Table 2.24 Nucleotide sequences of primers used for quantitative real-time PCR analysis of *PGRMC1*, *SARIP*, *progesterone receptor-related protein p23* and *Cdc42* in *P. monodon*

Gene/Primer	Sequence	T _m (°C)	Size (bp)
<i>Progesterin membrane receptor component 1 (PGRMC1)</i>			
Real-time	F: 5'- TTAATGGCAAGATCTTTGATGTCAC -3'	61.5	147
	F: 5'- AAGGAAGAGTACGATGACCTCAGTG -3'	62.2	
Standard	F: 5'- ATGGCCGGACGAGGGAGCGGA -3'	71.4	573
	R: 5'- CTAATCATCCGTCTTCGCTT -3'	54.8	
<i>Small androgen receptor interacting protein (SARIP)</i>			
Real-time	F: 5'- GAACGAAACTTAACGAGCAGTGTGA -3'	62.9	157
	R: 5'- ATCTCTTCCTGCTCTTTCTTCTTGC -3'	62.8	
<i>Progesterone receptor-related protein p23</i>			
Real-time	F: 5'- ACGAAGCAGCACTGGCTCAAAG -3'	64.4	108
	R: 5'- CATCTGCCGCATCATCTCCTC -3'	62.7	
Standard	F: 5'- ATGTCAACCACACAGTCT TTGCC -3'	61.4	501
	R: 5'- ACACAGTTACTCCAGGTCAGG -3'	58.1	
<i>cell division cycle 42 (Cdc42)</i>			
Real-time	F: 5'- AAATGCAGACCATTAAATGCGTAGT -3'	61.8	261
	R: 5'- GGGATACCACTGAGAAGCAGACTAA -3'	61.2	
Standard	F: 5'- CTGCTGGGGAGCGTGAGA -3'	59.8	605
	R: 5'- GCGTCCTACCCTACAGAACA -3'	55.1	
<i>EF-1α</i>			
Real-time	F: 5'- TCCGTCTTCCCCTTCAGGACGTC -3'	68.4	215
	R: 5'- CTTTACAGACACGTTCTTCACGTTG -3'	61.1	
Standard	F: 5'- CGAGCCCAGTACTAAGAGCCTA -3'	58.7	1183
	R: 5'- GACCAAGATCGACAGGCGTACT -3'	60.8	

2.11.2 Preparation of cRNA probes

2.11.2.1 Addition of RNA polymerase recognition sequence (RPRS) by PCR

For adding RPRS to *PGMRC1* and *Cdc42*, gene-specific forward and reverse primers containing T7-RPRS (TAATACGACTCACTATAGGG) were designed (Table 2.25). *Thrombospondin (TSP)* cRNA probes were also performed as the condition control. Fifty nanograms of recombinant plasmid containing the complete ORF of target transcripts were used as the template in a 50 µl reaction volume containing 1X *Ex Taq*TM Buffer (2.0 mM MgCl₂), 0.2 mM of each dNTP, 0.2 µM of each primer and 1 unit of *TaKaRa Ex Taq*TM (Takara). PCR was initially performed by predenaturation at 94°C for 2 minutes (*TSP* and *PGMRC1*) or 1 minute (*Cdc42*) followed by 40 cycles of denaturation at 94°C for 30 seconds (*TSP* and *PGMRC1*) or 15 seconds (*Cdc42*), annealing at 60°C (*TSP* and *PGMRC1*) or 55°C (*Cdc42*) for 30 seconds and a 72°C extension for 1 minute.

For adding RPRS to *small androgen receptor interacting protein (SARIP)* and *progesterone receptor-related protein p23 (PGp23)*, a particular gene segment was amplified using gene-specific primers without the RPRS. The amplified product of each gene was diluted 100 fold. Forward and reverse gene-specific primers containing T7-RPRS; TAATACGACTCACTATAGGG and SP6-RPRS; ATTTAGGTGACACTATAGAA) was then used for the addition of it RPRS to the target genes. The *vitellogenin (VTG)* cRNA probe was also synthesized and used as the control (Table 2.26). PCR were carried out using the same component described above except the sense and antisense probes were simultaneously synthesized. The thermal profiles were predenaturation at 94°C for 5 minutes followed by 35 cycles of denaturation at 94°C for 30 seconds, annealing at 58°C for 30 seconds and extension at 72°C for 2 minutes.

The PCR products were purified using MinElute PCR purification Kit (Qiagen). The concentrations of purified PCR product were estimated by comparing with the DNA marker after electrophoresis.

Table 2.25 Primer sequences for preparation of templates for synthesis of *Cdc42*, *PGMRC1* and *TSP* antisense and sense cRNA probes of *P. monodon*

Primer combinations	
For antisense cRNA probe	
PGMRC1-F	5': AGAGTCCTTCCTGGGCTCACTA :3' (541 bp)
PGMRC1/T7-R	5': TAATACGACTCACTATAGGGCTTTGGTGCCTTTGCTTCCTC :3'
Cdc42-F	5': TAAGACCTGCCTCCTCATCTCC :3' (561 bp)
Cdc42/T7-R	5': TAATACGACTCACTATAGGGTGCCTACCTACAGAACAA :3'
TSP-F	5': GACGAGTGTCTGGTGGCTAATG :3' (914 bp)
TSP/T7-R	5': TAATACGACTCACTATAGGGACCATCAAAGTCAGAGGTGCAA :3'
For sense cRNA probe	
PGMRC1/T7-F	5': TAATACGACTCACTATAGGGAGAGTCCTTCCTGGGCTCACTA :3'
PGMRC1-R	5': CTTTGGTGCCTTTGCTTCCTC :3' (541 bp)
Cdc42/T7-F	5': TAATACGACTCACTATAGGGTAAGACCTGCCTCCTCATCTCC :3'
Cdc42-R	5': TGCGTCCTACCCTACAGAACAA :3' (561 bp)
TSP/T7-F	5': TAATACGACTCACTATAGGGGACGAGTGTCTGGTGGCTAATG :3'
TSP-R	5': ACCATCAAAGTCAGAGGTGCAA :3' (914 bp)

Table 2.26 Primer sequences for preparation of *SARIP* and *VTG* antisense and sense cRNA probes of *P. monodon*

Primer combinations	
For sense and antisense cRNA probe	
SARIP-T7/F	5': TAATACGACTCACTATAGGGCTGGAGTCCATATATCCAGAGGAAT :3'
SARIP-R/SP6	5': ATTTAGGTGACACTATAGAATCTTCATCCTCGAGGTCTAAGTCAT :3' (650 bp)
PGp23-T7/F	5': TAATACGACTCACTATAGGGATGTCAACCACACAGTCTTTGC :3'
PGp23-R/SP6	5': ATTTAGGTGACACTATAGAAGAGTCTTCATCCTCGAGGTCATC :3' (464 bp)
VTG-T7/F	5': TAATACGACTCACTATAGGGACCGACCCTTGTATTCTCTAATGC :3'
VTG-R/SP6	5': ATTTAGGTGACACTATAGAAAGCCGTCAACATTTAGGCTATGTAA :3' (927 bp)

2.11.2.2 Synthesis of cRNA probes

For synthesis of *Cdc42*, *PGMRC1* and *TSP* antisense and sense cRNA probes, 1 µg of each product (derived from F/T7-R primers for antisense or T7-F/R primers for sense) was used as template for synthesis of antisense and sense cRNA probes using a Toyobo ScriptMAX kit (Toyobo) and PCR DIG labeling mix (Roche). The mixture was incubated at 42°C for 2 hours.

For *SARIP* and *VTG* cRNA probes, 300 ng of purified products, T7 or SP6 RNA polymerase (Takara, Japan) and PCR DIG labeling mix (Roche, Germany) were used for synthesis of sense and antisense cRNA probes, respectively. The mixture was incubated at 42°C (for T7) or 37°C (for SP6) for 2 hours. DNA was eliminated by treating cRNA probes with DNase I (TURBO DNA-free™ kit; Ambion) according to the manufacturer's protocols.

For *PGp23* cRNA probes, 1 µg of purified products were used for synthesis of sense and antisense cRNA probes using a DIG RNA Labeling Kit (Roche). The mixture was incubated at 37°C for 2 hours. DNA was eliminated by treated cRNA probes with 2 µl DNase I at 37°C for 15 minutes. The activity of enzymes was stopped by adding 2 µl of 0.2 M EDTA (pH 8.0).

The success of cRNA synthesis was determined by electrophoresis. The synthesized cRNA was purified using an RNeasy Mini Elute Clean up Kit (Qiagen) and the probe concentration was spectrophotometrically measured. The cRNA probe was stored at -80°C until needed.

2.11.2.3 Dot blot analysis (*Cdc42*, *PGMRC1* and *TSP*)

The quality of cRNA probes was determined before used for *in situ* hybridization. Plasmid DNA containing the target gene was 10 fold diluted to 10 ng/µl, 1 ng/µl, 100 pg/µl and 10 pg/µl. One microliter of each DNA solution was spotted on the nylon membrane. The spotted double stranded cDNA was denatured by alkaline treatment, neutralized and fixed using UV cross linking (0.12 joules/cm²). The membranes were pre-hybridization with the DIG easyHyb solution (Roche) at 50°C for 30 minutes and hybridized with the DIG easyHyb solution containing 100 ng/ml of the denatured DIG-labeled cRNA probe at 50°C for 3 hours. The membrane

was washed twice in 2X SSC (with 0.1% SDS) at room temperature for 5 minutes followed by 0.1X SSC (with 0.1% SDS) once at room temperature and twice at 68°C for 15 minutes. The membranes were briefly washed with TBS with 0.1% tween 20. The dot bot signal was detected as described for *in situ* hybridization.

2.11.3 Hybridization and detection

After deparaffinized, the sections were prehybridized in the hybridization buffer (50% Formamide, 2X SSC, 1 µg/µl tRNA, 1 µg/µl Salmon sperm DNA, 1 µg/µl BSA and 10% Dextran sulfate) (Wako) at 50°C for 30 minutes. The digoxigenin (DIG)-labeled sense or antisense cRNA probe was added to the hybridization buffer (pre-warmed at 50°C) and incubated overnight at 50°C. The sections were rinsed in 4X SSC twice at 50°C for 5 minutes, and 2X SSC containing 50% formamide at 50°C for 20 minutes. After equilibration in the RNase buffer (0.5M NaCl; 10mM Tris-HCl, pH8.0; 1mM EDTA) at 37°C for 30 minutes, single-strand RNA was digested with 10 µg/ml of RNase A at 37°C for 30 minutes. The sections were washed four times with the RNase A buffer at 37°C for 10 minutes. The sections were rinsed with 2X SSC four times at 50°C for 15 minutes and 0.2X SSC twice at 50°C for 20 minutes each. DIG was immunologically detected (anti-Digoxigenin-AP Fab fragment conjugated with alkaline phosphatase and NBT/BCIP) according to the manufacturer's instructions (Roche, Germany).

2.12 Production of the polyclonal antibody and western blot analysis

2.12.1 Polyclonal antibody raise against Cdc42

The polyclonal antibody (PcAb) against Cdc42 was purchased from a commercial company (Santa Cruz Biotechnology Inc.) (Table 2.27).

2.12.2 Production of the polyclonal antibody against PGMRC1

A synthetic peptide and polyclonal antibody was commercially carried out by Sigma. A synthetic C-terminal peptide (CEAKDTKAKTDD) (Table 2.27) of PGMRC1 of *P. monodon* conjugated with keyhole limpet hemocyanin was immunized into two rabbits during the intervals of 7 weeks. Titers of serum as examined at pre-immunized and after the fifth and sixth injections by ELISA.

Anti-PGMRC1 was purified using HiTrap NHS-activated HP affinity column chromatography according to the manufacturer's instruction (GE Healthcare). A synthetic peptide of PGMRC1 in the coupling buffer (0.2 M NaHCO₃, 0.5 M NaCl; pH 8.3) was coupled into the HiTrap NHS-activated HP column. The column was then alternately washed with Buffer A (0.5 M ethanolamine, 0.5 M NaCl; pH 8.3) and Buffer B (0.1 M acetate, 0.5 M NaCl; pH 4.0) to deactivate any excess active groups that were not coupled to the ligand and to wash out the non-specifically bound ligands. The filtered anti-PGMRC1 was adjusted to the composition of the start buffer (binding buffer) by buffer exchange using the PD-10 Desalting column.

Table 2.27 Detailed information of the polyclonal antibody against Cdc42 and PGMRC1

Antibody against	Source	Sequence	Company
Cdc42 (commercial available)	Rabbit Polyclonal antibody raised against amino acids 1-191 of Cdc42 of <i>Saccharomyces cerevisiae</i>	MQTLKCVVVG DGAVGKTCLLI SYTTNQFPADYVPTVFDNYAV TVMIGDEPYTLGLFDTAGQED YDRLRPLSYPSTDVFLVCFSVIS PPSFENVKEKWFPEVHHHCPG VPCLVVG TQIDLRDDKVIIEKL QRQRLRPITSEQGSRLARELKA VKYVECSALTQRGLKNVFDEA IVAAL EPPVIKSKKCAIL	Santa Cruz Biotechnology Inc.
PGMRC1 (synthesized antibody)	Synthetic peptide conjugated with KLH MBS Rabbit Polyclonal antibody raised against PGMRC1 of <i>P. monodon</i>	<u>CEAKDTKAKTDD</u>	Sigma

The ligands-coupled HiTrap NHS-activated HP column was connected to the AKTA Prime FPLC Protein Purification System (Pharmacia). The system was equilibrated by 5 ml of the binding buffer (10 mM sodium phosphate buffer; pH 7.0

and 0.15 M NaCl). The filtered anti-PGMRC1 was then injected into the system and the column was washed with 10 ml binding buffer. The anti-PGMRC1 was eluted from the column by adding 10 ml of the elution buffer (0.1 M Glycine-HCl; pH 2.7). The elution solution was fractionated in 1 ml each and the concentration of the purified anti-PGMRC1 was determined by the dye binding method (Bradford, 1976) using Bio-Rad Protein assay (Bio-Rad Laboratories). IgG was used as the protein standard. The purified solution was kept in PBS containing 1 mg/ml BSA (-) and stored at -20°C.

2.12.3 Sample preparation

Ovarian tissues of *P. monodon* were homogenized in the sample buffer (50 mM Tris-HCl; pH 7.5, 0.15 M NaCl) supplemented with the proteinase inhibitors cocktail (EDTA free; Roche). The homogenate was centrifuged at 12000g for 30 minutes at 4°C. The supernatant was transferred to a new tube. Protein concentrations of the tissues extract were determined by the dye binding method (Bradford, 1976). Twenty-five microliters of proteins were heated at 100°C for 5 min and immediately cooled on ice. Proteins were size-fractionated on a 15% SDS-PAGE (Laemmli, 1970).

2.12.4 Western blot analysis

Proteins separated with SDS-PAGE were transferred onto a PVDF membrane (Hybond P; GE Healthcare) (Towbin, 1979) in 25 mM Tris, 192 mM glycine (pH 8.3) buffer containing 10% methanol at a constant current of 350 mA for 1 hour. The membrane was treated in the DIG blocking solution (Roche) for 1 hour and incubated with the primary antibody (1:100 in the blocking solution) for 1 hour at room temperature. The membrane was washed 3 times with 1X Tris-buffer saline tween-20 (TBST; 50 mM Tris-HCl, 0.15 M NaCl, pH 7.5, 0.1% Tween-20) and incubated with goat anti rabbit IgG (H+L) conjugated with alkaline phosphatase (Bio-Rad Laboratories) at 1:3000 for 60 minutes and then washed 3 times with 1X TBST. Visualization of immunoreactional signals was carried out by incubating the membrane in NBT/BCIP (Roche) as a substrate. The color reaction was stopped by transferring the membrane into water.

2.13 Immunohistochemistry

The paraffin sections were prepared from pieces of ovaries fixed with 4% paraformaldehyde (Cdc42) or Davidson's fixative (PGMRC1). De-paraffinized sections were autoclaved in 0.01 M citric acid buffer (pH 6.0) containing 0.1% Tween-20 for 5 minutes. The sections were then incubated in the blocking solution I (3% H₂O₂ in methanol) for 15 min. After treatment in the blocking solution II (Roche) for 1 hour, sections were incubated with purified anti-PGMRC1 PcAb for 1 hour in a humid chamber. For Cdc42, the sections were incubated with different dilution of the antibody (at 1:30, 1:100 and 1:300). The sections were rinsed three times for 5 minutes with PBS(-), pH 7.2-7.4 (0.35 g NaH₂PO₄, 1.28 g Na₂HPO₄ and 8 g NaCl in 1000 ml of distilled H₂O) and incubated with goat anti-rabbit IgG conjugated with horse radish peroxidase (simple stain PO, Nichirei) for 30 minutes. The sections were again rinsed three times for 5 minutes with PBS(-), pH 7.2-7.4. Localization of antigen was visualized using diaminobenzidine (Wako) as the substrate. Tissue sections were also incubated with the normal sera (PGMRC1) or blocking solution II (Cdc42 and PGMRC1) to examine the specificity of antisera. The sections were dehydrated and mounted for long term storage.

2.14 *In vitro* expression of the full length cDNA using the bacterial expression system

2.14.1 Primers design

A primer pair was designed to amplify the full length cDNA of *Cdc42* and *progesterone receptor-related protein p23*. The forward primer containing *Nde* I site, and reverse primer containing *Bam* HI site and six Histidine residues encoded nucleotides were illustrated in Table 2.28.

2.14.2 Construction of recombinant plasmid in cloning and expression vectors

The full length cDNA of *Cdc42* and *progesterone receptor-related protein p23* were amplified by PCR, ligated to pGEM[®]-T Easy vector and transformed into *E. coli* JM109. Plasmid DNA was extracted from a positive clone and used as the template for amplification using 0.5 μM of each forward primer containing *Nde* I site,

and reverse primer containing *Bam* HI site and 6-repeated Histidine encoded nucleotides, 0.75-1.5 unit *Pfu* DNA polymerase (Promega) and 0.2 mM of each dNTPs. The thermal profiles were predenaturation at 95°C for 2 minutes followed by 25 cycles of denaturation at 95°C for 45 seconds, annealing at 60°C for 30 seconds, extension at 72°C for 4 minutes and final extension at 72°C for 7 minutes.

Table 2.28 Nucleotide sequences of primers used for *in vitro* expression of *Cdc42* and *progesterone receptor-related protein p23* of *P. monodon*

Primer	Sequence
Full length cDNA	
Cdc42	F: 5'- CTGCTGGGGAGCGTGAGA -3' R: 5'- GCGTCCTACCCTACAGAACA -3'
Progesterone receptor-related protein p23	F: 5'- <u>ATGTCA</u> ACCACACAGTCT TTGCC -3' R: 5'- ACACAGTTACTCCAGGTCAGG -3'
Full length cDNA containing restriction site and 6 repeated-Histidine encoded nucleotides	
Cdc42-Nde I	F:5'- CCGC <u>ATATGC</u> AGACCATTAATGCGTAGTGGT -3'
Cdc42-6His and Bam HI	R:5'- GGCGGATCCCTA <u>ATGATGATGATGATGATG</u> CAGAACAATACATTTCTTCGT -3'
Progesterone receptor-related protein p23-Nde I	F:5'- CCGC <u>ATATGT</u> CAACCACACAGTCTTTGCC -3'
Progesterone receptor-related protein p23-6His and Bam HI	R:5'- GGCGGATCCTTA <u>ATGATGATGATGATGATG</u> CTCCAGGTCAGGGAGATCGT -3'

*underline = *Nde* I or *Bam* HI restriction site, Double underlines = start or stop codon, dash line = Histidine usage codon

The amplification product was analyzed by agarose gel electrophoresis and the gel-eluted product was digested with *Nde* I and *Bam* HI. The digested DNA fragment was again analyzed by agarose gel electrophoresis and the gel-eluted product was ligated with pET-15b (for *Cdc42*) or pET-32a(+) (for *progesterone receptor-related protein p23*) expression vectors and transformed into *E. coli* JM109. Plasmid DNA of the positive clones was sequenced to confirm the orientation of recombinant clones. The corrected direction of plasmid DNA of *Cdc42* and *progesterone receptor-related protein p23* was subsequently transformed into *E. coli* BL21-CodonPlus (DE3)-RIPL (genotype strain: *E. coli* BF⁻*ompT hsdS*(r_B⁻m_B⁻) *dcm*⁺ Tet^r *gal*λ(DE3) *endA* The [*argU proL Cam*^r] [*argU ileY leuW Strep/Spec*^r]) and *E. coli* BL21 (DE3)plysS

(genotype strain: B F⁻ *dcm ompT hsdS*(r_B⁻ m_B⁻) *galλ* (DE3) [pLysS Cam^r]) competent cells, respectively.

2.14.3 Expression of recombinant proteins

A single colony of recombinant *E. coli* BL21-CodonPlus (DE3)-RIPL or *E. coli* BL21 (DE3)pLysS carrying desired recombinant plasmid was inoculated into 3 ml of LB medium, containing 50 µg/ml ampicillin and 50 µg/ml chloramphenicol at 37°C. Fifty microlitres of the overnight cultured was transferred to 50 ml of LB medium containing 50 µg/ml ampicillin 50 µg/ml chloramphenicol and further incubated to an OD₆₀₀ of 0.4-0.6. After IPTG induction (1.0 mM final concentration), appropriate volume of the culture corresponding to the OD of 1.0 was time-interval taken (0, 1, 2, 3, 4, 6 hours and overnight at 37°C) and centrifuged at 12000g for 1 minute. The pellet was resuspended in 1X PBS buffer and examined by 15% SDS-PAGE (Laemmli, 1970).

In addition, 20 ml of the IPTG induced-cultured cells at the most suitable time-interval were taken (6 hours or overnight at 37°C or lower), harvested by centrifugation 5000 rpm for 15 minutes and resuspended in the lysis buffer (0.05 M Tris-HCl; pH 7.5, 0.5 M Urea, 0.05 M NaCl, 0.05 M EDTA; pH 8.0 and 1 mg/ml lysozyme). The cell wall was broken by sonication using Digital Sonifier[®] sonicator Model 250 (BRANSON). The bacterial suspension was sonicated 2-3 times at 15-30% amplitude, pulsed on for 10 seconds and pulsed off for 10 seconds in a period off 2-5 minutes. Soluble and insoluble portions were separated by centrifuged at 14000 rpm for 30 minutes. The protein concentration of both portions was measured using a dye-binding assay (Bradford, 1972). Expression of the recombinant protein was electrophoretically analyzed by 15% SDS-PAGE.

2.14.4 Detection of recombinant proteins

Recombinant protein was analyzed in 15% SDS-PAGE. The electrophoresed proteins were transferred to a PVDF membrane (Hybond P; GE Healthcare) (Towbin, 1979). The membrane was washed three times with 1X Tris-buffer saline tween-20 (TBST; 25 mM Tris, 137 mM NaCl, 2.7 mM KCl and 0.05% tween-20) for 10 minutes, blocked with 20 ml of a blocking buffer (1.0 g of BSA in 20 ml of 1X TBST) and incubated for 1 hour at room temperature with gentle shaking. The membrane was

washed three times in 1X TBST and incubated with diluted Mouse Anti-His antibody IgG2a (GE Healthcare; 1:5,000) in the blocking buffer for 1 hour. The membrane was incubated with diluted goat anti-mouse IgG (H+L) conjugated with alkaline phosphatase (Promega, U.S.A.; 1:10,000) in the blocking buffer for 1 hour. Visualization of immunoreactional signals was carried out by incubating the membrane in NBT/BCIP (Roche) as a substrate. The color reaction was stopped by transferring the membrane into water.

2.14.5 Purification of recombinant proteins

Recombinant protein was purified by using a His GraviTrap kit (GE Healthcare). Initially 1 litre of IPTG-induced cultured at the optimal time and appropriate temperature was harvested by centrifugation at 5000 rpm for 15 minutes. The pellet was resuspended in the binding buffer (20 mM sodium phosphate, 500 mM NaCl, 20 mM imidazole, pH 7.4), sonicated and centrifuged at 14000 rpm for 30 minutes. The soluble and insoluble fractions were separated. Soluble fraction composed of the recombinant protein was loaded into column. The column was washed with 10 ml of binding buffer containing 20 mM imidazole (20 mM sodium phosphate, 500 mM NaCl, 20 mM imidazole, pH 7.4), 5 ml of the binding buffer containing 50 mM imidazole (20 mM sodium phosphate, 500 mM NaCl, 50 mM imidazole, pH 7.4) and 5 ml of the binding buffer containing 80 mM imidazole (20 mM sodium phosphate, 500 mM NaCl, 80 mM imidazole, pH 7.4). The recombinant protein was eluted with 6 ml of the elution buffer (20 mM sodium phosphate, 500 mM NaCl, 500 mM imidazole, pH 7.4). Each fraction of the washing and eluting step were analyzed by SDS-PAGE and western blotting. The purified proteins were stored at 4°C or -20°C for long term storage.

2.14.6 Polyclonal antibody production

Polyclonal antibody against progesterone receptor-related protein p23 was immunologically produced from the purified rPG23 protein in a rabbit by Faculty of Associated Medical Sciences, Changmai University. Western blot analysis was carried out to examine specificity and sensitivity of the antibody.

CHAPTER III

RESULTS

3.1 Construction of typical, normalized and suppression subtractive hybridization (SSH) cDNA libraries from ovaries of *P. monodon*

3.1.1 A typical ovarian cDNA library of *P. monodon*

A typical ovaries cDNA library was established for isolation of genes involving ovarian (and oocyte) development in *P. monodon*. Initially, mRNA was purified from total RNA extracted from vitellogenic ovaries of wild *P. monodon* broodstock. Five micrograms of mRNA was reversed transcribed and second-stranded synthesized using a ZAP-cDNA Synthesis and Cloning Kit (BD Biosciences Clontech). cDNA were then sized-fractionated by gel filtration (Sepharose CL-2B). Fractions were collected and a 5 µl aliquot of each fraction was examined in 5% native polyacrylamide gels. Fractions contained cDNA greater than 500 bp fragments, which were free from adaptors, were selected and pooled.

Size-selected cDNAs (>500 bp) were cloned into dephosphorylated *Eco* RI/*Xho* I-digested Uni-ZAP[®] XR and transfected into *E. coli* XL1-Blue MRF'. The lambda library was converted into the pBluescript library by *in vivo* excision. Recombinant clones were selected by a lacZ' system following standard protocols (Sambrook and Russell, 2001). Recombinant clones were randomly selected from those carrying insert sizes greater than 500 bp (Srisuparbh *et al.*, 2003) by colony PCR. Clones carrying the inserted sizes > 500 bp were further analyzed (Figure 3.1). Plasmid DNA is extracted and digested with *Eco* RI-*Xho* I (or *Eco* RI-*Apa* I) for qualification checked (Figure 3.2). The selected plasmid DNA of ESTs were unidirectional sequenced from the 5' direction on a MegaBase 1000 automated DNA sequencer (Amersham Biosciences). Nucleotide sequences were compared with those previously deposited in the GenBank using BLASTN and BLASTX.

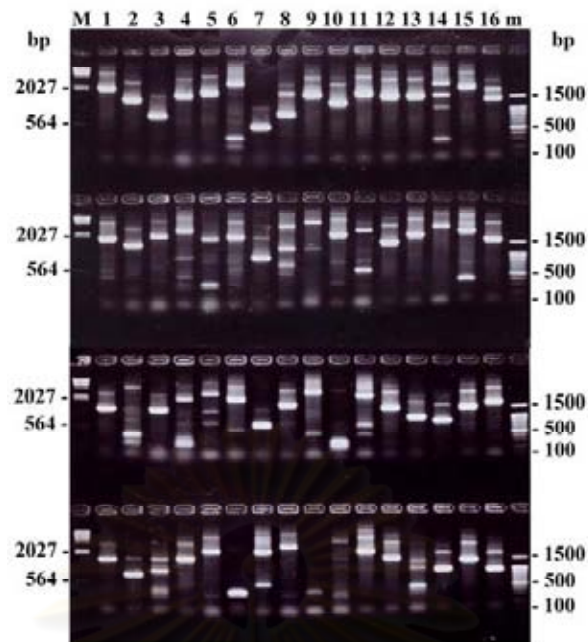


Figure 3.1 Estimation of insert sizes by colony PCR. Recombinant clones carrying insert sizes greater than 500 bp from the typical cDNA libraries of *P. monodon* were sequenced. Lanes M and m are λ -*Hind* III and a 100 bp DNA ladder, respectively.

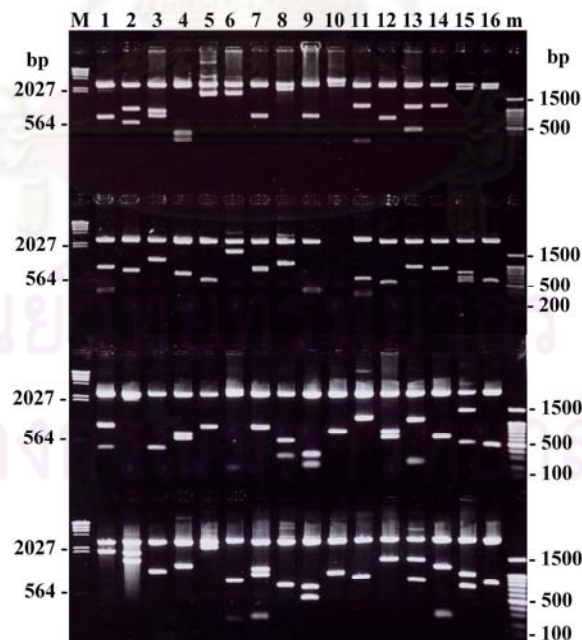


Figure 3.2 Recombinant plasmid DNA of the typical cDNA libraries of *P. monodon* digested with *Eco* RI-*Xho* I (or *Eco* RI-*Apa* I). Lanes M and m are λ -*Hind* III and 100 bp DNA ladder, respectively.

The primary titer of a cDNA library was approximately 4×10^6 pfu/ml. The first phase of EST analysis of a typical ovarian cDNA library was carried out. From 1051 recombinant clones sequenced, a total of 830 ESTs (79.0%) corresponded to known sequences in the GenBank (E-value $< 10^{-4}$) whereas the remaining sequences were regarded as novel (unknown) transcripts (21.0%, E-value $> 10^{-4}$). Homologues of *TSP* (79 clones, 7.5% of sequenced clones) and *peritrophin* (87 clones, 8.3%) were abundantly expressed in vitellogenic ovaries of *P. monodon* (Table 3.1).

Table 3.1 The percentage and number of clones found in the first phase of EST analysis of a typical ovarian cDNA library of *P. monodon*

Transcripts	Number of clones (%)
Known transcripts (excluding peritrophin and thrombospondin)	664 (63.2%)
Ovarian peritrophin	87 (8.3%)
Thrombospondin	79 (7.5%)
Unknown genes	221 (21.0%)
Total	1051 (100%)

Among known transcripts in the first phase of EST analysis of a typical ovarian cDNA library of *P. monodon*, ESTs categorized to members of signaling and communication were predominant (14.6%) followed by those classified as members of miscellaneous function (12.0%), unidentified function (10.1%), gene expression and protein synthesis (6.7%), metabolism (6.0%) and internal/external structure (5.0%) groups. The remaining ESTs allocated to other functional categories were accounted for less than 5.0% of the characterized ESTs in this library (Figure 3.3).

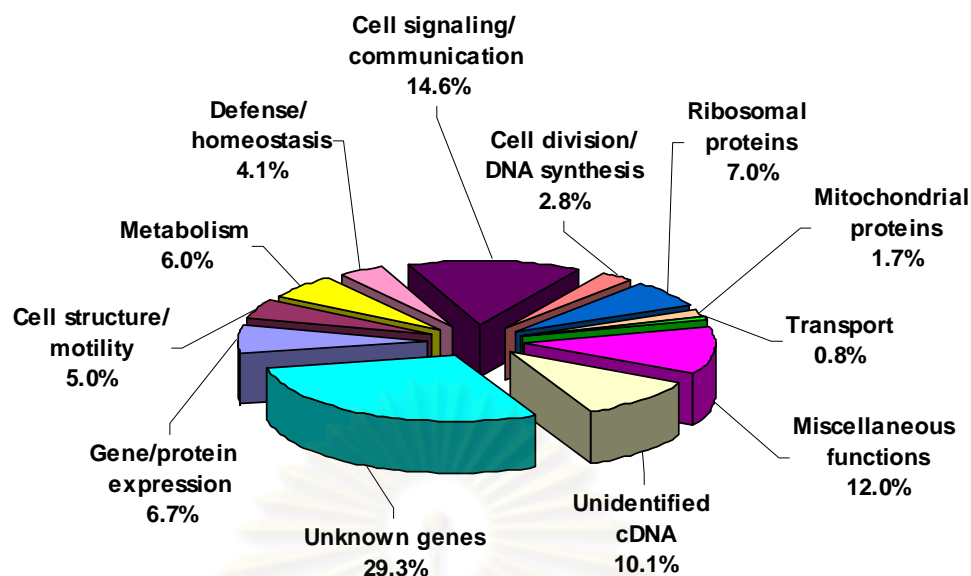


Figure 3.3 Classification of genes identified in the first phase of EST analysis of an ovarian cDNA libraries of *P. monodon* (E-value < 10^{-4}) owing to functional categories of their homologues.

The percent distributions of sequences in the first phase of a typical ovarian cDNA library were also classified according to 3 principal GO ontology categories. For the biological process, ESTs involved in the cellular process (e.g. *glutamate oxaloacetate transaminase 2*, *chicadae/profilin* and *ubiquitin-activating enzyme E1*) predominated (35.2%) followed by those involved in the metabolic process (e.g. *transcription factor Dp-2* also called *E2F dimerization partner 2*), *40S ribosomal protein S3a* and *mcm7 protein*, 27.6%). ESTs functional ontology involved in reproduction and reproductive process were found at 1.3% and 0.4% for the first phase of EST analysis, respectively.

For the cellular component category, ESTs involved in the cell part (e.g. *cathepsin D*, *modifier 1* and *chaperonin*) predominated (34.2%) followed by those play their roles in the organelles (e.g. *ribosomal protein L3*, *ATP/ADP translocase* and *adipophilin* also called *adipose differentiation-related protein, ADRP, isoform 3*, 24.5%).

For the molecular function category, ESTs involved in the binding function (45.2%, such as *L-3-hydroxyacyl-Coenzyme A dehydrogenase; short chain*, *RuvB-like protein 2* and *Calreticulin CG9429-PA isoform 1*) predominated followed by those involved in the catalytic activity (e.g. *AF479772_1 allergen Pen m 2*, *tissue specific transplantation antigen P35B* and *DNA mismatch repair protein Msh2 (MutS protein homolog 2) mismatch repair protein*, 27.2%) (Table 3.2; Figure 3.5).

Five hundred and fifty-three transcripts (96 contigs; from 594 transcripts and 457 singletons; 43.5%) were obtained after clustering analysis of 1051 ESTs from the first phase of EST analysis (Table 3.3).

Transcripts involved in reproduction found in the first phase of EST analysis of a typical ESTs ovarian cDNA library were identified using GO ontology function. These included *twin CG31137-PB, isoform B (carbon catabolite repressor protein)* and *oncoprotein nm23*. A homologues of sex-linked or sex differentiation-related transcripts found in the first phase of EST analysis of an ovarian cDNA library of *P. monodon* were investigated (Table 3.4).

Moreover, the full length cDNA of transcripts involved in important function were further characterized. These included *Cdc20* (biological process GO:0007096), *Cdc42* (biological process GO:0032501) and *small androgen receptor-interacting protein: a RWD domain containing 1*. Notably, *SARIP* is a thymus involution related protein that may indirectly affect AR signaling pathway in mammal but the actual function is unknown (Kang *et al.*, 2008)

In addition, transcripts involved in growth according to the GO ontology function were also identified including *ATP lipid-binding protein like protein*, *H3 histone, family 3A*, *tubulin beta-2 chain (beta-II tubulin) beta-II tubulin* and *glutaminyl-tRNA synthetase (glutamine--tRNA ligase) (GlnRS)*.

Surprisingly, *laminin beta chain* and *ubiquitin-conjugating enzyme (Ubc-2)* were classified into GO ontology functions involving both reproduction and growth.

Table 3.2 Classification of nucleotide sequences according to three principal GO categories of the first phase of EST analysis (1051 ESTs) of a typical ovarian cDNA library of *P. monodon*

Type	Term	Number of sequences	Percentages
Biological process	immune system process	1	0.2
	maintenance of localization	1	0.2
	multi-organism process	1	0.2
	reproductive process	2	0.4
	locomotion	2	0.4
	growth	5	1.1
	reproduction	6	1.3
	response to stimulus	10	2.2
	multicellular organismal process	17	3.7
	biological adhesion	18	3.9
	biological regulation	23	5.0
	developmental process	24	5.2
	establishment of localization	29	6.3
	localization	32	7.0
	metabolic process	127	27.6
cellular process	162	35.2	
Cellular component	extracellular region part	2	0.5
	envelope	11	2.6
	membrane-enclosed lumen	13	3.1
	extracellular region	27	6.4
	organelle part	54	12.7
	macromolecular complex	68	16.0
	organelle	104	24.5
	cell	145	34.2
Molecular function	antioxidant activity	2	0.7
	nutrient reservoir activity	2	0.7
	enzyme regulator activity	4	1.4
	molecular transducer activity	4	1.4
	transcription regulator activity	4	1.4
	transporter activity	13	4.4
	translation regulator activity	13	4.4
	structural molecule activity	39	13.3
	catalytic activity	80	27.2
	binding	133	45.2

Table 3.3 A summary of contigs and singletons creation and BLASTX score in the first phase of EST analysis (1051 ESTs) of a typical ovarian cDNA library of *P. monodon*

Contig/Singleton	Number of transcripts	BLASTX score			
		0	<100	100 - 200	≥ 200
Contigs with no. of ESTs					
2	48	9	7	9	23
3	15	4	2	1	8
4	8	0	1	1	6
5 to 9	13	3	3	2	5
10 to 49	9	3	0	0	6
≥ 50	3	0	0	1	2
Singleton	457	168	58	106	125

The relationship between the number of sequenced clones and the accumulative numbers of unique transcripts indicated that the discovery rate of new transcripts still did not reach a plateau of saturation and was greater than 10% after 1051 recombinant clones were sequenced (Figure 3.4). Therefore, additional unique transcripts can still be identified by sequencing a larger number of recombinant clones. The relatively high rate of gene discovery and a large number of transcripts obtained indicated that the established library is reasonably diversified. Homologues of sex-linked or sex differentiation-related transcripts found in the first phase of EST analysis of ovarian cDNA library of *P. monodon* was shown in Table 3.4.

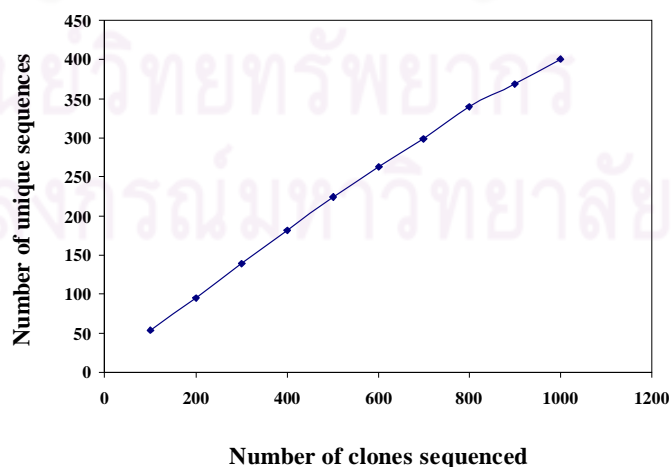


Figure 3.4 Number of unique sequences plotted as a function of the accumulative number of sequenced clones from the first phase of an ovarian cDNA library of *P. monodon*.

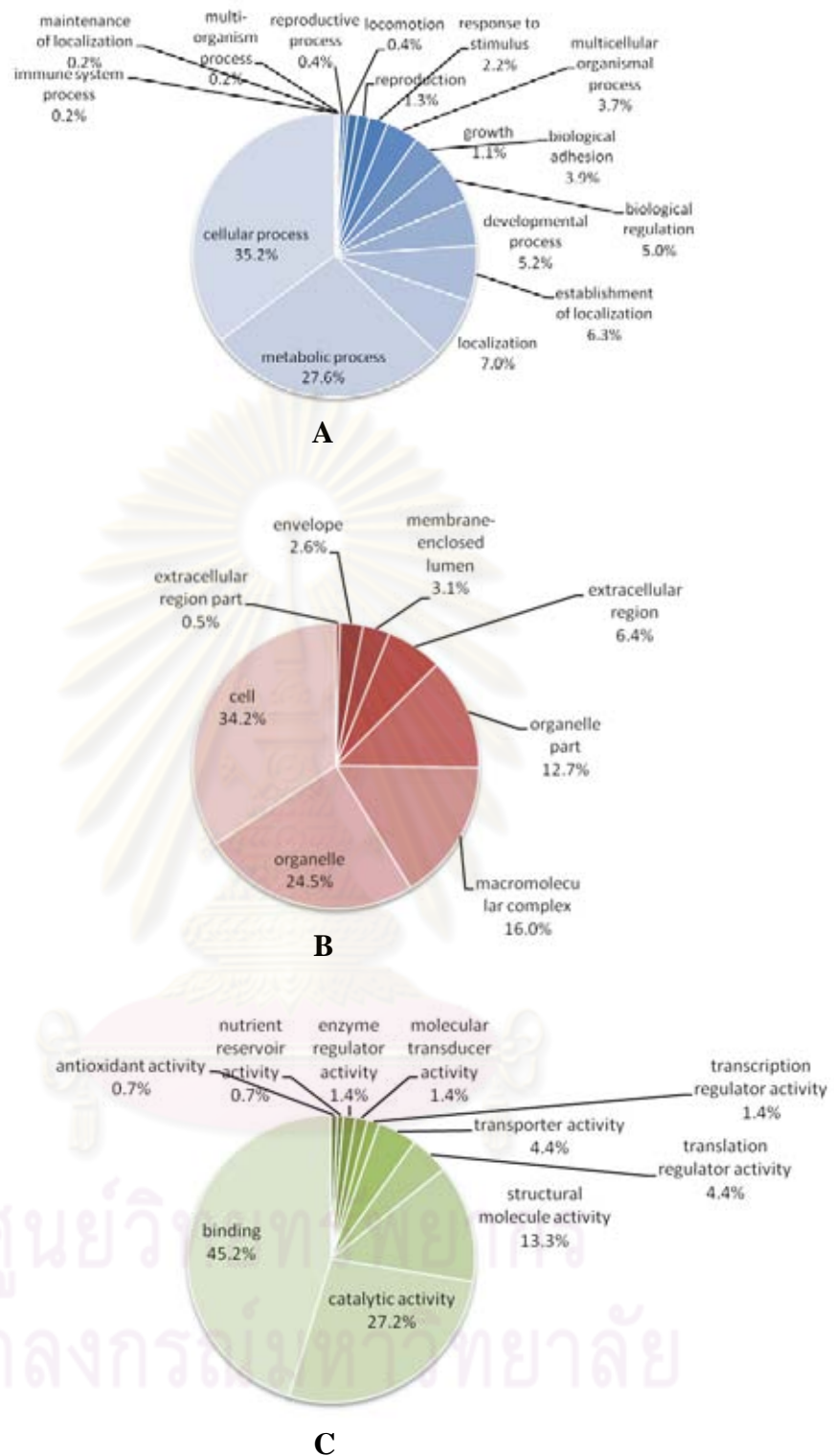


Figure 3.5 The percent distribution of nucleotide sequences according to three principal GO categories from the first phase of EST analysis (1051 ESTs) of a typical ovarian cDNA library of *P. monodon*. A-C are biological process, cellular component and molecular function categories, respectively.

Table 3.4 A summary of homologues of sex-linked or sex differentiation-related transcripts found in the first phase of EST analysis of an ovarian cDNA library of *P. monodon*

Transcripts*	Matched species	Size (bp)	E-value	Linked **
CG9946-PA	<i>Drosophila melanogaster</i>	738	3 x 10 ⁶⁵	X
Brain mitochondrial carrier protein 1	<i>Homo sapiens</i>	671	3 x 10 ⁴³	X
Thioredoxin peroxidase	<i>Homo sapiens</i>	923	7 x 10 ⁶⁸	X
NADPH-cytochrome P450 reductase	<i>Anopheles gambiae</i>	698	8 x 10 ²⁶	X
Phosphatidylinositol 4 kinase	<i>Caenorhabditis elegans</i>	725	3 x 10 ¹³	X
ENSANGP00000019081	<i>Anopheles gambiae</i>	452	6 x 10 ²²	X
Rab-protein 10 CG17060-PA	<i>Drosophila melanogaster</i>	892	1 x 10 ⁸⁸	X
Ubiquitin specific protease 9	<i>Mus musculus</i>	891	5 x 10 ⁵⁸	X
ENSANGP00000011950	<i>Anopheles gambiae</i>	866	2 x 10 ⁸⁷	X
Female sterile (1) M3	<i>Drosophila melanogaster</i>	884	2 x 10 ⁰⁷	X
Protein disulfide isomerase-related P5 precursor	<i>Caenorhabditis elegans</i>	651	3 x 10 ⁶¹	X
ENSANGP00000022750	<i>Anopheles gambiae</i>	666	2 x 10 ⁸⁹	X
Ribosomal protein L1, isoform D	<i>Drosophila melanogaster</i>	611	7 x 10 ⁶²	X
NADP-dependent leukotriene B4 12-hydroxydehydrogenase (15-oxoprostaglandin 13-reductase)	<i>Tribolium castaneum</i>	923	6 x 10 ³⁷	Not known
Nuclear autoantigenic sperm protein	<i>Homo sapiens</i>	639	5 x 10 ²⁵	1
X-linked eukaryotic translation initiation factor isoform 3	<i>Tribolium castaneum</i>	797	4 x 10 ⁹³	X
CG1681-PA	<i>Drosophila melanogaster</i>	452	2 x 10 ⁰⁹	X
Adenine nucleotide translocator 2	<i>Homo sapiens</i>	554	1 x 10 ⁹³	X
Chromobox protein	<i>Gallus gallus</i>	745	2 x 10 ⁴⁶	W
Small androgen receptor-interacting protein isoform 1	<i>Canis familiaris</i>	578	3 x 10 ³⁰	1
Vitellogenin	<i>Fenneropenaeus merguensis</i>	801	6 x 10 ⁹⁷	Not known
Ovarian lipoprotein receptor	<i>Panaeus semisulcatus</i>	923	4 x 10 ⁹⁴	Not known
Y-box protein Ct-p0	<i>Chironomus tentans</i>	846	3 x 10 ¹⁰	Not known
Polehole	<i>Drosophila melanogaster</i>	725	4 x 10 ⁰⁹	1
Zonadhesin precursor	<i>Homo sapiens</i>	653	1 x 10 ¹⁰	7

*GenBank accession number EE332433 – EE332457. **Localization in chromosomes of matched species

The second phase of EST analysis using a typical ovarian cDNA library was further carried out. From 1279 recombinant clones sequenced, a total of 970 ESTs (75.8%) corresponded to known sequences in the GenBank (E-value $< 10^{-4}$) whereas the remaining sequences were regarded as novel (unknown) transcripts (24.2%, E-value $> 10^{-4}$). Homologues of *TSP* (119 clones, 9.3% of sequenced clones) and *peritrophin* (118 clones, 9.2%) were abundantly expressed in vitellogenic ovaries of *P. monodon* (Table 3.5).

Table 3.5 The percentage and number of clones found in the second phase of EST analysis of a typical ovarian cDNA library of *P. monodon*

Transcripts	Number of clones (%)
Known transcripts (excluding peritrophin, thrombospondin and their precursors)	733 (57.3%)
Ovarian peritrophin 1 precursor	26 (2.0%)
Ovarian peritrophin 2 precursor	66 (5.2%)
Peritrophin 3 precursor	4 (0.3%)
Ovarian peritrophin	22 (1.7%)
Thrombospondin	119 (9.3%)
Unknown genes	309 (24.2%)
Total	1279 (100.0%)

The percent distributions of sequences from the second phase of EST analysis according to 3 principal GO ontology categories were analyzed. For the biological process category, ESTs functionally involved cellular process; e.g. *HEAT-like (PBS lyase) repeat containing 1*, *ferritin* and *cyclin A1*) was predominant (32.1%) followed by those in the metabolic process (e.g. *AKT interacting protein*, *heat shock protein 90* and *nuclear inhibitor of protein phosphatase*, 26.4%). EST involving reproduction and reproductive process were found at 1.5% and 1.0%, respectively.

For the cellular component category, EST functionally involved in the cell part (e.g. *Yip1 domain family; member 3*, *cyclin B* and *cytochrome c oxidase subunit*

I) predominated (33.9%) followed by ESTs exhibiting their functions in the organelles (24.3%).

For the molecular function category, ESTs displayed in the binding function (e.g. *calmodulin CG8472-PA; isoform A, platelet-activating factor acetylhydrolase isoform 1b alpha subunit* and *casein kinase 1 epsilon*) predominated (46.5%) followed by those exhibited the catalytic activity; e.g. *cathepsin C, ubiquitin carboxyl-terminal hydrolase 14 (ubiquitin thioesterase 14)* and *thyroid hormone receptor interactor 12 isoform 5*, 29.9%) (Table 3.6; Figure 3.6).

Six hundred and seventy-nine transcripts (125 contigs; from 725 transcripts and 554 singletons; 43.3%) were obtained after clustering analysis of ESTs from the second sequencing phase of a typical ovarian cDNA library (Table 3.7).

Transcripts functionally involved in reproduction from the second sequencing phase identified using GO ontology function were composed of *platelet-activating factor acetylhydrolase isoform 1b alpha subunit, protein mago nashi, neuralized CG11988-PB; isoform B, putative beta-NAC-like protein, hypothetical protein AaeL_AAEL003957, tubulin beta-2 chain (beta-II tubulin) beta-II tubulin, chicadae/profiling* and *oncoprotein nm23*.

The full length cDNA of *protein mago nashi* and *actin depolymerizing factor* and *cytochrome B5* (biological process GO:0006118) was further characterized.

In addition, transcripts involved in growth according to the GO ontology function including *poly [ADP-ribose] polymerase 1 (PARP-1) (ADPRT) (NAD(+)) ADP-ribosyltransferase 1) (Poly[ADP-ribose] synthetase 1)*, *ATP lipid-binding protein like protein* and *H3 histone, family 3A* were also identified.

Table 3.6 Classification of sequences according to three principal GO categories of the second phase of EST analysis (1279 ESTs) of an ovarian cDNA library of *P. monodon*

Type	Term	Number of sequences	Percentages
Biological process	immune system process	1	0.2
	rhythmic process	1	0.2
	locomotion	3	0.6
	growth	4	0.8
	reproductive process	5	1.0
	reproduction	8	1.5
	biological adhesion	13	2.5
	response to stimulus	19	3.6
	multicellular organismal process	31	5.9
	biological regulation	31	5.9
	developmental process	31	5.9
	establishment of localization	33	6.3
	localization	38	7.2
	metabolic process	139	26.4
	cellular process	169	32.1
Cellular component	extracellular region part	1	0.2
	envelope	14	3.0
	extracellular region	18	3.9
	membrane-enclosed lumen	21	4.6
	organelle part	64	13.9
	macromolecular complex	74	16.1
	organelle	112	24.3
	cell	156	33.9
Molecular function	motor activity	1	0.3
	antioxidant activity	1	0.3
	transcription regulator activity	2	0.7
	enzyme regulator activity	2	0.7
	molecular transducer activity	3	1.0
	translation regulator activity	6	2.1
	transporter activity	11	3.8
	structural molecule activity	42	14.6
	catalytic activity	86	29.9
	binding	134	46.5

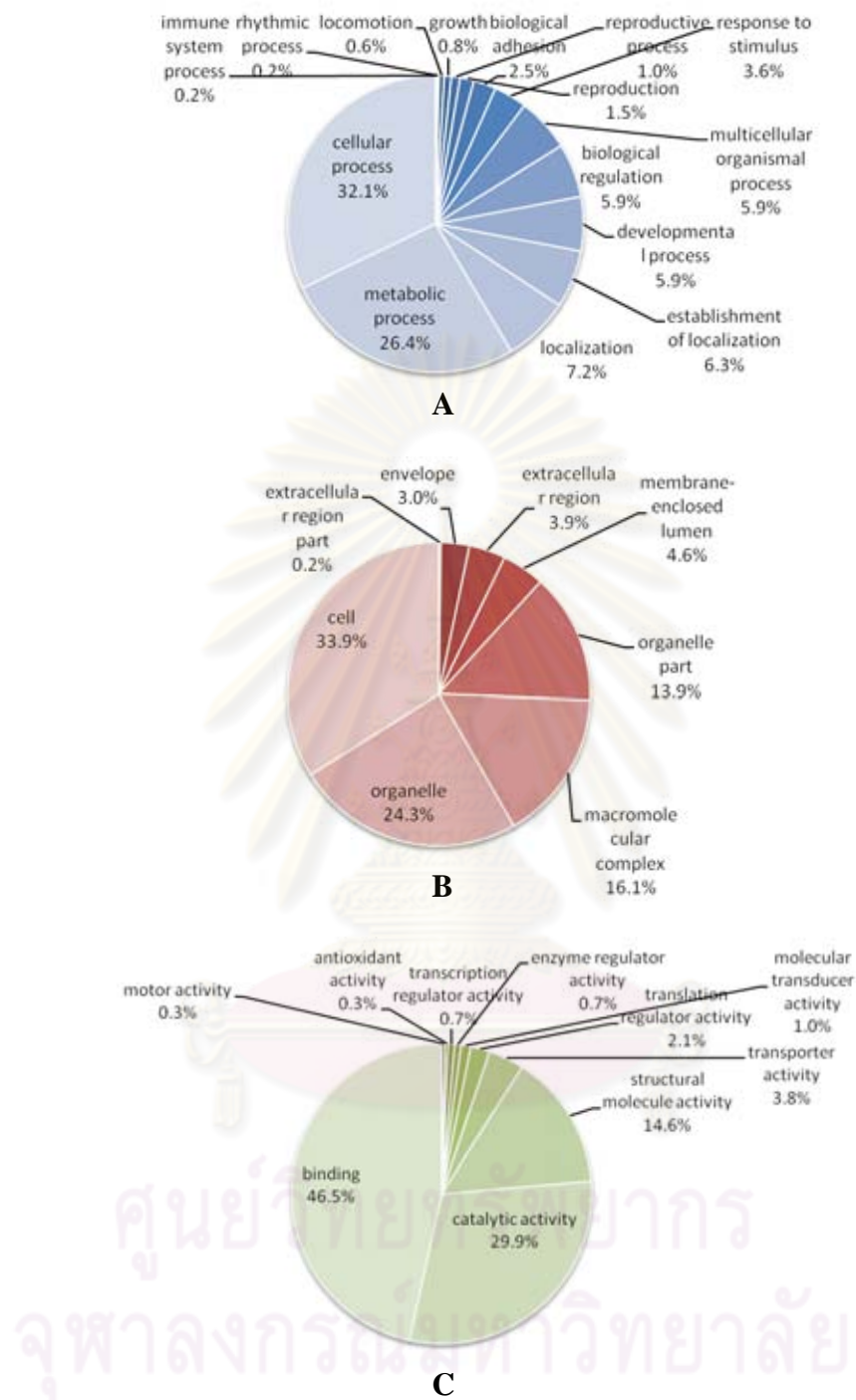


Figure 3.6 The percent distribution of nucleotide sequences according to three principal GO categories in the second phase of EST analysis (1279 ESTs) of a typical ovarian cDNA library of *P. monodon*. A-C are biological process, cellular component category and molecular function category, respectively.

Table 3.7 A summary of contigs and singletons creation and BLASTX score in the second phase of EST analysis (1279 ESTs) of a typical ovarian cDNA library of *P. monodon*

Contig/Singleton	Number of transcripts	BLASTX score			
		0	<100	100 – 200	≥ 200
Contigs with no. of ESTs					
2	61	15	4	8	34
3	20	1	2	6	11
4	9	2	1	3	3
5 to 9	19	7	0	0	12
10 to 49	14	1	3	2	7
≥ 50	2	0	0	1	1
Singleton	554	222	61	113	158

ESTs from the first and second phases of typical ovaries cDNA library was then analyzed simultaneously. From 2330 recombinant sequenced clones, a total of 1800 ESTs (77.3%) matched known sequences in the GenBank (E-value < 10^{-4}) whereas the remaining sequences were regarded as novel (unknown) transcripts (22.7%, E-value > 10^{-4}). The assembly of typical ESTs resulted in 230 contigs from 1,488 ESTs and 842 (36.1%) singletons. Homologues of *TSP* (198 clones, 8.5% of sequenced clones) and *peritrophin* (205 clones, 8.8%) were abundantly expressed in vitellogenic ovaries of *P. monodon* (Table 3.8).

Table 3.8 The percentage and number of clones found in both phases of a typical ovaries cDNA library

Transcripts	Number of clones
Known transcripts (excluding peritrophin and thrombospondin)	1397 (60.0%)
Ovarian peritrophin	205 (8.8%)
Thrombospondin	198 (8.5%)
Unknown genes	530 (22.7%)
Total	2330 (100%)

The percent distributions of nucleotide sequences in combined data of a typical ovarian cDNA library according to 3 principal GO ontology categories were examined. For the biological process category, ESTs involved in the metabolic process (e.g. *thrombospondin*, *AF510332_1 ovarian peritrophin 2 precursor* and *26S proteasome non-ATPase regulatory*) was predominant (30.3%) followed by those in

Table 3.9 Classification of sequences according to three principal GO categories in the first and second phases (2330 ESTs) of typical ovaries cDNA library

Type	Term	Number of sequences	Percentages
Biological process	growth	7	1.0
	reproduction	11	1.6
	response to stimulus	23	3.4
	multicellular organismal process	37	5.5
	biological regulation	47	7.0
	developmental process	47	7.0
	localization	54	8.0
	establishment of localization	54	8.0
	cellular process	191	28.3
	metabolic process	205	30.3
Cellular component	envelope	3	0.5
	extracellular region part	6	1.0
	membrane-enclosed lumen	16	2.6
	organelle part	19	3.1
	extracellular region	41	6.6
	macromolecular complex	103	16.6
	organelle	178	28.6
	cell	256	41.2
Molecular function	motor activity	1	0.2
	nutrient reservoir activity	2	0.4
	antioxidant activity	3	0.6
	molecular transducer activity	6	1.2
	transcription regulator activity	6	1.2
	enzyme regulator activity	7	1.4
	translation regulator activity	14	2.8
	transporter activity	20	4.1
	structural molecule activity	58	11.8
	catalytic activity	144	29.3
	binding	231	47.0

the cellular process (e.g. *putative mitochondrial ATP synthase gamma-subunit*, *heat shock cognate 70* and *elongation factor 1-alpha*, 28.3%). EST functionally involved in reproduction of the combined data of a typical ovarian cDNA library was 1.6%.

For the cellular component category, EST functionally involved in the cell part (e.g. *dendritic cell protein*, *lymphoid organ expressed yellow head virus receptor protein* and *SDA1 domain containing 1*) were predominant (41.2%) followed by those exhibited their functions in the organelles (e.g. *AGAP005098-PA*, *F1-ATP synthase beta subunit* and *Ras-related nuclear protein*, 28.6%).

For the molecular function category, ESTs displayed the binding function (e.g. *ATP lipid-binding protein like protein*, *eukaryotic translation initiation factor 5A* and *elongation factor 2*) predominated (47.0%) followed by those exhibited the catalytic activity (e.g. *thioredoxin peroxidase*, *putative mitochondrial ATP synthase gamma-subunit* and *MGC80929 protein isoform 1*, 29.3%, such as) (Table 3.9; Figure 3.7).

One thousand and seventy-two transcripts (230 contigs and 842 singletons; 36.1%) were obtained after clustering analysis (Table 3.10) and 679 ESTs (499 singletons; 21.4% and 180 contigs) significant matched known genes previously deposited in the GenBank (E-value < 10⁻⁴).

Table 3.10 A summary of contigs and singletons creation and BLASTX score in the first and second phases (2330 ESTs) of a typical ovarian cDNA library

Contig/Singleton	Number of transcripts	BLASTX score			
		0	<100	100 - 200	≥ 200
Contigs with no. of ESTs					
2	114	33	8	24	49
3	39	7	5	8	19
4	24	-	3	4	17
5 to 9	28	4	1	5	18
10 to 49	21	6	3	1	11
≥ 50	4	-	-	2	2
Singleton	842	343	98	181	220

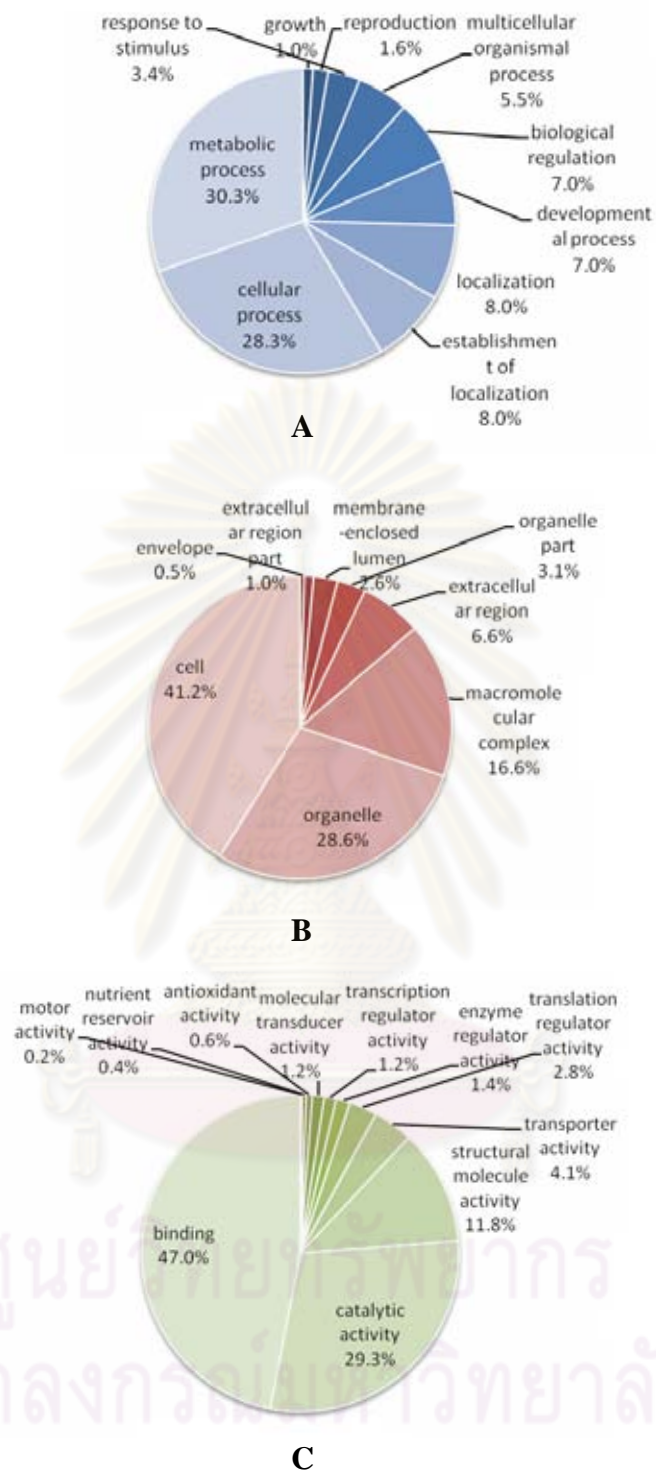


Figure 3.7 The percent distribution of nucleotide sequences according to three principal GO categories in both phases of typical ovaries cDNA library (2330 ESTs). A-C are biological process, cellular component and molecular function categories, respectively.

3.1.2 Construction of a normalized ovarian cDNA library of *P. monodon*

High redundancy of *TSP* and *peritrophin* were found in the typical ovarian cDNA library. To minimize highly redundant transcripts, a normalized cDNA library was constructed from the original ovarian cDNA library. The driver were prepared from the *in vivo* excision phagemid library and labeled with biotin. Hybridization was carried out between single-stranded phagemid and the labeled driver. The remaining single-stranded plasmids of rare expressed genes were removed from the hybrid using streptavidin beads and converted to double-strands by a proof-reading *Pfu* polymerase. The double-stranded cDNA inserts were then cloned into *Escherichia coli* XL-1 blue to propagate the normalized library.

Recombinant clones were randomly selected from those carrying insert sizes greater than 500 bp by colony (Figure 3.8). Plasmid DNA is extracted and digested with *Eco* RI-*Xho* I (or *Eco* RI-*Apa* I) and sequenced as described previously (Figure 3.9).

A total of 1778 ESTs was sequenced and 1413 ESTs (79.5%) significantly matched known sequences in the GenBank (E-value < 10^{-4}) whereas the remaining 365 ESTs (20.5%) were regarded as unknown transcripts (E-value > 10^{-4}). Sequence assembly of the normalized EST library resulted in 236 contigs from 1320 ESTs and 458 (25.8%) singletons. Surprisingly, homologues of *TSP* (176 clones, 9.9% of sequenced clones) and *peritrophin* (212 clones, 12.0%) were still highly redundant in the normalized cDNA library of *P. monodon* (Table 3.11).

The percent distributions of sequences following 3 principal GO ontology categories of the normalized ovaries cDNA library were also analyzed. For the biological process category, ESTs involved in the metabolic process (e.g. *dopamine N acetyltransferase*, *methionine-tRNA synthetase* and *QM protein*) predominated (33.8%) followed by those of the cellular process; *putative mitochondrial ATP synthase gamma-subunit*, *protein phosphatase 2 (formerly 2A)*, *catalytic subunit, alpha isoform* and *proliferating cell nuclear antigen*; 30.1%). ESTs functionally involved in reproduction was found at 2.3% of examined ESTs. This was higher than that of the typical ovarian cDNA library (1.6%).

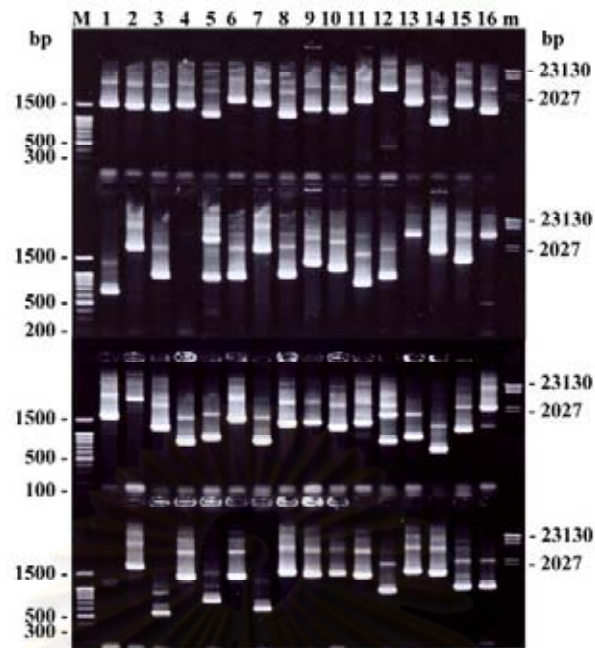


Figure 3.8 Colony PCR for determining recombinant clones carrying insert sizes greater than 500 bp from the normalized ovarian cDNA libraries of *P. monodon*. Lanes m and M are λ -*Hind* III and 100 bp DNA ladder, respectively.

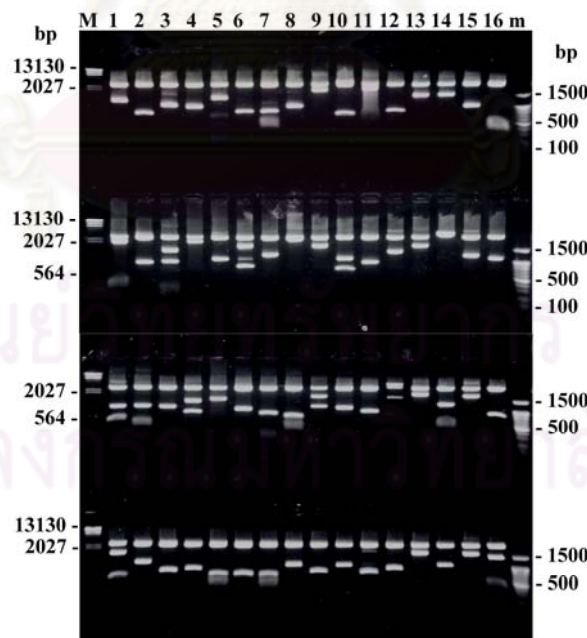


Figure 3.9 Digestion of plasmid DNA containing positive clones of the normalized ovarian cDNA libraries of *P. monodon*. Lanes M and m are λ -*Hind* III and 100 bp DNA ladder, respectively.

For the cellular component category, ESTs play the important role in the cell part was accounted for 40.4%. Examples of these transcripts were *vacuolar ATP synthase 16 kDa proteolipid subunit vacuolar H(+)-ATPase proteolipid subunit, dihydrolipoamide dehydrogenase and RAB14, member RAS oncogene family*. ESTs play their roles in the organelles was 28.8%. Examples of these ESTs were *dynein light chain-2 isoform 2, nudix (nucleoside diphosphate linked moiety X)-type motif 21 isoform 2 and H2A histone family, member V isoform 1*).

For the molecular function category, EST exhibited the binding function was predominant and accounted for 48.0% of examined ESTs. Examples of these transcripts were *ginner centromere protein antigens 135/155kDa, mannose-binding protein and Rac GTPase-activating protein 1*. This was followed by ESTs displayed the catalytic activity (e.g. *receptor for activated protein kinase C-like protein, S-adenosylmethionine synthetase and cytosolic manganese superoxide dismutase*, 27.0%) (Table 3.12; Figure 3.10).

Table 3.11 The percentage and number of clones found in the normalized ovaries cDNA library

Transcripts	Number of clones
Known transcripts (excluding peritrophin, thrombospondin and their precursors)	1024 (57.6%)
Ovarian Peritrophin 1 precursor	67 (3.8%)
Ovarian Peritrophin 2 precursor	113 (6.4%)
Ovarian peritrophin	32 (1.8%)
Thrombospondin	176 (9.9%)
Unknown genes	365 (20.5%)
Total	1778 (100.0%)

Four hundred and fifty-five ESTs (289 singletons and 166 contigs) was significantly similar to known genes previously deposited in the GenBank (E-value < 10^{-4}). Six hundred and seventy-nine transcripts (125 contigs; from 725 transcripts and 554 singletons; 43.3%) were obtained after clustering analysis (Table 3.13).

Table 3.12 Classification of sequences according to three principal GO categories in the normalized ovaries cDNA library (1778 ESTs)

Type	Term	Number of sequences	Percentages
Biological process	growth	3	0.7
	reproduction	10	2.3
	response to stimulus	14	3.2
	multicellular organismal process	18	4.1
	developmental process	21	4.8
	biological regulation	22	5.0
	localization	35	8.0
	establishment of localization	35	8.0
	cellular process	132	30.1
	metabolic process	148	33.8
	Cellular component	extracellular region part	2
envelope		2	0.5
membrane-enclosed lumen		6	1.5
organelle part		8	1.9
extracellular region		32	7.7
macromolecular complex		77	18.6
organelle		119	28.8
cell		167	40.4
Molecular function	antioxidant activity	1	0.3
	nutrient reservoir activity	2	0.6
	motor activity	2	0.6
	enzyme regulator activity	3	0.8
	molecular transducer activity	6	1.7
	translation regulator activity	12	3.4
	transporter activity	18	5.1
	structural molecule activity	45	12.6
	catalytic activity	96	27.0
	binding	171	48.0

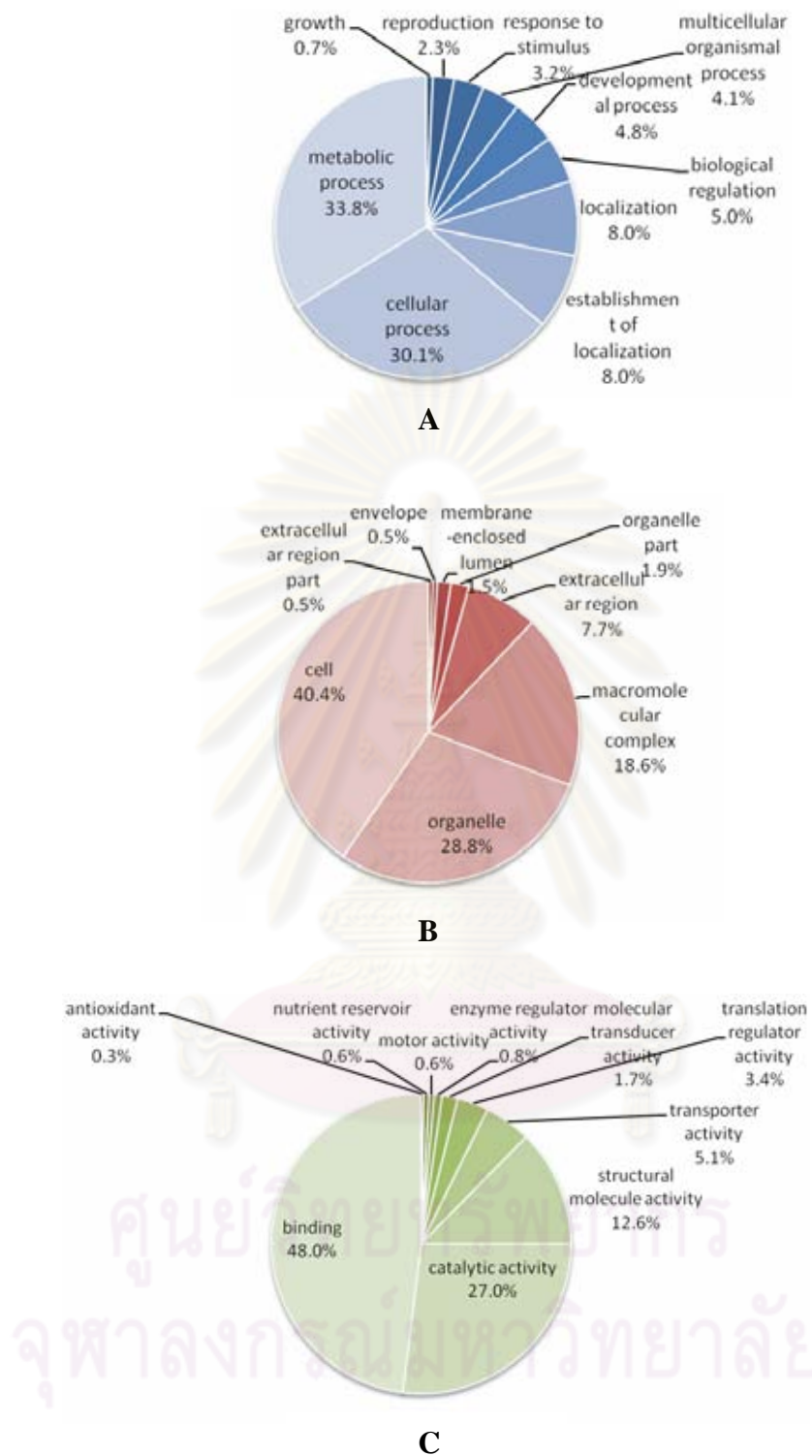


Figure 3.10 The percent distribution of nucleotide sequences among the three principal GO categories in the normalized ovaries cDNA library (1778 ESTs). A-C are biological process, cellular component category and molecular function category, respectively.

Table 3.13 A summary of contigs and singletons creation and BLASTX score in the normalized ovaries cDNA library (1778 ESTs)

Contig/Singleton	Number of transcripts	BLASTX score			
		0	<100	100 - 200	≥ 200
Contigs with no. of ESTs					
2	109	41	9	24	35
3	44	12	11	10	11
4	26	6	2	4	14
5 to 9	33	7	-	9	17
10 to 49	22	4	4	1	12
≥ 50	3	-	-	1	2
singleton	458	169	61	101	127

Transcripts functionally involved in reproduction according to the GO ontology function observed in the normalized ESTs ovarian cDNA library were *dynein light chain-2 isoform 2*, *Cofilin/actin-depolymerizing factor homolog (Protein D61) (Protein twinstar)*, *proliferating cell nuclear antigen*, *oncoprotein nm23*, *dihydrolipoamide dehydrogenase*, *vertebrate homocysteine-inducible; endoplasmic reticulum stress-inducible; ubiquitin-like domain member 1 (HERPUD1)*, *chicadae/profiling*, *egalitarian CG4051-PA isoform 1*, *CG8978-PA, isoform A (actin-related protein 2/3 complex subunit 1A)* and *ovarian serine protease*.

The full length cDNA of *actin depolymerizing factor*, *F-box*, *wd40 repeat domain binding protein* (biological process GO:0006512), *cyclin-dependent kinase 7* (molecular function GO:0004672) and *selenoprotein M precursor* (cellular component GO:0005783) was further characterized.

In addition, transcripts involved to growth according to the GO ontology function; *Zgc:85671 protein DnaJ (Hsp40) homolog; subfamily C member 2*, and *glutamyl(E)/glutaminyl(Q) tRNA synthetase family member (ers-1)* were also identified.

Interestingly, *ubiquitin-conjugating enzyme (Ubc-2)* was classified based on the GO ontology functions to both reproduction and growth subgroups. This transcript was also identified in the typical ESTs cDNA library.

3.1.3 Construction of suppression subtractive hybridization (SSH) cDNA libraries from mature and immature ovaries of *P. monodon* broodstock

Forward and reverse SSH cDNA libraries of mature and immature ovaries of *P. monodon* broodstock (cDNA of vitellogenic ovaries of broodstock shrimp having GSI = 5.689% as tester and cDNA of previtellogenic ovaries of broodstock shrimp having GSI = 1.434% as driver and *vice versa*) were carried out. Initially, first and second strand cDNA were separately synthesized from mRNA of vitellogenic and previtellogenic ovaries of *P. monodon* broodstock. Double strand cDNA of tester and driver was digested with *Rsa* I (Figure 3.11). Only digested testers were ligated with the adapter. Tester and driver were hybridized twice. Each subtracted cDNA was sequentially amplified twice using suppression PCR (Figure 3.12). The resulting products are ligated with pGEM[®]-T easy vector and transformed into *E. coli* JM109. Recombinant clones of both forward and reverse SSH libraries were identified by colony PCR (Figure. 3.13). Plasmid DNA is extracted (Figure. 3.14) and unidirectional sequenced.

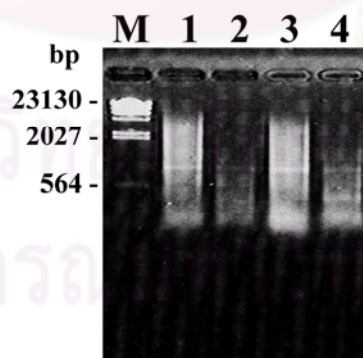


Figure 3.11 Agarose gel electrophoresis showing *Rsa*I digestion for SSH ovarian cDNA libraries of *P. monodon*. Lane M is λ -*Hind* III ladder, lanes 1 and 3 are undigested cDNA of mature and immature ovaries of *P. monodon* broodstock and lanes 2 and 4 are digested cDNA of mature and immature ovaries of *P. monodon* broodstock, respectively.

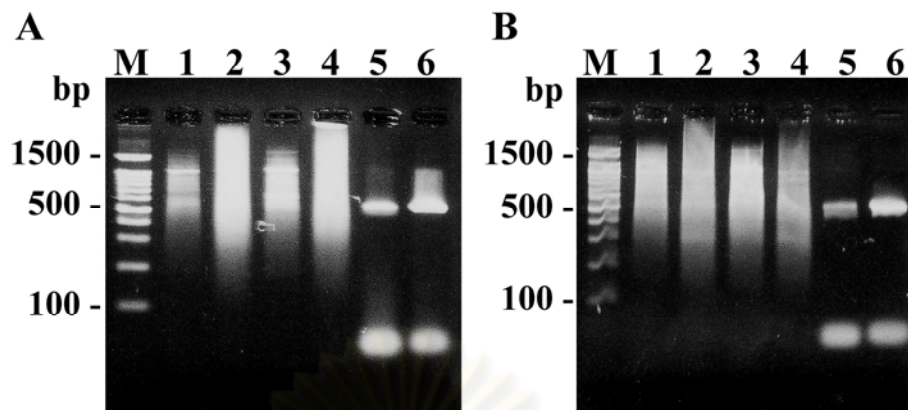


Figure 3.12 An agarose gel electrophoresis showing primary (A) and secondary (B) PCR amplification of subtracted (lanes 1 and 3) and unsorted (lanes 2 and 4) for forward (lanes 1-2; A and B) and reverse (lanes 3-4; A and B) SSH ovaries cDNA libraries of *P. monodon*. Lanes 5-6 are PCR controls of forward and reverse SSH libraries using *EF-1 α* primer. Lanes M is a 100 bp ladder.

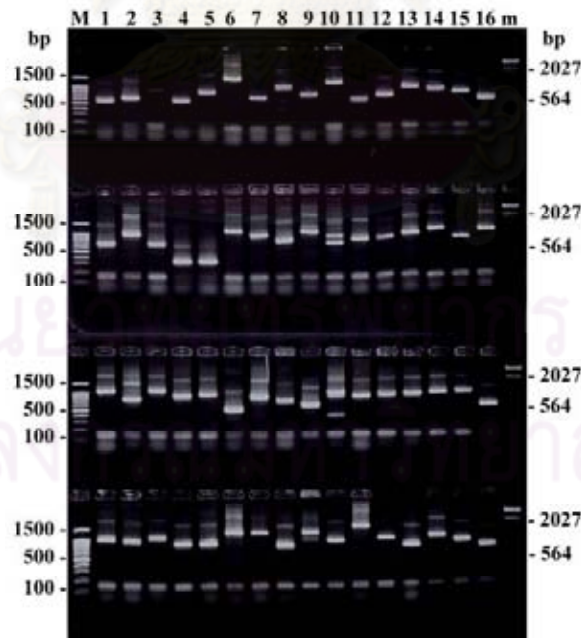


Figure 3.13 Colony PCR for determining recombinant clones carrying insert sizes greater than 300 bp the forward (lines 1-2) and reverse (lines 3-4) SSH ovarian cDNA libraries of *P. monodon*. Lane m and M are λ -*Hind* III and 100 bp DNA ladder, respectively.

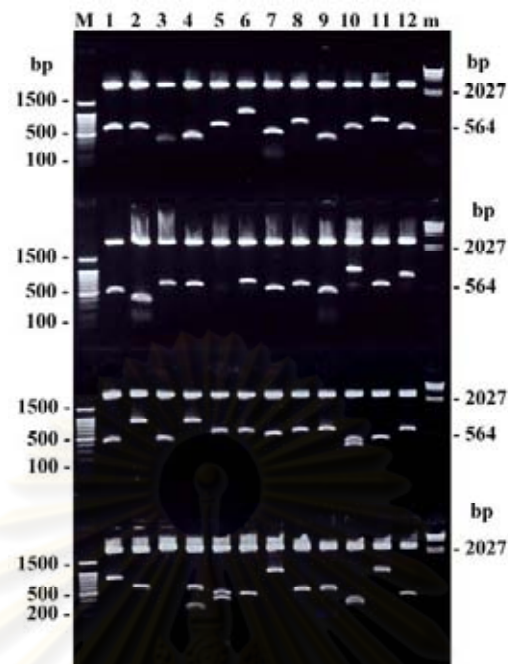


Figure 3.14 Digestion of plasmid DNA containing positive clones of the forward (lines 1-2) and reverse (lines 3-4) SSH ovarian cDNA libraries of *P. monodon*. Lanes m and M are λ -*Hind* III and 100 bp DNA ladder, respectively.

A total of 220 clones from the forward SSH ovarian library of *P. monodon* were unidirectional sequenced. A total of 71 clones (32.3%) corresponded to known sequences in the GenBank (E-value $< 10^{-4}$) whereas the remaining 149 ESTs were regarded as novel (unknown) transcripts (38.2%, E-value $> 10^{-4}$). Sequence assembly of this SSH library resulted in 16 contigs from 97 ESTs and 123 singletons (55.9%). Homologues of *TSP* (39 clones, 17.7% of sequenced clones) and *peritrophin* (26 clones, 11.8%) were abundantly expressed in this libraries (Table 3.14).

Table 3.14 The percentage and number of clones found in the forward SSH ovarian cDNA library of *P. monodon*

Transcripts	Number of clones
Known transcripts (excluding peritrophin, thrombospondin and their precursors)	71 (32.3%)
Ovarian Peritrophin 1 precursor	15 (6.8%)
Ovarian Peritrophin 2 precursor	9 (4.1%)
Ovarian peritrophin	2 (0.9%)
Thrombospondin	39 (17.7%)
Unknown genes	84 (38.2%)
Total	220 (100.0%)

The percent distributions of sequences following 3 principal GO categories of the forward SSH ovaries cDNA library was analyzed. For the biological process category, ESTs functional involved in the cellular process (e.g. *Chromosome-associated protein CG9802-PA; isoform A*, *keratinocyte associated protein 2* and *elongation factor 2*) predominated (33.3%) followed by those involved in the metabolic process (e.g. *26S proteasome regulatory subunit rpn2 isoform 2*, *eukaryotic initiation factor 4A* and *interleukin enhancer binding factor 2*, 27.0%). Reproduction-related ESTs was found at 2.7% of the examined sequences.

For the cellular component category, ESTs functioned in the cell part (e.g. *putative myosin II essential light chain*, *MCM2 minichromosome maintenance deficient 2*, *mitotin* and *40S ribosomal protein S2*) predominated (36.0%) followed by those functioned in the organelles (e.g. *coatamer protein complex*, *subunit beta*, *ATP synthase E chain* and *calreticulin*, 24.0%).

For the molecular function category, EST exhibited the binding function (e.g. *T-complex protein 1 subunit epsilon (TCP-1-epsilon) (CCT-epsilon)*, *translation initiation factor eif-2b* and *RNA binding motif protein 5 isoform 9*, 53.4%) were predominant followed by ESTs displayed the catalytic activity (e.g. *oncoprotein nm23*, *neuralized CG11988-PC; isoform C* and *peroxiredoxin*, 25.9%, such as) (Table 3.15; Figure 3.15).

Seventy-two transcripts (59 singletons; 26.8% and 13 contigs) significantly matched known genes previously deposited in the GenBank (E-value $< 10^{-4}$). One hundred and thirty-nine transcripts (16 contigs; from 97 transcripts and 123 singletons; 55.9%) were obtained after clustering analysis (Table 3.16).

Table 3.15 Classification of sequences according to three principal GO categories in the forward SSH ovaries cDNA library (220 ESTs)

Type	Term	Number of sequences	Percentages
Biological process	locomotion	1	0.9%
	rhythmic process	1	0.9%
	reproduction	3	2.7%
	establishment of localization	4	3.6%
	localization	5	4.5%
	response to stimulus	5	4.5%
	biological adhesion	6	5.4%
	multicellular organismal process	6	5.4%
	biological regulation	6	5.4%
	developmental process	7	6.3%
	metabolic process	30	27.0%
	cellular process	37	33.3%
Cellular component	extracellular region part	1	1.3%
	envelope	1	1.3%
	membrane-enclosed lumen	3	4.0%
	extracellular region	11	14.7%
	macromolecular complex	14	18.7%
	organelle	18	24.0%
	cell part	27	36.0%
Molecular function	motor activity	1	1.7%
	enzyme regulator activity	1	1.7%
	transporter activity	1	1.7%
	structural molecule activity	4	6.9%
	translation regulator activity	5	8.6%
	catalytic activity	15	25.9%
	binding	31	53.4%

A total of 232 ESTs from the reverse SSH ovarian library of *P. monodon* were unidirectional sequenced. A total of 67 clones sequenced (28.9%) corresponded to known sequences in the GenBank (E-value $< 10^{-4}$) whereas the remaining 165 ESTs (42.7%) were regarded as unknown transcripts (E-value $> 10^{-4}$). Sequence assembly of the reverse SSH transcripts resulted in 14 contigs from 142 ESTs and 90

singletons. Homologues of *TSP* (39 ESTs, 16.8% of sequenced clones) and *peritrophin* (27 ESTs, 11.6%) were abundantly expressed in the reverse SSH library of *P. monodon* (Table 3.17).

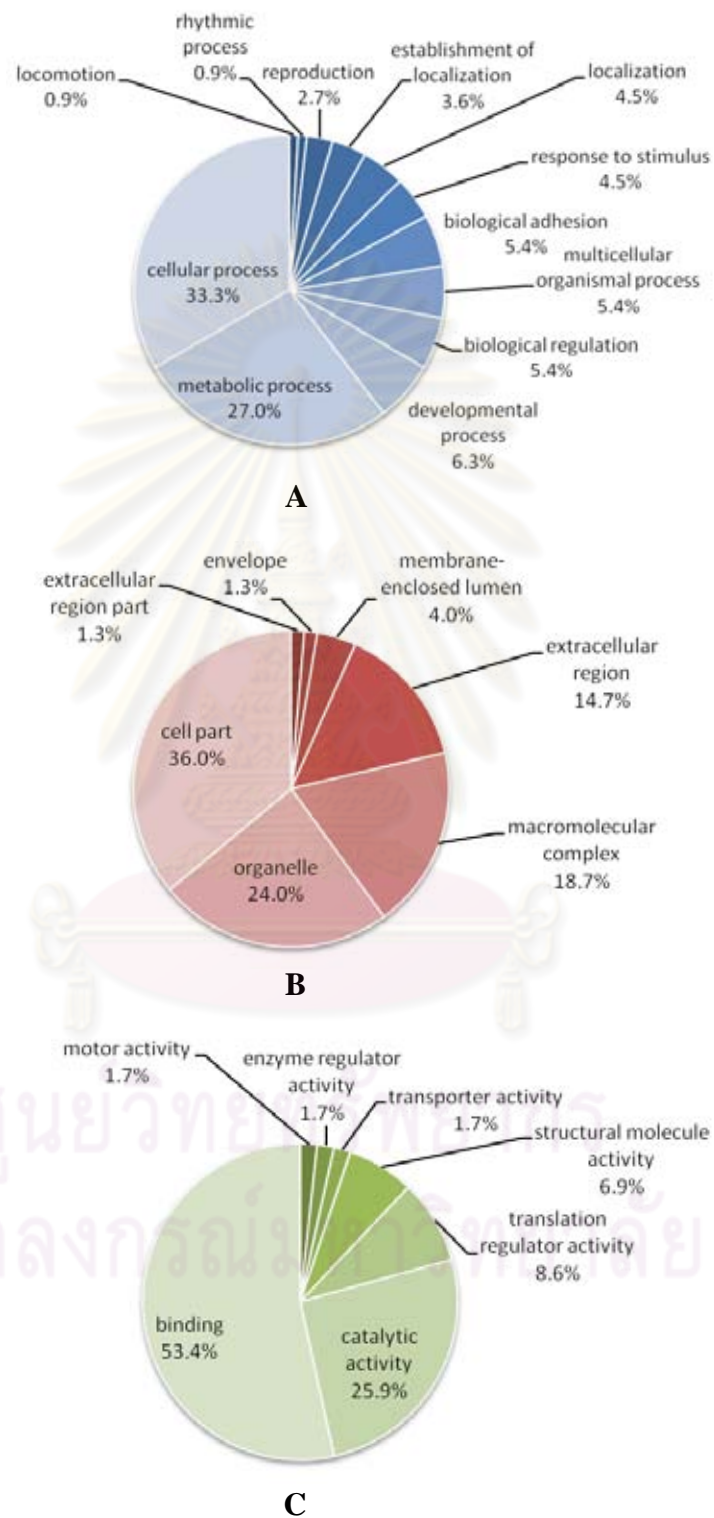


Figure 3.15 The percent distribution of nucleotide sequences according to three principal GO categories in the forward SSH ovaries cDNA library. A-C are biological process, cellular component category and molecular function category, respectively.

Table 3.16 A summary of contigs and singletons creation and BLASTX score in the forward SSH ovarian cDNA library (220 ESTs)

Contig/Singleton	Number of transcripts	BLASTX score			
		0	<100	100 - 200	≥ 200
Contigs with no. of ESTs					
2	7	1	3	-	3
3	1	1	-	-	-
4	2	-	1	-	1
5 to 9	4	1	-	-	3
10 to 49	2	-	-	-	2
≥ 50	-	-	-	-	-
Singleton	123	64	16	25	18

The percent distribution of nucleotide sequences according to 3 principal GO categories of the reverse SSH ovarian cDNA library was analyzed. For the biological process category, ESTs involved in the cellular process (e.g. *s-adenosylmethionine synthetase*, *F1-ATP synthase beta subunit* and *egalitarian CG4051-PA isoform 1*) predominated (32.5%) followed by those involved in the metabolic process (e.g. *elongation factor 1-alpha*, *40S ribosomal protein S6* and *calreticulin*, 26.3%). Reproduction-related ESTs was found in this library at 2.5% which is slightly lower than that of the reverse SSH library (2.7%).

For the cellular component category, ESTs functioned in the cell part (*ATP synthase subunit 9 mitochondrial precursor*, *70kD heat shock-like protein* and *40S ribosomal protein S6*) predominated (34.2%) followed by ESTs functioned in the extracellular region (e.g. *thrombospondin* and *ovarian peritrophin*, 26.3%).

For the molecular function category, ESTs displayed the binding function (e.g. *ferritin peptide*, *ATP synthase subunit 9 mitochondrial precursor* and *eukaryotic initiation factor 4A*; 53.3%) predominated followed by ESTs exhibited in the catalytic activity (e.g. *phosphatase 2C gamma*; *AGAP006171-PA*, *selenophosphate synthetase* and *70kD heat shock-like protein*; 31.1%, such as) (Table 3.18; Figure 3.16).

Table 3.17 The percentage and number of clones found in the reverse SSH ovaries cDNA library of *P. monodon*

Transcripts	Number of clones
Known transcripts (excluding peritrophin, thrombospondin and their precursors)	67 (28.9%)
Ovarian Peritrophin 1 precursor	9 (3.9%)
Ovarian Peritrophin 2 precursor	18 (7.7%)
Thrombospondin	39 (16.8%)
Unknown genes	99 (42.7%)
Total	232 (100.0%)

Table 3.18 Classification of sequences according to three principal GO categories in the reverse SSH ovaries cDNA library (232 ESTs)

Type	Term	Number of sequences	Percentages
Biological process	immune system process	1	1.3%
	reproduction	2	2.5%
	response to stimulus	3	3.8%
	developmental process	3	3.8%
	localization	3	3.8%
	establishment of localization	3	3.8%
	multicellular organismal process	4	5.0%
	biological regulation	5	6.3%
	biological adhesion	9	11.3%
	metabolic process	21	26.3%
	cellular process	26	32.5%
Cellular component	membrane-enclosed lumen	3	7.9%
	macromolecular complex	6	15.8%
	organelle part	6	15.8%
	extracellular region	10	26.3%
	cell part	13	34.2%
Molecular function	antioxidant activity	1	2.2%
	transporter activity	1	2.2%
	translation regulator activity	2	4.4%
	structural molecule activity	3	6.7%
	catalytic activity	14	31.1%
	binding	24	53.3%

Fifty-nine transcripts (50 singletons; 21.6% and 9 contigs) significant matched known genes previously deposited in the GenBank (E-value $< 10^{-4}$). One hundred and four transcripts (14 contigs; from 142 transcripts and 90 singletons; 38.8%) were obtained after clustering analysis (Table 3.19).

Table 3.19 A summary of contigs and singletons creation and BLASTX score in the reverse SSH ovarian cDNA library (232 ESTs)

Contig/Singleton	Number of transcripts	BLASTX score			
		0	<100	100 - 200	≥ 200
Contigs with no. of ESTs					
2	4	5	-	-	2
3	2	1	-	-	1
4	1	-	-	-	1
5 to 9	3	1	1	-	1
10 to 49	4	1	-	-	3
≥ 50	-	-	-	-	-
Singleton	90	40	9	30	11

Data of ESTs from the forward and reverse SSH ovarian cDNA libraries of *P. monodon* were analyzed together. From 452 recombinant clones sequenced, 269 ESTs (59.5%) corresponded to known sequences in the GenBank (E-value $< 10^{-4}$) whereas the remaining 183 ESTs were regarded as unknown transcripts (40.5%, E-value $> 10^{-4}$). Sequence assembly of subtractive ESTs resulted in 28 contigs from 251 ESTs and 201 singletons. Like other libraries, homologues of *TSP* (78 ESTs, 17.3% of examined sequences) and *peritrophin* (53 ESTs, 11.7%) were abundantly expressed in ovaries of *P. monodon* (Table 3.20).

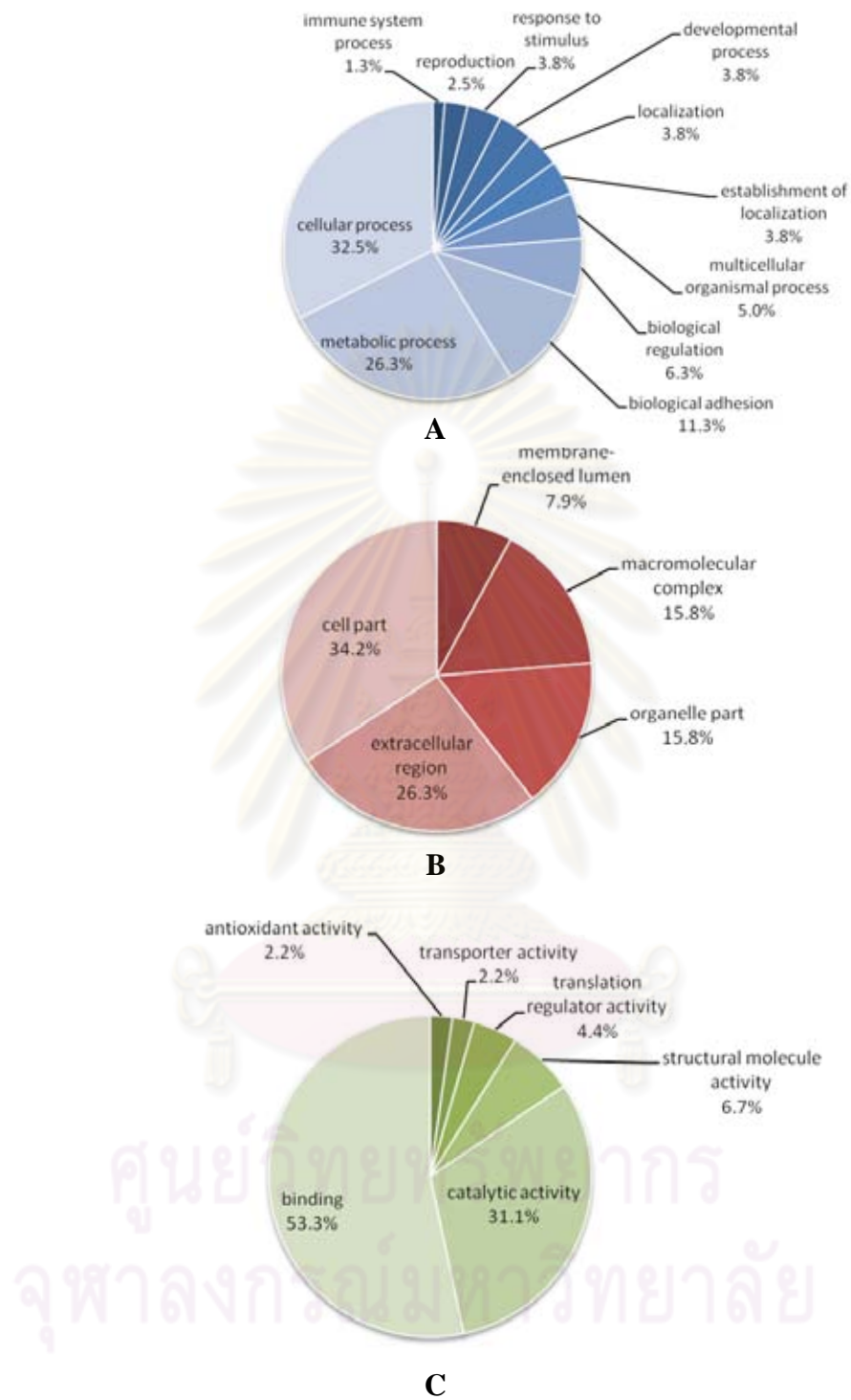


Figure 3.16 The percent distribution of nucleotide sequences according to three principal GO categories in the reverse SSH ovaries cDNA library. A-C are biological process, cellular component and molecular function categories, respectively.

The percent distributions of nucleotide sequences following 3 principal GO ontology categories of the forward and reverse SSH ovaries cDNA libraries were analyzed. For the biological process category, ESTs involved in the metabolic process was predominant; e.g. *anaphase promoting complex subunit 11 homolog*, *s-adenosylmethionine synthetase* and *T-complex protein 1 subunit epsilon (TCP-1-epsilon or CCT-epsilon)* (35.0%), followed by those involved in the cellular process (e.g. *acidic p0 ribosomal protein*, *MCM2 minichromosome maintenance deficient 2*, *mitotin* and *coatamer protein complex; subunit beta*; 25.2%). Reproduction-related ESTs were found at 2.4% of examined sequences of the combined SSH data. This was higher than that of the typical (1.6%) and normalized (2.3%) ovarian cDNA libraries of *P. monodon*.

For the cellular component category, EST functionally involved in the cell part (e.g. *putative myosin II essential light chain*, *ATP synthase E chain* and *checkpoint kinase 1*) predominated (35.5%) followed by those functionally displayed in the organelles (e.g. *selenoprotein M*, *keratinocyte associated protein 2* and *interleukin enhancer binding factor 2*; 25.5%).

For the molecular function category, ESTs displayed the binding function (e.g. *translation initiation factor eif-2b*, *RNA binding motif protein 5 isoform 9* and *selenophosphate synthetase*; 50.5%) predominated followed by those displayed the

Table 3.20 The percentage and number of clones found in the forward and reverse SSH ovarian cDNA libraries of *P. monodon*

Transcripts	Number of clones
Known transcripts (excluding peritrophin, thrombospondin and their precursors)	138 (30.5%)
Ovarian Peritrophin 1 precursor	24 (5.3%)
Ovarian Peritrophin 2 precursor	27 (6.0%)
Ovarian peritrophin	2 (0.4%)
Thrombospondin	78 (17.3%)
Unknown genes	183 (40.5%)
Total	452 (100.0%)

Table 3.21 Classification of sequences according to three principal GO categories in the forward and reverse SSH ovarian cDNA libraries (452 ESTs)

Type	Term	Number of sequences	Percentages
Biological process	reproduction	3	2.4
	response to stimulus	6	4.9
	biological regulation	8	6.5
	establishment of localization	8	6.5
	developmental process	8	6.5
	multicellular organismal process	8	6.5
	localization	8	6.5
	cellular process	31	25.2
	metabolic process	43	35.0
Cellular component	extracellular region part	1	0.9
	membrane-enclosed lumen	4	3.6
	organelle part	4	3.6
	extracellular region	15	13.6
	macromolecular complex	19	17.3
	organelle	28	25.5
	cell	39	35.5
	Molecular function	enzyme regulator activity	1
antioxidant activity		1	1.1
transporter activity		3	3.2
structural molecule activity		6	6.3
translation regulator activity		7	7.4
catalytic activity		29	30.5
binding		48	50.5

catalytic activity (e.g. *MGC80929 protein isoform 1*, *oncoprotein nm23* and *eukaryotic initiation factor 4A*30.5%) (Table 3.21; Figure 3.17).

One hundred and nine transcripts (93 singletons; 20.6% and 16 contigs) significant matched known genes in the GenBank (E-value < 10⁻⁴). Two hundred and twenty-nine transcripts (28 contigs from 251 transcripts and 201 singletons; 44.5%) were obtained after clustering analysis (Table 3.22).

Table 3.22 A summary of contigs and singletons creation and BLASTX score in the forward and reverse SSH ovarian cDNA libraries (452 ESTs)

Contig/Singleton	Number of transcripts	BLASTX score			
		0	<100	100 - 200	≥ 200
Contigs with no. of ESTs					
2	15	8	-	-	7
3	2	-	-	1	1
4	-	-	-	-	-
5 to 9	6	3	1	-	2
10 to 49	5	1	-	-	4
≥ 50	-	-	-	-	-
Singleton	201	108	22	55	16

Transcripts involved in reproduction from SSH ovarian cDNA libraries were identified according to the GO ontology function. These included, *CG8597-PA, isoform A (RNA binding motif protein 4)*, *neuralized CG11988-PC; isoform C* and *egalitarian CG4051-PA isoform 1* which was first identified in the SSH ovarian cDNA libraries of *P. monodon*.

The full length cDNA of functionally important transcripts such as, *anaphase promoting complex subunit 11 homolog* (biological process GO:0008152) and *selenoprotein M precursor* (cellular component GO:0005783) which were previously identified in the normalized ESTs cDNA library, were further characterized.

3.1.4 ESTs from all libraries

A total of 4560 clones (2330 ESTs from a typical library, 1778 ESTs from the normalized library and 452 clones from subtractive ovarian cDNA libraries) were analyzed. A total of 3482 ESTs (76.4%) matched known genes in the GenBank (E-value $< 10^{-4}$) whereas the remaining sequences were regarded as unknown transcripts (23.6%, E-value $> 10^{-4}$). Sequence assembly of all ESTs in this thesis resulted in 441 contigs from 3330 ESTs and 1231 (27.0%) singletons. Homologues of *TSP* (452 ESTs, 9.9% of sequenced ESTs) and *peritrophin* (470 clones, 10.3%) were abundantly expressed in ovaries of *P. monodon* (Table 3.23).

The percent distributions of all sequences according to 3 principal GO ontology categories were analyzed. For the biological process category, ESTs function involved in the cellular process (e.g. *Smt3 activating enzyme 2 CG7528-PA*, *pre-mRNA splicing factor SF3b 10 kDa subunit* and *nucleosome assembly protein 1 p56A*) predominated (32.8%) followed by those in the metabolic process; e.g. *glyoxylase 1*, *putative fructose 1,6-bisphosphate aldolase* and *DNA mismatch repair protein Msh2 (MutS protein homolog 2) mismatch repair protein* (25.4%). EST functionally involved in reproduction and reproductive process were found at 1.7 and 0.6%, respectively.

For the cellular component category, ESTs functioned in the cell part (e.g. *ADP ribosylation factor 79F CG8385-PB; isoform B*, *Rps16 protein* and *H3 histone, family 3A*; 34.3%, such as) were predominant followed by those played their function in the organelles (e.g. *ND4_15276 NADH dehydrogenase subunit 4*, *cytochrome c oxidase polypeptide Vb* and *Vacuolar ATP synthase 16 kDa proteolipid subunit*, 23.4%).

Table 3.23 The percentage and number of clones found in all ESTs ovarian cDNA libraries

Transcripts	Number of clones
Known transcripts (excluding peritrophin and thrombospondin)	2560 (56.2%)
Ovarian peritrophin	470 (10.3%)
Thrombospondin	452 (9.9%)
Unknown genes	1078 (23.6%)
Total	4560 (100.0%)

For the molecular function category, EST displayed the binding function (e.g. *ras-related protein Rab-10; putative*, *14-3-3-like protein* and *fruitless CG14307-PB; isoform B*; 49.0%) predominated followed by those displayed the catalytic activity (e.g. *protein phosphatase 2 (formerly 2A); catalytic subunit; alpha isoform*, *ribonucleotide reductase m2 polypeptide* and *L-3-hydroxyacyl-Coenzyme A dehydrogenase, short chain*; 29.5%) (Table 3.24; Figure 3.18).

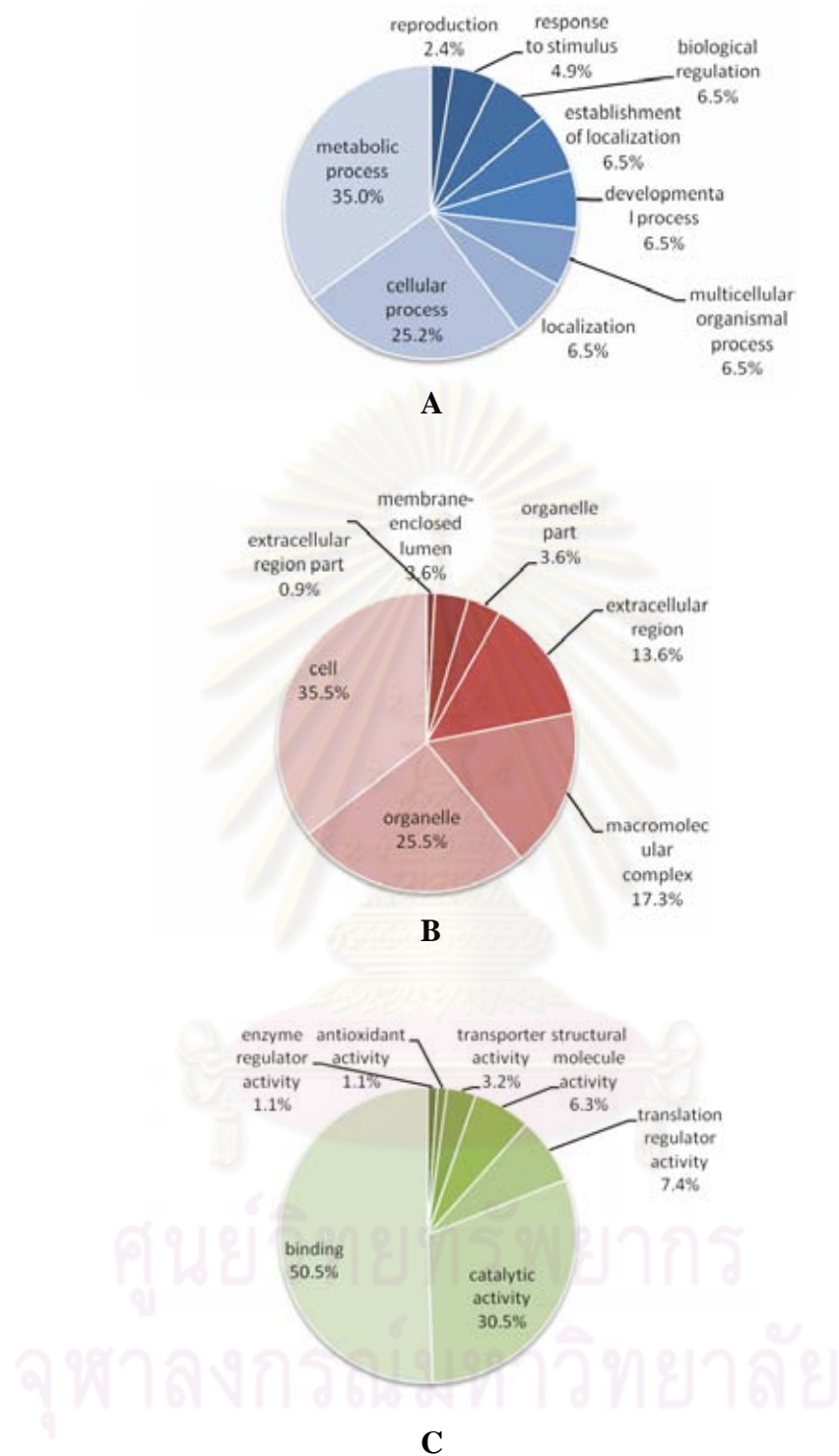


Figure 3.17 The percent distribution of nucleotide sequences according to three principal GO categories in the forward and reverse SSH ovaries cDNA library. A-C are biological process, cellular component and molecular function categories, respectively.

Table 3.24 Classification of nucleotide sequences according to three principal GO categories in all ESTs ovaries cDNA libraries (4560 ESTs)

Type	Term	Number of sequences	Percentages
Biological process	rhythmic process	1	0.1
	maintenance of localization	1	0.1
	multi-organism process	3	0.2
	immune system process	4	0.3
	locomotion	6	0.5
	reproductive process	7	0.6
	growth	9	0.7
	reproduction	21	1.7
	response to stimulus	38	3.2
	biological adhesion	50	4.2
	multicellular organismal process	64	5.3
	developmental process	68	5.7
	establishment of localization	73	6.1
	biological regulation	75	6.2
	localization	82	6.8
	metabolic process	305	25.4
	cellular process	394	32.8
Cellular component	extracellular region part	8	0.8
	envelope	30	3.0
	membrane-enclosed lumen	38	3.8
	extracellular region	67	6.7
	organelle part	129	12.8
	macromolecular complex	153	15.2
	organelle	235	23.4
	cell	345	34.3
Molecular function	antioxidant activity	3	0.4
	nutrient reservoir activity	3	0.4
	motor activity	4	0.6
	transcription regulator activity	5	0.7
	enzyme regulator activity	10	1.4
	molecular transducer activity	10	1.4
	translation regulator activity	21	2.9
	transporter activity	29	4.1
	structural molecule activity	69	9.7
	catalytic activity	211	29.5
	binding	350	49.0

In total, 1023 ESTs transcripts (692 singletons; 15.2% and 331 contigs) were significant similar to known genes previously deposited in the GenBank (E-value < 10^{-4}). One thousand six hundred and seventy-two transcripts (441 contigs; from 3330 transcripts and 1231 singletons) were obtained after clustering analysis (Table 3.25).

Table 3.25 A summary of contigs and singletons creation and BLASTX score in all ESTs ovaries cDNA libraries (4560 ESTs)

Contig/Singleton	Number of transcripts	BLASTX score			
		0	<100	100 - 200	≥ 200
Contigs with no. of ESTs					
2	206	67	18	50	71
3	72	14	9	17	32
4	38	9	3	10	16
5 to 9	76	12	6	15	43
10 to 49	36	8	2	3	23
≥ 50	13	0	1	4	8
Singleton	1,231	539	155	250	287

Function of all ESTs (4560 ESTs) were categorized following the GO ontology biological process and revealed 21 transcripts (14 singletons and 7 contigs) involved in reproduction. These included *egalitarian*, *proliferating cell nuclear antigen*, *actin-related protein 2/3 complex subunit 1 CG8978-PA isoform A*, *RNA binding motif protein 4 lark CG8597-PA*, *SUMO (ubiquitin-related) homolog family member (smo-1)*, *Ubiquitin-conjugating enzyme E2-17 kDa effete CG7425-PA*, *putative beta-NAC-like protein*, *hypothetical protein AaeL_AAEL003957*, *ovarian serine protease*, *carbon catabolite repressor protein twin CG31137-PB, isoform B*, *chicadae/profilin*, *neuralized CG11988-PB, isoform B*, *platelet-activating factor acetylhydrolase isoform 1b alpha subunit*, *nonmuscle myosin-II heavy chain zipper CG15792-PD, isoform D*, *dynein light chain-2 isoform 2*, *hypothetical protein LOC379247*, *oncoprotein nm23*, *dihydrolipoamide dehydrogenase*, *Tubulin beta-2 chain*, *Protein mago nashi* and *laminin beta chain*, respectively (Table 3.26). Moreover, ontological function of all ESTs (4560 ESTs) functionally involving growth in homologue species was investigated (Table 3.27).

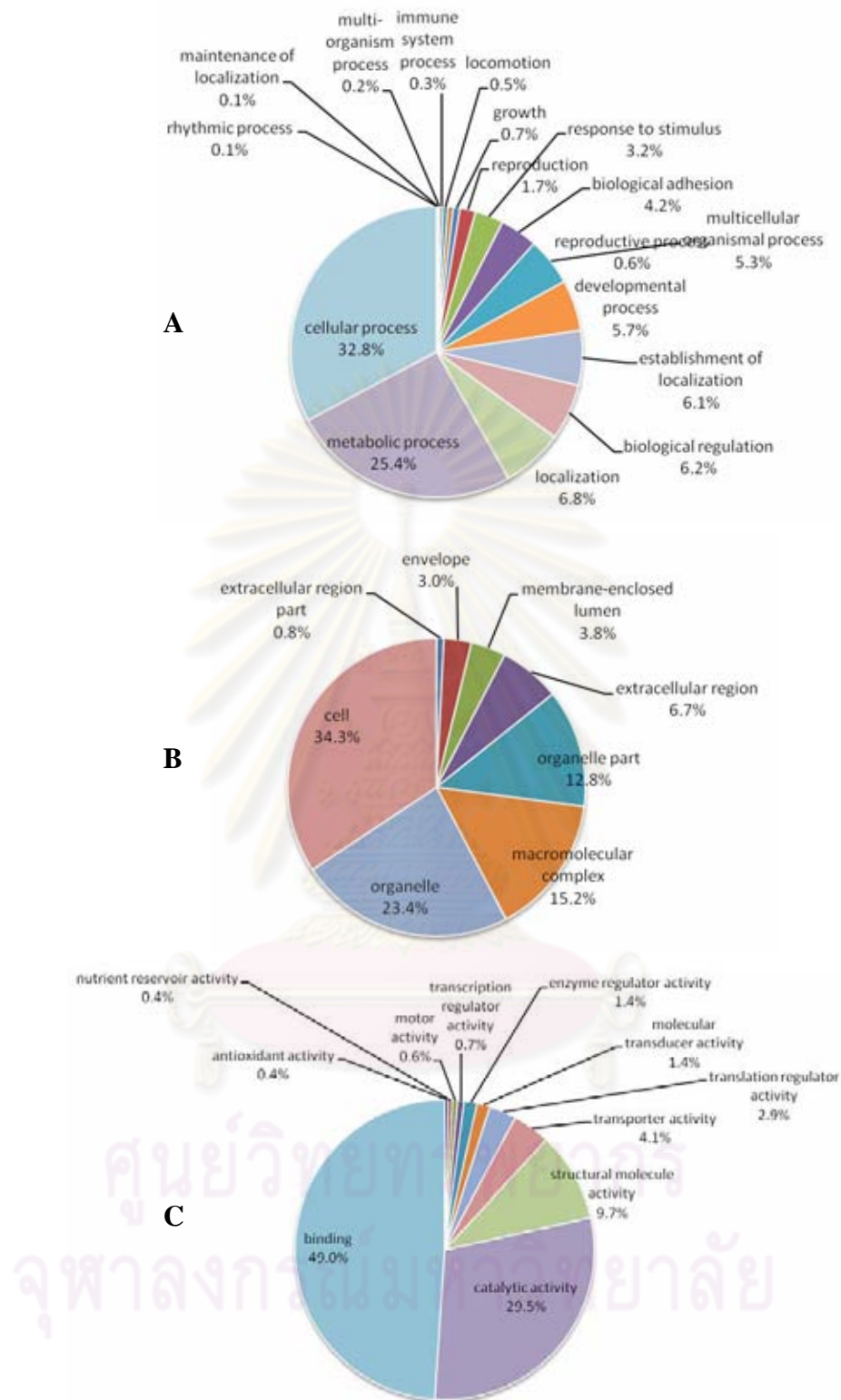


Figure 3.18 The percent distribution of nucleotide sequences according to three principal GO categories in the ESTs ovaries cDNA libraries. A-C are biological process, cellular component and molecular function categories, respectively.

Table 3.26 Ontological function of ESTs functionally involving reproduction in homologue species

Function	Putative transcripts	EST	Accession number
Cellular component			
Male and female pronucleus (GO:0001939 and GO:0001940)	Chromobox protein homolog 1 (Heterochromatin protein 1 homolog beta) (HP1 beta) (Modifier 1 protein)	AlIOV-CT333 (OV-N-S01-0035-W, OV-N-S01-1463-W)	XP_393875
Molecular function			
steroid binding (GO:0005496)	short-chain dehydrogenase	OV-N-N01-1067-W	XP_001655210.1
Biological process			
multicellular organism reproduction (GO:0032504)	oncprotein nm23	AlIOV-CT280 (OV-N-N01-0112-W, OV-N-N01-0359-W, OV-N-N01-0508-W, OV-N-N01-1050-W, OV-N-N01-1339- W, OV-N-N01-1517-W, OV-N-N01-1668-W, OV-N-N01- 1743-W, OV-N-S01-0497-W, OV-N-S01-0871-W, OV-N- S01-0984-W, OV-N-S01-1200-W, OV-N-S01-1507-W, OV- N-S01-2368-W, OV-N-S01-2593-W, OV-N-ST02-0102-W)	ABI93176.1
sexual reproduction (GO:0019953) and eggshell formation (GO:0030703)	proliferating cell nuclear antigen	AlIOV-CT153 (OV-N-N01-0180-W, OV-N-N01-0805-W, OV-N-N01-1098-W, OV-N-N01-1272-W)	ACA09718.1
sexual reproduction (GO:0019953)	twin CG31137-PB, isoform B (carbon catabolite repressor protein)	OV-N-S01-0359-W	NP_732967.1
sexual reproduction (GO:0019953)	platelet-activating factor acetylhydrolase isoform 1b alpha subunit	OV-N-S01-1769-W	XP_001651009.1
sexual reproduction (GO:0019953)	neuralized CG11988-PB, isoform B	OV-N-S01-2003-W	XP_001120035.1
sexual reproduction (GO:0019953)	CG8978-PA, isoform A (actin-related protein 2/3 complex subunit 1A)	OV-N-N01-1082-W	XP_971606.1
sexual reproduction (GO:0019953)	CG8597-PA, isoform A (RNA binding motif protein 4,lark)	OV-N-ST01-0125-W	XP_970745.1
sexual reproduction (GO:0019953)	ovarian serine protease	OV-N-N01-1787-W	NP_001037168.1
sexual reproduction (GO:0019953)	myosin-9	OV-N-ST01-0103-W	EEB15037.1
sexual reproduction (GO:0019953)	dynein light chain-2 isoform 2	AlIOV-CT28 (OV-N-N01-0149-W, OV-N-N01-0374-W, OV-N-N01-0470-W, OV-N-N01-1711-W)	XP_866843.1
sexual reproduction (GO:0019953)	vertebrate homocysteine-inducible, endoplasmic reticulum stress-inducible, ubiquitin-like domain member 1 (HERPUD1)	OV-N-N01-0391-W	CAK03951

Table 3.26 (cont.)

Function	Putative transcripts	EST	Accession number
sexual reproduction (GO:0019953)	dihydrolipoamide dehydrogenase	OV-N-N01-0376-W	NP_001003294.1
sexual reproduction (GO:0019953)	Tubulin beta-2 chain	AlIOV-CT215 (OV-N-N01-1682-W, OV-N-S01-1759-W, OV-N-S01-2251-W, OV-N-S01-2551-W)	Q94571
sexual reproduction and oocyte development (GO:0019953 and GO:0048599)	Profilin (Chickadee protein)	AlIOV-CT279 (OV-N-S01-0198-W, OV-N-S01-0831-W, OV-N-S01-1169-W, OV-N-S01-1528-W)	ABI93174.1
sexual reproduction and spermatogenesis (GO:0019953 and GO:0007283)	Ubiquitin- Conjugating Enzyme (Ubc-2): effete CG7425-PA	OV-N-S01-0547-W	XP_001120139.1
sexual reproduction and oocyte nucleus localization during oocyte axis determination (GO:0019953 and GO:0051663)	egalitarian CG4051-PA isoform 1	AlIOV-CT436 (OV-N-N01-0942-W, OV-N-ST02-0133-W)	XP_623215.1
sexual reproduction and female gonad development (GO:0019953 and GO:0008585)	Cofilin/actin-depolymerizing factor homolog (Protein D61) (Protein twinstar)	AlIOV-CT95 (OV-N-N01-0465-W, OV-N-N01-0526-W, OV-N-S01-2306-W, OV-N-S01-2307-W)	XP_968178.1
meiosis (GO:0007126)	DNA repair and recombination protein RAD54B (RAD54 homolog B)	OV-N-ST01-0068-W	XP_001915028.1
meiosis (GO:0007126)	checkpoint kinase 1	AlIOV-CT409 (OV-N-S01-2602-W, OV-N-ST01-0032-W)	NP_001091925.1
Hormone-mediated signaling (GO:0009755)	serine/threonine-protein kinase LATS1	OV-N-S01-0543-W	EEB15352.1
Response to hormone stimulus (GO:0009725)	serine-pyruvate aminotransferase	OV-N-S01-2642-W	XP_001862936.1
sex differentiation (GO:0007548)	SUMO (ubiquitin-related) homolog family member (smo-1)	OV-N-N01-1208-W	XP_392826.1
sex differentiation (GO:0007548)	putative beta-NAC-like protein	OV-N-S01-2561-W	XP_001607323.1
Reproduction (GO:0000003)	laminin beta chain	OV-N-S01-0522-W	AAK51547.1
Reproduction (GO:0000003)	Protein mago nashi	OV-N-S01-1895-W	XP_001120074.1
Reproduction (GO:0000003)	neutralized CG11988-PC, isoform C	OV-N-ST02-0046-W	NP_731310.1

Table 3.27 Ontological function of ESTs functionally involving growth in homologue species

Function	Putative transcripts	EST	Accession number
Biological process			
positive regulation of growth rate (GO:0040010)	Probable glutaminyl-tRNA synthetase (Glutamine--tRNA ligase) (GlnRS)	AlIOV-CT18 (OV-N-N01-0100-W, OV-N-S01-0015-W)	XP_972452.1
positive regulation of growth rate (GO:0040010)	H3 histone, family 3A	AlIOV-CT345 (OV-N-S01-0235-W, OV-N-S01-0582-W, OV-N-S01-1626-W)	NP_002098.1
positive regulation of growth rate (GO:0040010)	SUMO (ubiquitin-related) homolog family member (smo-1)	OV-N-N01-1208-W	XP_392826.1
positive regulation of growth rate (GO:0040010)	laminin beta chain	OV-N-S01-0522-W	AAK51547.1
negative regulation of cell growth (GO:0030308) and cell growth (GO:0016049)	Zgc:85671 protein DnaJ (Hsp40) homolog, subfamily C, member 2	AlIOV-CT117 (OV-N-N01-0720-W, OV-N-N01-0722-W)	AAH55125.1
regulation of growth (GO:0040008)	Poly [ADP-ribose] polymerase 1 (PARP-1) (ADPRT) (NAD(+) ADP-ribosyltransferase 1) (Poly[ADP-ribose] synthetase 1)	OV-N-S01-1952-W	1A26
Growth (GO:0040007)	ATP lipid-binding protein like protein	AlIOV-CT131 (OV-N-N01-0718-W, OV-N-N01-0833-W, OV-N-N01-0854-W, OV-N-N01-0944-W, OV-N-N01-1092-W, OV-N-N01-1211-W, OV-N-N01-1602-W, OV-N-S01-0506-W, OV-N-S01-0760-W, OV-N-S01-1562-W, OV-N-S01-2127-W, OV-N-S01-2180-W, OV-N-S01-2195-W, OV-N-ST02-0167-W)	BAB85212.1
Growth (GO:0040007)	Tubulin beta-2 chain	AlIOV-CT215 (OV-N-N01-1682-W, OV-N-S01-1759-W, OV-N-S01-2251-W, OV-N-S01-2551-W)	Q94571
Growth (GO:0040007)	Ubiquitin- Conjugating Enzyme (Ubc-2): effete CG7425-PA	OV-N-S01-0547-W	XP_001120139.1

3.2 Isolation and characterization of differentially displayed transcripts during ovarian development of *P. monodon* using RNA arbitrary primed (RAP)-PCR

3.2.1 Identification of candidate differential/stage-specific of differential ovarian development expression markers of RAP-PCR fragments

Forty-five primer combinations of the oligo-dT₍₁₆₎-overhang with A, C or G and arbitrary primers were screened against the first strand cDNA synthesized from mRNA of mature (GSI = 5.689%) and immature (GSI = 1.434%) ovaries and those of juveniles.

The amplified RAP-PCR fragments were size-fractionated through 5% denaturing polyacrylamide gels and silver-stained. Expression profiles of RAP-PCR were categorized to stage-specific, up-regulated, down-regulated and differential expressed (fluctuated expression levels) RAP-PCR fragments. The number of respective groups was 31, 5, 6 and 1 markers, respectively (Table 3.28). Bands from different groups of expression profiles (Figure 3.19) were gel-eluted, reamplified by the original primers and cloned.

Fourteen RAP-PCR fragments from oligo-dT₍₁₆₎-overhang with A, C or G and arbitrary primers were sequenced. Nucleotide sequences of all 14 candidate RAP-PCR markers were examined. A single sequence was obtained from each of a few fragments. However, more than one homologous sequences were obtained from each of several cloned fragments (Figures 3.20 – 3.42).

Similarity search was carried out. Several RAP-PCR sequences significantly matched previously deposited in the GenBank (E-value < 10⁻⁴). These were homologues of, for example, *B cell RAG associated protein*; *N-acetylgalactosamine 4-sulfate 6-O-sulfotransferase*, *DNA replication licensing factor MCM5*, *β-ketoacyl synthase*, *alpha-1,6-mannosyl-glycoprotein* *beta-1,2-N-acetylglucosaminyl transferase*, *putative* and *APEX nuclease (apurinic/aprimidinic endonuclease)* 2. Sequences showing E-value > 10⁻⁴ were regarded as an unknown transcript (Table 3.29).

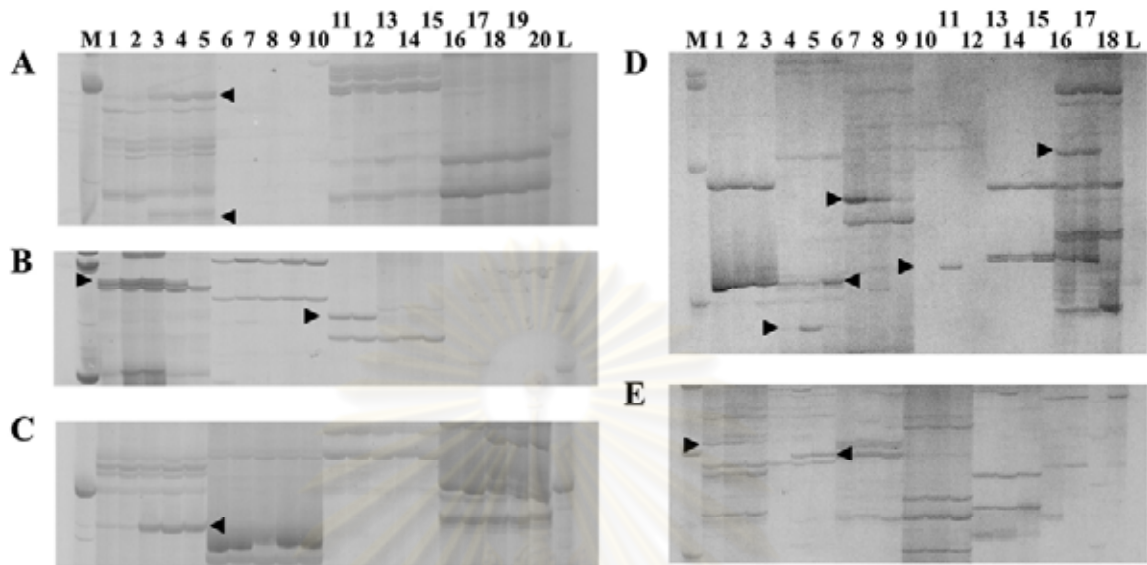


Figure 3.19 RAP-PCR patterns of transcripts expressed in mature (lanes 1 – 2, 6 - 7, 11 - 12 and 16 – 17; A – C and lanes 1, 4, 7, 10 and 13; D and E) and immature (lanes 5, 10, 15 and 20; A – C and lanes 2, 5, 8, 11 and 14; D and E) ovaries of wild broodstock and those of juveniles (lanes 3 - 4, 8 - 9, 13 - 14 and 18 – 19; A – C and lanes 3, 6, 9, 12 and 15; D and E) *P. monodon*. The amplification was performed using oligo-dT₍₁₆₎-overhang with G combined with UBC 191 (lanes 1 - 5; A), UBC 217 (lanes 6 - 10; A), UBC 222 (11 - 15; A), UBC 228 (16 - 20; A), UBC 268 (lanes 1 - 5; B), UBC 273 (lanes 6 - 10; B), UBC 299 (11 - 15; B), UBC 428 (16 - 20; B), UBC 457 (lanes 1 - 5; C), UBC 459 (lanes 6 - 10; C), OPA01 (11 - 15; C) and OPA02 (16 - 20; C) and oligo-dT₍₁₆₎-overhang with A combined with UBC299 (lanes 1 - 3; D), UBC457 (4 - 6; D), UBC459 (7 - 9; D), OPA01 (10 - 12; D), OPA09 (13 - 15; D), OPA02 (16 - 18; D), UBC 191 (lanes 1 - 3; E), UBC 222 (4 - 6; E), UBC 228 (7 - 9; E), UBC 268 (10 - 12; E) and UBC 273 (13 - 15; E). Arrowheads indicate candidate stage-specific/differential expressed markers further characterized. Lanes M and L are 100 bp and 50 bp ladders, respectively.

Table 3.28 A summary of candidate RAP-PCR fragments converted to SCA R markers

Category	Number of genes
Candidate stage-specific fragments	31
- Mature ovaries	11
- Immature ovaries	3
- Juvenile ovaries	1
- Both mature and immature ovaries	2
- Both mature and juvenile ovaries	2
- Both immature and juvenile ovaries	12
Candidate up-regulated fragments during ovarian development	6
Candidate down-regulated fragments during ovarian development	5
Differential expressed fragments (fluctuations of levels) during ovarian development	1
Total	43

TGTCAGCGGTCTCACCTGAGAGATTTGACCTCTTAGTCAAGAGCTCC**CTTGAATGTGGGAAAACC**GCACAACAGA
 ATACTCAGTGAGAACTTGTGCCTACAATAAAACATTGCAAAACGCTATGGGTGTTTCGTTTGTATAATGGGTGTAT
 AGTGTGTTTTTGTGCGACTGGCTGAAGGTGTTTCCCTCGAGAACAGGTGCTAGTTGTCAGAATGGAGGATTACCATC
 AAAATATGGTCTCTTCCCTAGCTACAATCTACAGTCATCTTGGCCTAAGACCTCTA**ACAGATGACGAAGAAGAGGT**
AGTCAACACAGCACCAATACACAATAAAAAGCAAGAGGAAAAAGACTGTAGGCAAGATGCTCAACTCCACCGCTGAC
A

Figure 3.20 Nucleotide sequence of a candidate stage-specific RAP-PCR fragment (mature ovaries, 381 bp) generated from oligo-dT₍₁₆₎G-UBC 299 primers. Positions of RAP-PCR primers were illustrated in boldface and underlined. Positions of the forward and those complementary with the reverse primer for RT-PCR were bold-italicized and underlined.

GACCGCTTGTGGTGAAAGAAGAACCTAAGGATGAGGACATAGAGCCTAATTGTGTCTTCCCAGGTGACACTCGGGA
 AACCCCAAATATCCTTCCCTGACGGTGACCGGCCAGC**TGACATTCCCTCCAGACGCT**GTCTCACCTCGGCTGTTGCTG
 TCACCGTGTGCTGCTGGTTCACCTGTATTAGGTGGACCAAGTCAAATCCCCTGAGTGCAAGGTTGCAGCAGCAGCAA
 AGATAGCTGCAGATATTGACAGTTCTCACGCTCTAACCAAGAAGTCAAAGCTGAACCTTGTGTAGCCGAGGCTTG
 TTCTAGCAAGAACAAGTCAAACGTGTTGGAAGTAGCCACAGAGGCTTTGGTCCCTGAAGATAAGGTACAGTTAGCT
 GCAGTGCCAGAGGTCCCCAATGTAACCT**TGTGCCTAAAGTAAAGTGAAGC**ATATATTCCTGAGGCTACAGACACTA
 AAGCTGCTGTCCCTGGGGATACAAAATCAGAAGCCTTAGTACCTGAGTCTGTTGACACAGAAGCTCTAGTTCCAGA
 AGACACAGTTGCTAAGGCATTTGAACCTGAGGCTTCTGAAGCTGCTATCCCTAAAGAAAAAGTCACAAAGGTCTCA
 GACCTGAACCCCATGCAGAGTCTCTGTTATAGAAAAGTCTGATATAACAGAATCTGCTACCATAAAGGATATTG
 TTTCAGAAGCTTCAGTTCAATTGGCCACTGTTCCAGAGGCAGCAGTTATTGAAGCTGCTATTCCAGGAGTTATTGA
 TGCTGAGGCTGTTGTTCCAGAGACGGCAGTAACTGAAGCTACTGTAACAAAATATTACAGACATTGATGGTG

Figure 3.21 Nucleotide sequence of a candidate stage-specific RAP-PCR fragment (mature ovaries, 831 bp) generated from oligo-dT₍₁₆₎G-OPA17 primers. Positions of RAP-PCR primers were illustrated in boldface and underlined. Positions of the forward and those complementary with the reverse primer for RT-PCR were bold-italicized and underlined.

GTCCACACGGAACACTTGCCTCTGTTTGGAGGAAGCA**GCCAAGGAGGTAGCAGATGA**GGTGACAGCACCCAGGCCTC
 AAGGAGAAGAGAAAGTTGAAGATATCCAAATAACACTCACCTCCGCCTCAAATCCTGTTGATGTCCGCAATCTGCA
 GTCTGAGGAGGTTAGCCGATTGGTGAAAGTAGCTGGTATTGTGGTTGCAGCCTCAGGGGTGAAGGCCAAGGCTCTG
 ACCTGACAGTGCAGTGTCTGCTGCCAGACCACAATCCCAACATTCCTGTCAAGCCTGGTCTTGAAGGATACC
 AGCTGCCAAGAAAGTGCAACACAGAGCAAGCAGGCCGTCCAAAGTGCCTCTAG**ATCCCTCTTCATTGTCCCTGA**
 TCGATGCACATGTGTGGACTACCAAGTTCTGAAGCTTCAGGAAGTACCTGAAAAATCTGCCACAGGGAGAGATGCCT
 CGTCACCTCCAACCTATGTTGACAGGTCTCTGTGAGCGTGTGTACCTGGGAACAGAGTCAAGTTTTGGGTA
 TTTACTCAATCAAGAAAATTGGTAAATCTACAAGAGGCTCAAGAGACAAGTTGCTGTAGGTATTCTGTCGCCCAT
 TCT**CCGTGTGGAC**

Figure 3.22 Nucleotide sequence of a candidate stage-specific RAP-PCR fragment (mature ovaries, 621 bp) generated from oligo-dT₍₁₆₎G-OPB08 primers. Positions of RAP-PCR primers were illustrated in boldface and underlined. Positions of the forward and those complementary with the reverse primer for RT-PCR were bold-italicized and underlined.

TGCTGGGACACGTGACAAGGAGAGAGGACGAGTACGTGGGCAAGAGGGTGAGGAGACTGGTGGTTGGGAGAAGAAA
 GAGGGGAAGACCGAAGAGGAGATGGGAGGATTGCATCAAGGAGGACATGGAGACGGCGGGAGTGACGGAGGGGAG
 GCCCTGGATAGGGCAGAGTGGAGGAGGAAGATCCGCACCGCGACCCCAAGTTGAACTGGGACAAAAGCCTTTTGT
 TTTTATTCTTCCATTTCTCTCTTAATTCCTTACTGCATCCTTTCCCAAGCAGCATTAATAAATTGTGAAGGCCA
 TCTAGCTCTTATTCA**GTCCACAGCAG**

Figure 3.23 Nucleotide sequence of a candidate stage-specific RAP-PCR fragment (immature ovaries, 329 bp) generated from oligo-dT₍₁₆₎A-OPB10 primers. Positions of RAP-PCR primers were illustrated in boldface and underlined.

CTGCTGGGACCCGAGGGAAGGAGGGATAGAAACAGGGAGATATTAATAGGAAACAAAGGGAGGGAAGTATACGGGAA
 GGAAGGACAGAGGCGCAGAGGAAAGGAATAGTATGAGGTGAGAGAGATAGAGAGACCGGAGGACCGAACAGCAGAG
 GAACAGAGAGGATGGAAGCTGGGATAGAGGGATGGGCTAGGGTCGATGATTCACGCATCTACTTAAACATTTACGA
 CAGGTCCCCCCCCCGTCCGCGTCAATGCCGTTAACGCTTGCCGTGTCAGGTAATTCGCAAGCCTTTGTATTTAT
 TGACACAAACGTTATG**GTCCACAGCAG**

Figure 3.24 Nucleotide sequence of another candidate stage-specific RAP-PCR fragment (immature ovaries, 331 bp) generated from oligo-dT₍₁₆₎G-OPB10 primers. Positions of RAP-PCR primers were illustrated in boldface and underlined.

CTGCTGGGACAAGGGTTTTGGTGTAGTAAGATCAATAAGTACTAGTTCTAGCCTTGCAAGAGAACTATTACCCTAC
 TGCTTACACTTTACACGGAATGAAGTACAAGCCATTTGTAGAACTGAATGCACCATTAACCTGGTGGGCAGAGCAC
 TTTAGTGTGCCTGATGCAGTCTTCCCAGAGATATCAAAACATGCTTTGTTAATTGGACAAGGAAATTCGGCCAAGT
 TGCTAGAGCTGAAGATGAATGGTCTGACTCATGAGGCTGGACATATAGAGTGCAACCCAGGAGCTTTCAAGTATCC
 TGAATTAATGCCAATA**GTCCACAGCAG**

Figure 3.25 Nucleotide sequence of an additional candidate stage-specific RAP-PCR fragment (immature ovaries, 330 bp) generated from oligo-dT₍₁₆₎G-OPB08 primers. Positions of RAP-PCR primers were illustrated in boldface and underlined.

CAGGCCCTTCAAATCACAAGATTCCAAACTTCTTGCATTAGAGATGATCTATTAAG**AGCTGTCTTGATTCTCTCGGA**
 TTTACGAGATGCAAATGAGGAAGAGGATTGTAGAGAGGAGGATGAACGTGTTCCGATGTAGTGCTGATATGAAAT
 GATGGTGTGGATGTATTTACGTAATAACCTTCTTCTTGTGTTCTTGGAGCAATGCTACTCTCTGTAAGATCTTGT
 ATGATATGTAATCCGGAGGGTATC**ATGGGGTTATGAAGCCGTT**CGAAGTATTATCATAAATTTCCA

Figure 3.26 Nucleotide sequence of a candidate stage-specific RAP-PCR fragments (immature ovaries, 294 bp) generated from oligo-dT₍₁₆₎G-OPA01 primers. Positions of RAP-PCR primers were illustrated in bold face and underlined. Positions of the forward and those complementary with the reverse primer for RT-PCR were bold-italicized and underlined.

CAGGCCCTTC**CAGGTGATCTATCCATTACTGTACG**TGTTACTGGTGTACTTTTGGACTGATCAACCCCTAGAGGCG
 CACAGGTTCTTCATGTTCAACACAATGTGTATCATGACATCACTAGTGGCACAGTCTCTCGGCTTGGCCATTGGTG
 CTTGTATGAATATACAGGGTGTGTGTTCTGGGTCTATAACATCCATTCTGT**GTTGCTCTTCTCGGGATTCTT**
 TGCTAATTTCTCAACCATCCAATATATCTAAGGTGGATAACATATATATCTTATGTAAGGTACGGGTTTT**GAGGG**
CCTG

Figure 3.27 Nucleotide sequence of another candidate stage-specific RAP-PCR fragments (immature ovaries, 308 bp) generated from oligo-dT₍₁₆₎G-OPA01 primers. Positions of RAP-PCR primers were illustrated in boldface and underlined. Positions of the forward and those complementary with the reverse primer for RT-PCR were bold-italicized and underlined.

CAGGCCCTTCCCATATCAAGAGAAAGTTTATGACTTCCCCCTCCCCGTTCTGTTCCGTTTCTTTTTTCATCTTCC
 AGTTC TAAAGGATGCAACAATGGGTATTTTTCCCTACTTACTTTATTTTGAGTCTTATTATCCTGCTTCGTAGAGA
 CAAAGTTCAGTGAATGTAAAGATAATGACTTCGTTCCCTGGCTATTAGGGAGGATTTTGGTATTTTATGCAAGTGTA
 CGTGTAGTTATTATACGTTACATATCCGTTGATATTAAGGTTTTTGTGTACAGAGAAAGAACCTTGACCATCAA
 TTTTTATTTTGTATTGTTGCATAATCCAT

Figure 3.28 Nucleotide sequence of additional candidate stage-specific RAP-PCR fragments (immature ovaries, 335 bp) generated from oligo-dT₍₁₆₎G-OPA01 primers. Positions of RAP-PCR primers were illustrated in boldface and underlined.

AGGCCGCTTA**GGATTGGGCAACCGAGTTATCA**GTAACCTCTGCGGCTTGTGCCACGGGCACACAAGCTATTTTAATG
 GGCCATGAGTATATTAACATGGCATGGCAAAACGTATGGTAGTGGGTAGCAGTGAATATGTGGATGCATATGTTT
 TCGGGGCGTTTGATTCTATGCGTGTTTTGTCCAGAAAGTTAATCATGAACCTGAAAAGAGCTTCCAGGCCAATGAG
 TAG**TA****CTGCGGGTGGCTTTGT**ACCGGGTTCGGGTGCCGGCGCACTGGTTTTTGAAGACTTGGATTTTGATTACAA
 CGTAATGCAACTATCTATGCAGAAGTTTTAGGTGGCTGTAATAACTCCGGTGGGCAGCGTGGAGGCGGCACAAATGA
 CGGCTCCCGCATCTGCAGGCGTTATTAATGCATCACCGATGCGCTCGAAAGCGCTGATATTACGGGTGACGATGT
 TGATTTGATA**AAGCGGCCCT**

Figure 3.29 Nucleotide sequence of a RAP-PCR fragment (294 bp) found in mature ovaries and those of juvenile generated from oligo-dT₍₁₆₎G-UBC268 primers. Positions of RAP-PCR primers were illustrated in boldface and underlined. Positions of the forward and those complementary with the reverse primer for RT-PCR were bold-italicized and underlined.

AGGCCGCTTAAGAGGCCAAGGGGAAATTAGCTGGTGAAATAACCGTTAAAAAATTTGCATTTTTTTTCC
CGGCATTCTGAATGGGGCTTTTAAACGGATATAATCCT**GGAGGACAGCAGAGTAAAAA**ATGTGTTTGTTTA
GGGTCCATTTCGAAGGAGTAACTAGTTATTAACTTCAAAGCAAAATCAGTTTAGAAAACAAAACAAATC
AAAGTAGTTACAAGTTATTCTCTGACAGAGCAAAACGATAGTAACTAGTTATTCACATAAAAACAATGT
AGAAAGCAAAACATGGAAGTAGGAACTAGCTATTTAGTTACACAAAACGTATTAATAGGTTAAACGAGG
AGTAAACGACATGCAAGGAAGTGAATCGTACCTCAATTACAAGGAGCTACTGAAATCTACATGTCTTGA
AGCGCGAACGGCTG**GAATGTTGACTGTCTGCTTTG**TTGTTTCACTTTT**CTAAGCGGCCT**

Figure 3.30 Nucleotide sequence of an another RAP-PCR fragment (474 bp) found in mature ovaries and those of juvenile generated from oligo-dT₍₁₆₎G-UBC268 primers. Positions of RAP-PCR primers were illustrated in boldface and underlined. Positions of the forward and those complementary with the reverse primer for RT-PCR were bold-italicized and underlined.

GCTGCGAGTGGAATATGCC**CAGGGACAGTGACCAAGACT**GTCTTAAACAAGGCTTGGCCAGATAAGTACG
GGCACTACCGGGAGCCACAGTTTACCCAAAATCAAACATCACTGGTGGTGGAAAGATCAACAGGTAGGGCG
AGCTGCAGTTATTTAGATTTGGAGCTAATTTGCCGAACACTCGTCATACAGTGGACGGGATAAGTATGG
TCGAGAAGATGAGTCTTTTGTTCGGACCATTGATCAAAGATGTGTTGAACTGATCCAAGGAAAAAA
TGGTGACTCACAGAACACTTGTGAATTTTTTTTATCATTTTCATCATAACGATTTATATAATCTTTT**A**
TCTACTATCACTCCTCGTTTCTCTATTTTATTGTACATTTACAAAATAATCATATATTTTACCTATCGG
TTATAATCATG**CTCGCAGCTT**

Figure 3.31 Nucleotide sequence of a RAP-PCR fragment (435 bp) found in immature ovaries and those of juvenile generated from oligo-dT₍₁₆₎G-UBC135 primers. Positions of RAP-PCR primers were illustrated in boldface and underlined. Positions of the forward and those complementary with the reverse primer for RT-PCR were bold-italicized and underlined.

AAGCTGCGAGTGGCCCCTGAACTGTTCCCTCAAGATGCTT**ATAGTTGGAGGTATTGACAG**AGTATATGAA
ATTGAAAAACAATTTAGGAATGAAAGTATTGATCTCACACACAACCCAGAGTTTACAACCTTGTGAATTT
TATATGGCTTATGCAGACTATAATGACTTGGATTGAGCTTACAGAGAAATTGGTGTGAGGAATGGTTTAT
AGTATTTTTGGTTTACATAAAAAGTGAATTTCCAGCCACAAGGACCAGAAGGTGAAGAATGGGAAATTTGAT
TTTT**AAACCTCCCTACCGAAGAAT**TACATGTTCCAGATCTTGAGAAGGAACTTAGTGTAACCTTCCA
GCCCCAGATCAGCTTAATTTCTGAGGAGGCACGTAACCTTTAAGTGACTTGTGTGAGAAGCATGGTGTGA
GAGTGCCCCCT**CTCGCAGCTT**

Figure 3.32 Nucleotide sequence of an another RAP-PCR fragment (437 bp) found in immature ovaries and those of juvenile generated from oligo-dT₍₁₆₎G-UBC135 primers. Positions of RAP-PCR primers were illustrated in boldface and underlined. Positions of the forward and those complementary with the reverse primer for RT-PCR were bold-italicized and underlined.

CGATGGCTTTCCCAATATATTTAACAGAGAGAAATTCAATGTATAGCACAATATTATGGAAAGACTTGACCAGTAC
 TAATAAATGGTGAATGAATCAAATAAATGGAACATTAAAAATGCATGAGTCGTGAGGAAGGAAATATAACACAAAAA
 GTAATGCTAATATATGGCAATGGTTATATCAAATCAATCATTTTTCTACCCAGTTTCTCCATAAAACACAAGACT
 TGGTCCCAAATTTGGAATCAGCTGGTCTTGGACCAACACTATTTGCCAAATCTCGGCTTAAAGAAGCATGGTTGT
 AACAAACATTCATAACTTCTTAAAAAAGACAAATAAATAAAAAGAAATCAAGAAATCTTAAACTAAATTC**AAAGC**
CATCG

Figure 3.33 Nucleotide sequence of a RAP-PCR fragment (385 bp) found in immature ovaries and those of juvenile generated from oligo-dT₍₁₆₎G-UBC191 primers. Positions of RAP-PCR primers were illustrated in boldface and underlined. Positions of the forward and those complementary with the reverse primer for RT-PCR were bold-italicized and underlined.

CGATGGCTTTAAGAATGCCTACAGTGTGAAAGTTCTCCCTTCTCTTAAAGAAGAAGAAACTATAACATTTAAGGTC
 ATCCTTGAGTTAGAGGAAGGTGATGGCGATCCTGTGT**CCTTCACTGTCCAGATTTCC**CGAGGCATAACCAAGGAC
 TTAGGGAACATAATGGTATCTCTCAAATGCACTGATATGCATAAAAAATATTTCTTTTACGATCTTTCGGATGTTGGA
 TACAATGCTACGTTACCATCGATTGCTCAGATAC**GAAGCGGTTGGAAGAAAAG**ATATTTCTTATTGAATAGAGAA
 ATCAACCGTCCAATTGACATTGGACCAGCTGTGCAAGGAGTCAACGGGTTCTTCAGTAGCAT**GAAGCCATCG**

Figure 3.34 Nucleotide sequence of another RAP-PCR fragment (377 bp) found in immature ovaries and those of juvenile generated from oligo-dT₍₁₆₎G-UBC191 primers. Positions of RAP-PCR primers were illustrated in boldface and underlined. Positions of the forward and those complementary with the reverse primer for RT-PCR were bold-italicized and underlined.

TGCCGAGCTGAGAACTACACAT**ATGATTATTTGGGCGGACT**CAACTCCTGCCTTTTGATCAGTGTCAATTGGTTC
 ACTCTGCTGCTCGATTTGTATATGGGCAGGAGCATCATATTAAGGTATCTTCTGCCTAGACGATTCTCAAATCC
 TCACTGTATCAGGATCACAGTATCAATCTTCTGTGAGAAAGTGTGATATCCCCAACATGACATGACAGC
 CAGTAGCTCTGATGGCAGCTGCCCTTTGCCGTAGCAATTCATAGAATCTTAATTTATAGATGCCA**CGCTCTGGTTT**
CTCAGGGTCTACATGTGGCAGTATACATTTATGACTGCTATTCTCAACTCTTTTCTTCTGTATCCCTCATAAGA
 TTTTGTGTGATGA**CAGCTCGGCA**

Figure 3.35 Nucleotide sequence of a RAP-PCR fragment (403 bp) found in immature ovaries and those of juvenile generated from oligo-dT₍₁₆₎G-OPA02 primers. Positions of RAP-PCR primers were illustrated in boldface and underlined. Positions of the forward and those complementary with the reverse primer for RT-PCR were bold-italicized and underlined.

TGCCGAGCTGTGAGGAGAAGGTCAACAATATGATTGCGGACTGAAGGGCACCATAGATAAGACAGAGTTGAAAGA
 CTTGGCCCTGACGGACATTTATGAAATGTATGAGTACAAGATGACTGCCATGGCACATGTGGAGATAACATTGAGA
 GATGCGCTGGCGGCAGCCGATGCGCAGAACAGACAGACCCACCCTCCATGCTACAGACAAGGGCTCAGAAAGACC
 ATCTGCGAAATCTTCTGCGCACGTGGGAACAGAACTCCAAGCATCTGAGAAGGACAAGAATGAACTGCAAGCAAC
 TATTTTCCAAGTGCAGAACT**CAGCTCGGCA**

Figure 3.36 Nucleotide sequence of another RAP-PCR fragment (334 bp) found in immature ovaries and those of juvenile generated from oligo-dT₍₁₆₎G-OPA02 primers. Positions of RAP-PCR primers were illustrated in boldface and underlined.

TCCACACGGCCAGAACTCCATTAACAGCTAGATCAAAATGGCAGAAGAAATTGGCTACCTGAAAAATGACCCG
 AATTTTGGCACTCGTGCCATCCACGAAGGCAATGAGCCGAGCAGTGGAAGTCCATGGCAGTTGTTCTCCA
 ATTTCCAT**GGCCACA****ACTTTCAAGCAGG**ATGGCCCAGCAGATTTTAAGGCATTTGAGTACGGTCGCTCTGGT
 AACCCAACAAGAACTGTGTGGAGAAATGTCTAGCAGCAACAGAGGAAGCCAAACACTGTATAACCTTTGCC
 TCTGGTTGGCTGCGACAACCACCATCACGCACTTGTCTCAGCTGGGGATCATGTGATTTCCAT**GATGAC**
CTGTATGGCGGCACCAACCGTTACTTCC**CCCGTGTGGAC**

Figure 3.37 Nucleotide sequence of a candidate up-regulated RAP-PCR fragment (499 bp) generated from oligo-dT₍₁₆₎G-OPB08 primers. Positions of RAP-PCR primers were illustrated in boldface and underlined. Positions of the forward and those complementary with the reverse primer for RT-PCR were bold-italicized and underlined.

CGGTCGAGGGCAGTTATGTGTACAAGGGAAACAAAATCTCCAAGGTCCTGCGGATGAGAAGGAAGCTCTTA
 CCTCAGATCTGATGGGCATGTTTGAAAAGCGAAGGTTCAAGAACTTCTGGTGTTCGCCAAGATTACCGTG
 ACGATGACCCAGCTTGTGAACGGCCTGGTGTCTTTGCAAAGCTCGAAGACTGCACCTGAATATTACTCTTGCA
 TCTCGCTTCAACATGGGTGGCTGCAGAGACTGTTTCATGTGCCCAGTGGAACGCTGTTCAACGAGGTAACAG
 GAGCTTGTGAAGATCCTTGCTCACGGACAATGGTGTGCTATGAGGAAGGCGGGTCCAGATCCCCTCGACG
 C

Figure 3.38 Nucleotide sequence of a candidate up-regulated RAP-PCR fragment (361 bp) generated from oligo-dT₍₁₆₎G-UBC459 primers. Positions of RAP-PCR primers were illustrated in boldface and underlined.

CGGTCGAGGGCGTGACCGTGAACAAGGTTCAAAATATAAACACCATCCATGCAGTTTATCCAATCGATCTTC
 CTAGCACAAAGGCCATTTACAAGAATGGCTT**GGGCACGGATACATCTACAA**AGACGGGAAAATGAAGCTGC
 TTATGGTCCGTAATATGTGGACAAATTCCATGCTCTGGATGTGCATGTGGAAGTAACCTCGACCGACACGAGTT
 GTGCCTGCTGTGCTAACGGTGAAGACTTTGCTTACCT**AGTGAAGGTCTCCAGGGTAA**CATTTGTGTTGGAG
 GCACTGGTGACCTTGCGTTTGTGAGTGTCTCAAACAGGTATTTCGACCTCTT**CCCTCGACGC**

Figure 3.39 Nucleotide sequence of a candidate up-regulated RAP-PCR fragment (349 bp) generated from oligo-dT₍₁₆₎G-UBC459 primers. Positions of RAP-PCR primers were illustrated in boldface and underlined. Positions of the forward and those complementary with the reverse primer for RT-PCR were bold-italicized and underlined.

CGACGCCCTGCAGATGGTAGGTCGTGCAAATAGACCTAATGATGATGAT**GAAGCCAAGTGTCTCAT**GTG
 TCATTCCTCAAAGAAGGACTACTTTAAGAAGTCTTGTATGAGCCTCTGCCCATCGAGAGCCATCTTGACCA
 TGCCCTCCGTGACCATTTCAATGCTGAGATTGTCACACGTACCATTGAAAACAAACAGGAGGCTGTGGACTA
 TGTCA**CTTGGACTTTCTTATACCGC**CGCATGACACAGAACCCCAATTACTATGGGCTA**CAGGGCGCTG**C

Figure 3.40 Nucleotide sequence of a candidate up-regulated RAP-PCR fragment (284 bp) generated from oligo-dT₍₁₆₎G-UBC457 primers. Positions of RAP-PCR primers were illustrated in boldface and underlined. Positions of the forward and those complementary with the reverse primer for RT-PCR were bold-italicized and underlined.

GCTTCCCCTTCAGCAAATCAGGAAACCCAATTATGTCCACT**TGTGGCTTCCTTGGCATCTG**TTGTTGACC
 CCAGGATCGCAGCGTCTGCAGCCAAGGCAGCCATGGATGAGTTCTGCAGGATTAAGGACGAGGTCCC
 CTGCTCTCCTTACTCGCACAT**CAAGAATGTCGCAGATAATGC**TGCCTCTAATGAAGGAAAGGTTGATC
 CCACTGCCGGCTTGGCCAAGTCCGGCATTGCTGGTACTGAACCAGAAGGTGAGGAGAAGAAGGAAGGG
 AAGCGCTTCCCCTTTCAGCAAATCAGGAAACCCAATTATGTCCACTGTGGCTTTCCTTGGCATCTGTTGTT
 GACCCAGGATCGCAGCGTCTGCAGCCAAGGCAGCCATGGATGAGTTCTGCAGGATTAAGGACGAGGT
 CCGGCTGCTCTCCTTACTCGCACAT**CAAGAATGTCGCAGATAATGC**TGCCTCTAATGAAGGAAAGGTT
 GATCCCCTGCGGGCTTGGCCAAGTCCGGCATTGCTGGCACTGAACCAGAAGGTGAGGAGAAGAAGG**AA**
GGGAAGC

Figure 3.41 Nucleotide sequence of a candidate down-regulated RAP-PCR fragment (560 bp) generated from oligo-dT₍₁₆₎G-UBC138 primers. Positions of RAP-PCR primers were illustrated in boldface and underlined. Positions of the forward and those complementary with the reverse primer for RT-PCR were bold-italicized and underlined.

TCTGTGCTGGTCACACGACTCGCAGCGCATATGTGTTGTAGGAGAAGGCCGGGGAAAGTTTGCCACGT
 TTTCATGATGGACACGGGAGCCTCGGTGAAAGGTGACCTTCTGGACA**CACCAAGGCTATCAACTCAGT**
 CTCTTGGAAAGCCGACCAGACCTTTCGCATTGCCACTGGCTCCGAGGATAACAAGTCTGCCTTCTATGA
 GGGTCCCTCCATTTGTCTTCAAGTGCACCAAAGCTGATCACACAAAATTTGTCCAGTCTGTACGGTACTC
 TCCAGATGGTGAGAAAATATGCCAC**GGGTGGATTTGATGGCAAG**GATCTTTGTCTACAATGGAAAGGATGC
 TGAACTCATCAAGGAAATGGGATCC**CCAGCACAGA**

Figure 3.42 Nucleotide sequence of a candidate differentially expressed marker (380 bp) generated from oligo-dT₍₁₆₎G-OPA14 primers. Positions of RAP-PCR primers were illustrated in boldface and underlined. Positions of the forward and those complementary with the reverse primer for RT-PCR were bold-italicized and underlined.

ศูนย์วิทยทรัพยากร
 จุฬาลงกรณ์มหาวิทยาลัย

Table 3.29 Candidate differentially expressed SCAR markers in *P. monodon* initially generated from RAP-PCR using an oligo-dT₍₁₆₎-overhang with A, C or G in combination with each of 45 arbitrary primers

RAP-PCR marker	Expression pattern*	Sequence patterns	Sizes (bp)	Transcripts homologues	Closest species	E-value	RT-PCR
oligo-dT ₍₁₆₎ G-UBC 299	M	1	381	<i>B cell RAG-associated protein; N-acetylgalactosamine 4-sulfate 6-O-sulfotransferase</i>	<i>Gallus gallus</i>	2x10 ⁻²⁰	Yes
oligo-dT ₍₁₆₎ G-OPA 17	M	1	1300	<i>hypothetical protein W02B8.3</i>	<i>Mus musculus</i>	2x10 ⁻⁰⁷	Yes
oligo-dT ₍₁₆₎ G-OPB 08	M	1	621	<i>DNA replication licensing factor MCM5</i>	<i>Aedes aegypti</i>	3x10 ⁻⁸³	Yes
oligo-dT ₍₁₆₎ A-OPB 10	I	1	329	<i>Unknown</i>			-
		2	331	<i>Unknown</i>			-
		3	332	<i>Unknown</i>			-
oligo-dT ₍₁₆₎ A-OPA 01	I	1	294	<i>Unknown</i>			Yes
		2	308	<i>ABC transporter</i>	<i>Drosophila melanogaster</i>	6x10 ⁻²⁸	Yes
		3	335	<i>Unknown</i>			-
oligo-dT ₍₁₆₎ G-UBC 268	M,J	1	474	<i>β-ketoacyl synthase</i>	<i>Tenacibaculum sp. MED152</i>	2x10 ⁻⁴¹	Yes
		2	474	<i>Unknown</i>			Yes
oligo-dT ₍₁₆₎ A-UBC135	I,J	1	435	<i>alpha -1,6-mannosyl-glycoprotein beta-1,2-N-acetylglucosaminyltransferase, putative</i>	<i>Caenorhabditis elegans</i>	1x10 ⁻⁰⁸	Yes
		2	437	<i>lysyl-tRNA synthetase</i>	<i>Danio rerio</i>	4x10 ⁻⁵⁶	Yes
oligo-dT ₍₁₆₎ A-UBC191	I,J	1	385	<i>Unknown</i>			-
		2	377	<i>Unknown</i>			Yes
oligo-dT ₍₁₆₎ A-OPA02	I,J	1	403	<i>APEX nuclease (apurinic/apyrimidinic endonuclease) 2</i>	<i>Xenopus tropicalis</i>	8x10 ⁻³¹	Yes
		2	334	<i>GA11764-PA</i>	<i>Apis mellifera</i>	2x10 ⁻⁰⁸	-
oligo-dT ₍₁₆₎ G-OPB 08	Up regulation	1	399	<i>cystathionine gamma-lyase</i>	<i>Rattus norvegicus</i>	6x10 ⁻⁴²	Yes
oligo-dT ₍₁₆₎ A-UBC 459	Up regulation	1	361	<i>Unknown</i>			-
		2	349	<i>Thrombospondin</i>	<i>Marsupenaeus japonicus</i>	1x10 ⁻²⁷	Yes
oligo-dT ₍₁₆₎ G-UBC 457	Down regulation	1	284	<i>U5 snRNP-specific protein, 200 kDa; U5 snRNP-specific protein, 200 kDa (DEXH RNA helicase family), partial</i>	<i>Gallus gallus</i>	5x10 ⁻⁴²	Yes
oligo-dT ₍₁₆₎ G-UBC 138	Down regulation	1	560	<i>Moiria CG18740-PA</i>	<i>Apis mellifera</i>	1x10 ⁻²⁶	Yes
oligo-dT ₍₁₆₎ G-OPA 14	Differential expression	1	380	<i>WD-repeat protein 1 (Actin-interacting protein 1) (AIP1)</i>	<i>Gallus gallus</i>	2x10 ⁻³⁶	Yes

*Expression patterns of original RAP-PCR: M = found in mature ovaries, I = found in immature ovaries and J = found in juveniles ovaries, - = not determined.

3.2.2 Preliminary examining expression patterns of genes related to ovarian development by RT-PCR

Sixteen sequence-specific primers were designed from nucleotide sequences of 13 identified RAP-PCR fragments. Transcripts were non-quantitatively examined using the cDNA template of ovaries of female juveniles and broodstock of *P. monodon* using RT-PCR analysis (Figures 3.43 - 3.44). Eleven primers generated the expected amplification product. Seven genes (*B cell RAG associated protein*, *hypothetical protein W02B8.3*, *DNA replication licensing factor MCM5*, *APEX nuclease* and *U5 snRNP-specific protein*, *ABC transporter* and *Moirra CG18740-PA*) showed a trend of differential expression between different ovarian developmental stages. Four genes (*Lysyl-tRNA synthetase*, *Unknown:oligo-dT₍₁₆₎A-UBC191*, *Cystathionine gamma-lyase*, and *Thrombospondin*) seemed to be comparable expression during ovarian development of *P. monodon* (Tables 3.30 and 3.31).

Table 3.30 A summary of expression patterns of various gene homologues or unknown transcripts analyzed by RT-PCR using primers derived from RAP-PCR

Category	Number of genes
Trend in differential expression levels between ovarian developmental stages	7
Comparable expression levels in different ovarian developmental stages	4
No amplification product	5
Total	16

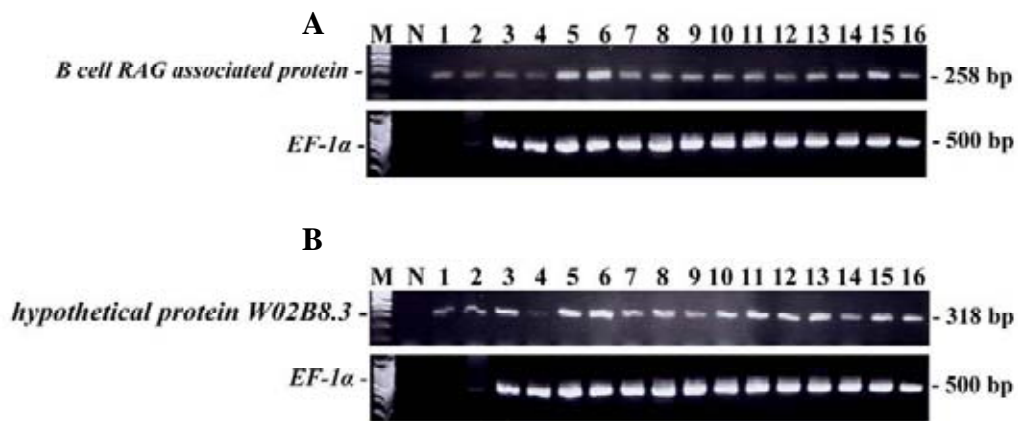


Figure 3.43 A 1.5% ethidium bromide-stained agarose gel showing RT-PCR result of *B cell RAG associated protein* (oligo-dT₍₁₆₎G-UBC 299) (A) and *hypothetical protein W02B8.3* (oligo-dT₍₁₆₎G-OPA 17) (B) using the first strand cDNA of *P. monodon* with different Gonado-Somatic Index (GSI). Lanes 3 - 14 are the first strand cDNA of ovaries of *P. monodon* with GSI = 5.689, 4.687, 3.017, 2.401, 2.018, 2.128, 1.894, 1.434, 1.100, 0.918, 0.870, 0.647, respectively. Lanes 15 - 16 are the first strand cDNA of ovaries of 4-months old *P. monodon*. Lanes 1 and 2 are genomic DNA using as template.

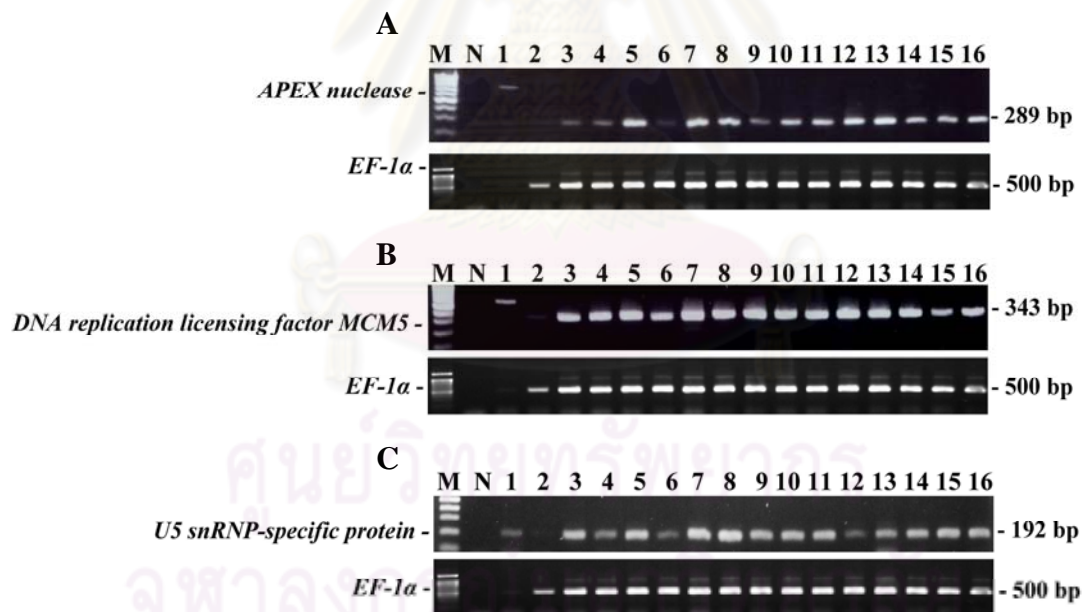


Figure 3.44 A 1.5% ethidium bromide-stained agarose gel showing RT-PCR result of *APEX nuclease* (oligo-dT₍₁₆₎A-OPA02) (A), *DNA replication licensing factor MCM5* (oligo-dT₍₁₆₎G-OPB 08) (B) and *U5 snRNP-specific protein* (oligo-dT₍₁₆₎G-UBC 457) (C) using the first strand cDNA of *P. monodon* with different Gonadosomatic Index (GSI). Lanes 3 - 14 are the first strand cDNA of *P. monodon* ovaries with GSI = 5.689, 4.687, 3.017, 2.401, 2.018, 2.128, 1.894, 1.434, 1.100, 0.918, 0.870, 0.647, respectively. Lanes 15 - 16 are the first strand cDNA of ovaries of 4-months old *P. monodon*. Lanes 1 and 2 are genomic DNA and the first strand cDNA of testes of *P. monodon* broodstock, respectively.

Table 3.31 A trend of expression levels of various genes isolated by RAP-PCR

Gene/Primer	Trends of expression screened by RT-PCR					
	Testes	Ovaries				
		Juveniles	Stage I (GSI<1.5)	Stage II (GSI 2.0-4.0)	Stage III (GSI 4.0-6.0)	Stage IV (GSI>6.0)
1. <i>B cell RAG - associated protein; N-acetylgalactosamine 4-sulfate 6-O-sulfotransferase</i>	ND	+	+	++	+	ND
2. <i>Hypothetical protein W02B8.3</i>	ND	+	++	++	+	ND
3. <i>DNA replication licensing factor MCM5</i>	+	++	+++	+++	++	ND
4. <i>ABC transporter</i>	+	+	+	++	++	ND
5. <i>APEX nuclease (apurinic/aprimidinic endonuclease) 2</i>	-	+	++	++	+	ND
6. <i>U5 snRNP-specific protein, 200 kDa; U5 snRNP-specific protein, 200 kDa (DEXH RNA helicase family), partial</i>	+	+	+	++	+	ND
7. <i>Moiria CG18740-PA</i>	-	++	++	+	+	ND
8 <i>Lysyl-tRNA synthetase</i>	ND	++	++	++	++	ND
9 <i>Unknown (oligo-dT₍₁₆₎A-UBC191)</i>	+++	+	+	+	+	ND
10 <i>Cystathionine gamma-lyase</i>	+	+	+	+	+	ND
11 <i>Thrombospondin</i>	-	+++	+++	+++	+++	ND
12 <i>Unknown (oligo-dT₍₁₆₎A-OPA 01)</i>	-	-	-	-	-	ND
13 <i>β-ketoacyl synthase</i>	-	-	-	-	-	ND
14 <i>Unknown (oligo-dT₍₁₆₎G-UBC 268)</i>	-	-	-	-	-	ND
15 <i>Alpha -1,6-mannosyl-glycoprotein beta-1,2-N-acetylglucosaminyltransferase, putative</i>	-	-	-	-	-	ND
16. <i>WD-repeat protein 1 (Actin-interacting protein 1) (AIP1)</i>	-	-	-	-	-	ND

ND = not determined, - = no amplification product, + = low level of expression, ++ = moderate level of expression., +++ = abundant level of expression

3.2.3 Semiquantitative RT-PCR to evaluate expression of different gene homologues in ovaries of broodstock *P. monodon*

Seven genes showed a trend of differential expression during ovarian development examined by non-quantitative RT-PCR. Relative expression levels of these genes during ovarian development of wild broodstock were further evaluated by semiquantitative RT-PCR. The optimal conditions on MgCl₂ and primer concentrations and amplification cycles were carefully examined (data not shown) and illustrated in Table 3.32. Two genes *ABC transporter* and *Moirai CG18740-PA* were not consistently amplified by semiquantitative RT-PCR.

Table 3.32 Optimal primer and MgCl₂ concentrations and the number of PCR cycles for semiquantitative analysis of various genes in *P. monodon*

Transcripts	Expected amplicons (bp)	Primer concentration (μM)	MgCl ₂ concentration (mM)	PCR cycles
From RAP-PCR marker				
<i>B cell RAG associated protein</i>	258	0.02	2.5	35
<i>Hypothetical protein W02B8.3</i>	318	0.04	1.5	30
<i>DNA replication licensing factor MCM5</i>	343	0.1	1.0	27
<i>APEX nuclease</i>	289	0.1	1.0	31
<i>U5 snRNP-specific protein</i>	192	0.04	1.0	28

Expression profiles of *B cell RAG associated protein* and *APEX nuclease* were similar. These transcripts were slightly down-regulated at stage II ovaries ($P < 0.05$). Expression of *B cell RAG associated protein* and *APEX nuclease* were slightly increased, but not significant, at more mature stages of ovarian development (stages III and IV, Figures 3.45 and 3.46, $P < 0.05$). Results indicated that high levels of *B cell RAG associated protein* and *APEX nuclease* may prevent ovarian development of *P. monodon*.

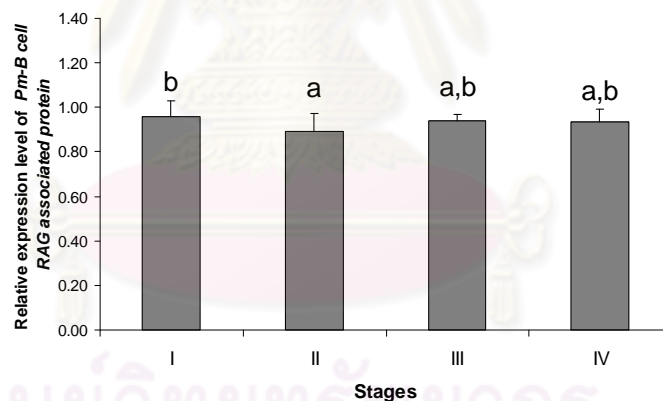
The expression levels of *U5 snRNP-specific protein* at stages I-III was comparable ($P > 0.05$). This transcript was down-regulated at stage IV ovaries (Figure

3.47). Accordingly, *U5 snRNP-specific protein* may contribute the final maturation of *P. monodon* ovaries.

The expression levels of *hypothetical protein W02B8.3* and *DNA replication licensing factor MCM5* were comparable during ovarian development of *P. monodon* broodstock ($P > 0.05$, Figures 3.48 and 3.49). Relatively abundant expression of these transcripts suggested their possible important roles to maintain development of ovaries of this species.

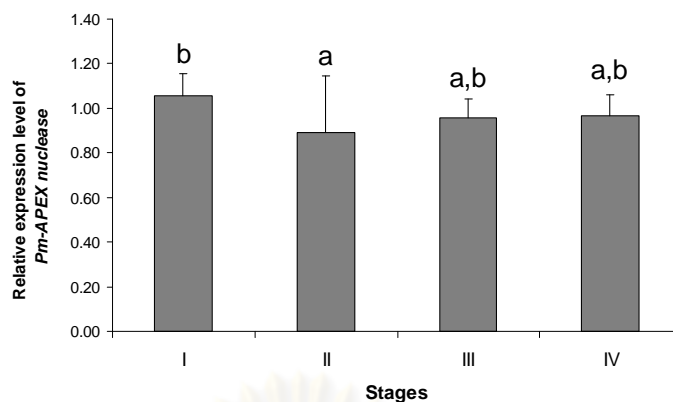
3.2.4 Tissue distribution analysis

Tissue distribution analysis of *B cell RAG-associated protein*, *APEX nuclease* and *U5 snRNP-specific protein* were carried out. *B cell RAG associated protein* was specifically expressed in ovaries but not other tissues of a female *P. monodon* broodstock (Figure 3.50A).



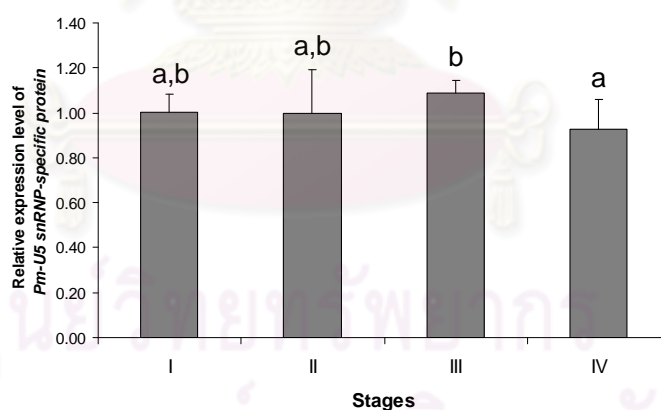
Ovarian stages	Expression levels	N
Stage I (GSI < 1.5)	0.9571±0.071 ^b	8
Stage II (GSI 2.0-4.0)	0.8903±0.083 ^a	5
Stage III (GSI 4.0-6.0)	0.9379±0.031 ^{a,b}	9
Stage IV (GSI > 6.0)	0.9366±0.056 ^{a,b}	12

Figure 3.45 Histograms showing the relative expression levels of *B cell RAG associated protein* in different ovarian developmental stages of normal *P. monodon* broodstock. The same letters indicate that the expression levels were not significantly different ($P > 0.05$). The relative expression levels and standard deviation in each stage of ovaries was also shown.



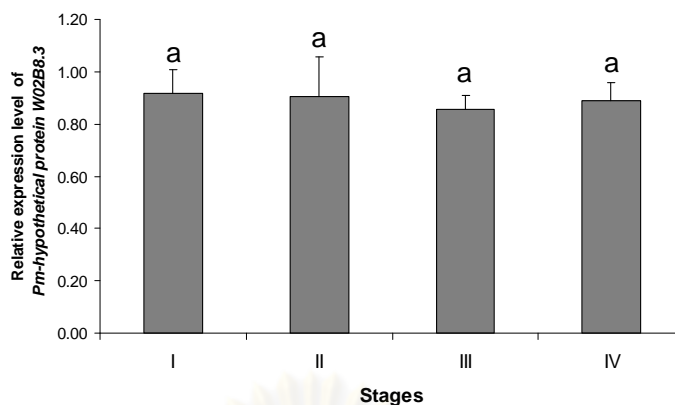
Ovarian stages	Expression levels	N
Stage I (GSI < 1.5)	1.0555±0.101 ^b	8
Stage II (GSI 2.0-4.0)	0.8904±0.253 ^a	5
Stage III (GSI 4.0-6.0)	0.9585±0.082 ^{a,b}	9
Stage IV (GSI > 6.0)	0.9652±0.097 ^{a,b}	12

Figure 3.46 Histograms showing the relative expression levels of *APEX nuclease* in different ovarian developmental stages of normal *P. monodon* broodstock. The same letters indicate that the expression levels were not significantly different ($P > 0.05$). The relative expression levels and standard deviation in each stage of ovaries was also shown.



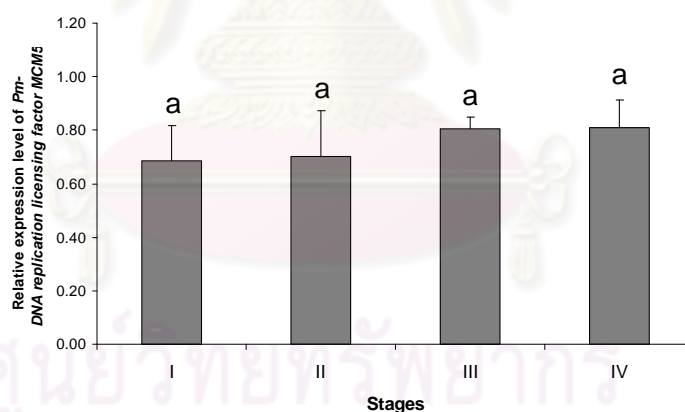
Ovarian stages	Expression levels	N
Stage I (GSI < 1.5)	1.0033±0.078 ^{a,b}	8
Stage II (GSI 2.0-4.0)	0.9977±0.192 ^{a,b}	5
Stage III (GSI 4.0-6.0)	1.0872±0.057 ^b	9
Stage IV (GSI > 6.0)	0.9252±0.137 ^a	12

Figure 3.47 Histograms showing the relative expression levels of *U5 snRNP-specific protein* in different ovarian developmental stages of normal *P. monodon* broodstock. The same letters indicate that the expression levels were not significantly different ($P > 0.05$). The number of relative expression levels and standard deviation was also shown.



Ovarian stages	Expression levels	N
Stage I (GSI<1.5)	0.9183±0.091 ^a	8
Stage II (GSI 2.0-4.0)	0.9059±0.149 ^a	5
Stage III (GSI 4.0-6.0)	0.8551±0.054 ^a	9
Stage IV (GSI>6.0)	0.8878±0.070 ^a	12

Figure 3.48 Histograms showing the relative expression levels of *hypothetical protein W02B8.3* in different ovarian developmental stages of normal *P. monodon* broodstock. The same letters indicate that the expression levels were not significantly different ($P > 0.05$). The number of relative expression levels and standard deviation was also shown.



Ovarian stages	Expression levels	N
Stage I (GSI<1.5)	0.6858±0.131 ^a	8
Stage II (GSI 2.0-4.0)	0.7013±0.173 ^a	5
Stage III (GSI 4.0-6.0)	0.8072±0.042 ^a	9
Stage IV (GSI>6.0)	0.8878±0.070 ^a	12

Figure 3.49 Histograms showing the relative expression levels of *DNA replication licensing factor MCM5* in different ovarian developmental stages of normal *P. monodon* broodstock. The same letters indicate that the expression levels were not significantly different ($P > 0.05$). The number of relative expression levels and standard deviation was also shown.

APEX nuclease was abundantly expressed in ovaries followed by testes and lower levels of expression were observed in other tissues. Extremely low expression of this transcript was observed in thoracic ganglion and eyestalk of female *P. monodon* broodstock (Figure 3.50B).

U5 snRNP-specific protein was highly expressed in ovaries and lymphoid organs of *P. monodon* broodstock. Moderate expression levels of this transcript were observed in testes, gills, heart, intestine, hepatopancreas, stomach, and epicutical. Rare expression levels of *U5 snRNP-specific protein* was observed in haemocytes, thoracic ganglion, eyestalk and pleopods (Figure 3.50C).

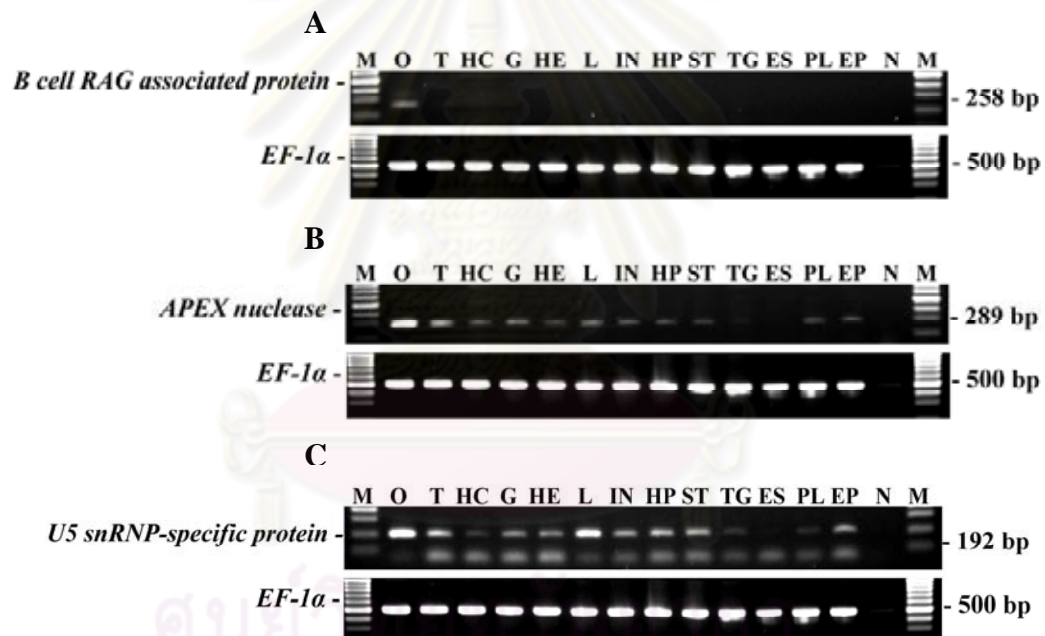


Figure 3.50 Tissue distribution analysis of *B cell RAG-associated protein* (A), *APEX nuclease* (B) and *U5 snRNP-specific protein* (C) using the first strand cDNA of ovaries of normal broodstock (O), testes (T), haemocytes (HC), gills (G), heart (HE), lymphoid organs (L), intestine (IN), hepatopancreas (HP), stomach (ST), thoracic ganglion (TG), eyestalks (ES), pleopods (PL) and epicutical (EP) *P. monodon* broodstock. Lanes M and N are a 100 bp DNA marker and the negative control (without the cDNA template), respectively. PCR was carried out at 25 cycles (35 cycles for *B cell RAG-associated protein*). *EF-1α* was successfully amplified from the same template.

3.3 Isolation and characterization of the full length cDNA of functionally important gene homologues of *P. monodon*

3.3.1 3' end terminal sequencing of original EST clones

Ten functionally important gene homologues (*cell division cycle 20*, *small androgen receptor-interacting protein: RWD domain containing 1*, *Rho family small GTP binding protein cdc42*, *cytochrome B5*, *Protein mago nashi*, *actin depolymerizing factor*, *f-box and wd-40 domain protein*, *Cyclin-dependent kinase 7*, *selenoprotein M precursor* and *anaphase promoting complex subunit 11*) were previously isolated by EST analysis. Similarity analysis indicated that the complete 5' portion of each gene, when compared with its gene homologue, was already obtained. Therefore, the 3' portion of each gene was further characterized by primer walking.

The full length cDNA of *P. monodon cell division cycle 20 (Pm-Cdc20)* was 2612 bp in length composing of an ORF of 1626 bp corresponding to a deduced protein of 541 amino acid and the 5' and 3' UTRs of 143 and 843 bp, respectively (Figure 3.51). It significantly matched *Cdc20* of *Branchiostoma floridae* (E-value = 5×10^{-149}). The predicted molecular mass and *pI* of the deduced Pm-Cdc20 protein was 59.52 kDa and 8.91, respectively. Pm-Cdc20 contained 7 WD40 (beta-transducin repeats; Trp-Asp (W-D) dipeptide) domains as the same as *F-box and wd40 repeat domain binding protein* (see below).

```

TTTTAAACTCCCTCTTCCCTCCGCTCTCTTATTATCTCCAAATATCGCCGCTTCCCTTCGC 60
CTTATCTTCCCTTTTATCGAAGGATAGTCTAGGGAGCAGCCAACAAAAGTAAAAAGAGAC 120
      M S H L Q F D A K L S E A 13
CAAATTCATAAATAAACGGCAAGATGTCACCTTCCAGTTTGCAGCTAAGCTAAGTGAAG 180
  L R M D G D L T R G P I P R W Q R K A M 33
CGTTAAGGATGGACGGAGATTTGACGAGGGGGCCAATCCCGAGGTGGCAGCGGAAGGCAA 240
  E Q G M Q Q L S I S N E N S F V N K S G 53
TGGAGCAGGGAATGCAACAGCTCTCCATAAGCAACGAAAACAGTTTTGTTAACAAGTCCG 300
  Y S S P K S G K T P R S G S F L E T K S 73
GTTATAGCAGTCCAAAGTCGGGTAAAACCCACGAAGCGGATCTTTCCTTGAGACCAAGA 360
  P G R G K S P S R S K S P G R R I P K L 93
GCCCTGGCCGAGGGAAGTCTCCAAGCAGGTCCAAGTCGCCAGGTTCGCAGGATTCCAAAGC 420
  T V R G A G Q K T P S L K T P A T P H N 113
TGACAGTTCGCGGTGCAGGCCAGAAGACTCCCTCTCTCAAACTCCCGCCACCCACATA 480
  Q Q D R F I P N R S T T D T E R S H H L 133
ACCAGCAAGACAGATTCATTCCAAACCGAAGCACCACAGATACGGAACGTTCACCAACC 540
  L V T S M E A S G G E K S A E E D E V S 153
TTTTGGTCACCAGCATGGAGGCTTCGGGAGGAGAAAAGTCTGCAGAGGAGGATGAAGTGT 600
  L Q Q K E Y Q E K M T E N L N D G I A P 173
CCCTGCAGCAGAAAGAATATCAGGAGAAGATGACAGAGAACCTAAACGATGGGATAGCAC 660
  E S R V L S F K S K A P Q A K E G H L N 193
CTGAGTCGAGGGTTTTGTCATTTAAGAGTAAGGCACCACAAGCAAAAAGAAGGACATTTGA 720

```

```

N H K V L Y S A G K P T V P K A A T T R 213
ACAATCACAAGTTCTCTACAGTGTGGAAAACCCACTGTGCCCAAGGCTGCCACAACAA 780
H I P N M P E K V L D A P E L L D D Y Y 233
GACACATTCCAACATGCCAGAAAAGGTTCTTGATGCTCCAGAACTTCTTGATGATTACT 840
L H L L D W S V N N H L A V A L G N S V 253
ATCTTCACCTTCTCGACTGGAGTGTGAACAACCACTTGGCTGTAGCTCTGGGAAATTCCGG 900
Y V W N A G D G S I T P L C Q L D D P D 273
TGTATGTTTGAATGCTGGCGATGGTTCATTACCCCCCTGTGCCAGCTGGATGACCCCG 960
Y I C S L S W I K E G N V L A I G N S S 293
ACTATATCTGCTCTCTGCTGGATTAAGGAAGGTAATGTGCTTGCCATTGGCAATAGCT 1020
G V T Q L W D V A Q Q K L V R S M G G H 313
CGGGTGTACACAGCTGTGGGATGTTGCACAACAGAAGCTTGTTCGCTCTATGGGTGGCC 1080
E S R V T T L S W N S Y I L S S G S R S 333
ACGAGAGCCGTGTCACCACCCTTTCCCTGGAACCTCGTACATCCTCTCCTCCGGCTCTCGCT 1140
G Q I F H H D V R V A E H H V A T L A G 353
CAGGACAGATTTCCACCATGATGTGAGTGGCTGAACATCATGTGGCGACCTTAGCTG 1200
H S Q E V C G L K W S P D G R L L A S G 373
GGCATTTCGAGGAGTCTGTGGTCTAAAGTGGTCTCCTGATGGGCGTTTGCCTCCGG 1260
G N D N Q V N I W D S M N T T P V H T L 393
GTGGAAATGACAATCAGGTAACATCTGGGATAGCATGAATACTACTCCGGTCCACACGC 1320
T Q H Q A A V K A V A W C P W Q N N L L 413
TAACTCAACATCAAGCTGCCGTTAAGGCTGTAGCTTGGTGTCCGTGGCAGAACAATCTCC 1380
A T G G G T A D R T I R L W N C T T G I 433
TTGCAACGGTGGAGGACTGCCACCCAGCATCAGATTGTGGAAGTGCACAAGTGGAA 1440
C L K D T T T N S Q V S S I V W S A H Y 453
TTTGCCTTAAAGATAACCACAACATAATTCTCAGGTGTCATCCATTGTTTGGTCTGCACACT 1500
K E F I S G H G F S N N Q L T I W K Y P 473
ACAAAGAGTTCATATCAGGCCATGGATTCTCTAACAATCAGCTGACCATCTGGAAGTACC 1560
S M A K V A D L T G H T G R V L E L C V 493
CATCTATGGCAAAGTGGCTGACCTCACAGGTACACAGGCAGAGTACTGGAGCTGTGTG 1620
S P D Q M V S A A A D E T I R M W K 513
TGTCTCCTGATGGCCAGATGGTAGTGAGTGCAGCTGCCGACGAGACCATCCGGATGTGGA 1680
C W A M D K K D K K Q A D A N K G H P I 533
AATGCTGGCCATGGACAAAAGGACAAGAAACAGGCCGATGCAAACAAGGCCATCCGA 1740
S M L A Q T I R * 541
TATCCATGCTTGGCTCAGACCATTTCGATTAAATTGTATGGTCAAGTCAGCCTTCCACCTCTT 1800
TCCTCTGTGTTTATCTTTATTATTACTATTAATATTATTATTATTATTATTATTATTATT 1860
ATTATTATTATTATTGATAGGTCATCATAGGGATTTTTTTTTTACATTCCCTAAACAATC 1920
ACCTGAGTGGGTGTTGTTTGAATTCCCTCTTTGCAAAATGTGATTTTATAAGATTTTCTAA 1980
AACATCAGGAATGAATGTACAGAATCTCATGTTAATTACCAAATCTATATCTCTTCAACT 2040
TTTAAATGTGTTTCATGGCAGACATGATATGATTTTCTTCTCAGATTTGATTTCTTGTA 2100
TTGGTTCACTCTTTAATATTTTGCATTAATGTGAAATGAATGTGACTTGCATCTTTGTT 2160
ATAAGAACTGCTAGATGTTTGTAAATGTCAGGGATCTACCATTTCTGCCTTACCTATGG 2220
TAGACTTTTATGTATTGGAAGTCTCCATCCATAAGATATGTAATATTTAGATACCAAT 2280
GACTTTTATTCGTCGAAAATGGAGATGGTAGAAGTCTCAAACTGCATAATTTCTTCTTGCA 2340
GCTGTAATAATACTTGTCTATTACCTATATAATTTATAAGCTTTAACAGGAATAAATTTT 2400
CAGTGATTTATGTGTGTCTGGTTTATGTATCACTATTGGATATTTTGTATAGATATAGTG 2460
TAGAATCAATTGCACAGATTATAGTACATTTGGTTGCCAGTACTTCCAAAGAACAGCCTCC 2520
TTTGTCTGTGCATTATGCCTTCTTAATTTCTGTAGCACTATTTTTTATGGCTTGAAT 2580
AAACATCACTTTGTTAAAAAATAAAAAAAAAA 2612

```

Figure 3.51 The full length cDNA and deduced protein sequences of *Pm-Cdc20* (2612 bp, ORF of 1626 bp corresponding to a deduced polypeptide of 541 aa) further sequenced from the original EST by 3' primer walking. The putative start (ATG) and stop (TAA) codons are illustrated in boldface and underlined. Two putative poly A additional signal are underlined. The predicted WD40 (beta-transducin repeats; Trp-Asp (W-D) dipeptide) domains (positions 216th – 257th, 262nd – 300th, 303rd – 340th, 344th – 383rd, 386th – 428th, 431st – 471st and 474th – 513th) are highlighted.


The full length cDNA of *P. monodon small androgen receptor-interacting protein isoform 1 (Pm-SARIP)* was 1366 bp in length composing of an ORF of 738 bp corresponding to a polypeptide of 245 amino acids and the 5' and 3' UTRs of 71 and 557 bp, respectively (Figure 3.52). It significantly matched *RWD domain-containing protein 1 (small androgen receptor-interacting protein)* of *Rattus norvegicus* (E-value = 2×10^{-40}). The predicted molecular mass and pI of the deduced Pm-SARIP protein was 28.54 kDa and 4.12, respectively. Pm-SARIP contained the RWD domain which functional interacting to the ubiquitin-conjugating enzyme domains.

The full length cDNA of *P. monodon cell division cycle 42 (Pm-Cdc42)* was 2195 bp in length composing of an ORF of 576 bp corresponding to a polypeptide of 191 amino acids and the 5' and 3' UTRs of 52 and 1567 bp, respectively (Figure 3.53). Its closes similarity was *Rho family small GTP binding protein, cdc42* of *Acyrtosiphon pisum* (E-value = 9×10^{-101}). The predicted molecular mass and pI of the deduced Pm-Cdc42 protein was 21.40 kDa and 6.16, respectively. Pm-Cdc42 contained a RHO domains involved in intracellular cell signaling processes.

The full length cDNA of *P. monodon cytochrome B5 (Pm-Cyt B5)* was 1539 bp in length composing of an ORF of 432 bp corresponding to a polypeptide of 143 amino acids and the 5' and 3' UTRs of 52 and 1055 bp, respectively (Figure. 3.54). The closest similar sequence of this transcript was *cytochrome b5* of *Strongylocentrotus purpuratus* (E-value = 4×10^{-36}). The predicted molecular mass and pI of the deduced Pm-Cyt B5 protein was 16.20 kDa and 4.51, respectively. Pm-Cyt B5 contained a Cyt-b5 domain which is transition metal ion binding and heme binding sites. The transmembrane domain of Pm-Cyt B5 was also found (WLVPVGLACLASIIYRMYAL) (Figure 3.55).

Most of the proteins with a b5-domain are linked to cell membranes, either directly or by forming part of membrane-associated complexes. The proximity of cell membranes to a heme-binding template pocket could have served to give rise to new ligand-binding pockets with specificity for membrane-soluble molecules such as steroids. Thus, Membrane-associated progesterone receptors (MAPRs), such as PGMRC1 (see below), may represent an adaptation by which cells could start making use of steroids as triggers for rapid response mechanisms (Mifsud and Bateman, 2002).

The full length cDNA of *P. monodon protein mago nashi* was 858 bp in length composing of an ORF of 444 bp corresponding to a polypeptide of 147 amino acids and the 5' and 3' UTRs of 27 and 387 bp, respectively (Figure 3.56). It significantly matched *protein mago nashi* of *Apis mellifera* (E-value = 5×10^{-76}). The predicted molecular mass and pI of the deduced Pm- protein mago nashi was 17.27 kDa and 5.72, respectively. Pm-Protein mago nashi contained Mago_nashi domains originally identified in *Drosophila* which is essential for female germlasm assembly (Newmark and Boswell, 1994).



```

GGCACGAGGGTCACGCTTTTGGGTTTCATGTGTTTCCTCCTAATTTCTTCTCTTC 60
      M T D Y K E E Q N N E I E A L E S 17
AATTATTCGTCATGACAGACTACAAGGAAGAACAGAATAACGAAATTGAGGCCCTGGAGT 120
      I Y P E E F E I I D I E P R H K F R I T 37
CCATATATCCAGAGGAATTGAGATAATTGATATAGAACCAAGGCACAAGTTCAGAATTA 180
      V K S E G S D P Y D E I Q T L P A T I I 57
CTGTCAAATCCGAAGGCTCTGATCCATATGATGAGATTGACAGCTTACCAGCAACTATTA 240
      L N F E Y T P T Y P D E P P V M E V T A 77
TCCTCAACTTTGAATACACTCCAACGTATCCAGATGAACCCCCAGTCATGGAAGTCACAG 300
      V E N I E E E E L D D L R T K L N E Q C 97
CTGTTGAAAACATAGAAGAGGAAGAGCTGGATGATTTAAGAACGAAACTTAACGAGCAGT 360
      E E N L G M V M V F T L V S Y S L E W L 117
GTGAGGAGAACCTGGGGATGGTCATGGTGTTCACGCTTGTCTCATACTCATTGGAGTGGC 420
      T T H M E G I A L S T K E E L D R K K K 137
TCACCACACACATGGAAGGTATTGCTCTCAGCACAAAGAAGAATTGGATCGCAAGAAGA 480
      E Q E E I D R K K F E G T R V T V E T F 157
AAGAGCAGGAAGAGATAGATCGGAAAAAGTTTGAAGGTACCAGAGTACTGTAGAAAACGT 540
      L A W K A K F D T E M Q A L R S E K D R 177
TTCTTGCTTGGAAGCAAAGTTTGATACGGAGATGCAAGCACTCCGATCTGAGAAAAGACA 600
      E D E K N K K P T G R E L F M K D V T L 197
GGGAGGATGAGAAGAACAAAAACCAACTGGTAGAGAGCTTTCATGAAGGACGTCACCTT 660
      N E S D L S F L G E G E G E V T V D E S 217
TGAATGAGTCGGATCTTAGCTTCTTGGTGAAGGAGAAGGTGAGGTGACTGTTGATGAGA 720
      L F Q D L D D L D L E D E D D E D Y V P 237
GTTTATCCAAGACCTGGATGACTTAGACCTCGAGGATGAAGATGACGAGGATTATGTTTC 780
      G A D D D I S D * 245
CAGGAGCGGATGATGACATATCTGATTAGAAACTTTAAATAAATATCATTTCATTATCAT 840
ATCTTTTTTTTCTCTCTCACTCTCGTGGTTTCCCATCATGAATTTGTTTTAGTCATGGAT 900
ACTGGCTCATGAATTTTTTTTTTTTCTTTCTTTCTTTTATACATCCGTTTT 960
TGCAGAAGATGTCTCTTCAAATGTAATGTTTGTGTTTCTTATTAGCTAAAATTAGC 1020
CCTCTTATTTATTTGGAAAAGTTGTTTTGATAATGCATTGTAAATAAACATTTAACAA 1080
AAATGGAGATTAAGTTCAGTTGTTTCAGAGGTTATTTAGTTGGGGAGTGTCCCGAAATTA 1140
TTATCTTTGTTTATTTGTTTGCATACAGAATTAGATCATGCAAATAGACAGTTGCTTAT 1200
AAAGACCATTTTTTTATTTTGTTCATTCACCATGATTGTTATTTTTTATACAGTTTAAA 1260
CCATTTGTATCAAGTTGTTTTACTTAGATTTTCATCAATAGAGGAGTCAAGTATGATGCAT 1320
TAGCCCTCAATAAAATGTTAAATCTGTAAAAAATAAAAAAAAAAAAAAAAAA 1366

```

Figure 3.52 The full length cDNA and deduced protein sequences of *Pm-SARIP* (1366 bp, ORF of 738 bp corresponding to a deduced polypeptide of 245 aa) further sequenced from the original EST by 3' primer walking. The putative start (ATG) and stop (TAG) codons are illustrated in boldface and underlined. Three putative poly A additional signal sites are underlined. The predicted RWD (RING finger and WD repeat containing proteins) domain (positions 10th – 120th) is highlighted.

	M Q T 3	
CAGCAGCGTCTCGGATGAACTACGCCAGCTGGCTGCTGGGGAGCGTGAGAA <u>ATG</u> CAGAC	60	
I K C V V V G D G A V G K T C L L I S Y	23	
CATTAAATGCGTAGTGGTGGGCGATGGAGCGGTGGGTAAGACCTGCCTCCTCATCTCCTA	120	
T T N K F P S E Y V P T V F D N Y A V T	43	
CACAACAAACAAGTTCCCTTCAGAAATATGTTCCACAGTATTTGACAACCTATGCTGTGAC	180	
V M I G G E P Y T L G L F D T A G Q E D	63	
TGTTATGATAGGAGGGGAGCCATACACATTAGGCCTTTTTGATACAGCTGGTCAGGAGGA	240	
Y D R L R P L S Y P Q T D V F L V C F S	83	
TTATGACAGACTGCGACCTTTAGCTATCCACAGACAGATGTTTTCTTAGTCTGCTTCTC	300	
V V S P S S F E N V K E K W V P E I T H	103	
AGTGGTATCCCCTTCGTCCCTTCGAGAATGTCAAGGAAAAGTGGGTACCAGAAATCACTCA	360	
H C Q K T P F L L V G T Q I D L R D D A	123	
CCACTGCCAGAAGACTCCATTCCCTCCTAGTAGGCACACAGATAGATTTGCGGGATGATGC	420	
A T V E K L A K N K Q K P I T Y E Q G D	143	
AGCAACCGTAGAAAAGCTGGCAAAGAATAAGCAGAAGCCAATCACCTACGAACAAGGGGA	480	
K L S R E L K A V K Y V E C S A L T Q K	163	
CAAGCTCAGTCGCGAGCTGAAGGCCGTCAAGTACGTGGAATGCTCCGCGCTCACACAGAA	540	
G L K N V F D E A I L A A L E P P E P Q	183	
GGGGCTGAAGAATGTATTTGATGAAGCAATTTCTCGCAGCCCTGGAGCCCCCAGAACCTCA	600	
R R R K C I V L *	191	
GAGACGAAGGAAAATGTATTGTTCTG <u>TAG</u> GGTAGGACGCATCTACGGTAGACCTTGGAGTG	660	
GCCCCAGGCTTAACAGATGCACAGATTGCCTTCAATGGTTCAGTAGGGGTTCTAGTGGAGT	720	
TGGTGATGCCTCTGAAGCTATTTAGACAAGAGAAACTTGATAACTGTATAAAATATATGAA	780	
GGATTTTATACTTGTGAAAGGGAAAAATGTCCACTATTTGGATGGTGGAAAGATGCCAAAGT	840	
TCAGATAACTTGCCGATCAAGTCAGGCTTAACGCAGCTTTGGGGCTAAACTCCATGGGGA	900	
ATGTGAGCAATCTAAGCACAAGAAAAGTGGCTGTTTGGGTCTTGAGCGTCGAGAGTCGCT	960	
TCACGCGAGGCAACTTCTCGCACAAGTCCCTCCCTCAGCCAGTCACTACTCTTGTGTGTT	1020	
CCCACCTTCCCTGTCCCTTATCCCTTGGGCCAGCACCCCTCCCTGTACCATTTGATGAACC	1080	
ATGGTTCCAGTTGGTTTGGCTTCCAGTTAGGTCGAGTGCCTTTGACTTTTATATAAACTT	1140	
GTCATATAAAATTTAATACCAAGACTGAAACACAAATATCATGTTGATTCCAATCATCTCTA	1200	
GATTTCTCAGATAATTCATTTAATTTCAAGAGAACTACAGTAATCAATAGCTCAGTATTTCA	1260	
AATTCTGATAGGCTTTTTTTTTCTAATTTTACCTTTCCCTATAGCTTATGGCATCTCATAA	1320	
CAAGTAATGAGTTTGAAGTGTGATAAAATGAATGAGTAACCAATATTTGTATGAGCTT	1380	
AACTTCTATATAACTGCCTCAGACTATCATATGTTTCCCTATTCTTACACGTACACGTCT	1440	
AGTGGCGTGACCTAGCATTGGTATCTTCTTTTTTATTATAACATTAGTGCAAACTTTTTA	1500	
GGAGGTTTGTCTAGGGACTATGGCTTGGTTTTGTGGGCTCAAAAACCAAGATAATCCTTG	1560	
AGACGAGACCAGTTATGATTTTAAGTATCAGTTTGTAAATTTTTTACAATATGGTGTGCC	1620	
TGAGTAAGAAAATAGGTTTGAAGTACGTGGCATTTATGCAAAGGGTTATCAATTTGTCAA	1680	
AAGAGTGAGAAAGCATTCTCTTTTCCAGTGTGTTGGTTTCATTTGGAACAGATTTGGCC	1740	
TCTTCTGCTCACTCTGGCCTTTCCCTCAGTAGTCATAGTGGGTATGAAGCCAGTCTGGGGA	1800	
AGTCTGATGTAGTGGAAATGGTTATATCAACTTGCATAGTTGGCTCAATTACAGGAAT	1860	
TGTTATTTTTGTACAAATTTCTAAATTTGAAAGTAGTGTCCATGATTTTTTAAATTTTTTG	1920	
CTACTTCAGACGTAGTAAGTTGATGGCACCCAGATGGTTGGTAACTACCTTGCCCTCGTCA	1980	
TACATTAACCTAACCCACCACTGGTGTGGGTGAAATATTTAATATCAGAATGTGTAGTT	2040	
GCCATGTTGACCATTCATATATGACAAAAACAAAAATTTATGGATTTTTGTCTTCATTTA	2100	
AAGTGTGATAAAAACCCTGATGATTTAGAAGGAAGTTTGGTGTATGGAGGGAGATACAAA	2160	
<u>TAAACCATTTGGATTGAAAAAAAAAAAAAAAAAAAA</u>	2195	

Figure 3.53 The full length cDNA and deduced protein sequences of *Pm-Cdc42* (2195 bp, ORF of 576 bp corresponding to a deduced polypeptide of 191 aa) further sequenced from the original EST by 3' primer walking. The putative start (ATG) and stop (TAG) codons are illustrated in boldface and underlined. The putative poly A additional signal site is underlined. The predicted RHO domain (positions 6th – 179th) is highlighted.

M G E 3

```

CCGGTATTCTGCAACGCCTTGCAAGATCAGTTCCCCGTGACTAGCGGAGACAATGGGGGGA 60
E S K D E Q I S N T T T K V Y T L A E I 23
AGAAAGTAAGGATGAACAAATTAGCAACACAACACTACAAAGGTGTACACCTTAGCGGAGAT 120
A E H K T T D S C W I V I H D K V Y D V 43
TGCGGAGCATAAAACAACAGATTTCGTGTTGGATTGTGATTCACGACAAAGTCTATGATGT 180
T K F L D E H P G G E E V L L E Q A G M 63
AACCAAATTTTTAGATGAGCATCCTGGAGGAGAGGAAGTGCTACTGGAGCAAGCAGGGAT 240
D T T E S F E D V G H S T D A R E M M T 83
GGACACCACAGAAAAGCTTTGAGGATGTTGGTCACTCTACTGATGCTCGGGAGATGATGAC 300
D Y Y L G E L S E E D K K H T Q D K G P 103
GGACTATTACCTTGGTGAACATAAGTGAGGAAGACAAGAAGCACACTCAAGATAAGGGTCC 360
K T W A Y D N N S N Q S A W K S W L V P 123
CAAAACCTGGGCATATGATAATAACTCCAATCAGAGTGCATGGAAGTCATGGTTGGTACC 420
V G L A C L A S I I Y R M Y A L P Q S S 143
TGTAGGCCTAGCATGTCTTGCATCAATTATCTACCGAATGTATGCCCTGCCACAGTCTAG 480
*
CTAATGTCAATGTTTCATGCCCTTGATCCATCTGAAGTACATTAGTCATTGTCTCCTTGT 540
TATCCACAGTGGTTTTACTTTTTAATTTTTTATATCCTCTTTGCTACTGTTCTTTTTTCCT 600
TCCTTTTCCATGTCTTTGTCAAAATGATAAGTGAGTCAATAATTTGTTTAAAGAGTGAA 660
ATATTTTACATTGTATTTGTATTTGCACACACACACACACACACACACACACACACACAC 720
ACACACACACACACACACACACACACACACACAGAACATGTATATGTATATAAAATCACATA 780
AATTTCCATATAAAATATACATGCAAGTATATTACCAAACTTGGAATCAATTTTTTTTCT 840
ATTTGGCATACAAAGAGACCTATCTTCCAATAATATAAGGAATTTTATGTCTGTCTTCAT 900
TATATTTTAATATATTCTAATGAACCTTTTTTTTTTACCATAACAAGAGACATTTTTTGTAGT 960
AACTAGTATAAATTACATTATCAATAGAACTCGTACATACATGTACTTTGGCAAGGGGAA 1020
TTGTGAGCCTTTTATTCTTAGGTAATACTCAGTCTCATTGTAAATTCAGATGCCATAATTC 1080
ATGAACCATTCTTTCTGGCAACTAACAATCAGGCCGTGACTAAATCTTATTTTTTACAGTG 1140
AATTGTGAAAATTGTGATAATAAGCCTTACATATCTGTTTGTGTTAAAGTGATTGTTCTG 1200
TCACGTGTATCAAGATCAATGTAAAAGTGTTCATACTAATACTATCTTCATTCCATCAAA 1260
ACTGGGAACAATGAGATCAGAATCTGATTTTTTCTTCTTTTAAATGTATTCGGATT 1320
GCAGAAGCATGTGTTTCGATATATATGGTGGCATTTTGATGGACATACAATGAAGTGCAT 1380
GTAATTTTGCACATGAGTATTACAGACATGTCTTCAGATGTGACAGGACAGAGTTCTGA 1440
TAGTTATATTTATATGTGATGCGTCTATGGTATTTTTGGAATGTTTTGTAACAGTATAGT 1500
CACAAATAATCCAGTCCATCCAAAAAAAAAAAAAAAAAAAAA 1539

```

Figure 3.54 The full length cDNA and deduced protein sequences of *Pm-cytochrome B5* (1539 bp, ORF of 432 bp corresponding to a deduced polypeptide of 143 aa) further sequenced from the original EST by 3' primer walking. The putative start (ATG) and stop (TAA) codons are illustrated in boldface and underlined. The predicted Cyt-b5 domain (positions 17th – 91st) is highlighted. The predicted transmembrane domain is indicated by double underlines (positions 120th – 139th).

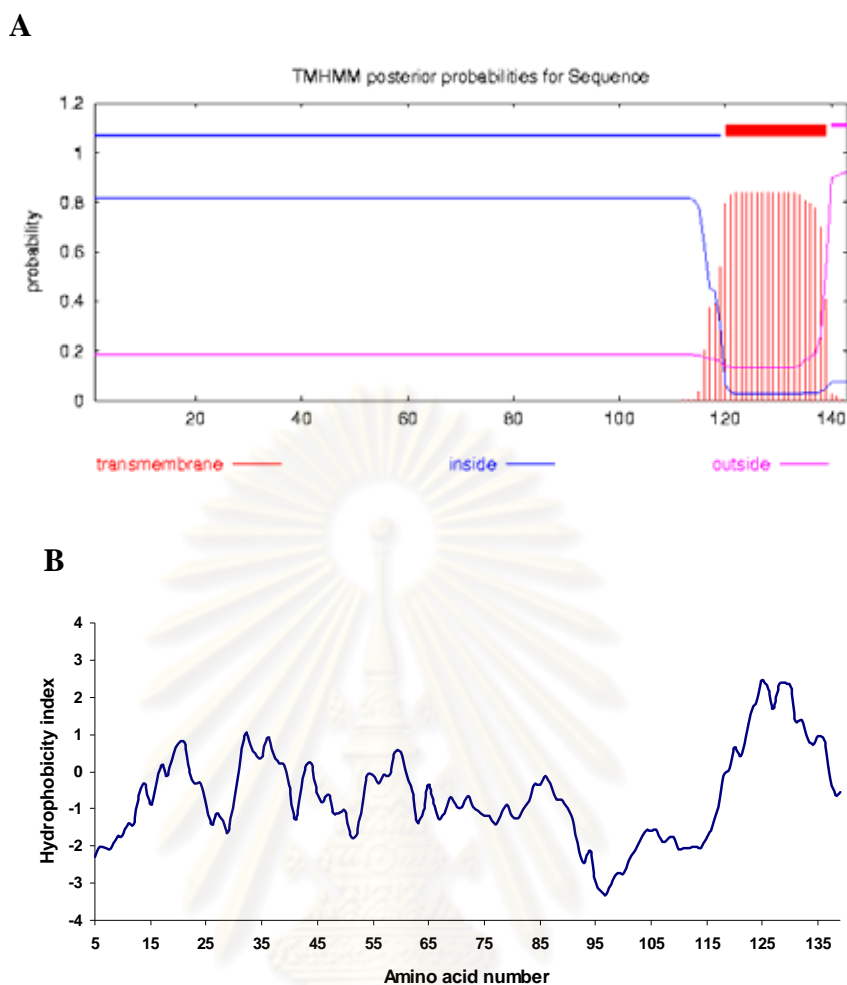


Figure 3.55 Diagrams showing outside, inside and transmembrane probability (A) and hydrophobicity analysis of deduced *Pm-cytochrome B5* protein according to Kyte and Doolittle (1982).

The full length cDNA of *P. monodon actin depolymerizing factor* (*Pm-actin depolymerizing factor*) was 1449 bp in length composing of an ORF of 447 bp corresponding to a polypeptide of 148 amino acids and the 5' and 3' UTRs of 23 and 979 bp, respectively (Figure 3.57). The closest similar sequence to *Pm-actin depolymerizing factor* was *Cofilin/actin-depolymerizing factor* of *Tribolium castaneum* (E-value = 2×10^{-52}). The predicted molecular mass and pI of the deduced *Pm-actin depolymerizing factor* was 17.13 kDa and 5.94, respectively. *Pm-actin depolymerizing factor* contained an ADF (Actin depolymerisation factor/cofilin-like domains) domain which involved actin-binding and remodeling of the actin cytoskeleton.


```

M G S N D F Y I R Y Y 11
AGACGCCGCAGCACGCGTCGACGCGCGATGGGCTCCAACGACTTCTACATTGCTATTAC 60
V G H K G K F G H E F L E F E F R P D G 31
GTCGGCCACAAAGGCAAATTTGGGCACGAATTCCTCGAGTTCGAGTTTAGACCAGATGGC 120
K L R Y A N N S N Y K N D V M I R K E A 51
AAACTTCGATATGCCAACAACTCCAAC TACAAGAACGATGTTATGATCCGTAAAGAGGCT 180
Y V H R C V M E E L K R I I D D S E I M 71
TATGTTTCATAGATGTGTCATGGAAGAGCTCAAGAGAATCATCGACGACTCAGAGATCATG 240
Q E D D A L W P Q P D R V G R Q E L E I 91
CAGGAGGATGATGCACTTTGGCCACAGCCTGACCGTGTGGGCCGGCAGGAGCTGGAGATT 300
V I G D E H I S F T T S K I G S L V D V 111
GTCATTGGTGATGAACACATCTCCTTCACTACCTCCAAGATTGGCTCACTCGTCGATGTT 360
N N S K D P D G L R C F Y Y L V Q D L K 131
AATAACTCCAAAGATCCAGATGGTTTGGAGATGCTTCTATTACCTCGTGCAGGACTTGAAG 420
C L V F S L I G L H F K I K P I * 147
TGCCTGGTGTCTCATTGATTGGTCTTCACTTCAAGATCAAGCCCATCTAAAGGGGATAACA 480
GCTTGTGATGTTGCATAGGTTGTCAGCAGTGAAAAACACATAATTTTTGGTTACTTTTTATA 540
GCTGTCAAAAAACTGTTATTACTCCTTTACCCCTCTAAAACAAAAGAAAACAAAAAGTAAGG 600
CAAAC TTTCTGGCTTTTAAGTAAAAGATTTGTTCTAGTTTTTACAATACTTTTTCTTTTC 660
TTTTTTTCAGCAGTATCATGTGTAGTATGATTTTTTAGTAAATCATATGCAGTGAGAGCTT 720
ATCATAATATATTTAATTTACAGATTATTAGGCAGGGTTTATTTCTTTGTTTTCAAGACAA 780
ATTTAAGTGATTGTTTATACAATACTTTTCATTGAGA ACTTGTATTTAAAATAACAACATT 840
AAAAAAAAAAAAAAAAAAAAA 858

```

Figure 3.56 The full length cDNA and deduced protein sequences of *Pm-Protein mago nashi* (858 bp, ORF of 444 bp corresponding to a deduced polypeptide of 147 aa) further sequenced from the original EST by 3' primer walking. The putative start (ATG) and stop (TAA) codons are illustrated in boldface and underlined. The predicted Mago_nashi domain (positions 5th – 147th) is highlighted.

The full length cDNA of *P. monodon-F-box and wd40 repeat domain binding protein* was 1841 bp in length composing of an ORF of 1506 bp corresponding to a polypeptide of 501 amino acids and the 5' and 3' UTRs of 49 and 175 bp, respectively (Figure. 3.58). Its significantly matched sequence was *F-box and wd-40 domain protein* of *Culex quinquefasciatus* (E-value = 0.0). The predicted molecular mass and pI of the deduced Pm-F-box and wd40 repeat domain binding protein was 61.12 kDa and 8.23, respectively. The predicted F-BOX domain was found in this deduced protein. This domain was first described as a sequence motif found in cyclin-F that interacts with the protein SKP1 (Bai *et al.*, 1996). Like Pm-Cdc20, the deduced Pm-F-box and wd40 repeat domain binding protein contained 7 WD40 (beta-transducin repeats; Trp-Asp (W-D) dipeptide) domains which are implicated in a variety of functions ranging from signal transduction and transcription regulation to cell cycle control and apoptosis.

```

M A S G V Q V A D A C T Q 13
GGAATTCGCCGTAGAGTAGCACGATGGCTTCCGGAGTACAAGTAGCAGATGCATGCACAC 60
A F L D I K K N K K Y R Y I I F H I K D 33
AGGCCTTTCTCGATATAAAAAAAAAACAAGAAATATAGGTACATCATATTCCACATTAAG 120
E K V I D I E K Y G D R D S S Y D D Y L 53
ATGAGAAAGTTATAGATATTGAAAAGTATGGTGACAGAGATAGTTCCTATGATGACTACT 180
K H L E E L G P D Q C R Y G L Y D F E Y 73
TGAAACATCTGGAAGAGTTGGGCCCTGACCAGTGCCGCTATGGTCTATATGACTTCGAGT 240
E H Q C Q G G T S D R T P K Q K L F L M S 93
ATGAGCACCAGTGCCAGGGAACATCAGATCGCACACCAAAGCAGAAGCTGTTCCCTGATGT 300
W C P D T A K I K K K M L Y S S S F D A 113
CCTGGTGCCAGACACTGCCAAAATTAAGAAGAAAATGCTTTACTCTTCAAGCTTTGATG 360
L K S A C E G I G K Y I Q A T D M A E A 133
CCCTCAAAAAGTGCATGTGAAGGCATTGGCAAATATATCCAGGCCACGGATATGGCTGAAG 420
S Y E C V L E K L R S T D R A * 148
CATCATACGAGTGTGTGTTGGAGAACTGCGTTCTACTGACCGTGCCTTAAACCTACTATG 480
GGAGGCCCTCACGAAAAGCAGCCCTTACCCTGTGTTTGTACTTTCCACCCTGGTGTA 540
CACTGGTCTCGGCTCTTGCCGACCCAACCTGCACTGTGAGGGGTCTTTCAGTACCACCCGC 600
ACTGCGGTCACTGCTGCCCTAGTCATGCCCGGCAGCAACTGTTTATCATGCTACCCACG 660
CAGCATCAGGGGACTCATTGTTTTATACTTCTGATTATATTTATTTTATTATAATTCAA 720
TTGGTTGGCATGTAGGTGGGTGGGCAGCAGTGTAGCACTGGTTCAGCTCTGGCTGTTAT 780
CCCATGATGAGTAGCATTGGCAAAGTCGAGACCCCATCTTTGATTATAATTCAAATGGTT 840
GGCATGTAGGTGGGTGGCAGCAGTGTAGCACTGGTTCAAGCTCTGGCTGTTATCCCATGA 900
TGAGTAGCATTGGCAAGTCGAGACCCCATCTTGTGAAGAATATGGACACAAGTGCCATCC 960
AGTGTGTTCTTCCAGGGAGACTTGTCTCTCTGAATTTCTGGCAAAGAATGTGGTTCAGTG 1020
GGTCTGCATTGATGATTGACTTGAAGTTGGTGGATTGTGCTGGAACGCTATACCAGTGT 1080
CGCCCCGTGCCACGTGTTGGCTGAGGCAAGTTTAGTATTACCTGAAGCTCTTCCATTTGT 1140
ATCTTTTGCATCACATCAGTGTGAAATATCAGTCTGCGTTCATTAAGTATAATATAAGCT 1200
TTATATAACGGAATCATGTTTATAGGCATTTGGCAAGTATTGGCTCAAAGTACATTTTGT 1260
AATTGACACTGCTCAAAAATCTTTTGTGTTGCACTGGCTGTTGCCCTTTGTCTGGAAAAAGGA 1320
ATTACCATTACTTAAAGGGTTTTGTATGATTTTTATTGTAGGATCATTGTCAACTTGTCTA 1380
AAATAAAATTTCTTTTTTAATAAAAAAAAAAAAAAAAAAAAAAAAAAAAAAAAAAAAAAAAA 1440
AAAAAAAAA 1449

```

Figure 3.57 The full length cDNA and deduced protein sequences of *Pm-actin depolymerizing factor* (1449 bp, ORF of 447 bp corresponding to a deduced polypeptide of 148 aa) further sequenced from the original EST by 3' primer walking. The putative start (ATG) and stop (TAA) codons are illustrated in boldface and underlined. The putative poly A additional signal site is underlined. The predicted ADF (Actin depolymerisation factor/cofilin-like) domain (positions 9th – 143rd) is highlighted.

```

M T V I 4
GGCACTGAACCACTTTTGGACGATAGTCTAGATTCAAGTTCAGTTGAGGCACCCATGACGGTGAT 60
Y D N N I S P M S V T T S V G I R S G D 24
TTACGACAACAACATATCCCCATGAGTGTACGACAAGTGTGGCATTTCGGAGTGGTGA 120
G G S G D N E E S E P M T T I P L T Q G S 44
TGTTGGCAGTGACAATGAGGAGTCGGAACCCATGACGACCATACCCCTGACAGAAGGTT 180
G G V R G G G G P R K K E S T A Q Y N 64
AGGGGGTGTACGGGGAGGGGGAGGGGGCCCGGAAGAAAGAGTCCACAGCTCAGTACAA 240
N E R E M C L H Y F D K W S E Q D H L E 84
TAATGAGCGAGAGATGTCTGCACTATTTTGACAAGTGGAGTGAGCAGGACCACCTAGA 300

```

```

I M E H L L S R M C H Y Q H G H I N A F 104
GATCATGGAGCACCTCTGTCCAGAATGTGCCACTATCAGCATGGACACATCAACGCCTT 360
L K P M L Q R D F I T L L P K K G L D H 124
CCTAAAGCCTATGCTCCAGAGAGATTTTATTACACTCTTGCCAAAAAAGGGTCTAGATCA 420
V A E K I L G Y L D A K S L R E A E L V 144
TGTAGCAGAAAAAATCTTAGGATATTTAGATGCCAAATCCTTGCAGAGAAGCAGAGTTGGT 480
C K E W H R V I A D G L L W K K L I E R 164
ATGTAAGAATGGCACAGGGTAATTGCAGATGGACTTCTATGGAAAAAATTGATAGAGAG 540
K V R T D P L W R G L S E R K G W G M Y 184
AAAAGTACGCACAGATCCTCTATGGAGAGGGCTCTCAGAACGAAAGGGGTGGGGTATGTA 600
L F K P R P G E Q H P G H S Y Y R K L Y 204
TCTCTTCAAACCACGGCCAGGAGAGCAACATCCTGGGCACTCTTATTATCGAAAGTTATA 660
P K I I Q D I Q T I E N N W R M G R H N 224
TCCTAAAATTATACAGGATATTCAAACCATAGAAAATAAATTGGAGAATGGGTAGACATAA 720
L Q R I N C R S E N S K G V Y C L Q Y D 244
TTTGCAAAGGATAAAATGTCGCTCAGAGAACTCCAAGGTGTCTACTGTTTACAATATGA 780
D Q K I V S G L R D N T I K I W D R T S 264
TGACCAGAAAATTGTCTCTGGTCTCCGAGATAACACCATCAAAAATTGGGATCGAACTTC 840
L Q C Y K V L T G H T G S V L C L Q Y D 284
GCTGCAGTGTTACAAGGTGTTGACGGGTACACAGGGTCAGTGTATGCCTCCAGTATGA 900
E R V I I S G S S D S T V R V W D V N T 304
TGAAAGGGTGATCATTAGCGGGTCTGTCAGATTCCACAGTCAGAGTGTGGGACGTGAACAC 960
G E M T N T L I H H C E A V L H L R F N 324
GGGCGAGATGACCAACACACTCACCACCAGTGTGAGGCAGTACTTCACTTACGCTTTAA 1020
N G M M V T C S K C D R S I A V W D M V S 344
CAATGGAATGATGGTCACTTGCTCAAAGGACCGTTCCATGCTGTCTGGGATATGGTATC 1080
P A E I N L R R V L V G H R A A V N V V 364
TCCGGCAGAAATCAACCTCAGACGGGTGCTAGTGGGTACCCGGGCAGCAGTTAATGTTGT 1140
D F D E K Y I V S A S G D R T I K V W S 384
TGATTTTGTAGAGAAATATATTGTCAGTGCATCTGGTGACAGAACAATCAAGGTGTGGAG 1200
T G T C E F V R T L N G H K R G I A C L 404
CACAGGAACCTGTGAATTTGTGCGGACGCTAAATGGTCAACAAGAGGGGCATTGCATGTCT 1260
Q Y R D R L V V S G S S D N T I R L W D 424
GCAGTATCGTGATAGACTTGTAGTCACTGCTCTTCAGATAATAACAATAAGGCTGTGGGA 1320
I E C G A C L R I L E G H E E L V R C I 444
CATTGAATGTGGTGCATGTTAAGAATTCTGGAAGGGCATGAAGAACTTGTACGATGCAT 1380
R F D N K R I V S G A Y D G K I K V W D 464
TCGCTTTTGACAACAAGAGGATCGTATCAGGAGCATATGATGGGAAGATCAAGGTTTGGGA 1440
L Q A A L D L R V P A G T L C L R T L V 484
CCTCCAAGCAGCGTTGGATCTTCGAGTGCCAGCTGGAACCTTATGTCTTCGAACTCTTGT 1500
E H S G R V F R L Q F D E F Q I V S S S 504
GGAACATTCCGGCCGAGTATTCCGCCTCCAGTTTGACGAGTTCAGATAGTGTCTGCTCGTC 1560
H D D T I L I W D F L N C S P P E A S G 524
CCACGATGATACATCCTCATCTGGGATTTCTCAACTGCTCCCCCAGAAGCGTCTGG 1620
T A G A R G G S P T C C D R S * 538
GACTGCCGGTGTCTCGAGGGGGATCACCCACCTGCGACAGAAGCTTAAATGCAGTGAAGACAT 1680
AGTGCACATTGTTTTGTTCCATTAAGAGGTCTCCTGGGCGTTGATGATCCTCAGGAGA 1740
TATTCTTGTAGCAACTTGCATCTACGGGATGTGCCTGCAGCTGTGAAAGAGACTTGAGTG 1800
ATGGAAGCTCGAGTGTCTCAAGAAAAAATAAAAAAAAAA 1841

```

Figure 3.58 The full length cDNA and deduced protein sequences of *Pm-F-box* and *wd40* repeat domain binding protein (1841 bp, ORF of 1506 bp corresponding to a deduced polypeptide of 501 aa) further sequenced from the original EST by 3' primer walking. The putative start (ATG) and stop (TAA) codons are illustrated in boldface and underlined. The predicted FBOX domain (positions 122nd – 161st) is gray-shaded. The predicted WD40 (beta-transducin repeats; Trp-Asp (W-D) dipeptide) domains (positions 224th – 261st, 264th – 301st, 304th – 341st, 347th – 384th, 387th – 424th, 427th – 464th and 476th – 513th) are dark-shaded.

The full length cDNA of *P. monodon-cyclin-dependent kinase 7 (Pm-Cdk7)* was 1407 bp in length composing of an ORF of 1062 bp corresponding to a polypeptide of 353 amino acids and the 5' and 3' UTRs of 10 and 335 bp, respectively (Figure 3.59). The closest similar sequence to *Pm-Cdk7* was *cyclin-dependent kinase 7* of *Drosophila melanogaster* (E-value = 1×10^{-122}). The predicted molecular mass and pI of the deduced Pm-Cdk7 protein was 40.12 kDa and 7.06, respectively. Pm-Cdk7 contained S_TKc (Serine/Threonine protein kinases, catalytic) domain involved in catalytic subunit which transfers the gamma phosphate from nucleotide triphosphates (often ATP) to one or more amino acid residues in the protein substrate side chain, resulting in a conformational change affecting functions of the target proteins (Hanks *et al.*, 1988).

The full length cDNA of *P. monodon-selenoprotein M precursor (Pm-SEPM)* was 904 bp in length composing of an ORF of 396 bp corresponding to a polypeptide of 131 amino acid residues and the 5' and 3' UTRs of 6 and 502 bp, respectively (Figure 3.60). It significantly matched *selenoprotein M* of *Litopenaeus vannamei* (E-value = 2×10^{-58}). The predicted molecular mass and pI of the deduced Pm-SEPM protein was 15.10 kDa and 7.75, respectively. The Pm- Pm-SEPM contained a Sep15_SelM domain that functions as thiol-disulphide isomerases involved in disulphide bond formation in the endoplasmic reticulum.

The full length cDNA of *P. monodon-anaphase promoting complex subunit 11 (Pm-APC11)* was 600 bp in length composing of an ORF of 255 bp corresponding to a polypeptide of 84 amino acids and the 5' and 3' UTRs of 1 and 387 bp, respectively (Figure 3.61). The closest similar sequence to *Pm-APC11* was *anaphase promoting complex subunit 11 homolog* of *Tribolium castaneum* (E-value = 1×10^{-41}). The predicted molecular mass and pI of the deduced *Pm-APC11* was 9.84 kDa and 7.99, respectively.

```

      M E V E Q E K K G R I R I E E K L 17
GGAAGACAGGATGGGAAGTAGAACAAAGAGAAGAAAGGAAGGATTAGAATAGAAGAAAAATT 60
  K R Y E K I D F L G E G Q F A T V Y K A 37
GAAGAGATATGAGAAGATCGATTTCTTGGGAGAAGGACAGTTTGCCACTGTATATAAGGC 120
  L D V E T K Q I V A V K K I K L G S R E 57
TCTTGATGTGGAGACCAAGCAGATAGTAGTGTCAAAAAGATCAAACCTAGGTAGCAGAGA 180
  E A R D G I N R T A L R E I K L L Q E V 77
GGAGGCAAGGGATGGCATCAACCGTACGGCTCTCCGAGAGATCAAGCTCTTGCAGGAGGT 240
  H H P N L I G L L D V F G Y K S N V S L 97
CCACCACCCAAACCTCATTGGCCTCCTCGATGTCTTTGGCTACAAGTCAAATGTGTGCGT 300
  V F D F M D T D L E V I I K D T D N I I 117
GGTGTGTTGATTTTCATGGATACAGATTTAGAGGTGATCATCAAGGACACAGACAACATCAT 360
  L T P S N I K A Y M I Q T L K G L E F L 137
CCTCACACCCCTCCAACATCAAAGCATATATGATCCAAACATTAAGGCTTGGAAATTCCT 420
  H L H W I L H R D L K P N N L L V N S D 157
GCATCTTCACTGGATCCTACACAGAGATCTGAAACCAAACCACTACTAGTCAATTCAGA 480
  G I L K I G D F G L A R F F G S P N R Q 177
TGGCATACTCAAAAATAGGAGATTTTGGTCTGGCAAGATTCTTTGGCTCTCCCAACAGACA 540
  Y S H Q V V T R W Y R S P E L L F G A R 197
GTATTCACATCAAGTAGTTACAAGATGGTACAGGAGTCCAGAGTTGCTGTTTGGCGCGAG 600
  S Y G T G V D M W A I G C I L A E M L V 217
ATCCTACGGCACAGGGGTAGACATGTGGGCGATTGGCTGTATCCTGGCGGAGATGTTGGT 660
  R C P Y F P G D S D L D Q L T R I F T A 237
TCGCTGTCCCTACTTCCCGGGTGACTCTGATCTAGACCAGCTTACCAGGATTTTCACTGC 720
  L G T P G D D D W P D M T K L P D Y V S 257
CCTAGGGACTCCTGGTGATGACGACTGGCCGGACATGACGAAACTTCCCGACTACGTATC 780
  F K H F E G S P L R D L F P A A S D D L 277
ATTCAAGCACTTCGAGGGTTCCCACTGCGAGACCTCTTTCCTGCTGCCAGTGATGACCT 840
  L Q L L G S L L T I N P M K R C S C T E 297
TCTCCAGCTATTGGGGTCTTTGCTCACTATTAATCCTATGAAACGATGCAGCTGTACTGA 900
  A L K M E Y F S N K P V P T P G P L L P 317
GGCTCTGAAGATGGAGTATTTTCAGCAATAAGCCTGTCCCGACACCAGGACCTCTTCTTCC 960
  L P P T I R Q R S E A E K P S L K R K I 337
TCTCCCACCAACCATTAGACAGAGAAGTGAGGCAGAAAAACCGTCCCTCAAGCGAAAGAT 1020
  I E E S G F G G S L A K K L Q F * 353
TATTGAAGAGTCTGGCTTTGGAGGTTCCCTTAGCAAAGAAGCTTCAATTCTAGTCCATACA 1080
  AGGAAGAGAAAAAGAAGCACTACCTCCTGATGTGCCAGCGTGACCTCGGTACTTAGTCGT 1140
  AAAGGTGAAAATAAAATTCCTTTAAATGAGGCAAGAAAGAGAGAGGCTGATTTATGAAAGT 1200
  GAATGATATTTATGTTGATGTTAATTTTTTTTCCCTCCGACATGTTAAAGACAAAGGGATG 1260
  ACAGTATTGTCTTTTATTTCTTTATTTACTTGAGTACTGTGTAATATATTGATGTTTCC 1320
  AGAAAGTGTGTTATTTTCTAAACCCAGTGGTATTATTGTAATCATTTCAGAATAAAATTT 1380
  TCATATAATAAAAAAAAAAAAAAAAAAAAAA 1407

```

Figure 3.59 The full length cDNA and deduced protein sequences of *Pm-Cdk 7* (1407 bp, ORF of 1062 bp corresponding to a deduced polypeptide of 353 aa) further sequenced from the original EST by 3' primer walking. The putative start (ATG) and stop (TAG) codons are illustrated in boldface and underlined. Two putative poly A additional signal sites are underlined. The predicted S_TKc (Serine/Threonine protein kinases, catalytic) domain (positions 20th – 304th) is highlighted.

```

      M A K R S L R L L L L L L G V A F S Y 18
GCAACCATGCGCGAAAAGGAGTCTCCGGCTCCTCCTCCTGCTGGGGGTAGCGTTCTCTTAT 60
T L A E E L R E T D I A K A R V E S C G 38
ACCCTCGCTGAAGAATTACGTGAGACTGATATTGCCAAGGCTCGCGTTGAGAGCTGCGGT 120
G U R L N R L P E V K K F I H E D I P L 58
GGATGACGTTTGAACAGGCTCCCCGAGGTGAAGAAATTCATCCACGAGGACATCCCCTC 180
F H N A K F K Q I G G A P P E L V L L N 78
TTCCATAATGCCAAGTTCAAGCAGATAGGAGGTGCTCCTCCAGAACTGGTTCTTCTCAAT 240
R F D Q V V E R L P L D K L S R E E C N 98
CGGTTTGATCAGGTTGTGGAGCGCTGCCCTGGATAAGTTGTCCCGCGAGGAGTGCAAT 300
K L M L K K G F Y K K N S P D E E V P E 118
AAACTCATGCTGAAGAAGGGATTCTATAAGAAGAATTCACCCGACGAGGAAGTCCCTGAA 360
E Y L N G P Y R E R E E L * 131
GAATACCTTAACGGGCTTATAGAGAGAGGGGAAGAACTGTAGATGAAACCTCGGGCAAAG 420
GCAATAAAAAACCATGTTCCCTTAGAAGCAATGTTGGTAACTGTTTCGTCAATTATTCATCG 480
TGGAACACATCTGTAGAAAATTCGAAGTCGTTAGACAGTGTCAAGTATAATAGTCAACTA 540
GTTAAATCAGAGCAGATAGTACTTAGATTTTATTTGTAGAAAATATCGAGTTTTTATATAA 600
GTAAAGCATCATGCAAGCTCCCCAAAATGCAGCTTACCAATTTTCGCTTCAAAAACGGAAC 660
ATGGAAGTACCGCACAAAATTCGGTCAGTGACATTTGTTACCAATATGGAGTCTCGGGGC 720
ACTCGAGGGAAGACACGATTTTCGACATGAAAAGGATCACGAAAAGGGTTCGACTCAAGT 780
GGTCCTTGGAAGCAAAGAATTATCTGGTTGCTTTCGAGTGTTTTGAGACGTTTGCATT 840
CCGTTGATTTTGTAGTTGTTTGAATAAAAATTTAATTTTAAAAAAAAAAAAAAAAAAAAA 900
AAAA 904

```

Figure 3.60 The full length cDNA and deduced protein sequences of *Pm-SEPM* (904 bp, ORF of 396 bp corresponding to a deduced polypeptide of 131 aa) further sequenced from the original EST by 3' primer walking. The putative start (ATG) and stop (TAG) codons are illustrated in boldface and underlined. Two putative poly A additional signal sites are underlined. The signal peptide is dot-underlined. The predicted Sep15_SelM domain (positions 31st - 107th) is highlighted.

```

      M K V K I K S W T G L A T C R W L A N D 20
CATGAAGGTGAAGATTAAATCCTGGACGGGATTGGCTACATGTCGGTGGTTGGCTAATGA 60
D S C G I C R M P F D G C C S D C R L P 40
TGACAGTTGTGGCATTGTAGGATGCCCTTTGATGGATGCTGCTCAGATTGTAGGTTGCC 120
G D D C P L V W G Q C S H C F H I H C I 60
AGGTGATGACTGCCCACTAGTGTGGGGCCAGTGTCTCACTGTTTCCATATTCCTGTCAT 180
M K W L Q S Q Q L H Q Q C P M C R Q E W 80
TATGAAGTGGCTTCAATCTCAACAGCTTACCAGCAGTGTCCAATGTGTGCGCAAGAGTG 240
K F K E * 84
GAAGTTTAAAGAATAACCTTTAAAATACTTTATATTTTGTACTGTTTCAAGACTCATA 300
AGTTGTGGGAGGAGTAAATTTGATGATTTGAAAGATATGGGTCACTCAAAGCATAGGGAC 360
TCGTCATCTGAGTCATTGGAGGAAAAACATAGAAGGAAACACAAAAAAGGCATAGGGAC 420
TCACCGTCTGAGTCATCGGAAGAAGAAGCAGCAGAAAAACAAAAAAGGCATAGGGAC 480
TCGTCGTCTGAATCTTTGGAGGAAGGACGTAGAAGAAGACAAAAAAGGCATAGGGAC 540
TCATCATCTGAGTCTTCGGAGGAAGAGCGCAGAAGAAAAACGAAAAAAAAAAAAAAAAAA 600

```

Figure 3.61 The full length cDNA and deduced protein sequences of *Pm-APC11* (600 bp, ORF of 255 bp corresponding to a deduced polypeptide of 84 aa) further sequenced from the original EST by 3' primer walking. The putative start (ATG) and stop (TAA) codons are illustrated in boldface and underlined.

3.3.2 Rapid Amplification of cDNA Ends-Polymerase Chain Reaction (RACE – PCR)

In addition, the full length cDNAs of 8 functionally important genes (*phosphatidylserine receptor*, *progesterone receptor related protein p23*, *Bystin*, *checkpoint kinase 1*, *Progesterin membrane receptor component 1*, *carbonyl reductase*, *Protein disulfide-isomerase precursor (PDI) (Prolyl 4-hydroxylase subunit beta)* (*Cellular thyroid hormone-binding protein*) (*p55*) (*Erp59*) and *gonadotropin-regulated long chain acyl-CoA synthetase*) were also characterized by RACE-PCR.

Approximately a 1200 bp fragment was obtained from 3' RACE-PCR of *phosphatidylserine receptor* (Figure 3.62; A). Nucleotide sequences of EST and 3' RACE products of this gene were assembled. The full length cDNA of *P. monodon phosphatidylserine receptor (Pm-PSR)* was 1862 bp in length consisting an ORF of 1170 bp corresponding to a polypeptide of 389 amino acids and the 5' and 3' UTRs of 194 and 500 bp, respectively (Figure 3.63). Its significantly closest sequence was *phosphatidylserine receptor* of *Apis mellifera* (E-value = 4×10^{-142}). The predicted molecular mass and *pI* of the deduced Pm-PSR was 45.32 kDa and 9.23, respectively. Pm-PSR contained a JmjC (jumonji-C) domain, part of the cupin metalloenzyme superfamily, which is functionally regulated chromatin reorganization processes (Clissold and Ponting, 2001).

An approximately 1400 bp fragment of 3' RACE-PCR of a *progesterone receptor related protein p23* was successfully amplified (Figure 3.62; B). Nucleotide sequences of EST and 3' RACE products of this gene were assembled. The full length cDNA of *P. monodon progesterone receptor related protein p23 (Pm-p23 like protein)* was 1943 bp in length composing of an ORF of 495 bp corresponding to a polypeptide of 164 amino acids and the 5' and 3' UTRs of 7 and 1441 bp, respectively (Figure 3.64). The closest similar sequence to *Pm-p23 like protein* was *p23 like protein* of *Nasonia vitripennis* (E-value = 7×10^{-46}). The predicted molecular mass and *pI* of the deduced Pm-p23 like protein was 19.07 kDa and 4.39, respectively. Pm-p23 like protein contained a CS domain but the function of this domain is unknown.

An approximately 1000 bp fragment was successfully amplified from 5' RACE-PCR of a *bystin* homologue (Figure 3.62; C). Nucleotide sequences of EST

and 5' RACE products of this gene were assembled. The full length cDNA of *P. monodon bystin isoform 1 (Pm-bystin1)* was 1553 bp in length composing of an ORF of 1365 bp corresponding to a polypeptide 454 amino acids and the 5' and 3' UTRs of 126 and 62 bp, respectively (Figure 3.65). Its significantly matched sequence was *bystin* of *Nasonia vitripennis* (E-value = 1×10^{-124}). The predicted molecular mass and pI of the deduced Pm-bystin1 was 52.43 kDa and 6.55, respectively. The Pm-bystin1 contained a Bystin domain. Bystin may be involved in implantation and trophoblast invasion because bystin is found along with trophinin and tastin in cells at human implantation sites and also in the intermediate trophoblasts at the invasion front in the placenta from early pregnancy (Tyarkowski *et al.*, 1976).

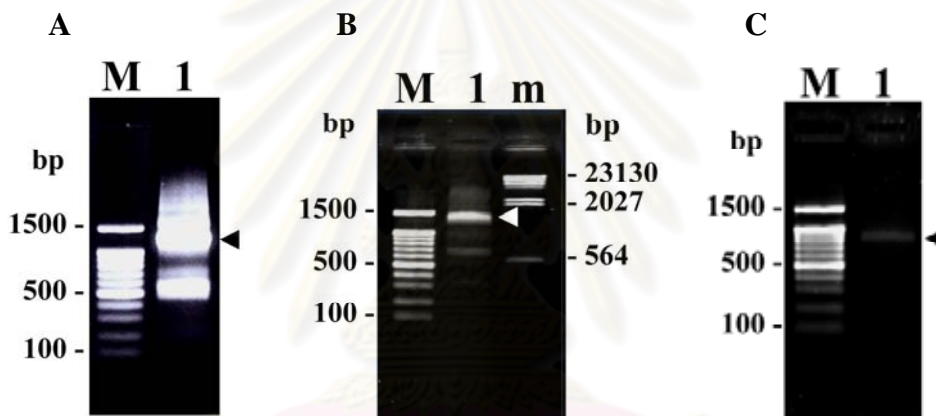


Figure 3.62 3' RACE-PCR products of *Pm-PSR* (A) and *Pm-p23 like protein* (B) and 5' RACE-PCR products of *Pm-bystin* (C). Arrowheads indicate bands selected for further analysis. A 100 bp DNA ladder (lanes M) and λ -*Hind* III (lane m) were used as the markers.

```

TTAACATGATTACGCCACCTCGAATTTAAACCTCACTAAAGGGAACAAACAGCTGGAGCT 60
CCACCGCGGTGGCGGCCGCTCTAGAACTAGTGGATCCCCCGGGCTGCAGGCTTTCCTCCT 120
GTTTTTGTCAAGCCCATGGATCACAGGTGCCGGAAGAGAGTGAGAGAAGCCAAAAAGAAA 180
      M D H R C R K R V R E A K K K A 16
GCGAGACCAGAATTATGGATCACAGGTGCCGGAAGAGAGTGAGAGAAGCCAAAAAGAAAAG 240
  R P E L C L E K G V W T K H D Y K N K F 36
CGAGACCAGAATTATGTTTAGAAAAGGCGTGTGGACAAAACATGACTACAAGAACAAGT 300
  D C S I D I V P D T V E R I H A N E V P 56
TTGACTGCTCTATAGACATTGTTCCAGATACAGTAGAACGCATTCATGCAAATGAGGTCC 360
  I E E F I E R Y E K P Y K P V V I E A V 76
CAATTGAAGAGTTTCATCGAGCGATATGAGAAGCCTTACAAACCAGTTGTTATTGAAGCGG 420
  T D N W K A R Y K W T L E R L Y K K Y R 96
TCACAGACAACCTGGAAGGCTCGATATAAGTGGACCCTAGAGAGGTTATACAAGAAATACA 480

```



```

  N Q K F K C G E D N E G Y S V K M K M K 116
GAAATCAGAAATTC AAGTGTGGAGAAGATAATGAAGGCTACAGCGTAAAGATGAAGATGA 540
  Y Y I E Y M K T T D D D S P L Y I F D S 136
AGTATTACATTGAATATATGAAGACAACAGATGATGATAGTCCACTCTATATATTTGATA 600
  S F G E H V R R K K L L E D Y D V P K Y 156
GCAGTTTTGGTGAGCATGTCCGTCGTAAAAAGCTTCTAGAAAGATTATGATGTGCCGAAAT 660
  F R D D L F K Y A G E D R R P P Y R W F 176
ATTTTCGAGATGATTTATTTAAGTATGCCGGTGAGGATAGACGCCCCCTTACCGCTGGT 720
  V M G P A R S G T G I H I D P L G T S A 196
TCGTCATGGGTCTGCTCGTTCAGGACCGGCATTCACATAGATCCTTTAGGAACTAGTC 780
  W N T L L R G H K R W C M F P T T D T P K 216
CTTGGAAATACGCTTCTCCGTGGTCAAAAAGATGGTGCATGTTCCCTACAGATACTCCCA 840
  E L I K V T S A E G G K Q V D E A I T W 236
AGGAGCTTATTAAGGTGACTTCTGCAGAAGGAGGGAAGCAAGTAGATGAAGCTATAACAT 900
  F S I I Y P R T K L P N W P E K Y K P L 256
GGTTCTCCATTATTTATCCTCGTACGAAACTTCCAAATTTGGCCAGAGAAATATAAGCCGC 960
  E L V Q H P G E T V F V P G G W W H V V 276
TGGAGTTGGTGCAGCATCCTGGTGAAACAGTATTTGTGCCTGGAGGCTGGTGGCATGTTG 1020
  I N L D N T I A I T Q N F A S C T N F P 296
TCATTAACCTTGACAATACAATTGCCATCACTCAGAACTTTGCTTCATGCACAAACTTCC 1080
  V V W H K T V R G R P K L S K K W L R I 316
CTGTTGTGTGGCACAAGACTGTGCGGGGCCGTCCAAAAGCTTTCAAAAAGTGGCTTCGAA 1140
  L R E K K P D L A V V A D S I D M S K S 336
TCTTAAGGGAGAAGAAGCCAGACCTAGCAGTTGTAGCAGATTCAATTGATATGAGCAAAA 1200
  C G M A S D S S S D S S S S S S S S S S S D 356
GCTGTGGAATGGCATCTGACTCCTCATCAGATTCATCTTCATCGTCTTCCCTCGTCTTCTG 1260
  E S S S S S V S D S G Q E S L P E H K 376
ATGAATCCTCATCCTCTGAGAGTGTTCAGACAGTGGTCAGGAGAGCTTACCAGAACATA 1320
  K K R R K T H N S P P R S * 389
AAAAGAAGAGGAGGAAGACACACAACCTCTCCTCCGAGGTCTTGAAGGGAGCCAGTCCAGCA 1380
GCGCTCTTGAAGACGGTGCTGCTGCTTCCGACTCTCCACTCCCCCTCTATCCTTCCAACAC 1440
CACCACCAAGGAATGTTTCTCCAGCTTGTGTCATGCTGCTTGTAAATGCACATTGGTTCT 1500
CACCTCGCATTCTAGGCATACAACAAAAGACATTGATACGATGAATTCCTCAGAGAGCATGT 1560
AGGATATACATATATATTTATATTACTGTCCACATTTTTTACTTTTTTATTGTATTACCC 1620
CAGAGCTTATATACCATCGGAATAACGTATACTATGTATTTGGTGAAAACTTTTAAGTGG 1680
AAGTATTAGATATTAATACATGTAACAGAAAAAAGGGTAAAAATATTTCCCTGAAACACAG 1740
GATGATAGATCAGATGTTTTGATTTATATATCTTGGTTGCTTATGTCAGCAAAAAGAAATA 1800
AATCATAAAAAAAAAACAATAAAATAAAACAAAATGACAAAAAAAAAAAAAAAAAAAAAAAAAA 1860
AA 1862

```

Figure 3.63 The full length cDNA and deduced protein sequences of *Pm-PSR* (1862 bp, ORF of 1170 bp corresponding to a deduced polypeptide of 389 aa) further characterized by 3' RACE-PCR. The putative start (ATG) and stop (TGA) codons are illustrated in boldface and underlined. The putative multiple and single poly A additional signal sites are underlined. The predicted JmjC (jumonji-C) domain (positions 142nd – 306th) is highlighted.

```

      M S T T Q S L P P P V T W A Q R K N 18
AAACACCATGTCAACCACACAGTCTTTGCCACCCCAGTGACATGGGCACAGCGAAAAAA 60
L I F L T I C V E D C K S P T I N I E A 38
TCTCATCTTCCTAACTATCTGTGTTGAAGACTGCAAACTCTCCACCATTAACATAGAAGC 120
D K V Y F K G T G G T E R K D Y E Y T Y 58
AGATAAGGTGTACTTCAAGGGCACAGGAGGCACTGAAAGAAAAGATTATGAATATACTTA 180
N L F K D I D T D K S R S F V R D R N I 78
CAACTTGTTTAAAGATATTGATACAGATAAAAAGCCGTAGTTTTGTACGAGATCGTAACAT 240
E L I L V K K E E G P Y W P H L L K E K 98
AGAGCTGATACTGGTCAAAAAAGAGGAGGGACCTTACTGGCCACACCTGCTTAAGGAGAA 300
T K Q H W L K V D F S R W K D E D S D 118
AACGAAGCAGCACTGGCTCAAAGTAGATTTTCAGCCGATGGAAGGACGAAGACGACAGTGA 360
D E E G Q N Q D L E E M M R Q M G G L G 138
CGATGAGGAGGGCCAGAACCAAGACTTGGAGGAGATGATGCGGCAGATGGGAGGTCTAGG 420
G G G D D R P S L D D L E D E D S D D D 158
TGGTGGCGGAGATGACAGGCCATCCCTCGATGACCTCGAGGATGAAGACTCCGACGACGA 480
D L P D L E * 164
CGATCTCCCTGACCTGGAGTAACTGTGTCAGTAGCCCAAAGAGGCCTTCGCAGACCACTT 540
CTTGCAAGTGGGTGCAAGTGATGCGTCGTGGTAAGCTGTCTGTACCTAAGTCAGTGTGT 600
GCGAATTCAGTTACCTCCAGATGGACAACCTTTGCTATGTGGGATCCACTGCAGTTGGAA 660
ACAATACAAAGAATATTGTCCCGCGGAGTTTTTTTTGTACACACAGTGTGACTAGGACTTG 720
ACTGCCCTCCTTGTGCAGGGTTCCAGTGAGCGTGGATTAGTGGCTCTTTTTCTTTTTCTCA 780
TTTTCTTTTTCTTTTCCAACCAACCTGCCATAAAAAGAAAACTAAATGAAATTTTTCCATTT 840
TCGTTTCCATATATACATAGCATAACAAGCAAGCTTGTTCAGAACAGTCCCTTCCAAA 900
CTTAGTTAGAATTTTTTTTTTTTTTTTACTTTTTGTTTTCTCAACGCTCTTGGCCTGGCAGCT 960
CTGGAGAGAAATGTGTCCCACCTTTCTGCCCTGCTAAAGAAAAGTGAATTTAAAATGGAA 1020
AGTGCTGTCTTTTATCATTTAAACTTCGCAATTTATCAGATAAGCAGATTTTTTTGTTTAA 1080
GAAACTACATGTTTAGCTTGCAAATATTCTCATCTTTACATGTCTGTTATATGGCAAAA 1140
CAAAACCAAAAAATCCACAATCCTGTGTAGGCCTTACATTTATTTTGTCAAGGTAC 1200
ATGGAGTTGGGTTTGATGAGAAAAATCATATTGATTGCCCTCAGCAGACCAATTTCTTGTG 1260
TTTTTGATGAGTCGTGATGTAATGAGTGAGTCTAGGCTATTCCCACGGCTTAGCACATGA 1320
AAACTTTGTAAGGTTATTTCTTATGTTTATATTTATTATTGTTAATTATAGATGTTTCAT 1380
TTTTCATTTTTTTAGAGGGAGGAAAAATGAATGTAACCTGGTAGTGTGCATGTGAAGAGT 1440
AAAAAACTAAAAGTTTATTATTCCTTGTATTTAAATGGGGACGTGAGTTCCTTGGTCTTACA 1500
AAGAGATCTCATAGAACCAGTGGATAGGGTACATCAGATGTTTGCTGCCCTTAGTGTCAA 1560
ATTTTATATACATGTATTATGTCATATCATTATGGAACCTAGAAATCAAAGTGTTTTTTAA 1620
GACATTGTGATTTTGTACCACCTGGGGTAAGTCTTTATATATATAATATATACTCTTGGC 1680
AGAACAGCATAACATACCTGAAGGTTTTCTTCCAATACACAAGTCATGATTCAAAGTGT 1740
TATAATCCTGTTTGTATAAGTTAATGAAAACCTAGATATTTCTTTTTTTCATCGCAGAAAT 1800
ATTTCCGATTAATTAATAATCTGTCTCTGTATATGATTTAAAGTCTTTTTTGAGTTGAAAAT 1860
TTAGTTTTGTATTTCTTTCTGCATGTAAGGGAGATGAAGGCAAAGAAACAATTTGAAAAA 1920
AAAAAAAAAAAAAAAAAAAAAAAAA 1943

```

Figure 3.64 The full length cDNA and deduced protein sequences of *Pm-p23* (1943 bp, ORF of 495 bp corresponding to a deduced polypeptide of 164 aa) further characterized by 3' RACE-PCR. The putative start (ATG) and stop (TAA) codons are illustrated in boldface and underlined. The predicted CS domain (positions 9th – 84th) is highlighted. A p23 signature (WPHLLKE; position 91st – 97th) is double-underlined.

```

GTTTCGCGGGACCTTGTGTCTGGCGGCACGTGTGGACGGAGGGTCTGTCTCACCTATAA 60
TCATTTGTTAATAATTCTGAATCCTCATAATCTTCACTATTATATCCTAATCCTTGAAG 120
  M G K I K R L Q N A G G K V P R P G 18
GTCAGAAATGGGGAAAGATTAACGTCTGCAGAATGCTGGTGGCAAAGTGCCTCGGCCAGGC 180
P L A E Q I E K S E Y A Q P S A R K K V 38
CCTCTAGCAGAGCAAATGAAAAATCTGAATATGCACAACCCCTCTGCAAGGAAGAAAGTT 240
R S Q R S D G D D E F V E G Q M G R S I 58
CGCAGCCAACGCTCTGATGGTGACGATGAATTTGTAGAAGCCAGATGGGGCGTAGCATC 300
L K Q S Q A Q L Q E V L F E D M E K D F 78
TTGAAACAGAGTCAGGCTCAATTGCAGGAGGTTCTTTTTGAAGACATGGAGAAGGACTTC 360
P P L G Q P V E K Y E R Q P Q K V S L S 98
CCACCTCTTGGGCAGCCGTTGAGAAATATGAGAGACAACCTCAGAAGGTGTCTCTCAGC 420
R K S K D A I D D E E S S D D E K E V N 118
CGAAAATCCAAAGATGCCATTGATGACGAGGAAAGCAGTGACGATGAGAAAGAGGTTAAT 480
E M D N P V P C N V D K V V N D F E K E 138
GAGATGGATAACCCCTGTACCTTGAATGTAGACAAAGTTGTAACGATTTTGAAGAGGAA 540
L D L A E D D M K I L E H F M N K D A Q 158
TTGGATTTAGCCGAAGATGACATGAAAATTCTGGAACACTTCATGAACAAAGACGCACAA 600
P Q K L A D M F R D K I T E K Q T D I R 178
CCCCAGAGAAAACCTAGCAGACATGTTCCGTGATAAAATCACGAAAAGCAGACAGACATC 660
Q S Q V N A S T V Q T V N L S P E V Q E 198
CAATCACAAGTGAATGCTAGCACTGTACAGACCGTTAACCTTAGTCCAGAGGTGCAAGAA 720
M C S Q I G N V L S K Y R S G P L P K M 218
ATGTGCTCACAGATTGGGAATGTCTTGTCAAATACAGAAGTGGACCCTTGCCAAAGATG 780
F K V I P K M R N W E E L V Y L T D P D 238
TTCAAGGTAATTCCAAGATGCGCAACTGGGAAGAAGCTCGTATACCTGACAGACCCTGAC 840
K W S A A A V Y Q G V R I F V S N L K E 258
AAGTGGTCTGCTGCTGTGTACCAGGGTGTAGAATATTTGTGAGTAACCTCAAGGAG 900
P M A Q R F F N L V L L P R I R D D I S 278
CCCATGGCACAGCGCTTCTCAACTTGGTCCTCCTCCTCGCATACGGGATGACATCTCC 960
Y Y K R L N F H L Y Q A M C K A L F K P 298
TACTACAAGCGCCTCAACTTCCATTTGTATCAGGCTATGTGCAAGGCCCTTTTCAAGCCA 1020
G A F F K G V L L P L C M S G T C T L R 318
GGTGCCTTCTTTAAAGGTGTTTTACTTCTCTGTGCATGTCCGGTACATGTACTCTTCGA 1080
E A I I V G S V I A K N H I P I L H S A 338
GAAGCTATTATTGTTGGTTCAGTAATTGCAAAGAACCACATACCAATTCTGCACTCGGCT 1140
A T I L K I A E M D Y S G A N S I F L R 358
GCAACGATACTGAAGATTGCTGAAATGGACTATTCTGGAGCAAATTCAATATTTTTGAGA 1200
I F F D K K Y A L P Y R V V D A C V Y H 378
ATATTTTTTTGATAAGAAATATGCCCTCCCATACAGAGTTGTTGATGCTTGTGTCTACCAT 1260
F M R F Q H D R R E L P V L W H Q A L L 398
TTTATGAGGTTCCAGCATGACCGCCGTGAACTGCCAGTTTGTGGCATCAAGCCTTGCTT 1320
V F F V Q R Y K E D M S P D Q K Q A I M D 418
GTATTTGTCCAAAGATACAAGGAAGATATGAGTCTGACCAGAAACAAGCCATCATGGAT 1380
V I K F H T H F T I T A E V R R E L L N 438
GTCATTAATTCACACTCATTTCACCATCACTGCCGAGGTGAGGAGAGAACTTCTGAAT 1440
S K C R G Q D D D M P M M V D E * 454
TCCAAGTGCAGAGGTCAAGATGATGATATGCCAATGATGGTTGATGAGTAGTGTATGGGA 1500
ATGGGAAAGAAATTAAGGAAATAAATATTTAAAACATAAAAAAAAAAAAAAAAAAAAA 1553

```

Figure 3.65 The full length cDNA and deduced protein sequences of *Pm-bystin isoform 1* (1553 bp, ORF of 1365 bp corresponding to a deduced polypeptide of 454 aa) further characterized by 5' RACE-PCR and 3' primer walking of the original EST clone. The putative start (ATG) and stop (TAG) codons are illustrated in boldface and underlined. The putative poly A additional signal site is underlined. The predicted Bystin domain (positions 152nd – 452nd) is highlighted.

An approximately 2000 bp fragment was obtained from 3' RACE-PCR of a *checkpoint kinase 1* (Figure 3.66; A). Nucleotide sequences of EST and 3' RACE products of this gene were assembled. The full length cDNA of *P. monodon checkpoint kinase 1 (Pm-Chk1)* was 2078 bp in length composing of an ORF of 1455 bp corresponding to a polypeptide of 484 amino acids and the 5' and 3' UTRs of 169 and 454 bp, respectively (Figure 3.67). *Pm-Chk1* significantly matched *Serine/threonine-protein kinase grp (Chk1)* of *Drosophila melanogaster* (E-value = 3×10^{-131}). The predicted molecular mass and pI of the deduced Pm-Chk1 was 54.61 kDa and 8.61, respectively. The Pm-Chk1 contained a S_TKc (Serine/Threonine protein kinases, catalytic) domain as also found in Pm-Cdk 7.

A 300 bp amplification fragment was obtained from 5' RACE-PCR of a *progesterone membrane receptor component 1* (Figure 3.66; B). Nucleotide sequences of EST and 5' RACE products of this gene were assembled. The full length cDNA of *P. monodon progesterone membrane receptor component 1 (Pm-PGMRC1)* was 2040 bp in length composing of an ORF of 573 bp corresponding to a polypeptide of 190 amino acids and the 5' and 3' UTRs of 19 and 1448 bp, respectively (Figure 3.68). Its significantly matched sequence was *progesterone receptor membrane component 1* of *Oryzias latipes* (E-value = 3×10^{-47}). The predicted molecular mass and pI of the deduced Pm-PGMRC1 protein was 21.00 kDa and 4.60, respectively. Pm-PGMRC1 contained Cytochrome b5-like Heme/Steroid binding domain which is ubiquitous electron transport proteins in animals, plants and yeasts. The transmembrane domain of Pm-PGMRC1 was also found (IFTSPLNVFLLGVCTVLIY) (Figure 3.69).

A 800 bp amplicon was obtained from 3' RACE-PCR of *carbonyl reductase* (Figure 3.66; C). Nucleotide sequences of EST and 3' RACE products of this gene were assembled. The full length cDNA of *P. monodon carbonyl reductase (Pm-carbonyl reductase)* was 1269 bp in length composing of an ORF of 861 bp corresponding to a polypeptide of 286 amino acid residues and the 5' and 3' UTRs of 57 and 351 bp, respectively (Figure 3.71). The closest similarity to *Pm-carbonyl reductase* was *carbonyl reductase 1-like* of *Tribolium castaneum* (E-value = 2×10^{-86}). The predicted molecular mass and pI of the deduced Pm-carbonyl reductase was 31.32 kDa and 7.69, respectively. Pm-carbonyl reductase contained an adh_short (alcohol dehydrogenase short chain) domain which involved to metabolic process and

oxidoreductase activity. Moreover, carbonyl reductase also exhibits the 20 beta-hydroxysteroid dehydrogenase activity which is recognized as a maturation inducing hormone which involved in final maturation and ovulation processes of vertebrate oocytes (Espey *et al.*, 2000 and Tanaka *et al.*, 2002).

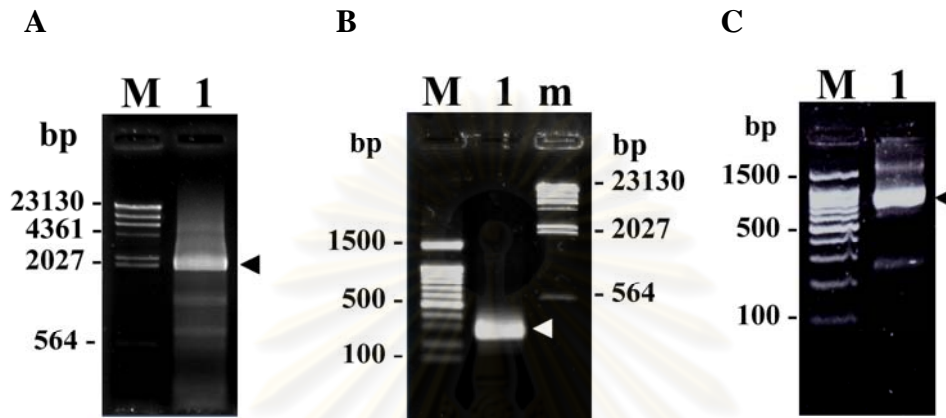


Figure 3.66 3' RACE-PCR products of *Pm-Chk1* (A), 5' RACE-PCR products of *Pm-PGMRC1* (B) and 3' RACE-PCR products of *Pm-carbonyl reductase* (C). Arrowheads indicate bands selected for further analysis. A 100 bp DNA ladder (lanes M, panels B and C) and λ -*Hind* III (lane M, panel A and m, panel B) were used as the markers.

```

GTCAGCGTGGCTTTTCATTCCCTCGCTGGAATTTCCCTCCGCTCAACCTCGGTCCGTCTGC 60
CGGCGACGCCCCCGCGGCCGAGATGTAGTTCCCCGAGCTCGGCCCTCCAGCGCAGACGCC 120
                                                                 M A G P 4
TTTTGTAGGTTATGTTGGCTAGAAAAGTGTGCAAAAAGACCAGCACCACCATGGCTGGGGCC 180
V T E F V V G W N V V Q T L G E G A F G 24
GGTCACCGAATTTGTGGTGGGGTGAACGTAGTCCAGACCCTTGGGGAGGGGGCCTTTGG 240
E V K L L I N K D T G E A V A M K M V D 44
AGAAGTAAAATTGCTAATCAATAAGGACACTGGGGAGGCAGTTGCCATGAAGATGGTGGA 300
L V K H P D A A D A V R K E I C L H R M 64
CTTGGTCAAACATCCAGATGCAGCAGATGCTGTGCGCAAGGAAATATGTCTGCACCGCAT 360
L K H A N I I K F Y G S R R E N S M Q Y 84
GTTAAACATGCAAAACATCATAAAATTTTATGGAAGTCGCCGTGAAAATTCATGCAGTA 420
M F L E Y A A G G E L F D R I E P D T G 104
CATGTTCCCTGGAATATGCTGCAGGTGGTGAACATTTGATCGTATTGAGCCTGACACGGG 480
M P C P H Q A Q K Y F R E L I S G V E Y L 124
CATGCCTCCCACATCAGGCACAGAAGTACTTCAGGGAATTGATCAGTGGTGTGGAATACCT 540
H G R G V T H R D L K P E N L L L D E N 144
CCATGGACGGGGTGTACACACCGGGATCTCAAGCCAGAGAACTTGCTGCTTGACGAGAA 600
D H L K I T D F G M A T L F R H N G K E 164
TGACCATCTTAAAATAACAGACTTTGGAATGGCCACTCTCTTCAGACACAATGGGAAGGA 660
R E L D R R C G T K P Y M A P E V L L R 184
ACGTGAATTGGATCGTTCGTTGTGGAACAAAACCATATATGGCTCCTGAAGTATTGCTGAG 720

```

```

P Y N A E P A D I W S C G V I L V A L L 204
ACCCTATAATGCTGAACCTGCAGATATTTGGTCTTGTGGAGTGATTCTTGTGGCACTGCT 780
A G E L P W D E P T F S C P E Y T A W K 224
AGCTGGTGAATTGCCATGGGATGAACCAACTTTTTCTTGTCCAGAATACACGGCCTGGAA 840
D R D C R L F T T T P W T K V D N L A L 244
AGACCGAGATTGTAGGTTGTTTCAACAACACACCTTGGACAAAGGTGGACAATCTGGCCCT 900
S L L R K V L N T V P R H R A T V P Q V 264
CTCTCTTTTGGCAAGGTATTGAATACTGTACCTAGGCATCGAGCAACAGTACCTCAGGT 960
K A H Q W F T K N Y H K S S G F G R S A 284
GAAAGCACATCAGTGGTTCACAAAGAATACTACCACAAAATCTTCAGGTTTTGGACGCAGTGC 1020
S N D S M T P T H T K R V C S E L E R E N 304
ATCGAATGACAGCATGACCCCTACTACCAAGCGTGTGTGCAGTGAGCTTGAACGGGAAAA 1080
S S F C L E D M S A R L A C S Q P E A P 324
CTCCTCATTCTGTTTTGGAAGACATGTCAGCACGGTTAGCATGTTTACAGCCAGAGGCCCC 1140
T S A S I N T V N G P N V D M G V V S F 344
TACATCTGCTTCAATTAATACTGTTAATGGTCTTAATGTAGACATGGGGGTTGTGAGCTT 1200
S Q P A Q P D Q L L L S S Q L T Q S T Q 364
CTCGCAACCAGCCCAACCTGACCAGCTGTTGCTCTCCTCTCAACTTACTCAAAGTACACA 1260
A S Q T P L Q R L V K R M T R L L V R T 384
AGCAAGTCAAACACCACTGCAGAGGCTTGTGAAACGCATGACTCGTTTGCCTTGTAAAGAC 1320
N L E D T L T H L E A L F N K M N Y T Y 404
CAACCTGGAGGACACCCCTAACTCACCTGGAAGCATTGTTCAACAAGATGAACTACACTTA 1380
R M H N V N V L T V T T L D R R G A Q L 424
TCGTATGCACAATGTCAATGTTCTTACTGTAACCACTCTGGATCGACGTGGAGCTCAACT 1440
V L K A S I L D M G Q H I L V D F R L S 444
TGTGCTGAAAGCAAGCATACTGGATATGGGCCAGCATAATCTTGTGGATTTTCAGACTTTT 1500
K G C G L D F K R H F L R I K E G L S H 464
AAAAGGATGGGATTTGATTTTAAACGACATTTTCTGCGAATTAAAGAGGTTTTATCTCA 1560
I V I K G P V T W N M A L A T N M L P A 484
TATAGTAATCAAGGGTCTGTAACTTGAATATGGCTCTAGCAACAAATATGCTACCAGC 1620
*
TAATTTGGACCCAGACAGAAAAATTTTTTGAAGTCTTTCAAAAATTTATATGCTGACTGTTA 1680
CTCATGCTTGTGTAAGATGTAAAATATTAGTCTTTAATGAATAAGCTATGATTTATACTC 1740
GGTTAAAGTATAAAAGTGTGTTGATATTGAATGTGTGATTAACCTTTGAAAGAATTGGATGT 1800
AAGACTGGTATGCCTGTAATAATTTTTCCCTGTCTAGATTAAGCATTTGGTTAACTTGAA 1860
AGGTGACCTCCCAGTAATAGTAGTATGGCAGAATGTTCCAGCAACATTGGCTGCCTGGAT 1920
AGGTAGTGAGTACCCATCTCAACAGTGTGCTGCGGTTGTAAGAGAAGTCTTGCTTTTGGAC 1980
CAGCCTTCTCTCTACTCTCGCAGGCAGAATTTCTAGTCTTTCACTGATGGGTGCTTACTTG 2040
CTTTTACCAAAAAAAAAAAAAAAAAAAAAAAAAAAAAAAAAAAAAA 2078

```

Figure 3.67 The full length cDNA and deduced protein sequences of *Pm-Chk1* (2078 bp, ORF of 1455 bp corresponding to a deduced polypeptide of 484 aa) further characterized by 3' RACE-PCR. The putative start (ATG) and stop (TAA) codons are illustrated in boldface and underlined. The predicted S_{TKc} (Serine/Threonine protein kinases, catalytic) domain (positions 12th – 270th) is highlighted.

M A D E G A D A V S I E E S 14

ACGCGGGGACTCGACTATC**ATG**GCGGACGAGGGAGCGGACGCCGTCTCCATCGAAGAGTC 60

F L G S L L K E I F T S P L N V F L L G 34

CTTCTGGGCTCACTACTCAAAGAAATATTCACCTCCCCTTAATGTGTTCCCTCTTGGG 120

V C T V L I Y K I F R S S D G S G G A T 54

TGTCTGTACCGTCCTCATCTATAAGATATTCGGTTCGTCCGATGGCAGTGGAGGAGCAAC 180

G P V E P P V P K M K R Q D M T L E Q L 74

AGGTCCAGTGGAACTCCTGTGCCCAAGATGAAACGACAGGACATGACCTTGGAGCAGTT 240

K Q Y D G M G E H G R V C V A V N G K I 94

GAAGCAGTATGATGGCATGGGGGAGCATGGGCGTGTATGTGTGGCAGTTAATGGCAAGAT 300

F D V T R G S K F Y G P G G P Y S A F A 114

CTTTGATGTCAACCGAGGCTCCAAGTTCTATGGCCAGGTGGGCCGTATTCTGCCTTTGC 360

G R D A T R A L A T F S V K D V K E E Y 134

TGGCCGAGATGCAACAAGAGCTCTGGCAACCTTCAGTGTAAAGGATGTAAAGGAAGAGTA 420

D D L S D L S S M Q M D S V R E W E M Q 154

CGATGACCTCAGTGACCTCTCCTCTATGCAGATGGACTCTGTCAGGGAATGGGAGATGCA 480

F T E K Y D Y I G K F L K P G E Q P T E 174

GTTACAGAAAAGTACGATTATATTTGGTAAATTTTTGAAACCAGGAGAACAGCCACAGA 540

Y S D D E E A K D T K A K T D D * 190

GTACTCAGATGATGAGGAAGCAAAGGACACCAAAGCGAAGACGGATGAT**TAG**ATGTAGTT 600

GAGGTGATTGCGCATTGCTGTATAGGTTAAGGCCTCTCGGTTCCACCAGACTCCAAAGCC 660

CTTGAGCATGGTCTTAAGATTAGGATGTGGACGTGAAAAAAGTAAAAAAAAAAAAAAAAA 720

AACCTCGTGCCGAATTCGGCACGAGGCGAAGCTGTACCTCTCGTGGTTCCTTGAAGC 780

CCACCTCAGGAAGCTCGTCAAGGAGGTCGTTAGCATCCCCCTGGTCTCGTCCGTCACGCA 840

GAAGGTCTCCACCACCCACGAGAAGCTTTGTAGTACGGTGCCGCTCTATGACTGGCTGAC 900

GGCGACCCGCGCTGTTGACGACGAAGGTGGTTCGCTTCGAAGGCTGAGGAGTACGCTGTGGT 960

CAAGACGTCAAGTCTCAAAGCGGAGGAACTGGGCTCCATGTGGTAGACAACCTTGAAGAA 1020

AAATTATCCTGTTATTGAGAAGCCTACCGAAGAGGTAGTAGAGCGGACTTCTGTTTACGT 1080

CCGCCAGAAGATCCAGCTGGGAAAGAGTCGCGTGGCTCCTATTCTGTAAGTCAAGCCAC 1140

CTGTGCGCAACAGAGGCTGCCATAAAGACTGCTGAGGTTGCTTGGGATACCTTGAAGAT 1200

AGACCGGAAGGAAAACTGGCTCGCTTCGATTGTCCAGCGCCACTGAGGACTCTATATAA 1260

CTATACATTTGGTCCAGCCTTGGCTAAAACGACTCGGCAGCTGCGCAACGGAAGGCCAAC 1320

AGTAAGAGCTNTGAGGCGTTCGCGCGGTGCACACAGCCGTTGAGAACCCTATCAAGCG 1380

CCGCCGGAAGGTTTCTCCACGCAAATCTACGAAGGACCAGCCAGTAGTGGTCTGTGGGC 1440

GTGGCTAATTAGTTTCTTGGCCGTGTTGGCTTGGCTTCGAGTCCCGCCACTCCTCCCC 1500

GGCGGAGCTCCCGAAGCTCGACCCGCGAACTGACCTCCAGCCCCAAGCAGCAGGAGGGAAC 1560

TACAGAGGACAAGAAGAGGAAGCTGTCTGACGTGGAAACGGAAGACGCCACCTCGGTCTGA 1620

GGAAATGAGTCACTTGGACCTTCTTACGACATGGACGACTACCGTTCAGACGAGGACCC 1680

CGACTATTGCGCAAGCGACACCTCCACCGACAGCTCGAGTACAGGTCGACGACCATGA 1740

GGAGAGCGAGGCGCCCTTACCGAGGACGACTTCAAGAAGGAACCCACGAAGGCCAGCGA 1800

AGGAGAACCTCGGTCCCTTGGGGCAGCAGCGCCCCGGGAGGCGAAAGCCAGCCAGTGTGAC 1860

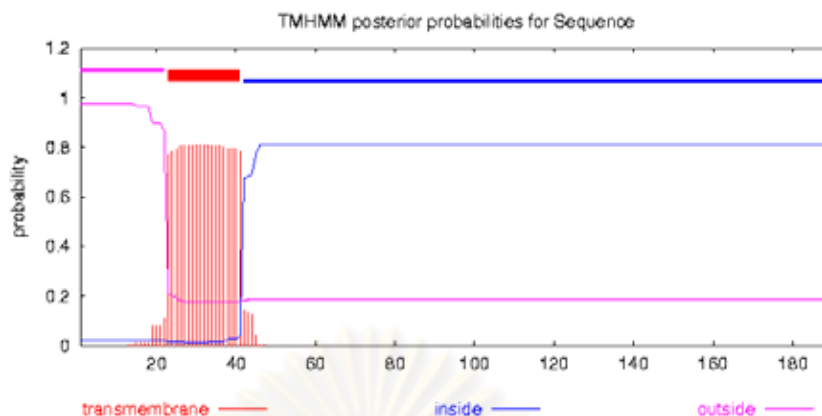
GACCAAGGTGTCCTGACGGTGGTTCGACACAGAGGACCAAGCCTGCGGAAGGGGATGCCCC 1920

CGAGGTTGGGAAGTCGGCGGCGGAGGTGGAGTAGGGATACGGATATTGTTATGACATTTA 1980

TATAAGTTTTTATTGTATTTTTTAATAACTAGTTTACTTCTATTAAAAAAAAAAAAAAAAA 2040

Figure 3.68 The full length cDNA and deduced protein sequences of *Pm-PGMRC1* (2040 bp, ORF of 573 bp corresponding to a deduced polypeptide of 190 aa) further characterized by 5' RACE-PCR and 3' primer walking of the original EST clone. The putative start (ATG) and stop (TAG) codons are illustrated in boldface and underlined. The predicted Cytochrome b5-like Heme/Steroid binding domain (positions 68th – 166th) is highlighted. The predicted transmembrane domain (positions 23rd – 41st) is double underlined.

A



B

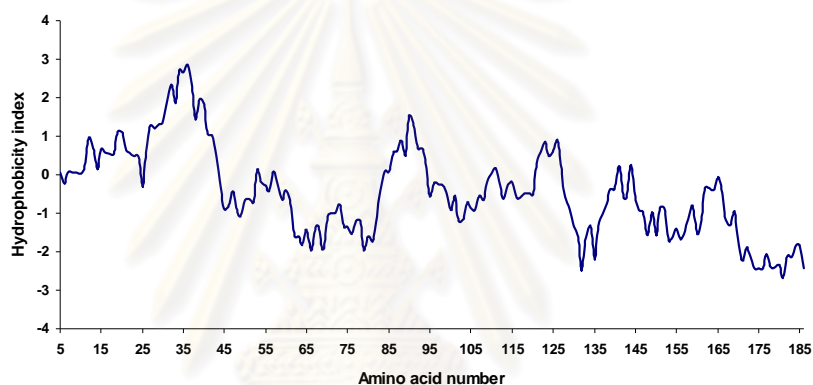


Figure 3.69 Diagrams showing outside, inside and transmembrane probability (A) and hydrophobicity analysis (B) of deduced Pm-PGMRC1 protein according to Kyte and Doolittle (1982).

```

Orangutan(CAH89877)  MAAEDVVATGADPSELESGLLLHEIFTSPLNLLLGLCIFLLYKIVRGD--QPAASGDS
Human(NP_006658)    MAAEDVVATGADPSDLESGLLLHEIFTSPLNLLLGLCIFLLYKIVRGD--QPAASGDS
Bovine(AAI18445)   MAAEDVAATGADTSELESGLLQEIFTSPLNLLLGLCIFLLYKIVRGD--QPAAS-DSD
Dog(XP_538151)     MAAEDVAATGADPSELEGGGLLHEIFTSPLNLLLGLCVFLLYKIVRGD--QPAAGGDS
Pig(NP_999076)     MAAEDVAATGADPSELEGGGLLHEIFTSPLNLLLGLCIFLLYKIVRGD--QPAAS-DSD
Mouse(O55022)      MAAEDVVATGADPSELEGGGLLHEIFTSPLNLLLGLCIFLLYKIVRGD--QPGASGND
Rat(NP_068534)     MAAEDVVATGADPSELEGGGLLQEIFTSPLNLLLGLCIFLLYKIVRGD--QPGASGND
Chicken(CAG31527)  MAAEPAMAGEEAVATEGGGLLEIVGSPNLSLLGLCLFLLYQILRGE--RPAAQ--PG
Xenopus t(AAH76926) MAEE-----GILQEIFTSPLNICLLCLCLYLLYKILRGD--KPQTENNE
Medaka(BAE47966)  MAE-----EAGEVTSAGIFQEIFTSPLNLTLLSLCLFLLYQIFRGD--RQPDFGEVE
Tetradon(CAF97306) MAEA-----EAGDTSGLLQEIFTSPLNLTLLSLCLFLLYKIVRGD--KQPDFAE
Zebra fish(AAH85558) MA-----EAVEQTSGLLQEIFTSPLNISLLCLCLFLLYKIIIRGD--KPADYGPVE
Trout(AAL49963)   MADT-----EGAEIYPGILQEIFTSPLNLSLLGLCIFLLYKIFRGD--KPADMGEVE
SeaUrchin(XM_778239) MALE-----ELMRELFLNPIINLGLLSVCGYLLYKIVRGN--RTPEPPQP
Tiger shrimp      MADEG--ADAVSIESFLGSLLEKIFTSPLNVFLLGVCTVLIYKIFRSSDGGSGATGPVE
**                :: *:. .*:* ** :* **:*:* *..
Orangutan(CAH89877)  DDEPPPLPRLKRRDFTPAELRRFDGVQDP-RILMAINGKVFDVTKGRKFGPEGPYGVFA
Human(NP_006658)    DDEPPPLPRLKRRDFTPAELRRFDGVQDP-RILMAINGKVFDVTKGRKFGPEGPYGVFA
Bovine(AAI18445)   DDEPPPLPRLKRRDFTPAELRRFDGVQDP-RILMAINGKVFDVTKGRKFGPEGPYGVFA
Dog(XP_538151)     DDEPPPLPRLKRRDFTPAELRRFDGVQDP-RILMAINGKVFDVTKGRKFGPEGPYGVFA
Pig(NP_999076)     DDEPPPLPRLKRRDFTPAELRRFDGVQDP-RILMAINGKVFDVTKGRKFGPEGPYGVFA
Mouse(O55022)      DDEPPPLPRLKRRDFTPAELRRFDGVQDP-RILMAINGKVFDVTKGRKFGPEGPYGVFA
Rat(NP_068534)     DDEPPPLPRLKRRDFTPAELRRYDGVQDP-RILMAINGKVFDVTKGRKFGPEGPYGVFA
Chicken(CAG31527)  EAGPPPLPKMRRDFTLEQLRPYDGVDRDP-RILMAVNGKVFDVTRASKFYGPDPGYGIFA

```



```

Xenopus t(AAH76926)      EQ----LPKMKRRDFTPAELKKEYDGVQNP-RILMAISGKVFVTRGKKFYGPEGPYGVFA
Medaka (BAE47966)       TP----LPKLKKRDFTLAELEKPYDGLQNP-RILMAVNGKVFVTRGKKFYGPEGPYGVFA
Tetradon(CAF97306)     KP----LPKMKKRDFTTAELEKPYDGLQNP-RILMAVNGKVFVTRGKKFYGPEGPYGVFA
Zebrafish(AAH85558)    EP----LPKLKKRDFTLADLQYDGLQNP-RILMAVNGKVFVTRGKKFYGPEGPYGVFA
Trout(AAL49963)        EP----LPKLKKRDFTLTELQPYDGLQNP-RILMAVNFVDFVTRGKKFYGPEGPYGVFA
SeaUrchin(XM_778239)   PR----LPKMKRKDFQVSELTEYDGLKNEGRILVAVNGKVFVSRGRKFFYGPEGPYGVFA
Tiger shrimp           PP----VPKMKRQDMTLEQLKQYDGMGEHGRVAVVNGKIFVDFVTRGSKFYGPGGYSVFA
                        :*::* :*: :* :*: :* :*: :* :*: :* :*: :* :*: :* :*: :*
Orangutan(CAH89877)    GRDASRGLATFCLDKKEALKDEYDDLSDLTAAQQETLSDWESQFTFKYHHV--GKLLKEGE
Human(NP_006658)       GRDASRGLATFCLDKKEALKDEYDDLSDLTAAQQETLSDWESQFTFKYHHV--GKLLKEGE
Bovine(AAI18445)      GRDASRGLATFCLDKKEALKDEYDDLSDLTAAQQETLSDWDSQFTFKYHHV--GKLLKDEGE
Dog(XP_538151)        GRDASRGLATFCLDKKEALKDEYDDLSDLTAAQQETLSDWDSQFTFKYHHV--GKLLKEGE
Pig(NP_999076)        GRDASRGLATFCLDKKEALKDEYDDLSDLTAAQQETLNDWDSQFTFKYHHV--GKLLKEGE
Mouse(O55022)         GRDASRGLATFCLDKKEALKDEYDDLSDLTAAQQETLSDWDSQFTFKYHHV--GKLLKEGE
Rat(NP_068534)        GRDASRGLATFCLDKKEALKDEYDDLSDLTAAQQETLNDWDSQFSSPSSITWGLLEGAE
Chicken(CAG31527)     GRDASRGLATFCLDKKEALRDDYDDLSDLNATQQETLRDWSQFTFKYHHV--GKLLKDEGE
Xenopus t(AAH76926)  GRDASRGLATFCLDKKEALKDITYDDLSDLTATQRETLSWWEAQFTFKYHHV--GKLLKDEGE
Medaka (BAE47966)     GRDASRGLATFCLDKESLKDDEYDDLSDLTAAQQETLSDWESQFTFKYDYV--GKLLKPEGE
Tetradon(CAF97306)   GRDASRGLATFCLDKKDALKDEHDDLSDLNASQWESLSDWEAQFTFKYDYI--GKLLKPEGE
Zebrafish(AAH85558)  GKDASRGLATFCLDKKEALKDTHDDLSDLNAMQWESLSEWETQFTQKYDYI--GKLLKPEGE
Trout(AAL49963)      GKDASRGLATFCLDKKEALKDTHDDLSDLNAMQWESLSEWETQFTQKYDYI--GKLLKAGE
SeaUrchin(XM_778239) GHIDASRALATFSLKEKTLKDEFDELSDLTSEQMDSVREWEMQFMKEYDYI--GKLLKPEGE
Tiger shrimp         GRDATRALATFVSKD--VKEEYDDLSDLSSMQMDSVREWEMQFTQKYDYI--GKFLKPEGE
                        :*::* :*: :* :*: :* :*: :* :*: :* :*: :* :*: :* :*: :*
Orangutan(CAH89877)    EPTVYSDEEPPKDESARKND-----
Human(NP_006658)      EPTVYSDEEPPKDESARKND-----
Bovine(AAI18445)     EPTVYSDEEPPKDESTRKND-----
Dog(XP_538151)       EPTVYSDEEAAKDENARKND-----
Pig(NP_999076)       EPTVYSDEEPPKDESARKND-----
Mouse(O55022)        EPTVYSDEEPPKDEETARKNE-----
Rat(NP_068534)       EPIVYSDEEQQMRLGLRVTEAVSGAYLFLYFAKSFVTFQSVFTTW
Chicken(CAG31527)    EPTVYSDEEKKDAQDAKKE-----
Xenopus t(AAH76926)  EPTEYTDDEDAKDTSDLKKN-----
Medaka (BAE47966)    EPTEYTDDEEGKDKAD-----
Tetradon(CAF97306)  EPAEYTDDEEGKDK-----
Zebrafish(AAH85558)  EPTEYTDDEEVKDKKKD-----
Trout(AAL49963)     EPTEYTDDEEVKDKKKD-----
SeaUrchin(XM_778239) EPTDYSDEEAAKDKDN-----
Tiger shrimp        QPTEYSDDEEAKDKAKTDD-----
                        :* :*: :* :*: :*

```

Figure 3.70 Multiple alignment of PM-PGMRC1 and other vertebrates and invertebrates PGMRC1 proteins. Identical residues across taxa are highlighted. Cysteine residues in each protein sequence are shaded.

```

                                                M 1
ATCGGCTTGAACCTCGCATTAGGCGGTGGTCTCGGGTTAGAAAGGAGCAAAGAGCATG 60
A G K R I A V V T G G N K G I G Y G I M 21
GCTGGAAAAGGATTGCTGTGGTGACTGGGGGCAATAAGGGAATTGGATATGGGATAATG 120
K E L C A K F D G I V Y L T A R D E G R 41
AAAGAGTTATGTGCCAAGTTTGACGGCATTGTGTATCTCACTGCCCGGGATGAAGGAAGG 180
G L A A V E E L K K L G F A P R F H Q L 61
GGCCTGGCAGCTGTTGAAGAACTCAAGAACTTGGCTTCGCTCCTCGTTTTTCATCAACTG 240
D I D N A D S I S K F T N Y I K N T Y G 81
GACATCGATAATGCTGACAGTATTTCAAATTTACAAACTATATAAAGAACACGTATGGA 300
G L D V L V N N A A I A Y K M A A T E P 101
GGACTTGATGTTCTAGTTAATAATGCAGCTATTGCCTACAAGATGGCAGCCACAGAACCT 360
F S E Q A E N T I R V N F F A T L A L C 121
TTTTTCGGAGCAAGCTGAAAATACCATTAGAGTGAACCTCTTTGCTACTTTGGCACTGTGT 420
R S L F P L L R P H A R V S T V S S S A 141
CGCAGTTTGTTCCTCACTCCTTAGACCACATGCTAGGGTGTCTACAGTATCAAGTTCTGCA 480
G H L S R I N G N E P Q A S A L R E K F 161
GGCCACCTTTTCACGCATCAATGGAAATGAACCACAGGCCTCTGCTCTCAGAGAGAAGTTT 540

```

```

A S P S L T E E E L S D L M N Q F V Q K 181
GCTTCACCATCTCTTACAGAAGAGGAACTTTCTGACCTCATGAACCAATTTGTACAAAAA 600
T K E G T W K E A G W P S S T Y V V S K 201
ACAAAAGAGGGAAACATGGAAGGAAGCTGGTTGGCCAAGCAGTACATATGTGGTGAGCAAA 660
V G V S A L T R I Q Q R A F D A D P R D 221
GTTGGCGTATCGGCTCTCACACGCATCCAGCAGAGAGCCTTTGATGCAGATCCTCGAGAT 720
D L V V N C S H P G Y V D T D M T S H K 241
GACCTTGTGGTGAACGTCTCACCCCTGGATATGTTGACACAGACATGACATCTCACAAG 780
G P L T I E Q G A V A P S Y L A L L P P 261
GGACCCTGACCATTGAGCAAGGAGCAGTAGCACCATCCTACTTGGCATTACTACCTCCA 840
N I K E P K G A Y L W Y E K Q V V D W V 281
AACATTAAGAACCAAAGGGAGCATATCTTTGGTATGAAAAGCAAGTTGTAGACTGGGTT 900
K G P M P * 286
AAGGGACCAATGCCTTGAAATTCAAAATGAACCTGCATATTACAAAAGGCATTATATGAGG 960
CACTGATTTATTAGTGAGATAATTTTTGTGTTATATTTTACAATGTTATCAAAGAATATT 1020
TAATTCTTATATTAATTATAATTTGTATCTCAATATACTGTTACTTTTGTAGAGGAAATATA 1080
TTAATGTATTCCACATATGGGTTAGAAATGGTGAATGTTTAATTCTCAACAAAATTACT 1140
GAGCCTTTTTTTCATTCTCTTTTTTGTGTTATTAATCTTTATTTGGATTTTGTAAAGTAAAA 1200
TATAATGTCTTTAAATAATAAAGTGGGATCCGCCAAAAAAAAAAAAAAAAAAAAAAAAAAAA 1260
AAAAAAAAA 1269

```

Figure 3.71 The full length cDNA and deduced protein sequences of *Pm-carbonyl reductase* (1269 bp, ORF of 831 bp corresponding to a deduced polypeptide of 275 aa) further characterized by 3' RACE-PCR. The putative start (ATG) and stop (TGA) codons are illustrated in boldface. The poly A additional signal site is underlined. The predicted adh_short (alcohol dehydrogenase short chain) domain (positions 5th – 166th) is highlighted.

A fragment of approximately 450 bp product was generated from 5' RACE-PCR of *protein disulfide-isomerase precursor* (Figure 3.72; A). Nucleotide sequences of EST and 5' RACE products of this gene were assembled. The full length cDNA of *P. monodon protein disulfide-isomerase precursor (PDI)* (*Prolyl 4-hydroxylase subunit beta*) (*Cellular thyroid hormone-binding protein*) (*p55*) (*Erp59*) (*Pm-PDI Erp59*) was 2220 bp in length composing of an ORF of 1506 bp corresponding to a polypeptide of 501 amino acids and the 5' and 3' UTRs of 71 and 643 bp, respectively (Figure 3.73). Its significantly matched sequence was *protein disulfide-isomerase precursor (PDI)* of *Tribolium castaneum* (E-value = 0.0). The predicted molecular mass and pI of the deduced Pm-PDI Erp59 was 55.17 kDa and 4.65, respectively. Pm-PDI Erp59 contained Calsequestrin, ERp29_N (endoplasmic reticulum protein 29_N) and Thioredoxin domains. Calsequestrin is the principal calcium-binding protein present in the sarcoplasmic reticulum of cardiac and skeletal muscle. It is a highly

acidic protein that is able to bind over 40 calcium ions and acts as an internal calcium store in muscle. ERp29 is a ubiquitously expressed endoplasmic reticulum protein, and is involved in the processes of protein maturation and protein secretion in this organelle. PDI Erp59 exists as a homodimeric protein. The *N*-terminal domain featured in this family is organized into a thioredoxin-like fold that resembles the a domain of human protein disulphide isomerase (PDI) (Baryshev *et al.*, 2006)

5' RACE-PCR of a *gonadotropin-regulated long chain acyl-CoA synthetase* generated a fragment of approximately 1200 bp in length (Figure 3.72; B). After assembly with nucleotide sequences of EST, a lack of amino acids sequences 330th – 519th of homologue transcript was predicted. Forward primer (5':-GAGTTGGGAAGATGTCGTGA-:3') was designed and used in combination of reverse primer for RT-PCR analysis to clarify the missing sequence. After RT-PCR, an approximately 1300 bp fragment was amplified (Figure 3.72; C). Nucleotide sequences derived from the former characterization and PCR product were assembled. The full length cDNA of *P. monodon gonadotropin-regulated long chain acyl-CoA synthetase (Pm-GRLC acyl-CoA synthetase)* was 3304 bp in length composing of an ORF of 1989 bp corresponding to a polypeptide of 662 amino acids and the 5' and 3' UTRs of 401 and 914 bp, respectively (Figure 3.74). *Pm-GRLC acyl-CoA synthetase* significantly matched *Acyl-CoA synthetase bubblegum family member 1* of *Gallus gallus* (E-value = 4×10^{-176}). The predicted molecular mass and pI of the deduced Pm-GRLC acyl-CoA synthetase was 72.85 kDa and 8.22, respectively. Pm-GRLC acyl-CoA synthetase contained AMP-binding domain functional involving in ATP-dependent adenylation.

A summary of full length cDNA examined by 3' primer walking and RACE-PCR is shown by Tables 3.33 and 3.34, respectively. Gene Ontology (GO) categories of these transcripts were also illustrated (Table 3.35). Putative *N*-link glycosylation sites, cAMP dependent protein kinase sites and the percentage of hydrophobic amino acid of each deduced protein is shown by Table 3.36.

Almost all proteins are regarded as glycoproteins whereas the putative *N*-linked glycosylation site was not found in the deduced anaphase promoting complex subunit 11, Cdc42, selenoprotein M precursor, actin depolymerizing factor, carbonyl reductase, PSR, p23-like protein, PGMRC1 and PDI Erp59 protein of *P. monodon*.

In addition, F-box and wd40 repeat domain binding protein, Cdk7, cytochrome B5, SARIP, selenoprotein M precursor, PSR, gonadotropin-regulated long chain acyl-CoA synthetase and PDI Erp59 contained a cAMP-dependent protein kinase phosphorylation site implied that these genes should play a functionally important role in the signal transduction pathway during oocyte/ovary development. Cyclic AMP (cAMP) is a key intracellular regulator of cell function in both prokaryotes and eukaryotes. One of the ways in which it regulates enzymes is by binding to and causing activation of cAMP-dependent protein kinases, which in turn activate or deactivate other enzymes by phosphorylating them (Kalderon and Rubin, 1989).

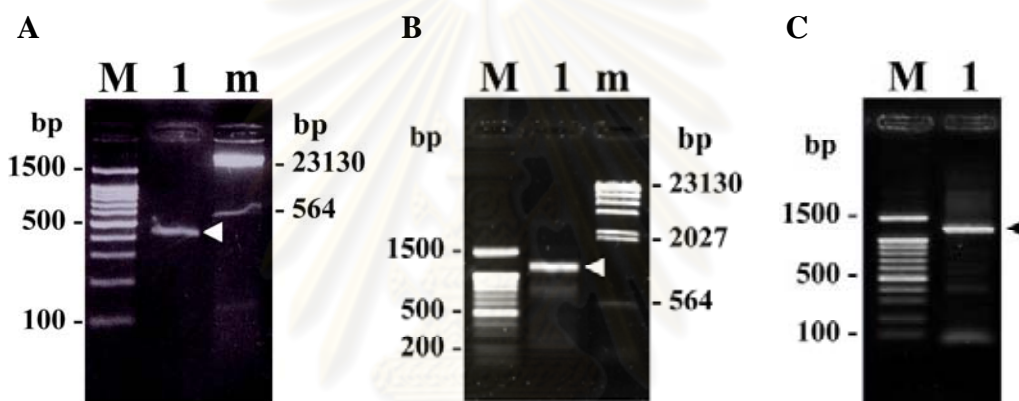


Figure 3.72 5' RACE-PCR products of *Pm-PDI Erp59* (A) and *Pm-gonadotropin-regulated long chain acyl-CoA synthetase* (B). C is the amplified transcript of *Pm-gonadotropin-regulated long chain acyl-CoA synthetase* using proof-reading DNA polymerase that were re-sequenced to clarify the missing amino acids sequences 330th – 519th of this gene initially obtained from RACE-PCR. Arrowheads indicate bands selected for further analysis. A 100 bp DNA ladder (lane M) and λ -*Hind* III (lane m) were used as the markers.

```

CTAATACGACTCACTATAGGGCAAGCAGTGGTATCAACGCAGAGTACGCGAGGGGTGACGA 60
      M R V G A T V A A V L V A S L V A 17
GAACTAGAACGATGAGGGTGGGAGCAACCGTCGCCGCGTCCTTGTGGCTTCCTTGGTGC 120
      S V G A D Q I A K E E G V L V L K T E N 37
CCTCTGTAGGGGCTGACCAGATCGCCAAAGAAGAGGGGGTGTGGTGTGAAGACGGAGA 180
      F K K A I E D N E F I L V E F Y A P W C 57
ATTTCAAGAAGGCGATAGAAGATAACGAATTTATCCTGGTTCGAGTTCTATGCACCATGGT 240
      G H C K A L A P E Y A K A A O K L E E M 77
GTGGCACTGAAGGCTCTTGCCCAAGGAGTATGCCAAGGCAGCTCAAAAGCTTGAAGAAA 300
      G S A I A L G K V D A T E E T E L A E E 97
TGGGATCTGCTATTGCACTGGGCAAAGTTGATGCCACAGAGGAAACCGAACTTGCTGAAG 360
      H G V R G Y P T L K F F R S G K S V D Y 117

```

```

AGCATGGTGTCCGAGGTTACCCACCCCTCAAGTTCTTCCGTTCTGGCAAATCTGTGCGACT 420
G G G R Q A D D I V N W L L K K T G P P 137
ATGGTGGTGGTTCGTCAGGCTGACGATATGTCAACTGGCTCTTGAAGAAAAGTGGTCCAC 480
A K P L A T V D D A K A F I A E K P V V 157
CTGCAAAGCCTTTGGCTACTGTAGATGCTAAGGCCTTATTGCTGAAAAGCCTGTGTG 540
I I G F F K D Q Q S D A A K Q F L A A A 177
TCATTATTGGTTTCTTCAAGGACCAGCAGTCTGATGCTGCCAAGCAGTTCTTGGCTGCTG 600
S A T D D H P F G I T S E E A L F T E Y 197
CTTCAGCCACTGATGACCATCCATTTGGAATTACCTCAGAGGAAGCTTTGTTCACTGAGT 660
G L S A D G G I I L F K D F D E G K N V Y 217
ATGGATTGAGTGTGCTGATGGTATCATTCTTCAAGGACTTCGATGAAGGCAAGAAATGTGT 720
E G E V T E D G V S K F V A A N S L P L 237
ATGAGGGTGGAGTGGTACTGAGGATGGTGTATCCAAGTTTGTGTGCAAACCTCTACCTC 780
V V D F N H E T A S K I F G G D I K S H 257
TTGTTGTGACTTCAACCATGAGACTGCATCAAAGATCTTGGTGGTGACATCAAGTCCC 840
L L I F L S K E A G H Y D T H L S A A T 277
ATCTCCTTATTTTCTGTCAAAGGAAGCTGGACATTATGATACTCACCTGAGTGTGCCA 900
A A A K G F K G E V L F V T I N T D E E 297
CTGCTGCTGCTAAGGGCTTCAAGGGAGAAGTTCTCTTTGTGACCATTAAACACAGATGAGG 960
D H S R I L E F F G M K K D E I P G L R 317
AGGATCACTCTCGCATCCTTGAATTCCTTCGCATGAAGAAGGATGAAATCCCAGGCCTCC 1020
I I K L E E D M A K Y K P D T Y D L S E 337
GTATTATCAAGTGGAGGAAGATATGGCCAAGTACAAGCCCATACTTATGACCTCAGCG 1080
S G L T G F V K S F L D G K L K Q H L L 357
AGAGTGGGCTTACCGGCTTCGTCAAGAGTTTCTTGGTGAAGGCTGAAGCAGCACCTTC 1140
S Q D L P E D W D K E P V K V L V S S N 377
TGTCTCAGGATCTGCCAGAAGACTGGGATAAAGAGCCAGTCAAGGTTCTGGTGTCTCTCAA 1200
F D E V A L N K E K D V L V E F Y A P W 397
ACTTCGATGAAGTTGCCTTGAACAAGGAGAAGGATGTCTTGTAGAGTTCTATGCACCAT 1260
C G H C K Q L A P I Y D O L G E K Y K D 417
GGTGTGGACACTGCAAACAGCTGGCACCTATCTATGATCAGCTAGGTGAAAAATACAAGG 1320
H D T I V V A K M D A T V N E L E H T K 437
ACCACGATACTATTGTTGTGGCGAAAATGGATGCTACAGTCAATGAGCTTGAGCATAACGA 1380
I Q S F P T L K L Y K K E T N E V V E Y 457
AGATTCAGTCCTTCCCAACCTTAAAACCTTACAAGAAGGAACTAATGAGGTTGTTGAAT 1440
N G E R T L A G M S K F L E T D G V Y G 477
ACAATGGAGAACGCACATGGCTGGAATGTCCAATTTTGGAAACTGATGGGGTTTATG 1500
Q A P P E D E D E E T D E D G D V P A 497
GCCAAGCGCCACCTGAGGATGAGGACGATGAGGAGACTGATGAGGATGGTGTGATGTGCCAG 1560
K D E L * 501
CAAAGGATGAACTTTAAAGAGGTTGAAAGTTGTTTTATGCGAGATAAATTGCTTTTGGTC 1620
CTAGCAGTATGACTACAAGAAAAGGTTTAAATTTTCTTGGATCCCATGAAAAATCGGTGCG 1680
AATAAGGGAAAGTAGTCGGTTTGAATGCTGGGATCAGTGTCTATAAAAAAATTTAGGTA 1740
CTTGATATCAAGTATTGACATCAAGTATTAACATCAGTGTACTTCTGTAGTGTTCAGTCA 1800
ATTTGGTTTCGAAGTGATTTGAAAAAGTTTATTTTTTACTACAGACATTCCTAATCATT 1860
AAGATATATTTTTGTACTTGGGGCATTCTAATATTTGTGACTGGAATAGGGAATGGTAC 1920
AAATCTGTTGATTAACAAGAAATGCTTTAAATTAGTATGTGTAACAACCTCATCCAAGGC 1980
TATGCAGTGTGTGGATGACAATGATGCTCGTCAAGTTATATTATTGTTAATTTTGGAC 2040
CCAGGCCTTGATGATAGCTTCAATGTCTCCACCAACTATCTCCCTGTACTTGGCACAAT 2100
GCTTCCCGTGGCCGTGTGTGTGTGAGTGTAAATGATGACAAAGGTCCTTGTGCAGTGTGA 2160
TGAATATACCAGTGACTTTTCCAATAAAAAGGAAAAAAGGGAAAAAAAAAAAAAAAAAAAAA 2220

```

Figure 3.73 The full length cDNA and deduced protein sequences of *Pm-PDI Erp59* (2220 bp, ORF of 1506 bp corresponding to a deduced polypeptide of 501 aa) further characterized by 5' RACE-PCR and 3' primer walking of the original EST clone. The putative start (ATG) and stop (TAA) codons are illustrated in boldface and underlined. The putative poly A additional signal site is underlined. The predicted Calsequestrin domain (positions 6th – 366th) is gray-shaded. The predicted ERp29_N (endoplasmic reticulum protein 29_N) domain (positions 224th – 261st) is gray-shaded and underlined. The predicted Thioredoxin domains (positions 29th – 133rd and 369th – 473rd) are dashed and underlined.

CGGGGGAGTGGATAGACGGCGCTCACCTGTGCTGCTCACCTGTGCCGCTCGCTGCCGCC 60
 TCCTGCCGCTGCCGCTCGAGTAGCCGAGTCTGCCCTGCCGCCACGGAAGGGACGCTT 20
 CCCTGCACGCGACCCGAAGGACGCCGCGCCGAGAGACAGATTTGTGCGCAGACGAATTGC 180
 GAGAGCGAGAAAAGAGCCTCTGAGAACTCGCGTCAGTGAATAAGCAGGAAGCAGAGCAGG 240
 ATAGCATAGAGTCCGTACAGTCATCGTCTTCGTCGTCGTCGTCGTCGTCGTCGTCGTCG 300
 CGTCGTCGGCCAGGCCAGAGACCCCCGAGACGACCTCCGCCCACTCGGCCAGCCCAGAGC 360
 CGGAGGAGCCCCCCTCGCCGCCAGCCACTCGGGCGGAG**ATG**TTCAAATCACCCCTGC 420
K A E Y L N G P D Q V I P T D R L K T W 27
 AGAAGGCGGAGTACCTCAATGGACCCGACCAGGTCATCCCAGCCAGCCGCTCAAGACGT 480
E P N G T T K L K I G D Q G V S A H T P 47
 GGGAGCCGAACGGCACAACCAAGCTGAAGATCGGGCAGCCAGGGTGTCTCCGCCACACGC 540
V S V P T L L K K A A E K F P T T N A L 67
 CCGTGTCTGTACCAACGCTGCTGAAAAAGGCTCGGGAGAAGTTTCCACCACCAACGCC 600
A V K R D G A W K F T T Y A E Y Y Q Q V 87
 TCGAGTGAAGCGAGATGGGGCTGGAATTCACCACTTACGCCGAGTACTACCAGCAAG 660
R T V A K A F I K L G L Q Q Y H G V C I 107
 TCCGCACAGTGGCTAAAGCCTTCATCAAGCTCGGCCTCCAGCAGTACCACGGGGTGTGCA 720
L G F N S P E W F I S D L A A V F A G G 127
 TCCTGGGCTTCAACTCCCCGAGTGGTTTCATCTCCGACCTGGCCGCCGTCTTCGCTGGGG 780
F A A G I Y T T N S P E A C E H C A K N 147
 GCTTCGCTGCCGAATCTACACCACCAATTCTCCTGAAGCTTGTGAACACTGTGCCAAAA 840
C E A Q I W V V E D Q K Q L D K V L K I 167
 ATGTGAAGCTCAGATATGGGTGGTGAAGATCAGAAGCAGTTGGACAAGGTCCTCAAGA 900
R G R L P S T R A I I Q Y S G K P T V E 187
 TCCGCGCCGCTCCCATCGACGCGGGCGATTCATTAGTACAGTGGGAAGCCCACTGTGG 960
G V L S W E D V V T L G K Q Q S D S E L 207
 AGGGCGTGTGAGTTGGGAAGATGTCGTGACGCTGGGGAAGCAGCAGTCAGACAGCGAGC 1020
E A R L R R I A V N Q C C T L I Y T S G 227
 TGGAGGCCAGGTTGCCGCGCATCGCGGTCAACCAGTGCTGCACCCTCATCTACACCTCCG 1080
T T G P P K G V M L S H D N I T W T A H 247
 GCACGACTGGCCCCCAAAGGGCGTCATGCTCAGCCACGACAACATCACCTGGACGGCCC 1140
A N C I N A D F H S G R E V I V S Y L P 267
 ACGCCAATGCATCAACGCCGACTTCCACTCTGGAAGGGAGGTCATCGTCAGCTACCTGC 1200
L S H V A A Q M A D L Y I T M Y A G A T 287
 CCCTCTCTCACGTCGCCGCACAAATGGCCGACTTGTACATCACGATGTATGCGGGAGCGA 1260
C Y F A Q P D A L K G S L G Q T L K E V 307
 CGTGCTACTTTCGCACAGCCCGACGCCCTGAAAGGAAGTCTTGGGCAAACCCCTCAAGGAAG 1320
R P T R F L G V P R V W E K I Y E K M M 327
 TCCGTCCAACACGATTCTTGGGCGTCCCTCGCGTCTGGGAGAAGATTTATGAGAAGATGA 1380
E V G R K T T G V K K S I A T W A K S V 347
 TGGAAGTCGGTCGCAAGACAACAGGAGTCAAGAAATCGATCGCCACTTGGGCCAAGTCTG 1440
G L E T S M R K Q Q Q D F S K S W G Y S 367
 TCGGGCTGGAGACCAGTATGCGCAAGCAGCAGCAGGACTTCTCTAAGTCTTGGGGTACT 1500
I A N A V V F K K I K G V L G L D R C E 387
 CCATCGCCAATGCAGTTGTTTTCAAGAAAATCAAAGGAGTCCCTTGGGCTGGACAGGTGTG 1560
L H L S G A A P I S P D I V R Y F H S L 407
 AATTGCACTTGTGAGGGCTGCTCCCATCTCCCCAGATATTGTGCGCTACTTCCACAGTC 1620
D I P L T E I Y G M S E S S G P H T I G 427
 TGGACATCCCTCTGACGGAGATTTATGGCATGTCTGAATCCTCCGGCCCCACACCATCG 1680
L E K A F K M G S C G R T V P G C Y T K 447
 GGCTGGAGAAGGCCTTCAAATGGGCAGCTGCGGGCGCACGGTGCCTGGCTGTTACACGA 1740
L D N P D A E G N G E V C M G G R H V S 467
 AGCTCGACAACCCGGACGCGGAGGGGAACGGAGAGGTGTGCATGGGCGGGCAGATGTGT 1800
M G Y L R M E E K T H E A I D D E G W L 487
 CCATGGGGTACTTGGCATGGAAGAGAAGACCCACGAAGCGATCGACGACGAGGGCTGGC 1860
H S G D I G K L D S D G F L Y I T G R I 507
 TGCCTCCGGGGACATCGGGAAGCTGGACAGCGATGGCTTTTGTATATCACGGGACGCA 1920
K E L I I T A G G E N I A P V I I E D N 527

```

TCAAAGAACTCATCATTACAGCTGGAGGAGAAAAATATTGCTCCAGTTATCATTGAAGACA 1980
L K A E L P S L S N S M L I G D K R K F 547
ACTTGAAGGCGGAATTACCTTCGCTAAGCAACAGCATGCTTATTGGTGACAAGCGGAAGT 2040
L S V L L T L K T N M N L D S G E P Q D 567
TCCTGTCTGTGCTTCTGACACTAAAGACCAATATGAACCTGGACTCCGGAGAGCCCCAGG 2100
T L S P A C I D W C R S V G S S A N T I 587
ACACACTCAGTCCGGCTTGCATCGATTGGTGTGCGAGCGTAGGGTCGTCCGCCAACACCA 2160
Q D I L A G P D A N V M R A I Q E A I D 607
TACAGGACATCCTCGCAGGACCCGATGCCAATGTAATGCGTGCAATCCAAGAGGCCATTG 2220
R A N K L A P S N A Q R I Q K W T V L P 627
ATCGGGCTAATAAACTGGCTCCTTCCAATGCTCAGAGAATTCAGAAGTGGACTGTGCTGC 2280
K D F S L P G G E L G P T M K L K R P V 647
CCAAAGACTTTTTCCTTGCCTGGCGGGGAGCTCGGGCCACCATGAAGCTAAAGCGACCAG 2340
V L Q K Y S E T I E R F Y E G * 662
TAGTTTTACAAAAATACAGCGAGACGATAGAAAAGATTCTACGAGGGTTAACATTCTTGTA 2400
GTCATCGAGCCCCCTTCTACCTTCTATAAACATGTTTTCTGTTACCGAAAAGAGTATATTT 2460
TTGAATGGAGCAGAAGCATGAACTTATTCACCTTTGAGGAAACCATCCACGTGTTTTCTTCG 2520
TGTGCACATCAAAACGAAGCATGTAGCTATAAGTATCCCATGGTGCATTTAATTTGAAGA 2580
GTAGATATTAATAAATACTTTTCATGTAAGTATGTTGCCATATGTGTATATTTATATA 2640
TTGCCATACAACCTACGGATGTCACCGATTCTTCAGGGGGAAACCTTACGTGTATTTACT 2700
TAAGCTCCTTATTCTCTGACGTTTAGCAGGACTGTGCATTTTCTCATTCAAACAGAATGC 2760
ATTAATTCACAGTAACATGTACAATGTCCCAGACACGTATGTTCCGCCAGATTAACCTGT 2820
AAATATTTTTTCTGCATACTGGAAACTGGGACCAAAGTGTTCCTCTGCAAGAACCTGGATG 2880
TTATTTAGAATTATGAACTAGAATAGAATTTTGAATGATTCTTAGCTAGTTCAGTTCGAGT 2940
AAACCTTCTGGGCTAGGTTTACGTTTACGGAAAGTGGCATTTGTGCAATTCACAGAGTTCT 3000
TATGATGAAAGGTTTGTACCCGCACAAGTTCGTTTAAATTTGAATTAACAAAAGTAGTATT 3060
GTAAACGTATATCAACTTAATATTCAGGGACATGAAAGCTGAGTACTTATTTTAGGTTAA 3120
GATTTTCGTTATCAATGCAATTTATGTACCTGCATCAGCACATTTGGTCCAGGATTTGGCAA 2180
TATTATTTTGGAGATGAAGCTACAGAGATTAGCCAATGTAATATGAATATGTTTGTATATT 3240
GAGTTTCGCTGTACTTGTTTTTGTGTATTATATGAGTAAATTAATAAATGTTTATACTAA 3300
AAAA 3304

```

Figure 3.74 The full length cDNA and deduced protein sequences of *Pm-gonadotropin-regulated long chain acyl-CoA synthetase* (3304 bp, ORF of 1989 bp corresponding to a deduced polypeptide of 662 aa) identified by 5' RACE-PCR and 3' direction sequencing. The putative start (ATG) and stop (TAA) codons are illustrated in boldface and underlined. The putative poly A additional signal site is underlined. The predicted AMP-binding domain (positions 79th – 540th) is highlighted.

จุฬาลงกรณ์มหาวิทยาลัย

Table 3.33 A summary of full length cDNA of genes expressed in ovaries of *P. monodon* characterized by 3' primer walking of original ESTs

Clone No.	Transcripts	Closest species	E-value	Full length
OV-N-S01-0197-W	<i>Cdc20</i>	<i>Branchiostoma floridae</i>	5×10^{-149}	2612 bp (ORF 541 amino acids, 1626 bp)
OV-N-S01-1107-W	<i>small androgen receptor-interacting protein: RWD domain containing 1</i>	<i>Rattus norvegicus</i>	2×10^{-40}	1364 bp (ORF 245 amino acids, 738 bp)
OV-N-S01-1131-W	<i>putative Rho family small GTP binding protein cdc42</i>	<i>Acyrtosiphon pisum</i>	9×10^{-101}	2195 bp (ORF 191 amino acids, 576 bp)
OV-N-S01-1852-W	<i>cytochrome B5</i>	<i>Strongylocentrotus purpuratus</i>	4×10^{-36}	1539 bp (ORF 143 amino acids, 432 bp)
OV-N-S01-1895-W	<i>Protein mago nashi</i>	<i>Apis mellifera</i>	5×10^{-76}	858 bp (ORF 147 amino acids, 444 bp)
OV-N-S01-2306-W, OV-N-S01-2307-W, OV-N-N01-0465-W, OV-N-N01-0526-W	<i>actin depolymerizing factor</i>	<i>Tribolium castaneum</i>	2×10^{-52}	1449 bp (ORF 148 amino acids, 447 bp)
OV-N-N01-0279-W, OV-N-N01-0479-W, OV-N-N01-1485-W	<i>f-box and wd-40 domain protein</i>	<i>Culex pipiens quinquefasciatus</i>	2×10^{-144}	1841 bp (ORF 501 amino acids, 1506 bp)
OV-N-N01-0378-W	<i>Cyclin-dependent kinase 7</i>	<i>Apis mellifera</i>	4×10^{-42}	817 bp (ORF 149 amino acids, 450 bp)
OV-N-N01-0438-W, OV-N-ST02-0024-W	<i>selenoprotein M precursor</i>	<i>Litopenaeus vannamei</i>	2×10^{-58}	904 bp (ORF 131 amino acids, 396 bp)
OV-N-ST02-0084-W	<i>anaphase promoting complex subunit 11 homolog</i>	<i>Tribolium castaneum</i>	1×10^{-41}	600 bp (ORF 84 amino acids, 255 bp)

Table 3.34 A summary of full length cDNA of genes expressed in ovaries of *P. monodon* characterized by RACE-PCR

Clone No.	Transcripts	Closest species	E-value	Full length
OV-N-S01-0046-W, OV-N-S01-2580-W	<i>phosphatidylserine receptor</i>	<i>Apis mellifera</i>	4×10^{-142}	1862 bp (ORF 389 amino acids, 1170 bp)
OV-N-S01-0802-W, OV-N-S01-2304-W	<i>progesterone receptor related protein p23</i>	<i>Nasonia vitripennis</i>	7×10^{-46}	1943 bp (ORF 164 amino acids, 495 bp)
OV-N-S01-1377-W	<i>Bystin</i>	<i>Nasonia vitripennis</i>	1×10^{-124}	1553 bp (ORF 454 amino acids, 1365 bp)
OV-N-S01-2602-W, OV-N-ST01-0032-W	<i>checkpoint kinase 1</i>	<i>Drosophila melanogaster</i>	3×10^{-131}	2078 bp (ORF 484 amino acids, 1455 bp)
OV-N-N01-0057-W, OV-N-N01-0381-W, OV-N-N01-1276-W, OV-N-N01-1549-W, OV-N-N01-1670-W	<i>Progesterin membrane receptor component 1</i>	<i>Oryzias latipes</i>	3×10^{-47}	2040 bp (ORF 190 amino acids, 573 bp)
OV-N-ST02-0071-W	<i>carbonyl reductase</i>	<i>Tribolium castaneum</i>	2×10^{-86}	1269 bp (ORF 275 amino acids, 831 bp)
OV-N-S01-0017, 0171, 0210, 0280, 0569, 0820, 1180, 1232, 1324, 2329, 2454, 2641-W, OV-N-N01- 0010, 0114, 0417, 0426, 0492, 0543, 0917, 0993, 1683-W, OV-N-ST01-0105-W	<i>Protein disulfide-isomerase precursor (PDI) (Prolyl 4-hydroxylase subunit beta) (Cellular thyroid hormone-binding protein) (p55) (Erp59)</i>	<i>Tribolium castaneum</i>	0.0	2220 bp (ORF 501 amino acids, 1506 bp)
GL-H-S01-0591-LF	<i>gonadotropin-regulated long chain acyl-CoA synthetase</i>	<i>Gallus gallus</i>	4×10^{-176}	3304 bp (ORF 662 amino acids, 1989 bp)

Table 3.35 GO ontology function, probability site in the cells and signal peptide prediction of the full length cDNA characterized in this study

No.	Transcripts	Function	Probability site			Signal peptide
			Inside of the cells	transmembrane	outside of the cells	
1	<i>F-box and wd40 repeat domain binding protein</i>	ubiquitin cycle (biological_process GO:0006512)	-	-	1 - 538	-
2	<i>Cdk7</i>	protein kinase activity (molecular_function GO:0004672)	-	-	1 - 353	-
3	<i>Cdc20</i>	regulation of exit from mitosis (biological_process GO:0007096)	-	-	1 - 541	-
4	<i>Protein mago nashi</i>	Reproduction (biological_process GO:0000003)	-	-	1 - 147	-
5	<i>Anaphase promoting complex subunit 11</i>	metabolic process (biological_process GO:0008152)	1 - 84	-	-	-
6	<i>Cdc42</i>	multicellular organismal process (biological_process GO:0032501)	-	-	1 - 191	-
7	<i>cytochrome B5</i>	electron transport (biological_process GO:0006118)	1 - 119	120 - 139	140 - 143	-
8	<i>SARIP</i>	Unknown	-	-	1 - 245	-
9	<i>selenoprotein M precursor</i>	endoplasmic reticulum (cellular_component GO:0005783)	-	-	1 - 131	1 - 21
10	<i>actin depolymerizing factor</i>	female gonad development (biological_process GO:0008585)	-	-	1 - 148	-
11	<i>carbonyl reductase</i>	carbonyl reductase (NADPH) activity (molecular_function GO:0004090)	-	-	1 - 286	-
12	<i>Chk1</i>	cell cycle checkpoint (biological_process GO:0000075)	-	-	1 - 484	-
13	<i>PSR</i>	cell differentiation (biological_process GO:0030154)	-	-	1 - 389	-
14	<i>p23-like protein</i>	p23 binds heat shock protein (Hsp)90 and participates in the folding of a number of Hsp90 clients, including the progesterone receptor. p23 also has a passive chaperoning activity and in addition may participate in prostaglandin E synthesis (Tanioka <i>et al.</i> , 2000)	-	-	1 - 164	-
15	<i>gonadotropin-regulated long chain acyl-CoA synthetase</i>	Long-chain-fatty-acid-CoA ligase activity (molecular_function GO:0004467)	-	-	1 - 662	-
16	<i>Bystin isoform 1</i>	cell adhesion (biological_process GO:0007155) and pregnancy (GO:0007565)	-	-	1 - 454	-
17	<i>PGMRC1</i>	progesterone binding protein	1 - 22	23 - 41	42 - 190	-
18	<i>PDI Erp59</i>	protein folding (biological_process GO:0006457)	-	-	1 - 501	-

Table 3.36 N-link glycosylation site, cAMP dependent protein kinase site and the percentage of hydrophobic amino acid of the full length cDNA characterized in this study

No.	Transcripts	N-Link glycosylation site (N-X-S/T)	cAMP dependent protein kinase site (K/R-K/R-X-S/T)	Hydrophobicity (%)					total
				V	L	I	M	P	
1	<i>F-box and wd40 repeat domain binding protein</i>	NIS; aa 8 th -10 th , NCS; aa 516 th -518 th	KKES; aa positions 56 th -59 th	6.9	9.1	6.5	2.4	3.0	27.9
2	<i>Cdk7</i>	NRT; aa 64 th -66 th , NVS; aa 94 th -96 th	KRCS; aa positions 291 st -294 th	4.8	13.0	6.8	2.3	5.9	32.8
3	<i>Cdc20</i>	NKS; aa 50 th -52 nd , NRS; aa 121 st -123 rd NSS; aa 291 st -293 rd , NTT; aa 386 th -388 th NCT; aa 428 th -430 th	-	5.9	8.3	3.9	2.6	5.0	25.7
4	<i>Protein mago nashi</i>	NNS; aa 37 th -39 th , NNS; aa 112 th -114 th	-	6.8	8.2	8.2	2.7	3.4	29.3
5	<i>anaphase promoting complex subunit 11</i>	-	-	2.4	7.1	4.8	4.8	4.8	23.9
6	<i>Cdc42</i>	-	-	10.5	9.4	4.2	1.0	6.3	31.4
7	<i>cytochrome B5</i>	NTT; aa 12 th -14 th , NNS; aa 110 th -112 th NQS; aa 113 th -115 th	KKHT; aa positions 95 th -98 th	5.6	7.0	4.2	3.5	2.8	23.1
8	<i>SARIP</i>	NES; aa 198 th -200 th	KKPT; aa positions 183 rd -186 th	5.3	9.0	5.3	2.9	4.1	26.6
9	<i>selenoprotein M precursor</i>	-	KKNS; aa positions 108 th -111 th	5.3	16.0	3.1	1.5	6.1	32.0
10	<i>actin depolymerizing factor</i>	-	-	2.7	7.4	6.1	2.7	2.0	20.9
11	<i>carbonyl reductase</i>	-	-	7.3	8.7	4.5	2.1	5.6	28.2
12	<i>Chk1</i>	NCS; aa 226 th -228 th	-	7.0	11.6	3.1	3.7	5.2	30.6
13	<i>PSR</i>	-	RRKT; aa positions 379 th -382 nd	6.4	5.4	4.9	2.1	6.4	25.2
14	<i>p23-like protein</i>	-	-	3.7	9.1	4.3	2.4	4.9	24.2
15	<i>gonadotropin-regulated long chain acyl-CoA synthetase</i>	NGT; aa 30 th -33 rd , NIT; aa 241 st -243 rd	RKTT; aa positions 331 st -334 th	6.2	8.8	6.3	2.4	5.0	28.7
16	<i>bystin isoform 1</i>	NAS; aa 183 rd -185 th , NLS; aa 191 st -193 rd	-	7.5	8.1	5.3	4.4	5.5	30.8
17	<i>PGMRC1</i>	-	-	6.8	6.8	3.2	3.7	4.7	25.2
18	<i>PDI Erp59</i>	-	KKET; aa positions 448 th -451 st	7.6	9.0	4.4	1.2	3.8	26.0

3.4 Expression profiles of *Pm-PGMRC1* and *Pm-Cdc42* in different ovarian stages and various tissues of *P. monodon* examined by northern blot analysis

A single band reflecting only one isoform of *Pm-PGMRC1* (approximately 2000 bp comparable to that inferred from RACE-PCR) was observed from northern blot analysis. *Pm-PGMRC1* in ovaries of both juvenile and broodstock was more abundantly expressed than other tissues (e.g. gill and hepatopancreas of female broodstock and testes of male broodstock). This indicated that *Pm-PGMRC1* should play the important role on reproduction of female shrimp. In contrast, multiple isoforms of *Pm-Cdc42* was observed and tissue-specific isoforms of *Pm-Cdc42* were not found (Figure 3.75).



Figure 3.75 Northern blot analysis of *Pm-PGRMCI* (upper) and *Pm-Cdc42* (middle) transcripts using total RNA isolated from ovaries of juvenile (lane 1), normal and eyestalk-ablated broodstock (Pre-Vg, lanes 2 and 6; Vg, lanes 3 and 7; ECR, lanes 4 and 8 and LCR; lanes 5 and 9, respectively) and various tissues of broodstock-sized *P. monodon*; testes (T), hemocytes (HC), gills (G), heart (HE), lymphoid organs (L), intestine (IN), hepatopancreas (HP), stomach (ST), thoracic ganglion (TG), eyestalks (ES) and pleopods (PL). Lanes M = RNA marker *18S rRNA* (5 µg of total RNA) in various tissues was used as the control (lower).

3.5 Genomic DNA organization of functionally important gene homologues of *P. monodon*

3.5.1 Genomic DNA preparation

Genomic DNA was extracted from pleopods of *P. monodon* using a proteinase K/phenol/chloroform extraction method. The quality of extracted genomic DNA was

examined by agarose gel electrophoresis (Figure 3.76). Generally, high molecular weight DNA was observed along with partially degraded DNA. The quantity of genomic DNA was spectrophotometrically estimated. The ratio between OD₂₆₀ to OD₂₈₀ ratio was approximately 1.8 indicating the acceptable quality of the extracted DNA.



Figure 3.76 A 1.0% ethidium bromide-stained agarose gel showing genomic DNA extracted from pleopods of *P. monodon* (lanes 1 - 4) and 100 ng of λ DNA (lane M).

3.5.2 Characterization of genomic sequence of *Pm-Cdc42*

Genomic organization of *Pm-Cdc42* was characterized by overlapping amplification of genomic DNA sequences. The *Pm-Cdc42* gene was composed of 4 exons and 3 introns spanning 5214 bp in length. The length of each intron was 695 bp (intron 1), 1897 bp (intron 2) and 306 bp (intron 3), respectively (Figure 3.77). The GC content of exons (43-51%) was much greater than that of introns (27-35%). The boundaries of all intron followed the GT/AG rule. Introns 1 and 3 of the *Pm-Cdc42* gene interrupt the ORFs between two codons (type 0 intron), whereas intron 2 interrupt the ORFs within the same codons (type 1 intron) (Table 3.37).

A

	M	Q	T	3
CAGCAGCGTCTCGGATGAACTACGCCAGCTGGCTGCTGGGGAGCGTGAGAAATGCAGAC				60
I K C V V V G D G A V G K T C L L I S Y				23
CATTAAATGCGTAGTGGTGGGCGATGGAGCGGTGGGTAAGACCTGCCTCCTCATCTCCTA				120
T T N K F P S E Y V P T				35
CACAACAAACAAGTTCCTTCAGAATATGTTCCACAGtaagtgtaatggtcgttgttg				180
ttgatcctgtataatctatattatattttcttatatctataaataagtgtatttctata				240
atatttatgtttatatttagttatggttgtaattaattatagtaattaattattgtggg				300
tagtctaataatcaacaacaggaggaggggggctattagaatagaagatatatagt				360
cagcactactgatatatgatatgaattctgataattattataatggaggggaatttaaatt				420

gttctaattccaaaaatatccaaaaaaaattttctttatgttttttaatttttcttatt 480
aagctaattcatggccaaaatcaaaggggaatttggaaaaaatggggatttttttaatatta 540
atltatttttcttggcaaaaaaaaaaatgggattgttttaagttttggtttctcattaaat 600
ttggtaatatataaattttaaggtggattagggaaactccggtgaaccttggcggactaaaa 660
gggtttcttctgaataaaaacgttggtttggtttaaaaggggaaccccaatttggcggaaa 720
tggcggttcccttctggttttgggtgtaggaaaggaaagttgctggaaatgcaatgtgtg 780
tgtatttatgtgggagggagaatgcagtttgaggaacattgtgtgttatattgactcttc 840
V F D N Y A V T V M I G G E P Y 51
ctccttccacagGTATTTGACAACATGCTGTGACTGTTATGATAGGAGGGGAGCCATAC 900
T L G L F D T A G 60
ACATTAGGCCTTTTTGATACAGCTGgtaagtaacacgggttgttgttgttttgttgtagt 960
aataacagcaacaatatttttctattatgtttatltatltatltatltatltatataaagact 1020
cgtctaaagttactcaatgacatattgactcctcctcagtttggatgtataggagggc 1080
cgtggcccccttctcattagtgaatagacagacctgttattgtactctacatgatcacttg 1140
atltctaaccctaaaggttataacctctcataataacaattagttgcaccataaggaaata 1200
ctttgataccttttaattcttctgcaaatacatttgtgatacaattacttctctatgcaat 1260
tataaatgagccagtggaagaatataaaagataaaacaggatatagactgaagacaatta 1320
tgaattagataaataggtagaattgagaaaaaatagcaattgatgaaaaggtaaatttgag 1380
aagaatcaaactcctgttctcaagttatgagttggattttatltatlttltgtcaaattgtga 1440
caactctcctaagttgcctgttacctatgtttcagttgaaataggaaaacgaacaataact 1500
ttgaactttctgatcacatgatagttatgtaatcagcaatgtactagaaacataaatt 1560
atgaaaattgatggaaactgtgaaacttggaaagaattgttaattgaattaaatcaaagat 1620
cattattaattaacagttgtgaaaaaaaaatataatgtgattaaatcaatggatataa 1680
cagggccttccatttatccagaatgaatggagagtaacttttagttctgcaaaaagccat 1740
atggcaaaggtcatccctcaaggtgcaatatctggaagacaagtgattgagaatataataa 1800
tatgtgggtttgaataatlttatgcatatctcctcacaagagagcatctaaaaataaaa 1860
tgcattgctgggtgcttcttcatcctctcctccttctgttcatccaagaaagcattaatcc 1920
atltcatggttttccatgtaattgtgacgtatttccatgaattccttcaagtgctagtcaagc 1980
ctgatcatagtgatgaatgatttctcatggaaggtgtctggcatgtctccccgtctagatcc 2040
tcaacagttggaagctctcctgcttatatgtggctagccagctgatgcaacattgtcaca 2100
ttcaaagtgaataaacacgatgtgactttatcacgttgattttttagccataaatggact 2160
tcggattccttttctcatgatacttgacaatgctgaggcataaaagtgggggtcaacattg 2220
ggaacaggctctccttttccatttagtggtgtttaggaagccagagctagacaggaggca 2280
ttgtctgaatccttagtaaaatctaggaattggctgccactgtttccatcggtttttcttg 2340
aagatcctgaagtttaagagattctgattacttttgagtgaagtgtgagaccggatta 2400
agacctatltttgtatltttaaataaagaataagttataagttccatcatcatacac 2460
aaaaaccacacacaatagaaactgtgaaaatgtatataatataatccattgaatttttaatt 2520
aaccatcaccgcccggtaacagaaatccgtgagcttgataagggttcatgtttgagccgc 2580
cgtggtcacagcatgatacttaattgtaattttcatgtttgtgatgctcttggagtgagta 2640
cgtggtagggtccccagttcctttccacggagagtgccggtgttaccttttaggttagca 2700
gtagtaaaattattgatlttacagggtaaatactagccagaaaaagggaactattataaaa 2760
atataccttttttgctaaagagacgaattcagacatagaaaagatcactcggcttgaaag 2820
gcctatlttatcaggaatccataagtcttttgttgttaattccatgcatatltccccccac 2880
Q E D Y D R L R P L S Y P Q T D V F L 79
agGTCAGGAGGATTATGACAGACTGCGACCTCTTAGCTATCCACAGACAGATGTTTTCTT 2940
V C F S V V S P S S F E N V K E K 96
AGTCTGCTTCTCAGTGGTATCCCCTTCGTCCTTCGAGAATGTCAAGGAAAAGgtgagagc 3000
gaaggacaatlttctgttggtaatlttgaacacgctccgtctctgttttaggcattcaa 3060
gagctttgaaaaaaggaatgtaatacaggggtgggaaaagtattlttggtttgaataat 3120
gtgggtatlttcaaactcgaagtaagaaaaatagataagtaaatgaatggttatataataa 3180
aaaaaaggggggtggggaataccaacaatlttcttggtttttatataatataatataat 3240
atataatataatataatataatataatataatataatataatataatataatataat 3300
W 97
ccagttttgctaactctttttgattttgtacatgaaatccttgttttcccttccctacagTG 3360
V P E I T H H C Q K T P F L L V G T Q I 117
GGTACCAGAAATCACTCACCCTGCCAGAAGACTCCATTCTCCTAGTAGGCACACAGAT 3420
D L R D D A A T V E K L A K N K Q K P I 137
AGATTTGCGGGATGATGCAGCAACCGTAGAAAAGCTGGCAAAGAATAAGCAGAAGCCAAT 3480
T Y E Q G D K L S R E L K A V K Y V E C 157
CACCTACGAACAAGGGGACAAGCTCAGTCGCGAGCTGAAGGCCGTCAAGTACGTGGAATG 3540
S A L T Q K G L K N V F D E A I L A A L 177

```

CTCCGCGCTCACACAGAAGGGGCTGAAGAATGTATTTGATGAAGCAATTCTCGCAGCCCT 3600
E P P E P Q R R R K C I V L * 191
GGAGCCCCCAGAACCTCAGAGACGAAGGAAATGTATTGTTCTGTAGGGTAGGACGCATCT 3660
ACGGTAGACCTTGGAGTGGCCCCAGGCTTAACAGATGCACAGATTGCCTTCAATGGTCAG 3720
TAGGGGTTCTAGTGGAGTTGGTGATGCCCTCTGAAGCTATTTAGACAAGAGAACTTGATA 3780
ACTGTATAAATATATGAAGGATTTTATACTTGTGAAAGGGAAAAATGTCCACTATTGGAT 3840
GGTGAAGATGCCAAAGTTCAGATAACTTGCCGATCAAGTCAGGCTTAACGCAGCTTTGG 3900
GGCTAAACTCCATGGGGAATGTGAGCAATCTAAGCACAAGAAAACTGGCTGTTTGGGTCT 3960
TGAGCGTCGAGAGTCGTCTGCACGCAGGCAACTTCTCGACAAGCTCCTCCCTCAGCCAG 4020
TCACTACCTGTTTGTGTTCCACCTTCCCTGTCCCTTATCCCTGGGCCAGCACCCCTCCC 4080
TGTACCATTTGATGAACCATGGTCCAGTTGGTTGGCTTCCAGTTAGGTCGAGTGTCTCT 4140
TGACTTTCATATAAACTTGTTCATATAAAATTTAATACCAAGACTGAACACAAATATCATGT 4200
TGATTCCAATCATCTCTAGATTTCTCAGATAAATTCATTTAATTCAAGAGAACTACAGTAA 4260
TCAATAGCTCAGTATTCAAATTCGATAGGCTTTTTTTTTTCTAATTTTACCTTTCTATA 4320
GCTTATGGCATCTCATAACAAGTAATGAGTTTAGAAGTGTGATAAAATGAATGAGTAAC 4380
CAATATTTGTATGAGCTTAACTTCTATATAACTGCCTCAGACTATCATATGTTTCTTAT 4440
TCTTACACGTACACGTCTAGTGGCGTGTACCTAGCATTGGTATCTTCTTTTTTATTATAA 4500
CATTAGTGCAAACTTTTAGGAGGTTTGTCTAGGGACTATGGCTTGGTTTTGTGGGCTCAA 4560
AAACCAAGATAATCCTTGAGACGAGACCAGTTATGATTTTAAGTATCAGTTTGTTAATTT 4620
TTTACAATATGGTGTGCCTGAGTAAGAAAATAGGTTTGAAGTACGTGGCATTATGCAAAA 4680
GGTTTATCAATTTGTCAAAGAGTGGAGAAGCATTCTTTTTCCAGTGTGTTGGTTTTCA 4740
TTTGAACAGATTTGGCCTCTTCTGCTCACTCTGGCCTTTCTCAGTAGTCATAGTGGGT 4800
ATGAAGCCAGTCTGGGGAAGTCTGATGTAGTGGAAATGGTTATATATCAACTTGCATAGT 4860
TGGCTCAATTACAGGAATTGTTATTTTTGTACAAATCTAAATTTGAAAGTAGTGTCCA 4920
TGATTTTTTAAATTTTTGCTACTTCAGACGTAGTAAGTTGATGGCACCCAGATGGTTGGT 4980
AACTACCTTGCCTCGTCATACATTAACCTAACCACCCTGGTGTGGGTGAAATATTTA 5040
ATATCAGAATGTGTAGTTGCCATGTTGACCATTGCATATATGACAAAAACAAAAATTTAT 5100
GGATTTTGTCTTCATTTAAAGTGTGATAAAACCCTGATGATTTAGAAGGAAGTTTGGTGT 5160
TATGGAGGGAGATACAAAATAAACCATTTGGATTGAAAAAAAAAAAAAAAAAAAAA 5214

```

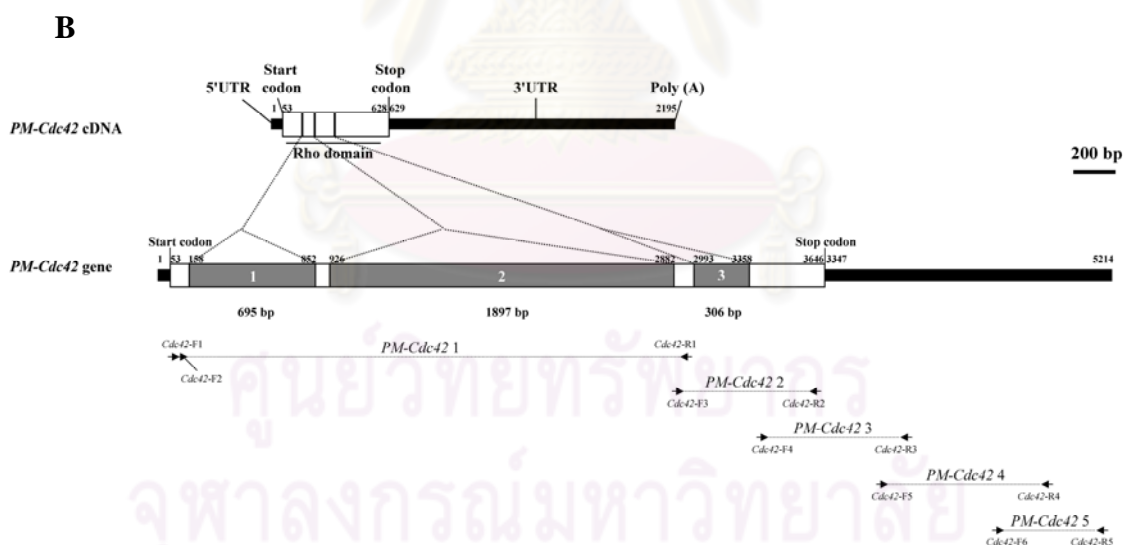


Figure 3.77 Organization of genomic sequence of *Pm-Cdc42* (A). Coding nucleotides and deduced amino acids of each exon are capitalized. Introns are highlighted, and illustrated with lower letters. The putative start, stop codons and the poly A additional signal site are bolded-underlined. The predicted Rho domain is indicated by double-underlined. B. Diagram showing organization of *Pm-Cdc42* cDNA and genomic DNA. Primers used for identification of genomic sequences and the corresponding clones are also shown.

Table 3.37 GC content and length of exons and introns in *Pm-Cdc42* genes

Exon	Nucleotides position	GC content (%)	Intron	Nucleotide position	GC content (%)	Type	GT/AG rule
1	1-827 (827 bp)	50	1	828-926 (99 bp)	31	0	Yes
2	927-1131 (205 bp)	43	2	1132-1230 (99 bp)	35	1	Yes
3	1231-1329 (99 bp)	46	3	1330-1474 (145 bp)	27	0	Yes
4	1475-1623 (149 bp)	51					

3.5.3 Characterization of the *SARIP* genes

Genomic organization of *Pm-SARIP* was also characterized by overlapping amplification of genomic DNA sequences. The *Pm-SARIP* gene was composed of 5 exons and 4 introns covering 5937 bp in length. The length of each intron was 2646 bp (intron 1), 163 bp (intron 2), 453 bp (intron 3) and 1309 bp (intron 4), respectively (Figure 3.78). The GC content of exons (41-49%) was much greater than that of introns (23-33%). The boundaries of all intron followed the GT/AG rule. Introns 1 and 4 of the *Pm-SARIP* gene interrupt the ORFs between two codons (type 0 intron), whereas introns 2 and 3 interrupt the ORFs within the same codons (type 1 intron) (Table 3.38).

A

```

GGCACGAGGGTCACGCTTTTGGGTTTCATGTGTTTCCTCCTAATTTCTATTTTCTCTTC 60
      M T D Y K E E Q N N E I E A L E S 17
AATTATTCGTCATGACAGACTACAAGGAAGAACAGAATAACGAAATTGAGGCCCTGGAGT 120
      I Y P E E F E I
CCATATATCCAGAGGAATTTGAGAGtaagtgtaaatcatacctaattaaggtcaaatac 180
cgtttgatattaatcaccaatagtaattagcatttcttcaagaattattaccctgctctg 240
aaattaggtaattatTTTTgTTTTaggtattagtcacgaattatgagcacaacgatta 300
gagatTTTgagtagcattacaagtgatttCCTTgaacataTTTactTgcctgtatttaa 360
gattatcaggaattctggTTTTagtcgttCactTaaactctaaaagctggagcctagaatt 420
gttcgaaacaaggctgtgtattggTcaatggaactcttaagattgtcgtaaatattctt 480
ttatttaatatagatatattggTgtgtgtaaattcctcgacctgagagtatacaatttagat 540
atagaataatattcattagaaatTTTgtaaaaattcctataaaaagctgtataggTTTTa 600
aagaaaatctaagttggtcataaagTTTTattgagtgatgagcagcatttcaagtaataca 660
cagacgtgcagttattctcaatcaccaaatTcaatataatctcaaaatgcaatgttgcca 720
attgtacaaaattcattctgtaaatatctataacagatggctgtcttactctatacata 780
attagtTTTTgccttacttatacctttatttattgtccaatttcatcttacctatattgcaa 840
agtaataaatggcatacaccataTTTctactacctgcacatcaggcacaaggcatacctg 900
ttcagctcataaatattattatTTTTtaggtctctgtTTTTcattggTcactatgtTTTTga 960
atatcaagtaagcattattcctaaaatgccataaccatctcataTTTTgtTTTTgtatatga 1020
ctgagaaaaataaaataaatgtatttagcaacacaaccaaagatgggaaactagagcagag 1080
tgccaacatcatcctcgcccatcgtcgtcgtcgttgccatcgtcatcgccatcgttatcg 1140
tcatcatcaacatcaacaataatgatattaaataaaaaataataatgaaaaaggctaa 1200
ttgtgatgatgatgctaataattaccattatcattgttattattattattatttttattat 1260

```


tatccttggttattattatcattgtcataataattattcataatattactacaattgccat 1320
 cccttgatcattatcatcatcatcattatgaacattctagttgctgttaacatcatct 1380
 aaagccactccgcacataactctttgggcaagatccaccattcacagccatctttgtgt 1440
 ttaccatctctcagactgaagtgaatagactatagtagatttagttatgtgaaattaga 1500
 cagtttctcaaactagactttacttggcattattttgaaccacttagctatcatcctta 1560
 aaagcctctgctatagctctggggcagttgcagcatgcaacattttttgcatgaggtgact 1620
 gtaatatgaatagagaattcaaatttgggaagtagcttttagtaacattcttatttttttc 1680
 ttgtatattattatattggttgtgttctcttcagatcctctctcaactaattccaatgtg 1740
 atagtagcatattgttaacaatcacattgaccttgtgtcatcaatcctcagacaaaaggc 1800
 cagaaaactttcaccatgtataatgtgataaagtagagctggaacttgtttcctacttga 1860
 tgaaaatttgcttggaaatctcagcaagctcttaattgaggttggcttggcttggctgga 1920
 cattgacaggtgtaaaactattgtatccattattatttgggtatgttactactcatttg 1980
 gtcagcaatacagcctaaggaattgagaaatattatttctattaccctgtttatctgt 2040
 ggtatttcaatggcaaatagtagataaagaaagtagttggtattatataatataaccaac 2100
 catatatcatgtttacatttcatgacgtaatacaaaatcctgtttcatttatcatgagat 2160
 atatgcacaaaatcccttgagtacttatatccactggaagtgatccagattctagtcaa 2220
 ttaaggaactagctggagtttaccttggcagaatttatataatggctgacatccagg 2280
 cagtgacttcaagttatctctttgtaacttgtacctcagtgcaacacttaggact 2340
 gaggtttggtaggagatttggttatcagcattgtgttgacactcttttgggtcaggctg 2400
 ttttcaagaccactcaacagttgcattagcataatctgacgaaacaaacagtaatgc 2460
 agcaactataggaaaattcagcctaagttcacttgggtctcccaagcttagctctatct 2520
 ttcagtacatactgaggtgaagacaatgtttgctgggtgggtgttggggggcagatcctcc 2580
 cgtcaagccccatcttttttaataatgaatttgggtatatactgtacagaataaacctttt 2640
 tattatggataactaattgtactttttcatctttttcaggtatgaagatgtaagattac 2700
 tttgtaaagggtaccagtaacagcaaaaatataaaactaaaaaatatggatggaattagag 2760
I D I E P R H K F R 35
 ccactgatgacttcccttttttattttacagTAATTGATATAGAACCAAGGCACAAGTTCA 2820
I T V K S E G S D P Y D E I Q T L P A T 55
 GAATTACTGTCAAATCCGAAGGCTCTGATCCATATGATGAGATTGAGACGTTACCAGCAA 2880
I I L N F E Y T P T Y P D E P P V M E V 75
 CTATTATCCTCAACTTTGAATACACTCCAACGTATCCAGATGAACCCCGATCATGGAAG 2940
T A V E N I E E E E L D D L R T K L N E 95
 TCACAGCTGTTGAAAACATAGAAGAGGAAGAGCTGGATGATTTAAGAACGAACTTAACG 3000
Q 96
 AGCAGgtactttgttgatgcatttcttgattatgccttgaacactggccagaatatcttg 3060
 gttaatgggggtcaagatgattgttgtaagttttccctatatattagaattatagaaaaga 3120
C E E N 100
 gcattgtgtctattattcctactttttcaaaatataaaatattttacagTGTGAGGAGAAC 3180
L G M V M V F T L V S Y S L E W L T T H 120
 CTGGGGATGGTCATGGTGTTCACGCTTGTCTCATACTCATTGGAGTGGCTCACACACAC 3240
M E G I A L S T K E E L D R K K K E Q E 140
 ATGGAAGGTATTGCTCTCAGCACCAAGAAGAATTGGATCGCAAGAAGAAAGAGCAGGAA 3300
E I D R 144
 GAGATAGATCGGgtgagcgggtcataactaacttggagaaccatctctcattgtagcagaa 3360
 tctttatttggttcatattttccacttaagatattgttaagtgtgggtggatatttagtgat 3420
 ttgctaattgtttgagaatgcatttagatgttttttacaggacgtagctatgtaaaattt 3480
 tagctgaatattttatgaactgctaataaaactcattctgcataaagactttttcttgg 3540
 ttgtggtgataatttttttatttttattttctttatttttctgtccgaggttcaacaa 3600
 tatgcctttattcatttggcaaaaagagaaaaagatttgatagagttggttattcatat 3660
 tagaagaaatcatattaaggactattgtaccgtacaaggacaatatttagtattaataca 3720
K K F E G 149
 ttaatctttatgaccatgggtgagttatatacctttatcctcacagAAAAAGTTTGAAGGT 3780
T R V T V E T F L A W K A K F D T E M Q 169
 ACCAGAGTGACTGTAGAAACGTTTCTTGCTTGGAAAGCAAAGTTTGATACGGAGATGCAA 3840
A L R S E K D R E D E K N K K P T G R E 189
 GCACTCCGATCTGAGAAAGACAGGGAGGATGAGAAGAACAACCAACTGGTAGAGAG 3900
L F M K D V T L N E S D L S F L G E G 208
 CTCTTCATGAAGGACGTCACCTTTGAATGAGTCGGATCTTAGCTTCCTTGGTGAAGgttag 3960
 tgccttgcaaatgatacatatttttttctgtttatactgtcttttatccatgcatggt 4020
 gttattggtaaagattgtctctttaaagcctaaccagtgacaggtgccttataattattct 4080
 gtacagattagaagccaatattttcccttgtgctcatattaatcctctttttgattgaa 4140

```

cttgatcccttttagaaatgcctggacttaccatacagccatttttaagttaaagacattat 4200
tgacctatgttgaacttcatgtaccatctaccagctaggtagtagtctttcaagtttgaat 4260
ttgtcctccacttgctattcctcttcttgtactcgtcagaaaaggagatctgagagatag 4320
aaattatcattagaacatttttaaacactactcgtgggttttgtgatcagtactgttaaagg 4380
tagtttttagggctagtttctcctgcagtaattagtggttttcttatatagattttataagtgt 4440
tgacaggtttcaaacttagagtagtatttagtagttccagtttctgccatccattcaggc 4500
ccaatcacgatttttacatttctgcatgaatttgaagcttctgcaactcctcccagaca 4560
aagacaatagcagccatcttcattttatttaatttctgtcttgatattgtgctgtagaag 4620
atctgtgctattagactatttttattgataaatggaaaagaatatgttcatgcaaatatt 4680
tataacatgatacatagaaagtttatccttgaattattgtagtcttctttgaatatttat 4740
tatattttagtaaagtaactaataatgtagatgaggatgcttgtgtgatttctgggacccaa 4800
catgcaaacagtgtaggaagcttgcggatgaggcttcttaataaaggcagtacttctact 4860
tatggaatgtacaaaactccttggttgggtgccttgtttacaggagagaggtgggtggcag 4920
aaaaagtgctggcattcatagtttctgattgatttgcataatgcccaggcagattttac 4980
tccttttttattttcatatggaatattgtgatttgaatattaaatgttattttctctt 5040
cctgctgtagttgtcatatttaacagttattattattttatgtgtatattttcagagctc 5100
atacagttgtttctaaactgcaaatattttatgcttggtaaattatcttctttttctctc 5160
actttctcaatattattttcttctcatttctctctatctttgatttattttcttttctgtg 5220
                                     E G E V T 213
ctacaaatgtttgtctcttttctcactgaacttggttttttccagGAGAAGGTGAGGTGAC 5280
V D E S L F Q L D D L D L E D E D D E D 233
TGTTGATGAGAGTTTATTCCAAGACCTGGATGACTTAGACCTCGAGGATGAAGATGACGA 5340
Y V P G A D D D D I S D * 245
GGATTATGTTCCAGGAGCGGATGATGACATATCTGATTAGAAACTTTAAATAAATATCAT 5400
TTCATTATCATATCTTTTTTTCTCTCTCACTCTCGTGGTTTCCCATCATGAATTTGTTT 5460
TAGTCATGGATACTGGCTCATGAATTTTTTTTTTTTTCTTTCTTTCTTTCTTTTTTTTAT 5520
ACATCCGTTTATTTGCAGAAGATGTCTCTTCAAATGTAATGTTTGTGTTTGTCTTATTAG 5580
CTAAAATTAGCCCTCTTATTTATTTGGAAAAGTTGTTTTGATAATGCATTTGTAATAAAA 5640
CATTTAAACAAAAATGGAGATTACTTTCAGTTGTTTTCAGAGGTTATTTAGTTGGGGAGTGT 5700
CACCGAAATTATTATCTTTGTTTATTTGTTTTGCATACAGAATTAGATCATGCAAAATAGA 5760
CAGTTGCTTATAAAGACCATTTTTTTATTTTTGTTTTCAATCACCATGATTGTTATTTTTTA 5820
TACAGTTTAAACCATTTGTATCAAGTTGTTTTTACTTAGATTTTCATCAATAGAGGAGTCA 5880
GTATGATGCATTAGCCCTCAATAAAAATGTTAAATCTGTAAAAAAAAAAAAAAAAAAAAA 5937

```

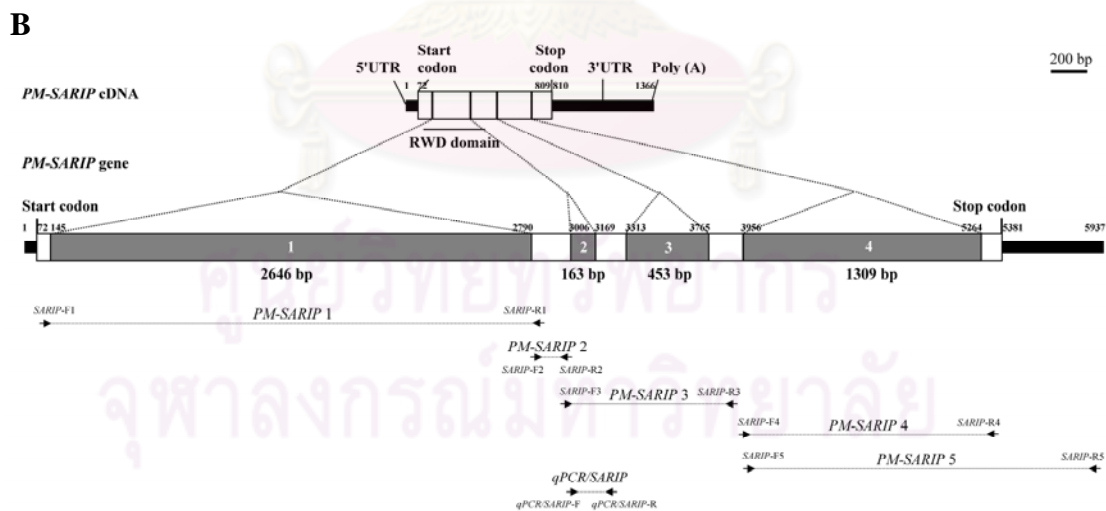


Figure 3.78 Organization of the *Pm-SARIP* gene (A). Coding nucleotides and deduced amino acids of each exon are capitalized. Introns are shaded, and illustrated with lower letters. The putative start, stop codons and the poly A additional signal site are bolded-underlined. The predicted RWD domain is indicated by double-underline. B. Diagram showing organization of *Pm-Cdc42* cDNA and genomic DNA. Primers used for identification of genomic sequences and the corresponding clones are also shown.

Table 3.38 GC content and length of exons and introns in *Pm-SARIP* gene

Exon	Nucleotides position	GC content (%)	Intron	Nucleotide position	GC content (%)	Type	GT/AG rule
1	1-827 (827 bp)	41	1	828-926 (99 bp)	33	1	Yes
2	927-1131 (205 bp)	40	2	1132-1230 (99 bp)	30	0	Yes
3	1231-1329 (99 bp)	49	3	1330-1474 (145 bp)	29	0	Yes
4	1475-1623 (149 bp)	43	4	1475-1623 (149 bp)	32	1	Yes
5	1475-1623 (149 bp)	45					



ศูนย์วิทยุทรัพยากร
จุฬาลงกรณ์มหาวิทยาลัย

3.6 Examination of expression patterns of genes functionally related to ovarian development of *P. monodon* by RT-PCR

3.6.1 Total RNA extraction

Total RNA from ovaries and testes and other tissues of *P. monodon* were extracted. The quality and quantity of total RNA were determined by spectrophotometry and agarose gel electrophoresis (Figure 3.79; A). The ratio of OD₂₆₀/ OD₂₈₀ of the extracted RNA was 1.8 – 2.0 indicating that its quality was acceptable for further applications. Agarose gel electrophoresis showed discrete ribosomal RNA bands reflecting good quality of total RNA. The first strand cDNA was successfully synthesized as illustrated by 1.2% agarose gel electrophoresis (Figure 3.79; B).

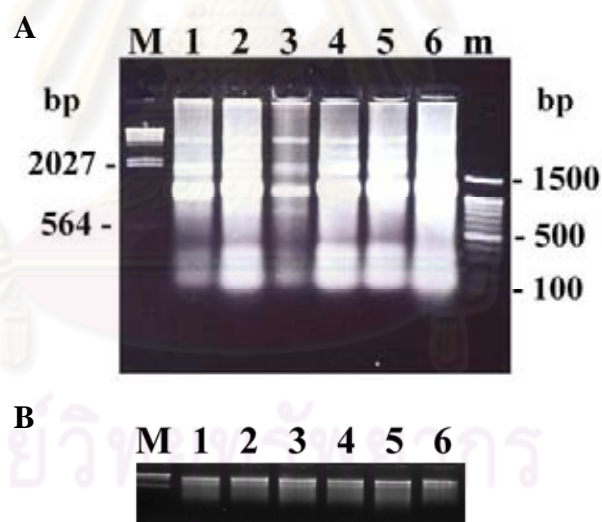


Figure 3.79 A 1.0% ethidium bromide-stained agarose gel showing the quality of total RNA extracted from ovaries of *P. monodon* broodstock (A) and the synthesized first strand cDNA (B). Lanes M and m are λ -Hind III and 100 DNA ladder, respectively. Lanes 1 - 6 are total RNA individually extracted from ovaries of each *P. monodon* broodstock.

3.6.2 RT-PCR and tissue distribution analysis of genes functionally related to ovarian development

Expression of 31 genes from ovarian cDNA libraries (29 genes) of normal shrimp and of a temperature-stressed gill cDNA library (1 gene) and *Vibrio* challenged of hemocytes library (1 gene) was examined by RT-PCR.

Seventeen genes were differentially expressed during ovarian development of wild normal broodstock of *P. monodon*. Expression profiles of 14 genes including *Progesterone receptor-related protein p23*, *Progesterin receptor membrane component 1 (PGMRC1)*, *Vitellogenin*, *26S proteasome regulatory subunit rpn2*, *CWF19-like 2*, *DNA replication licensing factor mcm2*, *Neuralized protein*, *Keratinocytes associated protein 2*, *CG17161-PA: Ser/Thr kinase chk1*, *Selenoprotein M precursor*, *carbonyl reductase*, *RNA polymerase I associated factor 53 isoform 1*, *Selenophosphate synthetase* and *Egalitarian* were correlated (up- or down-regulated following ovarian developmental stages) with stages of ovarian development (Figures 3.80 and 3.81; A; Tables 3.39 and 3.40).

Expression of 9 genes (*Cell division cycle 42 (Cdc42)*, *OV-N-ST01-0012-W*, *OV-N-ST02-0010-W*, *Small androgen receptor interacting protein (SARIP)*, *Procollagen-proline, 2-oxoglutarate 4-dioxygenase (protein disulfide isomerase; thyroid hormone binding protein p55) (P4HB)*, *GA17699-PA*, *Citrate synthase*, *Neutral alpha-glucosidase AB precursor* and *cytochrome c oxidase polypeptide IV*) was comparable between different stages of ovarian development (Figures 3.81; B and 3.82; Tables 3.39 and 3.40).

Nonspecific amplification products were observed from RT-PCR of *phospholipid phospholipase C beta isoform*, *M-phase inducer phosphatase (String protein Cdc25-like protein)*, *coatomer protein complex*, *OV-N-ST02-0006-W* and *thioesterase superfamily member 2*.

Progesterone receptor-related protein p23, *progesterin receptor membrane component 1 (PGMRC1)* and *vitellogenin* were up-regulated at later stages of ovarian development of *P. monodon* (Table 3.40).

DNA replication licensing factor mcm2, *CWF19-like 2*, *keratinocytes associated protein 2*, *26S proteasome regulatory subunit rpn2*, *CG17161-PA: Ser/Thr kinase chk1*, *selenoprotein M precursor*, *neuralized protein*, *Egalitarian* and *carbonyl reductase* were down-regulated during ovarian development of *P. monodon* (Figures 3.80 and 3.81; A).

Although expression levels of *gonadotropin regulated long chain Acyl-CoA synthetase*, *vitellogenin receptor* and *OV-N-ST01-0022-W* (unknown transcript) were differentially expressed during ovarian development, their profiles did not correlated with ovarian stages (Figure 3.83).

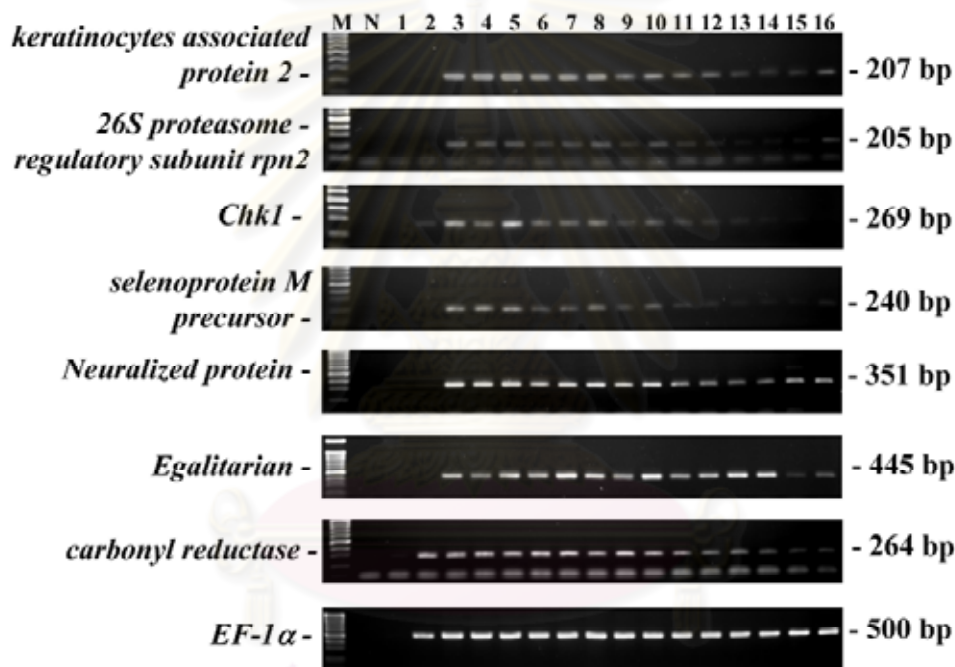


Figure 3.80 RT-PCR of *keratinocytes-associated protein 2*, *26S proteasome regulatory subunit rpn2*, *Chk1*, *selenoprotein M precursor*, *Neuralized protein*, *Egalitarian* and *carbonyl reductase* using the first strand cDNA template of *P. monodon* having different GSI values. These transcripts were differentially expressed during ovarian development of *P. monodon*.

Lanes 3 - 14 are the first strand cDNA template from ovaries of *P. monodon* having GSI = 1.12, 0.77, 1.10, 2.15, 2.58, 2.95, 4.62, 5.25, 5.38, 9.36, 11.21 and 12.55, respectively. Lanes 15 - 16 are the first strand cDNA template from ovaries of 4-month olds *P. monodon*. Lanes 1 and 2 are genomic DNA template and the first strand cDNA template from testes of *P. monodon* broodstock, respectively. PCR was carried out for 25 cycles and *EF 1-α* (500 bp) was used as the positive control. Lanes M and N are a 100 bp DNA marker and the negative control (without the cDNA template), respectively.

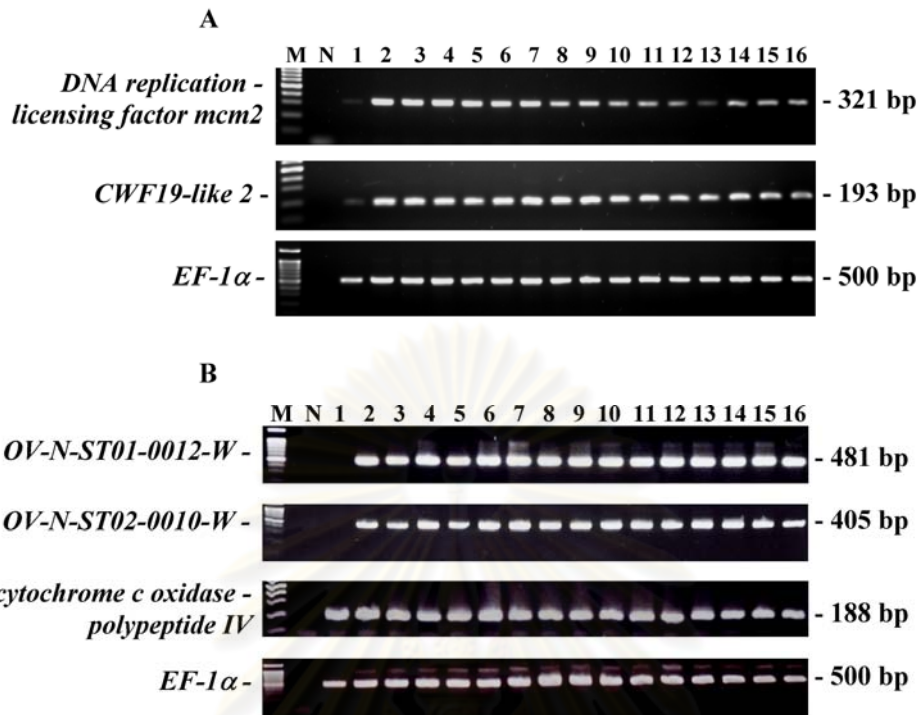


Figure 3.81 RT-PCR of *DNA replication - licensing factor mcm2* and *CWF19-like 2* (A) and *OV-N-ST01-0012-W* and *OV-N-ST02-0010-W* regarded as unknown transcripts, *cytochrome c oxidase polypeptide IV* (A) using the first strand cDNA template of *P. monodon* having with different GSI values. Differential (A) or comparable (B) expression profiles during ovarian developmental stages were observed.

A; Lanes 2 - 13 are the first strand cDNA template from ovaries of *P. monodon* having GSI = 1.12, 0.77, 1.10, 2.15, 2.58, 2.95, 4.62, 5.25, 5.38, 9.36, 11.21 and 12.55, respectively. Lanes 1 is the first strand cDNA template from testes of *P. monodon* broodstock.

B; Lanes 2 - 13 are the first strand cDNA template from ovaries of *P. monodon* having GSI = 5.689, 4.687, 3.017, 2.401, 2.018, 2.128, 1.894, 1.434, 1.100, 0.918, 0.870, 0.647, respectively. Lanes 1 are genomic DNA template of *P. monodon*. Lanes 14 - 16 are the first strand cDNA of ovaries of 4-month olds *P. monodon*.

PCR was carried out for 25 cycles and *EF 1-α* (500 bp) was used as the positive control. Lanes M and N are a 100 bp DNA marker and the negative control (without the cDNA template), respectively.

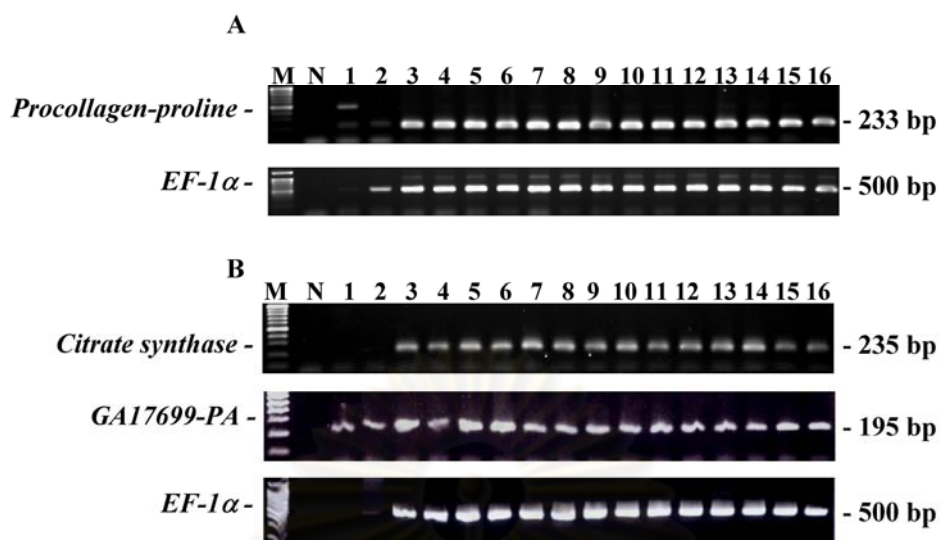


Figure 3.82 RT-PCR of *procollagen-proline* (A) and *citrate synthase*, *GAI7699-PA* (B) using the first strand cDNA of *P. monodon* having different GSI values. Expression patterns of each gene were comparable among different stages of *P. monodon*.

A; Lanes 3 - 14 are the first strand cDNA template from ovaries of *P. monodon* having GSI = 1.12, 0.77, 1.10, 2.15, 2.58, 2.95, 4.62, 5.25, 5.38, 9.36, 11.21 and 12.55, respectively. Lanes 1 and 2 are genomic DNA and the first strand cDNA template of testes of *P. monodon* broodstock, respectively.

B; Lanes 3 - 14 are the first strand cDNA template from ovaries of *P. monodon* having GSI = 5.689, 4.687, 3.017, 2.401, 2.018, 2.128, 1.894, 1.434, 1.100, 0.918, 0.870, 0.647, respectively. Lanes 1 and 2 are genomic DNA template of *P. monodon*. Lanes 15 - 16 are the first strand cDNA template from ovaries of 4-month olds *P. monodon*.

PCR was carried out at 25 cycles and *EF 1-α* (500 bp) was used as the positive control. Lanes M and N are a 100 bp DNA marker and the negative control (without the cDNA template), respectively.

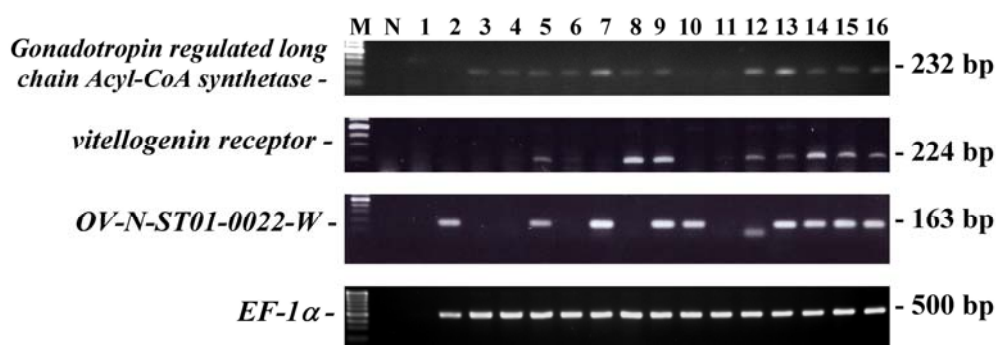


Figure 3.83 RT-PCR of *gonadotropin-regulated long chain Acyl-CoA synthetase*, *vitellogenin receptor* and *OV-N-ST01-0022-W* using the first strand cDNA template of ovaries *P. monodon*. These transcripts were differentially expressed during ovarian development of *P. monodon*.

Lanes 3 - 14 are the first strand cDNA template from ovaries of *P. monodon* having GSI = 5.689, 4.687, 3.017, 2.401, 2.018, 2.128, 1.894, 1.434, 1.100, 0.918, 0.870, 0.647, respectively. Lanes 15 - 16 are the first strand cDNA of ovaries of 4-month olds *P. monodon*. Lane 1 is a genomic DNA using as template.

Table 3.39 A summary of expression patterns of various gene homologues during ovarian development of *P. monodon* preliminary analyzed by RT-PCR

Category	Number of genes
Differential expression during ovarian development	17
- Correlated with ovarian developmental stages	14
- Not correlated with ovarian developmental stages	3
Comparable expression between different ovarian developmental stages	9
Non-specific amplification products	5
Total	31

Interestingly, *Pm-SARIP* was specifically expressed in gonads where a greater expression level was observed in ovaries than testes of *P. monodon* (Figure 3.84; A).

VTG was abundantly expressed in ovaries and hepatopancreas but not in other tissues of *P. monodon* broodstock. Extremely level of this transcript was also observed in ovaries of juvenile *P. monodon* (Figure 3.84; B).

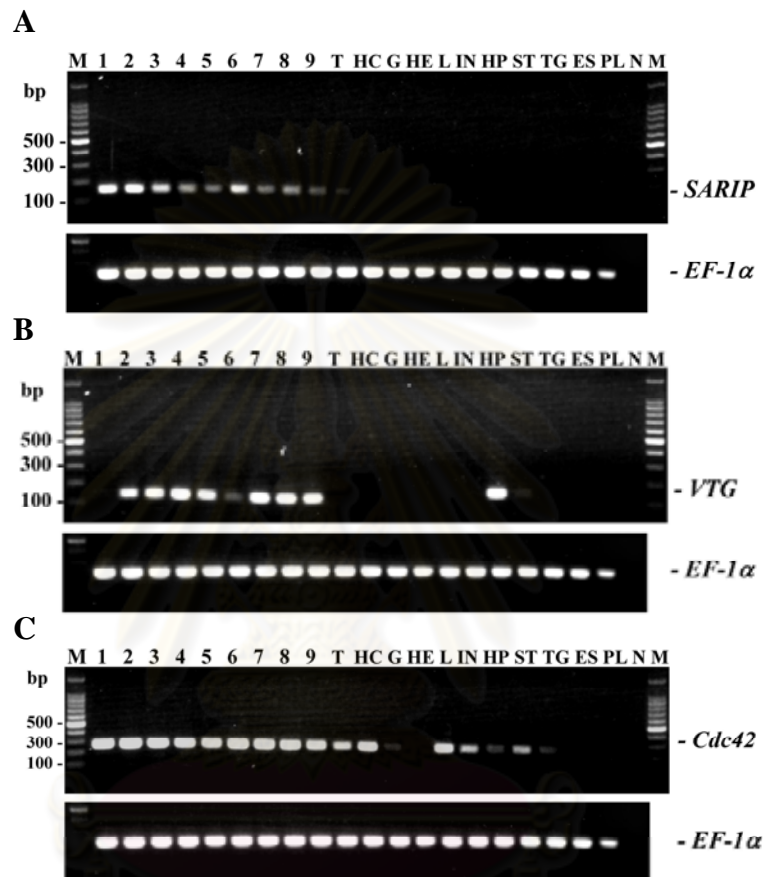


Figure 3.84 A 1.5% ethidium bromide-stained agarose gel showing results from tissue distribution analysis of *SARIP* (A), *VTG* (B) and *Cdc42* (C) transcripts using the first strand cDNA of ovaries of juvenile (lane 1), normal and eyestalk-ablated broodstock (previtellogenic, lanes 2 and 6; vitelligenic, lanes 3 and 7; early cortical rod, lanes 4 and 8 and late cortical rod ovaries, lanes 5 and 9) and various tissues of broodstock-sized *P. monodon*; testes (T), hemocytes (HC), gills (G), heart (HE), lymphoid organs (L), intestine (IN), hepatopancreas (HP), stomach (ST), thoracic ganglion (TG), eyestalks (ES), pleopods (PL) and epicutical (EP). *EF-1 α* was successfully amplified from the same template (E). Lanes M and N are a 100 bp DNA marker and the negative control, respectively.

Likewise, high expression levels of *Pm-Cdc42* were found in ovaries of juvenile and broodstock and testes, hemocytes, and lymphoid organs. Lower expression levels were observed in intestine and stomach. The expression of this transcript was extremely low in gill, hepatopancreas and thoracic ganglion. *Pm-Cdc42* was not expressed in eyestalk and pleopod of *P. monodon* (Figure 3.84; C).

Tissue expression analysis also indicated that *Pm-PGMRC1* was more abundantly expressed in ovaries of both juveniles and broodstock *P. monodon*. A relatively high level of expression was also found in hepatopancreas and lower expression was observed in the remaining tissues including testes of a male broodstock (Figure 3.85; A).

Expression levels of *p23-like protein* were observed in all stages of ovaries and testes, and various tissues (hemocytes, gill, lymphoid organ, intestine, hepatopancreas, stomach and thoracic ganglion). A low expression level of *p23-like protein* was found in eyestalk. Expression of this transcript was not observed in heart and pleopod of broodstock-sized *P. monodon* (Figure 3.85; B).

Carbonyl reductase was more abundantly expressed in ovaries than other tissues. However, this transcript seemed not to be expressed found in pleopods of broodstock-sized *P. monodon*. Low expression levels of *carbonyl reductase* were observed in eyestalk and heart of broodstock-sized *P. monodon* (Figure 3.85; C).

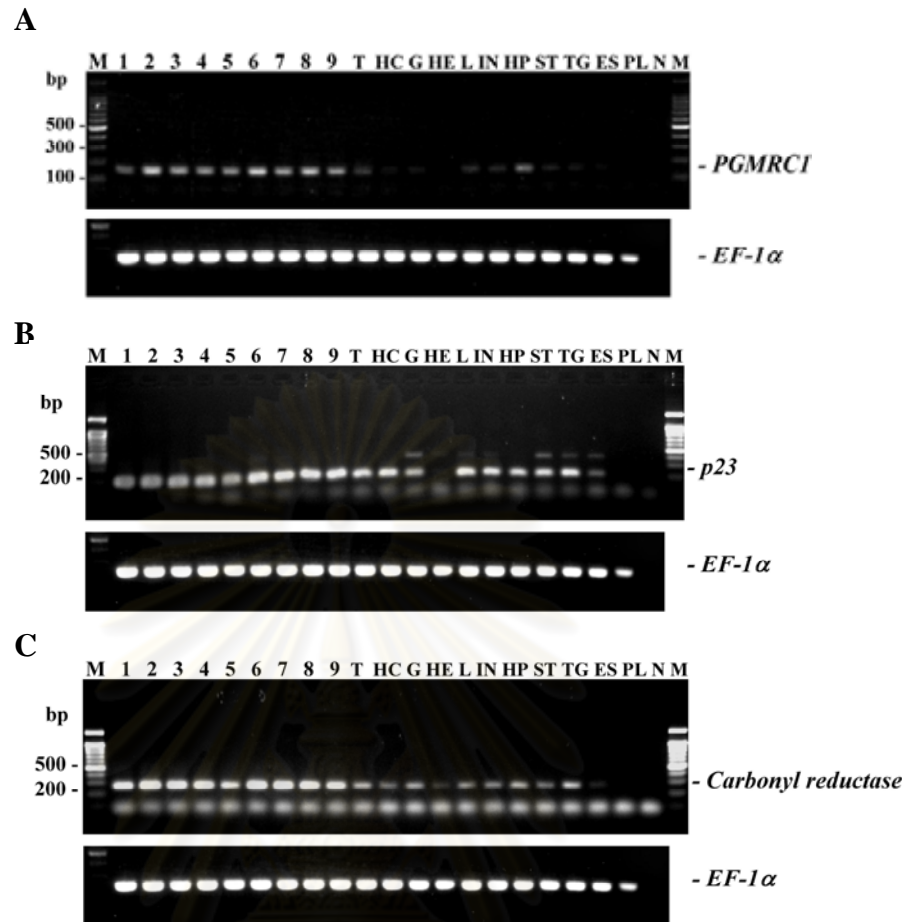


Figure 3.85 A 1.5% ethidium bromide-stained agarose gel showing results from tissue distribution analysis of *PGMRC1* (A), *p23-like protein* (B) and *carbonyl reductase* (C) transcripts using the first strand cDNA of ovaries of juvenile (lane 1), normal and eyestalk-ablated broodstock (previtellogenic, lanes 2 and 6; vitelligenic, lanes 3 and 7; early cortical rod, lanes 4 and 8 and late cortical rod ovaries, lanes 5 and 9) and various tissues of broodstock-sized *P. monodon*; testes (T), haemocytes (HC), gills (G), heart (HE), lymphoid organs (L), intestine (IN), hepatopancreas (HP), stomach (ST), thoracic ganglion (TG), eyestalks (ES) and pleopods (PL). *EF-1α* was successfully amplified from the same template (E). Lanes M and N are a 100 bp DNA marker and the negative control, respectively.

Table 3.40 Expression profiles and tissue distribution analysis of various genes during ovarian development of *P. monodon*

Gene/Primer	Tissue distribution analysis	Trends of expression screened by RT-PCR						
		Testes	Ovaries					
			Juveniles	Stage I (GSI<1.5)	Stage II (GSI 2.0-4.0)	Stage III (GSI 4.0-6.0)	Stage IV (GSI>6.0)	
1. Progesterone receptor-related protein p23	O, T, HC, G, L, IN, HP, ST, TG and ES	+	++	++	+++	+++	+++	
2. Progestin receptor membrane component 1 (PGMRC1)	O, T, HC, G, L, IN, HP, ST, TG and ES	+	+	++	++	++	+++	
3. Vitellogenin	O, HP and ST	-	-	+	+	+++	+++	
4. 26S proteasome regulatory subunit rpn2	ND	+	++	+++	+++	+++	++	
5. CWF19-like 2	ND	+	+++	+++	+++	+++	++	
6. DNA replication licensing factor mcm2	ND	+	++	+++	+++	++	+	
7. Neuralized protein	ND	-	++	+++	+++	++	+	
8. Keratinocytes associated protein 2	ND	+	+	+++	++	++	+	
9. CG17161-PA: Ser/Thr kinase chk1	ND	+	+	+++	++	++	+	
10. Selenoprotein M precursor	ND	+	+	+++	++	++	+	
11. carbonyl reductase	O, T, HC, G, HE, L, IN, HP, ST, TG and ES	+	+	++	++	++	+	
12. RNA polymerase I associated factor 53 isoform 1	ND	-	+	++	++	+	ND	
13. Selenophosphate synthetase	ND	+	+	+++	++	++	ND	
14. Egalitarian	ND	-	+	++	++	++	+	
15. Gonadotropin-regulated long chain acyl-CoA synthetase	ND	+	+	++ (3 in 5)	++	+	ND	
16. Low density lipoprotein receptor; vitellogenin receptor	ND	-	+	++ (4 in 5)	++ (2 in 5)	+1 in 2)	ND	
17. OV-N-ST01-0022-W	ND	-	+	++ (3 in 5)	++ (2 in 5)	++ (1 in 2)	ND	

Table 3.40 (Cont.)

Gene/Primer	Tissue distribution analysis	Trends of expression screened by RT-PCR						
		Testes	Ovaries					
			Juveniles	Stage I (GSI<1.5)	Stage II (GSI 2.0-4.0)	Stage III (GSI 4.0-6.0)	Stage IV (GSI>6.0)	
18. <i>Cell division cycle 42 (Cdc42)</i>	O, T, HC, G, L, IN, HP, ST and TG	+	+	++	++	++	++	
19. <i>OV-N-ST01-0012-W</i>	ND	-	+++	+++	+++	+++	ND	
20. <i>OV-N-ST02-0010-W</i>	ND	+	+++	+++	+++	+++	ND	
21. <i>Small androgen receptor interacting protein (SARIP)</i>	O > T	+	++	++	++	++	ND	
22. <i>Procollagen-proline, 2-oxoglutarate 4-dioxygenase (protein disulfide isomerase; thyroid hormone binding protein p55) (P4HB)</i>	ND	+	++	++	++	++	ND	
23. <i>GAI7699-PA</i>	ND	+	++	++	++	++	ND	
24. <i>Citrate synthase</i>	ND	-	+	++	++	++	ND	
25. <i>Neutral alpha-glucosidase AB precursor</i>	ND	-	+	++	++	++	ND	
26. <i>cytochrome c oxidase polypeptide IV</i>	ND	+	+	+	+	+	ND	
27. <i>Phospholipid phospholipase C beta isoform</i>	ND	NS	NS	NS	NS	NS	NS	
28. <i>M-phase inducer phosphatase (String protein Cdc25-like protein)</i>	ND	-	NS	NS	NS	NS	ND	
29. <i>Coatomer protein complex</i>	ND	ND	NS	NS	NS	NS	ND	
30. <i>OV-N-ST02-0006-W</i>	ND	NS	NS	NS	NS	NS	ND	
31. <i>Thioesterase superfamily member 2</i>	ND	ND	NS	NS	NS	NS	ND	

* ND = not determined, NS = non specific amplification products, + = low level of expression, ++ = moderate level of expression, +++ = abundant level of expression

3.6.3 Determining expression patterns of ovarian and testicular forms *PGMRC1* in ovaries and testes of *P. monodon* broodstock

Three different forms of *PGMRC1* sharing an identical ORF but different length of overlapping 3' UTRs were previously identified in testes of *P. monodon*. In this study, a single form of *PGMRC1* was identified in ovaries of *P. monodon*. Multiple alignments indicated that these transcripts have the same length of ORF with polymorphism for only 2 amino acids in the ovarian form. However, the 3' UTR region of the ovarian form was obviously different from the testicular forms. Therefore, primers designed from the ORFs generated mixed products from different forms of *PGMRC1*. The expression patterns of *PGMRC1* in ovaries and testes of juvenile shrimp were comparable whereas preferable expression of *PGMRC1* in ovaries than testes was observed in *P. monodon* broodstock (Figure 3.86).

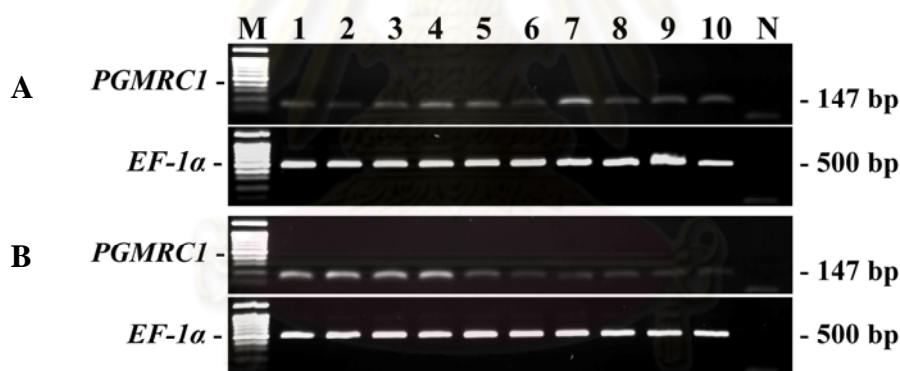


Figure 3.86 A 1.5% ethidium bromide-stained agarose gel showing RT-PCR of *PGMRC1* using the first strand cDNA of testes and ovaries of juveniles and broodstock of *P. monodon*.

Lanes 1 – 5 and 6 – 10 (A) are the first strand cDNA of ovaries and testes of juvenile *P. monodon*, respectively. Lanes 1 – 5 and 6 – 10 (B) are the first strand cDNA of ovaries and testes of *P. monodon* broodstock. Lanes M and N are a 100 bp DNA marker and the negative control (without the cDNA template), respectively. *EF 1-α* (500 bp) was used as the positive control.

A homologue of *PGMRC1* was identified from suppression subtractive hybridization (SSH) libraries of cDNA from testes (Leelatanawit *et al.*, 2008) of *P. monodon*. Previously, three isoforms of *P. monodon progesterone membrane receptor component 1: PM-PGMRC1-s* (1980 bp), *PM-PGMRC1-m* (2848 bp), and *PM-PGMRC1-l* (2971 bp), with an identical ORF of 573 bp corresponding to a deduced polypeptide of 190 amino acids, were successfully identified in male *P. monodon*. In the present study, one isoform of *PGMRC1* in female *P. monodon* was identified and the full length cDNA was successfully characterized. Only 1 amino acid residue (V for ovarian isoform and A for testis isoform at position 88th) of the ovarian and testis isoforms of deduced *Pm-PGMRC1* were different. 3'UTR of ovarian *Pm-PGMRC1* isoform was not same as any testes *Pm-PGMRC1* isoforms (Figure 3.87).

```

M A D E G A D A V S I E E S 14
ACGCGGGGACTCGACTATCATGGCGGACGAGGGAGCGGACGCCGTCTCCATCGAAGAGTC 60
F L G S L L K E I F T S P L N V F L L G 34
CTTCCTGGGCTCACTACTCAAAGAAATATTCACCTCCCCACTTAATGTGTTCCTCTGGG 120
V C T V L I Y K I F R S S D G S G G A T 54
TGCTGTACCGTCCCTCATCTATAAGATATTCGTTCCGTCCGATGGCAGTGGAGGAGCAAC 180
G P V E P P V P K M K R Q D M T L E Q L 74
AGGTCCAGTGAACCTCCTGTGCCAAGATGAAACGACAGGACATGACCTTGGAGCAGTT 240
K Q Y D G M G E H G R V C V A V N G K I 94
GAAGCAGTATGATGGCATGGGGGAGCATGGGCGTGTATGTGGCAGTTAATGGCAAGAT 300
F D V T R G S K F Y G P G G P Y S A F A 114
CTTTGATGTCACCCGAGGCTCCAAGTTCATGGCCAGGTGGGCCGTATTCTGCCTTTGC 360
G R D A T R A L A T F S V K D V K E E Y 134
TGGCCGAGATGCAACAAGAGCTCTGGCAACCTTCAGTGTAAAGGATGTAAGGAGYTA 420
D D L S D L S S M Q M D S V R E W E M Q 154
CGATGACCTCAGTGACCTCCTCTATGCAGATGGACTCTGTCCAGGAATGGGAGATGCA 480
F T E K Y D Y I G K F L K P G E Q P T E 174
GTTACAGAAAAGTACGATATATGGTAAATTTTGAAAACGAGGAGAACCACCCACAGA 540
Y S D D E E A K D T K A K T D D * 190
GTACTCAGATGATGAGGAAGCAAAGGACACCAAAGCGAAGACGGATGATTAGATGTAGTT 600

TTPM-PGMRC1-M GAGGTGATTGCGCATTGCTGTATAGGTTAAGGCCTCTCGGTTCCACCAGACTCCAAGGCC 660
TTPM-PGMRC1-L GAGGTGATTGCGCATTGCTGTATAGGTTAAGGCCTCTCGGTTCCACCAGACTCCAAGGCC 660
TTPM-PGMRC1-S GAGGTGATTGCGCATTGCTGTATAGGTTAAGGCCTCTCGGTTCCACCAGACTCCAAGGCC 660
OVPM-PGMRC1.2040 GAGGTGATTGCGCATTGCTGTATAGGTTAAGGCCTCTCGGTTCCACCAGACTCCAAGGCC 660
*****

TTPM-PGMRC1-M CTTGAGCATGGTCTTAAGATTAGGATGTGGACGTGAAAAAAGTAAAAAAGAAAAAAG 720
TTPM-PGMRC1-L CTTGAGCATGGTCTTAAGATTAGGATGTGGACGTGAAAAAAGTAAAAAAGAAAAAAG 720
TTPM-PGMRC1-S CTTGAGCATGGTCTTAAGATTAGGATGTGGACGTGAAAAAAGTAAAAAAGAAAAAAG 720
OVPM-PGMRC1.2040 CTTGAGCATGGTCTTAAGATTAGGATGTGGACGTGAAAAAAGTAAAAAAGAAAAAAG 720
*****

TTPM-PGMRC1-M AACCCC---ACTCAATTAGTCACTAA-TGATACGGTGTGATGGAAAAGCCTACATTAGG 776
TTPM-PGMRC1-L AACCCC---ACTCAATTAGTCACTAA-TGATACGGTGTGATGGAAAAGCCTACATTAGG 776
TTPM-PGMRC1-S AACCCC---ACTCAATTAGTCACTAA-TGATACGGTGTGATGGAAAAGCCTACATTAGG 776
OVPM-PGMRC1.2040 AACCCCTCGTGCCGAATTCGGCAGGCGAAGCTGTACC--TCTCGTGGTCTGTTCTGAAG 779
*****
* * * * *

TTPM-PGMRC1-M TTGGGGGTTGGAGGTTTA--AACTATATGTAAACTACTACTTTTATATTTTCTCAT-- 832
TTPM-PGMRC1-L TTGGGGGTTGGAGGTTTA--AACTATATGTAAACTACTACTTTTATATTTTCTCAT-- 832
TTPM-PGMRC1-S TTGGGGGTTGGAGGTTTA--AACTATATGTAAACTACTACTTTTATATTTTCTCAT-- 832
OVPM-PGMRC1.2040 CCCACCTCAGGAAGCTCGTCAAGGAGGTCGTTAGCATCCCCTGGTCTCGTCCGTCACGC 839
* * * * *

TTPM-PGMRC1-M --AAGGGGCTAATTAATCCCAAATATGTTCTCAATAAAGATTGTCTACTTTGAACAATTT 890
TTPM-PGMRC1-L --AAGGGGCTAATTAATCCCAAATATGTTCTCAATAAAGATTGTCTACTTTGAACAATTT 890
TTPM-PGMRC1-S --AAGGGGCTAATTAATCCCAAATATGTTCTCAATAAAGATTGTCTACTTTGAACAATTT 890
OVPM-PGMRC1.2040 AGAAGGTCTCCACCACCCAGAGGACTTTGTAGTACGG--TGCCGCTCTATGACTGGCT 897
* * * * *

```


TTPM-PGMRC1-M ATCGATATGTGGTGACTTTGGTTAGTCTGGGTGAGCCATGAAAGTTTGAGTAGGAGGAGC 950
 TTPM-PGMRC1-L ATCGATATGTGGTGACTTTGGTTAGTCTGGGTGAGCCATGAAAGTTTGAGTAGGAGGAGC 950
 TTPM-PGMRC1-S ATCGATATGTGGTGACTTTGGTTAGTCTGGGTGAGCCATGAAAGTTTGAGTAGGAGGAGC 950
 OVPM-PGMRC12040 GACGGCG-ACCGCGTGTGACGACGAAGTGGTGCCTCGAAGGCTGAG---GAGTACG 953
 * * * * *
 TTPM-PGMRC1-M AGGAGGTGACAAGATCAGTCATTATCAGGCTTATTGGGGTATTTTCATAAGGTATA-ATCT 1009
 TTPM-PGMRC1-L AGGAGGTGACAAGATCAGTCATTATCAGGCTTATTGGGGTATTTTCATAAGGTATA-ATCT 1009
 TTPM-PGMRC1-S AGGAGGTGACAAGATCAGTCATTATCAGGCTTATTGGGGTATTTTCATAAGGTATA-ATCT 1009
 OVPM-PGMRC12040 CTGTGGTCAAGACGTCAGTCTCAAAGCGGAGGAACTGGGCTCCATGTGGTAGACAAC 1013
 * * * * *
 TTPM-PGMRC1-M TGCAGTAAAAATG---GAAAAATAAGTCTCTTACAAAGGAGAGAGAAGGCTGATAGATA 1065
 TTPM-PGMRC1-L TGCAGTAAAAATG---GAAAAATAAGTCTCTTACAAAGGAGAGAGAAGGCTGATAGATA 1065
 TTPM-PGMRC1-S TGCAGTAAAAATG---GAAAAATAAGTCTCTTACAAAGGAGAGAGAAGGCTGATAGATA 1065
 OVPM-PGMRC12040 TGAAGAAAAATTATCTGTTATTGAGAAGCCTACCGAAGAGGTAGTAGAGCGGACTCTG 1073
 * * * * *
 TTPM-PGMRC1-M TGCAGCTTTGTAGACCAATGCAAGCAACAAGTATGTGTATACAGATTAATATAATTATAG 1125
 TTPM-PGMRC1-L TGCAGCTTTGTAGACCAATGCAAGCAACAAGTATGTGTATACAGATTAATATAATTATAG 1125
 TTPM-PGMRC1-S TGCAGCTTTGTAGACCAATGCAAGCAACAAGTATGTGTATACAGATTAATATAATTATAG 1125
 OVPM-PGMRC12040 TTTACGTCGCCAGAAGATCCAGCTGGGAAAGAGTCCGCTGGCCCTCTATTCTGTAAAGTC 1133
 * * * * *
 TTPM-PGMRC1-M AAGTAATTATTGAAGGATTGGATCCCAATTGAAACACAGCACCTACCAAACTTATCCTATT 1185
 TTPM-PGMRC1-L AAGTAATTATTGAAGGATTGGATCCCAATTGAAACACAGCACCTACCAAACTTATCCTATT 1185
 TTPM-PGMRC1-S AAGTGATTATTGAAGGATTGGATCCCAATTGAAACACAGCACCTACCAAACTTATCCTATT 1185
 OVPM-PGMRC12040 AAGCCACCTGTCGCGCAACAGAGCTGC-----CATAAAGACTGCTGAGGTTGCT----- 1183
 * * * * *
 TTPM-PGMRC1-M GTGTGATATATTT-GTATAGAT-GGTTGAAATGTTGTTTTGTGTTGGAATAAATGAATCAT 1243
 TTPM-PGMRC1-L GTGTGATATATTT-GTATAGAT-GGTTGAAATGTTGTTTTGTGTTGGAATAAATGAATCAT 1243
 TTPM-PGMRC1-S GTGTGATATATTT-GTATAGAT-GGTTGAGATGTTGTTTTGTGTTGGAATAAATGAATCAT 1243
 OVPM-PGMRC12040 -TGCGATACCTTGAGGATAGACCGAAGGAAAACCTGGCTCGCTTCGATTG-----TCCC 1236
 * * * * *
 TTPM-PGMRC1-M AGTAGTTTTGAAAATGTTTATGAGAATG-ATTGGATATAGTTTATGAATGAGCAGCCC 1302
 TTPM-PGMRC1-L AGTAGTTTTGAAAATGTTTATGAGAATG-ATTGGATATAGTTTATGAATGAGCAGCCC 1302
 TTPM-PGMRC1-S AGTAGTTTTGAAAATGTTTATGAGAATG-ATTGGATATAGTTTATGAATGAGCAGCCC 1302
 OVPM-PGMRC12040 AGCGCCACTGAGGACT-CTATATAACTATACATTTGGTCCAGCCCTGGCTAAAACGACTC 1295
 * * * * *
 TTPM-PGMRC1-M AAAGATGATGAGTTGGGAAGAGTGCA---AGTGCAAGGAATTCATCCTCAAATCAAACCTT 1359
 TTPM-PGMRC1-L AAAGATGATGAGTTGGGAAGAGTGCA---AGTGCAAGGAATTCATCCTCAAATCAAACCTT 1359
 TTPM-PGMRC1-S AAAGATGATGAGTTGGGAAGAGTGCA---AGTGCAAGGAATTCATCCTCAAATCAAACCTT 1359
 OVPM-PGMRC12040 GGCAGCTGCGCAACGGGAAGGCGAACCTAAGAGCTNTGAGG-CGTTCTGGCGCGGTGCA 1354
 * * * * *
 TTPM-PGMRC1-M TCAGCCTTATAGAATACTGACAGAGGACTCATAATTGCTGGTCTGACTCAGAGTTATTTT 1419
 TTPM-PGMRC1-L TCAGCCTTATAGAATACTGACAGAGGACTCATAATTGCTGGTCTGACTCAGAGTTATTTT 1419
 TTPM-PGMRC1-S TCAGCCTTATAGAATACTGACAGAGGACTCATAATTGCTGGTCTGACTCAGAGTTATTTT 1419
 OVPM-PGMRC12040 ACAGCCGTTGAGAACCCTATCAAGCGCCGCGGAAAGGTTCTCCACGCAAACTACG--A 1412
 * * * * *
 TTPM-PGMRC1-M ATACCTAACCTCTTGCCAGCATGGCATGATCCCATCCTTTTCTAATCTACCATGATTTA 1479
 TTPM-PGMRC1-L ATACCTAACCTCTTGCCAGCATGGCATGATCCCATCCTTTTCTAATCTACCATGATTTA 1479
 TTPM-PGMRC1-S ATACCTAACCTCTTGCCAGCATGGCATGATCCCATCCTTTTCTAATCTACCATGATTTA 1479
 OVPM-PGMRC12040 AGGACCAGCCAGTAGTGGTCTGTGGGCGTGGCTAATTAGTTTC--TTGGCCGTG-TTTG 1469
 * * * * *
 TTPM-PGMRC1-M TATTGTACTGTGGATACTCAGTGTGGATCCTTTATTTCAGTCAATGTTTAAACATGTAA 1539
 TTPM-PGMRC1-L TATTGTACTGTGGATACTCAGTGTGGATCCTTTATTTCAGTCAATGTTTAAACATGTAA 1539
 TTPM-PGMRC1-S TATTGTACTGTGGATACTCAGTGTGGATCCTTTATTTCAGTCAATGTTTAAACATGTAA 1539
 OVPM-PGMRC12040 GCTTG-GCTTCGAGTCCC-----GCCACTCCTC-CGGGGAGCTCCCGAAGCTCGA 1521
 * * * * *
 TTPM-PGMRC1-M ATATAGTGTGTTCAACCGTTGCCAAGTCCCTGAAAAGACGTCCTCCAAATCTGCCTGCCTAT 1599
 TTPM-PGMRC1-L ATATAGTGTATTCAACCGTTGCCAAGTCCCTGAAAAGACGTCCTCCAAATCTGCCTGCCTAT 1599
 TTPM-PGMRC1-S ATATAGTGTATTCAACCGTTGCCAAGTCCCTGAAAAGACGTCCTCCAAATCTGCCTGCCTAT 1599
 OVPM-PGMRC12040 CCGCGAAGTACCTCCAGCCCCAAGCAGCAGGAGGAACTACAGAGGACAAAGAAGAGGAA 1581
 * * * * *
 TTPM-PGMRC1-M CACGTTTTGGGAATGGTAAATGACTTAGATATTGGAATGAGAGTGCAAGGGGATTATCTAT 1659
 TTPM-PGMRC1-L CACGTTTTGGGAATGGTAAATGACTTAGATATTGGAATGAGAGTGCAAGGGGATTATCTAT 1659
 TTPM-PGMRC1-S CACGTTTTGGGAATGGTAAATGACTTAGATATTGGAATGAGAGTGCAAGGGGATTATCTAT 1659
 OVPM-PGMRC12040 GCTGTCTGACG-TGGAACCGGA---AGACGCCCTCGGTGAGGAAATGATCCTAG 1637
 * * * * *
 TTPM-PGMRC1-M TTTTCTAGAAGTT-TAGAGAGATAATGTTAACATGATTACTCTGA--ACTTACTGTTG 1716
 TTPM-PGMRC1-L TTTTCTAGAAGTT-TAGAGAGATAATGTTAACATGATTACTCTGA--ACTTACTGTTG 1716
 TTPM-PGMRC1-S TTTTCTAGAAGTT-TAGAGAGATAATGTTAACATGATTACTCTGA--ACTTACTGTTG 1716
 OVPM-PGMRC12040 ACCTTCTTACAGCATGGACGACTACCGTTCAGACGAGGACCCCGACTATTCCGCAAGCG 1697
 * * * * *
 TTPM-PGMRC1-M AGTGTTTTTCAGTACTCTTTTCTA--ACGAGTCTTTAGATGACATGTAGGTTCTGGCACA 1774
 TTPM-PGMRC1-L AGTGTTTTTCAGTACTCTTTTCTA--ACGAGTCTTTAGATGACATGTAGGTTCTGGCACA 1774
 TTPM-PGMRC1-S AGTGTTTTTCAGTACTCTTTTCTA--ACGAGTCTTTAGATGACATGTAGGTTCTGGCACA 1774
 OVPM-PGMRC12040 A-CACCTCCACCAGCAGCTCGAGTACAGTCCGACCGACCATGAGGAGGCGGAGCGCCC 1756
 * * * * *
 TTPM-PGMRC1-M ACATGTGAAAGATGTATCTCGAGAGACAACAGGATCATAATGCTGCCTTGTAACTGTTTC 1834
 TTPM-PGMRC1-L ACATGTGAAAGATGTATCTCGAGAGACAACAGGATCATAATGCTGCCTTGTAACTGTTTC 1834

```

TTPM-PGMRC1-S          ACATGTGAAAGATGTATCTCGAGAGACAACAGGATCATAATGCTGCCTTGTAACTGTTC 1834
OVPM-PGMRC12040       TT-CACCGAGGACG-ACCTCAAGAAAGGAAC----CCACGAAGGCCAGCGAAGGAGAACCT 1810
          * * * * * * * * * * * * * * * * * * * *
TTPM-PGMRC1-M          TTCATCTTTAAGCAAGTAAGGCCTTTAGGTAGTGTGTCAGTCATT--GTAAAGAGTTTGT 1892
TTPM-PGMRC1-L          TTCATCTTTAAGCAAGTAAGGCCTTTAGGTAGTGTGTCAGTCATT--GTAAAGAGTTTGT 1892
TTPM-PGMRC1-S          TTCATCTTTAAGCAAGTAAGGCCTTTAGGTAGTGTGTCAGTCATT--GTAAAGAGTTTGT 1892
OVPM-PGMRC12040       CGGTCTCTGGGGCAGCAGCGCCCCGGGAGGGCAAAGCAGCCAGGTGACGACCAAGGTG 1870
          * * * * * * * * * * * * * * * * * * * *
TTPM-PGMRC1-M          TGA--GAAATGAAGGCAT-AAACACTAGGCTTAGTTGACTGGGGACTGTTTCATCATTCA 1949
TTPM-PGMRC1-L          TGA--GAAATGAAGGCAT-AAACACTAGGCTTAGTTGACTGGGGACTGTTTCATCATTCA 1949
TTPM-PGMRC1-S          TGA--GAAATGAAGGCAT-AAACACTAGGCTTAGTTGACTGGGGACTGTTTCATCATTCA 1949
OVPM-PGMRC12040       TCCTGACGGTGGTGCACCCAGAGGACAAGCCT-GCGGAAGGGGATGCCCCGAGGTTGG 1929
          * * * * * * * * * * * * * * * * * * * *
TTPM-PGMRC1-M          GAAATTTGTACAAAAA----AAAAAAGTTATGACTTGCTCT-----CTTAAGTAAATTC 1999
TTPM-PGMRC1-L          GAAATTTGTACAAAAA----AAAAAAGTTATGACTTGCTCT-----CTTAAGTAAATTC 1999
TTPM-PGMRC1-S          GAAATTTGTACAAAAA----AAAAAAGTTATGACTTGCTCT-----CTTAAGTAAATTC 1987
OVPM-PGMRC12040       GAAGTCGGCGGCGGAGGTGGAGTAGGGATACGGATATTGTTATGACATTTATATAAGTTT 1989
          * * * * * * * * * * * * * * * * * * * *
TTPM-PGMRC1-M          CTTGGCACTAAAAGAAAAGAGGTGTTTTTAATAAGAATAAGATGATTGGGCATATAGAT 2059
TTPM-PGMRC1-L          CTTGGCACTAAAAGAAAAGAGGTGTTTTTAATAAGAATAAGATGATTGGGCATATAGAT 2059
TTPM-PGMRC1-S          -----
OVPM-PGMRC12040       TATTGTATTTTTAATAACTAGTTTACTTCTATTTAAAAAATAAATAAATAAATAAATAA 2040
          -----
TTPM-PGMRC1-M          TTATATGCTTTGTACCTCCAGCCAGTAGAGGTAATAAGATTATGCTAACAGCTTCTAT 2119
TTPM-PGMRC1-L          TTATATGCTTTGTACCTCCAGCCAGTAGAGGTAATAAGATTATGCTAACAGCTTCTAT 2119
TTPM-PGMRC1-S          -----
OVPM-PGMRC12040       -----
TTPM-PGMRC1-M          GTTCAACAGGATTATATTTTTGATGTTGTAGTTGATTACCCCTTATAAACGTATGAAGAAA 2179
TTPM-PGMRC1-L          GTTCAACAGGATTATATTTTTGATGTTGTAGTTGATTACCCCTTATAAACGTATGAAGAAA 2179
TTPM-PGMRC1-S          -----
OVPM-PGMRC12040       -----
TTPM-PGMRC1-M          TGTTCATTTTAAAGCTTACGAGTTTTTCATTTCTTATAAAAACTGATAAACAGAAAGTTGA 2239
TTPM-PGMRC1-L          TGTTCATTTTAAAGCTTACGAGTTTTTCATTTCTTATAAAAACTGATAAACAGAAAGTTGA 2239
TTPM-PGMRC1-S          -----
OVPM-PGMRC12040       -----
TTPM-PGMRC1-M          ATGAGTGTCTTCTCCCATGGCTTGATGGTTGCAACACTAGATGTATATGATCAAGGCTTT 2299
TTPM-PGMRC1-L          ATGAGTGTCTTCTCCCATGGCTTGATGGTTGCAACACTAGATGTATATGATCAAGGCTTT 2299
TTPM-PGMRC1-S          -----
OVPM-PGMRC12040       -----
TTPM-PGMRC1-M          CCTTCTTTTCACACATCAATGTTTGATAAAAGGCAGTTGTGAAAGGAAGATCCAGGAAGC 2359
TTPM-PGMRC1-L          CCTTCTTTTCACACATCAATGTTTGATAAAAGGCAGTTGTGAAAGGAAGATCCAGGAAGC 2359
TTPM-PGMRC1-S          -----
OVPM-PGMRC12040       -----
TTPM-PGMRC1-M          TTCCACTAATGGCTTAAAAGCCTGATAAGTGAGTGTATTCTTAACAAAGGAACGCCGA 2419
TTPM-PGMRC1-L          TTCCACTAATGGCTTAAAAGCCTGATAAGTGAGTGTATTCTTAACAAAGGAACGCCGA 2419
TTPM-PGMRC1-S          -----
OVPM-PGMRC12040       -----
TTPM-PGMRC1-M          GGCAGCTGTTGCAGTGCCTGGTGGTGTAAAGGTCCTGGGGGATGTGATCTTCATTGATGAT 2479
TTPM-PGMRC1-L          GGCAGCTGTTGCAGTGCCTGGTGGTGTAAAGGTCCTGGGGGATGTGATCTTCATTGATGAT 2479
TTPM-PGMRC1-S          -----
OVPM-PGMRC12040       -----
TTPM-PGMRC1-M          CTAGATTTATCATTATAAGGTATACTACTTTTGTATGTTTCAATTTTGTATTTTTTCATAT 2539
TTPM-PGMRC1-L          CTAGATTTATCATTATAAGGTATACTACTTTTGTATGTTTCAATTTTGTATTTTTTCATAT 2538
TTPM-PGMRC1-S          -----
OVPM-PGMRC12040       -----
TTPM-PGMRC1-M          CCTTTATTTTCTATTTTATTTATTTTCTTTTCTTTTCTTTCCATATAGGGAGAATTTATATT 2599
TTPM-PGMRC1-L          CCTTTATTTTCTATTTTATTTATTTTCTTTTCTTTTCTTTCCATATAGGGAGAATTTATATT 2598
TTPM-PGMRC1-S          -----
OVPM-PGMRC12040       -----
TTPM-PGMRC1-M          TTGGACATCAGAGTTTCGTGAGCTGGAAATTCCTGTAATTGTGTGTGCATACCAAGTTTTT 2659
TTPM-PGMRC1-L          TTGGACATCAGAGTTTCGTGAGCTGGAAATTCCTGTAATTGTGTGTGCATACCAAGTTTTT 2658
TTPM-PGMRC1-S          -----
OVPM-PGMRC12040       -----
TTPM-PGMRC1-M          GGCTAGCTATATCCAGCAATCTGTTCATTTGGCATTCCCTGAAAGTTGCTCTTCAGGCTTT 2719
TTPM-PGMRC1-L          GGCTAGCTATATCCAGCAATCTGTTCATTTGGCATTCCCTGAAAGTTGCTCTTCAGGCTTT 2718
TTPM-PGMRC1-S          -----
OVPM-PGMRC12040       -----

```

```

TPM-PGMRC1-M      GCGTGAAGGAGTTGATTTAACTTTGTGATATTTAGAGAAGCAGAATTTGTATTTATATTT 2779
TPM-PGMRC1-L      GCGTGAAGGAGTTGATTTAACTTTGTGATATTTAGAGAAGCAGAATTTGTATTTATATTT 2778
TPM-PGMRC1-S      -----
OVPM-PGMRC12040  -----

TPM-PGMRC1-M      TTTACACATTGTCAATGTAGTTTGATAATATCCACATGGAACAAATGTTAAAAAAAAAAAA 2839
TPM-PGMRC1-L      TTTACACATTGTCAATGTAGTTTGATAATATCCACATGGAACAAATGTTAAAAAAGGAAA 2838
TPM-PGMRC1-S      -----
OVPM-PGMRC12040  -----

TPM-PGMRC1-M      AAAAA-----AAAAAAAAAAAA----- 2854
TPM-PGMRC1-L      AAAAAAGTCTGTGTAATAAAGGAAAACCTTCTCCAATAGATGAAAGTTTTTCATTTATGTACA 2898
TPM-PGMRC1-S      -----
OVPM-PGMRC12040  -----

TPM-PGMRC1-M      -----
TPM-PGMRC1-L      GTTGAGTGTAAATATTGTTCTAAATGAAATCAATAAATTTACCCAATAAAAAAAAAAAAA 2958
TPM-PGMRC1-S      -----
OVPM-PGMRC12040  -----

TPM-PGMRC1-M      -----
TPM-PGMRC1-L      AAAAAAAAAAAAAAAAAAAAAA 2978
TPM-PGMRC1-S      -----
OVPM-PGMRC12040  -----

```

Figure 3.87 The sequence alignments between the full length cDNA of *Pm-PGMRC1* initially characterized one isoform from ovaries (OVPM-PGMRC12040) and three isoforms from testes (TPM-PGMRC1-S, -M and -L) of *P. monodon*. The difference of an amino acid residue of deduced PM-PGMRC1 between ovarian and testis isoforms was illustrated in underlined.

To identify whether ovarian and testicular isoforms were specifically expressed in different gonadal tissues or not, expression profiles of *PGMRC1* transcripts in ovaries and testes of *P. monodon* juveniles and broodstock were estimated by RT-PCR using ovarian or testicular specific primers.

RT-PCR indicated that both ovarian and testicular forms of *PGMRC1* were co-expressed in each gonadal tissue. The former was more abundantly expressed in ovaries but expressed in a lower level in testes (Figure 3.88; A). The latter was expressed in the opposite direction (Figure 3.88; B). The results suggested that the ovarian and testicular forms of *PGMRC1* should be encoded from different loci.

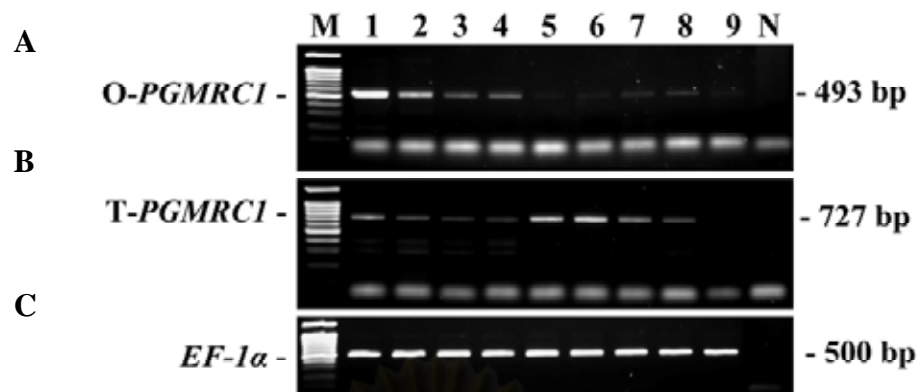


Figure 3.88 A 1.5% ethidium bromide-stained agarose gel showing RT-PCR of *PGMRC1* transcript using primers specifically amplified an ovarian form (A) and testicular forms (B) of *PGMRC1* against the first strand cDNA from ovaries and testes of *P. monodon*.

Lanes 1 & 2 (A, B and C) = juvenile ovaries. Lanes 3 & 4 (A, B and C) = broodstock ovaries. Lanes 5 & 6 (A, B and C) = juvenile testes. Lanes 7 & 8 (A, B and C) = broodstock testes. Lanes M and N are a 100 bp DNA marker and the negative control (without the cDNA template), respectively. Lane 9 is genomic DNA of *P. monodon*. *EF 1- α* (500 bp, C) was used as the positive control.

3.7 Semiquantitative RT-PCR of functionally important genes during ovarian development of *P. monodon*

Expression levels of 5 genes identified by SSH ovarian libraries; *keratinocytes associated protein 2*, *Ser/Thr kinase chk1*, *DNA replication licensing factor mcm2* (forward library), *selenoprotein M precursor* and *egalitarian* (reverse library) were determined using semiquantitative RT-PCR analysis. This technique requires optimization of several parameters including concentration of primers, $MgCl_2$, and the number of PCR cycles.

Primers for the target genes were designed. The non-quantitative RT-PCR was carried out by reaction recipes and conditions (annealing temperature of 53°C) previously used for screening of expression patterns of various genes. *EF-1 α* gene was used as an internal control.

3.7.1 Optimization of primer concentration, MgCl₂ concentration and cycle numbers

RT-PCR of each gene was carried out with fixed components except primer concentrations (between 0.02-0.4 μ M, data not shown). Lower concentrations may result in non-quantitative amplification whereas higher concentrations of primer may leave a large amount of unused primers which could give rise to non-specific amplification products. The suitable concentration of primers for each gene is shown by Table 3.41.

The optimal concentration of MgCl₂ (between 1.0-4.0 mM, data not shown) for each primer pairs was carefully examined using the amplification conditions with the optimized primer concentration. The concentration of MgCl₂ that gave the highest yields and specificity for each PCR product was chosen (Table 3.41).

The number of amplification cycles was important because the product reflecting the expression level should be measured quantitatively before reaching a plateau amplification phase. At the plateau stage, transcripts initially present at different levels may give equal intensity of the amplification products. In this experiment, RT-PCR of each gene was performed using the conditions that primers and MgCl₂ concentrations were optimized between 22 - 35 cycles (data not shown). The number of cycles that gave the highest yield before the product reached a plateau phase of amplification was chosen (Table 3.41).

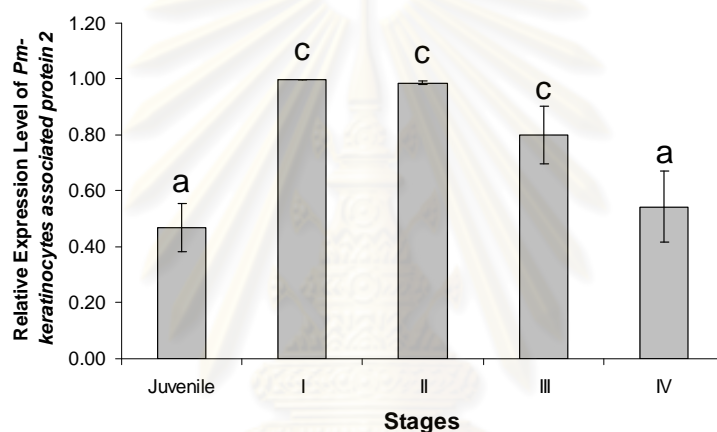
Table 3.41 Optimal primer and MgCl₂ concentrations and the number of PCR cycles for semiquantitative analysis of expression levels of functionally important genes in *P. monodon*

Transcripts	Expected amplicons (bp)	Primer concentration (μ M)	MgCl ₂ concentration (mM)	PCR cycles
From ovaries cDNA library				
<i>keratinocytes associated protein 2</i>	207	0.2	1.5	22
<i>Ser/Thr kinase chk1</i>	269	0.2	1.5	27
<i>DNA replication licensing factor mcm2</i>	321	0.2	1.5	24
<i>selenoprotein M precursor</i>	240	0.2	1.5	22
<i>Egalitarian</i>	313	0.15	1.5	24
Normalized transcripts				
<i>Elongation factor 1-α</i>	500	0.1	1.5	22

3.7.2 Semi-quantitative RT-PCR analysis

3.7.2.1 *keratinocytes associated protein 2*

The expression level of *keratinocytes associated protein 2* in stages I (GSI < 1.5), II (GSI = 2.0 - 4.0) and III (GSI = 4.0 - 6.0) of *P. monodon* broodstock was significantly greater than that of juvenile *P. monodon* ($P < 0.05$). *Keratinocytes associated protein 2* was down-regulated at the final stage of ovarian development ($P < 0.05$) (Figure 3.89).

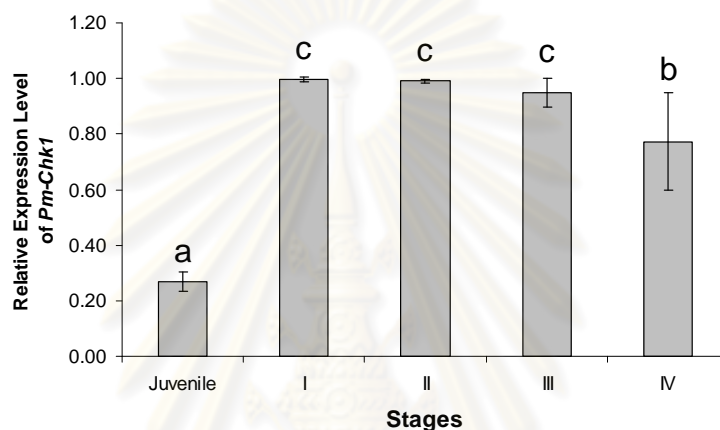


Ovarian stages	Expression levels \pm SD	N
Juveniles	0.4696 \pm 0.086 ^a	3
Stage I (GSI < 1.5)	0.9988 \pm 0.000 ^c	3
Stage II (GSI 2.0-4.0)	0.9855 \pm 0.007 ^c	3
Stage III (GSI 4.0-6.0)	0.8009 \pm 0.103 ^c	3
Stage IV (GSI > 6.0)	0.5430 \pm 0.128 ^a	3

Figure 3.89 Histograms showing relative expression levels of *keratinocytes associated protein 2* in different ovarian developmental stages of *P. monodon*. The same letters indicate that the relative expression levels were not significantly different ($P > 0.05$). Relative expression levels and standard deviation of each group of samples are also shown.

3.7.2.2 Ser/Thr kinase *chk1*

The expression level of *Ser/Thr kinase chk1* in ovaries of *P. monodon* broodstock was significantly greater than that of juveniles ($P < 0.05$). Like *keratinocytes associated protein 2*, this transcript was down-regulated at stage IV (GSI > 6.0 , $P < 0.05$) but the level was still greater than that of juveniles ($P < 0.05$) (Figure 3.90).

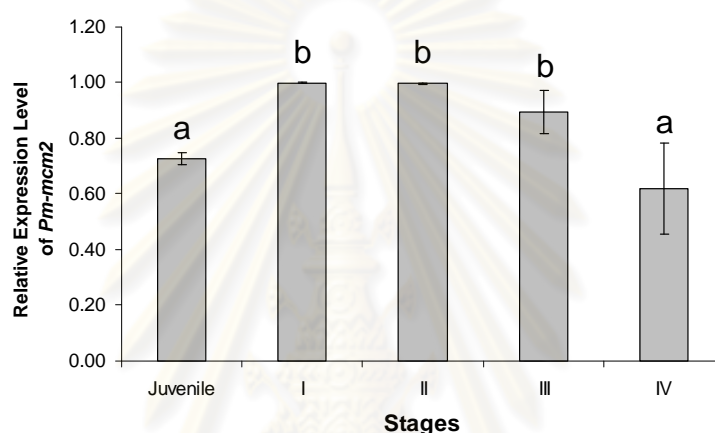


Ovarian stages	Expression levels \pm SD	N
Juveniles	0.2701 \pm 0.034 ^a	3
Stage I (GSI < 1.5)	0.9948 \pm 0.009 ^c	3
Stage II (GSI 2.0-4.0)	0.9901 \pm 0.005 ^c	3
Stage III (GSI 4.0-6.0)	0.9479 \pm 0.052 ^c	3
Stage IV (GSI > 6.0)	0.7731 \pm 0.176 ^b	3

Figure 3.90 Histograms showing relative expression levels of *chk1* in different ovarian developmental stages of *P. monodon*. The same letters indicate that the relative expression levels were not significantly different ($P > 0.05$). Relative expression levels and standard deviation of each group of samples are also shown.

3.7.2.3 DNA replication licensing factor *mcm2*

The expression level of *DNA replication licensing factor mcm2* in stages I (GSI < 1.5), II (GSI = 2.0 - 4.0) and III (GSI = 4.0 - 6.0) of *P. monodon* broodstock was significantly greater than that of juvenile *P. monodon* ($P < 0.05$). *DNA replication licensing factor mcm2* was down-regulated at the final stage of ovarian development ($P < 0.05$) (Figure 3.91).

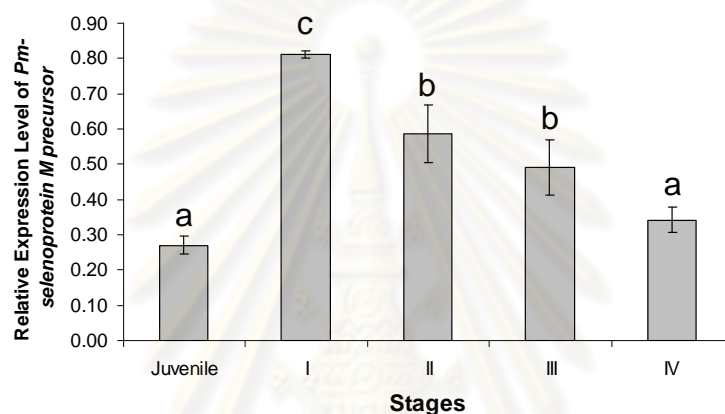


Ovarian stages	Expression levels \pm SD	N
Juveniles	0.7263 \pm 0.021 ^a	3
Stage I (GSI < 1.5)	0.9999 \pm 0.000 ^b	3
Stage II (GSI 2.0-4.0)	0.9964 \pm 0.003 ^b	3
Stage III (GSI 4.0-6.0)	0.8950 \pm 0.077 ^b	3
Stage IV (GSI > 6.0)	0.6190 \pm 0.165 ^a	3

Figure 3.91 Histograms showing relative expression levels of *DNA replication licensing factor mcm2* in different ovarian developmental stages of *P. monodon*. The same letters indicate that the relative expression levels were not significantly different ($P > 0.05$). Relative expression levels and standard deviation of each group of samples are also shown.

3.7.2.4 Selenoprotein *M* precursor

The expression level of *selenoprotein M precursor* at stages I, II and III ovaries of broodstock was greater than that of juvenile *P. monodon* ($P < 0.05$). Interestingly, the highest expression level was found at stage I ovaries (GSI < 1.5). Its levels were significantly decreased at stages II and III ovaries and further decreased at the mature stage ($P < 0.05$) (Figure 3.92).

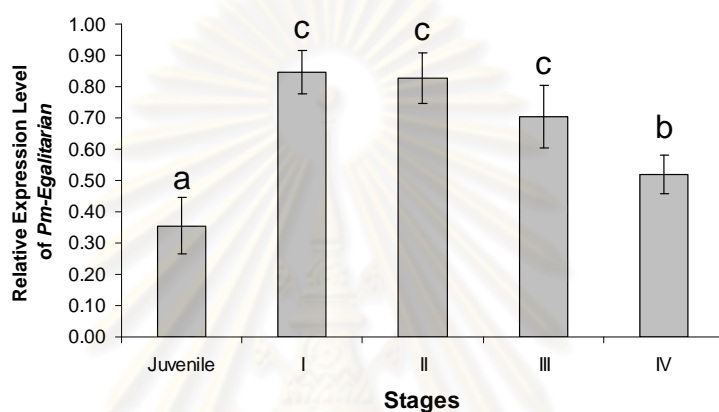


Ovarian stages	Expression levels \pm SD	N
Juveniles	0.2705 \pm 0.026 ^a	3
Stage I (GSI < 1.5)	0.8105 \pm 0.010 ^c	3
Stage II (GSI 2.0-4.0)	0.5856 \pm 0.082 ^b	3
Stage III (GSI 4.0-6.0)	0.4918 \pm 0.079 ^b	3
Stage IV (GSI > 6.0)	0.3425 \pm 0.035 ^a	3

Figure 3.92 Histograms showing relative expression levels of *selenoprotein M precursor* in different ovarian developmental stages of *P. monodon*. The same letters indicate that the relative expression levels were not significantly different ($P > 0.05$). Relative expression levels and standard deviation of each group of samples are also shown.

3.7.2.5 Egalitarian

The expression level of *egalitarian* in ovaries of *P. monodon* broodstock was significantly greater than that of juveniles ($P < 0.05$). Like *Ser/Thr kinase chk1*, this transcript was down-regulated at stage IV (GSI > 6.0 , $P < 0.05$) but the level was still greater than that of juveniles ($P < 0.05$) (Figure 3.93).



Ovarian stages	Expression levels \pm SD	N
Juveniles	0.3553 \pm 0.090 ^a	3
Stage I (GSI < 1.5)	0.8455 \pm 0.070 ^c	3
Stage II (GSI 2.0-4.0)	0.8257 \pm 0.081 ^c	3
Stage III (GSI 4.0-6.0)	0.7044 \pm 0.100 ^c	3
Stage IV (GSI > 6.0)	0.5202 \pm 0.062 ^b	3

Figure 3.93 Histograms showing relative expression levels of *Egalitarian* in different ovarian developmental stages of *P. monodon*. The same letters indicate that the relative expression levels were not significantly different ($P > 0.05$). Relative expression levels and standard deviation of each group of samples are also shown.

3.8 Examination of expression levels of interesting genes related with ovarian development of *P. monodon* by Quantitative real-time PCR

The expression levels of *progesterone receptor-related protein p23* (*Pm-p23*), *progesterin receptor membrane component1* (*Pm-PGMRC1*), *small androgen receptor interacting protein* (*Pm-SARIP*) and *cell division cycle 42* (*Pm-Cdc42*), in ovaries of normal and unilateral eyestalk-ablated *P. monodon* broodstock and *Pm-PGMRC1* in ovaries of 5-HT treated juvenile *P. monodon* were quantitatively estimated by real-time PCR (Figure 3.98 - 3.102).

The standard curves used for quantitative real-time PCR analysis of interesting transcripts are shown by Figures 3.94 - 3.97. High R^2 values and efficiency of amplification of examined transcripts were found. Therefore, these standard curves were acceptable to be used for quantitative estimation of the mRNA levels of *Pm-p23*, *Pm-PGMRC1*, *Pm-SARIP* and *Pm-Cdc42*.

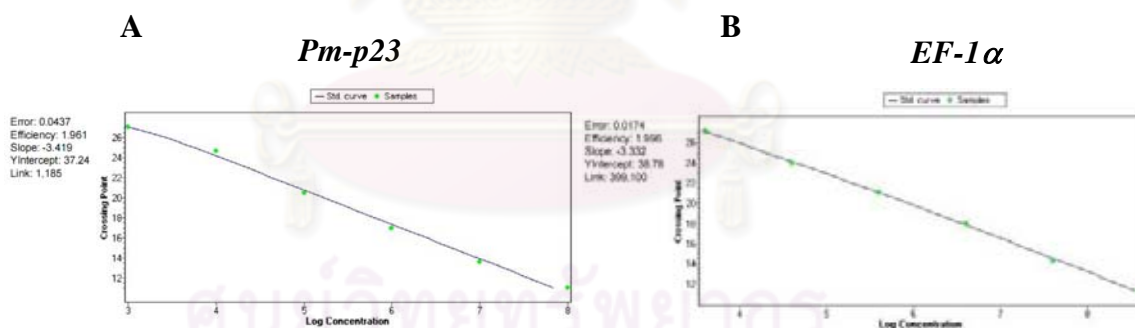


Figure 3.94 Standard curves of *Pm-p23* (A; $R^2 = 0.995$, efficiency = 96.1% or (\log_2) 1.961 and equation; $Y = -3.419 \cdot \log(X) + 37.24$) and *EF-1α* (B; $R^2 = 0.999$, efficiency = 99.6% or (\log_2) 1.996 and equation; $Y = -3.322 \cdot \log(X) + 38.78$) using 10-fold dilution of plasmid DNA of *Pm-p23* and *EF-1α* ($10^3 - 10^8$ copy). *EF-1α* was used as a reference transcript.

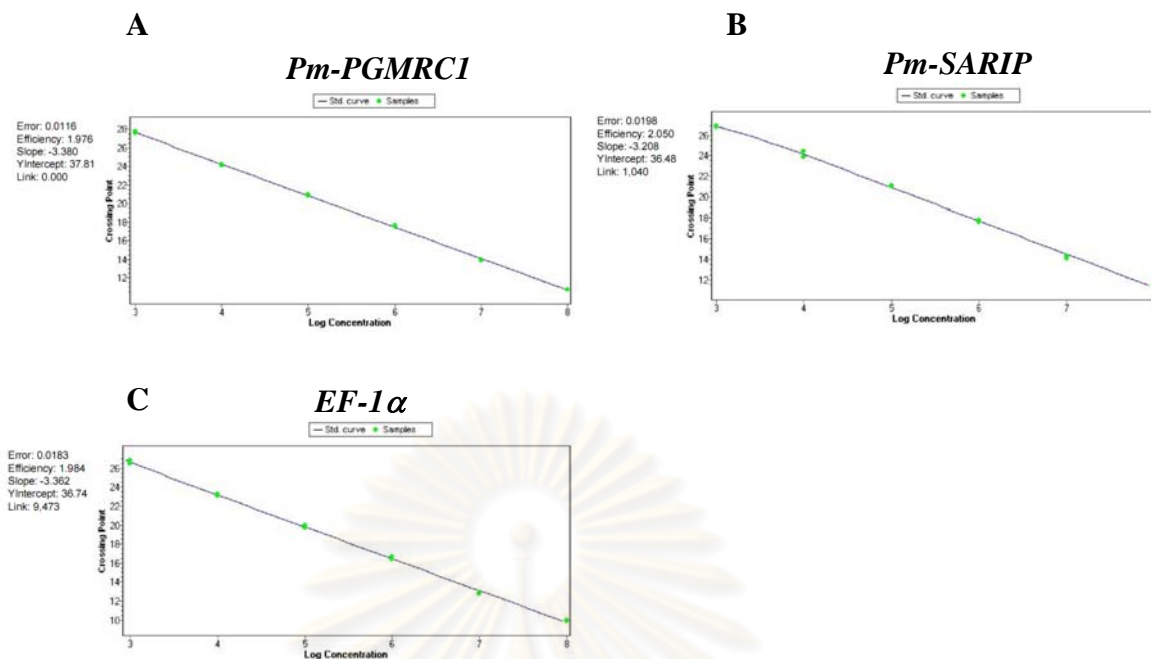


Figure 3.95 Standard curve of *Pm-PGMRC1* (A; $R^2 = 0.999$, efficiency = 97.6% or (\log_2) 1.976 and equation; $Y = -3.380 * \log(X) + 37.81$), *Pm-SARIP* (B; $R^2 = 0.998$, efficiency = 105.0% or (\log_2) 2.050 and equation; $Y = -3.208 * \log(X) + 36.48$) and *EF-1α* (C; $R^2 = 0.999$, efficiency = 98.4% or (\log_2) 1.984 and equation; $Y = -3.362 * \log(X) + 36.74$) using 10-fold dilution of plasmid DNA of *Pm-PGMRC1* or *Pm-SARIP* or *EF-1α* (10^3 – 10^8 copy). *EF-1α* was used as a reference transcript.

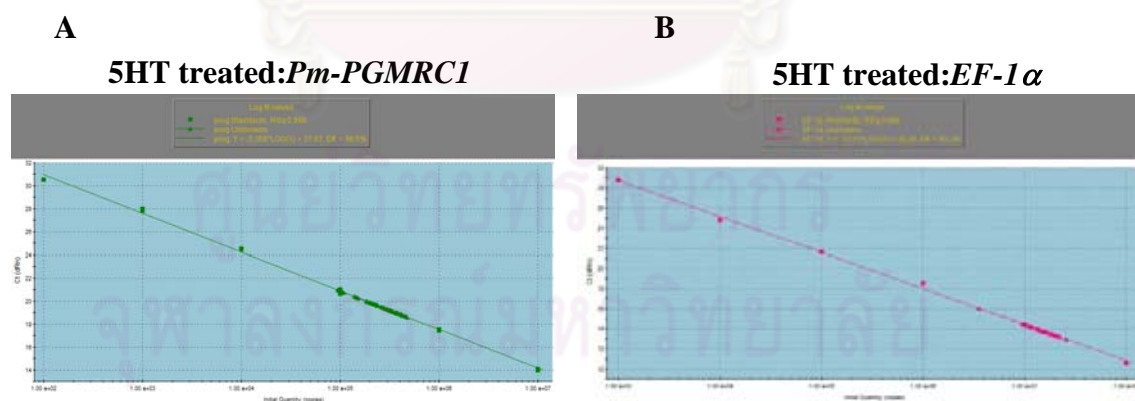


Figure 3.96 Standard curve of *Pm-PGMRC1* (A; $R^2 = 0.998$, efficiency = 90.3% and equation; $-3.579 * \log(X) + 39.48$) and *EF-1α* (B; $R^2 = 0.998$, efficiency = 98.5% and equation $Y = -3.358 * \log(X) + 37.67$) for examined expression profiles of *Pm-PGMRC1* transcript in ovaries of 5-HT treated juvenile *P. monodon*. *EF-1α* was used as a reference transcript.

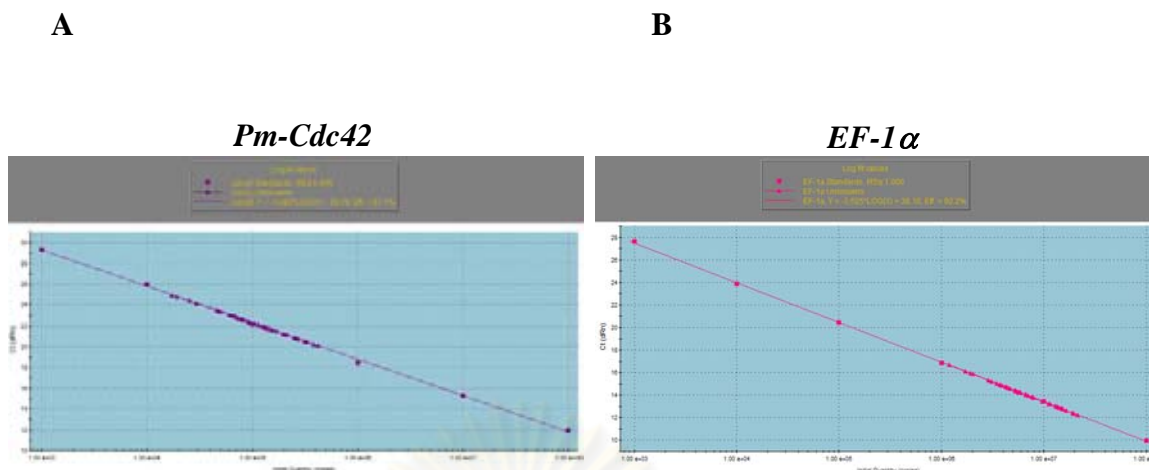
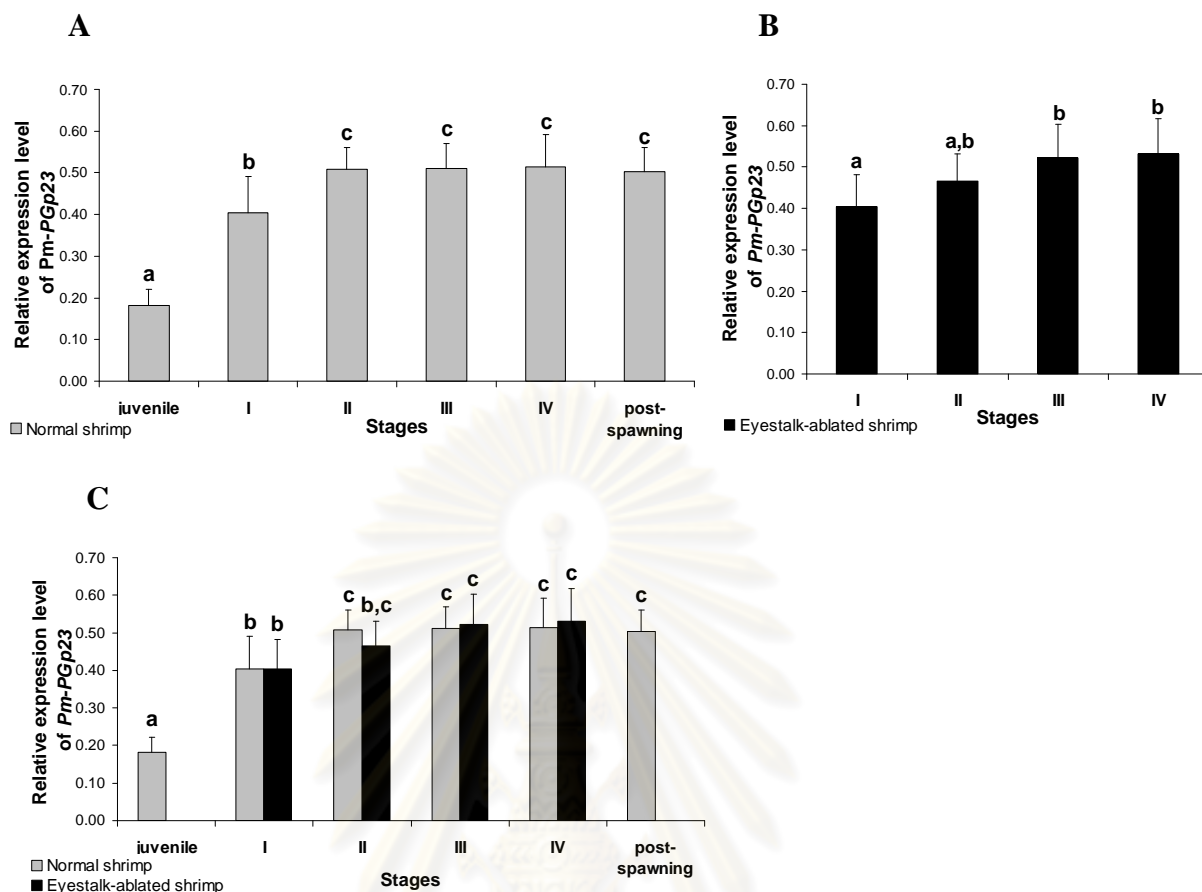


Figure 3.97 Standard curve of *Pm-Cdc42* (A; $R^2 = 0.999$, efficiency = 93.1% and equation; $Y = -3.498 * \log(X) + 39.79$) and *EF-1α* (B; $R^2 = 1.000$ efficiency = 92.2% and equation; $Y = -3.525 * \log(X) + 38.10$) for examined expression profiles of *Pm-Cdc42* transcript using 10-fold dilution of plasmid DNA of *Pm-Cdc42* and *EF-1α* ($10^3 - 10^8$ copy). *EF-1α* was used as a reference transcript.

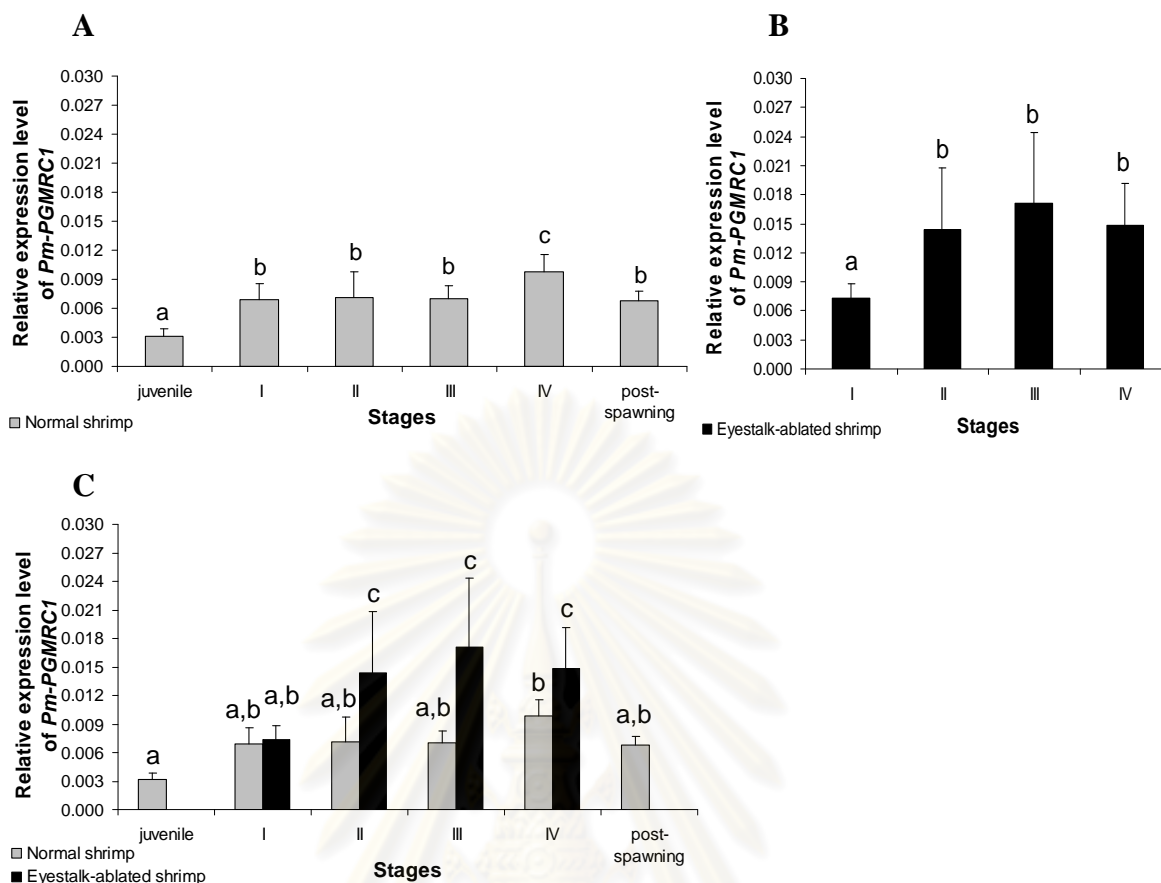
The expression levels of *Pm-p23* in ovaries of both normal and eyestalk-ablated broodstock were significantly greater than that of juveniles (4 month-olds shrimp) ($P < 0.05$). *Pm-p23* was up-regulated at stage II ovaries of normal and at stage III ovaries of eyestalk ablated *P. monodon* broodstock ($P < 0.05$). The expression levels of this gene were comparable at the subsequent stages within each sample group. The mRNA level of *Pm-p23* after spawning was not significantly different from stages I-IV ovaries of normal broodstock ($P > 0.05$) (Figure 3.98). Results clearly indicated that eyestalk ablation had no direct effects on transcription of *p23* in ovaries of *P. monodon* broodstock.

Like *Pm-p23*, the expression levels of *Pm-PGMRC1* in ovaries of both normal and eyestalk-ablated broodstock were clearly greater than that of juveniles (4 month-olds shrimp) ($P < 0.05$). In adults, *Pm-PGRMC1* was up-regulated at the mature stage (stage IV) in normal broodstock ($P < 0.05$). Its expression level was decreased to the normal level at the post-spawning stage ($P < 0.05$) (Figure 3.99). Interestingly, *Pm-PGRMC1* was up-regulated since stage II ovaries in eyestalk ablated *P. monodon* broodstock. The expression level of *Pm-p23* in each of stages II – IV of eyestalk-ablated broodstock was greater than that of normal broodstock ($P < 0.05$)



Ovarian stage	Relative expression level	N	Relative expression level	N
	Normal		Eyestalk-ablated	
Juveniles	0.1810±0.040 ^a	6	-	-
Stage I (GSI < 1.5)	0.4046±0.087 ^b	8	0.4039±0.078 ^a	6
Stage II (GSI 2.0 – 4.0)	0.5079±0.053 ^c	7	0.4653±0.066 ^{a,b}	4
Stage III (GSI 4.0 - 6.0)	0.5109±0.059 ^c	7	0.5216±0.081 ^b	10
Stage IV (GSI > 6.0)	0.5144±0.077 ^c	9	0.5318±0.086 ^b	11
post-spawning (GSI 1.86 – 3.49)	0.5027±0.059 ^c	6	-	-

Figure 3.98 Histograms showing the relative expression profiles of *Pm-p23* during ovarian maturation of normal (A), unilateral eyestalk ablated (B) *P. monodon* broodstock. Data of normal and eyestalk-ablated broodstock were also analyzed together (C). Expression levels were measured as the absolute copy number of *Pm-PGp23* mRNA (25 ng template) and normalized by that of *EF-1 α* mRNA (0.5 ng template). Each bar corresponds to a particular ovarian stage. The same letters indicate that the expression levels were not significantly different ($P > 0.05$). Relative expression levels and standard deviation were also shown.



Ovarian stage	Relative expression level		N	Relative expression level		N
	Normal	Eyestalk-ablated		Normal	Eyestalk-ablated	
Juveniles	0.0031±0.001 ^a	-	5	-	-	
Stage I (GSI < 1.5)	0.0069±0.002 ^b	0.0073±0.001 ^a	9	0.0073±0.001 ^a	6	
Stage II (GSI 2.0 – 4.0)	0.0071±0.003 ^b	0.0144±0.006 ^b	7	0.0144±0.006 ^b	5	
Stage III (GSI 4.0 - 6.0)	0.0070±0.001 ^b	0.0171±0.007 ^b	6	0.0171±0.007 ^b	8	
Stage IV (GSI > 6.0)	0.0098±0.002 ^c	0.0148±0.004 ^b	10	0.0148±0.004 ^b	10	
post-spawning (GSI 1.86 - 3.49)	0.0068±0.001 ^b	-	6	-	-	

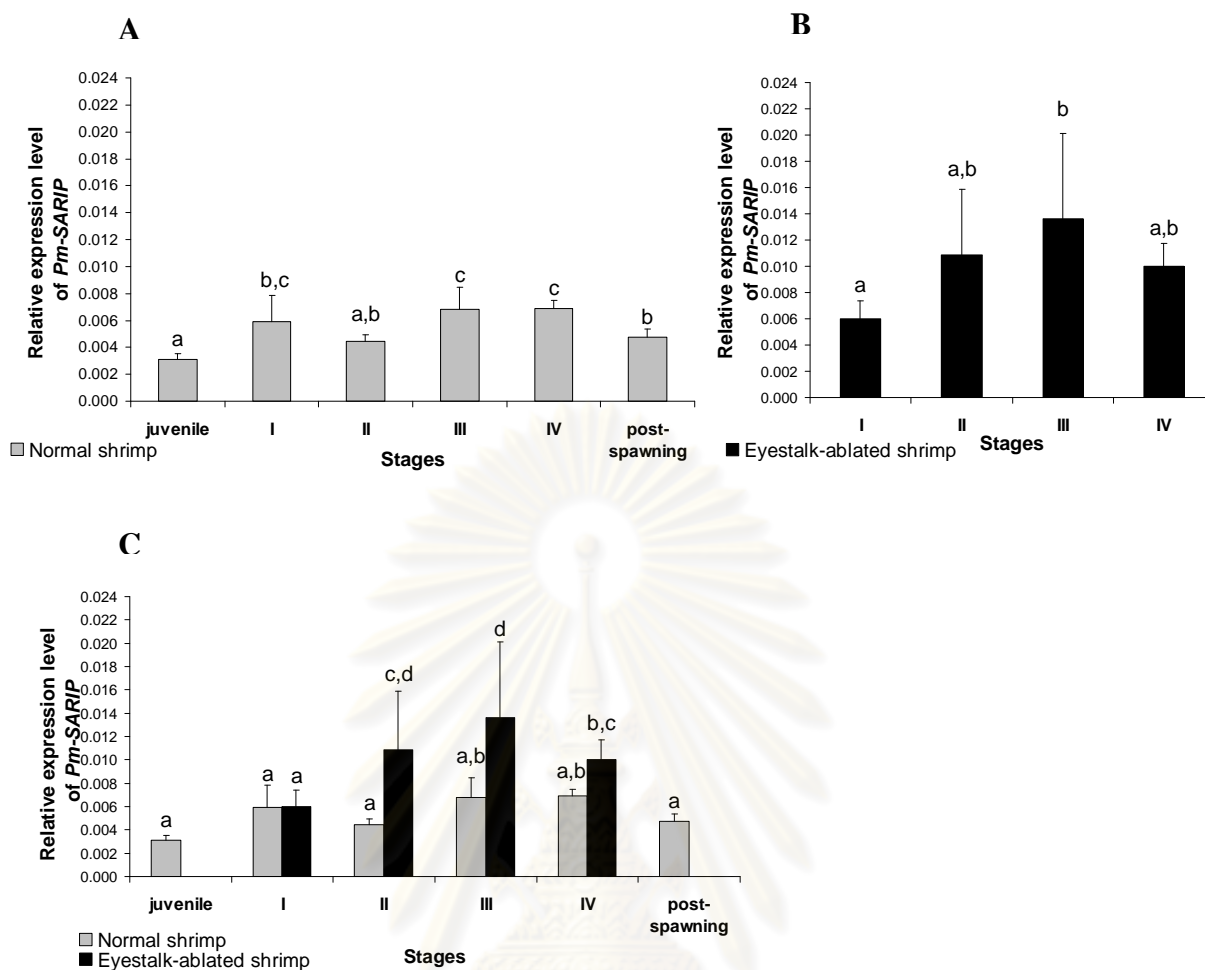
Figure 3.99 Histograms showing the relative expression profiles of *Pm-PGMRC1* during ovarian maturation of normal (A), unilateral eyestalk ablated (B) *P. monodon* broodstock. Data of normal and eyestalk-ablated broodstock were also analyzed together (C). Expression levels were measured as the absolute copy number of *Pm-PGMRC1* mRNA (25 ng template) and normalized by that of *EF-1 α* mRNA (25 ng template). Each bar corresponds to a particular ovarian stage. The same letters indicate that the expression levels were not significantly different ($P > 0.05$). Relative expression levels and standard deviation were also shown.

(Figure 3.99). Results from this study strongly suggested that eyestalk ablation positively affects transcription of *PGMRC1* in ovaries of *P. monodon* broodstock.

Pm-SARIP in ovaries of normal and eyestalk-ablated broodstock were significantly higher than that of juveniles (4 month-olds shrimp) ($P < 0.05$). In normal broodstock, expression levels of *Pm-SARIP* at stages III and IV ovaries was slightly greater than those at stages I and II ovaries ($P > 0.05$). This transcript was significantly decreased to be the same as that of stages I and II after spawning ($P < 0.05$). Interestingly, *Pm-SARIP* was up-regulated at stage II, III and IV ovaries of eyestalk ablated *P. monodon* broodstock ($P < 0.05$). The mRNA levels of *Pm-SARIP* in stages II and III of eyestalk-ablated were greater than those in ovaries of normal broodstock (Figure 3.100). Results also clearly suggested that transcription of *Pm-SARIP* in ovaries of broodstock was affected by eyestalk ablation.

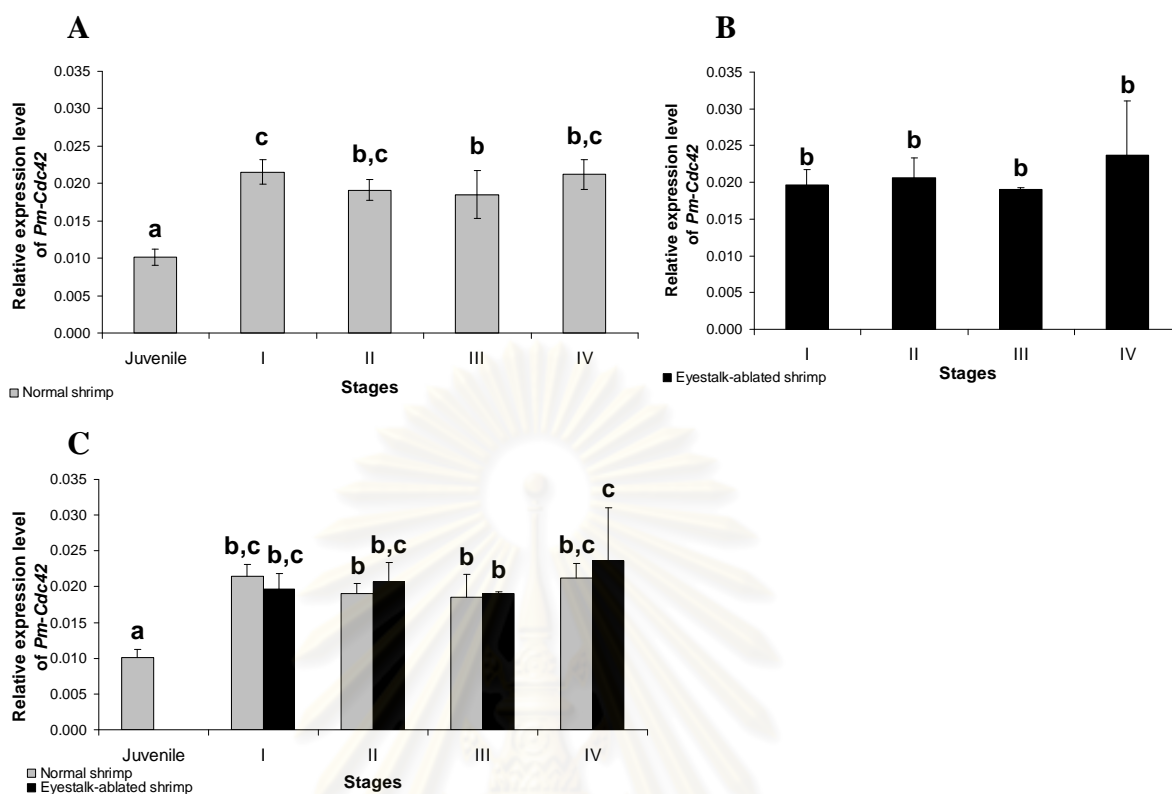
Like other genes in this study, the expression levels of *Pm-Cdc42* in ovaries of normal and eyestalk-ablated broodstock were significantly greater than that of juveniles ($P < 0.05$). In normal broodstock, *Pm-Cdc42* was not significantly different at stage I, II and IV ovaries ($P > 0.05$) but the level was significantly decreased at stage III ovaries compared to the early developmental stage (I, $P < 0.05$). The mRNA level of *Pm-Cdc42* in eyestalk-ablated broodstock was not significantly different throughout the ovarian development ($P > 0.05$) (Figure 3.101). Moreover, the expression levels of *Pm-Cdc42* in the same stages of ovaries of normal and eyestalk-ablated broodstock was not significantly different when different groups of samples were statistically considered together ($P > 0.05$).

Moreover, the expression levels of *Pm-PGMRC1* in ovaries of 5-HT treated *P. monodon* juveniles were also carried out. The level of *Pm-PGMRC1* transcript in each treatment was not significantly different ($P > 0.05$) (Figure 3.102). It is premature at this stage to conclude that 5-HT has no effects on expression of *Pm-PGMRC1*. Accordingly, effects of 5-HT on expression of *Pm-PGMRC1* should be further carried out in *P. monodon* broodstock.



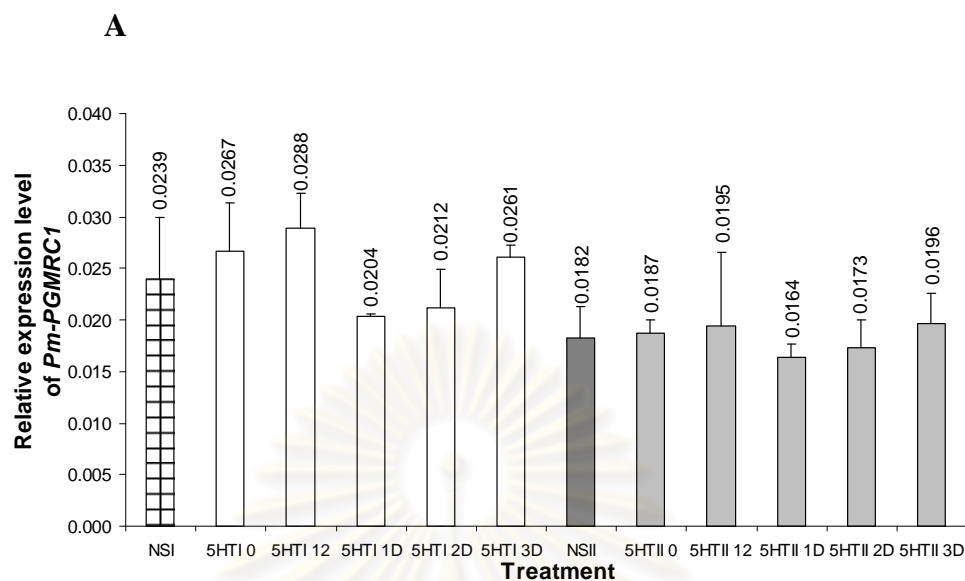
Ovarian stage	Relative expression level	N	Relative expression level	N
	Normal		Eyestalk-ablated	
Juveniles	0.0031±0.000 ^a	5	-	-
Stage I (GSI < 1.5)	0.0059±0.002 ^{b,c}	10	0.0060±0.001 ^a	6
Stage II (GSI 2.0 - 4.0)	0.0045±0.001 ^{a,b}	5	0.0109±0.005 ^{a,b}	5
Stage III (GSI 4.0 - 6.0)	0.0068±0.002 ^c	7	0.0136±0.007 ^b	10
Stage IV (GSI > 6.0)	0.0069±0.001 ^c	9	0.0100±0.002 ^{a,b}	9
post-spawning (GSI 1.86 – 3.49)	0.0048±0.001 ^b	5	-	-

Figure 3.100 Histograms showing the relative expression profiles of *Pm-SARIP* during ovarian maturation of normal (A), unilateral eyestalk ablated (B) *P. monodon* broodstock. Data of normal and eyestalk-ablated broodstock were also analyzed together (C). Expression levels were measured as the absolute copy number of *Pm-SARIP* mRNA (25 ng template) and normalized by that of *EF-1 α* mRNA (25 ng template). Each bar corresponds to a particular ovarian stage. The same letters indicate that the expression levels were not significantly different ($P > 0.05$). Relative expression levels and standard deviation were also shown.



Ovarian stage	Relative expression level		N	Relative expression level		N
	Normal			Eyestalk-ablated		
Juveniles	0.01014±0.001 ^a		4	-		-
Stage I (GSI < 1.5)	0.02152±0.002 ^c		5	0.01964±0.002 ^b		6
Stage II (GSI 2.0 - 4.0)	0.01908±0.001 ^{b,c}		6	0.02068±0.003 ^b		4
Stage III (GSI 4.0 - 6.0)	0.01849±0.003 ^b	0.01	3	904±0.000 ^b	10	10
Stage IV (GSI > 6.0)	0.02121±0.002 ^{b,c}		5	0.02366±0.007 ^b		11

Figure 3.101 Histograms showing the relative expression profiles of *Pm-Cdc42* during ovarian maturation of normal (A), unilateral eyestalk ablated (B) *P. monodon* broodstock. Data of normal and eyestalk-ablated broodstock were also analyzed together (C). Expression levels were measured as the absolute copy number of *Pm-Cdc42* mRNA (25 ng template) and normalized by that of *EF-1 α* mRNA (25 ng template). Each bar corresponds to a particular ovarian stage. The same letters indicate that the expression levels were not significantly different ($P > 0.05$). Relative expression levels and standard deviation were also shown.

**B**

Samples	Average	N
NSI	0.02393±0.0060 ^{b,c,d,e}	3
5HTI 0	0.02667±0.0046 ^{c,d,e}	3
5HTI 12	0.02884±0.0034 ^e	3
5HTI 1D	0.02036±0.0002 ^{b,c,d,e}	3
5HTI 2D	0.02119±0.0038 ^{b,c,d,e}	3
5HTI 3D	0.02611±0.0012 ^{c,d,e}	3
NSII	0.01823±0.0030 ^{a,b,c,d}	3
5HTII 0	0.01866±0.0013 ^{a,b,c,d}	3
5HTII 12	0.01946±0.0071 ^{b,c,d}	3
5HTII 1D	0.01643±0.0012 ^{a,b}	3
5HTII 2D	0.01732±0.0027 ^{a,b,c}	3
5HTII 3D	0.01962±0.0029 ^{b,c,d}	3

Figure 3.102 Expression profiles of *Pm-PGMRC1* in ovaries of 5-HT treated juvenile *P. monodon*. The levels were measured as the absolute copy number of *Pm-PGMRC1* and normalized by that of *EF-1 α* . Each bar corresponds to a particular time intervals after injection with 5-HT. White bars = shrimp injected once with 5-HT; gray bars = shrimp injected twice with 5-HT; NS = shrimp injected with 0.85% NaCl (the control).

3.9 Localization of sex-related transcripts in ovaries of *P. monodon* broodstock

3.9.1 Quantification of the cRNA probes

The amount of cRNA probes was estimated by dot blot analysis. The antisense *TSP* probe was used as the positive control and gave the positive signal between 10 pg - 10 ng. The antisense and sense probes of *Pm-PGMRC1* and *Pm-Cdc42* gave the signal from 100 pg - 10 ng (Figure 3.103). An appropriate amount of the cRNA probe of each transcript was applied for examination of transcriptional localization using *in situ* hybridization.

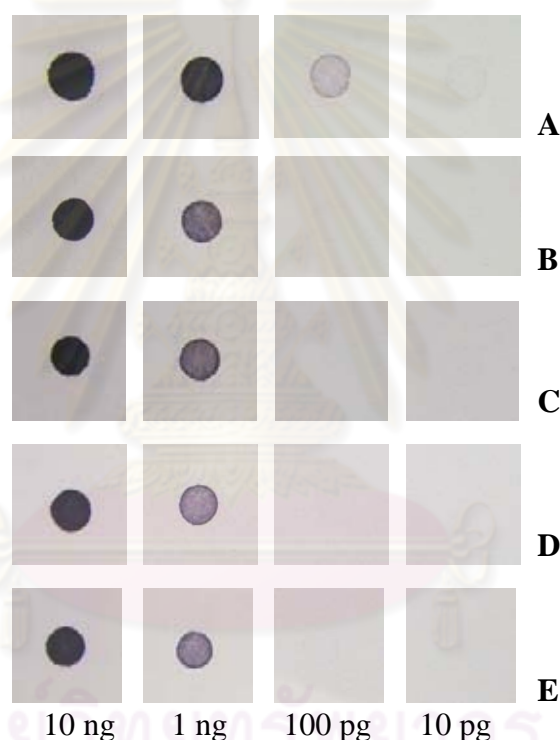


Figure 3.103 Dot blot hybridization using the antisense *Pm-TSP* probe (A), antisense *Pm-PGMRC1* probe (B), sense *Pm-PGMRC1* probe (C), antisense *Pm-Cdc42* probe (D) and sense *Pm-Cdc42* probe (E).

3.9.2 *In situ* hybridization (ISH)

The cellular localization of *Pm-Cdc42*, *Pm-PGMRC1*, *Pm-SARIP* and *Pm-p23* transcripts in ovaries of *P. monodon* broodstock was determined by *in situ*

hybridization. Localization of highly abundant transcripts; *Pm-TSP* and *Pm-VTG*, were also carried out as the positive control. Adjacent sections were probed with sense and antisense probes. No signal was observed with the sense strand probe (specificity control) for *Pm-Cdc42*, *Pm-SARIP* and *Pm-p23* (Figures 3.108 and 3.110 - 3.112; A). However, the positive signal was observed when the tissue section was hybridized with the sense probe of *PGMRC1* (Figure 3.109; A).

The antisense *Pm-PGMRC1*, *Pm-Cdc42*, *Pm-p23*, *Pm-TSP* and *Pm-SARIP* probes gave a clear signal in ooplasm of previtellogenic oocytes (Figures 3.104 and 3.105, 3.108 – 3.112; B and C and Table 3.42). Generally, oocytes at the late previtellogenic stage showed weaker positive signals than early previtellogenic oocytes. Positive signals were not detected from CR oocytes. In the germinative zone, oogonia did not display positive signals for any transcripts. Ovaries at younger stages that are located close to the germinative zone showed the earliest expression of the transcripts for *Pm-TSP* (Figure 3.104; B). The antisense *Pm-VTG* probe gave a clear signal in the cytoplasm of follicular cells (Figures 3.106 - 3.107; B and C).

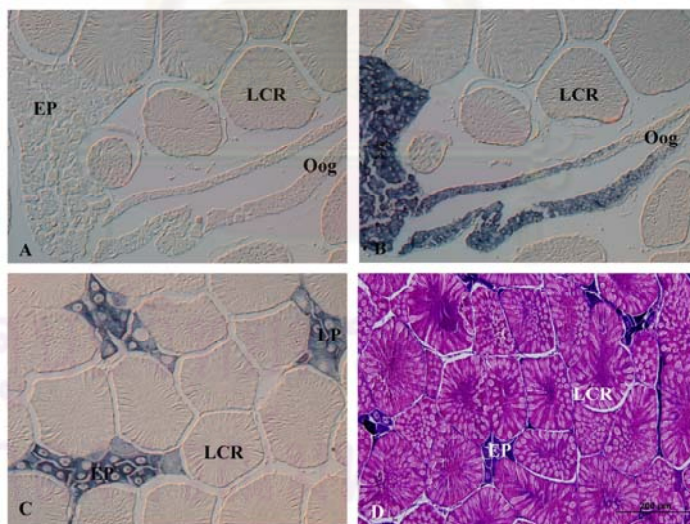


Figure 3.104 Localization of *Pm-TSP* transcript during ovarian development of normal *P. monodon* broodstock visualized by *in situ* hybridization using the sense *Pm-TSP* probe (A), antisense *Pm-TSP* probe (B and C). Conventional HE staining was carried out for identification of oocyte stages (D). EP = early previtellogenic oocytes; LCR = late cortical rod oocytes and Oog = oogonia.

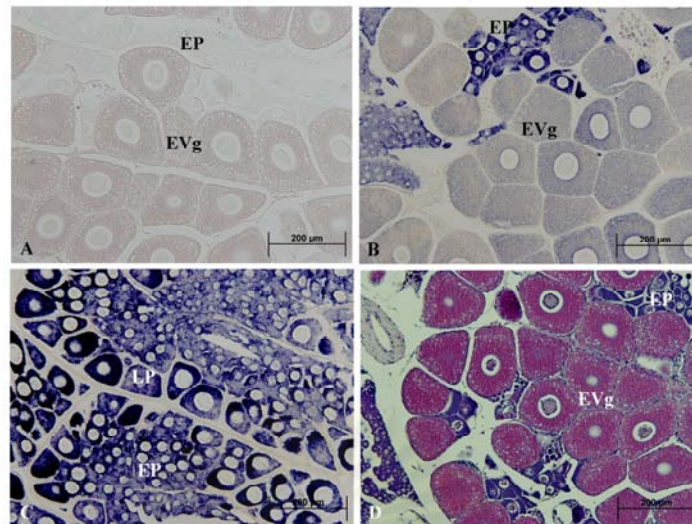


Figure 3.105 Localization of *Pm-TSP* transcript during ovarian development of eyestalk-ablated *P. monodon* broodstock visualized by *in situ* hybridization using the sense *Pm-TSP* probe (A), antisense *Pm-TSP* probe (B and C). Conventional HE staining was carried out for identification of oocyte stages (D). EP = early previtellogenic oocytes; LP = late previtellogenic oocytes; EVg = early vitellogenic oocytes.

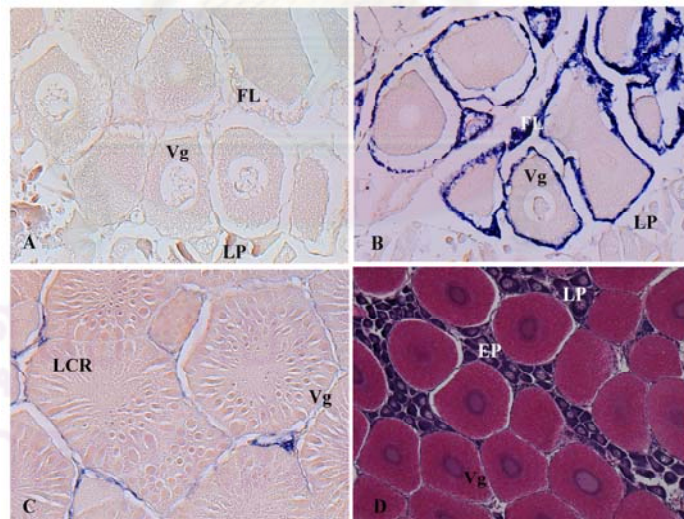


Figure 3.106 Localization of *Pm-VTG* transcript during ovarian development of normal *P. monodon* broodstock visualized by *in situ* hybridization using the sense *Pm-VTG* probe (A), antisense *Pm-VTG* probe (B and C). Conventional HE staining was carried out for identification of oocyte stages (D). EP = early previtellogenic oocytes; LP = late previtellogenic oocytes; Vg = vitellogenic oocytes; LCR = late cortical rod oocytes; FL = follicular layers.

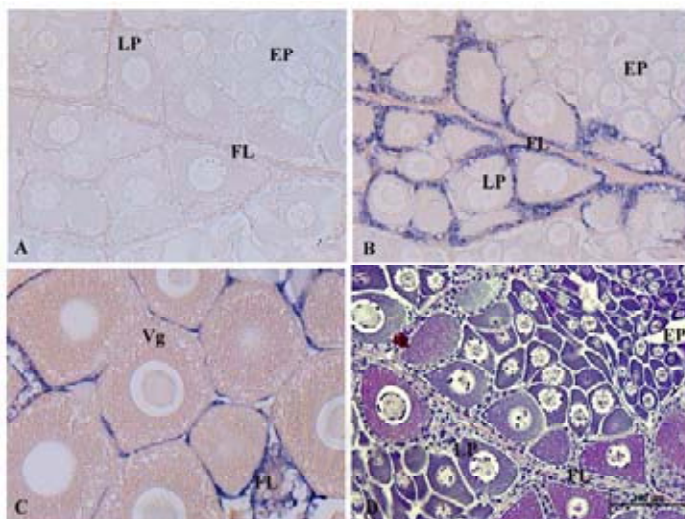


Figure 3.107 Localization of *Pm-VTG* transcript during ovarian development of eyestalk-ablated *P. monodon* broodstock visualized by *in situ* hybridization using the sense *Pm-VTG* probe (A), antisense *Pm-VTG* probe (B and C). Conventional HE staining was carried out for identification of oocyte stages (D). EP = early previtellogenic oocytes; LP = late previtellogenic oocytes; Vg = vitellogenic oocytes; FL = follicular layers.

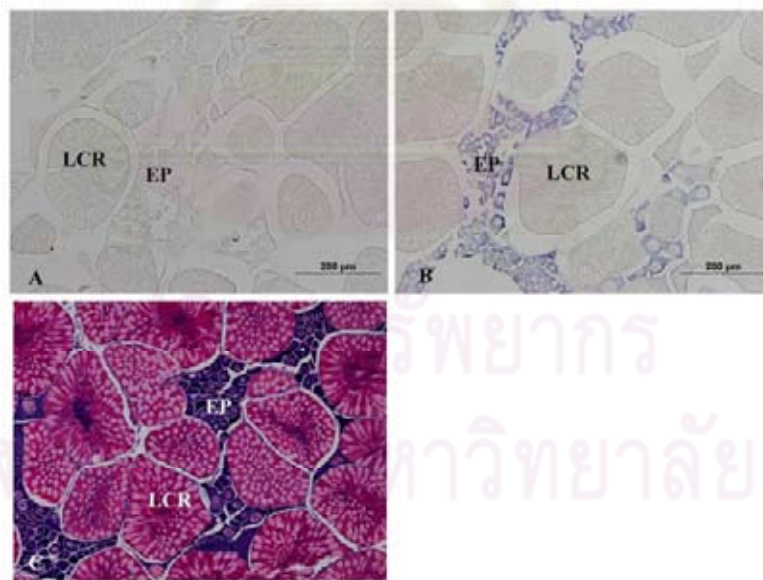


Figure 3.108 Localization of *Pm-Cdc42* transcript during ovarian development of normal *P. monodon* broodstock visualized by *in situ* hybridization using the sense *Pm-Cdc42* probe (A), antisense *Pm-Cdc42* probe (B). Conventional HE staining was carried out for identification of oocyte stages (C). EP = early previtellogenic oocytes; LCR = late cortical rod oocytes.

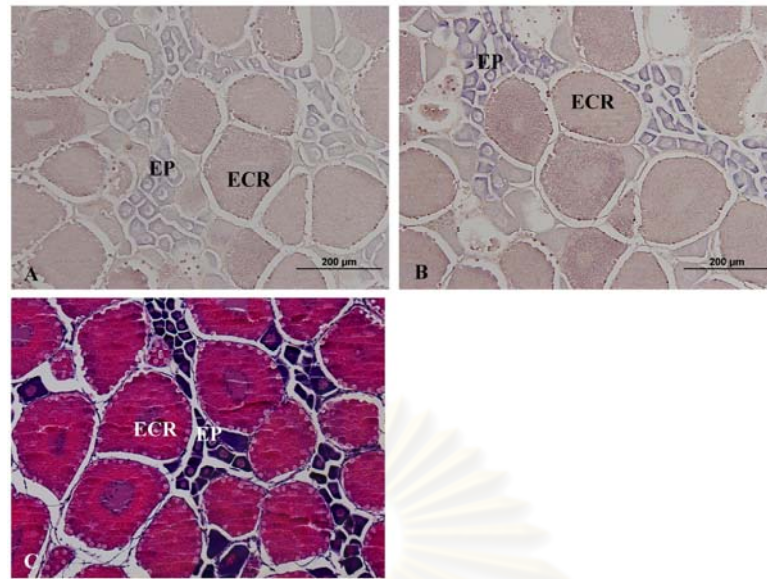


Figure 3.109 Localization of *Pm-PGMRC1* transcript during ovarian development of normal *P. monodon* broodstock visualized by *in situ* hybridization using the sense *Pm-PGMRC1* probe (A), antisense *Pm-PGMRC1* probe (B). Conventional HE staining was carried out for identification of oocyte stages (C). EP = early previtellogenic oocytes; ECR = early cortical rod oocytes.

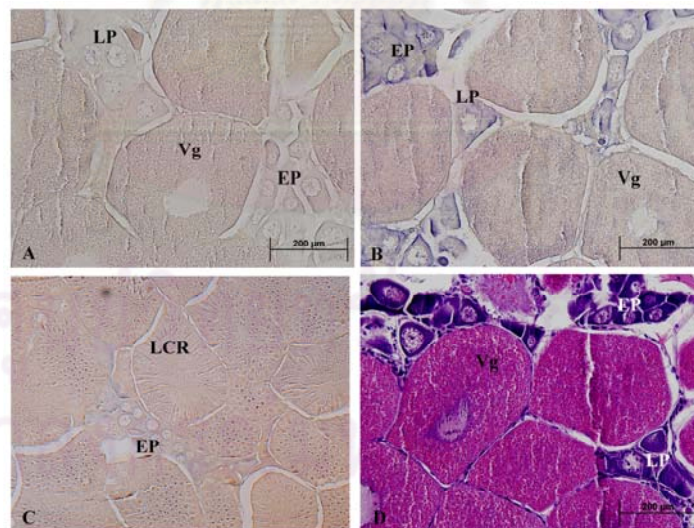


Figure 3.110 Localization of *Pm-SARIP* transcript during ovarian development of normal *P. monodon* broodstock visualized by *in situ* hybridization using the sense *Pm-SARIP* probe (A), antisense *Pm-SARIP* probe (B and C). Conventional HE staining was carried out for identification of oocyte stages (D). EP = early previtellogenic oocytes; LP = late previtellogenic oocytes; Vg = vitellogenic oocytes; LCR = late cortical rod oocytes.

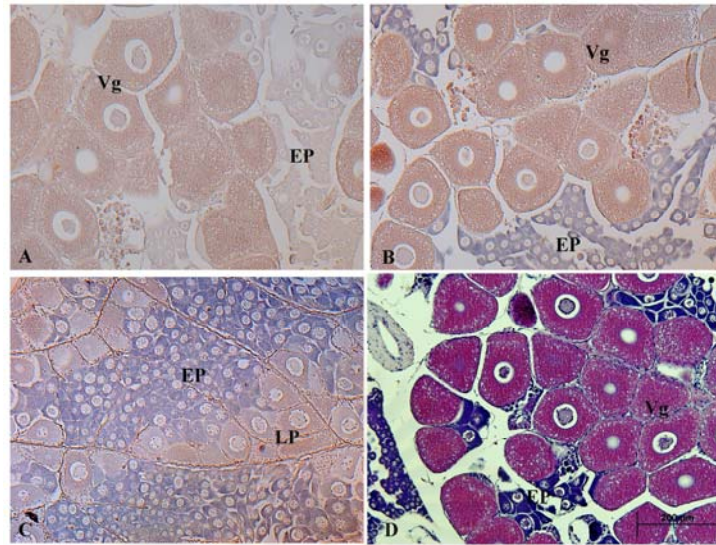


Figure 3.111 Localization of *Pm-SARIP* transcript during ovarian development of eyestalk-ablated *P. monodon* broodstock visualized by *in situ* hybridization using the sense *Pm-SARIP* probe (A), antisense *SARIP* probe (B and C). Conventional HE staining was carried out for identification of oocyte stages (D). EP = early previtellogenic oocytes; LP = late previtellogenic oocytes; Vg = vitellogenic oocytes.

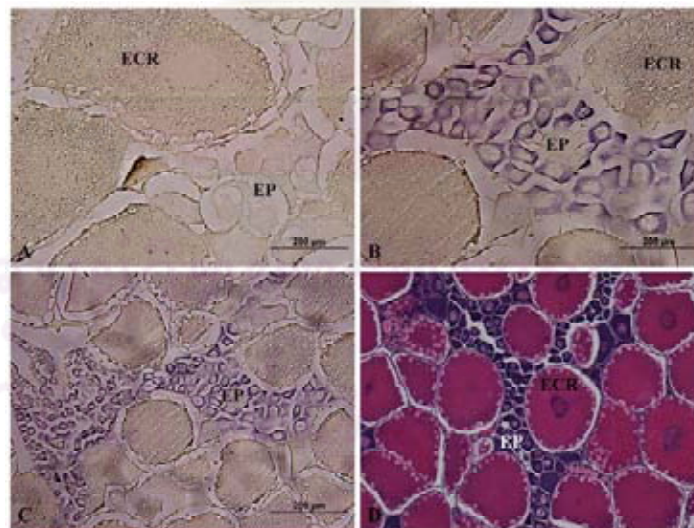


Figure 3.112 Localization of *Pm-p23* transcript during ovarian development of normal *P. monodon* broodstock visualized by *in situ* hybridization using the sense *Pm-PGMRC1* probe (A), antisense *Pm-p23* probe (B and C). Conventional HE staining was carried out for identification of oocyte stages (D). EP = early previtellogenic oocytes; ECR = early cortical rod oocytes.

As described previously, localization of *Pm-PGMRC1*, *Pm-Cdc42*, *Pm-TSP*, *Pm-SARIP* and *Pm-p23* was not observed in more mature (cortical rod and mature) stages of oocytes and follicular cells. This further indicated cell-type specific expression of these transcript in ovaries of *P. monodon* broodstock. Contradictory expression patterns based on quantitative real-time PCR and *in situ* hybridization on the disappearance of hybridized signals of *Pm-PGMRC1*, *Pm-Cdc42*, *Pm-TSP*, *Pm-SARIP* and *Pm-p23* in ooplasm of the later stages of oocytes may be due to significantly increasing oocytes sizes as oogenesis proceeded. In addition, the sensitivity of real-time PCR on detecting gene expression is much greater than that of *in situ* hybridization.

Table 3.42 Localization of sex-related transcripts in ovaries of *P. monodon* visualized by *in situ* hybridization.

Transcripts	Localization	Visualized stage
<i>Pm-Cdc42</i>	ooplasm of oocytes	Previtellogenic
<i>Pm-PGMRC1</i>	ooplasm of oocytes	Previtellogenic
<i>Pm-SARIP</i>	ooplasm of oocytes	Previtellogenic
<i>Pm-p23</i>	ooplasm of oocytes	Previtellogenic
<i>Pm-TSP</i>	ooplasm of oocytes	Previtellogenic
<i>Pm-VTG</i>	cytoplasm of follicular cells	previtellogenic, vitellogenic, cortical rods

3.10 Expression profiles and localization of Cdc42 and PGMRC1 proteins during ovarian development of *P. monodon*

The anti-PGMRC1 was purified using HiTrap NHS-activated HP affinity column chromatography to eliminate high molecular weight proteins and those possible causing non-specific signals from western blot analysis.

The positive bands corresponding to monomeric and dimeric forms (21 and 42 kDa, respectively) of Pm-PGMRC1 were successfully detected by western blot analysis. The former was expressed slightly greater in ovaries of juveniles and

previtellogenic oocytes than those of other ovarian stages of shrimp broodstock whereas the latter was more abundantly expressed in the opposite direction (Figure 3.113; C).

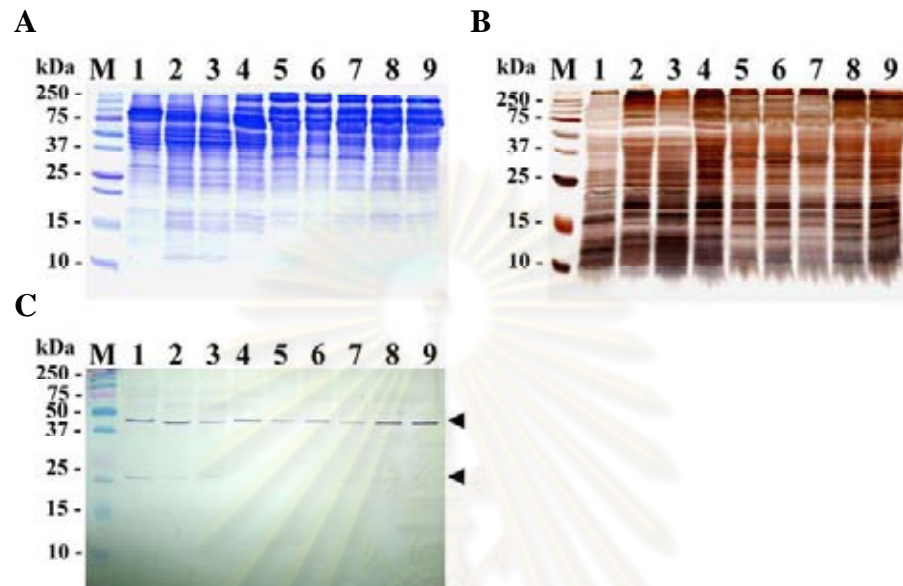


Figure 3.113 Western blotting analysis of purified anti-PGMRC1 PcAb (dilution 1:100; expected MW approximately 21 kDa) for a monomer and 42 kDa a dimer of PGMRC1) (C) using total protein extracted from ovaries of *P. monodon* broodstock. Ovarian proteins (30 μ g) were size-fractionated by 15% SDS-PAGE and visualized by coomassie brilliant blue (A) and silver (B) staining.

Lane 1 = ovaries of 4 month-old shrimp, lanes 2-3 = previtellogenic ovaries (GSI = 1.19 and 1.75%, respectively), lanes 4-6 = vitellogenic ovaries (GSI = 3.31, 4.61 and 5.75%, respectively), lanes 7-9 = CR ovaries (GSI = 7.32, 11.19 and 11.66%, respectively). Lanes M = protein standard.

In contrast, several positive bands were found from western blot analysis of total ovarian proteins of *P. monodon* with the commercially available Cdc42 PcAb with a dilution ratio of 1:100. Notably, the deduced Pm-Cdc42 protein does not contain any *N*-linked glycosylation site. The expected target band of 21.40 kDa was preferentially expressed in immature stages of ovaries (Figure 3.114; C). Positive

bands of 27, 50, 70 and 80 kDa in size were further analyzed by LC-MS/MS. While a 27 kDa protein was significantly matched allergen Pen m2 protein of *P. monodon* (V-S-S-T-L-S-S-L-E-G-E-L-K; E value = 6.5×10^{-9}), a 50 kDa protein was significantly matched Y-box binding protein isoform 2 of *Tribolium castaneum* (G-N-E-A-A-N-V-T-G-P-G-G-E-A-V-K; E value = 6.2×10^{-5}). In addition, a 80 kDa protein was significantly matched hemocyanin of *P. monodon* (I-D-V-S-N-N-K-G-Q-E-V-L-A-T-V-R; E value = 6.6×10^{-5}) whereas a 70 kDa fragment was not significantly similar to any protein.

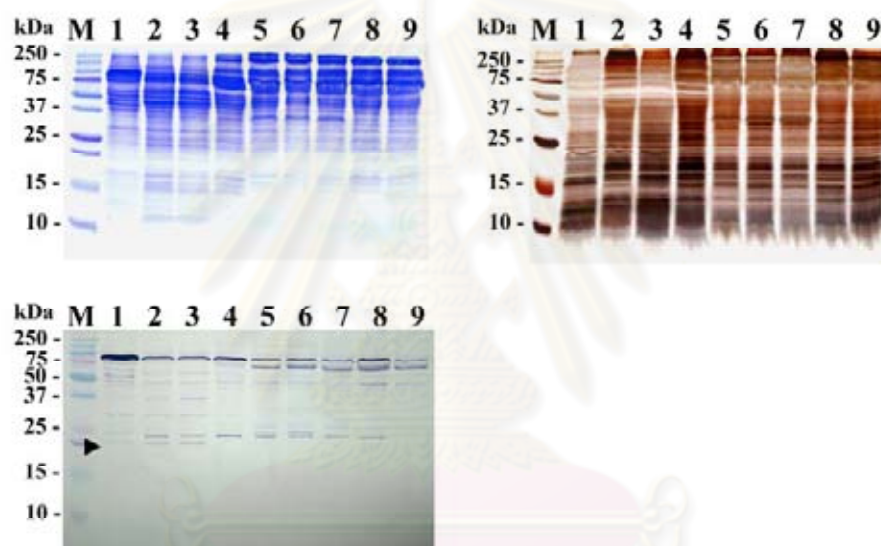


Figure 3.114 Western blotting analysis of anti-Cdc42 PcAb (dilution 1:100; expected MW approximately 21.40 kDa) (C) using total protein extracted from ovaries of *P. monodon*. Ovarian proteins (30 μ g) were size-fractionated by 15% SDS-PAGE and visualized by coomassie brilliant blue (A) and silver (B) staining.

Lane 1 = ovaries of 4 month-old shrimp, lanes 2-3 = previtellogenic ovaries (GSI =1.19 and 1.75%, respectively), lanes 4-6 = vitellogenic ovaries (GSI =3.31, 4.61 and 5.75%, respectively), lanes 7-9 = CR ovaries (GSI = 7.32, 11.19 and 11.66%, respectively). Lanes M = protein standard.

Interestingly, positive immunohistological signals of Pm-PGMRC1 were only detected in the follicular layer (FL) and cell membrane of follicular cells (Figures 3.115 and 3.116, D - F). No immunoreactivity was found in ovaries when incubated with the blocking solution (the negative control, Figures 3.115 and 3.116; B). Nevertheless, the false positive signal was detected when tissue sections were incubated with normal sera (Figures 3.115 and 3.116; C). However, the signals were lower than those from hybridization with Pm-PGMRC1 PcAb.

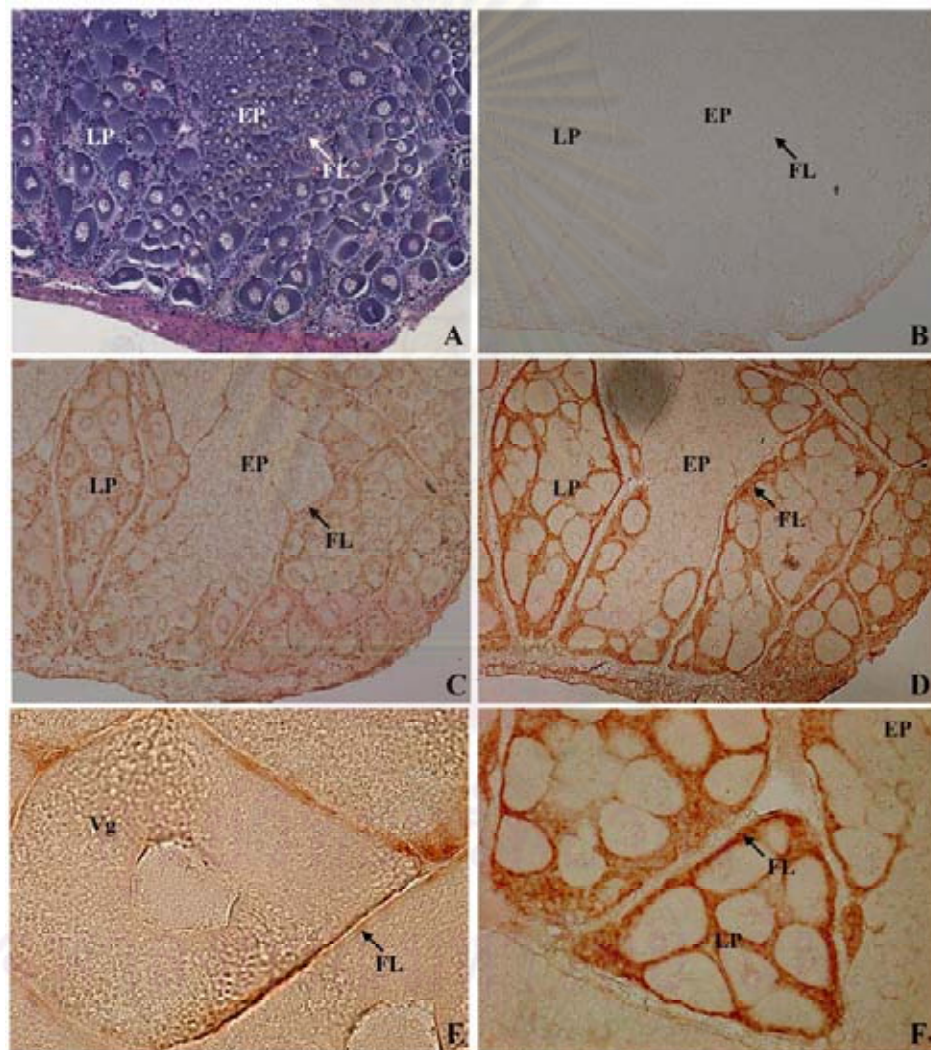


Figure 3.115 Immunohistochemical localization of PGMRC1 protein in ovaries of wild *P. monodon* broodstock using purified anti-PGMRC1 PcAb (D-F). Immunoreactive proteins were detected only in follicle cells. Hematoxylin and eosin staining (A) of tissue sections was carried out classification of oocyte stages. The blocking solution (B) and normal sera (C) were used as negative and positive control, respectively. EP = early perinucleolus stage; LP = late perinucleolus stage; Vg = vitellogenic stage; FL = follicular layer.

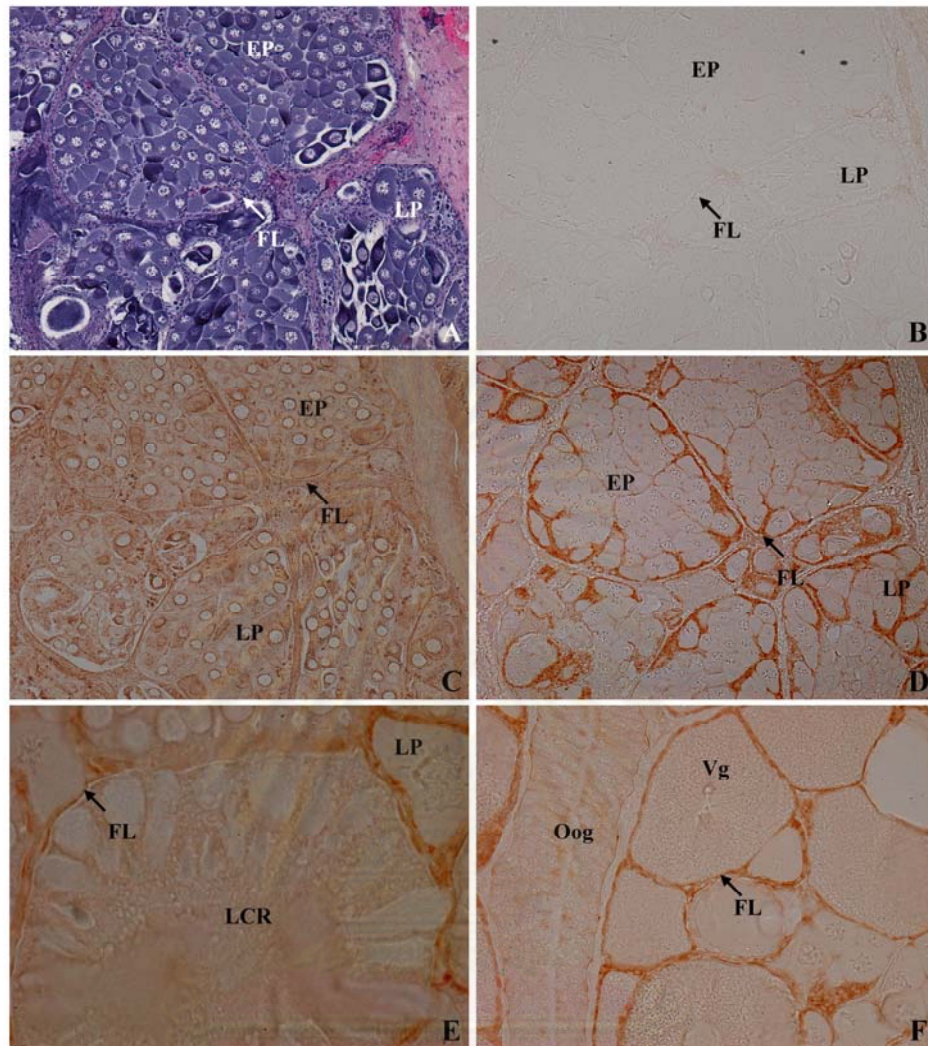


Figure 3.116 Immunohistochemical localization of PGMRC1 protein in ovaries of eyestalk-ablated broodstock *P. monodon* using purified anti-PGMRC1 PcAb (D-F). Immunoreactive proteins were detected only in follicle cells. Hematoxylin and eosin staining (A) of tissue sections was carried out for classification of oocyte stages. The blocking solution (B) and normal sera (C) were used as negative and positive control, respectively. EP = early perinucleolus stage; LP = late perinucleolus stage; Vg = vitellogenic stage; ; LCR = late cortical rod stage; ; Oog = oogonia; FL = follicular layer.

As can be seen from Figure 3.117, positive immunohistochemical signals of Pm-Cdc42 were detected in oogonia (Oog), cytoplasm of previtellogenic oocytes (P) and follicular layer (FL) (Figure 3.117; B and D). No immunoreactivity was found in ovaries when incubated with the blocking solution (the negative control, Figure 3.117; A and C).

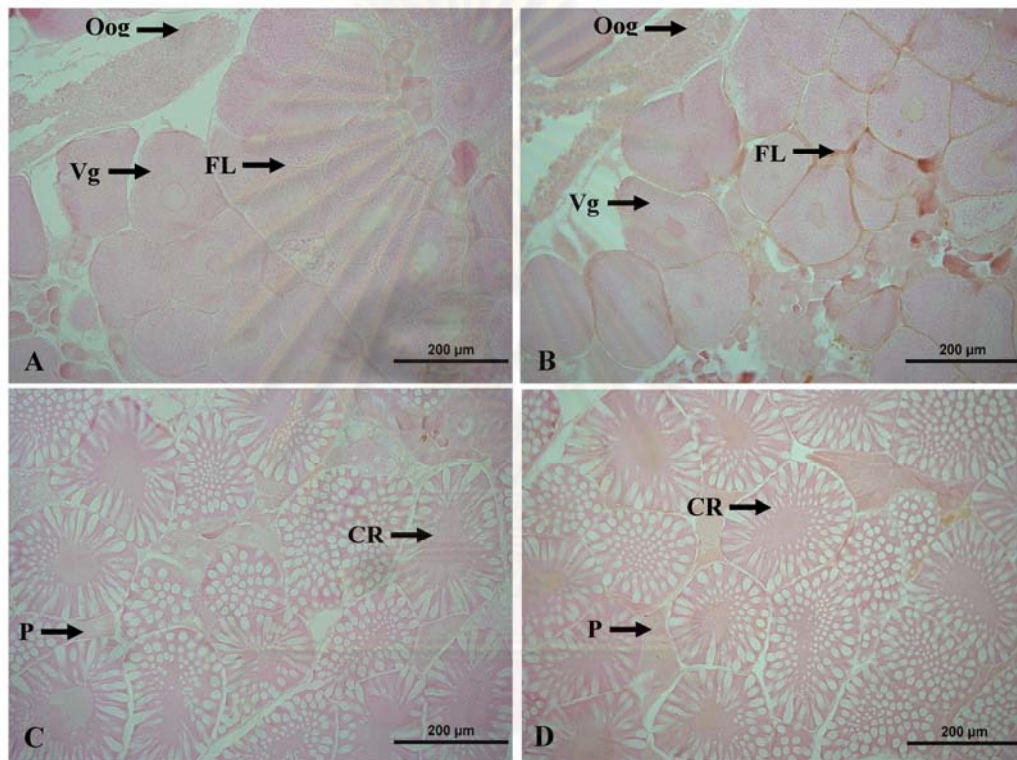


Figure 3.117 Immunohistochemical localization of Pm-Cdc42 protein in ovaries of *P. monodon* broodstocks using commercially available anti-Cdc42 PcAb (B and D). Immunoreactive proteins were detected only in oogonia (Oog), previtellogenic oocytes (P) and follicular layer (FL). The blocking solution (A and C) was used as the negative control. Vg = vitellogenic oocytes; CR = cortical rod oocytes.

3.11 *In vitro* expression of recombinant Cdc42 and p23 proteins using the bacterial expression system

3.11.1 Construction of recombinant plasmids

Recombinant plasmids carrying the entire ORF of *cell division cycle 42* (*Cdc42*) and *progesterone receptor related protein p23* (*p23*) were prepared for *in vitro* expression of the corresponding protein. A primer pair was designed to amplify cDNA representing each mature peptide. The amplified full length cDNA of *Cdc42* and *p23* was ligated to pGEM[®]-T easy vector and transformed into *E. coli* JM109. Plasmid DNA of the selected clone was used as the template for amplification using a forward primer containing *Nde* I restriction site, and a reverse primer containing *Bam* HI restriction site and six-repeated Histidine encoded nucleotides by *Pfu* DNA polymerase (Figure 3.118). The amplification product was digested with *Nde* I and *Bam* HI and the product was electrophoresed. The gel-eluted product was ligated with pET-15b (for *Cdc42*) or pET-32a(+) (for *p23*) expression vectors and transformed into *E. coli* JM109.

Plasmid DNA of the positive clone was sequenced to confirm the orientation of recombinant clones. Plasmid DNA was extracted from a clone carrying the correct direction of *Cdc42* and *p23* genes and transformed into *E. coli* BL21-CodonPlus (DE3)-RIPL and *E. coli* BL21 (DE3)plysS competent cells, respectively.

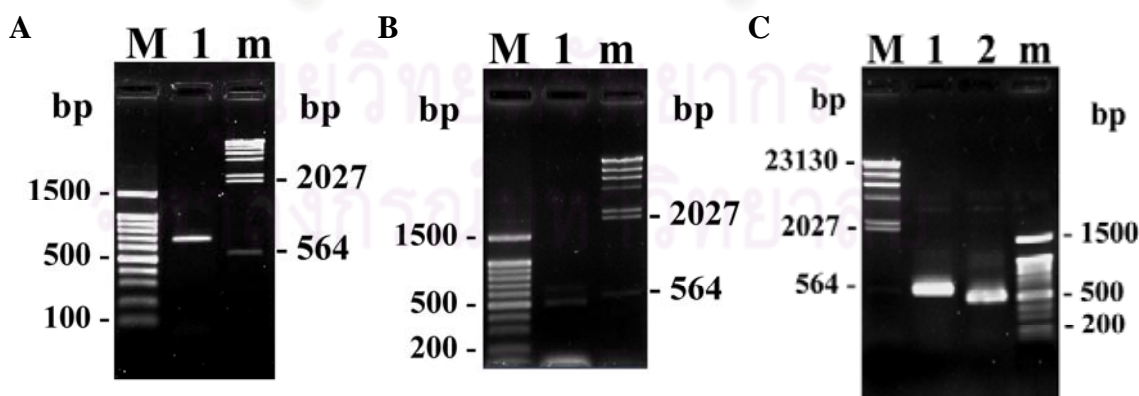


Figure 3.118 RT-PCR of the mature transcript of *Cdc42* (A) and *p23* (B). Fragments were cloned and sequenced. A hundred-fold dilution of plasmid DNA was used as the template to amplify the ORF overhang with *Nde* I-*Bam* HI of each gene overhang (C; lane 1 and 2 are *Cdc42* and *p23* fragments, respectively).

3.11.2 *In vitro* expression of recombinant protein

Expression of 3 recombinant clones of Cdc42 (21.40 kDa) and p23 (19.07 kDa) were induced by 1 mM IPTG at 37°C for 3 and 6 hours. Expression of the recombinant protein was observed at 3 hours after IPTG induction. Recombinant Cdc42 and p23 were stably expressed at 6 hours post induction (Figures 3.119 A and B).

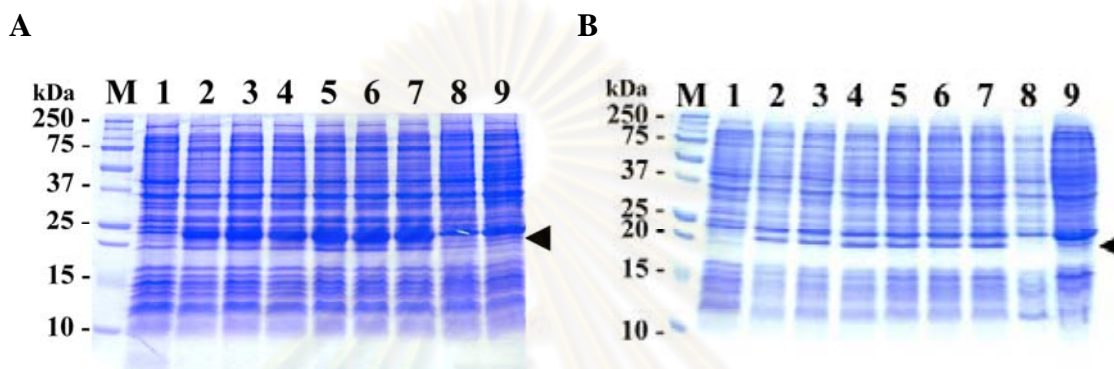


Figure 3.119 A 15% SDS-PAGE showing *in vitro* expression of three recombinant clones of Cdc42 (A) and p23 (B) of *P. monodon* at 0 hr (lanes 1; A and B), 3 hours (lanes 2-4; A and B) and 6 hours (lanes 5-7; A and B) after IPTG induction (1 mM). A pET-15b (Cdc42; A) or pET-32a(+) (p23; B) vectors in *E. coli* BL21-CodonPlus (DE3)-RIPL (Cdc42; A) or *E. coli* BL21 (DE3)plysS (lanes 8; A and B) and *E. coli* BL21-CodonPlus (DE3)-RIPL (Cdc42; A) or *E. coli* BL21 (DE3)plysS (lanes 9; A and B) were included as the control.

A recombinant clone of each protein was selected and the expression profile of the corresponding recombinant protein was examined at 37°C for 0, 1, 2, 3, 4, 6 hours and overnight after IPTG induction. Recombinant Cdc42 and p23 were overexpressed since 1 hour after IPTG induction (Figures 3.120 and 3.121). The expression level of recombinant Cdc42 was highest when cultured overnight (Figure 3.120). In contrast, the expression level of recombinant p23 was comparable between time intervals (1, 2, 3, 4, 6 hours and overnight) after IPTG induction (Figure 3.121).

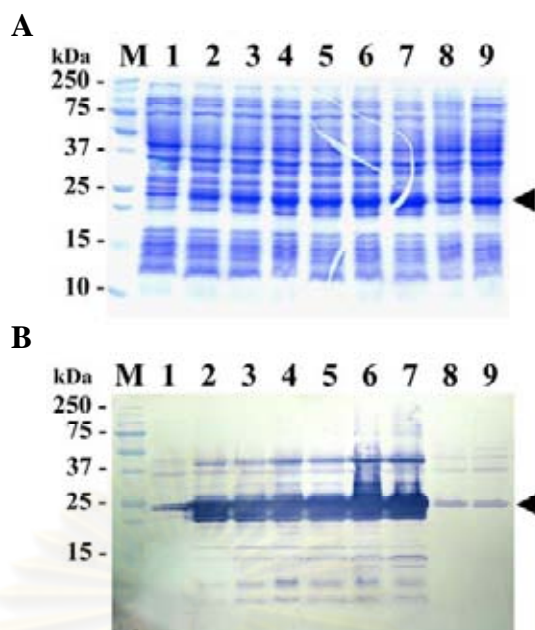


Figure 3.120 *In vitro* expression of Cdc42 of *P. monodon* at 0, 1, 2, 3, 4, 6 hours and overnight after induction with 1 mM IPTG (lanes 1-7) analyzed by 15% SDS-PAGE (A) and Western blot analysis (B). A pET-15b vector in *E. coli* BL21-CodonPlus (DE3)-RIPL (lanes 8; A and B) and *E. coli* BL21-CodonPlus (DE3)-RIPL (lanes 9; A and B) were included as the control.

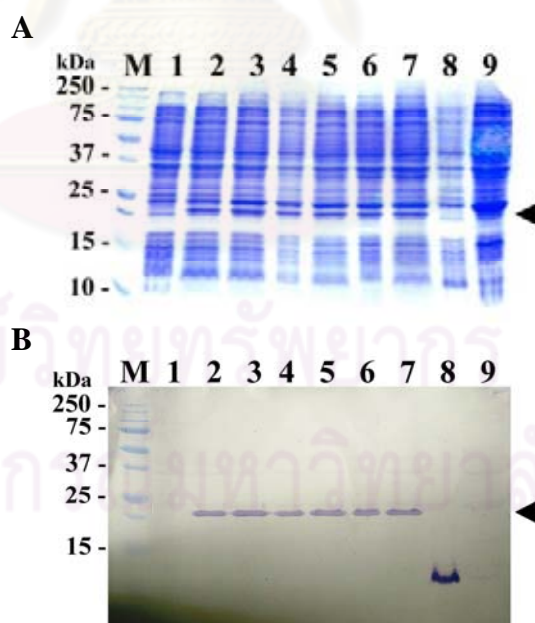


Figure 3.121 *In vitro* expression of p23 of *P. monodon* at 0, 1, 2, 3, 4, 6 hours and overnight after induction with 1 mM IPTG (lanes 1-7) analyzed by 15% SDS-PAGE (A) and Western blot analysis (B). A pET-15b vector in *E. coli* BL21-CodonPlus (DE3)-RIPL (lanes 8; A and B) and *E. coli* BL21-CodonPlus (DE3)-RIPL (lanes 9; A and B) were included as the control.

For determination of expressed proteins, an aliquot of the IPTG-induced culture ($OD = 1$) of each protein was collected. The soluble and insoluble protein fractions of each gene were analyzed by 15% SDS-PAGE and Western blot analysis. Recombinant Cdc42 cultured at 30°C for 6 hours after IPTG induction was mainly expressed in an insoluble form and a lower level of recombinant Cdc42 was expressed in the soluble form (Figure 3.122). Expression of recombinant p23 cultured at 30°C for 6 hours after IPTG induction was in the opposite direction (Figure 3.123).

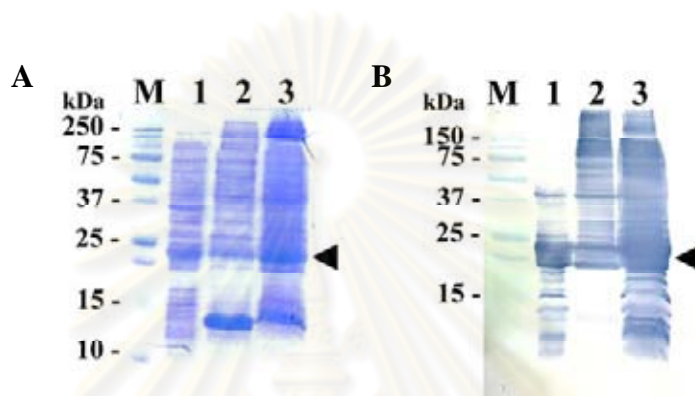


Figure 3.122 A 15% SDS-PAGE (A) and Western blot analysis (B) showing expression of recombinant Cdc42 in a recombinant clone cultured at 30°C for 6 hours after IPTG induction (1 mM). Arrowheads indicated the expected protein products. Lanes 1-3 are whole cells ($OD_{600} = 1.0$), a soluble protein fraction (50 μg protein), and an insoluble protein fraction (50 μg protein), respectively.

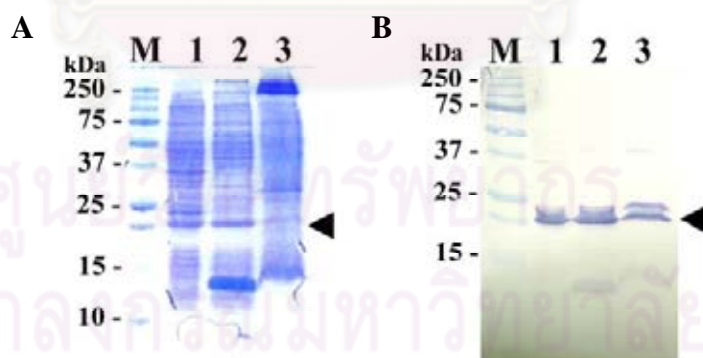


Figure 3.123 A 15% SDS-PAGE (A) and Western blot analysis (B) showing expression of recombinant p23 in a recombinant clone cultured at 30°C for 6 hours after IPTG induction (1 mM). Arrowheads indicated the expected protein products. Lanes 1-3 are whole cells ($OD_{600} = 1.0$), a soluble protein fraction (50 μg protein), and an insoluble protein fraction (50 μg protein), respectively.

To promote the possible expression of each recombinant protein in the soluble form, the cultured temperature was decreased. As a result, recombinant Cdc42 and p23 was cultured overnight after IPTG induction at 20 and 25°C, respectively. The large portion of recombinant Cdc42 protein was expressed in the soluble form (Figure 3.124). Interestingly, recombinant p23 was expressed as the soluble protein in a low culture condition (Figure 3.125). Therefore, the above conditions were used for further purification of recombinant Cdc42 and p23 proteins.

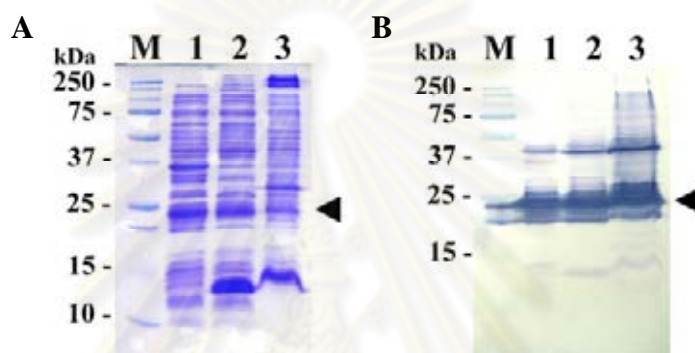


Figure 3.124 A 15% SDS-PAGE (A) and Western blot analysis (B) showing expression of recombinant Cdc42 in the clone cultured at 20°C overnight after IPTG induction (1 mM). Arrowheads indicated the expected protein products. Lanes 1-3 are whole cells ($OD_{600} = 1.0$), a soluble protein fraction (50 μ g protein), and an insoluble protein fraction (50 μ g protein), respectively.

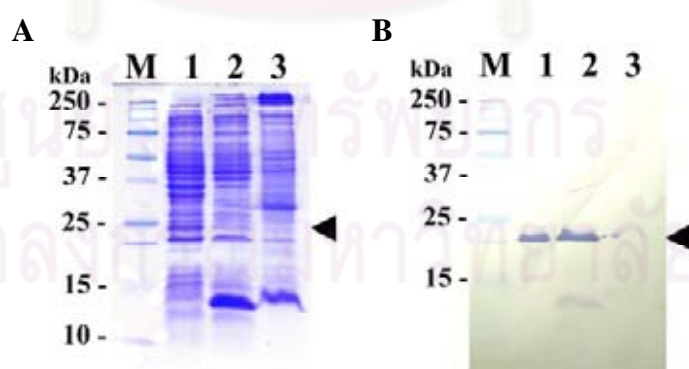


Figure 3.125 A 15% SDS-PAGE (A) and Western blot analysis (B) showing expression of recombinant p23 in a clone cultured at 25°C overnight after IPTG induction (1 mM). Arrowheads indicated the expected protein products. Lanes 1-3 are whole cells ($OD_{600} = 1.0$), a soluble protein fraction (50 μ g protein), and an insoluble protein fraction (50 μ g protein), respectively.

3.11.3 Purification of recombinant proteins

The soluble fractions of both recombinant Cdc42 and p23 were purified as native proteins. Recombinant proteins were run through the column three times. The first washing step was carried out using 10 ml of the binding buffer (20 mM sodium phosphate and 500 mM NaCl) including 20 mM imidazole, pH 7.4. In addition, the second and third washing steps were carried out using the binding buffer including 50 and 80 mM imidazole, pH 7.4 in a volume of 5 ml each. The recombinant proteins were eluted from the column with 6 ml of the elution buffer (20 mM sodium phosphate, 500 mM NaCl and 500 mM imidazole, pH 7.4). Aliquots of 1 ml were collected from washing and elution of the purified protein. The collected fractions were analyzed by 15% SDS-PAGE and Western blot analysis (Figures 3.126 and 3.127). The fractions kept at 4°C were concentrated by ultrafiltration and the obtained protein were subjected to polyclonal antibody production in rabbit.

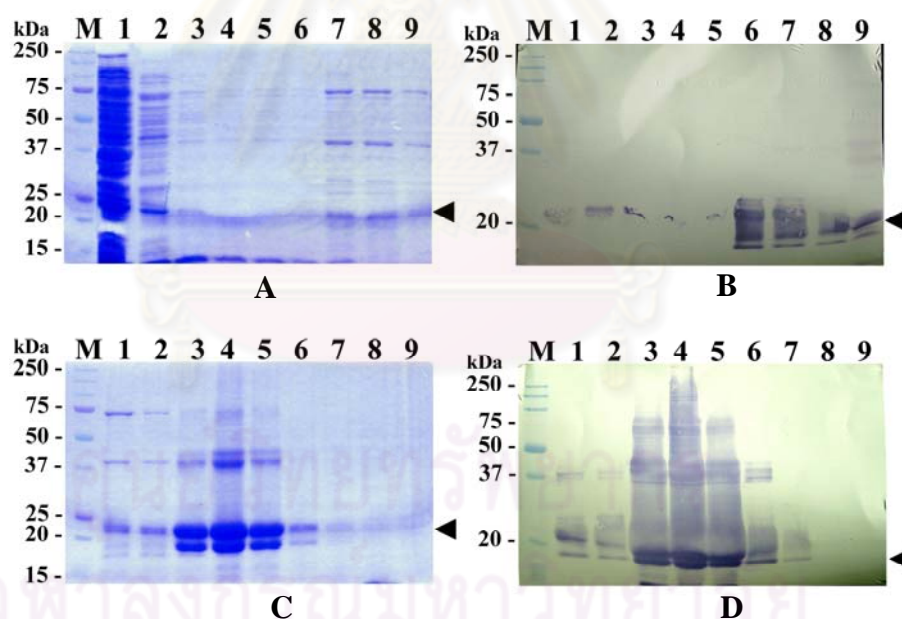


Figure 3.126 Purification of recombinant Cdc42 of *P. monodon* (cultured overnight at 20°C). Recombinant proteins were examined by a 15% SDS-PAGE (A and C) and Western blot analysis (B and D).

A and B; lane 1 is the soluble fraction after pass through the column, lanes 2 - 6 are the first washing solution fractions 1, 3, 5, 7 and 9 and lanes 7 - 9 are the second washing solution fractions 1, 3 and 5, respectively. C and D; lanes 1 - 3 are the third washing solution fractions 1, 3, and 5 and lanes 4 - 9 are eluted protein fractions 1-6, respectively.

The purified recombinant Cdc42 from the 5th fraction of the binding buffer containing 80 mM imidazole, pH 7.4 (Figure 3.126 lane 3; C and D) was concentrated and size-fractionated by 15% SDS-PAGE. For p23, the purified proteins from fractions 1-5 of the binding buffer containing 80 mM imidazole, pH 7.4 (Figure 3.127 lanes 1 - 3; C and D) were pooled and concentrated.

After electrophoresis, the expected band of each protein was excised from the gel and electroeluted with the protein elution buffer (25 mM Tris, 192 mM glycine, and 0.1% SDS) using an Electro-Eluter (model 422, Bio-Rad). Non-purified and purified recombinant proteins were sent to Faculty of Associated Medical Sciences, Chiangmai University, for production of the polyclonal antibody in rabbit.

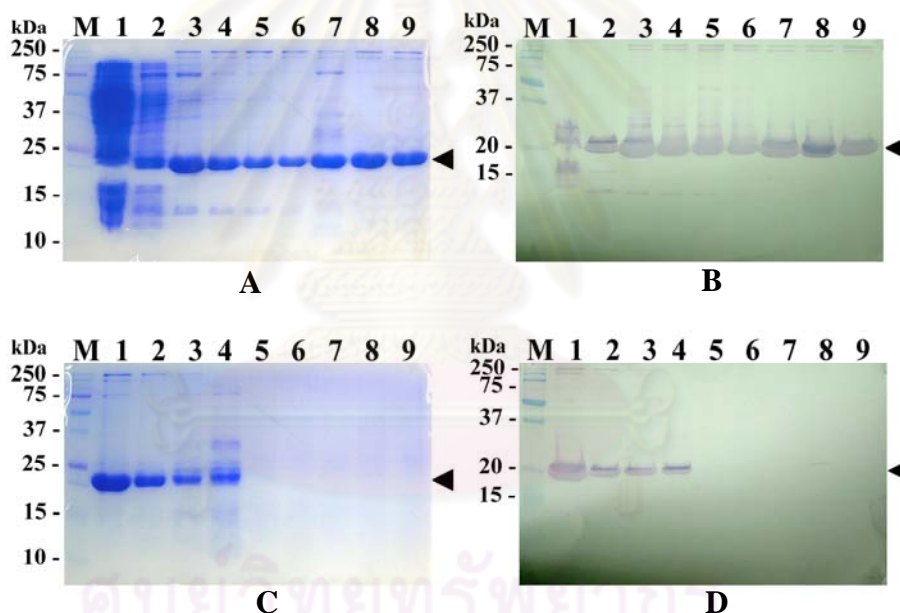


Figure 3.127 Purification of recombinant p23 of *P. monodon* (cultured overnight at 20°C). Recombinant proteins were examined by a 15% SDS-PAGE (A and C) and Western blot analysis (B and D).

A and B; lane 1 is the soluble fraction after pass through the column, lanes 2 - 6 are the first washing solution fractions 1, 3, 5, 7 and 9 and lanes 7 - 9 are the second washing solution fractions 1, 3 and 5, respectively. C and D; lanes 1 - 3 are the third washing solution fractions 1, 3, and 5 and lanes 4 - 9 are eluted protein fractions 1-6, respectively.

Anti-Cdc42 and anti-p23 polyclonal antibodies (PcAb) were successfully produced but the titer of anti-Cdc42 PcAb after the third immunization was quite low (Table 3.43). After additional immunization, the titers of both anti-Cdc42 and anti-p23 PcAb was comparably high (Table 3.44). Rabbits were sacrificed and their serum was collected, filtrated through 0.22 μ M membrane and kept at -20 °C.

Table 3.43 Titers of polyclonal antibodies using indirect ELISA assay and read the optical density at 450 nm after rabbits were immunized with recombinant Cdc42 and p23 for 3 times

Dilution of serum	Polyclonal antibody			
	Cdc42		P23	
	Pre-immunized serum (OD ₄₅₀)*	Immunized serum (OD ₄₅₀)**	Pre-immunized serum (OD ₄₅₀)	Immunized serum (OD ₄₅₀)
1:500	0.055	0.342	0.061	1.918
1:2000	0.043	0.281	0.049	1.566
1:8000	0.037	0.075	0.046	1.041
1:32000	0.036	0.070	0.043	0.396

*Pre-immunized serum = serum from normal rabbit

**Immunized serum = serum from rabbit injected with the recombinant protein

Table 3.44 Titers of polyclonal antibodies using indirect ELISA assay and read the optical density at 450 nm after rabbits were immunized with recombinant Cdc42 and p23 for 4 times

Dilution of serum	Polyclonal antibody			
	Cdc42		P23	
	Pre-immunized serum (OD ₄₅₀)*	Immunized serum (OD ₄₅₀)**	Pre-immunized serum (OD ₄₅₀)	Immunized serum (OD ₄₅₀)
1:500	0.062	2.638	0.035	2.880
1:2000	0.044	1.641	0.032	2.656
1:8000	0.040	0.683	0.033	1.923
1:32000	0.042	0.241	0.033	0.828

*Pre-immunized serum = serum from normal rabbit

**Immunized serum = serum from rabbit injected with the recombinant protein

3.11.4 Expression profiles of p23 protein during ovarian development of *P. monodon*

Anti-p23 PcAb was tested for its specificity by Western blot analysis. A positive band was obtained along with several discrete bands (data not shown). These positive bands should be further characterized whether they are the complex of p23 and its partners or nonspecific signals of anti-p23 PcAb.

To examine levels of p23 during ovarian development of *P. monodon*, Western blot analysis of this protein was carried out. After transferring, a portion of the PVDF membrane containing proteins with the molecular weight > 37 kDa was excised and the smaller proteins were analyzed by Western blotting (Figure 3.128).

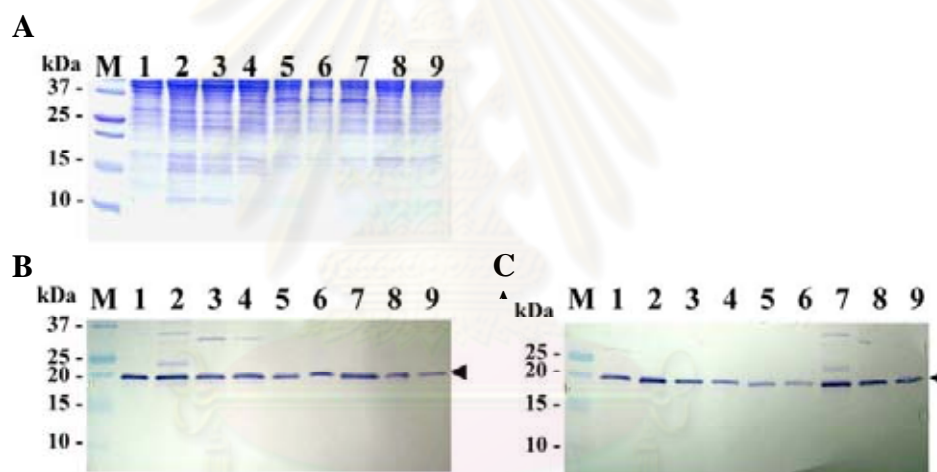


Figure 3.128 SDS-PAGE (A) and Western blotting analysis of anti-p23 PcAb (dilution 1:300, expected MW approximately 19.04 kDa; B and C) using total protein extracted from ovaries of *P. monodon* broodstock. Ovarian proteins (30 µg) were size-fractionated by 15% SDS-PAGE and visualized by coomassie brilliant blue.

Lanes 1; B and C = ovaries of 4 months-old shrimps, lanes 2; B and C = stage I ovaries (GSI = 0.89 and 1.08%, respectively), lanes 3-4; B and C = stage II ovaries (GSI = 2.24, 2.15%, 3.31% and 2.95%, respectively), lanes 5; B = stage III ovaries (GSI = 5.91%), lane 5, C; lanes 6, B and C = stage IV ovaries (GSI = 10.41%, 11.19% and 11.21%, respectively). Lanes 7-9 = positive controls of each membrane (lanes 7-9; B and C = stage I, II and IV ovaries (GSI = 1.08 and 0.89%, 2.95 and 3.31% and 10.41% and 11.19%, respectively). Lanes M = protein standard.

The discrete bands corresponding to a monomeric form (approximately 19.04 kDa) of *P. monodon* p23 were successfully detected. The immunological signal in ovaries of 4 months-old shrimp was greater than that in stages I, III and IV ovaries of broodstock. In broodstock, the p23 protein level in stage II ovaries was increased from stage I ovaries and the expression level of this protein was decreased when oocyte development proceeds (Figure 3.128; B and C and Table 3.45). Notably, statistical analysis was not performed because only 2 individuals from each ovarian stage (except stage II) were examined.

Table 3.45 The intensity of p23 signals in different stages of ovaries of *P. monodon* from Western blot analysis

Stage of samples	Intensity	Average	SD
4 months-old shrimps ovaries	372506.2361 444539.7357	408522.99	50935.4
Stage I ovaries (GSI = 0.89%)	441496.0207 335336.2275	388416.12	75066.3
Stage II ovaries (GSI = 2.24%)	594430.2327 483647.8894 505501.4476 426608.9127	502547.12	69701.8
Stage III ovaries (GSI = 5.91%)	392110.5767	392110.577	-
Stage IV ovaries (GSI = 10.41%)	265575.1079 257984.9952 245806.3998	256455.50	9972.71

Anti-Cdc42 PcAb yielded non-specific immunological fragments from Western blot analysis (data not shown). Therefore, expression of this protein during ovarian development of *P. monodon* was not further examined.

CHAPTER IV

DISCUSSION

Molecular mechanisms and functional involvement of genes and proteins in ovarian development of *P. monodon* is necessary for better understanding the reproductive maturation of *P. monodon* in captivity to resolve the major constraint of this economically important species.

The major obstacle in the development of shrimp maturation technology is the limited knowledge of the molecular events of ovarian maturation of shrimp (Benzie, 1998). Over the past few decades, there have been many studies on the characterization of vitellogenin/vitellin and the elucidation of the process of vitellogenesis in penaeid shrimp (Longyant *et al.*, 2000; Tsutsui *et al.*, 2000). Intensive studies have also been conducted on molecular endocrinology of shrimp reproduction, particularly on GIH and methylfarnesoate (MF) (e.g., Silva Gunawardene *et al.*, 2001; Gu *et al.*, 2002; Yamano *et al.*, 2004). These studies begin to reveal a better picture of the endocrine control of ovarian maturation in shrimp. However, reproductive maturation of penaeid shrimp is still not well understood. Detailed understanding of the molecular events during ovarian development is crucial in further applications on the control of ovarian maturation in shrimp.

An EST approach (single-pass sequencing of randomly selected clones from cDNA libraries) has been successfully applied and recognized as an effective method for discovery of immune related genes in shrimp (Gross *et al.*, 2001; Rojtinnakorn *et al.*, 2002; Shen *et al.*, 2004; Supungul *et al.*, 2004). Recently, ESTs from ovaries and testes of *P. monodon* were reported (Leeelatanawit *et al.*, 2004). However, only 157 clones from subtractive cDNAs of ovaries and 61 clones from those of testes were characterized.

An initial step toward understanding molecular mechanisms of ovarian (and oocyte) maturation and sex differentiation in *P. monodon* is the identification and characterization of sex-specific/differential expression genes in ovaries of this economically important species. In this study, 4560 ESTs including 2330 ESTs from a

typical ovarian cDNA library, 1778 EST from the normalized ovarian cDNA library and 452 ESTs from SSH ovarian cDNA libraries were unidirectional sequenced. Additional transcripts were also identified by RAP-PCR. The expression profiles of interesting genes/proteins were examined in different stages of ovarian development of *P. monodon*.

Isolation and characterization of functionally important gene homologues in the typical ovarian cDNA libraries of *P. monodon*

From 1051 and 1279 of the first and second phases of typical ovaries ESTs sequenced, a total of 830 and 970 ESTs (79.0 and 75.8%) corresponded to known sequences in the GenBank whereas 221 and 309 ESTs (21.0 and 24.2%, E-value > 10⁻⁴) were regarded as unknown transcripts. A relatively large number of unique sequences (1072, 46.0%) including 230 contigs and 842 singletons were obtained. *Thrombospondin* (198 clones, 8.5% of examined ESTs) and *peritrophin* (205 ESTs, 8.8%) were highly redundant in this and other ovarian cDNA libraries.

In *P. monodon*, *TSP* was specifically expressed in ovaries ($N = 20$) but not in testes ($N = 22$) of broodstock-sized *P. monodon* (Leelatanawit *et al.*, 2004). Recently, complete sequences of three closely related *TSP* homologues encoding the major cortical rod proteins of 1114, 1032, and 991 amino acids (GenBank accession numbers AB121209, AB121210, and AB121211) were isolated and characterized in *M. japonicus* (Yamano *et al.*, 2004). *MjTSP* protein levels dramatically increased after eyestalk ablation (Okumura *et al.*, 2006).

Peritrophin is a major component of cortical rods and the precursor of the jelly layer of shrimp eggs. *Peritrophin* is highly expressed during oocyte development of marine shrimp (Khayat *et al.*, 2001). Synthesis of *peritrophin* in ovaries of *P. semisulcatus* is inhibited by crustacean hyperglycemic hormone (CHH) purified from the sinus gland extract of *M. japonicus* (Avarre *et al.*, 2001). *Peritrophin* was not differentially expressed between ovaries and testes of *P. monodon* broodstock (Leelatanawit *et al.*, 2004) and between different stages of ovarian development of *M. japonicus* after eyestalk ablation (Okumura *et al.*, 2006).

Sizes of cDNA inserts in a typical ovarian cDNA library were relatively large. As a result, several full length transcripts of functionally important genes

including *chromobox protein (CBX)* (ORF of 570 bp, encoding a polypeptide of 189 aa), *cyclophilin 1* (519 bp, 172 aa), *cytochrome c oxidase subunit Va* (462 bp, 153 aa), *eIF-5A* (474 bp, 157 aa), *histone 1* (411 bp, 136 aa), *histone H2A variant* (399 bp, 132 aa), *profilin* (381 bp, 126 aa), *signal peptidase complex; sid2895p* (540 bp, 179 aa), *stress-associated endoplasmic reticulum protein 1* (201 bp, 66 aa) and *thioredoxin peroxidase* (591 bp, 196 aa), homologues were discovered (GenBank accession numbers EE332458-EE332467). Interestingly, ESTs representing *Cdc20*, *Cdc42*, *SARIP*, *cytochrome B5*, *protein mago nashi* and *bystin*, *phosphatidylserine receptor* and *p23* homologues were isolated from this library.

Early gonad maturity is a ubiquitous problem which devalues the product quality of the river prawn, *Macrobrachium nipponense*. A high-quality cDNA library of ovaries was constructed. A total of 3256 ESTs longer than 100 bp were identified. The cluster and assembly analyses yielded 1514 unique sequences including 414 contigs and 1168 singletons. Approximately 719 (47.49%) unique sequences were identified as orthologs of genes from other organisms. By sequence comparability analysis, 28 important genes involved in reproductive and development functions including *cathepsin B*, *chromobox protein*, *Cdc2*, *cyclin B*, *DEAD box protein* and *ADF/cofilin protein* were expressed. Peritrophin consisting of cortical rods was also found in this species. The identification of these EST sequences in *M. nipponense* would improve an understanding on the genes that regulate reproduction and development in this species (Wu *et al.*, 2008).

Isolation and characterization of functionally important gene homologues in the normalized ovarian cDNA libraries of *P. monodon*

Generally, sequencing cDNAs from standard cDNA libraries is ineffective for discovering rare expressed genes, when intermediately and highly expressed cDNAs would be sequenced redundantly (Maruyama and Sugano, 1994).

A normalized ovarian cDNA library of *P. monodon* was constructed from the typical ovarian cDNA library using the biotinylated Cap-Trapper method. However, homologues of *TSP* (176 ESTs, 9.9% of sequenced clones) and *peritrophin* (212 clones, 12.0%) were more abundant than those in the conventional library (8.5

and 8.4%, respectively) indicating that normalization for reducing abundantly expressed transcripts was not successful.

Sequence assembly of ESTs from the normalized library yielded 694 unique transcripts (39.0%) composing of 236 contigs (from 1320 ESTs) and 458 singletons. The percentage of ESTs corresponded to known sequences in the GenBank (E-value < 10^{-4}) was 79.5% (1413 ESTs) which slightly higher than those from the typical ovaries cDNA library of *P. monodon* (77.3%; 1800 ESTs). The percentage of unique sequences of this library was lower than that of the typical library (46.0%) indicating that normalization of the typical EST library was unsuccessful.

Five EST (OV-N-N01-0057-W, OV-N-N01-0381-W, OV-N-N01-1276-W, OV-N-N01-1549-W and OV-N-N01-1670-W) representing *P. monodon* *PGMRC1*, two EST representing *f-box* and *wd-40 domain protein* and an EST representing *cyclin-dependent kinase 7* (*cdk7*) were found in the normalized but not other ovarian cDNA libraries.

Isolation and characterization of functionally important gene homologues in SSH ovarian cDNA libraries of *P. monodon*

Suppression subtractive hybridization (SSH), a technique combining suppression Polymerase Chain Reaction (PCR) with hybridization technology, is widely used to isolate differentially expressed genes in two closely related samples/specimens/species (Diatchenko *et al.*, 1996). Accordingly, SSH should facilitate the identification of genes involved in ovarian development of *P. monodon*. These genes may be candidates for molecular markers, which could assist the domestication and selective breeding programs of *P. monodon*.

In the present study, two SSH cDNA libraries were constructed between vitellogenesis (forward subtractive library using previtellogenic ovary cDNA as the driver) and previtellogenic (reverse subtractive library using vitellogenic ovary cDNA as the driver) ovaries of *P. monodon* broodstock. Sequence assembly yielded a relatively large number of unique transcripts; 16 unique contigs and 123 singletons for the forward SSH library and 14 unique contigs and 90 singletons from the reverse SSH library. Homologues of *TSP* (39 and 39 clones, 17.7 and 16.8%) and *peritrophin*

(26 and 27 clones, 11.8 and 11.6%) were abundantly expressed in ovaries of *P. monodon*.

Excluding unknown transcripts and *TSP* and *peritrophin* homologues, 23 singletons, e.g. *coatamer protein complex, subunit beta*; *T-complex protein 1 subunit epsilon (TCP-1-epsilon) (CCT-epsilon)*, *zipper CG15792-PD; isoform D, CWF19-like 2*; *cell cycle control* and *putative myosin II essential light chain*, were found only in the forward SSH library but not in reverse SSH and other ESTs libraries. Two contigs; *selenophosphate synthetase* (clone numbers OV-N-ST02-0118-W, OV-N-ST02-0130-W) and *phosphatase 2C gamma* (clone numbers OV-N-ST02-0142-W, OV-N-ST02-0172-W) and 19 singletons, e.g., *carbonyl reductase 1-like*, *anaphase promoting complex subunit 11 homolog*, *peptidylprolyl isomerase D (cyclophilin D)*, *splicing factor*, *arginine/serine-rich 7* and *C-type lectin*, were found only in the reverse SSH library but not in other EST libraries. Only *40S ribosomal protein S6* and *calreticulin* were found in both SSH libraries, suggesting that subtraction of cDNAs from different stages of *P. monodon* ovaries were successful.

EST analysis using SSH cDNA libraries was also reported in *P. monodon*. Leelatanawit *et al.* (2004), a total of 218 clones from subtractive suppression hybridization (SSH) cDNA libraries between ovaries and testes of *P. monodon* broodstock were unidirectional sequenced. Most expressed genes in ovaries encoded *thrombospondin (TSP)*, 45 clones accounting for 28.7% of total investigated ESTs), *peritrophin* (17 clones, 10.8%), and unknown transcripts (78 clones, 49.7%). Conversely, almost all of the ESTs in *P. monodon* testes were unknown transcripts (59 clones, 96.7%).

More recently, Leelatanawit *et al.* (2008) constructed SSH cDNA libraries of broodstock and juvenile testes of *P. monodon*. The 178 and 187 clones from the forward and reverse SSH libraries were unidirectional sequenced. From these, 37.1% and 53.5% ESTs significantly matched known genes (E-value < 1×10^{-4}). *Peritrophin* and *TSP* which are abundantly expressed in ovaries of *P. monodon* were not found in the subtractive testis cDNA libraries. Relatively large numbers of genes encoding ribosomal proteins were found in both libraries (16 and 11 accounting for 8.9 and 5.6%, respectively).

Identification of candidate differential/stage-specific of differential ovarian development expression markers

RNA fingerprinting using arbitrarily primed PCR (RAP-PCR) (Welsh *et al.*, 1992) and differential display reverse transcription PCR (DDRT-PCR) (Liang and Pardee, 1992) and cDNA-AFLP (Bachem *et al.*, 1996) allow a semiquantitative simultaneous comparison of differentially expressed transcripts in a large number of RNA samples.

Recently, RAP-PCR was used to identify differentially expressed genes during ovarian maturation of *Metapenaeus ensis*. From a screening of 700 clones in a cDNA library of the shrimp ovary by the products of RAP-PCR of different maturation stages, 91 fragments with differentially expressed pattern as revealed by dot-blot hybridization were isolated and sequenced. Forty-two of these fragments show significant sequence similarity to known gene products and the differentially expressed pattern of 10 putative genes were further characterized via northern hybridization. Putative glyceraldehyde-3-phosphate dehydrogenase, arginine kinase, translationally controlled tumor protein, actin, keratin, high mobility group protein DSP1, heat shock protein 70, nucleoside diphosphate kinase, peptidyl-prolyl cis-trans isomerase and glutathione peroxidase are differentially expressed during ovarian development of *M. ensis* (Lo *et al.*, 2007).

Although RAP-PCR is a rapid and convenient method for identifying differentially expressed genes, it generates a high level of false positives and is biased for high copy-number mRNA (Bertioli *et al.*, 1995). Therefore differential expression of RAP-PCR should be further confirmed by semiquantitative RT-PCR or real-time PCR.

In this study, 45 primer combinations of the oligo-dT₍₁₆₎-overhang with A, C or G and arbitrary primers were screened against the first strand cDNA synthesized from mRNA of mature (GSI = 5.689%) and immature (GSI = 1.434%) ovaries and those of juveniles. Several transcripts showing a trend of differential expression during ovarian development of *P. monodon* were cloned and sequenced. Semiquantitative RT-PCR revealed that *B cell RAG associated protein*, *APEX nuclease* and *U5 snRNP-specific protein* were down-regulated at stage I and stage IV

of ovarian development, respectively. This suggested that lower level of these transcripts allowed progression of oocyte development of *P. monodon*. Moreover, *B cell RAG associated protein* specifically expressed in ovaries but not in testes and other tissues of a female broodstock.

Gender-specific gene expression has been reported in the nodule worm (*Oesophagostomum dentatum*) using RAP-PCR. A total of 31 differentially expressed bands between sexes were cloned and sequenced. Northern blot analysis indicated that ESTs significantly matched *vitellogenin-5* and *endonuclease III* of *C. elegans* were expressed solely in *O. dentatum* females (Boag *et al.*, 2000).

Transcription in germ cells during oogenesis follows a carefully regulated programs corresponding to a series of developmental events of oocytes (Qiu and Yamano, 2005; Qui *et al.*, 2005). Khamnamtong *et al.* (2006) identified sex-specific (and differential) expression markers in ovaries and testes of *P. monodon* by RAP-PCR. Five (*FI-4*, *FI-44*, *FIII-4*, *FIII-39* and *FIII-58*) differential display-derived unknown transcripts revealed female-specific expression patterns in ovaries of 3-month-old juveniles and broodstock. This result implied that these unknown genes should contribute to gonadal development and/or sex differentiation of *P. monodon*.

Tissue-specific transcription is important during development and during maturation of specific cell types from stem cells in the adults. *B cell RAG associated protein* was only expressed in ovaries but not in testes of *P. monodon* juveniles and broodstock. Ovary-specific transcription of *PM-polehole* suggested its essential role for ovarian but not testicular development of *P. monodon*. More importantly, results from tissue expression analysis further indicated that this transcript should mainly contribute to female germ cell development and can potentially be used as a biomarker to enhance an understanding of developmental and reproductive processes in the female germ line of *P. monodon*.

Full length cDNAs of functionally important genes in ovaries of *P. monodon*

The full length cDNA of *SARIP*, *PGMRC1*, *p23* and *Cdc42* transcripts and another functional important transcripts (such as, *PSR*, *Bystin*, *chk1*, *carbonyl reductase*, *protein disulfide-isomerase precursor PDI*, also called *prolyl 4-*

hydroxylase subunit beta, cellular thyroid hormone-binding protein (p55) (*Erp59*), *gonadotropin-regulated long chain acyl-CoA synthetase*, *Cdc20*, *protein mago nashi*, *actin depolymerizing factor*, *f-box and wd-40 domain protein*, *Cyclin-dependent kinase 7*, *selenoprotein M precursor* and *anaphase promoting complex subunit 11 homolog*) were successfully identified.

The putative *N*-linked glycosylation site (N-X-S/T) was not found in the deduced anaphase promoting complex subunit 11, *Cdc42*, selenoprotein M precursor, actin depolymerizing factor, carbonyl reductase, PSR, p23-like protein, PGMRC1 and PDI *Erp59* proteins of *P. monodon*. This indicated that these genes can be *in vitro* expressed in the bacterial expression system with the possibility to retain protein activity.

In addition, the deduced F-box and wd40 repeat domain binding protein, *Cdk7*, cytochrome B5, SARIP, selenoprotein M precursor, PSR, gonadotropin-regulated long chain acyl-CoA synthetase and PDI *Erp59* proteins contained a cAMP-dependent protein kinase phosphorylation site (K/R-K/R-X-S/T) implied that these genes should play a functionally important role in the signal transduction pathway during oocyte/ovary development.

Using DDRT-PCR and EST segment ligation, a novel mouse thymus involution related *Rwdd1* gene (or *SARIP*) was identified. The deduced ORF encoded a protein of 243 amino acid residues containing an RWD domain at the N terminus. The expression level of *Rwdd1* could affect the transactivation activity of androgen receptor (AR) in transiently transfected thymic epithelial cells. In mice, *Rwdd1* is a thymus involution related protein that may indirectly affect AR signaling pathway (Kang *et al.*, 2008).

Cdc42, a member of the small GTPases superfamily, acts in the control of the oocyte maturation pathway. The GDP-bound *Cdc42* greatly facilitates progesterone-induced maturation, whereas its GTP-bound form completely blocks meiotic maturation of oocytes (Cau *et al.*, 2000). In mouse, *Cdc42* also involved in MI spindle assembly and migration completion of meiosis I (Na and Zernicka-Goetz, 2006) but it was involved in control of spindle organization and positioning in

Xenopus. Cdc42 is also required for the cortical polarization that occurs prior to polar body extrusion (Ma *et al.*, 2006).

The presence of vertebrate-type steroids has been documented in almost all invertebrate groups including crustaceans (Lehoux and Sandor 1970; Lafont 1991). Nevertheless, steroid receptors have not been reported in penaeid shrimp.

Nuclear p23 was first characterized and named as an essential component of the Hsp90 molecular chaperone complex with the progesterone receptor (Johnson and Toft, 1994). Nuclear p23 binds the ATP-bound form of Hsp90 and blocks its ATPase activity, thereby stabilizing that state and thus client protein binding (Felts and Toft, 2003). Tissue distribution analysis shows that *p23* was observed in a variety of tissues of *P. monodon* broodstock suggests that its function in *P. monodon* not only acts as the progesterone receptor, but also act as chaperones in the folding and processing of proteins.

Recently, Mourot *et al.* (2006) characterized the full length cDNA of PGMRC1 (ORF of 546 nucleotide deduced to a polypeptide of 181 amino acids with one predicted transmembrane domain) and mPR- β (1080 nucleotides, 359 amino acids with eight predicted transmembrane domains) in the rainbow trout (*Oncorhynchus mykiss*). Both membrane-bound receptor transcripts was similarly expressed at the highest levels in the middle of vitellogenesis and down regulated during late vitellogenetic and mature stages. Levels of PGMRC1 mRNA were not upregulated by the hormonal (17,20 β P) treatment.

A homologue of PGMRC1 was identified from suppression subtractive hybridization (SSH) libraries of cDNA from juvenile and broodstock ovaries (this study) and testes (Leelatanawit *et al.*, 2008) of *P. monodon*. Previously, three isoforms of *P. monodon* progestin membrane receptor component 1: *PM-PGMRC1-s* (1980 bp), *PM-PGMRC1-m* (2848 bp), and *PM-PGMRC1-l* (2971 bp), with an identical ORF of 573 bp corresponding to a deduced polypeptide of 190 amino acids, were successfully identified in male *P. monodon*. Interestingly, the testis forms of *PM-PGMRC1* showed a greater expression level in testes of juvenile than broodstock of *P. monodon* ($P < 0.05$).

In contrast, a single isoform of ovarian *PGMRC1* with comparable to that inferred from RACE-PCR was observed from northern blot analysis. *PGMRC1* in ovaries of both juvenile and broodstock was more abundantly expressed than other tissues (e.g. gill and hepatopancreas of female broodstock and testes of male broodstock). This strongly indicated that *PGMRC1* should also play the important role on reproductive maturation of female shrimp. Only a single amino acid residue (V for ovarian isoform and A for testis isoform, position 88 of the deduced proteins) of the ovarian and testis isoforms of deduced *Pm*-PGMRC1 were different. Nucleotide sequence alignments and RT-PCR using isoform-specific primers indicated that these isoforms should be transcribed from different loci.

The Cyt-b5 domain functionally important for ubiquitous electron transportation in heme-binding protein and progesterone receptor (Ozols, J., 1989; Meyer *et al.*, 1996) was found in the deduced *PM*-PGMRC1. Most of the proteins with a Cyt-b5-domain are linked to cell membranes, either directly or by forming part of membrane-associated complexes (Mifsud and Bateman, 2002).

One potential transmembrane domain (amino acid residues 23rd - 41st) was identified in the deduced *Pm*-PGMRC1 as previously reported in mammalian (Gerdes, *et al.*, 1998) and the rainbow trout (Mourot *et al.*, 2006). Thus, results from this study for gene and amino acid sequence analysis and hydrophobicity analysis support the suggestion that *Pm*-PGMRC1 is similar to other known PGMRC1 previously described in various species.

Expression patterns of various transcripts isolated by EST analysis during ovarian development of *P. monodon*

Semiquantitative RT-PCR showed that *Pm-chk1*, *Pm-selenoprotein M precursor*, *Pm-keratinocytes associated protein 2*, *Pm-DNA replication licensing factor mcm2* and *Pm-egalitarian* were significantly down-regulated at stage IV ovaries (GSI > 6.0, $P < 0.05$). Generally, these transcripts involved in the cell division cycles. Therefore, they may play the important role on progression of ovarian development and lower levels of these genes may be necessary for the final maturation of *P. monodon* oocytes.

Quantitative real-time PCR indicated that *Cdc42* and *p23* play their important roles during the early stage of ovarian development. Eyestalk ablation did not alter expression patterns of these reproductively related genes in ovaries of *P. monodon*.

SARIP and *PGMRC1* played the important role in the late stage of ovarian development of normal *P. monodon* broodstock. Therefore, these gene products should involve in the final oocyte maturation in *P. monodon*. Results from the present study were concordant with the progesterone levels in ovaries of *P. monodon* examined by GC-MS where the highest level was found in mature ovaries (Fairs *et al.*, 1990).

Expression patterns of *SARIP* and *PGMRC1* in eyestalk-ablated of *P. monodon* broodstock revealed that these transcripts positively responded to eyestalk-ablation. Accordingly, these transcripts may be used as molecular indicators for investigation the progression in final maturation stage of *P. monodon* broodstock. Overexpression of *PGMRC1* also indicated that potent progesterone can induce oocyte maturation of *P. monodon*.

Female progesterone receptor knockout mice exhibited higher level of *PGRMCI* than the wild-type controls (Krebs *et al.*, 2000). The *PGRMCI* promoter does not contain a progesterone response element but it does possess a glucocorticoid response element (GRE) through which progesterone can mediate its suppressive effect on *PGRMCI* expression. Accordingly, progesterone (P4) exerts a modest down regulation of in *PGRMCI* the reporter gene assay (Cairns *et al.*, 1991). The findings clearly point to a specific role of progesterone in regulation of *PGRMCI* transcription.

Biogenic amines (e.g serotonin or 5-HT, epinephrine and dopamine) and peptide neuroregulators are known to modulate the release of neuropeptide hormones from the sinus gland (Alfaro *et al.*, 2004). Effects of exogenous 5-HT on the reproductive performance of *P. monodon* was recently examined. Domesticated shrimp treated with 5-HT (50 µg/g body weight) administration exhibited comparable ovarian maturation and spawning rates with eyestalk-ablated shrimp ($P < 0.05$) (Wongprasert *et al.*, 2006).

In present study, the expression levels of *Pm-PGMRC1* in ovaries of 5-HT treated *P. monodon* juveniles were also carried out. The level of *Pm-PGMRC1* transcript in each treatment was not significantly different ($P > 0.05$). It is premature at this stage to conclude that 5-HT has no effects on expression of *Pm-PGMRC1*. Accordingly, effects of 5-HT on expression of *Pm-PGMRC1* should be further carried out in *P. monodon* broodstock.

Interestingly, tissue distribution analysis revealed that *Pm-SARIP* was specifically expressed in gonads where a greater expression level was observed in ovaries than testes of *P. monodon*, whereas *Pm-PGMRC1*, *Pm-Cdc42* and *Pm-carbonyl reductase* were more abundantly expressed in ovaries of both juveniles and broodstock *P. monodon*. The results strongly recommended that these transcripts play important roles in ovarian development of *P. monodon*.

Unilateral eyestalk ablation is used commercially to induce ovarian maturation of penaeid shrimp but the technique leads to an eventual loss in egg quality and death of the spawner (Benzie, 1998; Okumura, 2004). Therefore, predictable maturation and spawning of captive penaeid shrimp without the use of eyestalk ablation is a long-term goal for the industry (Quackenbush, 2001). Taken the available information together, induced reproductive maturation of captive female *P. monodon* may be carried out by administration of serotonin and/or appropriate forms of progesterone (progestins). Effects of hormones and neurotransmitters on ovarian development and maturation of *P. monodon* broodstock should be further performed *in vivo*.

To evaluate the possible roles of examined gene products at a particular stage of ovarian development, gene expression profiles were considered. Functional involvement of each gene was inferred from its initially significant up- or down-regulation during ovarian development of *P. monodon*. Accordingly, *B cell RAG associated protein* and *APEX nuclease* should play their important roles in stage II ovaries of normal *P. monodon* broodstock. Likewise, *p23* may play an important role in stages II and III ovaries of normal and eyestalk-ablated *P. monodon* broodstock, respectively. *Cdc42* and *SARIP* should play their roles in stage III ovaries of both normal and eyestalk-ablated *P. monodon* broodstock. In contrast, *PGMRC1* plays an important role in stage IV ovaries of normal broodstock and stage II ovaries of

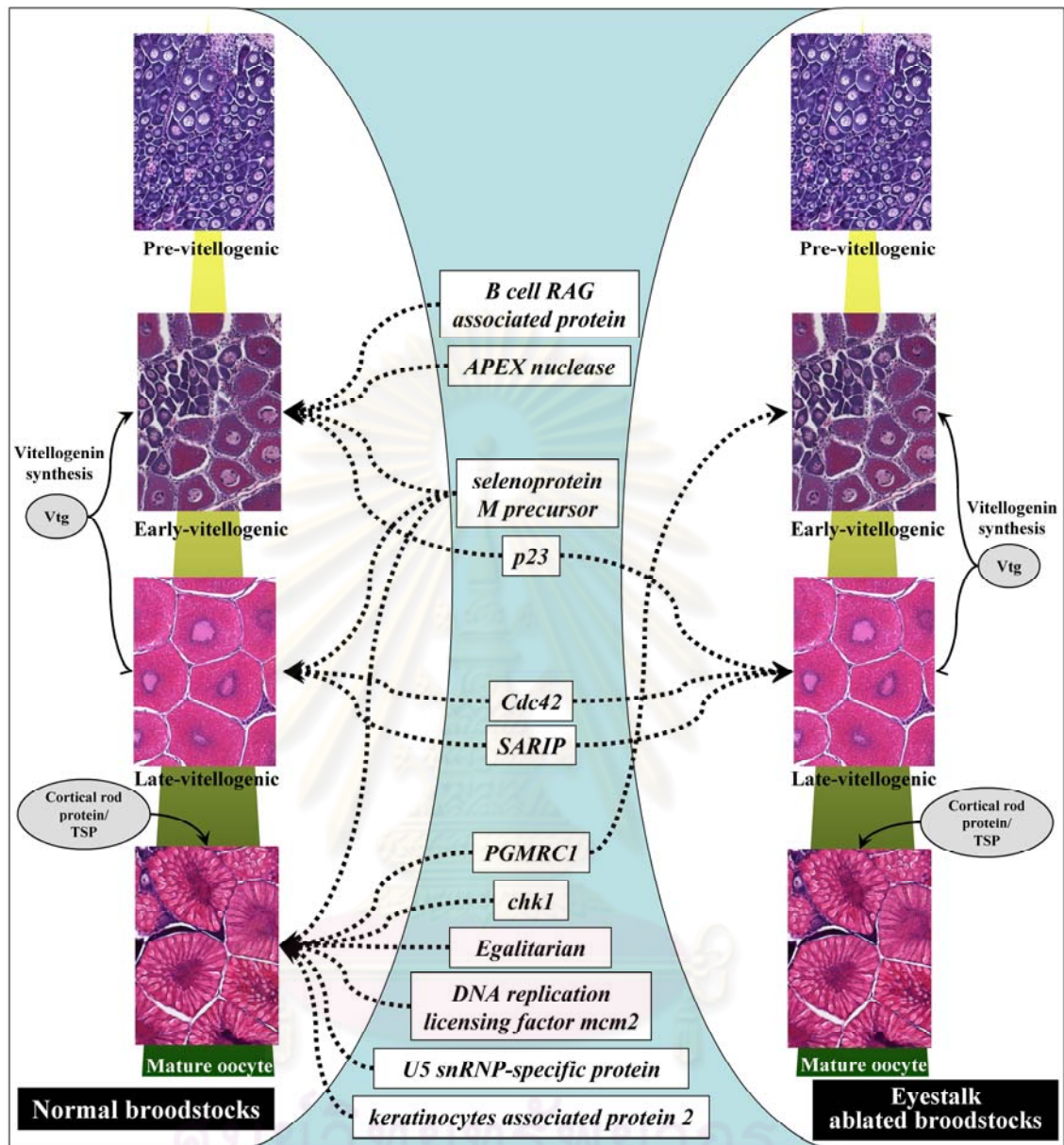


Figure 4.1 A diagram proposing functional involvement of various reproduction-related genes during ovarian development of normal and eyestalk-ablated *P. monodon* broodstock. The prediction was deduced from the expression profile of each gene. Vitellogenin (Vtg), cortical rod protein (CRP) and thrombospondin (TSP) were previously reported to be related with ovarian development of penaeid shrimp.

eyestalk-ablated broodstock. *Chk1*, *egalitarian*, *DNA replication licensing factor mcm2*, *U5 snRNP-specific protein* and *keratinocytes associated protein 2* should play their important roles in stage IV ovaries of normal broodstock. Interestingly, *selenoprotein M precursor* plays a prolonged role in stage II, III and IV ovaries of *P. monodon* broodstock (Figure 4.1).

Localization of gene products in ovaries of *P. monodon*

Localization of various genes was carried out using *in situ* hybridization and *Pm-TSP* and *Pm-VTG* transcripts were included as the protocol control. Clear positive signal was observed from the antisense probe of an abundantly expressed *Pm-TSP* and *Pm-VTG* transcripts in both normal and eyestalk-ablated shrimps. The result suggested that *in situ* hybridization technique set up in this study is successful.

In the germinative zone, oogonia did not display positive signals of *Pm-TSP* transcripts. Young oocytes located close to the germinative zone showed the earliest expression of *Pm-TSP* transcripts. In the immature ovary, strong signals were observed in cytoplasm of the early previtellogenic oocytes and slightly decreased in subsequent stages but not observed in CR oocyte stages. The results were in agreement with those reported in *M. japonicus* (Yamano *et al.*, 2004).

The signals of *Pm-VTG* were only detected in the follicle cells surrounding the late previtellogenic oocytes of *P. monodon*. This result was consistent with those previously reported in *M. japonicus* (Tsutsui *et al.*, 2000). The VTG protein analyzed was localized in ooplasm of vitellogenic oocytes and follicular cells of *P. monodon* ovaries (Tiu *et al.*, 2008).

The detection of rare transcripts can enhance by increasing the hybridization time up to 40 hours (Braissant and Wahli, 1998). Due to low signals of *Pm-PGMRC1* and *Pm-SARIP*, the detection time was extended to overnight at 4°C. From this step, the signal was clearly observed from the antisense probe. Unfortunately, the *Pm-PGMRC1* sense probe gave a non-specific signal in cytoplasm of previtellogenic oocytes of *P. monodon*.

Pm-Cdc42, *Pm-PGMRC1*, *Pm-SARIP* and *Pm-p23* transcripts were localized in the ooplasm of previtellogenic oocytes where late previtellogenic oocytes showed weaker signals than early previtellogenic oocytes. Positive signals were not detected in CR oocytes, oogonia in the germinative zone and follicular cells. The disappearance of hybridized signals of these transcripts in ooplasm of the later stages of oocytes may be due to significantly increasing oocytes sizes as oogenesis proceeded.

In the rainbow trout (*Onchorynchus mykiss*), *PGMRC1* mRNA was localized in the ooplasm of previtellogenic oocytes. Surprisingly, no signal was observed in mid-vitellogenic oocytes. On the other hand, real-time PCR showed that *PGMRC1* reached the highest expression level in mid-vitellogenic oocytes. This may be due to a dramatic volume increase over 100-fold during vitellogenesis of *O. mykiss* oocytes resulted in the lack of hybridized signals (Mourot *et al.* 2006). In addition, the sensitivity of real-time PCR on detecting gene expression is much greater than that of *in situ* hybridization.

Nonpurified PcAbs generated the positive signals along with non-specific immunoreactive bands. After affinity-chromatographic purification, Anti-Pm-PGMRC1 PcAb yielded only a target band and western blot analysis revealed two positive signals corresponding to the monomeric and dimeric forms of Pm-PGMRC1 but more intense signals of the dimeric than monomeric forms were observed throughout a reproductive cycle of *P. monodon*. It has been reported that PGRMC1 often detected as a 56-kDa dimer accompanying with a 28-kDa monomer in rat ovaries (Selmin *et al.*, 1996) and pig spermatozoa (Meyer *et al.*, 1996). In contrast, several positive bands were observed from immunohistochemistry of Pm-Cdc42. Accordingly, the positive bands may represent different forms of Cdc42 and should be further analyzed by peptide fragmentation using mass spectrometry to verify its suspected results.

Immunohistochemistry revealed positive signals of the PGMRC1 protein only in the follicular layer and cell membrane of follicular cells. Nevertheless, the false positive signal was also detected when tissue sections were incubated with normal sera. It was hypothesized that PGMRC1 was synthesized by oocytes and transported to other cell types after protein translation. In contrast, Pm-Cdc42 were

detected in oogonia (Oog), cytoplasm of previtellogenic oocytes (P) and follicular layer (FL).

PGRMC1 was present at the extracellular surface of the plasma membrane of the immature rat ovaries (Peluso *et al.*, 2006). Furthermore, PGRMC1 is found in the inner acrosomal membrane of porcine spermatozoa (Losel *et al.*, 2004) and both cytoplasm and the nucleus of human HeLa cell (Beausoleil *et al.*, 2004).

***In vitro* expression of recombinant Pm-p23 and Pm-Cdc42 and polyclonal antibody production**

Recombinant Cdc42 and p23 were successfully expressed *in vitro* and purified using Ni affinity chromatography. The purified proteins were subjected to the polyclonal antibody production in rabbit. Western blot analysis indicated that Pm-p23 in ovaries of juvenile and previtellogenic ovaries of broodstock was greater than later stages of ovaries. This illustrated that Pm-p23 was essential for the early stage of ovarian development. In contrast, Anti-Pm-Cdc42 yielded several non-specific bands as previously observed when the commercial available PcAb of yeast Cdc42 was used. Localization of Pm-p23 in different stages of oocytes should be examined.

Expression of functionally important gene homologues and the potential to be applied as biomarkers to monitor reproductive maturation of *P. monodon*

Reduced spawning potential of *P. monodon* in captivity and degree of maturation of *P. monodon* in captivity crucially prohibits several applications to improve efficiency of culture and management including the development of effective selective breeding programs of this species (Withyachumnarnkul *et al.*, 1998).

Ovarian maturation in penaeid shrimps involves formation of cortical rods (CRs) in the peripheral crypts of oocytes at final stages of oocyte development. CRs first microscopically appear as spherical structures in fully yolk-invested oocytes one to two days before spawning. They then extend toward the center of the oocytes, forming a rod-like shape. At the time of spawning the contact of eggs with seawater stimulates the release of CRs outward, which results in the formation of a jelly layer that surrounds the fertilized eggs within 15 minutes after spawning (Wallis *et al.*,

1990). The jelly layer is thought to function as a barrier against polyspermy and between the egg and the external environment.

Yamano *et al.* (2004) pointed out that ovaries of *P. japonicus*, in most cases, start to develop in the reproductive season but fail to reach the necessary stage required by the formation of CRs. Accordingly, ovaries are degenerate without spawning. Ovarian development of penaeid shrimps may not pass through to the accumulation of yolk substances or in some cases to the stage after yolk accumulation is achieved. Further studies about mechanisms controlling formation of CRs is, therefore, required to control maturation of *P. monodon* in captivity successfully.

In the present study, a large number of cDNA including sex-related transcripts in ovaries of *P. monodon* were identified. The expression profiles of various genes in ovaries of normal and eyestalk-ablated *P. monodon* broodstock implied that several genes may have contributed ovarian development and maturation in *P. monodon*. Functionally analysis of genes/proteins involving ovarian development can be further carried out for better understanding of the reproductive maturation of female *P. monodon* in captivity.

CHAPTER V

CONCLUSION

1. A total of 4560 clones (2330 clones from a typical, 1778 clones from a normalized and 452 clones from subtractive ovarian cDNA libraries) were unidirectional sequenced and 3482 (76.4%) ESTs significantly matched known genes previously deposited in the GenBank (E-value $< 10^{-4}$). Sequence assembly of all ESTs generated 441 unique contigs and 1231 (27.0%) singletons.
2. RAP-PCR was carried out for identification of differentially expressed transcripts during ovarian development of *P. monodon*. Fourteen candidate RAP-PCR fragments were cloned and sequenced. Semi-quantitative RT-PCR indicated that the expression level of *B cell RAG associated protein* and *APEX nuclease* at stage I ovaries was greater than that of subsequent stages ($P < 0.05$). In contrast, *U5 snRNP-specific protein* was down-regulated at stage IV ovaries ($P < 0.05$).
3. The full length cDNA of *SARIP*, *PGMRC1*, *p23*, *Cdc42*, *PSR*, *Bystin*, *chk1*, *carbonyl reductase*, *Protein disulfide-isomerase precursor (PDI)*, *gonadotropin-regulated long chain acyl-CoA synthetase*, *Cdc20*, *protein mago nashi*, *actin depolymerizing factor*, *f-box and wd-40 domain protein*, *Cyclin-dependent kinase 7*, *selenoprotein M precursor* and *anaphase promoting complex subunit 11 homolog* were successfully characterized.
4. Expression patterns of 31 gene homologues were examined using RT-PCR. Seventeen genes (*p23*, *PGMRC1*, *vitellogenin*, *26S proteasome regulatory subunit rpn2*, *CWF19-like 2*, *DNA replication licensing factor mcm2*, *Neuralized protein*, *Keratinocytes associated protein 2*, *chk1*, *Selenoprotein M precursor*, *carbonyl reductase*, *RNA polymerase I associated factor 53 isoform 1*, *Selenophosphate synthetase* and *egalitarian*) exhibited a trend of differential expression during ovarian development of wild *P. monodon* broodstock.
5. Expression levels of 5 gene homologues from SSH ovarian cDNA libraries were examined using semi-quantitative RT-PCR. *Pm-chk1*, *Pm-selenoprotein M precursor*,

Pm-keratinocytes associated protein 2, *Pm-DNA replication licensing factor mcm2* and *Pm-egalitarian* were significantly down-regulated at stage IV ovaries (GSI > 6.0, $P < 0.05$). Therefore, these genes may play an important role in oocyte development rather than the final maturation of oocytes.

6. Quantitative real-time PCR indicated that *Pm-p23* was up-regulated at the early stage ($P < 0.05$) whereas *Pm-Cdc42* was down-regulated at stage III ($P < 0.05$) of ovarian development. Eyestalk ablation did not alter the expression pattern of *Pm-p23* ($P > 0.05$) but caused increasing levels of *Pm-Cdc42* at stage III and IV ovaries of *P. monodon* ($P < 0.05$). In contrast, *Pm-SARIP* and *Pm-PGMRC1* were differentially expressed in ovaries of normal broodstock ($P < 0.05$). Eyestalk ablation resulted in earlier and greater expression levels of these genes in ovaries of eyestalk-ablated broodstock than normal broodstock ($P < 0.05$). Results suggested that *Pm-SARIP* and *Pm-PGMRC1* may be used as bioindicators for monitoring progression of oocyte maturation of *P. monodon* broodstock.

7. *In situ* hybridization illustrated that *Pm-Cdc42*, *Pm-PGMRC1*, *Pm-SARIP* and *Pm-p23* transcripts were localized in the ooplasm of previtellogenic oocytes. Immunohistochemistry revealed positive signals of the Pm-PGMRC1 protein in the follicular layer and cell membrane of follicular cells suggesting that Pm-PGMRC1 may be synthesized by oocytes and transported to other cell types after translation.

8. Recombinant Pm-Cdc42 and Pm-p23 proteins were successfully expressed *in vitro*. Polyclonal antibodies (PcAb) of these recombinant proteins were successfully produced. Western blot analysis indicated that the level of p23 was decreased as oogenesis progressed whereas anti-Pm-Cdc42 PcAb yielded non-specific signals. Results strongly confirmed functional importance of p23 gene products during vitellogenesis of *P. monodon* oocytes.

REFERENCES

- Abe, S.-I. 1987. Differentiation of spermatogenic cells from vertebrates *in vitro*. Int. Rev. Cytol. 109: 159-209.
- Adams, M. D., Kelley, J. M., Gocayne, J. D., Dubnick, M., Polymeropoulos, M. H., Xiao, H., Merril, C. R., Wu, A., Olde, B., Moreno, R. F., Kerlavage, A. R., McCombie, W. R., and Venter, J. C. 1991. Complementary DNA sequencing: expressed sequence tags and human genome project. Science. **252** : 1651-1656.
- AIMS, Manual for the Determination of Egg Fertility in *Penaeus monodon* [Online]. 2009. Available from: <http://www.aims.gov.au/pages/research/mdef/mdef-00.html> [2009, February 20].
- Alfaro, J., Zuniga, G., and Komen, J. 2004. Induction of ovarian maturation and spawning by combined treatment of serotonin and a dopamine antagonist, spiperone in *Litopenaeus stylirostris* and *Litopenaeus vannamei*. Aquaculture. 236 : 511-522.
- Altschul, S. F., Gish, W., Miller, W., Myers, E. W., and Lipman, D. J. 1990. Basic local alignment search tool. J. Mol. Biol. 215 : 403-410.
- Anderson, I., and Brass, A. 1998. Searching DNA databases for similarities to DNA sequences: when is a match significant? Bioinformatics 14(4) : 349-356.
- Avarre, J.-C., Khayat, M., Michelis, R., Nagasawa, H., Tietz, A. and Lubzens, E. 2001. Inhibition of de novo synthesis of a jelly layer precursor protein by crustacean hyperglycemic hormone family peptides and posttranscriptional regulation by sinus gland extracts in *Penaeus semisulcatus* ovaries. Gen. Comp. Endocrinol. 124 : 257-268.
- Bachem, C. W. B., Vander Hoeven, R. S., deBruijin, S. M., Vreugdenhil, D., Zabeau, M., and Visser, R. G. F. 1996. Visualisation of differential gene expression using a novel method of RNA fingerprinting based on AFLP: analysis of gene expression during tuber development. Plant J. 9 : 745-753.

- Bai, C., Sen, P., Hofmann, K., Ma, L., Goebel, M., Harper, J. W., and Elledge, S. J. 1996. SKP1 connects cell cycle regulators to the ubiquitin proteolysis machinery through a novel motif, the F-box. Cell. 86(2) : 263–274.
- Barr, F., and Emanuel, B. 1990. Application of a subtraction hybridization technique involving photo activatable biotin and organic extraction to solution hybridization analysis of genomic DNA. Anal.Biochem. 186 : 369-373.
- Baryshev, M., Sargsyan, E., and Mkrtchian, S. 2006. ERp29 is an essential endoplasmic reticulum factor regulating secretion of thyroglobulin. Biochem. Biophys. Res. Commun. 340(2) : 617-24.
- Bauchau, A. G. 1981. Crustaceans. In: Ratcliffe N. A., and Rowley, A. F. (editors). Invertebrate blood cells. Academic Press, London and New York. pp. 385-420.
- Beausoleil, S. A., Jedrychowski, M., Schwartz, D., Elias, J. E., Villen, J., Li, J., and et al. 2004. Large-scale characterization of HeLa cell nuclear phosphoproteins. Proc. Natl. Acad. Sci. USA. 101 : 12130-12135.
- Benzie, J. A. H. 1997. A review of the effect of genetics and environment on the maturation and larval quality of the giant tiger prawn *Penaeus monodon*. Aquaculture. 155 : 69-85.
- Benzie, J. A. H. 1998. Penaeid genetics and biotechnology. Aquaculture. 164 : 23-47.
- Bertioli, D. J., Schlichter, U. H., Adams, M. J., Burrows, P. R., Steinbiss, H. H., and Antoniw, J. F. 1995. An analysis of differential display shows a strong bias towards high copy number mRNAs. Nucleic Acids Res. 23 : 4520-4523.
- Boag, P. R., Newton, S. E., Hansen, N-P., Christensen, C. M., Nansen, P. and Gasser, R. B. (2000) Isolation and characterization of sex-specific transcripts from *Oesophagostomum dentatum* by RNA arbitrarily-primed PCR. Mol. Biochem. Parasitol. 108 : 217-224.
- Bonaldo, M., Lennon, G., and Soares, M. 1996. Normalization and subtraction: Two approaches to facilitate gene discovery. Genome Res. 6 : 791-806.
- Bradford, M. M. 1976. A rapid and sensitive method for the quantitation of microgram quantities of protein utilizing the principle of protein-dye binding. Anal. Biochem. 72 : 248-254.

- Braissant, O., and Wahli, W. 1998. A simplified *in situ* hybridization protocol using non-radioactively labeled probes to detect abundant and rare mRNAs on tissue sections. Biochemica. 1 : 10-16.
- Brusca, R. C., and Brusca, G. J. 1990. Invertebrates. Sinauer Associates, Inc., Massachusetts, 922 pp.
- Cahill, M. A. 2007. Progesterone receptor membrane component 1: an integrative review. J. Steroid Biochem. Mol. Biol. 150 : 16-36.
- Cairns, C., Gustafsson, J. A., and Carlstedt-Duke, J. 1991. Identification of protein contact sites within the glucocorticoid/progestin response element. Mol. Endocrinol. 5 : 598-604.
- Callard, G. V. 1991. Spermatogenesis. In: Pang, K.T., Schreibman, M.P. (Eds.) Vertebrate endocrinology; fundamentals and biochemical implication, Vol 4 Part A. San Diego: Academic Press. pp. 303-341.
- Carninci, P., Shibata, Y., Hayatsu, N., Sugahara, Y., Shibata, K., Itoh, M., Konno, H., Okazaki, Y., Muramatsu, M. and Hayashizaki, Y. 2000. Normalization and subtraction of cap-trapper-selected cDNAs to prepare full-length cDNA libraries for rapid discovery of new genes. Genome Res. 10 : 1617-1630.
- Cau, J., Faure, S., Vigneron, S., Labbe, J. C., Delsert, C., and Morin, N. 2000. Regulation of *Xenopus* p21-activated kinase (X-PAK2) by Cdc42 and maturation-promoting factor controls *Xenopus* oocyte maturation. J. Biol. Chem. 275 : 2367-2375.
- Chan, S.-M., Gu, P. L., Chu, K. H., and Tobe, S. S. 2003. Crustacean neuropeptide genes of the CHH/MIH/GIH family: implications from molecular studies. Gen. Comp. Endocrinol. 134 : 214-219.
- Chang, E. S. 1993. Comparative endocrinology of molting and reproduction: insects and crustaceans. Annu. Rev. Entomol. 38 : 161-180.
- Clifford, H. C., and Preston, N. P. 2006. Genetic improvement; in Operating Procedures for Shrimp Farming: Global Shrimp OP Survey Results and Recommendations, pp. 73-77. Global Aquaculture Alliance, St. Louis, USA.
- Clissold, P. M., and Ponting, C. P. 2001. JmjC Cupin metalloenzyme-like domains in jumonji, hairless and phospholipase A₂β. Trends Biochem Sci. 26 : 7-9.

- Coman, G. J., Arnold, S. J., Peixoto, S., Crocos, P. J., Coman, F. E., and Preston, N. P. 2006. Reproductive performance of reciprocally crossed wild-caught and tank reared *Penaeus monodon* broodstock. Aquaculture. 252 : 372-384.
- Cuzon, G. Guillaume, J., and Cahu, C. 1994. Composition, preparation and utilization of feeds for Crustacea. Aquaculture. 124 : 253-267.
- De Kleijn, D. P. V., and Van Herp, F. 1995. Molecular biology of neurohormonal precursors in the eyestalks of crustacean. Comp. Biochem. Physiol. B. 112 : 573-579.
- Diatchenko, L., Lau, Y. C., Campbell, A. P., Chenchik, A., Moqadam, F., Hung, B., Lukyanov, S., Lukyanov, K., Gurskay, N., Sverdlov, E. D. and Siebert, P. D. 1996. Suppression subtractive hybridization: a method for generating differentially regulated or tissue-specific cDNA probes and libraries. Proc. Natl. Acad. Sci. USA. 93 : 6025-6030.
- Diwan, A. D., Joseph, S., and Ayyappan, S. 2009. Physiology of reproduction, breeding and culture of tiger shrimp *Penaeus monodon* (Fabricius). Narendra Publishing House, 1st edition. 292 pp.
- Donzelli, M., and Draetta, G. F. 2003. Regulating mammalian checkpoints through Cdc25 inactivation. EMBO Rep. 4 : 671-677.
- Espey, L. L., Yoshioka, S., Russel, D., Ujioka, T., Vladu, B., Skelsey, M., Fujii, S., Okamura, H., and Richards, J. S. 2000. Characterization of ovarian carbonyl reductase gene expression during ovulation in the gonadotropin-primed immature rat. Biol. Reprod. 62 : 390-397.
- FAO, Fishery Statistic [Online]. 2009. Available from: <http://www.fao.org/fishery/statistics/en> [2009, February 20].
- Fairs, N. J., Quinlan P. T., and Goad L. J. 1990. Changes in ovarian unconjugated and conjugated steroid titers during vitellogenesis in *Penaeus monodon*. Aquaculture. 89 : 83-99.
- Fargnoli, J., Holbrook, N., and Fornace Jr., A. 1990. Low-ratio hybridization subtraction. Anal. Biochem. 187 : 364-73.
- Felts, S. J., and Toft, D. O. 2003. p23, a simple protein with complex activities. Cell Stress Chaperones. 8 : 108-113

- Fernandes, M. S., Brosens, J. J., and Gellersen, B. 2008. Honey, we need to talk about the membrane progesterin receptors. Steroids 73 : 43-53.
- Frohman, M. A., Dush, M. K., and Martin, G. R. 1988. Rapid production of full-length cDNAs from rare transcripts: amplification using a single gene-specific oligonucleotide primer. Proc. Natl. Acad. Sci. U.S.A. 85 : 8998-9002.
- Garcia-Ranea, J. A., Mirey, G., Camonis, J., and Valencia, A. 2002. p23 and Hsp20/ α -crystallin proteins define a conserved sequence domain present in other eukaryotic protein families. FEBS Lett. 529 : 162-167.
- Gerdes, D., Wehling, M., Leube, B., and Falkenstein, E. 1998. Cloning and tissue expression of two putative steroid membrane receptors. Biol. Chem. 379 : 907-911.
- Gross, P. S., Bartlett, T. C., Browdy, C. L., Chapman, R. W. and Warr, G. W. 2001. Immune gene discovery by expressed sequence tag analysis of hemocytes and hepatopancreas in the Pacific white shrimp, *Litopenaeus vannamei* and the Atlantic white shrimp, *L. setiferus*. Dev. Comp. Immunol. 25 : 565-577.
- Gu, P. L., Tobe, S. S., Chow, B. K., Chu, K. H., He, J. G., and Chan, S. M. 2002. Characterization of an additional molt inhibiting hormone-like neuropeptide from the shrimp *Metapenaeus ensis*. Peptides. 23 : 1875-1883.
- Hanks, S. K., Quinn, A. M., and Hunter, T. 1988. The protein kinase family: conserved features and deduced phylogeny of the catalytic domains. Science. 241(4861) : 42-52.
- Harrison, K. E. 1990. The role of nutrition in maturation, reproduction and embryonic development of decapod crustaceans: A review. J. Shellfish Res. 9 : 1-28.
- Huang, X., and Madan, A. 1999. CAP3: A DNA sequence assembly program. Genome Res. 9 : 868-877.
- Ibarra, A. M., Racotta, I. S., Arcos, F. G., and Palacios E. 2007. Progression the genetics of reproductive performance in Penaeid shrimp. Aquaculture. 268 : 23-43.

- Jarayabhand, P., Uraiwan, S., Klinbunga, S., Tassanakajon, A., Srimukda, P., Pattanachan, P., Panakulchaiwit, R. and Menasveta, P. 1998. Estimated heritabilities for early growth rate of the black tiger prawn, *Penaeus monodon*, Fabricius. In: Felgel, T. (ed.), *Advances in Shrimp Biotechnology*, National Center for Genetic Engineering and Biotechnology, Bangkok, pp. 67-70.
- Johnson, J. L., Beito, T. G., Krco, C. J., and Toft, D. O. 1994. Characterization of a novel 23-kilodalton protein of inactive progesterone receptor complexes. Mol Cell Biol. 14(3) : 1956-1963.
- Johnson, J. L., and Toft, D. O. 1994. A novel chaperone complex for steroid receptors involving heat shock proteins, immunophilins, and p23. J. Biol. Chem. 269 : 24989-24993.
- Johnson, P. T. 1980. Histology of the blue crab, *Callinectes sapidus*. A model for the Decapoda. Praeger. New York. 440 pp.
- Kalderon, D., and Rubin, G. M. 1989. cGMP-dependent protein kinase genes in *Drosophila*. J. Biol. Chem. 264 : 10738-10748.
- Kang, N., Duan, L., Tang, L., Liu, S., Li, C., Li, Y., Liu, Q., Hu, Y., Cui, L., and He, W. 2008. Identification and characterization of a novel thymus aging related protein *rwdd1*. Cell Mol. Immunol. 5(4) : 279-85.
- Karlsson-Rosenthal, C., and Jonathan, B. A. M. 2006. Cdc25: mechanisms of checkpoint inhibition and recovery. Trends Cell Biol. 16(6) : 285-92.
- Khamnamtong, B., Klinbunga, S. and Menasveta, P. 2005. Species identification of five penaeid shrimps using PCR-RFLP and SSCP analyses of 16S ribosomal DNA. J. Biochem. Mol. Biol. 38 : 491-499.
- Khayat, M., Babin, P. J., Funkenstein, B., Sammar, M., Nagasawa, H., Tietz, A. and Lubzens, E. 2001. Molecular characterization and high expression during oocyte development of a shrimp ovarian cortical rod protein homologous to insect intestinal peritrophins. Biol. Reprod. 64 : 1090-1099.
- King, J. E. 1948. A study of the reproductive organs of the common marine shrimp, *Penaeus setiferus* (Linnaeus). Biol. Bull. 94 : 244-262.

- Klinbunga, S. 1996. Genetic variation and population structure of the giant tiger shrimp (*Penaeus monodon* Fabricius). PhD's thesis. University of Stirling, Scotland. 356 pp.
- Klinbunga, S., Penman, D.J., McAndrew, B.J., and Tassanakajon, A. 1999. Mitochondrial DNA diversity in three populations of the giant tiger shrimp, *P. monodon*. Mar. Biotechnol. 1(2) : 113-121.
- Krebs, C. J., Jarvis, E. D., Chan, J., Lydon, J. P., Ogawa, S., and Pfaff, D. W. 2000. A membrane-associated progesterone-binding protein, 25-Dx, is regulated by progesterone in brain regions involved in female reproductive behaviors. Proc. Natl. Acad. Sci. USA. 97 : 12816-21.
- Kyte, J., and Doolittle, R. 1982. A simple method for displaying the hydropathic character of a protein. J. Mol. Biol. 157 : 105-132.
- Laemmli, U. K. 1970. Cleavage of structural proteins during the assembly of the head of bacteriophage T4. Nature. 227(5259) : 680-685.
- Lafont, R. 1991. Reversal endocrinology or "hormones" seeking functions. Insect Biochem. 21 : 697-721.
- Lee, D. O'C., and Wickins, J. F. 1992. Crustacean farming. Blackwell Scientific Publications, The University Press, Cambridge. 392 pp.
- Leelatanawit, R., Klinbunga, S., Puanglarp, N., Tassanakajon, A., Jarayabhand, P., Hirono, I., Aoki, T., and Menasveta, P. 2004. Isolation and characterization of differentially expressed genes in ovaries and testes of the giant tiger shrimp (*Penaeus monodon*). Mar. Biotechnol. 6: S506-S510.
- Leelatanawit, R., Klinbunga, S., Hirono, I., Aoki, T., and Menasveta, P. 2008. Suppression subtractive hybridization (SSH) for isolation and characterization of genes related with testicular development of the giant tiger *Penaeus monodon*. BMB Reports. 41(11) : 796-802.
- Lehoux, J. G., and Sandor, T. 1970. The occurrence of steroids and steroid-metabolising enzyme system in invertebrates. Steroids. 16 : 141-171.
- Liang, P., and Pardee, A. B. 1992. Differential display of eukaryotic messenger RNA by means of the polymerase chain reaction. Science. 257 : 967-971.

- Limsuwan, C. 2004. Diseases of Pacific white shrimp (*Litopenaeus vannamei*) cultured in Thailand. Proceeding of the JSPS-NRCT International Symposium Joint Seminar 2004: Management of Food Safety in Aquaculture and HACCP. pp. 36-41, Kasetsart University, Thailand.
- Liu, Z. J., and Cordes, J. F. 2004. DNA marker technologies and their applications in aquaculture genetics. Aquaculture 238 : 1-37.
- Lo, T. S., Cui, Z. X., Mong, L. Y., Wong, W. L., Chan, S. M., Kwan, H. S., and Chu, K. H. 2007. Molecular coordinated regulation of gene expression during ovarian development in the penaeid shrimp. Marine Biotechnol. 9 : 459-468.
- Longyant, S., Sithigorngul, P., Thammapalerd, N., Sithigorngul, W., and Menasveta, P. 2000. Characterization of vitellin and vitellogenin of giant tiger prawn *Penaeus monodon* using monoclonal antibodies specific to vitellin subunits. Invert. Reprod. Dev. 37 : 211-221.
- Lopez, C., Piegu, B., Cooke, R., Delseny, M., Tohme, J., and Verdier, V. 2005. Using cDNA and genomic sequences as tools to develop SNP strategies in cassava (*Manihot esculenta* Crantz). Theor. Appl. Genet. 110 : 425-431.
- Losel, R., Dorn-Beineke, A., Falkenstein, E., Wehling, M., and Feuring, M. 2004. Porcine spermatozoa contain more than one membrane progesterone receptor. Int. J. Biochem. Cell. Biol. 36 : 1532-41.
- Ma, C., Benink, H. A., Cheng, D., Montplaisir, V., Wang, L., Xi, Y., Zheng, P.-P., Bement, W. M., and Liu, X. J. 2006. Cdc42 activation couples spindle positioning to first polar body formation in oocyte maturation. Curr. Biol. 16 : 214-220.
- MacIntosh, G. C, Wilkerson, C., Green, P. J. 2001. Identification and analysis of analysis of Arabidopsis expressed sequence tags characteristic of non-coding RNAs. Plant Physiol. 127(3) : 765-776.
- Maller, J. L. 2003. Signal transduction: Fishing at the cell surface. Science. 300(5619) : 594-595.
- Maruyama, K. and Sugano, S. 1994. Oligo-capping: A simple method to replace the cap structure of eukaryotic mRNAs with oligoribonucleotides. Gene. 138 : 171-174.

- Marsden, G. E., Mather, P. B., and Richardson, N. A. 2007. Captivity, ablation and starvation of the prawn *Penaeus monodon* affects protein and lipid content in ovary and hepatopancreas tissues. Aquaculture. 271(1-4) : 507-515.
- Maxam, A.M., and Gilbert, W. 1977. A new method for sequencing DNA. Proc. Natl. Acad. Sci. 74 : 560.
- Meusy, J. J., and Payen, G. G. 1988. Female reproduction in Malacostracan Crustacea. Zool. Sci. 5 : 217-265.
- Meyer, C., Schmid, R., Scriba, P. C., and Wehling, M. 1996. Purification and partial sequencing of high-affinity progesterone-binding site(s) from porcine liver membranes. Eur. J. Biochem. 239 : 726-731.
- Mifsud, W., and Bateman, A. 2002. Membrane-bound progesterone receptors contain a cytochrome b5-like ligand-binding domain. Genome Biol. 3(12) : 1-5.
- Miura, T., Higuchi, M., Ozaki, Y., Ohta, T., and Miura, C. 2006. Progesterone is an essential factor for the initiation of the meiosis in spermatogenic cells of the eel. Proc. Natl. Acad. Sci. USA. 103 : 7333-7338.
- Morimoto, R. I. 2002. Dynamic remodeling of transcription complexes by molecular chaperones. Cell. 110 : 281-284.
- Motoh, H. 1984. Biology and ecology of *Penaeus monodon*. Proceedings of the First International Conference on the Culture of Penaeid Prawns/Shrimp. SEAFDEC Aquaculture Department, Iloilo City. pp. 27-36.
- Motoh, H., Buri, P. 1980. Development of the external genitalia of the giant prawn, *Penaeus monodon*. Bull. Jap. Soc. Sci. Fish. 46 : 149-155.
- Mourot, B., Nguyen, T., Fostier, A., and Bobe, J. 2006. Two unrelated putative membrane-bound progesterone receptors, progesterone membrane receptor component 1 (PGMRC1) and membrane progesterone receptor (mPR) beta, are expressed in the rainbow trout oocyte and exhibit similar ovarian expression patterns Reprod. Biol. Endocrinol. 4(6) : 1-14.
- Murray, A. W. 2004. Recycling the cell cycle: cyclins revisited. Cell. 116 : 221-234.

- Na, J., and Zernicka-Goetz, M. 2006. Asymmetric positioning and organization of the meiotic spindle of mouse oocytes requires CDC42 function. Curr. Biol. 16 : 1249-1254.
- Nagabhushanam, R., Joshi, P. K., and Kulkarni, G. K., 1980. Induced spawning in the prawn *Parapenaeopsis stylifera* (H. Milne Edwards) using a steroid hormone 17α -hydroxyprogesterone. Indian J. Mar. Sci. 9 : 227.
- Newmark, P., and Boswell, R. 1994. The mago nashi locus encodes an essential product required for germ plasm assembly in *Drosophila*. Development. 120(5) : 1303-1313.
- Okumura, T. 2004. Perspectives on hormonal manipulation of shrimp reproduction. JARQ 38 : 49-54.
- Okumura, T., Kim, Y. K., Kawazoe, I., Yamano, K., Tsutsui, N. and Aida, K. 2006. Expression of vitellogenin and cortical rod proteins during induced ovarian development by eyestalk ablation in the kuruma prawn, *Marsupenaeus japonicus*. Comp. Biochem. Physiol. A 143 : 246-253.
- Pardue, M. L., and Gall, J. G. 1969. Molecular hybridization of radioactive DNA to the DNA of cytological preparations. Proc. Natl. Acad. Sci. USA. 64 : 600-604.
- Peluso, J. J., Pappalardo, A., Losel, R., and Wehling, M. 2006. Progesterone membrane receptor component 1 expression in the immature rat ovary and its role in mediating progesterone's antiapoptotic action. Endocrinology. 147 : 3133-40.
- Pertea, G., Huang, X., Liang, F., Antonescu, V., Sultana, R., Karamycheva, S., Lee, Y., White, J., Cheung, F., Parvizi, B., Tsai, J., and Quackenbush, J. 2003. TIGR Gene Indices clustering tools (TGICL): a software system for fast clustering of large EST datasets. Bioinformatics. 19(5) : 651-652 .
- Pongtippatee-Taweepreda, P., Chavadej, J., Plodpai, P., Pratoomchart, B., Sobhon, P., Weerachatanukul, W., and Withyachumnarnkul, B. 2004. Egg activation in the black tiger shrimp *Penaeus monodon*. Aquaculture. 234: 183-198.
- Primavera, J. H. 1990. External and internal anatomy of adult penaeid prawns/shrimps. SEAFDEC, Aquaculture Department, The Philippines, Poster.

- Qiu, G-F. and Yamano, K. 2005. Three forms of cyclin B transcripts in the ovary of the kuruma prawn *Marsupenaeus japonicus*: Their molecular characterizations and expression profiles during oogenesis. Comp. Biochem. Physiol. B. 141 : 186-195.
- Qiu, G-F., Yamano, K., and Unuma, T. 2005. Cathepsin C transcripts are differentially expressed in the final stages of oocyte maturation in kuruma prawn *Marsupenaeus japonicus*. Comp. Biochem. Physiol. B. 140 : 171-181.
- Qiu, L., Jiang, S., Zhou, F., Zhang, D., Huang, J., and Guo, Y. 2008. Molecular cloning and mRNA expression of cyclophilin A gene in black tiger shrimp (*Penaeus monodon*). Mol. Biol. Rep. 35(3) : 431-8.
- Quackenbush, L. S. 2001. Yolk synthesis in the marine shrimp, *Penaeus vannamei*. Comput. Biol. 41(3) : 458-464.
- Quinitio, E. T., Hara, A. Yamaguchi, K., and Fuji, A. 1994. Changes in the steroid hormone and vitellogenin levels during the gametogenic cycle of the giant tiger shrimp, *Penaeus monodon*. Comp. Biochem. Physiol. C. 109 : 21-26.
- Rao, B. R., Wiest, W. G., and Allen, W. M. 1974. Progesterone "receptor" in human endometrium, Endocrinology. 95 : 1275-1281.
- Rao, L. H., Kathirvel, M., Ravichandran, P., and Sivagnanam, S. 1995. Development of broodstock of tiger prawn *Penaeus monodon* in captivity. CIBA Bulletin. 6 : 1-10.
- Rodriguez, E. M., Medesani, D. A., Greco, L. L., and Fingerman, M. 2002. Effects of some steroids and other compounds on ovarian growth of the red swam crayfish, *Procambarus clarkii*, during early vitellogenesis. J. Exp. Zool. 292 : 82-87.
- Rojtinnakorn, J., Hirono, I., Itami, T., Takahashi, Y. and Aoki, T. 2002. Gene expression in haemocytes of kuruma prawn, *Penaeus japonicus* in response to infection with WSSV by EST approach. Fish Shellfish Immunol. 13 : 69-83.
- Rosenberry, B. 1997. World Shrimp Farming 1997. Shrimp News International, San Diego. 284 pp.
- Rouleau, N., Reeben, M., Palvimo, J. J., and Janne, O. A. 1999. A small novel protein interacts with androgen receptor. The EMBL GenBank DDBJ databases [Submitted].

- Saiki, R. K., Bugawan, T. L., Horn, G. T., Mullis, K. B., and Erlich, H. A. 1986. Analysis of enzymatically amplified beta-globin and HLA-DQ alpha DNA with allele-specific oligonucleotide probes. Nature. 324(6093) : 163-166.
- Sambrook, J. and Russell, D. W. 2001. Molecular Cloning: A Laboratory Manual, 3rd ed., Cold Spring Harbor Laboratory Press, New York, USA.
- Sanger, F., Nicklen, S., and Coulson, A.R. 1977. DNA sequencing with chain-terminating inhibitors. Proc. Natl. Acad. Sci. 74 : 5463.
- Selmin, O., Lucier, G. W., Clark, G. C., Tritscher, A. M., Vanden-Heuvel, J. P., Gastel, J. A., Walker, N. J., Sutter, T. R., and Bell, D. A. 1996. Isolation and characterization of a novel gene induced by 2,3,7,8-tetrachlorodibenzo-p-dioxin in rat liver. Carcinogenesis. 17 : 2609-2615.
- Shen, Y. Q., Xiang, J. H., Wang, B., Li, F. H. and Tong, W. 2004. Discovery of immune related factors in *Fenneropenaeus chinensis* by annotation of ESTs. Prog. Nat. Sci. 14 : 47-54.
- Silva Gunawardene, Y. I. N., Chow, B. K. M., He, J. G., and Chan, S. M. 2001. The shrimp FAMET cDNA is encoded for a putative enzyme involved in the methylfarnesoate (MF) biosynthetic pathway and is temporally expressed in the eyestalk of different sexes. Insect. Biochem. Mol. Bio. 131 : 1115-1124.
- Srisuparbh, D., Klinbunga, S., Wongsiri, S. and Sittipraneed, S. (2003) Isolation and characterization of major royal jelly cDNAs and proteins of the honey bee (*Apis cerana*). J. Biochem. Mol. Biol. 36 : 572-579.
- Staelens, J., Rombaut, D., Vercauteren, I., Argue, B., Benzie, J., and Vuylsteke, M. 2008. High density linkage maps and sex-linked markers for the black tiger shrimp (*Penaeus monodon*). Genetics. 179(2) : 917-925.
- Supungul, P., Klinbunga, S., Pichyangkura, R., Hirono, I., Aoki, T. and Tassanakajon, A. 2004. Antimicrobial peptides discovered in the black tiger shrimp *Penaeus monodon* by using the EST approach. Dis. Aquat. Org. 61 : 123-135.
- Tanaka, M., Nakajin, S., Kobayashi, D., Fukuda, S., Guan, G., Todo, T., Senthilkumaran, B., and Nagahama, Y. 2002. Teleost ovarian carbonyl reductase-like 20 β -hydroxysteroid dehydrogenase: potential role in the

- production of maturation-inducing hormone during final oocyte maturation. Biol. Reprod. 66 : 1498-1504.
- Tanioka, T., Nakatani, Y., Semmyo, N., Murakami, M., and Kudo, I. 2000. Molecular identification of cytosolic prostaglandin E₂ synthase that is functionally coupled with cyclooxygenase-1 in immediate prostaglandin E₂ biosynthesis. J. Biol. Chem. 275 : 32775-32782.
- Tiu, S. H. K., Benzie, J., and Chan, S.-M. 2008. From hepatopancreas to ovary: molecular characterization of a shrimp vitellogenin receptor involved in the processing of vitellogenin. Biol. Reprod. 79(1) : 66-74.
- Towbin, H., Starhelin, T., and Gordon, J. 1979. Electrophoretic transfer of proteins from polyacrylamide gels to nitrocellulose sheets: procedure and some applications. Proc. Natl. Acad. Sci. USA 76 : 4350-4354.
- Treerattrakool, S., Panyim, S., Chan, S.-M., Withyachumnarnkul, B., and Udomkit, A. 2007. Molecular characterization of gonad-inhibiting hormone of *Penaeus monodon* and elucidation of its inhibitory role in vitellogenin expression by RNA interference Federa. Eur. Biochem. Soc. 275(5) : 970-980.
- Tyarkowski, T. K., Napowski, J., and Baczyk, K. 1976. Disturbances in electrolyte transport before the onset of uranyl acetate induced renal kidney failure. Kidney Int (suppl 6) : S144–S152.
- Tsukimura, B., and Kamemoto, F. I. 1991. *In vitro* stimulation of oocytes by presumptive mandibular organ secretions in the shrimp, *Penaeus vannamei*. Aquaculture. 92 : 59-66.
- Tsutsui, N., Kawazoe, I., Ohira, T., Jasmani, S., Yang, W. J., Wilder, M. N., and Aida, K. 2000. Molecular characterization of a cDNA encoding vitellogenin and its expression in the hepatopancreas and ovary during vitellogenesis in the kuruma prawn, *Penaeus japonicus*. Zool. Sci. 17 : 651-660.
- VanGuilder, H. D., Vrana, K. E., and Freeman, W. M. 2008. "Twenty-five years of quantitative PCR for gene expression analysis". Biotechniques. 44 : 619-626.
- Verlhac, M.-H., and Dumont, J. 2008. Interactions between chromosomes, microfilaments and microtubules revealed by the study of small GTPases in a big cell, the vertebrate oocyte. Mol. Cell. Endocri. 282(1-2) : 12-17.

- Welsh, J., Chada, K., Dalal, S. S., Cheng, R., Ralph, D., and McClelland, M. 1992. Arbitrarily primed PCR fingerprinting of RNA. Nucleic Acids Res. 20 : 4965-4970.
- Welsh, J. and McClelland, M. 1990. Fingerprinting genomes using PCR with arbitrarily primers. Nucleic Acids Res. 18 : 7213-7218.
- Whitefield, C. W., Band, M. R., Bonaldo, M. F., Kumar, C. G., Liu, L., Pardinas, J. R., Robertson, M., Soares, M. B., and Robinson, G. E. 2002. Annotated expressed sequence tags and cDNA microarrays for studies of brain and behaviour in the honey bee. Genome Res. 12 : 555-566.
- Williams, J. G., Kubelik, A. R., Livak, K.J., Rafalski, J. A., and Tingey, S. V. 1990. DNA polymorphisms amplified by arbitrary primers are useful as genetic markers. Nucleic Acids Res. 18 : 6531-6535.
- Withyachumnarnkul, B., Boonsaeng, V., Flegel, T.W., Panyim, S., and Wongteerasupaya C. 1998. Domestication and selective breeding of *Penaeus monodon* in Thailand. In Felgel, T. (Ed.), Proceedings to the Special Session on Advances in Shrimp Biotechnology, The Fifth Asian Fisheries Forum: International Conference on Fisheries and Food Security Beyond the Year 2000, pp. 73-77. 11-14 November 1998. Thailand: Chiangmai.
- Wongprasert, K., Asuvapongpatana, S., Poltana, P., Tiensuwan, M., and Withyachumnarnkul, B. 2006. Serotonin stimulates ovarian maturation and spawning in the black tiger shrimp *Penaeus monodon*. Aquaculture. 261 : 1447-1454.
- Wu, P., Qi, D., Chen, L., Zhang, H., Zhang, X., Qin, J. G., and Hu, S. 2008. Gene discovery from an ovary cDNA library of oriental river prawn *Macrobrachium nipponense* by ESTs annotation. Comp. Biochem. Physiol. D. 4(2) : 111-120.
- Yamano, K., Qiu, G. F., and Unuma, T. 2004. Molecular cloning and ovarian expression profiles of thrombospondin, a major component of cortical rods in mature oocytes of penaeid shrimp, *Marsupenaeus japonicus*. Biol. Reprod. 70 : 1670-1678.
- Yano, I. 1985. Induced ovarian maturation and spawning in greasyback shrimp, *Metapenaeus ensis*, by progesterone. Aquaculture. 47: 223-229.

- Yano, I. 1987. Effect of 17- α -OH-progesterone on vitellogenin secretion in kuruma prawn, *Penaeus japonicus*. Aquaculture. 61: 46-57.
- Yano, I. 1988. Oocyte development in the kuruma prawn *Penaeus japonicus*. Mar. Biol. 99 : 547-553.
- Yano, I. 1998. Hormonal control vitellogenesis in Penaeid shrimp. In: T.W. Flegel, Editor, Advances in Shrimp Biotechnology, National Center for Genetic Engineering and Biotechnology, Bangkok, pp. 29-31.
- Young, N. J., Quinlan, P. T., and Goad, L. J. 1992. Cholesteryl esters in the decapod crustacean, *Penaeus monodon*. Comp. Biochem. Physiol. B. 102 : 761-768.
- Zhang, Y., and Lees, E. 2001. Identification of an overlapping binding domain on Cdc20 for Mad2 and anaphase-promoting complex: model for spindle checkpoint regulation. Mol. Cell. Biol. 21(15) : 5190-9.
- Zhu, Y., Bond, J., and Thomas, P. 2003a. Identification, classification and partial characterization of genes in humans and other vertebrates homologous to a fish membrane progesterin receptor. Proc. Natl. Acad. Sci. U.S.A. 100 : 2237-2242.
- Zhu, Y., Rice, C. D., Pang, Y., Pace, M., and Thomas, P. 2003b. Cloning, expression and characterization of a novel membrane progesterin receptor and evidence it is an intermediary in meiotic maturation of fish oocytes. Proc. Natl. Acad. Sci. USA. 100 : 2231-2236.
- Zhu, Y., Hanna, R. N., Schaaf, M. J. M., Spink, H. P., and Thomas, P. 2008. Candidates for membrane progesterin receptors-Past approaches and future challenges. Comp. Biochem. Physiol C. 148(4) : 381-389.
- Zirkin, B. R. 1993. Regulation of spermatogenesis in the adult mammals: gonadotropin and androgens. In: Desjardins, C., Ewing, L.L. (Eds.), Cell and Molecular Biology of the Testis. New York: Oxford University Press. pp. 166-188.



APPENDICES

ศูนย์วิทยทรัพยากร
จุฬาลงกรณ์มหาวิทยาลัย



APPENDIX A

ศูนย์วิทยทรัพยากร
จุฬาลงกรณ์มหาวิทยาลัย

Table A1 Contigs creation of the of the typical, normalized and SSH cDNA library of *P. monodon*

Input Sequence	Accession Number	Hit Item	Closest Species	e-value	Bit-score	% Identity	Predicted Full Length	Row Labels	Count of Input Sequence	Input Sequence
Contig1		NO HIT		0	0	0		1	9	OV-N-N01-0002-W, OV-N-N01-0099-W, OV-N-N01-0219-W, OV-N-N01-0832-W, OV-N-N01-1694-W, OV-N-S01-0294-W, OV-N-S01-1497-W, OV-N-S01-2133-W, OV-N-ST01-0004-W- is in OV-N-N01-0002-W
Contig2	XP_001849762.1	peroxidase	<i>Culex pipiens quinquefasciatus</i>	2.00E-20	102	39	Full-length	2	3	OV-N-N01-0007-W, OV-N-S01-1355-W, OV-N-S01-2355-W
Contig3	XP_969584.1	CG10576-PA, isoform A	<i>Tribolium castaneum</i>	2.00E-79	298	65	Full-length	3	2	OV-N-N01-0009-W, OV-N-N01-0627-W
Contig4	XP_393509.2	CG3731-PB, isoform B	<i>Apis mellifera</i>	2.00E-82	307	74	Full-length	4	2	OV-N-N01-0014-W, OV-N-N01-1034-W
Contig5	XP_001120969.1	CG14972-PA	<i>Apis mellifera</i>	1.00E-40	168	46	Full-length	5	2	OV-N-N01-0021-W, OV-N-N01-0973-W
Contig6		NO HIT		0	0	0		6	6	OV-N-N01-0022-W, OV-N-N01-1277-W, OV-N-N01-1299-W, OV-N-N01-1442-W, OV-N-N01-1598-W, OV-N-S01-1297-W
Contig7	XP_624048.1	casein kinase 2 beta	<i>Apis mellifera</i>	1.00E-97	359	85	Full-length	7	4	OV-N-N01-0035-W, OV-N-N01-0409-W, OV-N-N01-0856-W, OV-N-S01-0040-W
Contig8	NP_001090293.1	hypothetical protein LOC779202	<i>Xenopus laevis</i>	4.00E-35	150	38	Full-length	8	2	OV-N-N01-0036-W, OV-N-S01-0014-W
Contig9	XP_001636913.1	predicted protein	<i>Nematostella vectensis</i>	3.00E-40	167	42	Full-length	9	2	OV-N-N01-0038-W, OV-N-N01-1240-W
Contig10	XP_624088.1	Putative actin-interacting protein 1 (AIP1)	<i>Apis mellifera</i>	2.00E-37	160	66	5'-sequenced partial	10	2	OV-N-N01-0042-W, OV-N-S01-0161-W
Contig11		NO HIT		0	0	0		11	2	OV-N-N01-0047-W, OV-N-S01-0295-W
Contig12		NO HIT		0	0	0		12	2	OV-N-N01-0048-W, OV-N-N01-0661-W
Contig13	AAV66932.1	cytochrome c oxidase polypeptide Vb	<i>Ixodes scapularis</i>	5.00E-32	140	56	Full-length	13	2	OV-N-N01-0051-W, OV-N-S01-1760-W
Contig14		NO HIT		0	0	0		14	4	OV-N-N01-0059-W, OV-N-N01-1523-W, OV-N-S01-1223-W, OV-N-S01-1536-W
Contig15	XP_001648450.1	hypothetical protein AaeL_AAEL004113	<i>Aedes aegypti</i>	7.00E-28	126	38	Full-length	15	2	OV-N-N01-0063-W, OV-N-N01-0646-W
Contig16	NP_038299.1	CYTB_15276 cytochrome b	<i>Penaeus monodon</i>	1.00E-143	510	82	Ambiguous	16	3	OV-N-N01-0072-W, OV-N-N01-0925-W, OV-N-S01-1741-W
Contig17	XP_001631720.1	predicted protein	<i>Nematostella vectensis</i>	6.00E-19	98	41	Full-length	17	3	OV-N-N01-0037-W, OV-N-N01-0090-W, OV-N-N01-1221-W
Contig18	XP_972452.1	Probable glutaminyl-tRNA synthetase (Glutamine--tRNA ligase) (GlnRS)	<i>Tribolium castaneum</i>	6.00E-39	163	43	Full-length	18	2	OV-N-N01-0100-W, OV-N-S01-0015-W
Contig19		NO HIT		0	0	0		19	2	OV-N-N01-0108-W, OV-N-S01-0616-W
Contig20		NO HIT		0	0	0		20	3	OV-N-N01-0118-W, OV-N-N01-0775-W, OV-N-N01-1053-W
Contig21	XP_001647767.1	hypothetical protein AaeL_AAEL015379	<i>Aedes aegypti</i>	1.00E-10	69	79	Full-length	21	2	OV-N-N01-0119-W, OV-N-N01-0754-W
Contig22	AAX55747.1	mannose-binding protein	<i>Pacifastacus leniusculus</i>	1.00E-27	127	47	Full-length	22	4	OV-N-N01-0120-W, OV-N-N01-0293-W, OV-N-S01-0837-W, OV-N-S01-1283-W
Contig23	AAV83539.2	ovarian peritrophin	<i>Fenneropenaeus merguensis</i>	1.00E-105	383	57	Full-length	23	67	OV-N-N01-0125-W, OV-N-N01-0131-W, OV-N-N01-0186-W, OV-N-N01-0379-W, OV-N-N01-0400-W, OV-N-N01-0497-W, OV-N-N01-0575-W, OV-N-N01-0625-W, OV-N-N01-0657-W, OV-N-N01-0700-W, OV-N-N01-0734-W, OV-N-N01-0750-W, OV-N-N01-0870-W, OV-N-N01-0882-W, OV-N-N01-0887-W, OV-N-N01-1004-W, OV-N-N01-1097-W, OV-N-N01-1290-W- is in OV-N-N01-0400-W, OV-N-N01-1291-W, OV-N-N01-1429-W, OV-N-N01-1509-W,

Table A1 (Cont.)

Input Sequence	Accession Number	Hit Item	Closest Species	e-value	Bit-score	% Identity	Predicted Full Length	Row Labels	Count of Input Sequence	Input Sequence
										OV-N-N01-1529-W, OV-N-N01-1622-W, OV-N-N01-1635-W, OV-N-N01-1656-W, OV-N-N01-1693-W, OV-N-N01-1732-W, OV-N-N01-1759-W, OV-N-S01-0041-W, OV-N-S01-0063-W, OV-N-S01-0081-W, OV-N-S01-0083-W, OV-N-S01-0127-W, OV-N-S01-0159-W, OV-N-S01-0330-W, OV-N-S01-0415-W, OV-N-S01-0447-W, OV-N-S01-0607-W, OV-N-S01-0648-W, OV-N-S01-0679-W, OV-N-S01-0729-W, OV-N-S01-0761-W, OV-N-S01-0956-W, OV-N-S01-1029-W, OV-N-S01-1057-W, OV-N-S01-1063-W, OV-N-S01-1123-W, OV-N-S01-1194-W, OV-N-S01-1301-W, OV-N-S01-1322-W, OV-N-S01-1383-W, OV-N-S01-1412-W, OV-N-S01-1447-W, OV-N-S01-1555-W, OV-N-S01-1858-W, OV-N-S01-1935-W, OV-N-S01-1964-W, OV-N-S01-1981-W, OV-N-S01-2178-W, OV-N-S01-2227-W, OV-N-S01-2265-W, OV-N-S01-2294-W, is in OV-N-N01-0400-W, OV-N-S01-2335-W, OV-N-S01-2405-W, OV-N-S01-2447-W, OV-N-S01-2473-W, OV-N-S01-2566-W
Contig24		NO HIT		0	0	0		24	4	OV-N-N01-0132-W, OV-N-N01-0304-W, OV-N-N01-0337-W, OV-N-N01-0795-W
Contig25	AAH87825.1	Gstt1-prov protein	<i>Xenopus tropicalis</i>	6.00E-19	88	43	Full-length	25	2	OV-N-N01-0134-W, OV-N-S01-0735-W
Contig26		NO HIT		0	0	0		26	2	OV-N-N01-0138-W, OV-N-N01-1559-W
Contig27	XP_001360270.1	GA15451-PA	<i>Drosophila pseudoobscura</i>	7.00E-51	202	72	Ambiguous	27	6	OV-N-N01-0141-W, OV-N-N01-0675-W, OV-N-N01-1028-W, OV-N-N01-1357-W, OV-N-N01-1477-W, OV-N-N01-1768-W
Contig28	XP_866843.1	dynein light chain-2 isoform 2	<i>Canis familiaris</i>	3.00E-37	158	84	Full-length	28	4	OV-N-N01-0149-W, OV-N-N01-0374-W, OV-N-N01-0470-W, OV-N-N01-1711-W
Contig29	XP_966852.1	CG12070-PA, isoform A isoform 1	<i>Tribolium castaneum</i>	2.00E-46	137	43	Full-length	29	2	OV-N-N01-0150-W, OV-N-N01-0864-W
Contig30	NP_990661.1	inner centromere protein antigens 135/155kDa	<i>Gallus gallus</i>	1.00E-18	96	46	Full-length	30	2	OV-N-N01-0152-W, OV-N-N01-0848-W
Contig31	XP_392726.1	Ribosomal protein S9 CG3395-PA, isoform A	<i>Apis mellifera</i>	4.00E-74	282	86	Full-length	31	8	OV-N-N01-0154-W, OV-N-N01-0482-W, OV-N-N01-0551-W, OV-N-N01-0992-W, OV-N-N01-1790-W, OV-N-S01-0311-W, OV-N-S01-0489-W, OV-N-S01-1884-W
Contig32		NO HIT		0	0	0		32	22	OV-N-N01-0106-W, OV-N-N01-0156-W, OV-N-N01-0203-W, OV-N-N01-0535-W, OV-N-N01-0552-W, OV-N-N01-0678-W, OV-N-N01-0948-W, OV-N-N01-1043-W, OV-N-N01-1179-W, OV-N-N01-1204-W, OV-N-N01-1206-W, OV-N-N01-1435-W, OV-N-S01-0221-W, OV-N-S01-0372-W, OV-N-S01-0485-W, OV-N-S01-0633-W, OV-N-S01-0655-W, OV-N-S01-1018-W, OV-N-S01-1308-W, OV-N-S01-2231-W, OV-N-S01-2469-W, OV-N-S01-2540-W
Contig33	NP_610484.1	CG8801 CG8801-PA	<i>Drosophila melanogaster</i>	3.00E-85	316	78	Full-length	33	3	OV-N-N01-0157-W, OV-N-N01-0187-W, OV-N-N01-0538-W
Contig34		NO HIT		0	0	0		34	2	OV-N-N01-0160-W, OV-N-N01-1075-W
Contig35	ABG67961.1	eukaryotic initiation factor 4A	<i>Callinectes sapidus</i>	3.00E-54	215	89	Ambiguous	35	2	OV-N-N01-0162-W, OV-N-ST02-0164-W

Table A1 (Cont.)

Input Sequence	Accession Number	Hit Item	Closest Species	e-value	Bit-score	% Identity	Predicted Full Length	Row Labels	Count of Input Sequence	Input Sequence
Contig36	XP_001335480.1	Prt1 homolog	<i>Danio rerio</i>	3.00E-63	243	64	Full-length	36	3	OV-N-N01-0163-W, OV-N-N01-1311-W, OV-N-N01-1755-W
Contig37		NO HIT		0	0	0		37	4	OV-N-N01-0169-W, OV-N-N01-0591-W, OV-N-S01-0745-W, OV-N-S01-2256-W
Contig38		NO HIT		0	0	0		38	2	OV-N-N01-0174-W, OV-N-N01-1416-W
Contig39	BAD92217.1	ribosomal protein L5 variant	<i>Homo sapiens</i>	8.00E-78	292	69	Full-length	39	5	OV-N-N01-0179-W, OV-N-N01-0257-W, OV-N-N01-0621-W, OV-N-N01-0893-W, OV-N-S01-0534-W
Contig40		NO HIT		0	0	0		40	2	OV-N-N01-0182-W, OV-N-N01-1138-W
Contig41	NP_989274.1	protein phosphatase 2 (formerly 2A), catalytic subunit, alpha isoform	<i>Xenopus tropicalis</i>	1.00E-100	368	92	Full-length	41	2	OV-N-N01-0198-W, OV-N-N01-1066-W
Contig42		NO HIT		0	0	0		42	3	OV-N-N01-0202-W, OV-N-S01-1042-W, OV-N-ST01-0200-W
Contig43	XP_001892369.1	hypothetical protein	<i>Brugia malayi</i>	2.00E-34	147	36	Full-length	43	6	OV-N-N01-0204-W, OV-N-N01-0316-W, OV-N-N01-0320-W, OV-N-N01-0741-W, OV-N-N01-0742-W, OV-N-N01-1038-W
Contig44		NO HIT		0	0	0		44	6	OV-N-N01-0208-W, OV-N-N01-0311-W, OV-N-N01-0842-W, OV-N-S01-1540-W, OV-N-S01-1670-W, OV-N-S01-2409-W
Contig45	XP_001625547.1	predicted protein	<i>Nematostella vectensis</i>	8.00E-05	43	60	Full-length	45	2	OV-N-N01-0215-W, OV-N-N01-0866-W
Contig46		NO HIT		0	0	0		46	2	OV-N-N01-0220-W, OV-N-N01-0346-W
Contig47		NO HIT		0	0	0		47	2	OV-N-N01-0224-W, OV-N-N01-0636-W
Contig48		NO HIT		0	0	0		48	2	OV-N-N01-0230-W, OV-N-N01-1507-W
Contig49	XP_310188.3	AGAP009508-PA	<i>Anopheles gambiae str. PEST</i>	4.00E-58	226	67	Full-length	49	7	OV-N-N01-0233-W, OV-N-N01-0517-W, OV-N-N01-0523-W, OV-N-N01-1188-W, OV-N-N01-1391-W, OV-N-S01-0680-W, OV-N-S01-1547-W
Contig50	Q94571	Tubulin beta-2 chain (Beta-II tubulin) beta-II tubulin	<i>Homarus americanus</i>	6.00E-67	256	98	Full-length	50	2	OV-N-N01-0235-W, OV-N-S01-1378-W
Contig51	AAV66871.1	pre-mRNA splicing factor SF3b 10 kDa subunit	<i>Ixodes scapularis</i>	5.00E-31	138	82	Full-length	51	5	OV-N-N01-0241-W, OV-N-N01-0263-W, OV-N-N01-1700-W, OV-N-N01-1802-W, OV-N-S01-2166-W
Contig52		NO HIT		0	0	0		52	2	OV-N-N01-0245-W, OV-N-S01-2182-W
Contig53	AAL62468.1	ribosomal protein L3	<i>Spodoptera frugiperda</i>	5.00E-48	194	81	Full-length	53	7	OV-N-N01-0247-W, OV-N-N01-0485-W, OV-N-N01-0515-W, OV-N-N01-0651-W, OV-N-N01-0791-W, OV-N-S01-0492-W, OV-N-S01-1287-W
Contig54	CAJ81953.1	ribonucleotide reductase m2 polypeptide	<i>Xenopus tropicalis</i>	1.00E-93	345	70	Full-length	54	2	OV-N-N01-0250-W, OV-N-S01-1826-W
Contig55	XP_001600649.1	eukaryotic translation initiation factor 4 gamma, 2	<i>Nasonia vitripennis</i>	2.00E-85	320	48	5'-sequenced partial	55	6	OV-N-N01-0252-W, OV-N-S01-0818-W, OV-N-S01-1012-W, OV-N-S01-1156-W, OV-N-S01-1217-W, OV-N-S01-1736-W
Contig56		NO HIT		0	0	0		56	2	OV-N-N01-0253-W, OV-N-S01-1940-W
Contig57	XP_001608115.1	conserved hypothetical protein	<i>Nasonia vitripennis</i>	5.00E-67	256	58	5'-sequenced partial	57	2	OV-N-N01-0254-W, OV-N-N01-1013-W
Contig58		NO HIT		0	0	0		58	2	OV-N-N01-0264-W, OV-N-N01-1342-W
Contig59	ABB89953.1	vitellogenin	<i>Penaeus monodon</i>	1.00E-165	582	98	Full-length	59	6	OV-N-N01-0265-W, OV-N-N01-0305-W, OV-N-N01-0670-W

Table A1 (Cont.)

Input Sequence	Accession Number	Hit Item	Closest Species	e-value	Bit-score	% Identity	Predicted Full Length	Row Labels	Count of Input Sequence	Input Sequence
Contig60	ABW79798.1	vitellogenin receptor	<i>Penaeus monodon</i>	1.00E-159	562	95	Full-length	60	2	W, OV-N-N01-1224-W, OV-N-N01-1300-W, OV-N-S01-1049-W
Contig61	XP_975408.1	CG3412-PA	<i>Tribolium castaneum</i>	1.00E-129	464	80	Full-length	61	3	OV-N-N01-0268-W, OV-N-S01-0395-W
Contig62	AAL62468.1	ribosomal protein L3	<i>Spodoptera frugiperda</i>	1.00E-122	441	74	Full-length	62	8	OV-N-N01-0279-W, OV-N-N01-1485-W, OV-N-S01-0479-W, OV-N-N01-0287-W, OV-N-S01-0055-W, OV-N-S01-0374-W, OV-N-S01-0638-W, OV-N-S01-1000-W, OV-N-S01-1151-W, OV-N-S01-1348-W, OV-N-S01-1825-W
Contig63		NO HIT		0	0	0		63	2	OV-N-N01-0302-W, OV-N-N01-1798-W
Contig64	ABN04118.1	ATP/ADP translocase	<i>Marsupenaeus japonicus</i>	1.00E-141	506	93	Full-length	64	26	OV-N-N01-0330-W, OV-N-N01-0370-W, OV-N-N01-0398-W, OV-N-N01-0699-W, OV-N-N01-0763-W, OV-N-N01-0826-W, OV-N-N01-0845-W, OV-N-N01-0899-W, OV-N-N01-1095-W, OV-N-N01-1297-W, OV-N-N01-1407-W, OV-N-N01-1660-W, OV-N-N01-1666-W, OV-N-N01-1726-W, OV-N-S01-0739-W, OV-N-S01-0854-W, OV-N-S01-0865-W, OV-N-S01-1075-W, OV-N-S01-1104-W, OV-N-S01-1269-W, OV-N-S01-1419-W, OV-N-S01-1428-W, OV-N-S01-1575-W, OV-N-S01-1779-W, OV-N-S01-1849-W, OV-N-S01-2440-W
Contig65	AAV37462.1	cyclin B	<i>Marsupenaeus japonicus</i>	6.00E-93	342	90	Full-length	65	4	OV-N-N01-0345-W, OV-N-N01-0653-W, OV-N-N01-1561-W, OV-N-S01-2524-W
Contig66	XP_001581848.1	conserved hypothetical protein	<i>Trichomonas vaginalis G3</i>	1.00E-07	59	26	Full-length	66	2	OV-N-N01-0356-W, OV-N-S01-0495-W
Contig67		NO HIT		0	0	0		67	24	OV-N-N01-0054-W, OV-N-N01-0240-W, OV-N-N01-0357-W, OV-N-N01-0529-W, OV-N-N01-0994-W, OV-N-N01-1030-W, OV-N-N01-1090-W, OV-N-N01-1143-W, OV-N-N01-1365-W, OV-N-N01-1466-W, OV-N-N01-1649-W, OV-N-N01-1766-W, OV-N-S01-0120-W, OV-N-S01-0484-W, OV-N-S01-0557-W- is in OV-N-N01-1090-W, OV-N-S01-0560-W, OV-N-S01-0567-W, OV-N-S01-1035-W, OV-N-S01-1120-W, OV-N-S01-1745-W, OV-N-S01-1801-W, OV-N-S01-1980-W, OV-N-S01-2035-W, OV-N-S01-2619-W
Contig68	CAD29196.1	triosephosphate isomerase	<i>Archaeopotamobius sibiriensis</i>	1.00E-101	370	88	Full-length	68	6	OV-N-N01-0191-W, OV-N-N01-0363-W, OV-N-N01-0364-W, OV-N-N01-0784-W, OV-N-N01-1541-W, OV-N-S01-1026-W
Contig69		NO HIT		0	0	0		69	2	OV-N-N01-0367-W, OV-N-N01-1564-W
Contig70		NO HIT		0	0	0		70	2	OV-N-N01-0368-W, OV-N-N01-1704-W
Contig71		NO HIT		0	0	0		71	3	OV-N-N01-0372-W, OV-N-N01-0403-W, OV-N-N01-0597-W
Contig72	XP_001370185.1	uncharacterized hematopoietic stem/progenitor cells protein MDS033	<i>Monodelphis domestica</i>	6.00E-28	126	59	Full-length	72	2	OV-N-N01-0373-W, OV-N-S01-1863-W
Contig73		NO HIT		0	0	0		73	2	OV-N-N01-0375-W, OV-N-S01-1251-W
Contig74	XP_001602414.1	ENSANGP00000011417	<i>Nasonia vitripennis</i>	2.00E-38	161	43	Full-length	74	3	OV-N-N01-0380-W, OV-N-N01-0444-W, OV-N-S01-1090-W
Contig75	XP_975650.1	CG9066-PA	<i>Tribolium castaneum</i>	4.00E-37	157	50	Full-length	75	5	OV-N-N01-0057-W, OV-N-N01-0381-W, OV-N-N01-1276-W, OV-N-N01-1549-W, OV-N-N01-1670-W
Contig76		NO HIT		0	0	0		76	4	OV-N-N01-0388-W, OV-N-N01-0445-W, OV-N-N01-0919-W, OV-N-N01-1303-W

Table A2 Singletons creation of the of the typical, normalized and SSH cDNA library of *P. monodon*

Input Sequence	Accession Number	Hit Item	Closest Species	e-value	Bit-score	%Identity	Predicted Full Length
OV-N-N01-0003-W		NO HIT		0	0	0	Full-length
OV-N-N01-0005-W	XP_001602354.1	conserved hypothetical protein	<i>Nasonia vitripennis</i>	3.00E-35	150	70	Full-length
OV-N-N01-0011-W	XP_971520.1	CG6778-PB, isoform B	<i>Tribolium castaneum</i>	3.00E-61	237	67	5'-sequenced partial
OV-N-N01-0017-W	XP_971725.1	Tyrosine-protein phosphatase non-receptor type 13 (Protein-tyrosine phosphatase 1E) (PTP-E1) (hPTPE1) (PTP-BAS) (Protein-tyrosine phosphatase PTP1) (Fas-associated protein-tyrosine phosphatase 1) (FAP-1)	<i>Tribolium castaneum</i>	1.00E-12	76	43	Full-length
OV-N-N01-0018-W		NO HIT		0	0	0	Full-length
OV-N-N01-0019-W	XP_001605394.1	CG9977-PA	<i>Nasonia vitripennis</i>	1.00E-79	298	86	Short full-length
OV-N-N01-0020-W	XP_001605101.1	CG2212-PA	<i>Nasonia vitripennis</i>	3.00E-73	277	62	5'-sequenced partial
OV-N-N01-0028-W	AAT46564.1	Ran-binding protein	<i>Marsupenaeus japonicus</i>	8.00E-66	252	100	Full-length
OV-N-N01-0032-W	XP_001122253.1	kismet CG3696-PA, isoform A	<i>Apis mellifera</i>	1.00E-33	145	41	Full-length
OV-N-N01-0039-W		NO HIT		0	0	0	
OV-N-N01-0043-W		NO HIT		0	0	0	5'-sequenced partial
OV-N-N01-0050-W		NO HIT		0	0	0	Full-length
OV-N-N01-0060-W	BAE92940.1	anti-lipoplysaccharide factor like protein	<i>Marsupenaeus japonicus</i>	6.00E-09	64	29	Full-length
OV-N-N01-0061-W	CAM15108.1	acyl-Coenzyme A dehydrogenase, C-4 to C-12 straight chain	<i>Danio rerio</i>	1.00E-102	372	80	Full-length
OV-N-N01-0064-W	XP_309710.1	AGAP010984-PA	<i>Anopheles gambiae str. PEST</i>	2.00E-40	168	46	5'-sequenced partial
OV-N-N01-0067-W	XP_001607922.1	amine oxidase	<i>Nasonia vitripennis</i>	6.00E-13	77	29	Full-length
OV-N-N01-0071-W		NO HIT		0	0	0	Full-length
OV-N-N01-0076-W	XP_392777.2	CG6443-PA	<i>Apis mellifera</i>	5.00E-48	193	54	Full-length
OV-N-N01-0077-W	XP_397092.2	small bristles CG1664-PA	<i>Apis mellifera</i>	2.00E-15	85	28	Full-length
OV-N-N01-0083-W	XP_788763.1	SEC13-like 1 (<i>S. cerevisiae</i>)	<i>Strongylocentrotus purpuratus</i>	2.00E-18	95	74	5'-sequenced partial
OV-N-N01-0085-W	XP_309608.4	AGAP004055-PA	<i>Anopheles gambiae str. PEST</i>	2.00E-82	307	78	Full-length
OV-N-N01-0086-W		NO HIT		0	0	0	
OV-N-N01-0089-W	XP_001605370.1	ubiquitin fusion degradaton protein	<i>Nasonia vitripennis</i>	1.00E-76	288	73	5'-sequenced partial
OV-N-N01-0096-W		NO HIT		0	0	0	Full-length
OV-N-N01-0097-W	XP_001120950.1	CG8009-PA, isoform A	<i>Apis mellifera</i>	2.00E-37	158	69	Full-length
OV-N-N01-0102-W	XP_393212.2	hu li tai shao CG9325-PB, isoform B	<i>Apis mellifera</i>	2.00E-26	121	42	Full-length
OV-N-N01-0103-W		NO HIT		0	0	0	
OV-N-N01-0109-W	XP_623806.1	COP9 constitutive photomorphogenic homolog subunit 5 isoform 1	<i>Apis mellifera</i>	2.00E-92	341	84	5'-sequenced partial
OV-N-N01-0116-W	XP_781099.2	TUBA	<i>Strongylocentrotus purpuratus</i>	1.00E-20	102	29	Short full-length
OV-N-N01-0144-W	AAH87495.1	ARL3 protein	<i>Xenopus laevis</i>	1.00E-72	275	85	5'-sequenced partial
OV-N-N01-0145-W	AAN17670.1	thrombospondin	<i>Penaeus monodon</i>	1.00E-83	311	88	Full-length
OV-N-N01-0158-W	XP_001639738.1	predicted protein	<i>Nematostella vectensis</i>	1.00E-57	225	75	Full-length
OV-N-N01-0159-W		NO HIT		0	0	0	
OV-N-N01-0167-W		NO HIT		0	0	0	Full-length
OV-N-N01-0185-W		NO HIT		0	0	0	Full-length
OV-N-N01-0188-W	XP_971200.1	CG2260-PA	<i>Tribolium castaneum</i>	3.00E-63	243	55	Full-length
OV-N-N01-0195-W	XP_395115.3	CG31992-PA, isoform A, partial	<i>Apis mellifera</i>	2.00E-25	118	42	Full-length
OV-N-N01-0199-W	XP_001201460.1	hypothetical protein	<i>Strongylocentrotus purpuratus</i>	2.00E-08	62	28	Full-length
OV-N-N01-0201-W		NO HIT		0	0	0	Full-length
OV-N-N01-0209-W	AAU12181.1	G protein s alpha subunit	<i>Litopenaeus vannamei</i>	1.00E-104	379	100	Full-length
OV-N-N01-0213-W		NO HIT		0	0	0	Full-length
OV-N-N01-0216-W		NO HIT		0	0	0	Full-length
OV-N-N01-0223-W	AAN17670.1	thrombospondin	<i>Penaeus monodon</i>	4.00E-64	246	59	Ambiguous
OV-N-N01-0229-W		NO HIT		0	0	0	Short full-length
OV-N-N01-0238-W		NO HIT		0	0	0	

Table A2 (Cont.)

Input Sequence	Accession Number	Hit Item	Closest Species	e-value	Bit-score	%Identity	Predicted Full Length
OV-N-N01-0239-W	NP_001012594.1	heat shock 70kDa protein 4-like	<i>Gallus gallus</i>	3.00E-36	154	41	Full-length
OV-N-N01-0242-W		NO HIT		0	0	0	
OV-N-N01-0246-W	XP_001897655.1	RNA recognition motif containing protein	<i>Brugia malayi</i>	7.00E-05	50	26	Full-length
OV-N-N01-0259-W	YP_001110913.1	hypothetical protein HVAV3e_gp060	<i>Heliothis virescens ascovirus 3e</i>	2.00E-07	58	21	Full-length
OV-N-N01-0267-W	XP_001353323.1	GA19031-PA	<i>Drosophila pseudoobscura</i>	6.00E-32	140	78	Full-length
OV-N-N01-0269-W		NO HIT		0	0	0	Full-length
OV-N-N01-0273-W		NO HIT		0	0	0	
OV-N-N01-0274-W	NP_001084373.1	selenocysteine tRNA activating factor	<i>Xenopus laevis</i>	3.00E-47	190	54	Full-length
OV-N-N01-0278-W		NO HIT		0	0	0	
OV-N-N01-0280-W	XP_975769.1	CG4169-PA isoform 2	<i>Tribolium castaneum</i>	2.00E-27	124	35	Full-length
OV-N-N01-0282-W		NO HIT		0	0	0	Full-length
OV-N-N01-0286-W	NP_001080558.1	hypothetical protein LOC380250	<i>Xenopus laevis</i>	3.00E-09	65	47	Ambiguous
OV-N-N01-0290-W		NO HIT		0	0	0	Full-length
OV-N-N01-0291-W	XP_969770.1	CG9403-PA, isoform A	<i>Tribolium castaneum</i>	8.00E-07	56	34	Short full-length
OV-N-N01-0294-W	XP_968356.1	H326	<i>Tribolium castaneum</i>	8.00E-30	124	47	Full-length
OV-N-N01-0296-W	XP_625126.2	histone aminotransferase 1	<i>Apis mellifera</i>	9.00E-58	225	54	Full-length
OV-N-N01-0297-W		NO HIT		0	0	0	Full-length
OV-N-N01-0298-W	XP_001607669.1	heat shock protein 20.6 isoform 1	<i>Nasonia vitripennis</i>	1.00E-56	221	69	Ambiguous
OV-N-N01-0300-W	XP_001628185.1	predicted protein	<i>Nematostella vectensis</i>	3.00E-54	214	50	Full-length
OV-N-N01-0301-W		NO HIT		0	0	0	Full-length
OV-N-N01-0307-W		NO HIT		0	0	0	Full-length
OV-N-N01-0309-W		NO HIT		0	0	0	Ambiguous
OV-N-N01-0312-W	ABG11961.1	tail muscle elongation factor 1 gamma	<i>Procambarus clarkii</i>	2.00E-89	331	72	Full-length
OV-N-N01-0313-W	XP_792559.1	hypothetical protein	<i>Strongylocentrotus purpuratus</i>	7.00E-24	113	35	Full-length
OV-N-N01-0314-W		NO HIT		0	0	0	Ambiguous
OV-N-N01-0317-W		NO HIT		0	0	0	Full-length
OV-N-N01-0322-W		NO HIT		0	0	0	5'-sequenced partial
OV-N-N01-0325-W	AAN17670.1	thrombospondin	<i>Penaeus monodon</i>	1.00E-69	265	86	Full-length
OV-N-N01-0326-W		NO HIT		0	0	0	Full-length
OV-N-N01-0329-W	BAC92764.1	thrombospondin	<i>Marsupenaeus japonicus</i>	1.00E-46	188	66	Full-length
OV-N-N01-0343-W	XP_001502237.1	hypothetical protein	<i>Equus caballus</i>	4.00E-59	230	62	Full-length
OV-N-N01-0348-W		NO HIT		0	0	0	Full-length
OV-N-N01-0350-W	AAN17670.1	thrombospondin	<i>Penaeus monodon</i>	7.00E-88	325	89	Ambiguous
OV-N-N01-0354-W	XP_001627537.1	predicted protein	<i>Nematostella vectensis</i>	1.00E-09	66	55	Full-length
OV-N-N01-0361-W		NO HIT		0	0	0	Full-length
OV-N-N01-0369-W		NO HIT		0	0	0	5'-sequenced partial
OV-N-N01-0376-W	NP_001003294.1	dihydroliipoamide dehydrogenase	<i>Canis lupus familiaris</i>	3.00E-79	296	71	Full-length
OV-N-N01-0378-W	XP_001657865.1	cak1	<i>Aedes aegypti</i>	3.00E-88	327	79	5'-sequenced partial
OV-N-N01-0386-W	XP_001602190.1	ENSANGP00000017163	<i>Nasonia vitripennis</i>	4.00E-16	87	66	Full-length
OV-N-N01-0391-W	NP_001079560.1	hypothetical protein LOC379247	<i>Xenopus laevis</i>	1.00E-13	79	48	Full-length
OV-N-N01-0393-W	XP_701018.2	hypothetical protein	<i>Danio rerio</i>	8.00E-18	93	44	Full-length
OV-N-N01-0429-W	XP_501932.1	hypothetical protein	<i>Yarrowia lipolytica</i>	3.00E-11	71	47	Full-length
OV-N-N01-0431-W		NO HIT		0	0	0	Full-length
OV-N-N01-0437-W		NO HIT		0	0	0	Short full-length
OV-N-S01-0025-W	NP_035434.1	RuvB-like protein 2	<i>Mus musculus</i>	5.00E-56	122	57	Full-length
OV-N-S01-0027-W		NO HIT		0	0	0	Full-length

Table A2 (Cont.)

Input Sequence	Accession Number	Hit Item	Closest Species	e-value	Bit-score	%Identity	Predicted Full Length
OV-N-S01-0029-W	AAP92780.1	hepatopancreas kazal-type proteinase inhibitor	<i>Penaeus monodon</i>	3.00E-21	104	44	Full-length
OV-N-S01-0031-W		NO HIT		0	0	0	Full-length
OV-N-S01-0033-W	XP_001121889.1	JTBR CG1935-PA	<i>Apis mellifera</i>	2.00E-19	98	36	Full-length
OV-N-S01-0034-W		NO HIT		0	0	0	Full-length
OV-N-S01-0036-W		NO HIT		0	0	0	Full-length
OV-N-S01-0038-W	NP_751894.1	MBD2-interacting zinc finger	<i>Mus musculus</i>	1.00E-36	155	41	Full-length
OV-N-S01-0039-W	NP_001087562.1	MGC84654 protein	<i>Xenopus laevis</i>	3.00E-08	61	41	5'-sequenced partial
OV-N-S01-0049-W	BAC92762.1	thrombospondin	<i>Marsupenaeus japonicus</i>	2.00E-69	264	60	Full-length
OV-N-S01-0050-W		NO HIT		0	0	0	
OV-N-S01-0058-W	AAI26031.1	Narg1l protein	<i>Xenopus laevis</i>	1.00E-79	298	77	5'-sequenced partial
OV-N-S01-0067-W	BAE42496.1	unnamed protein product	<i>Mus musculus</i>	6.00E-74	279	78	Full-length
OV-N-S01-0068-W	NP_001012901.1	solute carrier family 25 (mitochondrial carrier, brain), member 14	<i>Gallus gallus</i>	1.00E-50	202	57	Full-length
OV-N-S01-0071-W	AAZ66372.1	thrombospondin	<i>Fenneropenaeus chinensis</i>	9.00E-62	239	56	Full-length
OV-N-S01-0076-W		NO HIT		0	0	0	
OV-N-S01-0079-W		NO HIT		0	0	0	Full-length
OV-N-S01-0085-W	AAN17670.1	thrombospondin	<i>Penaeus monodon</i>	1.00E-65	251	63	Full-length
OV-N-S01-0092-W	XP_001373175.1	insulinoma protein (rig)	<i>Monodelphis domestica</i>	7.00E-38	159	63	Full-length
OV-N-S01-0110-W	XP_392689.2	Calreticulin CG9429-PA isoform 1	<i>Apis mellifera</i>	4.00E-29	130	80	Full-length
OV-N-S01-0113-W		NO HIT		0	0	0	Full-length
OV-N-S01-0115-W	XP_001623641.1	predicted protein	<i>Nematostella vectensis</i>	2.00E-09	65	29	Ambiguous
OV-N-S01-0119-W	XP_001372216.1	basalin	<i>Monodelphis domestica</i>	4.00E-05	51	27	Full-length
OV-N-S01-0121-W		NO HIT		0	0	0	Full-length
OV-N-S01-0123-W		NO HIT		0	0	0	
OV-N-S01-0124-W		NO HIT		0	0	0	
OV-N-S01-0138-W		NO HIT		0	0	0	Full-length
OV-N-S01-0142-W	XP_393377.3	transcription factor Dp-2 (E2F dimerization partner 2)	<i>Apis mellifera</i>	2.00E-41	171	69	Full-length
OV-N-S01-0146-W	AAL26579.1	AF429977_1 ribosomal protein S3A	<i>Spodoptera frugiperda</i>	2.00E-62	240	64	Ambiguous
OV-N-S01-0147-W	ABW23211.1	ribosomal protein rps21	<i>Eurythoe complanata</i>	4.00E-28	127	81	Full-length
OV-N-S01-0151-W	NP_001036574.1	CG34140 CG34140-PA	<i>Drosophila melanogaster</i>	1.00E-11	73	53	Full-length
OV-N-S01-0157-W	AAN17670.1	thrombospondin	<i>Penaeus monodon</i>	3.00E-80	300	87	Full-length
OV-N-S01-0181-W		NO HIT		0	0	0	Full-length
OV-N-S01-0188-W	XP_971174.1	NADPH--cytochrome P450 reductase (CPR) (P450R)	<i>Tribolium castaneum</i>	6.00E-35	149	62	Ambiguous
OV-N-S01-0192-W		NO HIT		0	0	0	Full-length
OV-N-S01-0197-W	AAO85336.1	Cdc20	<i>Branchiostoma floridae</i>	1.00E-07	59	32	Full-length
OV-N-S01-0202-W		NO HIT		0	0	0	
OV-N-S01-0207-W		NO HIT		0	0	0	
OV-N-S01-0218-W		NO HIT		0	0	0	Full-length
OV-N-S01-0222-W		NO HIT		0	0	0	
OV-N-S01-0223-W		NO HIT		0	0	0	
OV-N-S01-0226-W	AAN17670.1	thrombospondin	<i>Penaeus monodon</i>	7.00E-89	329	80	Full-length
OV-N-S01-0227-W	XP_972821.1	CG7004-PA, isoform A	<i>Tribolium castaneum</i>	2.00E-11	72	58	Full-length
OV-N-S01-0229-W	XP_392695.2	Polycomb protein Suz12 (Suppressor of zeste 12 protein homolog)	<i>Apis mellifera</i>	7.00E-32	140	40	Full-length
OV-N-S01-0231-W	XP_967480.1	CG6647-PA, isoform A isoform 1	<i>Tribolium castaneum</i>	7.00E-75	282	63	Full-length
OV-N-S01-0236-W	AAH44204.1	Cry5 protein	<i>Danio rerio</i>	2.00E-54	214	50	Full-length
OV-N-S01-0237-W		NO HIT		0	0	0	
OV-N-S01-0239-W		NO HIT		0	0	0	Full-length
OV-N-S01-0241-W		NO HIT		0	0	0	

Table A2 (Cont.)

Input Sequence	Accession Number	Hit Item	Closest Species	e-value	Bit-score	%Identity	Predicted Full Length
OV-N-S01-0242-W		NO HIT		0	0	0	
OV-N-S01-0243-W		NO HIT		0	0	0	Full-length
OV-N-S01-0245-W		NO HIT		0	0	0	Ambiguous
OV-N-S01-0246-W		NO HIT		0	0	0	
OV-N-S01-0251-W		NO HIT		0	0	0	
OV-N-S01-0252-W	XP_623706.1	CG5970-PA	<i>Apis mellifera</i>	1.00E-64	248	64	Full-length
OV-N-S01-0256-W		NO HIT		0	0	0	Full-length
OV-N-S01-0257-W	XP_968135.1	cytokine induced protein 29 kDa	<i>Tribolium castaneum</i>	3.00E-11	71	29	Full-length
OV-N-S01-0258-W	XP_001604284.1	AMPK-beta subunit	<i>Nasonia vitripennis</i>	3.00E-35	125	41	Full-length
OV-N-S01-0262-W		NO HIT		0	0	0	Ambiguous
OV-N-S01-0264-W		NO HIT		0	0	0	Full-length
OV-N-S01-0266-W		NO HIT		0	0	0	Full-length
OV-N-S01-0268-W	NP_957139.1	hypothetical protein LOC393818	<i>Danio rerio</i>	2.00E-47	191	86	Full-length
OV-N-S01-0269-W		NO HIT		0	0	0	5'-sequenced partial
OV-N-S01-0270-W	XP_001627003.1	predicted protein	<i>Nematostella vectensis</i>	8.00E-20	100	40	Full-length
OV-N-S01-0271-W		NO HIT		0	0	0	
OV-N-S01-0274-W	XP_395525.3	CG9461-PA	<i>Apis mellifera</i>	2.00E-88	327	75	Full-length
OV-N-S01-0292-W		NO HIT		0	0	0	Full-length
OV-N-S01-0296-W		NO HIT		0	0	0	Full-length
OV-N-S01-0297-W	NP_001103952.1	hypothetical protein LOC798203	<i>Danio rerio</i>	7.00E-17	90	49	Full-length
OV-N-S01-0300-W		NO HIT		0	0	0	
OV-N-S01-0301-W	XP_001599430.1	CNOT1	<i>Nasonia vitripennis</i>	2.00E-87	299	76	Ambiguous
OV-N-S01-0304-W	XP_001231886.1	KIAA0367	<i>Gallus gallus</i>	3.00E-25	117	64	Full-length
OV-N-S01-0305-W	XP_970329.1	PRP39 pre-mRNA processing factor 39 homolog	<i>Tribolium castaneum</i>	7.00E-50	199	53	Full-length
OV-N-S01-0306-W	XP_395256.3	eukaryotic initiation factor 5C CG2922-PG, isoform G	<i>Apis mellifera</i>	2.00E-51	204	48	Ambiguous
OV-N-S01-0309-W		NO HIT		0	0	0	5'-sequenced partial
OV-N-S01-0310-W		NO HIT		0	0	0	
OV-N-S01-0317-W	ABC86571.1	vitellogenin	<i>Fenneropenaeus chinensis</i>	1.00E-103	299	95	Full-length
OV-N-S01-0318-W	CAF96633.1	unnamed protein product	<i>Tetraodon nigroviridis</i>	2.00E-49	198	65	Full-length
OV-N-S01-0321-W	XP_001623402.1	predicted protein	<i>Nematostella vectensis</i>	1.00E-53	212	57	Full-length
OV-N-S01-0324-W		NO HIT		0	0	0	
OV-N-S01-0325-W	XP_394497.2	CG7275-PA	<i>Apis mellifera</i>	2.00E-38	161	43	Full-length
OV-N-S01-0335-W	Q86UY6	NAT11_HUMAN N-acetyltransferase 11 N-acetyltransferase 11	<i>Homo sapiens</i>	6.00E-36	153	50	Full-length
OV-N-S01-0337-W		NO HIT		0	0	0	Full-length
OV-N-S01-0342-W	AAN17670.1	thrombospondin	<i>Penaeus monodon</i>	2.00E-66	254	86	Full-length
OV-N-S01-0344-W		NO HIT		0	0	0	Short full-length
OV-N-S01-0350-W		NO HIT		0	0	0	Full-length
OV-N-S01-0352-W	XP_001513326.1	ubiquitin specific peptidase 9, X-linked, isoform 2	<i>Ornithorhynchus anatinus</i>	6.00E-50	200	82	Full-length
OV-N-S01-0354-W		NO HIT		0	0	0	5'-sequenced partial
OV-N-S01-0358-W		NO HIT		0	0	0	Full-length
OV-N-S01-0359-W	NP_732967.1	twin CG31137-PB, isoform B	<i>Drosophila melanogaster</i>	2.00E-34	148	56	Full-length
OV-N-S01-0363-W	AAN17670.1	thrombospondin	<i>Penaeus monodon</i>	4.00E-79	296	67	Ambiguous
OV-N-S01-0366-W		NO HIT		0	0	0	Full-length
OV-N-S01-0382-W	XP_001661360.1	hypothetical protein Aael_AAEL002340	<i>Aedes aegypti</i>	3.00E-10	68	32	Full-length
OV-N-S01-0384-W	XP_001118393.1	PWP2 periodic tryptophan protein homolog	<i>Macaca mulatta</i>	1.00E-58	228	50	Full-length
OV-N-S01-0386-W	XP_001606115.1	ubiquitin-conjugating enzyme E2	<i>Nasonia vitripennis</i>	4.00E-75	283	92	Full-length
OV-N-S01-0390-W	XP_001865121.1	mitochondrial 28S ribosomal protein S5	<i>Culex pipiens quinquefasciatus</i>	3.00E-69	264	59	Full-length

Table A2 (Cont.)

Input Sequence	Accession Number	Hit Item	Closest Species	e-value	Bit-score	%Identity	Predicted Full Length
OV-N-S01-0394-W		NO HIT		0	0	0	Full-length
OV-N-S01-0397-W	XP_001603205.1	ferrochelatase	<i>Nasonia vitripennis</i>	1.00E-91	338	67	Full-length
OV-N-S01-0399-W		NO HIT		0	0	0	Full-length
OV-N-S01-0412-W		NO HIT		0	0	0	Full-length
OV-N-S01-0416-W	XP_972190.1	CG18572-PA, isoform A	<i>Tribolium castaneum</i>	5.00E-73	276	65	Full-length
OV-N-S01-0419-W	XP_623495.1	Vacuolar ATP synthase catalytic subunit A, osteoclast isoform (V-ATPase subunit A 2) (Vacuolar proton pump alpha subunit 2) (V-ATPase 69 kDa subunit 2) (Isoform HO68) isoform 1	<i>Apis mellifera</i>	8.00E-79	295	75	Full-length
OV-N-S01-0426-W		NO HIT		0	0	0	
OV-N-S01-0428-W	XP_971434.1	CG1966-PA	<i>Tribolium castaneum</i>	6.00E-08	60	41	Full-length
OV-N-S01-0429-W	XP_001850447.1	rabconnectin	<i>Culex pipiens quinquefasciatus</i>	5.00E-29	130	36	Short full-length
OV-N-S01-0430-W		NO HIT		0	0	0	
OV-N-S01-0431-W		NO HIT		0	0	0	
OV-N-S01-0435-W	XP_523227.2	Tetraspanin 3	<i>Pan troglodytes</i>	5.00E-06	54	30	Full-length
OV-N-S01-0438-W	XP_001622223.1	predicted protein	<i>Nematostella vectensis</i>	2.00E-51	204	52	Full-length
OV-N-S01-0449-W	AAZ66372.1	thrombospondin	<i>Fenneropenaeus chinensis</i>	4.00E-83	310	61	Full-length
OV-N-S01-0451-W		NO HIT		0	0	0	5'-sequenced partial
OV-N-S01-0454-W	XP_969059.1	CG10161-PB	<i>Tribolium castaneum</i>	2.00E-61	237	58	Full-length
OV-N-S01-0456-W		NO HIT		0	0	0	
OV-N-S01-0459-W	XP_001652256.1	dihydropteridine reductase	<i>Aedes aegypti</i>	2.00E-66	254	59	Full-length
OV-N-ST01-0062-W		NO HIT		0	0	0	5'-sequenced partial
OV-N-ST01-0063-W	XP_532143.2	mitochondrial ribosomal protein L2	<i>Canis familiaris</i>	2.00E-20	101	59	Full-length
OV-N-ST01-0068-W	NP_001085120.1	hypothetical protein LOC432195	<i>Xenopus laevis</i>	4.00E-58	226	67	Ambiguous
OV-N-ST01-0069-W	NP_001006467.1	coatamer protein complex, subunit beta	<i>Gallus gallus</i>	8.00E-58	225	68	Full-length
OV-N-ST01-0071-W	XP_001515199.1	T-complex protein 1 subunit epsilon (TCP-1-epsilon) (CCT-epsilon)	<i>Ornithorhynchus anatinus</i>	9.00E-81	302	79	Ambiguous
OV-N-ST01-0090-W		NO HIT		0	0	0	Full-length
OV-N-ST01-0092-W		NO HIT		0	0	0	
OV-N-ST01-0095-W		NO HIT		0	0	0	Full-length
OV-N-ST01-0096-W		NO HIT		0	0	0	
OV-N-ST01-0097-W		NO HIT		0	0	0	
OV-N-ST01-0098-W		NO HIT		0	0	0	5'-sequenced partial
OV-N-ST01-0103-W	XP_623323.2	zipper CG15792-PD, isoform D	<i>Apis mellifera</i>	9.00E-88	325	75	Full-length
OV-N-ST01-0109-W	XP_001656982.1	chaperonin	<i>Aedes aegypti</i>	4.00E-22	107	85	Full-length
OV-N-ST01-0110-W		NO HIT		0	0	0	Full-length
OV-N-ST01-0112-W		NO HIT		0	0	0	Full-length
OV-N-ST01-0113-W		NO HIT		0	0	0	
OV-N-ST01-0114-W		NO HIT		0	0	0	
OV-N-ST01-0120-W		NO HIT		0	0	0	
OV-N-ST01-0122-W		NO HIT		0	0	0	Full-length
OV-N-ST01-0125-W	XP_970745.1	CG8597-PA, isoform A	<i>Tribolium castaneum</i>	2.00E-35	151	47	Ambiguous
OV-N-ST01-0127-W		NO HIT		0	0	0	Full-length
OV-N-ST01-0129-W	XP_396786.3	domino CG9696-PD, isoform D	<i>Apis mellifera</i>	3.00E-52	207	93	Ambiguous
OV-N-ST01-0132-W		NO HIT		0	0	0	Full-length
OV-N-ST01-0135-W		NO HIT		0	0	0	Full-length
OV-N-ST01-0137-W	AAN17670.1	thrombospondin	<i>Penaeus monodon</i>	1.00E-52	208	84	Full-length
OV-N-ST01-0142-W		NO HIT		0	0	0	5'-sequenced partial
OV-N-ST01-0144-W		NO HIT		0	0	0	Full-length

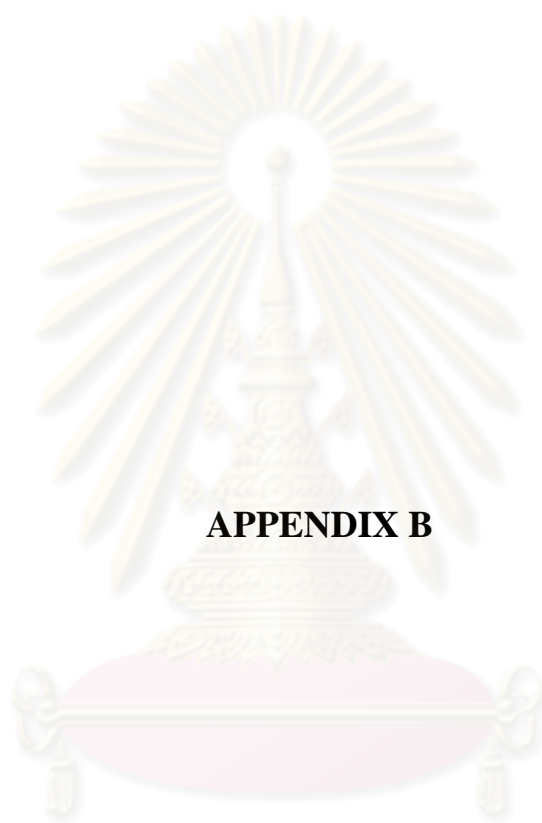
Table A2 (Cont.)

Input Sequence	Accession Number	Hit Item	Closest Species	e-value	Bit-score	%Identity	Predicted Full Length
OV-N-ST01-0148-W	XP_972190.1	CG18572-PA, isoform A	<i>Tribolium castaneum</i>	7.00E-20	100	49	Full-length
OV-N-ST01-0150-W		NO HIT		0	0	0	Full-length
OV-N-ST01-0151-W		NO HIT		0	0	0	
OV-N-ST01-0152-W		NO HIT		0	0	0	Full-length
OV-N-ST01-0156-W	XP_973593.1	CG8444-PA	<i>Tribolium castaneum</i>	3.00E-06	55	26	Full-length
OV-N-ST01-0158-W		NO HIT		0	0	0	Full-length
OV-N-ST01-0161-W		NO HIT		0	0	0	Full-length
OV-N-ST01-0162-W		NO HIT		0	0	0	
OV-N-ST01-0163-W		NO HIT		0	0	0	Full-length
OV-N-ST01-0165-W		NO HIT		0	0	0	Full-length
OV-N-ST01-0167-W		NO HIT		0	0	0	Full-length
OV-N-ST01-0168-W		NO HIT		0	0	0	
OV-N-ST01-0169-W		NO HIT		0	0	0	Full-length
OV-N-ST01-0173-W	BAF91418.1	elongation factor 1-alpha	<i>Upogebia major</i>	1.00E-88	328	90	Full-length
OV-N-ST01-0176-W		NO HIT		0	0	0	Full-length
OV-N-ST01-0178-W		NO HIT		0	0	0	Ambiguous
OV-N-ST01-0180-W		NO HIT		0	0	0	Full-length
OV-N-ST01-0181-W	XP_001508889.1	CWF19-like 2, cell cycle control (S. pombe)	<i>Ornithorhynchus anatinus</i>	1.00E-53	211	55	Full-length
OV-N-ST01-0182-W	ABM55540.1	putative myosin II essential light chain	<i>Maconellicoccus hirsutus</i>	3.00E-12	75	89	Full-length
OV-N-ST01-0183-W		NO HIT		0	0	0	Full-length
OV-N-ST01-0184-W	XP_541362.2	Zinc finger protein 208	<i>Canis familiaris</i>	5.00E-27	123	35	Full-length
OV-N-ST01-0186-W		NO HIT		0	0	0	Full-length
OV-N-ST01-0187-W		NO HIT		0	0	0	Full-length
OV-N-ST01-0189-W		NO HIT		0	0	0	Full-length
OV-N-ST01-0195-W		NO HIT		0	0	0	
OV-N-ST01-0196-W	XP_970124.1	CG3861-PA, isoform A	<i>Tribolium castaneum</i>	3.00E-66	253	84	Ambiguous
OV-N-ST01-0197-W	CAG12715.1	unnamed protein product	<i>Tetraodon nigroviridis</i>	6.00E-20	100	31	Full-length
OV-N-ST01-0198-W	NP_730978.1	sec23 CG1250-PA, isoform A	<i>Drosophila melanogaster</i>	2.00E-56	221	72	5'-sequenced partial
OV-N-ST01-0202-W		NO HIT		0	0	0	Full-length
OV-N-ST01-0204-W		NO HIT		0	0	0	Ambiguous
OV-N-ST01-0209-W		NO HIT		0	0	0	Full-length
OV-N-ST01-0211-W	XP_001167558.1	RNA binding motif protein 5 isoform 9	<i>Pan troglodytes</i>	3.00E-23	111	37	Ambiguous
OV-N-ST01-0212-W		NO HIT		0	0	0	
OV-N-ST01-0213-W	XP_316032.4	AGAP005990-PA	<i>Anopheles gambiae str. PEST</i>	8.00E-27	122	39	Full-length
OV-N-ST01-0214-W		NO HIT		0	0	0	
OV-N-ST01-0216-W		NO HIT		0	0	0	Full-length
OV-N-ST01-0219-W	NP_001025397.1	hypothetical protein LOC568840	<i>Danio rerio</i>	5.00E-26	120	40	Full-length
OV-N-ST01-0220-W		NO HIT		0	0	0	
OV-N-ST01-0226-W		NO HIT		0	0	0	Full-length
OV-N-ST01-0227-W		NO HIT		0	0	0	Short full-length
OV-N-ST01-0229-W		NO HIT		0	0	0	5'-sequenced partial
OV-N-ST01-0230-W	XP_539018.2	inhibitor of Brutons tyrosine kinase	<i>Canis familiaris</i>	1.00E-08	62	54	Full-length
OV-N-ST01-0231-W		NO HIT		0	0	0	Full-length
OV-N-ST02-0004-W		NO HIT		0	0	0	
OV-N-ST02-0005-W		NO HIT		0	0	0	
OV-N-ST02-0007-W		NO HIT		0	0	0	Full-length
OV-N-ST02-0009-W	XP_623732.1	CG2807-PA isoform 1	<i>Apis mellifera</i>	6.00E-42	173	74	Ambiguous

Table A2 (Cont.)

Input Sequence	Accession Number	Hit Item	Closest Species	e-value	Bit-score	%Identity	Predicted Full Length
OV-N-ST02-0028-W	BAC92764.1	thrombospondin	<i>Marsupenaeus japonicus</i>	9.00E-21	102	82	Ambiguous
OV-N-ST02-0038-W	XP_001846040.1	conserved hypothetical protein	<i>Culex pipiens quinquefasciatus</i>	8.00E-29	129	70	Ambiguous
OV-N-ST02-0042-W		NO HIT		0	0	0	
OV-N-ST02-0059-W		NO HIT		0	0	0	5'-sequenced partial
OV-N-ST02-0067-W		NO HIT		0	0	0	Full-length
OV-N-ST02-0071-W	XP_973193.1	carbonyl reductase 1-like	<i>Tribolium castaneum</i>	2.00E-45	184	60	Full-length
OV-N-ST02-0073-W		NO HIT		0	0	0	Full-length
OV-N-ST02-0078-W		NO HIT		0	0	0	5'-sequenced partial
OV-N-ST02-0084-W	XP_972421.1	anaphase promoting complex subunit 11 homolog	<i>Tribolium castaneum</i>	3.00E-37	157	81	Short full-length
OV-N-ST02-0087-W		NO HIT		0	0	0	Full-length
OV-N-ST02-0088-W	AAZ66372.1	thrombospondin	<i>Fenneropenaeus chinensis</i>	6.00E-08	60	65	Full-length
OV-N-ST02-0094-W		NO HIT		0	0	0	
OV-N-ST02-0120-W		NO HIT		0	0	0	5'-sequenced partial
OV-N-ST02-0123-W	XP_001356421.1	GA12460-PA	<i>Drosophila pseudoobscura</i>	8.00E-06	53	28	Full-length
OV-N-ST02-0127-W		NO HIT		0	0	0	Full-length
OV-N-ST02-0129-W	XP_001603266.1	conserved hypothetical protein	<i>Nasonia vitripennis</i>	3.00E-22	107	34	Full-length
OV-N-ST02-0132-W	NP_001002065.1	peptidylprolyl isomerase D (cyclophilin D)	<i>Danio rerio</i>	1.00E-20	102	38	Ambiguous
OV-N-ST02-0136-W		NO HIT		0	0	0	Full-length
OV-N-ST02-0140-W		NO HIT		0	0	0	5'-sequenced partial
OV-N-ST02-0147-W	XP_001504331.1	hypothetical protein	<i>Equus caballus</i>	1.00E-13	79	32	Full-length
OV-N-ST02-0149-W	XP_001122800.1	splicing factor, arginine/serine-rich 7	<i>Apis mellifera</i>	1.00E-36	155	72	Full-length
OV-N-ST02-0150-W	AAAY18083.1	interleukin enhancer binding factor 2	<i>Tetraodon nigroviridis</i>	2.00E-25	118	72	Full-length
OV-N-ST02-0154-W	AAF34332.1	peritrophin-like protein 2	<i>Penaeus semisulcatus</i>	3.00E-29	131	73	Full-length
OV-N-ST02-0156-W		NO HIT		0	0	0	Full-length
OV-N-ST02-0159-W		NO HIT		0	0	0	
OV-N-ST02-0163-W	XP_001603904.1	ENSANGP00000010063	<i>Nasonia vitripennis</i>	2.00E-24	115	47	Ambiguous
OV-N-ST02-0168-W	XP_624169.1	CG7338-PA	<i>Apis mellifera</i>	1.00E-36	155	42	Full-length
OV-N-ST02-0180-W		NO HIT		0	0	0	
OV-N-ST02-0181-W	XP_690005.2	hypothetical protein	<i>Danio rerio</i>	3.00E-50	200	45	Ambiguous
OV-N-ST02-0184-W		NO HIT		0	0	0	Full-length
OV-N-ST02-0185-W	ABI97374.1	C-type lectin	<i>Litopenaeus vannamei</i>	4.00E-05	51	35	Full-length
OV-N-ST02-0196-W	XP_393540.2	CG14224-PA	<i>Apis mellifera</i>	4.00E-18	94	63	Ambiguous
OV-N-ST02-0199-W		NO HIT		0	0	0	Full-length
OV-N-ST02-0200-W		NO HIT		0	0	0	Full-length
OV-N-ST02-0204-W	XP_001121013.1	HLA-B-associated transcript 3	<i>Apis mellifera</i>	2.00E-20	101	72	Full-length
OV-N-ST02-0206-W	XP_001606424.1	CG5814-PA	<i>Nasonia vitripennis</i>	6.00E-35	149	57	Full-length
OV-N-ST02-0211-W	XP_697518.2	hypothetical protein	<i>Danio rerio</i>	4.00E-33	143	83	5'-sequenced partial
OV-N-ST02-0212-W		NO HIT		0	0	0	Ambiguous
OV-N-ST02-0216-W		NO HIT		0	0	0	Full-length
OV-N-ST02-0217-W		NO HIT		0	0	0	
OV-N-ST02-0220-W	XP_975438.1	CG15814-PA, isoform A	<i>Tribolium castaneum</i>	8.00E-24	112	60	Ambiguous
OV-N-ST02-0223-W		NO HIT		0	0	0	Short full-length
OV-N-ST02-0225-W		NO HIT		0	0	0	Full-length
OV-N-ST02-0229-W		NO HIT		0	0	0	Full-length
OV-N-ST02-0231-W	XP_001605290.1	ENSANGP00000018564	<i>Nasonia vitripennis</i>	1.00E-16	89	53	Full-length

*The complete data are available on request.



APPENDIX B

ศูนย์วิทยทรัพยากร
จุฬาลงกรณ์มหาวิทยาลัย

Table B1 Classification of sequences among the three principal GO categories of the typical, normalized and SSH ovaries cDNA libraries of *P. monodon*

Level	GO ID	Term	Type	#Seqs	Graph Score	Sequences
2	GO:0000003	reproduction	biological_process	21	3.19	AlIOV-CT436, AlIOV-CT153, OV-N-N01-1082-W, OV-N-ST01-0125-W, OV-N-N01-1208-W, OV-N-S01-0547-W, OV-N-S01-2561-W, AlIOV-CT95, OV-N-N01-1787-W, OV-N-S01-0359-W, AlIOV-CT279, OV-N-S01-2003-W, OV-N-S01-1769-W, OV-N-ST01-0103-W, AlIOV-CT28, OV-N-N01-0391-W, AlIOV-CT280, OV-N-N01-0376-W, AlIOV-CT215, OV-N-S01-1895-W, OV-N-S01-0522-W
3	GO:0019953	sexual reproduction	biological_process	16	2.41	AlIOV-CT436, AlIOV-CT153, OV-N-N01-1082-W, OV-N-ST01-0125-W, OV-N-N01-1787-W, OV-N-S01-0359-W, OV-N-S01-0547-W, AlIOV-CT279, OV-N-S01-2003-W, OV-N-S01-1769-W, AlIOV-CT95, OV-N-ST01-0103-W, AlIOV-CT28, OV-N-N01-0391-W, OV-N-N01-0376-W, AlIOV-CT215
4	GO:0030707	ovarian follicle cell development	biological_process	4	2.18	AlIOV-CT153, OV-N-S01-2003-W, AlIOV-CT95, OV-N-ST01-0103-W
4	GO:0007548	sex differentiation	biological_process	4	1.3	OV-N-N01-1208-W, OV-N-S01-0547-W, OV-N-S01-2561-W, AlIOV-CT95
5	GO:0044454	nuclear chromosome part	cellular_component	6	1.93	AlIOV-CT345, AlIOV-CT329, AlIOV-CT420, OV-N-N01-1623-W, OV-N-S01-1179-W, AlIOV-CT333
5	GO:0043159	acrosomal matrix	cellular_component	1	1	OV-N-N01-0376-W
5	GO:0030660	Golgi-associated vesicle membrane	cellular_component	2	0.72	OV-N-S01-1103-W, OV-N-ST01-0198-W
5	GO:0000785	chromatin	cellular_component	8	6.65	AlIOV-CT345, AlIOV-CT110, AlIOV-CT253, AlIOV-CT329, AlIOV-CT420, OV-N-N01-1623-W, OV-N-S01-1179-W, AlIOV-CT333
5	GO:0030132	clathrin coat of coated pit	cellular_component	1	1	OV-N-S01-1118-W
5	GO:0044448	cell cortex part	cellular_component	1	0.6	OV-N-ST01-0103-W
5	GO:0005654	nucleoplasm	cellular_component	13	5.46	OV-N-S01-0359-W, OV-N-S01-0142-W, OV-N-N01-0956-W, AlIOV-CT333, OV-N-S01-1537-W, OV-N-S01-1699-W, OV-N-S01-1777-W, AlIOV-CT329, AlIOV-CT420, OV-N-N01-1623-W, OV-N-S01-1179-W, OV-N-S01-0025-W, OV-N-N01-0440-W
5	GO:0000428	DNA-directed RNA polymerase complex	cellular_component	1	1.08	OV-N-N01-0956-W
5	GO:0005802	trans-Golgi network	cellular_component	1	1	AlIOV-CT342
5	GO:0005751	mitochondrial respiratory chain complex IV	cellular_component	1	1	AlIOV-CT13
5	GO:0005746	mitochondrial respiratory chain	cellular_component	9	7	AlIOV-CT13, AlIOV-CT4, AlIOV-CT403, OV-N-S01-1263-W, OV-N-S01-2062-W, AlIOV-CT16, AlIOV-CT191, AlIOV-CT274, AlIOV-CT411
5	GO:0030659	cytoplasmic vesicle membrane	cellular_component	4	0.86	OV-N-S01-1103-W, OV-N-ST01-0198-W, OV-N-N01-1530-W, OV-N-ST01-0069-W
5	GO:0030131	clathrin adaptor complex	cellular_component	1	1	OV-N-S01-1118-W
5	GO:0000775	chromosome, pericentric region	cellular_component	1	0.6	AlIOV-CT333
5	GO:0005815	microtubule organizing center	cellular_component	3	1.8	AlIOV-CT280, OV-N-S01-0543-W, OV-N-S01-1769-W
5	GO:0016023	cytoplasmic membrane-bounded vesicle	cellular_component	6	1.73	OV-N-S01-1103-W, OV-N-ST01-0198-W, OV-N-N01-1530-W, OV-N-ST01-0069-W, OV-N-S01-1118-W, OV-N-N01-1042-W
5	GO:0005758	mitochondrial intermembrane space	cellular_component	2	2	AlIOV-CT130, OV-N-S01-2062-W
5	GO:0005637	nuclear inner membrane	cellular_component	1	0.36	OV-N-N01-1780-W
5	GO:0016461	unconventional myosin complex	cellular_component	2	2	OV-N-ST01-0103-W, OV-N-ST01-0182-W
5	GO:0030663	COPI coated vesicle membrane	cellular_component	2	1.2	OV-N-N01-1530-W, OV-N-ST01-0069-W
5	GO:0000152	nuclear ubiquitin ligase complex	cellular_component	1	0.6	OV-N-ST02-0084-LF

Table B1 (Cont.)

Level	GO ID	Term	Type	#Seqs	Graph Score	Sequences
5	GO:0000123	histone acetyltransferase complex	cellular_component	1	0.36	OV-N-S01-0025-W
5	GO:0005773	vacuole	cellular_component	5	1.66	AlIOV-CT121, OV-N-S01-0575-W, AlIOV-CT240, OV-N-N01-0376-W, OV-N-N01-1134-W
5	GO:0005759	mitochondrial matrix	cellular_component	11	8.52	AlIOV-CT331, AlIOV-CT4, OV-N-S01-0390-W, OV-N-S01-2557-W, OV-N-N01-0376-W, OV-N-N01-1178-W, OV-N-S01-1295-W, OV-N-S01-2281-W, OV-N-S01-2642-W, OV-N-ST01-0196-W, AlIOV-CT83
5	GO:0000314	organellar small ribosomal subunit	cellular_component	2	1.2	OV-N-S01-0390-W, OV-N-S01-2557-W
5	GO:0042579	microbody	cellular_component	1	0.6	OV-N-S01-2642-W
5	GO:0019717	synaptosome	cellular_component	1	1	OV-N-S01-1870-W
5	GO:0005685	snRNP U1	cellular_component	1	1	OV-N-S01-0305-W
5	GO:0015934	large ribosomal subunit	cellular_component	12	8	AlIOV-CT27, AlIOV-CT49, AlIOV-CT163, AlIOV-CT268, AlIOV-CT297, AlIOV-CT350, AlIOV-CT379, AlIOV-CT398, OV-N-N01-1716-W, OV-N-S01-2635-W, AlIOV-CT286, AlIOV-CT380
5	GO:0032302	MutSbeta complex	cellular_component	1	1	OV-N-S01-0999-W
5	GO:0016323	basolateral plasma membrane	cellular_component	2	0.43	OV-N-N01-1040-W, OV-N-S01-1889-W
5	GO:0030120	vesicle coat	cellular_component	4	2.4	OV-N-S01-1103-W, OV-N-ST01-0198-W, OV-N-N01-1530-W, OV-N-ST01-0069-W
5	GO:0030127	COPII vesicle coat	cellular_component	2	2	OV-N-S01-1103-W, OV-N-ST01-0198-W
5	GO:0031301	integral to organelle membrane	cellular_component	2	1.2	OV-N-N01-1780-W, OV-N-S01-2185-W
5	GO:0005743	mitochondrial inner membrane	cellular_component	23	16.92	AlIOV-CT13, AlIOV-CT4, AlIOV-CT403, OV-N-S01-1263-W, OV-N-S01-2062-W, AlIOV-CT16, AlIOV-CT191, AlIOV-CT274, AlIOV-CT411, AlIOV-CT64, AlIOV-CT83, AlIOV-CT136, AlIOV-CT146, AlIOV-CT264, AlIOV-CT392, OV-N-N01-0645-W, OV-N-S01-0318-W, OV-N-S01-0468-W, OV-N-S01-0827-W, OV-N-S01-0851-W, OV-N-S01-1295-W, AlIOV-CT429, AlIOV-CT378
5	GO:0016021	integral to membrane	cellular_component	25	22.44	OV-N-N01-1763-W, OV-N-S01-1124-W, OV-N-N01-1780-W, OV-N-S01-2185-W, AlIOV-CT16, AlIOV-CT64, AlIOV-CT84, AlIOV-CT121, AlIOV-CT131, AlIOV-CT146, AlIOV-CT191, AlIOV-CT337, AlIOV-CT392, OV-N-N01-0645-W, OV-N-N01-0655-W, OV-N-N01-1134-W, OV-N-S01-0022-W, OV-N-S01-0068-W, OV-N-S01-0231-W, OV-N-S01-0568-W, OV-N-S01-0575-W, OV-N-S01-0962-W, OV-N-S01-1082-W, OV-N-S01-1255-W, OV-N-S01-2448-W
5	GO:0005967	mitochondrial pyruvate dehydrogenase complex	cellular_component	1	1	AlIOV-CT331
5	GO:0005794	Golgi apparatus	cellular_component	10	7.23	OV-N-ST01-0069-W, OV-N-ST01-0198-W, AlIOV-CT276, AlIOV-CT384, AlIOV-CT431, OV-N-N01-0985-W, OV-N-S01-0812-W, OV-N-S01-1103-W, OV-N-N01-1530-W, AlIOV-CT342
5	GO:0030014	CCR4-NOT complex	cellular_component	1	1	OV-N-S01-0359-W
5	GO:0010369	chromocenter	cellular_component	1	0.6	AlIOV-CT333
5	GO:0005753	mitochondrial proton-transporting ATP synthase complex	cellular_component	2	1.2	AlIOV-CT429, AlIOV-CT378
5	GO:0005730	nucleolus	cellular_component	12	10.72	OV-N-N01-0956-W, OV-N-N01-1662-W, AlIOV-CT206, AlIOV-CT234, AlIOV-CT297, OV-N-N01-0429-W, OV-N-S01-0321-W, OV-N-S01-1952-W, OV-N-S01-2104-W, OV-N-S01-2635-W, OV-N-ST02-0094-LF, OV-N-ST02-0150-W
5	GO:0005829	cytosol	cellular_component	37	17.48	AlIOV-CT31, AlIOV-CT137, AlIOV-CT154, AlIOV-CT188, AlIOV-CT323, AlIOV-CT354, AlIOV-CT399, OV-N-N01-1214-W, OV-N-S01-0092-W, OV-N-S01-0268-W, AlIOV-CT375, AlIOV-CT27, AlIOV-CT49, AlIOV-CT163, AlIOV-CT268, AlIOV-CT297, AlIOV-CT350, AlIOV-CT379, AlIOV-CT398, OV-N-N01-1716-W, OV-N-S01-2635-W, OV-N-S01-0704-W, AlIOV-CT307, OV-N-N01-0660-W, OV-N-S01-0553-W, AlIOV-CT126, AlIOV-CT308, AlIOV-CT335, AlIOV-CT384, OV-N-N01-0393-W, OV-N-N01-0985-W, OV-N-S01-0025-W, OV-N-S01-0807-W, OV-N-S01-1291-W, OV-N-S01-1931-W, OV-N-S01-2123-W, AlIOV-CT96
5	GO:0005874	microtubule	cellular_component	8	7.6	AlIOV-CT215, AlIOV-CT28, AlIOV-CT50, AlIOV-CT123, AlIOV-CT266, OV-N-S01-0904-W, OV-N-S01-1143-W, OV-N-S01-1769-W
5	GO:0005761	mitochondrial ribosome	cellular_component	2	1.2	OV-N-S01-0390-W, OV-N-S01-2557-W
5	GO:0005905	coated pit	cellular_component	1	0.6	OV-N-S01-1118-W

Table B1 (Cont.)

Level	GO ID	Term	Type	#Seqs	Graph Score	Sequences
5	GO:0005819	spindle	cellular_component	5	3.8	OV-N-S01-0543-W, OV-N-S01-1227-W, AIOV-CT215, AIOV-CT333, OV-N-S01-1769-W
5	GO:0005747	mitochondrial respiratory chain complex I	cellular_component	3	3	AIOV-CT403, OV-N-S01-1263-W, OV-N-S01-2062-W
5	GO:0044445	cytosolic part	cellular_component	26	10.8	AIOV-CT31, AIOV-CT137, AIOV-CT154, AIOV-CT188, AIOV-CT323, AIOV-CT354, AIOV-CT399, OV-N-N01-1214-W, OV-N-S01-0092-W, OV-N-S01-0268-W, AIOV-CT375, AIOV-CT27, AIOV-CT49, AIOV-CT163, AIOV-CT268, AIOV-CT297, AIOV-CT350, AIOV-CT379, AIOV-CT398, OV-N-N01-1716-W, OV-N-S01-2635-W, OV-N-S01-0704-W, AIOV-CT307, OV-N-N01-0660-W, OV-N-S01-0553-W, AIOV-CT96
5	GO:0031461	cullin-RING ubiquitin ligase complex	cellular_component	1	0.6	OV-N-S01-1798-W
5	GO:0030286	dynein complex	cellular_component	1	0.6	AIOV-CT28
5	GO:0005694	chromosome	cellular_component	12	6.96	AIOV-CT345, OV-N-S01-2611-W, AIOV-CT329, AIOV-CT420, OV-N-N01-1623-W, OV-N-S01-1179-W, AIOV-CT110, AIOV-CT253, AIOV-CT333, AIOV-CT145, AIOV-CT427, OV-N-ST01-0001-W
5	GO:0032421	stereocilium bundle	cellular_component	1	0.6	OV-N-S01-2261-W
5	GO:0005813	centrosome	cellular_component	3	3	AIOV-CT280, OV-N-S01-0543-W, OV-N-S01-1769-W
5	GO:0005665	DNA-directed RNA polymerase II, core complex	cellular_component	1	1	OV-N-N01-0956-W
5	GO:0005856	cytoskeleton	cellular_component	23	13.75	OV-N-S01-0558-W, OV-N-S01-1343-W, OV-N-ST01-0103-W, OV-N-ST01-0182-W, AIOV-CT28, OV-N-S01-1393-W, OV-N-S01-0543-W, OV-N-S01-1227-W, AIOV-CT342, OV-N-N01-1082-W, AIOV-CT215, OV-N-S01-1769-W, AIOV-CT50, AIOV-CT123, AIOV-CT266, OV-N-S01-0904-W, OV-N-S01-1143-W, AIOV-CT262, AIOV-CT279, OV-N-N01-1040-W, OV-N-S01-2261-W, AIOV-CT333, AIOV-CT280
5	GO:0044449	contractile fiber part	cellular_component	2	1.2	OV-N-ST01-0103-W, AIOV-CT384
5	GO:0005795	Golgi stack	cellular_component	1	1	OV-N-ST01-0198-W
5	GO:0016471	vacuolar proton-transporting V-type ATPase complex	cellular_component	1	0.6	OV-N-N01-1134-W
5	GO:0005763	mitochondrial small ribosomal subunit	cellular_component	2	2	OV-N-S01-0390-W, OV-N-S01-2557-W
5	GO:0030867	rough endoplasmic reticulum membrane	cellular_component	1	0.6	AIOV-CT364
5	GO:0033176	proton-transporting V-type ATPase complex	cellular_component	1	0.36	OV-N-N01-1134-W
5	GO:0000228	nuclear chromosome	cellular_component	6	1.16	AIOV-CT345, AIOV-CT329, AIOV-CT420, OV-N-N01-1623-W, OV-N-S01-1179-W, AIOV-CT333
5	GO:0044452	nucleolar part	cellular_component	2	1.2	OV-N-N01-0956-W, OV-N-N01-1662-W
5	GO:0030126	COPI vesicle coat	cellular_component	2	2	OV-N-N01-1530-W, OV-N-ST01-0069-W
5	GO:0005684	U2-dependent spliceosome	cellular_component	1	0.6	OV-N-S01-0305-W
5	GO:0030054	cell junction	cellular_component	4	1.99	OV-N-N01-1040-W, OV-N-S01-1889-W, OV-N-S01-0962-W, AIOV-CT180
5	GO:0032420	stereocilium	cellular_component	1	1	OV-N-S01-2261-W
5	GO:0031227	intrinsic to endoplasmic reticulum membrane	cellular_component	1	0.6	OV-N-S01-2185-W
5	GO:0048471	perinuclear region of cytoplasm	cellular_component	4	4	AIOV-CT192, AIOV-CT342, AIOV-CT399, OV-N-S01-2003-W
5	GO:0005798	Golgi-associated vesicle	cellular_component	4	0.86	OV-N-S01-1103-W, OV-N-ST01-0198-W, OV-N-N01-1530-W, OV-N-ST01-0069-W
5	GO:0042598	vesicular fraction	cellular_component	5	3	AIOV-CT93, AIOV-CT280, OV-N-N01-0800-W, OV-N-S01-0022-W, OV-N-S01-0568-W

Table B1 (Cont.)

Level	GO ID	Term	Type	#Seqs	Graph Score	Sequences
5	GO:0005783	endoplasmic reticulum	cellular_component	21	17.66	OV-N-S01-2185-W, AIIOV-CT236, OV-N-N01-0800-W, AIIOV-CT339, AIIOV-CT364, AIIOV-CT84, AIIOV-CT228, AIIOV-CT292, AIIOV-CT368, AIIOV-CT401, AIIOV-CT431, OV-N-N01-0020-W, OV-N-N01-0985-W, OV-N-S01-0022-W, OV-N-S01-0110-W, OV-N-S01-0568-W, OV-N-S01-1082-W, OV-N-S01-1255-W, OV-N-S01-1405-W, OV-N-S01-2148-W, OV-N-ST01-0198-W
5	GO:0005811	lipid particle	cellular_component	16	16	AIIOV-CT4, AIIOV-CT13, AIIOV-CT100, AIIOV-CT130, AIIOV-CT163, AIIOV-CT268, AIIOV-CT282, AIIOV-CT292, AIIOV-CT307, AIIOV-CT354, AIIOV-CT368, AIIOV-CT401, AIIOV-CT429, AIIOV-CT442, OV-N-N01-0280-W, OV-N-S01-1607-W
5	GO:0000275	mitochondrial proton-transporting ATP synthase complex, catalytic core F(1) nucleoplasm part	cellular_component	1	1	AIIOV-CT378
5	GO:0044451	dynein complex	cellular_component	11	5.77	OV-N-S01-0359-W, OV-N-S01-0142-W, OV-N-N01-0956-W, OV-N-S01-1699-W, OV-N-S01-1777-W, AIIOV-CT329, AIIOV-CT420, OV-N-N01-1623-W, OV-N-S01-1179-W, OV-N-S01-0025-W, OV-N-N01-0440-W
5	GO:0005869	dynein complex	cellular_component	1	1	OV-N-S01-1393-W
5	GO:0000276	mitochondrial proton-transporting ATP synthase complex, coupling factor F(o)	cellular_component	1	1	AIIOV-CT429
5	GO:0000313	organellar ribosome	cellular_component	2	0.72	OV-N-S01-0390-W, OV-N-S01-2557-W
5	GO:0030118	clathrin coat	cellular_component	1	1.2	OV-N-S01-1118-W
5	GO:0033179	proton-transporting V-type ATPase, VO domain	cellular_component	1	0.6	OV-N-N01-1134-W
5	GO:0005750	mitochondrial respiratory chain complex III	cellular_component	1	1	AIIOV-CT4
5	GO:0005634	nucleus	cellular_component	81	54.61	OV-N-S01-0359-W, OV-N-S01-0142-W, OV-N-N01-0956-W, AIIOV-CT333, OV-N-S01-1537-W, OV-N-N01-1763-W, OV-N-S01-1124-W, AIIOV-CT345, OV-N-N01-1780-W, OV-N-S01-1952-W, AIIOV-CT33, AIIOV-CT39, AIIOV-CT51, AIIOV-CT65, AIIOV-CT106, AIIOV-CT110, AIIOV-CT145, AIIOV-CT153, AIIOV-CT163, AIIOV-CT175, AIIOV-CT217, AIIOV-CT232, AIIOV-CT250, AIIOV-CT253, AIIOV-CT280, AIIOV-CT353, AIIOV-CT399, AIIOV-CT408, AIIOV-CT409, AIIOV-CT442, OV-N-N01-0378-W, OV-N-N01-0510-W, OV-N-N01-0680-W, OV-N-N01-0800-W, OV-N-N01-0908-W, OV-N-N01-1232-W, OV-N-S01-0523-W, OV-N-S01-0543-W, OV-N-S01-0706-W, OV-N-S01-0743-W, OV-N-S01-0827-W, OV-N-S01-0888-W, OV-N-S01-1119-W, OV-N-S01-1291-W, OV-N-S01-1395-W, OV-N-S01-1498-W, OV-N-S01-1991-W, OV-N-S01-2611-W, OV-N-ST01-0001-W, OV-N-ST01-0068-W, OV-N-ST01-0125-W, OV-N-S01-1699-W, OV-N-S01-0229-W, OV-N-S01-1777-W, OV-N-S01-0999-W, AIIOV-CT329, AIIOV-CT420, OV-N-N01-1623-W, OV-N-S01-1179-W, OV-N-N01-1662-W, AIIOV-CT206, AIIOV-CT234, AIIOV-CT297, OV-N-N01-0429-W, OV-N-S01-0321-W, OV-N-S01-2104-W, OV-N-S01-2635-W, OV-N-ST02-0094-LF, OV-N-ST02-0150-W, OV-N-S01-0025-W, AIIOV-CT381, OV-N-N01-0440-W, AIIOV-CT78, OV-N-S01-1769-W, AIIOV-CT211, AIIOV-CT242, OV-N-N01-0109-W, OV-N-S01-0305-W, OV-N-S01-0067-W, OV-N-S01-0550-W, OV-N-ST02-0084-LF
5	GO:0032301	MutSalpa complex	cellular_component	1	1	OV-N-S01-0999-W
5	GO:0043292	contractile fiber	cellular_component	2	0.72	OV-N-ST01-0103-W, AIIOV-CT384
5	GO:0000922	spindle pole	cellular_component	2	2	OV-N-S01-0543-W, OV-N-S01-1227-W
5	GO:0031229	intrinsic to nuclear inner membrane	cellular_component	1	0.6	OV-N-N01-1780-W
5	GO:0005938	cell cortex	cellular_component	1	0.36	OV-N-ST01-0103-W
5	GO:0005739	mitochondrion	cellular_component	48	23.94	AIIOV-CT331, AIIOV-CT4, OV-N-S01-0390-W, OV-N-S01-2557-W, OV-N-N01-0376-W, OV-N-N01-1178-W, OV-N-S01-1295-W, OV-N-S01-2281-W, OV-N-S01-2642-W, OV-N-ST01-0196-W, AIIOV-CT130, OV-N-S01-2062-W, AIIOV-CT13, AIIOV-CT403, OV-N-S01-1263-W, AIIOV-CT16, AIIOV-CT191, AIIOV-CT274, AIIOV-CT411, AIIOV-CT64, AIIOV-CT83, AIIOV-CT136, AIIOV-CT146, AIIOV-CT264, AIIOV-CT392, OV-N-N01-0645-W, OV-N-S01-0318-W, OV-N-S01-0468-W, OV-N-S01-0827-W, OV-N-S01-0851-W, OV-N-S01-0068-W, AIIOV-CT99, AIIOV-CT131, AIIOV-CT173, AIIOV-CT214, AIIOV-CT280, AIIOV-CT289, AIIOV-CT337, OV-N-N01-0343-W, OV-N-N01-0895-W, OV-N-S01-0829-W, OV-N-S01-1025-W, OV-N-S01-1601-W, OV-N-S01-1893-W, OV-N-S01-

Table B1 (Cont.)

Level	GO ID	Term	Type	#Seqs	Graph Score	Sequences
						2058-W, OV-N-S01-2561-W, AIOV-CT429, AIOV-CT378
5	GO:0005657	replication fork	cellular_component	4	1.44	AIOV-CT329, AIOV-CT420, OV-N-N01-1623-W, OV-N-S01-1179-W
5	GO:0004091	carboxylesterase activity	molecular_function	2	2	OV-N-N01-0020-W, OV-N-N01-1042-W
5	GO:0032555	purine ribonucleotide binding	molecular_function	72	27.36	AIOV-CT33, AIOV-CT50, AIOV-CT123, AIOV-CT180, AIOV-CT204, AIOV-CT215, AIOV-CT246, AIOV-CT258, AIOV-CT265, AIOV-CT266, AIOV-CT280, AIOV-CT353, AIOV-CT384, OV-N-N01-0144-W, OV-N-N01-0209-W, OV-N-N01-0977-W, OV-N-N01-1101-W, OV-N-N01-1778-W, OV-N-S01-0591-W, OV-N-S01-0741-W, OV-N-S01-0829-W, OV-N-S01-0904-W, OV-N-S01-1143-W, OV-N-S01-1987-W, OV-N-S01-2267-W, OV-N-ST01-0173-W, AIOV-CT35, AIOV-CT121, AIOV-CT126, AIOV-CT130, AIOV-CT142, AIOV-CT167, AIOV-CT194, AIOV-CT250, AIOV-CT262, AIOV-CT287, AIOV-CT292, AIOV-CT307, AIOV-CT329, AIOV-CT343, AIOV-CT351, AIOV-CT401, AIOV-CT409, AIOV-CT420, AIOV-CT425, AIOV-CT427, AIOV-CT435, OV-N-N01-0378-W, OV-N-N01-0660-W, OV-N-N01-0822-W, OV-N-N01-1134-W, OV-N-N01-1623-W, OV-N-S01-0067-W, OV-N-S01-0142-W, OV-N-S01-0419-W, OV-N-S01-0543-W, OV-N-S01-0553-W, OV-N-S01-0575-W, OV-N-S01-0997-W, OV-N-S01-0999-W, OV-N-S01-1179-W, OV-N-S01-1291-W, OV-N-S01-1421-W, OV-N-S01-1495-W, OV-N-S01-1567-W, OV-N-S01-1923-W, OV-N-S01-1959-W, OV-N-S01-2026-W, OV-N-ST01-0068-W, OV-N-ST01-0071-W, OV-N-ST01-0103-W, OV-N-ST02-0150-W
5	GO:0016790	thiolester hydrolase activity	molecular_function	2	1.2	OV-N-S01-0352-W, OV-N-N01-1042-W
5	GO:0008379	thioredoxin peroxidase activity	molecular_function	1	1	AIOV-CT261
5	GO:0030554	adenyl nucleotide binding	molecular_function	53	20.4	AIOV-CT35, AIOV-CT121, AIOV-CT126, AIOV-CT130, AIOV-CT142, AIOV-CT167, AIOV-CT194, AIOV-CT246, AIOV-CT250, AIOV-CT262, AIOV-CT280, AIOV-CT287, AIOV-CT292, AIOV-CT307, AIOV-CT329, AIOV-CT343, AIOV-CT351, AIOV-CT401, AIOV-CT409, AIOV-CT420, AIOV-CT425, AIOV-CT427, AIOV-CT435, OV-N-N01-0378-W, OV-N-N01-0660-W, OV-N-N01-0822-W, OV-N-N01-1101-W, OV-N-N01-1134-W, OV-N-N01-1623-W, OV-N-S01-0067-W, OV-N-S01-0142-W, OV-N-S01-0419-W, OV-N-S01-0543-W, OV-N-S01-0553-W, OV-N-S01-0575-W, OV-N-S01-0997-W, OV-N-S01-0999-W, OV-N-S01-1291-W, OV-N-S01-1421-W, OV-N-S01-1495-W, OV-N-S01-1567-W, OV-N-S01-1923-W, OV-N-S01-1959-W, OV-N-S01-2026-W, OV-N-ST01-0068-W, OV-N-ST01-0071-W, OV-N-ST01-0103-W, OV-N-ST02-0150-W, OV-N-N01-0061-W, OV-N-N01-0376-W, OV-N-N01-1178-W, OV-N-S01-2281-W
5	GO:0016861	intramolecular oxidoreductase activity, interconverting aldoses and ketoses	molecular_function	1	0.6	AIOV-CT68
5	GO:0042803	protein homodimerization activity	molecular_function	3	3	AIOV-CT126, OV-N-S01-0999-W, OV-N-S01-2642-W
5	GO:0016668	oxidoreductase activity, acting on sulfur group of donors, NAD or NADP as acceptor	molecular_function	2	1.2	OV-N-N01-0376-W, OV-N-S01-2123-W
5	GO:0004129	cytochrome-c oxidase activity	molecular_function	3	3	AIOV-CT13, AIOV-CT191, OV-N-S01-0967-W
5	GO:0016758	transferase activity, transferring hexosyl groups	molecular_function	3	1.44	OV-N-N01-0800-W, OV-N-S01-0568-W, OV-N-S01-1082-W
5	GO:0009309	amine biosynthetic process	biological_process	2	0.35	OV-N-S01-2642-W, AIOV-CT435
5	GO:0007166	cell surface receptor linked signal transduction	biological_process	12	5.81	AIOV-CT7, OV-N-N01-0144-W, OV-N-N01-0209-W, OV-N-N01-1778-W, AIOV-CT192, OV-N-S01-1227-W, AIOV-CT343, OV-N-S01-0991-W, OV-N-S01-1923-W, OV-N-S01-1991-W, AIOV-CT310, OV-N-S01-2003-W
5	GO:0051028	mRNA transport	biological_process	4	3.6	OV-N-S01-0067-W, AIOV-CT436, OV-N-N01-1763-W, OV-N-S01-1124-W
5	GO:0048878	chemical homeostasis	biological_process	8	1.09	OV-N-S01-2062-W, AIOV-CT399, AIOV-CT41, AIOV-CT54, AIOV-CT406, OV-N-N01-0985-W, OV-N-S01-2126-W, OV-N-N01-0376-W

Table B1 (Cont.)

Level	GO ID	Term	Type	#Seqs	Graph Score	Sequences
5	GO:0044242	cellular lipid catabolic process	biological_process	3	1.08	AlIOV-CT83, OV-N-S01-0318-W, OV-N-S01-2281-W
5	GO:0007127	meiosis I	biological_process	1	0.6	OV-N-ST01-0068-W
5	GO:0051298	centrosome duplication	biological_process	1	0.6	AlIOV-CT145
5	GO:0048546	digestive tract morphogenesis	biological_process	1	0.08	OV-N-ST01-0103-W
5	GO:0007422	peripheral nervous system development	biological_process	2	2	AlIOV-CT192, OV-N-S01-2003-W
5	GO:0048667	neuron morphogenesis during differentiation	biological_process	5	1.22	OV-N-S01-1411-W, OV-N-N01-1082-W, OV-N-N01-0908-W, OV-N-S01-1699-W, AlIOV-CT95
5	GO:0030239	myofibril assembly	biological_process	2	1.6	OV-N-ST01-0103-W, OV-N-S01-1088-W
5	GO:0007031	peroxisome organization and biogenesis	biological_process	1	0.6	OV-N-S01-2642-W
5	GO:0035304	regulation of protein amino acid dephosphorylation	biological_process	1	0.6	OV-N-S01-1699-W
5	GO:0045216	cell-cell junction assembly and maintenance	biological_process	1	0.6	OV-N-N01-1040-W
5	GO:0046530	photoreceptor cell differentiation	biological_process	3	0.86	OV-N-N01-1337-W, AlIOV-CT192, OV-N-S01-2003-W
5	GO:0006891	intra-Golgi vesicle-mediated transport	biological_process	1	1	OV-N-N01-1530-W
5	GO:0016056	rhodopsin mediated signaling pathway	biological_process	1	0.22	OV-N-S01-1227-W
6	GO:0030658	transport vesicle membrane	cellular_component	2	0.72	OV-N-S01-1103-W, OV-N-ST01-0198-W
6	GO:0005700	polytene chromosome	cellular_component	1	0.6	AlIOV-CT333
6	GO:0030133	transport vesicle	cellular_component	2	0.43	OV-N-S01-1103-W, OV-N-ST01-0198-W
6	GO:0030662	coated vesicle membrane	cellular_component	4	1.44	OV-N-S01-1103-W, OV-N-ST01-0198-W, OV-N-N01-1530-W, OV-N-ST01-0069-W
6	GO:0012507	ER to Golgi transport vesicle membrane	cellular_component	2	1.2	OV-N-S01-1103-W, OV-N-ST01-0198-W
6	GO:0030176	integral to endoplasmic reticulum membrane	cellular_component	1	1	OV-N-S01-2185-W
6	GO:0055029	nuclear DNA-directed RNA polymerase complex	cellular_component	1	1.8	OV-N-N01-0956-W
6	GO:0030055	cell-substrate junction	cellular_component	2	0.72	OV-N-N01-1040-W, OV-N-S01-1889-W
6	GO:0005666	DNA-directed RNA polymerase III complex	cellular_component	1	1	OV-N-N01-0956-W
6	GO:0015629	actin cytoskeleton	cellular_component	5	3.12	OV-N-ST01-0103-W, OV-N-ST01-0182-W, AlIOV-CT28, OV-N-S01-1393-W, OV-N-N01-1082-W
6	GO:0030135	coated vesicle	cellular_component	5	1.22	OV-N-S01-1103-W, OV-N-ST01-0198-W, OV-N-N01-1530-W, OV-N-ST01-0069-W, OV-N-S01-1118-W
6	GO:0005792	microsome	cellular_component	5	5	AlIOV-CT93, AlIOV-CT280, OV-N-N01-0800-W, OV-N-S01-0022-W, OV-N-S01-0568-W
6	GO:0005680	anaphase-promoting complex	cellular_component	1	1	OV-N-ST02-0084-LF
6	GO:0015630	microtubule cytoskeleton	cellular_component	16	11.74	OV-N-S01-0543-W, OV-N-S01-1227-W, AlIOV-CT342, OV-N-S01-0558-W, OV-N-S01-1343-W, AlIOV-CT215, OV-N-S01-1769-W, AlIOV-CT28, AlIOV-CT50, AlIOV-CT123, AlIOV-CT266, OV-N-S01-0904-W, OV-N-S01-1143-W, OV-N-S01-1393-W, AlIOV-CT333, AlIOV-CT280

Table B1 (Cont.)

Level	GO ID	Term	Type	#Seqs	Graph Score	Sequences
6	GO:0005721	centric heterochromatin	cellular_component	1	1	AlIOV-CT333
6	GO:0046930	pore complex	cellular_component	2	1.2	OV-N-N01-1763-W, OV-N-S01-1124-W
6	GO:0005701	polytene chromosome chromocenter	cellular_component	1	1	AlIOV-CT333
6	GO:0000323	lytic vacuole	cellular_component	2	0.82	AlIOV-CT240, OV-N-N01-0376-W
6	GO:0000220	vacuolar proton-transporting V-type ATPase, VO domain	cellular_component	1	1	OV-N-N01-1134-W
6	GO:0005777	peroxisome	cellular_component	1	1	OV-N-S01-2642-W
6	GO:0019005	SCF ubiquitin ligase complex	cellular_component	1	1	OV-N-S01-1798-W
6	GO:0030016	myofibril	cellular_component	2	0.82	OV-N-ST01-0103-W, AlIOV-CT384
6	GO:0031674	I band	cellular_component	1	0.6	OV-N-ST01-0103-W
6	GO:0043189	H4/H2A histone acetyltransferase complex	cellular_component	1	0.6	OV-N-S01-0025-W
6	GO:0030134	ER to Golgi transport vesicle	cellular_component	2	0.72	OV-N-S01-1103-W, OV-N-ST01-0198-W
6	GO:0016604	nuclear body	cellular_component	1	0.6	OV-N-S01-1699-W
6	GO:0005639	integral to nuclear inner membrane	cellular_component	1	1	OV-N-N01-1780-W
6	GO:0045120	pronucleus	cellular_component	2	2.2	AlIOV-CT381, AlIOV-CT333
6	GO:0000792	heterochromatin	cellular_component	2	1.42	AlIOV-CT345, AlIOV-CT333
6	GO:0000790	nuclear chromatin	cellular_component	2	0.82	AlIOV-CT345, AlIOV-CT333
6	GO:0005912	adherens junction	cellular_component	3	1.72	OV-N-N01-1040-W, OV-N-S01-1889-W, AlIOV-CT180
6	GO:0030018	Z disc	cellular_component	1	1	OV-N-ST01-0103-W
6	GO:0005911	intercellular junction	cellular_component	2	1.6	OV-N-S01-0962-W, OV-N-N01-1040-W
6	GO:0005876	spindle microtubule	cellular_component	1	1	AlIOV-CT215
6	GO:0005868	cytoplasmic dynein complex	cellular_component	1	1	AlIOV-CT28
6	GO:0030137	COPI-coated vesicle	cellular_component	2	0.72	OV-N-N01-1530-W, OV-N-ST01-0069-W
6	GO:0005791	rough endoplasmic reticulum	cellular_component	1	0.36	AlIOV-CT364
6	GO:0043596	nuclear replication fork	cellular_component	4	2.4	AlIOV-CT329, AlIOV-CT420, OV-N-N01-1623-W, OV-N-S01-1179-W
6	GO:0000803	sex chromosome	cellular_component	1	0.36	AlIOV-CT345
6	GO:0005736	DNA-directed RNA polymerase I complex	cellular_component	1	1	OV-N-N01-0956-W
6	GO:0030017	sarcomere	cellular_component	2	1.36	OV-N-ST01-0103-W, AlIOV-CT384
6	GO:0016298	lipase activity	molecular_function	1	0.22	AlIOV-CT223
6	GO:0004672	protein kinase activity	molecular_function	9	4.73	OV-N-S01-1421-W, OV-N-N01-0378-W, OV-N-S01-0997-W, AlIOV-CT7, AlIOV-CT343, AlIOV-CT409, OV-N-S01-0543-W, OV-N-S01-1923-W, OV-N-S01-2026-W
6	GO:0005506	iron ion binding	molecular_function	11	10.6	AlIOV-CT16, AlIOV-CT41, AlIOV-CT54, AlIOV-CT157, AlIOV-CT191, AlIOV-CT306, AlIOV-CT404, OV-N-N01-0630-W, OV-N-N01-0985-W, OV-N-S01-2062-W, AlIOV-CT406

Table B1 (Cont.)

Level	GO ID	Term	Type	#Seqs	Graph Score	Sequences
6	GO:0004865	type 1 serine/threonine specific protein phosphatase inhibitor activity	molecular_function	1	1	OV-N-S01-1699-W
6	GO:0003756	protein disulfide isomerase activity	molecular_function	1	1	AlIOV-CT368
6	GO:0003994	aconitate hydratase activity	molecular_function	1	1	OV-N-N01-0985-W
6	GO:0004618	phosphoglycerate kinase activity	molecular_function	1	1	OV-N-S01-2139-W
6	GO:0018738	S-formylglutathione hydrolase activity	molecular_function	1	1	OV-N-N01-1042-W
6	GO:0019787	small conjugating protein ligase activity	molecular_function	9	5.8	OV-N-N01-1520-W, AlIOV-CT192, OV-N-S01-0547-W, OV-N-S01-1255-W, OV-N-S01-1591-W, OV-N-S01-1798-W, OV-N-S01-2003-W, OV-N-S01-2459-W, OV-N-ST02-0084-LF
6	GO:0005507	copper ion binding	molecular_function	1	1	AlIOV-CT191
6	GO:0003690	double-stranded DNA binding	molecular_function	2	1.6	OV-N-S01-0999-W, AlIOV-CT106
6	GO:0046592	polyamine oxidase activity	molecular_function	1	1	OV-N-N01-0067-W
6	GO:0004807	triose-phosphate isomerase activity	molecular_function	1	1	AlIOV-CT68
6	GO:0003697	single-stranded DNA binding	molecular_function	2	2	OV-N-S01-0743-W, OV-N-S01-0999-W
6	GO:0008081	phosphoric diester hydrolase activity	molecular_function	2	0.79	OV-N-S01-0744-W, AlIOV-CT223
6	GO:0004614	phosphoglucomutase activity	molecular_function	1	1	OV-N-S01-2126-W
6	GO:0031267	small GTPase binding	molecular_function	1	0.22	OV-N-S01-2267-W
6	GO:0030955	potassium ion binding	molecular_function	1	1	AlIOV-CT194
6	GO:0004812	aminoacyl-tRNA ligase activity	molecular_function	4	3.8	OV-N-N01-0757-W, OV-N-S01-1959-W, AlIOV-CT148, OV-N-S01-0142-W
6	GO:0046870	cadmium ion binding	molecular_function	1	1	AlIOV-CT44
6	GO:0004022	alcohol dehydrogenase activity	molecular_function	1	1	OV-N-N01-0849-W
6	GO:0004748	ribonucleoside-diphosphate reductase activity	molecular_function	2	2	AlIOV-CT54, AlIOV-CT157
6	GO:0004298	threonine endopeptidase activity	molecular_function	2	2	OV-N-S01-0704-W, OV-N-S01-0807-W
6	GO:0004756	selenide, water dikinase activity	molecular_function	1	1	AlIOV-CT435
6	GO:0003887	DNA-directed DNA polymerase activity	molecular_function	1	1	OV-N-S01-1537-W
6	GO:0003857	3-hydroxyacyl-CoA dehydrogenase activity	molecular_function	1	1	AlIOV-CT83
6	GO:0016791	phosphoric monoester hydrolase activity	molecular_function	5	2.04	OV-N-S01-1187-W, AlIOV-CT145, AlIOV-CT440, OV-N-S01-0991-W, AlIOV-CT41

Table B1 (Cont.)

Level	GO ID	Term	Type	#Seqs	Graph Score	Sequences
6	GO:0016509	long-chain-3-hydroxyacyl-CoA dehydrogenase activity	molecular_function	1	1	AlIOV-CT83
6	GO:0004069	aspartate transaminase activity	molecular_function	2	2	OV-N-S01-0515-W, OV-N-S01-1295-W
6	GO:0032356	oxidized DNA binding	molecular_function	1	0.6	OV-N-S01-0999-W
6	GO:0004697	protein kinase C activity	molecular_function	1	1	OV-N-S01-1421-W
6	GO:0003950	NAD+ ADP-ribosyltransferase activity	molecular_function	1	1	OV-N-S01-1952-W
6	GO:0008324	cation transmembrane transporter activity	molecular_function	15	4.78	AlIOV-CT4, AlIOV-CT392, AlIOV-CT121, AlIOV-CT131, AlIOV-CT321, AlIOV-CT327, OV-N-N01-0822-W, OV-N-N01-1134-W, OV-N-S01-0419-W, OV-N-S01-0575-W, AlIOV-CT378, AlIOV-CT13, AlIOV-CT191, OV-N-S01-0967-W, OV-N-N01-1701-W
6	GO:0004491	methylmalonate-semialdehyde dehydrogenase (acylating) activity	molecular_function	1	1	AlIOV-CT173
6	GO:0004332	fructose-bisphosphate aldolase activity	molecular_function	1	1	AlIOV-CT369
6	GO:0008143	poly(A) binding	molecular_function	2	2	OV-N-N01-0680-W, OV-N-N01-1168-W
6	GO:0004615	phosphomannomutase activity	molecular_function	1	1	OV-N-S01-1505-W
6	GO:0003899	DNA-directed RNA polymerase activity	molecular_function	1	1	OV-N-N01-0956-W
6	GO:0008746	NAD(P) transhydrogenase activity	molecular_function	1	1.2	OV-N-N01-1701-W
6	GO:0030145	manganese ion binding	molecular_function	2	2	AlIOV-CT41, OV-N-N01-0343-W
6	GO:0004177	aminopeptidase activity	molecular_function	1	1	OV-N-S01-0580-W
6	GO:0004197	cysteine-type endopeptidase activity	molecular_function	3	2.6	OV-N-S01-1968-W, AlIOV-CT283, OV-N-S01-2530-W
6	GO:0032561	guanyl ribonucleotide binding	molecular_function	26	15.6	AlIOV-CT33, AlIOV-CT50, AlIOV-CT123, AlIOV-CT180, AlIOV-CT204, AlIOV-CT215, AlIOV-CT246, AlIOV-CT258, AlIOV-CT265, AlIOV-CT266, AlIOV-CT280, AlIOV-CT353, AlIOV-CT384, OV-N-N01-0144-W, OV-N-N01-0209-W, OV-N-N01-0977-W, OV-N-N01-1101-W, OV-N-N01-1778-W, OV-N-S01-0591-W, OV-N-S01-0741-W, OV-N-S01-0829-W, OV-N-S01-0904-W, OV-N-S01-1143-W, OV-N-S01-1987-W, OV-N-S01-2267-W, OV-N-ST01-0173-W
6	GO:0032559	adenyl ribonucleotide binding	molecular_function	49	30	AlIOV-CT35, AlIOV-CT121, AlIOV-CT126, AlIOV-CT130, AlIOV-CT142, AlIOV-CT167, AlIOV-CT194, AlIOV-CT246, AlIOV-CT250, AlIOV-CT262, AlIOV-CT280, AlIOV-CT287, AlIOV-CT292, AlIOV-CT307, AlIOV-CT329, AlIOV-CT343, AlIOV-CT351, AlIOV-CT401, AlIOV-CT409, AlIOV-CT420, AlIOV-CT425, AlIOV-CT427, AlIOV-CT435, OV-N-N01-0378-W, OV-N-N01-0660-W, OV-N-N01-0822-W, OV-N-N01-1101-W, OV-N-N01-1134-W, OV-N-N01-1623-W, OV-N-S01-0067-W, OV-N-S01-0142-W, OV-N-S01-0419-W, OV-N-S01-0543-W, OV-N-S01-0553-W, OV-N-S01-0575-W, OV-N-S01-0997-W, OV-N-S01-0999-W, OV-N-S01-1179-W, OV-N-S01-1291-W, OV-N-S01-1421-W, OV-N-S01-1495-W, OV-N-S01-1567-W, OV-N-S01-1923-W, OV-N-S01-1959-W, OV-N-S01-2026-W, OV-N-ST01-0068-W, OV-N-ST01-0071-W, OV-N-ST01-0103-W, OV-N-ST02-0150-W
6	GO:0019783	small conjugating protein-specific protease activity	molecular_function	1	0.36	OV-N-S01-0352-W
6	GO:0015405	P-P-bond-hydrolysis-driven transmembrane transporter activity	molecular_function	10	1.77	AlIOV-CT121, AlIOV-CT131, AlIOV-CT321, AlIOV-CT327, OV-N-N01-0822-W, OV-N-N01-1134-W, OV-N-S01-0419-W, OV-N-S01-0575-W, AlIOV-CT378, AlIOV-CT364

Table B1 (Cont.)

Level	GO ID	Term	Type	#Seqs	Graph Score	Sequences
6	GO:0004576	oligosaccharyl transferase activity	molecular_function	2	1.2	OV-N-S01-0568-W, OV-N-S01-1082-W
6	GO:0019205	nucleobase, nucleoside, nucleotide kinase activity	molecular_function	1	0.6	AlIOV-CT280
6	GO:0004054	arginine kinase activity	molecular_function	2	2	AlIOV-CT134, AlIOV-CT149
6	GO:0004448	isocitrate dehydrogenase activity	molecular_function	2	1.2	AlIOV-CT81, AlIOV-CT419
6	GO:0051903	S-(hydroxymethyl)glutathione dehydrogenase activity	molecular_function	1	1	OV-N-N01-0849-W
6	GO:0030350	iron-responsive element binding	molecular_function	1	1	OV-N-N01-0985-W
6	GO:0004634	phosphopyruvate hydratase activity	molecular_function	1	1	AlIOV-CT96
6	GO:0004519	endonuclease activity	molecular_function	1	0.22	OV-N-S01-1495-W
6	GO:0008757	S-adenosylmethionine-dependent methyltransferase activity	molecular_function	1	0.6	OV-N-N01-0537-W
6	GO:0008415	acyltransferase activity	molecular_function	6	2.28	AlIOV-CT315, OV-N-S01-0318-W, OV-N-S01-0335-W, AlIOV-CT140, AlIOV-CT331, AlIOV-CT264
6	GO:0004527	exonuclease activity	molecular_function	2	0.82	OV-N-N01-0343-W, OV-N-S01-0888-W
6	GO:0019202	amino acid kinase activity	molecular_function	2	1.2	AlIOV-CT134, AlIOV-CT149
6	GO:0004108	citrate (Si)-synthase activity	molecular_function	1	1	OV-N-ST01-0196-W
6	GO:0004361	glutaryl-CoA dehydrogenase activity	molecular_function	1	1	OV-N-N01-1178-W
6	GO:0008270	zinc ion binding	molecular_function	16	16	AlIOV-CT4, AlIOV-CT329, AlIOV-CT332, AlIOV-CT339, AlIOV-CT420, OV-N-N01-0630-W, OV-N-N01-0849-W, OV-N-N01-1623-W, OV-N-N01-1639-W, OV-N-S01-1103-W, OV-N-S01-1179-W, OV-N-S01-1255-W, OV-N-S01-1421-W, OV-N-S01-1952-W, OV-N-ST01-0198-W, OV-N-ST02-0084-LF
6	GO:0004300	enoyl-CoA hydratase activity	molecular_function	1	1	AlIOV-CT83
6	GO:0004221	ubiquitin thiolesterase activity	molecular_function	1	1	OV-N-S01-0352-W
6	GO:0004322	ferroxidase activity	molecular_function	1	1	AlIOV-CT406
6	GO:0004550	nucleoside diphosphate kinase activity	molecular_function	1	1	AlIOV-CT280
6	GO:0004540	ribonuclease activity	molecular_function	1	0.22	OV-N-S01-1495-W
6	GO:0004252	serine-type endopeptidase activity	molecular_function	1	0.6	OV-N-S01-2286-W
6	GO:0019901	protein kinase binding	molecular_function	1	0.6	OV-N-N01-1530-W
6	GO:0004013	adenosylhomocysteinase activity	molecular_function	1	1	AlIOV-CT183
6	GO:0042625	ATPase activity, coupled to transmembrane movement of ions	molecular_function	9	3.24	AlIOV-CT121, AlIOV-CT131, AlIOV-CT321, AlIOV-CT327, OV-N-N01-0822-W, OV-N-N01-1134-W, OV-N-S01-0419-W, OV-N-S01-0575-W, AlIOV-CT378
6	GO:0032036	myosin heavy chain binding	molecular_function	2	2	OV-N-S01-1227-W, OV-N-ST01-0182-W
6	GO:0005537	mannose binding	molecular_function	1	1	OV-N-N01-0800-W

Table B1 (Cont.)

Level	GO ID	Term	Type	#Seqs	Graph Score	Sequences
6	GO:0043015	gamma-tubulin binding	molecular_function	1	1	AlIOV-CT280
6	GO:0005546	phosphatidylinositol-4,5-bisphosphate binding	molecular_function	1	1	AlIOV-CT279
6	GO:0008121	ubiquinol-cytochrome-c reductase activity	molecular_function	1	1	AlIOV-CT4
6	GO:0032027	myosin light chain binding	molecular_function	1	1	OV-N-ST01-0103-W
6	GO:0000217	DNA secondary structure binding	molecular_function	1	0.6	OV-N-S01-0999-W
6	GO:0000030	mannosyltransferase activity	molecular_function	1	1.2	OV-N-N01-0800-W
6	GO:0042626	ATPase activity, coupled to transmembrane movement of substances	molecular_function	9	1.94	AlIOV-CT121, AlIOV-CT131, AlIOV-CT321, AlIOV-CT327, OV-N-N01-0822-W, OV-N-N01-1134-W, OV-N-S01-0419-W, OV-N-S01-0575-W, AlIOV-CT378
6	GO:0016462	pyrophosphatase activity	molecular_function	49	11.3	AlIOV-CT50, AlIOV-CT114, AlIOV-CT123, AlIOV-CT204, AlIOV-CT215, AlIOV-CT258, AlIOV-CT265, AlIOV-CT266, AlIOV-CT353, AlIOV-CT384, OV-N-N01-0977-W, OV-N-S01-0591-W, OV-N-S01-0741-W, OV-N-S01-0829-W, OV-N-S01-0904-W, OV-N-S01-1143-W, OV-N-ST01-0173-W, AlIOV-CT121, AlIOV-CT131, AlIOV-CT321, AlIOV-CT327, OV-N-N01-0822-W, OV-N-N01-1134-W, OV-N-S01-0419-W, OV-N-S01-0575-W, OV-N-S01-0067-W, OV-N-ST02-0094-LF, OV-N-S01-0025-W, OV-N-S01-2185-W, AlIOV-CT378, AlIOV-CT329, AlIOV-CT420, OV-N-N01-1623-W, OV-N-S01-1179-W, AlIOV-CT35, AlIOV-CT287, AlIOV-CT307, AlIOV-CT425, OV-N-S01-1567-W, OV-N-S01-2348-W, AlIOV-CT250, AlIOV-CT401, AlIOV-CT427, OV-N-S01-0999-W, AlIOV-CT28, OV-N-N01-0660-W, OV-N-ST01-0103-W, OV-N-ST01-0182-W, OV-N-S01-1291-W
6	GO:0018478	malonate-semialdehyde dehydrogenase (acetylating) activity	molecular_function	1	1	AlIOV-CT173
6	GO:0032405	MutLalpha complex binding	molecular_function	1	1	OV-N-S01-0999-W
6	GO:0008017	microtubule binding	molecular_function	1	1	OV-N-S01-1769-W
6	GO:0004536	deoxyribonuclease activity	molecular_function	2	1.13	AlIOV-CT280, OV-N-S01-0888-W
6	GO:0050136	NADH dehydrogenase (quinone) activity	molecular_function	4	2.4	AlIOV-CT274, AlIOV-CT337, AlIOV-CT411, OV-N-S01-2062-W
6	GO:0008453	alanine-glyoxylate transaminase activity	molecular_function	1	1	OV-N-S01-2642-W
6	GO:0004190	aspartic-type endopeptidase activity	molecular_function	2	1.6	AlIOV-CT240, AlIOV-CT290
6	GO:0004729	protoporphyrinogen oxidase activity	molecular_function	1	1	OV-N-S01-0468-W
6	GO:0050679	positive regulation of epithelial cell proliferation	biological_process	1	1	AlIOV-CT280
6	GO:0006334	nucleosome assembly	biological_process	3	3	AlIOV-CT110, AlIOV-CT253, AlIOV-CT345
6	GO:0046939	nucleotide phosphorylation	biological_process	1	0.6	AlIOV-CT280
6	GO:0042775	organelle ATP synthesis coupled electron transport	biological_process	7	4.2	AlIOV-CT13, AlIOV-CT4, AlIOV-CT274, AlIOV-CT411, OV-N-N01-0376-W, OV-N-S01-1263-W, OV-N-S01-2062-W
6	GO:0008585	female gonad development	biological_process	1	1	AlIOV-CT95

***The complete data are available on request.**

APPENDIX C

Table C1 Raw data and relative expression levels of *B cell RAG associated protein* in different ovarian developmental stages of *P. monodon* based on semiquantitative RT-PCR analysis

Sample Groups		Densities of bands		Ratio of gene / <i>EF-1a</i>	Average	STDEV
		<i>B cell RAG</i> associated protein	<i>EF-1a</i>			
BD-Stage I	BUFOV3	261122.758	311553.119	0.838132	0.9571	0.071
	BUFOV6	332014.166	340808.668	0.974195		
	BUFOV4	299375.590	331477.676	0.903155		
	AGYLOV3	304569.510	334521.655	0.910463		
	BUFOV7	323451.901	336712.800	0.960617		
	BUFOV5	326520.140	328877.145	0.992833		
	AGYLOV1	333220.036	326521.596	1.020515		
	AGYLOV4	333547.080	315572.836	1.056958		
BD-Stage II	AGYLOV2	251574.120	323532.399	0.777586	0.8903	0.083
	BFNOV32	288733.032	303073.486	0.952683		
	ASPOV10	279896.973	336401.997	0.832031		
	ASPOV6	313314.165	342993.555	0.913470		
	BFNOV32	337691.525	346141.489	0.975588		
BD-Stage III	BFNOV38	319425.486	347851.052	0.918282	0.9379	0.031
	BFNOV33	322108.819	349338.124	0.922055		
	BFNOV35	318744.354	347891.902	0.916217		
	BFNOV31	307765.318	345878.797	0.889807		
	BFNOV4/1	330013.222	348809.907	0.946112		
	BFNOV18	333138.589	336327.971	0.990517		
	BFNOV3	302875.380	310679.861	0.974879		
	BFNOV4	309886.387	332732.930	0.931337		
	BFNOV23	326608.191	342996.153	0.952221		
BD-Stage IV	BFNOV24	306050.957	344142.965	0.889313	0.9366	0.056
	BFNOV5	305534.186	351929.978	0.868168		
	BFNOV1	347932.510	349088.892	0.996687		
	BFNOV2	321535.863	351668.230	0.914316		
	BFNOV14	320678.421	345509.907	0.928131		
	BFNOV10	328653.474	334919.884	0.981290		
	BFNOV12	327107.143	328078.621	0.997039		
	BFNOV21	334144.774	326722.245	1.022718		
	BFNOV15	248072.967	292843.793	0.847117		
	BFNOV20	274511.438	302705.776	0.906859		
	BFNOV17	284254.625	308287.358	0.922044		
	BFNOV13	321924.962	333307.428	0.965850		

Table C2 Raw data and relative expression levels of *APEX nuclease* in different ovarian developmental stages of *P. monodon* based on semi-quantitative RT-PCR analysis

Sample Groups		Densities of bands		Ratio of gene / <i>EF-1α</i>	Average	STDEV
		<i>APEX nuclease</i>	<i>EF-1α</i>			
BD-Stage I	BUFOV3	208487.587	250037.906	0.833824	1.0555	0.101
	BUFOV6	273776.569	250678.671	1.092141		
	BUFOV4	294795.392	261587.380	1.126948		
	AGYLOV3	287560.419	272096.759	1.056831		
	BUFOV7	275240.420	262688.816	1.047781		
	BUFOV5	275607.906	265109.486	1.039600		
	AGYLOV1	293511.007	248571.112	1.180793		
	AGYLOV4	267524.698	250934.652	1.066113		
BD-Stage II	AGYLOV2	145628.017	262150.155	0.555514	0.8904	0.253
	BFNOV32	279170.473	238731.303	1.169392		
	ASPOV10	246653.896	275205.658	0.896253		
	ASPOV6	204257.106	278227.668	0.734137		
	BFNOV32	298581.488	272262.692	1.096667		
BD-Stage III	BFNOV38	289547.692	281321.831	1.029240	0.9585	0.082
	BFNOV33	267570.580	273953.601	0.976700		
	BFNOV35	269371.971	297967.573	0.904031		
	BFNOV31	262967.265	283269.965	0.928327		
	BFNOV4/1	241131.758	271806.902	0.887144		
	BFNOV18	240080.635	277742.788	0.864399		
	BFNOV3	238020.955	266193.026	0.894167		
	BFNOV4	250285.233	238290.441	1.050337		
	BFNOV23	279208.655	255657.715	1.092119		
	BD-Stage IV	BFNOV24	248944.912	261248.528		
BFNOV5		183080.315	258475.705	0.708308		
BFNOV1		268996.249	261316.567	1.029388		
BFNOV2		248234.538	252645.657	0.982540		
BFNOV14		267813.575	245136.088	1.092510		
BFNOV10		236635.822	255726.806	0.925346		
BFNOV12		229885.982	242426.709	0.948270		
BFNOV21		235628.656	227777.139	1.034470		
BFNOV15		186333.791	200535.224	0.929182		
BFNOV20		212355.823	214482.211	0.990086		
BFNOV17		229495.073	217577.426	1.054774		
BFNOV13		215827.159	231063.264	0.934061		

Table C3 Raw data and relative expression levels of *U5 snRNP-specific protein* in different ovarian developmental stages of *P. monodon* based on semiquantitative RT-PCR analysis

Sample Groups		Densities of bands		Ratio of gene / <i>EF-1α</i>	Average	STDEV
		<i>U5 snRNP-specific protein</i>	<i>EF-1α</i>			
BD-Stage I	BUFOV3	234006.975	250037.906	0.916156	1.0033	0.078
	BUFOV6	237065.903	250678.671	0.928132		
	BUFOV4	268246.798	261587.380	1.050208		
	AGYLOV3	286866.263	272096.759	1.123105		
	BUFOV7	265000.101	262688.816	1.037497		
	BUFOV5	274897.334	265109.486	1.076245		
	AGYLOV1	243525.636	248571.112	0.953423		
	AGYLOV4	240518.671	250934.652	0.941650		
BD-Stage II	AGYLOV2	185970.187	262150.155	0.728088	0.9977	0.192
	BFNOV32	219496.349	238731.303	0.859346		
	ASPOV10	289231.531	275205.658	1.132365		
	ASPOV6	289043.227	278227.668	1.131628		
	BFNOV32	290446.531	272262.692	1.137122		
BD-Stage III	BFNOV38	294003.495	281321.831	1.151048	1.0872	0.057
	BFNOV33	296532.335	297967.573	1.160948		
	BFNOV35	275727.512	283269.965	1.079496		
	BFNOV31	263724.744	271806.902	1.032504		
	BFNOV4/1	267561.083	277742.788	1.047523		
	BFNOV18	253492.511	266193.026	0.992444		
	BFNOV3	288658.227	238290.441	1.130120		
	BFNOV4	275351.441	255657.715	1.078023		
	BFNOV23	284252.334	261248.528	1.112871		
	BD-Stage IV	BFNOV24	285049.477	258475.705		
BFNOV5		269070.726	261316.567	1.053434		
BFNOV1		268369.833	252645.657	1.050690		
BFNOV2		267504.208	245136.088	1.047301		
BFNOV14		263904.119	255726.806	1.033206		
BFNOV10		236193.136	242426.709	0.924715		
BFNOV12		238736.886	227777.139	0.934674		
BFNOV21		212067.777	200535.224	0.830263		
BFNOV15		180313.847	214482.211	0.705943		
BFNOV20		190049.562	217577.426	0.744059		
BFNOV17		220903.224	231063.264	0.864854		
BFNOV13		234006.975	250037.906	0.916156		
			255422.540			
			(average)*			

* Ratio of gene / *EF-1 α* were examined using average of bands density of *EF-1 α*

Table C4 Raw data and relative expression levels of *hypothetical protein W02B8.3* in different ovarian developmental stages of *P. monodon* based on semiquantitative RT-PCR analysis

Sample Groups		Densities of bands		Ratio of gene / <i>EF-1α</i>	Average	STDEV
		<i>hypothetical protein W02B8.3</i>	<i>EF-1α</i>			
BD-Stage I	BUFOV3	239804.810	311553.119	0.769708	0.9183	0.091
	BUFOV6	325176.376	340808.668	0.954132		
	BUFOV4	278344.440	331477.676	0.839708		
	AGYLOV3	328129.636	334521.655	0.980892		
	BUFOV7	286595.648	336712.800	0.851158		
	BUFOV5	307698.136	328877.145	0.935602		
	AGYLOV1	314816.890	326521.596	0.964153		
	AGYLOV4	331670.515	315572.836	1.051011		
BD-Stage II	AGYLOV2	209717.121	323532.399	0.648211	0.9059	0.149
	BFNOV32	294075.720	303073.486	0.970312		
	ASPOV10	318417.183	336401.997	0.946538		
	ASPOV6	319437.622	342993.555	0.931323		
	BFNOV32	357644.944	346141.489	1.033233		
BD-Stage III	BFNOV38	313591.542	347851.052	0.901511	0.8551	0.054
	BFNOV33	298957.112	349338.124	0.855782		
	BFNOV35	301550.445	347891.902	0.866794		
	BFNOV31	276721.729	345878.797	0.800054		
	BFNOV4/1	267980.485	348809.907	0.768271		
	BFNOV18	309592.129	336327.971	0.920507		
	BFNOV3	249265.175	310679.861	0.802322		
	BFNOV4	303067.221	332732.930	0.910842		
	BFNOV23	298356.599	342996.153	0.869854		
BD-Stage IV	BFNOV24	283725.758	344142.965	0.824442	0.8878	0.070
	BFNOV5	286175.135	351929.978	0.813159		
	BFNOV1	337447.218	349088.892	0.966651		
	BFNOV2	305975.499	351668.230	0.870069		
	BFNOV14	290615.208	345509.907	0.841120		
	BFNOV10	306481.873	334919.884	0.915090		
	BFNOV12	303646.269	328078.621	0.925529		
	BFNOV21	255429.424	326722.245	0.781794		
	BFNOV15	256377.116	292843.793	0.875474		
	BFNOV20	298196.965	302705.776	0.985105		
	BFNOV17	307066.488	308287.358	0.996040		
	BFNOV13	286286.857	333307.428	0.858927		

Table C5 Raw data and relative expression levels of *DNA replication licensing factor MCM5* in different ovarian developmental stages of *P. monodon* based on semiquantitative RT-PCR analysis

Sample Groups		Densities of bands		Ratio of gene / <i>EF-1α</i>	Average	STDEV
		<i>DNA replication licensing factor MCM5</i>	<i>EF-1α</i>			
BD-Stage I	BUFOV3	164502.094	250037.906	0.657909	0.6858	0.131
	BUFOV6	190180.113	250678.671	0.758661		
	BUFOV4	154557.608	261587.380	0.590845		
	AGYLOV3	117493.001	272096.759	0.431806		
	BUFOV7	170926.461	262688.816	0.650680		
	BUFOV5	210727.282	265109.486	0.794869		
	AGYLOV1	193845.091	248571.112	0.779838		
	AGYLOV4	206118.936	250934.652	0.821405		
BD-Stage II	AGYLOV2	105171.614	262150.155	0.401188	0.7013	0.173
	BFNOV32	168935.030	238731.303	0.707637		
	ASPOV10	224290.919	275205.658	0.814994		
	ASPOV6	222359.771	278227.668	0.799201		
	BFNOV32	213349.637	272262.692	0.783617		
BD-Stage III	BFNOV38	229378.177	281321.831	0.815359	0.8072	0.042
	BFNOV33	225590.249	273953.601	0.823462		
	BFNOV35	215596.135	297967.573	0.723556		
	BFNOV31	224042.633	283269.965	0.790916		
	BFNOV4/1	221688.460	271806.902	0.815610		
	BFNOV18	224525.643	277742.788	0.808394		
	BFNOV3	205917.595	266193.026	0.773565		
	BFNOV4	207421.246	238290.441	0.870456		
	BFNOV23	215586.001	255657.715	0.843260		
	BFNOV24	222914.913	261248.528	0.853268		
BD-Stage IV	BFNOV5	216003.661	258475.705	0.835683	0.8878	0.070
	BFNOV1	217733.169	261316.567	0.833216		
	BFNOV2	216880.636	252645.657	0.858438		
	BFNOV14	123865.877	245136.088	0.505294		
	BFNOV10	218831.753	255726.806	0.855725		
	BFNOV12	213786.746	242426.709	0.881861		
	BFNOV21	204757.163	227777.139	0.898936		
	BFNOV15	167591.066	200535.224	0.835719		
	BFNOV20	169359.844	214482.211	0.789622		
	BFNOV17	156112.302	217577.426	0.717502		
	BFNOV13	190716.998	231063.264	0.825389		

APPENDIX D

Table D1 Raw data and relative expression levels of *Keratinocytes associated protein 2* in different ovarian developmental stages of *P. monodon* based on semi quantitative RT-PCR analysis

Sample Groups		Densities of bands		Ratio of gene / <i>EF-1α</i>	Average	STDEV
		<i>Keratinocytes associated protein 2</i>	<i>EF-1α</i>			
Juvenile	JNOV6	408617.7352	409230.5505	0.998503	0.4696	0.086
	JNOV7	408894.4018	409362.7634	0.998856		
	JNOV8	408899.9573	409328.0295	0.998954		
BD-Stage I	AGYLOV4	401460.3285	409400.0183	0.980607	0.9988	0.000
	AGYLOV3	401140.3285	408268.6457	0.982540		
	AGYLOV1	406425.1428	409117.9455	0.993418		
BD-Stage II	BFNOV38	315227.7449	403926.6287	0.780408	0.9855	0.007
	BFNOV35	370014.7762	405633.9117	0.912189		
	BFNOV31	289907.3772	408242.0351	0.710136		
BD-Stage III	BFNOV4	280751.8226	408687.4132	0.686960	0.8009	0.103
	BFNOV23	200870.3494	402193.5754	0.499437		
	BFNOV24	179038.1295	404507.3010	0.442608		
BD-Stage IV	BFNOV10	171841.8339	408970.0463	0.420182	0.5430	0.128
	BFNOV20	170000.0000	405428.5896	0.419309		
	BFNOV13	227963.6799	400393.5753	0.569349		

Table D2 Raw data and relative expression levels of *Ser/Thr kinase chk1* in different ovarian developmental stages of *P. monodon* based on semi quantitative RT-PCR analysis

Sample Groups		Densities of bands		Ratio of gene / <i>EF-1α</i>	Average	STDEV
		<i>Ser/Thr kinase chk1</i>	<i>EF-1α</i>			
Juvenile	JNOV6	409300.0488	409230.5505	1.000170	0.2701	0.034
	JNOV7	403015.6509	409362.7634	0.984495		
	JNOV8	409258.5594	409328.0295	0.999830		
BD-Stage I	AGYLOV4	407416.0060	409400.0183	0.995154	0.9948	0.009
	AGYLOV3	401927.7075	408268.6457	0.984469		
	AGYLOV1	405350.4029	409117.9455	0.990791		
BD-Stage II	BFNOV38	385037.6346	403926.6287	0.953237	0.9901	0.005
	BFNOV35	404435.5092	405633.9117	0.997046		
	BFNOV31	364771.6747	408242.0351	0.893518		
BD-Stage III	BFNOV4	345470.3115	408687.4132	0.845317	0.9479	0.052
	BFNOV23	362549.7729	402193.5754	0.901431		
	BFNOV24	231619.4871	404507.3010	0.572597		
BD-Stage IV	BFNOV10	125722.7177	408970.0463	0.307413	0.7731	0.176
	BFNOV20	97370.2819	405428.5896	0.240166		
	BFNOV13	105156.7693	400393.5753	0.262634		

Table D3 Raw data and relative expression levels of *DNA replication licensing factor mcm2* in different ovarian developmental stages of *P. monodon* based on semiquantitative RT-PCR analysis

Sample Groups		Densities of bands		Ratio of gene / <i>EF-1α</i>	Average	STDEV
		<i>DNA replication licensing factor mcm2</i>	<i>EF-1α</i>			
Juvenile	JNOV6	409300.0488	409230.5505	1.000170	0.7263	0.021
	JNOV7	409246.4685	409362.7634	0.999716		
	JNOV8	409300.0488	409328.0295	0.999932		
BD-Stage I	AGYLOV4	406753.1349	409400.0183	0.993535	0.9999	0.000
	AGYLOV3	406609.1843	408268.6457	0.995935		
	AGYLOV1	408953.6290	409117.9455	0.999598		
BD-Stage II	BFNOV38	369761.5256	403926.6287	0.915418	0.9964	0.003
	BFNOV35	389079.3056	405633.9117	0.959188		
	BFNOV31	330778.5580	408242.0351	0.810251		
BD-Stage III	BFNOV4	315589.9142	408687.4132	0.772204	0.8950	0.077
	BFNOV23	257724.2283	402193.5754	0.640796		
	BFNOV24	179607.4288	404507.3010	0.444015		
BD-Stage IV	BFNOV10	305322.5055	408970.0463	0.746564	0.6190	0.165
	BFNOV20	295176.0846	405428.5896	0.728059		
	BFNOV13	281951.8855	400393.5753	0.704187		

Table D4 Raw data and relative expression levels of *selenoprotein M precursor* in different ovarian developmental stages of *P. monodon* based on semiquantitative RT-PCR analysis

Sample Groups		Densities of bands		Ratio of gene / <i>EF-1α</i>	Average	STDEV
		<i>selenoprotein M precursor</i>	<i>EF-1α</i>			
Juvenile	JNOV6	326978.9403	409230.5505	0.799009	0.2705	0.026
	JNOV7	335070.7343	409362.7634	0.818518		
	JNOV8	333126.6319	409328.0295	0.813838		
BD-Stage I	AGYLOV4	211707.6702	409400.0183	0.517117	0.8105	0.010
	AGYLOV3	229973.3093	408268.6457	0.563289		
	AGYLOV1	276697.4070	409117.9455	0.676327		
BD-Stage II	BFNOV38	195210.7489	403926.6287	0.483283	0.5856	0.082
	BFNOV35	232977.9244	405633.9117	0.574355		
	BFNOV31	170596.9053	408242.0351	0.417882		
BD-Stage III	BFNOV4	155465.6248	408687.4132	0.380402	0.4918	0.079
	BFNOV23	134671.7808	402193.5754	0.334843		
	BFNOV24	126272.2945	404507.3010	0.312163		
BD-Stage IV	BFNOV10	108778.4502	408970.0463	0.265981	0.3425	0.035
	BFNOV20	99999.0000	405428.5896	0.246650		
	BFNOV13	119697.9362	400393.5753	0.298951		

Table D5 Raw data and relative expression levels of *egalitarian* in different ovarian developmental stages of *P. monodon* based on semiquantitative RT-PCR analysis

Sample Groups		Densities of bands		Ratio of gene / <i>EF-1α</i>	Average	STDEV
		<i>egalitarian</i>	<i>EF-1α</i>			
Juvenile	JNOV6	343490.7636	409230.5505	0.839358	0.3553	0.090
	JNOV7	318974.0976	409362.7634	0.779197		
	JNOV8	375756.8340	409328.0295	0.917985		
BD-Stage I	AGYLOV4	306269.6337	409400.0183	0.748094	0.8455	0.070
	AGYLOV3	334255.3472	408268.6457	0.818714		
	AGYLOV1	372425.2865	409117.9455	0.910313		
BD-Stage II	BFNOV38	251941.9568	403926.6287	0.623732	0.8257	0.081
	BFNOV35	331137.7878	405633.9117	0.816346		
	BFNOV31	274822.9085	408242.0351	0.673186		
BD-Stage III	BFNOV4	240355.0524	408687.4132	0.588115	0.7044	0.100
	BFNOV23	203754.1606	402193.5754	0.506607		
	BFNOV24	188419.0420	404507.3010	0.465799		
BD-Stage IV	BFNOV10	125593.4486	408970.0463	0.307097	0.5202	0.062
	BFNOV20	121666.3654	405428.5896	0.300093		
	BFNOV13	183632.4350	400393.5753	0.458630		

APPENDIX E

Table E1 Relative expression levels of *p23* in different ovarian developmental stages of *P. monodon* based on Quantitative real-time PCR analysis

Sample Groups		Mean conc.		Ratio (target / <i>EF-1α</i>)	Average	STDEV
		<i>p23</i>	<i>EF-1α</i>			
Juvenile	JNOV5	1.39E+06	6.80E+07	0.1185	0.1810	0.04027
	JNOV6	4.99E+06	1.38E+08	0.2180		
	JNOV7	3.77E+06	1.12E+08	0.2000		
	JNOV8	1.81E+06	4.74E+07	0.2230		
	JNOV9	1.86E+06	6.41E+07	0.1695		
	JNOV10	3.06E+06	1.15E+08	0.1570		
N:BD-Stage I	BUFOV3	8.10E+06	1.14E+08	0.4315	0.4046	0.086948
	BUFOV6	-	-	-		
	BUFOV4	8.80E+06	1.08E+08	0.4990		
	AGYLOV3	4.99E+06	9.19E+07	0.3265		
	BUFOV7	1.39E+06	2.18E+07	0.3715		
	BUFOV5	-	-	-		
	AGYLOV1	8.00E+06	9.95E+07	0.4925		
	AGYLOV4	8.90E+06	1.42E+08	0.3835		
	AGYLOV2	3.96E+06	9.29E+07	0.2545		
	BFNOV32	4.70E+06	5.91E+07	0.4780		
N:BD-Stage II	ASPOV10	5.95E+06	8.20E+07	0.4405	0.5079	0.052581
	ASPOV6	8.10E+06	9.13E+07	0.5400		
	BFNOV38	3.44E+06	4.15E+07	0.4945		
	BFNOV33	2.40E+06	3.25E+07	0.4350		
	BFNOV35	4.25E+06	4.51E+07	0.5650		
	BFNOV31	4.77E+06	5.21E+07	0.5500		
	BFNOV4/1	2.69E+06	3.01E+07	0.5300		
N:BD-Stage III	BFNOV18	7.35E+05	9.32E+06	0.4520	0.5109	0.058721
	BFNOV3	2.31E+06	2.82E+07	0.4830		
	BFNOV4	2.40E+06	2.82E+07	0.5000		
	BFNOV23	3.60E+06	3.91E+07	0.5500		
	BFNOV24	2.31E+06	2.31E+07	0.5900		
	BFNOV5	2.50E+06	2.63E+07	0.5650		
	BFNOV1	2.16E+06	2.92E+07	0.4360		
N:BD-Stage IV	BFNOV2	1.13E+06	1.29E+07	0.5050	0.5144	0.07716
	BFNOV14	1.61E+06	1.74E+07	0.5450		
	BFNOV10	1.53E+06	1.79E+07	0.4965		
	BFNOV12	1.33E+06	1.55E+07	0.5000		
	BFNOV21	1.32E+06	1.85E+07	0.4140		
	BFNOV15	1.13E+06	1.09E+07	0.6050		
	BFNOV20	1.07E+06	9.43E+06	0.6550		

	BFNOV16	-	-	-		
	BFNOV17	6.15E+05	8.13E+06	0.4335		
	BFNOV13	1.03E+06	1.25E+07	0.4760		
N:BD Post-spawning	BFNOV30	3.00E+06	3.88E+07	0.4600	0.5027	0.05859
	BFNOV36	3.48E+06	5.00E+07	0.4160		
	BFNOV34	4.15E+06	4.63E+07	0.5400		
	BFNOV37	4.12E+06	5.05E+07	0.4900		
	BFNOV39	3.68E+06	3.83E+07	0.5750		
	BFNOV40	3.71E+06	3.88E+07	0.5350		
EA:BD-Stage I	BFEOV18	2.07E+06	3.55E+07	0.3565	0.4039	0.07766
	YLBOV01	8.60E+06	1.11E+08	0.4900		
	YLBOV06	2.22E+06	3.00E+07	0.4530		
	BFEOV15	2.43E+06	5.07E+07	0.2930		
	YLBOV05	5.15E+06	6.91E+07	0.4680		
	YLBOV08	4.39E+06	7.52E+07	0.3630		
EA:BD-Stage II	BFEOV19	1.22E+06	1.80E+07	0.4070	0.4653	0.06634
	BFEOV17	-	-	-		
	YLBOV07	1.86E+06	2.21E+07	0.5150		
	BFEOV16	1.86E+06	2.14E+07	0.5300		
	YLBOV04	2.02E+06	3.01E+07	0.4090		
EA:BD-Stage III	BFEOV21	2.02E+06	2.72E+07	0.4525	0.5216	0.08091
	YLBOV02	1.86E+06	2.82E+07	0.4010		
	YLBOV03	1.88E+06	2.21E+07	0.5200		
	BFEOV08	5.00E+06	5.00E+07	0.6300		
	BFEOV05	3.99E+06	4.10E+07	0.6050		
	BFEOV02	2.47E+06	2.76E+07	0.5500		
	BFEOV11	1.69E+06	2.38E+07	0.4305		
	BFEOV03	3.05E+06	3.04E+07	0.6200		
	BFEOV20	1.20E+06	1.36E+07	0.5300		
	BFEOV04	1.15E+06	1.45E+07	0.4765		
EA:BD-Stage IV	BFEOV01	1.15E+06	1.62E+07	0.4280	0.5318	0.08588
	BFEOV07	3.32E+06	3.95E+07	0.5200		
	BFEOV06	1.42E+06	1.98E+07	0.4330		
	BFEOV24	1.41E+06	1.70E+07	0.5050		
	BFEOV10	2.39E+06	3.03E+07	0.4850		
	BFEOV12	2.14E+06	2.13E+07	0.6150		
	BFEOV13	2.75E+06	2.61E+07	0.6500		
	BFEOV22	7.75E+05	1.04E+07	0.4440		
	BFEOV23	6.40E+05	7.41E+06	0.5100		
	BFEOV09	7.10E+05	6.43E+06	0.6600		
	BFEOV14	4.87E+05	5.37E+06	0.6000		

Table E2 Relative expression levels of *PGMRC1* in different ovarian developmental stages of *P. monodon* based on Quantitative real-time PCR analysis

Sample Groups		Mean conc.		Ratio (target / <i>EF-1α</i>)	Average	STDEV
		<i>PGMRC1</i>	<i>EF-1α</i>			
Juvenile	JNOV5	9.96E+04	9.76E+06	0.003460	0.003124	0.00071
	JNOV6	1.79E+05	1.84E+07	0.003310		
	JNOV7	1.43E+05	1.21E+07	0.004040		
	JNOV8	-	-	-		
	JNOV9	6.37E+04	8.88E+06	0.002420		
	JNOV10	1.33E+05	1.89E+07	0.002390		
N:BD-Stage I	BUFOV3	2.80E+05	1.86E+07	0.005150	0.006898	0.00171
	BUFOV6	7.75E+04	3.10E+06	0.008570		
	BUFOV4	2.82E+05	1.57E+07	0.006160		
	AGYLOV3	2.91E+05	1.47E+07	0.006800		
	BUFOV7	7.58E+04	3.53E+06	0.007350		
	BUFOV5	7.88E+04	3.07E+06	0.008790		
	AGYLOV1	2.79E+05	1.62E+07	0.005910		
	AGYLOV4	-	-	-		
	AGYLOV2	2.62E+05	9.89E+06	0.009140		
	BFNOV32	1.94E+05	1.57E+07	0.004210		
N:BD-Stage II	BFNOV38	-	-	-	0.007076	0.00268
	BFNOV33	1.02E+05	5.29E+06	0.006560		
	ASPOV10	1.94E+05	1.21E+07	0.005520		
	BFNOV35	1.21E+05	7.69E+06	0.005390		
	ASPOV6	2.31E+05	1.72E+07	0.004580		
	BFNOV31	1.42E+05	9.81E+06	0.004940		
	BFNOV4/1	7.63E+04	2.50E+06	0.010500		
N:BD-Stage III	BFNOV18	4.58E+04	1.78E+06	0.008800	0.006976	0.00134
	BFNOV3	7.93E+04	4.62E+06	0.005860		
	BFNOV4	7.50E+04	4.58E+06	0.005570		
	BFNOV23	1.26E+05	6.28E+06	0.006900		
	BFNOV24	6.42E+04	2.83E+06	0.007750		
	BFNOV5	9.01E+04	4.22E+06	0.007320		
	BFNOV1	7.73E+04	2.26E+06	0.011800		
N:BD-Stage IV	BFNOV2	6.10E+04	2.29E+06	0.009110	0.009826	0.00170
	BFNOV14	7.02E+04	2.92E+06	0.008230		
	BFNOV10	7.49E+04	3.06E+06	0.008390		
	BFNOV12	6.02E+04	2.77E+06	0.007430		
	BFNOV21	8.23E+04	2.65E+06	0.010700		
	BFNOV15	4.58E+04	1.68E+06	0.009340		
	BFNOV20	5.28E+04	1.61E+06	0.011300		
	BFNOV16	3.53E+04	1.30E+06	0.009260		
	BFNOV17	4.68E+04	1.30E+06	0.012400		
	BFNOV13	6.13E+04	1.75E+06	0.012100		

N:BD Post-spawning	BFNOV30	1.34E+05	6.52E+06	0.007050	0.006773	0.00096
	BFNOV36	1.20E+05	5.49E+06	0.005480		
	BFNOV34	1.25E+05	7.46E+06	0.008180		
	BFNOV37	1.08E+05	6.14E+06	0.005990		
	BFNOV39	1.15E+05	5.44E+06	0.007240		
	BFNOV40	1.11E+05	5.65E+06	0.006700		
EA:BD-Stage I	BFEOV18	2.21E+05	3.76E+06	0.006190	0.007332	0.00148
	YLBOV01	6.64E+05	7.53E+06	0.009400		
	YLBOV06	2.06E+05	2.75E+06	0.007930		
	BFEOV15	2.46E+05	4.82E+06	0.005370		
	YLBOV05	4.77E+05	7.40E+06	0.006840		
	YLBOV08	5.44E+05	7.01E+06	0.008260		
EA:BD-Stage II	BFEOV19	1.12E+05	1.60E+06	0.007310	0.014378	0.00642
	BFEOV17	1.73E+05	2.01E+06	0.009080		
	YLBOV07	1.67E+05	1.30E+06	0.013600		
	BFEOV16	1.52E+05	7.78E+05	0.020800		
	YLBOV04	2.58E+05	1.31E+06	0.021100		
	YLBOV02	2.26E+05	7.91E+05	0.030700		
EA:BD-Stage III	BFEOV21	1.86E+05	1.86E+06	0.010600	0.017075	0.00731
	YLBOV02	2.26E+05	7.91E+05	0.030700		
	YLBOV03	1.68E+05	1.38E+06	0.013200		
	BFEOV08	-	-	-		
	BFEOV05	3.75E+05	3.63E+06	0.011100		
	BFEOV02	2.19E+05	2.20E+06	0.010600		
	BFEOV11	1.81E+05	1.11E+06	0.017400		
	BFEOV03	2.79E+05	1.24E+06	0.024200		
	BFEOV20	1.04E+05	5.89E+05	0.018800		
	BFEOV04	-	-	-		
EA:BD-Stage IV	BFEOV01	-	-	-	0.014840	0.00432
	BFEOV07	3.01E+05	2.89E+06	0.011100		
	BFEOV06	1.49E+05	1.57E+06	0.010000		
	BFEOV24	1.67E+05	1.29E+06	0.013700		
	BFEOV10	2.42E+05	1.51E+06	0.017100		
	BFEOV12	1.76E+05	1.35E+06	0.013900		
	BFEOV13	2.49E+05	1.86E+06	0.014200		
	BFEOV22	9.82E+04	6.27E+05	0.016600		
	BFEOV23	7.60E+04	3.30E+05	0.024500		
	BFEOV09	8.25E+04	5.12E+05	0.017100		
	BFEOV14	4.03E+04	4.17E+05	0.010200		

Table E3 Relative expression levels of *SARIP* in different ovarian developmental stages of *P. monodon* based on Quantitative real-time PCR analysis

Sample Groups		Mean conc.		Ratio (target / <i>EF-1α</i>)	Average	STDEV
		<i>SARIP</i>	<i>EF-1α</i>			
Juvenile	JNOV5	1.20E+05	9.76E+06	0.00316	0.00313	0.0004
	JNOV6	2.02E+05	1.84E+07	0.00275		
	JNOV7	1.71E+05	1.21E+07	0.00357		
	JNOV8	9.76E+04	7.17E+06	0.00353		
	JNOV9	8.97E+04	8.88E+06	0.00262		
	JNOV10	-	-	-		
N:BD-Stage I	BUFOV3	3.37E+05	1.86E+07	0.00445	0.00591	0.0019
	BUFOV6	7.31E+04	3.10E+06	0.00624		
	BUFOV4	3.17E+05	1.57E+07	0.00497		
	AGYLOV3	3.17E+05	1.47E+07	0.00531		
	BUFOV7	8.32E+04	3.53E+06	0.00620		
	BUFOV5	7.50E+04	3.07E+06	0.00645		
	AGYLOV1	3.19E+05	1.62E+07	0.00485		
	AGYLOV4	2.84E+05	6.94E+06	0.01020		
	AGYLOV2	2.90E+05	9.89E+06	0.00730		
	BFNOV32	1.94E+05	1.57E+07	0.00309		
N:BD-Stage II	BFNOV38	-	-	-	0.00447	0.0005
	BFNOV33	1.24E+05	5.29E+06	0.00467		
	ASPOV10	9.48E+04	1.21E+07	0.00481		
	BFNOV35	2.32E+05	7.69E+06	0.00487		
	ASPOV6	1.46E+05	1.72E+07	0.00377		
	BFNOV31	2.62E+05	9.81E+06	0.00421		
	BFNOV4/1	-	-	-		
N:BD-Stage III	BFNOV18	8.49E+04	1.78E+06	0.00609	0.00681	0.0016
	BFNOV3	6.39E+04	4.62E+06	0.01010		
	BFNOV4	9.62E+04	4.58E+06	0.00912		
	BFNOV23	8.89E+04	6.28E+06	0.00543		
	BFNOV24	1.37E+05	2.83E+06	0.00507		
	BFNOV5	6.66E+04	4.22E+06	0.00559		
	BFNOV1	9.83E+04	2.26E+06	0.00624		
N:BD-Stage IV	BFNOV2	8.63E+04	2.29E+06	0.00741	0.00690	0.0006
	BFNOV14	6.37E+04	2.92E+06	0.00681		
	BFNOV10	7.53E+04	3.06E+06	0.00621		
	BFNOV12	7.17E+04	2.77E+06	0.00591		
	BFNOV21	6.14E+04	2.65E+06	0.00658		
	BFNOV15	-	-	-		
	BFNOV20	6.56E+04	1.61E+06	0.00697		
	BFNOV16	4.12E+04	1.30E+06	0.00708		
	BFNOV17	3.36E+04	1.30E+06	0.00758		
	BFNOV13	3.59E+04	1.75E+06	0.00753		

N:BD Post-spawning	BFNOV30	1.32E+05	6.52E+06	0.00520	0.00476	0.0006
	BFNOV36	-	-	-		
	BFNOV34	1.10E+05	7.46E+06	0.00382		
	BFNOV37	1.24E+05	6.14E+06	0.00521		
	BFNOV39	1.08E+05	5.44E+06	0.00515		
	BFNOV40	9.64E+04	5.65E+06	0.00443		
	EA:BD-Stage I	BFEOV18	5.28E+05	3.76E+06		
YLBOV01		2.07E+06	7.53E+06	0.00844		
YLBOV06		5.64E+05	2.75E+06	0.00667		
BFEOV15		7.70E+05	4.82E+06	0.00511		
YLBOV05		1.30E+06	7.40E+06	0.00547		
YLBOV08		1.27E+06	7.01E+06	0.00569		
EA:BD-Stage II		BFEOV19	3.10E+05	1.60E+06	0.00643	0.01088
	BFEOV17	3.36E+05	2.01E+06	0.00556		
	YLBOV07	4.16E+05	1.30E+06	0.01060		
	BFEOV16	3.85E+05	7.78E+05	0.01660		
	YLBOV04	6.08E+05	1.31E+06	0.01520		
EA:BD-Stage III	BFEOV21	4.85E+05	1.86E+06	0.00857	0.01361	0.0065
	YLBOV02	5.30E+05	7.91E+05	0.02220		
	YLBOV03	4.43E+05	1.38E+06	0.01080		
	BFEOV08	9.65E+05	3.25E+06	0.00947		
	BFEOV05	8.12E+05	3.63E+06	0.00720		
	BFEOV02	5.00E+05	2.20E+06	0.00744		
	BFEOV11	4.44E+05	1.11E+06	0.01330		
	BFEOV03	5.90E+05	1.24E+06	0.01560		
	BFEOV20	2.53E+05	5.89E+05	0.01470		
	BFEOV04	3.08E+05	3.90E+05	0.02680		
EA:BD-Stage IV	BFEOV01	-	-	-	0.01001	0.0017
	BFEOV07	6.91E+05	2.89E+06	0.00772		
	BFEOV06	4.98E+05	1.57E+06	0.00998		
	BFEOV24	3.29E+05	1.29E+06	0.00850		
	BFEOV10	5.87E+05	1.51E+06	0.01270		
	BFEOV12	4.44E+05	1.35E+06	0.01090		
	BFEOV13	5.57E+05	1.86E+06	0.00978		
	BFEOV22	1.94E+05	6.27E+05	0.01070		
	BFEOV23	-	-	-		
	BFEOV09	1.77E+05	5.12E+05	0.01190		
	BFEOV14	9.21E+04	4.17E+05	0.00791		

Table E4 Relative expression levels of *Cdc42* in different ovarian developmental stages of *P. monodon* based on Quantitative real-time PCR analysis

Sample Groups		Mean conc.		Ratio (target / <i>EF-1a</i>)	Average	STDEV
		<i>Cdc42</i>	<i>EF-1a</i>			
Juvenile	JNOV1	1.37E+05	1.38E+07	0.009960	0.010135	0.0011
	JNOV2	1.46E+05	1.65E+07	0.008837		
	JNOV3	2.51E+05	2.19E+07	0.011423		
	JNOV4	1.97E+05	1.91E+07	0.010322		
N:BD-Stage I	AGYL03	2.68E+05	1.24E+07	0.021629	0.021523	0.0016
	PMBF2	2.58E+05	1.37E+07	0.018846		
	AGYL01	3.26E+05	1.50E+07	0.021711		
	AGYL04	4.23E+05	1.89E+07	0.022392		
	AGYL02	3.14E+05	1.36E+07	0.023037		
N:BD-Stage II	BFN1OV4/1	9.57E+04	5.40E+06	0.017713	0.019078	0.0014
	BFN1OV4	1.27E+05	6.43E+06	0.019703		
	BFN1OV3	1.71E+05	8.01E+06	0.021307		
	BFN2OV5	1.14E+05	6.29E+06	0.018156		
	BFN1OV1	1.06E+05	5.92E+06	0.017938		
	BFN1OV2	4.56E+04	2.32E+06	0.019651		
N:BD-Stage III	BFN3OV9	4.71E+04	3.18E+06	0.014821	0.018495	0.0032
	BFN3OV8	9.15E+04	4.42E+06	0.020697		
	BFN3OV6	8.19E+04	4.10E+06	0.019966		
N:BD-Stage IV	BFN3OV12	6.97E+04	3.81E+06	0.018306	0.021207	0.0020
	BFN4OV15	4.92E+04	2.14E+06	0.022963		
	BFN3OV11	2.92E+04	1.28E+06	0.022876		
	BFN4OV16	2.54E+04	1.26E+06	0.020151		
	BFN4OV13	1.73E+04	7.94E+05	0.021739		
EA:BD-Stage I	YLBOV1	3.82E+05	1.86E+07	0.020505	0.019643	0.0021
	YLBOV6	1.71E+05	1.01E+07	0.016851		
	YLBOV8	6.09E+04	3.16E+06	0.019287		
	YLBOV5	2.73E+05	1.25E+07	0.021928		
EA:BD-Stage II	YLBOV4	1.27E+05	6.58E+06	0.019291	0.020683	0.0027
	YLBOV7	8.00E+04	5.57E+06	0.014372		
	YLBOV3	1.33E+05	6.66E+06	0.019925		
	BFEA2OV5	1.28E+05	6.09E+06	0.020962		
	BFEA2OV8	2.12E+05	9.19E+06	0.023083		
	BFEA1OV2	1.55E+05	6.77E+06	0.022843		
	BFEA1OV4	1.15E+05	5.45E+06	0.021111		
	BFEA2OV7	6.43E+04	2.89E+06	0.022283		
	BFEA2OV6	1.43E+05	6.40E+06	0.022276		
	BFEA3OV12	1.26E+05	6.65E+06	0.018879		
EA:BD-Stage III	BFEA2OV10	1.35E+05	7.03E+06	0.019203	0.019041	0.0002
	BFEA1OV9	1.93E+04	6.02E+05	0.032073		
EA:BD-Stage IV	BFEA1OV1	7.39E+04	3.62E+06	0.020414	0.023664	0.0073
	BFN4OV14	6.76E+04	3.66E+06	0.018503		

Table E4 Relative expression levels of *PGMRC1* in the time-course for 12, 24, 48 and 72 hours post treatment of 5-HT in juvenile *P. monodon* based on Quantitative real-time PCR analysis

Sample Groups	Mean conc.		Ratio (target / <i>EF-1α</i>)	Average	STDEV
	<i>PGMRC1</i>	<i>EF-1α</i>			
NSI 0-1	4.39E+05	1.58E+07	2.78E-02	0.023925	0.00596069
NSI 0-2	3.84E+05	2.56E+07	1.50E-02		
NSI 0-4	4.41E+05	1.52E+07	2.90E-02		
5HTI 0-1	4.00E+05	1.42E+07	2.82E-02	0.026673	0.00463881
5HTI 0-4	4.29E+05	2.18E+07	1.97E-02		
5HTI 0-5	4.43E+05	1.38E+07	3.21E-02		
5HTI12-3	3.20E+05	1.35E+07	2.37E-02	0.028838	0.00340721
5HTI12-4	3.62E+05	1.09E+07	3.34E-02		
5HTI12-5	3.37E+05	1.15E+07	2.94E-02		
5HTI1D-1	2.66E+05	1.32E+07	2.01E-02	0.020364	0.00024288
5HTI1D-2	2.37E+05	1.17E+07	2.03E-02		
5HTI1D-5	2.14E+05	1.03E+07	2.07E-02		
5HTI2D-1	3.87E+05	1.57E+07	2.48E-02	0.021195	0.00377081
5HTI2D-2	2.45E+05	1.58E+07	1.55E-02		
5HTI2D-4	2.23E+05	9.59E+06	2.33E-02		
5HTI3D-1	4.31E+05	1.56E+07	2.76E-02	0.026106	0.00116173
5HTI3D-2	4.55E+05	1.73E+07	2.64E-02		
5HTI3D-2	4.50E+05	1.85E+07	2.44E-02		
NSII 0-1	3.09E+05	2.25E+07	1.37E-02	0.018234	0.00299881
NSII 0-2	3.28E+05	1.68E+07	1.95E-02		
NSII 0-4	4.06E+05	1.89E+07	2.14E-02		
5HTII 0-1	3.33E+05	2.00E+07	1.66E-02	0.018657	0.00134028
5HTII 0-2	4.18E+05	2.17E+07	1.93E-02		
5HTII 0-3	2.39E+05	1.19E+07	2.00E-02		
5HTII 12-1	1.07E+05	3.55E+06	3.01E-02	0.019461	0.00709368
5HTII 12-4	1.98E+05	1.47E+07	1.35E-02		
5HTII 12-5	2.10E+05	1.42E+07	1.48E-02		
5HTII 1D-1	2.91E+05	1.59E+07	1.83E-02	0.016427	0.00123646
5HTII 1D-2	2.38E+05	1.53E+07	1.56E-02		
5HTII 1D-3	2.50E+05	1.62E+07	1.54E-02		
5HTII 2D-3	3.11E+05	2.03E+07	1.53E-02	0.017324	0.00271959
5HTII 2D-4	2.84E+05	1.33E+07	2.14E-02		
5HTII 2D-5	3.16E+05	2.08E+07	1.52E-02		
5HTII 3D-1	3.20E+05	1.80E+07	1.78E-02	0.019619	0.00293531
5HTII 3D-2	3.70E+05	1.54E+07	2.40E-02		
5HTII 3D-3	2.33E+05	1.37E+07	1.70E-02		

APPENDIX F

Table F1 The percentage of GSI and another data of *p. monodon* using in this thesis

No.	Body weight (g.)	Gonad weight (g.)	GSI (%)	Total length (cm.)	Original codes	Gonad colour	Remark
1	115.28	0.32	0.27	23.5	BUFOV03	light white	Stage I
2	76.37	0.47	0.61	23.0	BUFOV06	light white	Stage I
3	105.70	0.70	0.66	24.5	BUFOV04	light white	Stage I
4	99.96	0.77	0.77	23.5	AGYLOV03	white	Stage I
5	170.28	1.46	0.86	-	PMBF2	white	Stage I
6	112.35	1.00	0.89	23.0	BUFOV07	light yellow	Stage I
7	82.71	0.90	1.08	21.5	BUFOV05	turbid white	Stage I
8	157.33	1.73	1.10	27.0	AGYLOV01	white + light pink	Stage I
9	104.97	1.18	1.12	23.0	AGYLOV04	white	Stage I
10	120.58	1.60	1.33	23.5	AGYLOV02	white	Stage I
11	186.69	2.69	1.44	26.0	BFNOV32	yellow	Stage I
12	188.30	2.76	1.47	-	PMBF1	light yellow	Stage I
13	218.71	4.70	2.15	28.0	BFNOV38	light green + yellow	Stage II
14	205.67	4.61	2.24	27.5	BFNOV33	light yellow	Stage II
15	128.74	2.25	2.25	24.5	ASPOV10	light yellow	Stage II
16	205.05	5.29	2.58	28.0	BFNOV35	light yellow	Stage II
17	149.64	2.68	2.68	26.7	ASPOV06	light yellow	Stage II
18	208.54	6.16	2.95	26.0	BFNOV31	light green	Stage II
19	181.30	6.00	3.31	28.5	BFNOV04/1	yellow + green	Stage II
20	159.80	6.40	4.01	27.7	BFNOV07	light green	Stage III
21	187.10	8.27	4.42	30.0	BFNOV18	green + yellow	Stage III
22	173.40	8.00	4.61	28.0	BFNOV03	green	Stage III
23	164.50	7.60	4.64	27.5	BFNOV04	green	Stage III
24	230.93	12.12	5.28	32.0	BFNOV23	green + yellow	Stage III
25	235.98	12.69	5.37	33.0	BFNOV24	green	Stage III
26	172.30	9.90	5.75	28.0	BFNOV05	green	Stage III
27	172.60	10.20	5.91	28.0	BFNOV01	green	Stage III
28	136.40	8.40	6.16	26.5	BFNOV09	dark green	Stage IV
29	133.20	8.30	6.23	26.0	BFNOV08	green	Stage IV
30	176.20	12.90	7.32	29.0	BFNOV06	dark green	Stage IV
31	272.20	20.30	7.46	32.0	BFNOV02	green	Stage IV
32	152.20	12.80	8.42	27.0	BFNOV14	green	Stage IV
33	139.90	13.10	9.36	25.5	BFNOV10	dark green	Stage IV
34	162.20	16.20	9.99	28.0	BFNOV12	dark green	Stage IV
35	166.90	16.70	10.01	27.5	BFNOV11	light green	Stage IV
36	239.86	24.98	10.41	33.0	BFNOV21	green	Stage IV
37	207.40	23.20	11.19	30.5	BFNOV15	dark green	Stage IV
38	232.57	26.08	11.21	30.0	BFNOV20	green	Stage IV
39	156.10	18.20	11.66	27.0	BFNOV16	dark green	Stage IV
40	252.11	31.30	12.41	30.0	BFNOV17	green	Stage IV
41	158.60	19.90	12.55	27.5	BFNOV13	dark green	Stage IV
42	300.12	10.47	3.49	32.5	BFNOV30	light green + yellow	post-spawn

Table F1 (cont.)

No.	Body weight (g.)	Gonad weight (g.)	GSI (%)	Total length (cm.)	Original codes	Gonad colour	Remark
43	194.49	3.61	1.86	27.5	BFNOV36	light yellow + little green	post-spawn
44	256.40	8.39	3.27	29.5	BFNOV34	light yellow	post-spawn
45	264.70	7.66	2.89	30.0	BFNOV37	light yellow	post-spawn
46	285.97	8.30	2.90	32.0	BFNOV39	yellow	post-spawn
47	200.79	5.18	2.58	28.0	BFNOV40	light yellow	post-spawn
48	236.51	1.79	0.76	27.50	BFEOOV18	white	Eyestalk-ablated; Stg I
49	111.00	1.00	0.90	24.50	YLBOV01	white + light yellow	Eyestalk-ablated; Stg I
50	163.00	2.00	1.22	25.00	YLBOV06	white	Eyestalk-ablated; Stg I
51	272.20	3.71	1.36	30.00	BFEOOV15	yellow	Eyestalk-ablated; Stg I
52	125.00	2.00	1.60	24.50	YLBOV05	white + light yellow	Eyestalk-ablated; Stg II
53	118.00	2.00	1.69	24.50	YLBOV08	white	Eyestalk-ablated; StgII
54	173.37	4.72	2.72	25.50	BFEOOV19	light green + yellow	Eyestalk-ablated; Stg II
55	252.03	7.16	2.84	29.50	BFEOOV17	green + yellow	Eyestalk-ablated; Stg II
56	151.00	5.00	3.31	25.00	YLBOV07	light green	Eyestalk-ablated; Stg II
57	291.39	10.31	3.54	30.50	BFEOOV16	green	Eyestalk-ablated; Stg II
58	164.00	6.00	3.66	26.00	YLBOV04	light green	Eyestalk-ablated; Stg II
59	193.65	8.82	4.55	27.00	BFEOOV21	dark green	Eyestalk-ablated; Stg III
60	153.00	7.00	4.57	25.50	YLBOV02	light green	Eyestalk-ablated; Stg III
61	125.00	6.00	4.80	25.00	YLBOV03	light green	Eyestalk-ablated; Stg III
62	118.80	5.90	4.97	24.50	BFEOOV08	green	Eyestalk-ablated; Stg III; BIOTEC shrimp
63	186.50	9.40	5.04	27.50	BFEOOV05	light green	Eyestalk-ablated; Stg III
64	196.90	10.00	5.08	29.50	BFEOOV02	light green + yellow	Eyestalk-ablated; Stg III
65	96.20	4.90	5.09	23.30	BFEOOV11	green	Eyestalk-ablated; Stg III; BIOTEC shrimp
66	182.70	9.40	5.15	28.00	BFEOOV03	yellow + little green	Eyestalk-ablated; Stg III
67	278.23	14.37	5.16	29.50	BFEOOV20	dark green + little yellow	Eyestalk-ablated; Stg III
68	197.40	10.80	5.47	29.50	BFEOOV04	light green + yellow	Eyestalk-ablated; Stg III
69	229.60	14.60	6.36	30.00	BFEOOV01	green + yellow	Eyestalk-ablated; StgIV
70	220.10	14.00	6.36	28.50	BFEOOV07	light green + yellow	Eyestalk-ablated; StgIV
71	170.20	11.60	6.82	27.00	BFEOOV06	light green + yellow	Eyestalk-ablated; StgIV
72	365.38	25.08	6.86	33.00	BFEOOV24	green	Eyestalk-ablated; StgIV
73	116.40	8.00	6.87	25.50	BFEOOV10	dark green	Eyestalk-ablated; StgIV; BIOTEC shrimp
74	128.70	8.90	6.92	25.20	BFEOOV12	dark green	Eyestalk-ablated; StgIV; BIOTEC shrimp
75	188.20	13.80	7.35	27.50	BFEOOV13	dark green	Eyestalk-ablated; StgIV
76	167.54	14.33	8.55	25.00	BFEOOV22	dark green	Eyestalk-ablated; StgIV
77	256.34	22.41	8.74	29.50	BFEOOV23	dark green	Eyestalk-ablated; StgIV
78	249.50	22.30	8.94	31.50	BFEOOV09	light green	Eyestalk-ablated; StgIV
79	115.60	12.80	11.07	23.50	BFEOOV14	dark green	Eyestalk-ablated; StgIV; BIOTEC shrimp

BIOGRAPHY

Miss Rachanimuk Preechaphol was born on August 20, 1980 in Chonburi. She graduated with the degree of Bachelor of Science from the Faculty of Agricultural Technology at King Mongkut's Institute of Technology Ladkrabang in 2000 and the degree of Master of Science (Biotechnology) at the Program of Biotechnology, Chulalongkorn University in 2004. She has studied for the Degree of Doctor of Philosophy in Biotechnology, Chulalongkorn University since 2004.

Publications from this thesis

International publications

1. Klinbunga, S., **Preechaphol, R.**, Thumrunthanakit, S., Leelatanawit, R., Aoki, T., Jarayabhand, P., and Menasveta, P. (2006). Genetic diversity of the giant tiger shrimp (*Penaeus monodon*) in Thailand revealed by PCR-SSCP of polymorphic EST-derived markers. *Biochem Genet.* 44: 222-36.
2. **Preechaphol, R.**, Leelatanawit, R., Sittikankeaw, K., Klinbunga, S., Khamnamtong, B., Puanglarp, N., and Menasveta, P. (2007). Expressed sequence tag analysis for identification and characterization of sex-related genes in the giant tiger shrimp *Penaeus monodon*. *J Biochem Mol Biol.* 40: 501-10.
3. **Preechaphol, R.**, Leelatanawit, R., Wongsurawat, T., Klinbunga, S. and Menasveta, P. (2009). Expressed sequence tag analysis for isolation of genes functionally related to ovarian development of the giant tiger shrimp *Penaeus monodon* (in preparation).
4. **Preechaphol, R.**, Klinbunga, S., Wongsurawat, T., and Menasveta, P. (2009). Suppression subtractive hybridization (SSH) for isolation and characterization of reproduction-related genes of the giant tiger *Penaeus monodon* (in preparation).
5. **Preechaphol, R.**, Klinbunga, S., Wongsurawat, T., and Menasveta, P. (2009). Isolation of differentially expressed genes during ovarian development of the giant tiger shrimp *Penaeus monodon* using RNA arbitrarily primed-polymerase chain reaction (RAP-PCR) (in preparation).

6. **Preechaphol, R.**, Klinbunga, S., Yamano, K., and Menasveta, P. (2009). Molecular cloning and expression analysis of *progesterone receptor membrane component 1 (PGMRC1)* of the giant tiger shrimp *Penaeus monodon* (in preparation).
7. **Preechaphol, R.**, Klinbunga, S., Yamano, K., and Menasveta, P. (2009). Molecular cloning and characterization of *cell division cycle 42 (Cdc42)* downregulated during ovarian development of the giant tiger shrimp *Penaeus monodon* (in preparation).
8. **Preechaphol, R.**, Klinbunga, S., Yamano, K., and Menasveta, P. (2009). Potential roles of a *small androgen receptor interacting protein (SARIP)* gene in ovarian development of the giant tiger shrimp *Penaeus monodon* (in preparation).
9. **Preechaphol, R.**, Klinbunga, S., and Menasveta, P. (2009). Isolation and characterization of *progesterone receptor-related protein p23 (PRp23)* differentially expressed during ovarian development of the giant tiger shrimp *Penaeus monodon* (in preparation).

International conferences

1. **Preechaphol, R.**, Yamano, K., Klinbunga, S., and Menasveta, P. (2008). Isolation and characterization of *cell division cycle 42 (CDC42)* and *progesterone receptor membrane component 1 (PGMRC1)* differentially expressed during ovarian development the giant tiger shrimp *Penaeus monodon*. 5th World Fisheries Congress (WFC), 20-24 October 2008, Pacifico, Yokohama, Japan (Oral presentation).
2. **Preechaphol, R.**, Yamano, K., Klinbunga, S., and Menasveta, P. (2008). Potential roles of *small androgen receptor interacting protein (SARIP)*, *progesterone receptor membrane component 1 (PGMRC1)* and *cell division cycle 42 (Cdc42)* in ovarian development of the giant tiger shrimp *Penaeus monodon*. The 8th Asia-Pacific Marine Biotechnology Conference (APMBC), 12-15 November 2008, BEXCO/Busan, South Korea (Poster presentation).
3. **Preechaphol, R.**, Klinbunga, S., and Menasveta, P. (2009). Isolation and characterization of *progesterone receptor-related protein p23 (PRp23)* differentially expressed during ovarian development of the giant tiger shrimp *Penaeus monodon*. The 10th International Symposium on Genetics in Aquaculture (ISGA 2009), 22-26 June 2009, Bangkok Convention Centre & Sofitel Centara Grand Hotel, Bangkok, Thailand.

National conferences

1. **Preechaphol, R.**, Klinbunga, S., and Menasveta, P. (2005). Isolation and Characterization of Differentially Expressed Genes in Ovaries of the Giant Tiger Shrimp (*Penaeus monodon*). 31st Congress on Science and Technology of Thailand, 18–20 October 2005, Nakornratchasima, Thailand (Oral presentation).
2. **Preechaphol, R.**, Leelatanawit, R., Sittikankaew, K., Klinbunga, S., and Menasveta, P. (2006). Expressed sequence tag analysis for isolation and characterization of sex differentiation-related genes in the giant tiger shrimp (*penaeus monodon*). 32nd Congress on Science and Technology of Thailand, 10–12 October 2006, Queen Sirikit National Convention Center (QSNCC), Thailand (Oral presentation).
3. **Preechaphol, R.**, Yamano, K., Klinbunga, S., and Menasveta, P. (2008). Isolation and characterization of *cell division cycle 42 (CDC42)* and *progesterone receptor membrane component 1 (PGMRC1)* differentially expressed during ovarian development the giant tiger shrimp *Penaeus monodon*. NSTDA Annual Conference 2008 (NAC 2008), 28-30 March 2008, BIOTEC Science Park, Thailand (Oral presentation).
4. **Preechaphol, R.**, Yamano, K., Klinbunga, S., and Menasveta, P. (2009). Potential roles of *small androgen receptor interacting protein (SARIP)*, *progesterone receptor membrane component 1 (PGMRC1)* and *cell division cycle 42 (cdc42)* in ovarian development of the giant tiger shrimp *Penaeus monodon*. The RGJ-Ph.D. Congress X, 3-5 April 2009, Jomtien Palm Beach Hotel&Resort, Pattaya, Chonburi, Thailand (oral presentation).